

Contents

No. 1 JULY 1968

CHARLES MAYO GOSS. On Movement of Muscles by Galen of Pergamon	1
JOYCE E. SHRIVER, BENNETT M. STEIN AND MALCOLM B. CARPENTER. Central Projections of Spinal Dorsal Roots in the Monkey. I. Cervical and Upper Thoracic Dorsal Roots ..	27
MALCOLM B. CARPENTER, BENNETT M. STEIN AND JOYCE E. SHRIVER. Central Projections of Spinal Dorsal Roots in the Monkey. II. Lower Thoracic, Lumbosacral and Coccygeal Dorsal Roots	75
JAMES T. IRVING AND JAMES A. BOND. The Subcutaneous Implantation of Autogenous Rat Molars ..	119
J. V. KANNANKERIL AND L. V. DOMM. Development of the Gonads in the Female Japanese Quail	131
MARY A. BONNEVILLE. Observations on Epidermal Differentiation in the Fetal Rat	147
ERNEST N. ALBERT AND DANIEL C. PEASE. An Electron Microscopic Study of Uterine Arteries During Pregnancy ..	165
RUTH ELLEN BULGER AND BENJAMIN F. TRUMP. Renal Morphology of the English Sole (<i>Parophrys vetulus</i>) ..	195

No. 2 SEPTEMBER 1968

DANIEL O. GRANEY. The Uptake of Ferritin by Ileal Absorptive Cells in Suckling Rats. An Electron Microscope Study ..	227
ROBERT F. DYER. Morphological Features of Brown Adipose Cell Maturation <i>in vivo</i> and <i>in vitro</i>	255
J. B. GAVIN. The Ultrastructure of the Crevicular Epithelium of Cat Gingiva	283
WILLIAM G. SELIGER AND WAYNE F. SMITH. The Fine Structure of the Adrenal Cortex of the 13-Lined Ground Squirrel ..	297
WENCESLAO CALVO. The Innervation of the Bone Marrow in Laboratory Animals	315
J. M. BEDFORD. Ultrastructural Changes in the Sperm Head during Fertilization in the Rabbit	329
VINCENT DE ANGELIS. Autoradiographic Investigation of Calvarial Growth in the Rat	359
WALTER J. BO, D. LOUISE ODOR AND MARTHA ROTHROCK. The Fine Structure of Uterine Smooth Muscle of the Rat Uterus at Various Time Intervals Following a Single Injection of Estrogen	369

No. 3 NOVEMBER 1968

WINTER PATRICK LUCKETT. Morphogenesis of the Placenta and Fetal Membranes of the Tree Shrews (Family Tupaiidae)	385
THOMAS D. CLARKE, ALLEN D. ASHBURN AND W. LANE WILLIAMS. Cortisone-induced Hypertension and Cardiovascular Lesions in Mice	429
J. DAVIES AND CAROLE D. BROADUS. Studies on the Fine Structure of Ovarian Steroid-secreting Cells in the Rabbit. I. The Normal Interstitial Cells	441
J. M. PAPADIMITRIOU AND M. N-I. WALTERS. Fluid Flow in the Liver Demonstrated with Horse Radish Peroxidase	475
JAMES C. PETTERSEN AND ROBERT J. ROSE. Marginal Zone and Germinal Center Development in the Spleens of Neonatally Thymectomized and Nonthymectomized Young Rats	489
ERLE K. ADRIAN, JR. Cell Division in Injured Spinal Cord	501
J. TOOZE AND H. G. DAVIES. Light and Electron Microscopic Observations on the Spleen and the Splenic Leukocytes of the Newt <i>Triturus cristatus</i>	521
INDEX TO VOLUME 123	557

No. 2 SEPTEMBER 1968

DANIEL O. GRANEY. The Uptake of Ferritin by Ileal Absorptive Cells in Suckling Rats. An Electron Microscope Study . .	227
ROBERT F. DYER. Morphological Features of Brown Adipose Cell Maturation <i>in vivo</i> and <i>in vitro</i>	255
J. B. GAVIN. The Ultrastructure of the Crevicular Epithelium of Cat Gingiva	283
WILLIAM G. SELIGER AND WAYNE F. SMITH. The Fine Structure of the Adrenal Cortex of the 13-Lined Ground Squirrel . .	297
WENCESLAO CALVO. The Innervation of the Bone Marrow in Laboratory Animals	315
J. M. BEDFORD. Ultrastructural Changes in the Sperm Head during Fertilization in the Rabbit	329
VINCENT DE ANGELIS. Autoradiographic Investigation of Calvarial Growth in the Rat	359
WALTER J. BO, D. LOUISE ODOR AND MARTHA ROTHROCK. The Fine Structure of Uterine Smooth Muscle of the Rat Uterus at Various Time Intervals Following a Single Injection of Estrogen	369

On Movement of Muscles by Galen of Pergamon

CHARLES MAYO GOSS

The George Washington University, School of Medicine, Washington, D. C.

ABSTRACT Galen begins with definitions, giving the special differentiating characteristics of nerves, muscles, tendons, aponeuroses, fascia, and other connective tissue elements. He demonstrates that contraction is the specific activity of muscles. It occurs voluntarily through impulses from the brain carried by the nerves. Protagonists and antagonists are described and demonstrated by experiments with severing individuals and groups as well as with a model made of articulated bones and thongs attached in proper places to represent muscles. Attention is called to passive motion of muscles. The action of gravity is related to muscular action. Sustained contraction of muscles is called tonic activity. The effect of habit on muscles and the subconscious control of voluntary muscles are explained. Visceral organs and blood vessels are under the control of nature rather than the brain, and are thus contrasted with the muscles.

A translation of this treatise is important because it gives the reader an opportunity to judge for himself the validity of the criticism that Galen did not distinguish between nerves, tendons, and ligaments. Within the first few pages it becomes evident that he understood their differences both structurally and functionally to a surprising degree, although he is puzzled over the termination of the motor nerves because he had no microscope with which to follow them.

The title of the treatise is misleading to the modern reader because it does not mention the nervous system. Galen pictured the muscles as instruments of the brain, controlled through the nerves. In demonstrating this he introduced a large amount of information concerning the activity of the brain which is useful in understanding some of his other treatises, especially those dealing with psychiatry.

In the translation an attempt has been made to follow the Greek of the Kuhn (1821-1835) edition as literally as possible and at the same time convert it into an approach to easily readable English. Two words have been particularly difficult to translate, namely, *PSYCHE* and *PHYSIS*. Galen used the former to designate the organ which exerts voluntary control over the various structures of the body, especially the muscles. In so doing he contrasts these structures with others not under this control, but which are the province of nature, that is, the *PHYSIS*. The word

PSYCHE, therefore, will be translated brain and *PHYSIS* nature. He occasionally used another word for the brain, *ENKEPHALON*, but by this he meant the dissectable structure in the head contrasted with the spinal cord. Still another word is used for the more dynamic and less corporeal concept of the brain, namely *NOUS*, and this is translated mind in order to emphasize this distinction.

The following typographical conventions will be used:

The numbers in square brackets refer to the pages in volume 4 of the Kuhn edition (1821-1833).

Greek words taken directly into English are transliterated into Roman Capitals.

Greek words are given their Greek endings.

Titles of Galen's own works appear in quotes.

Modern anatomical terms, where appropriate, are taken from the 1965 *Nomina Anatomica*, italicized, and placed in parentheses.

Editorial comments and explanations are enclosed in square brackets.

BOOK ONE

Chapter I

Voluntary motion in the various parts of the body is brought about by the contraction of muscles. Their number is so great, however, that they cannot be counted with ease, for they unite with one another, some

soon as they join with the muscles, the nerves divide in many directions, some divisions go to one part, others to others, and at last, completely separating into delicate membranous fibers [INAS], they form a plexus through all the body of the muscle. The fascia by which the muscles are united and bound with the bones gives rise to the membranes which surround them and penetrate the flesh of the muscle. It appears to me, therefore, as if the muscle were a region [372] irrigated by several conduits, that is, by the first mentioned conduit, the nerve, and by two others, one the conduit for blood which is hot, thin, and vaporous, and the other for thicker and colder blood. The former of these is called the artery, the latter the vein. These same conduits, having their sources [ARCHE], from the heart, and from the liver, permeate the substance of the muscle and through them the muscle becomes not simply a place, but a vegetative being [PHYTOS = plant].

Through the third conduit, that from the great source, it becomes not simply a living thing but something in addition to a vegetative being, by acquiring sensation and the power of voluntary motion, attributes by which the animal is differentiated from the non-animal. Through these powers the muscle has become an instrument of the brain [PSYCHIKON ORGANON] exactly as it has become a natural or living one [PHYSIKON] through the arteries and veins, for the motions of the arteries and veins are simply living or natural and without impulse, but those of the muscles are voluntary and by impulse. Whether you say the movements of the muscles arise by deliberate choice or act of free will or by intention makes little difference, for the one object at which we must aim with all these terms [373] is to distinguish the notion of muscles from that of the arteries and veins. If it is not sufficient to point out the difference in words, you may demonstrate what you wish.

Why do we say that the muscle is not an organ of sensation, but solely of motion, and why does it not partake equally of both? Is it because voluntary movement could not occur in animals without the muscles, so that a muscle is the proper

organ of motion, but sensation resides in all the sensitive parts and independent of muscles? For whichever of them shares the nerve, that, at any rate, has sensation. It has been clearly stated, then, what the muscle is, namely, that it is the instrument of voluntary motion. It was stated, also, where the source is from which its motion arises, as well as how it comes from the brain through the nerves. It was stated also how the latter as well as the binding tissues ramify with it.

Chapter II

It still remains for us to speak concerning the nature of the tendons in order that nothing will remain obscure for the [374] discussions to follow. It was mentioned above, the constitution of tendons is a mixture of binding tissue and nerve. The elaboration of this was set aside, but now will be presented. Tendon is harder than nerve by as much as it is softer than binding tissue, but the bulk of its substance is great enough to be formed of both. Binding tissues are all without sensation, but all nerves are sensitive. The tendon is not insensitive because it contains nerve but it is not as sensitive as nerve because it is not solely nerve. To the extent that it has the nature of binding tissue, the accuracy of sensation is blunted. The tendon arises from the tail [insertion] of the muscle. Attaching to its head, however, are both nerve and binding tissue and they are distributed to the whole muscle making it reasonable that the tendon is formed from both.

The way to learn this more distinctly is through dissection, for then you would see clearly that the origin which they call the head of the muscle is more sinewy [NEUROEIDES = nerve-like], the middle, more flesh-like, [375] is called the belly of the muscle, and thereafter it becomes more and more sinewy in proportion to the beginning until finally the lower end seems more sinewy than the head. The nerve, having reached it at its origin, is distributed in small subdivisions; these in turn dividing into others and again the latter divide into still others, until this division advances in such a degree as to end in membranous and very thin fibers. Continuing farther, in

seeming to appear single, and some, although ending in many tendons, remain entities, however many the tendons seem to be. Because of this and because they are of diverse shapes and attach to dissimilar parts, it is quite difficult to investigate the manner of their moving. This may also be to some extent because they are secured to the moveable parts at different and often opposite places. [368] Thus, they insert, some above, others below, some in front, others behind, some on one side or some on the other. Accordingly, if a whole muscle has been cut into by a wound not too slight nor near the surface, some of the motions of the part to which it is attached are interrupted. Also, when its injuries are of many kinds, it becomes most difficult to comprehend the manner in which it moves. For example, if one or another of the muscles in the legs has been cut, a person may be unable to bend, straighten, raise, lower, or turn the limb about. In a similar manner, inflammations, scars, necroses, and bruises, or indurations affecting a whole muscle have the same effect, not only on the legs but also on the hands. For involvement of some of the muscles would cause loss of power to raise, others to bend, extend, or lower the hands, or twist them to either side or turn them backward. The same thing happens if the tendons are affected. (The more recent observers call them aponeuroses of muscles because, I think, they see the muscles [369] coming to an end in them.) The nature of tendon is something of a mixture and is intermediate between fascia [SUNDESMOS binding tissue or connective tissue] and nerve. Fascia, at least in its specific meaning, not as the name commonly implies (probably refers to ligament), is a nerve-like substance, always seen associated with bone, intervening between either bones or muscles, clearly its name (i.e., binding tissue) comes from its purpose.

Nerve [NEURON] or sinew [TONOS], on the other hand, originates from the brain [ENKEPHALON] or spinal marrow (cord). (Although one organ, it has been called by two names from its functions because it produces bending and pulling.) The consistency of its substance may be imagined if you think of the brain as having been

compressed and packed close, thereby becoming harder. The substance of the spinal cord is similar to the brain but, having been compressed, it has become hard. Indeed, within the brain itself, the posterior portion which is continuous with the spinal cord is harder than the anterior part, and some nerves which are softer than others will not seem to you to differ from the spinal cord.

The marrow in the other bones is not the same, for it is wet and almost liquid. You might compare it most of all [370] to fat in softness. Moreover, you will not find any nerve either soft or hard arising from this latter marrow, nor is it clothed by the meninges of the brain and spinal cord. Arteries and veins do not form a plexus through it as they do in the brain and spinal cord, nor is it associated with any muscle. There is an important association between the brain or spinal cord and all muscles, however, for each must receive a nerve from either the brain or the spinal cord.

This nerve appears small but it is, indeed, not slight in power. This you may observe as a result of injuries to it, for either cutting, compressing, contusing, scarring, necrosing, or binding with a ligature would eliminate all motion and sensation from its associated muscle. When it is inflamed, however, convulsions and delirium are caused in not a few persons. Some individuals, being thus afflicted and meeting one of the more skilled physicians, have had the nerve cut and straightway were relieved of the convulsions and delirium. Henceforth the muscle to [371] which the nerve ran was insensible and useless for motion.

Thus in the nerves, some great power resides flowing to them from the great source [ARCHE]. The power is not inherent in the nerves nor does it stem directly from them. You may demonstrate this especially well if you cut any one of these nerves or the spinal cord itself. Then whatever part is above the cut and connected to the brain [ENCEPHALON] will retain the powers of the source, while all the part below can supply no sensation or motion. The nerves, being analogous to conduits, carry power to the muscles from some fount of the brain. As

son as they join with the muscles, the nerves divide in many directions, some divisions go to one part, others to others, and at last, completely separating into delicate membranous fibers [INĀS], they form a plexus through all the body of the muscle. The fascia by which the muscles are united and bound with the bones gives rise to the membranes which surround them and penetrate the flesh of the muscle. It appears to me, therefore, as if the muscle were a region [372] irrigated by several conduits, that is, by the first mentioned conduit, the nerve, and by two others, one the conduit for blood which is hot, thin, and porous, and the other for thicker and colder blood. The former of these is called the artery, the latter the vein. These same conduits, having their sources [ARCHE], from the heart, and from the liver, permeate the substance of the muscle and through them the muscle becomes not simply a place, but a vegetative being [PHYTOS = plant].

Through the third conduit, that from the great source, it becomes not simply a living being but something in addition to a vegetative being, by acquiring sensation and the power of voluntary motion, attributes by which the animal is differentiated from the non-animal. Through these powers the muscle has become an instrument of the brain [PSYCHIKON ORGANON] exactly as it has become a natural or living one [PHYSIKON] through the arteries and veins, for the motions of the arteries and veins are simply living or natural and without impulse, but those of the muscles are voluntary and by impulse. Whether you say the movements of the muscles arise by deliberate choice or act of free will or by intention makes little difference, for the one object at which we must aim with all these terms [373] is to distinguish the motion of muscles from that of the arteries and veins. If it is not sufficient to point out the difference in words, you may demonstrate what you wish.

Why do we say that the muscle is not an organ of sensation, but solely of motion, and why does it not partake equally of both? Is it because voluntary movement would not occur in animals without the muscles, so that a muscle is the proper

organ of motion, but sensation resides in all the sensitive parts and independent of muscles? For whichever of them shares the nerve, that, at any rate, has sensation. It has been clearly stated, then, what the muscle is, namely, that it is the instrument of voluntary motion. It was stated, also, where the source is from which its motion arises, as well as how it comes from the brain through the nerves. It was stated also how the latter as well as the binding tissues ramify with it.

Chapter II

It still remains for us to speak concerning the nature of the tendons in order that nothing will remain obscure for the [374] discussions to follow. It was mentioned above, the constitution of tendons is a mixture of binding tissue and nerve. The elaboration of this was set aside, but now will be presented. Tendon is harder than nerve by as much as it is softer than binding tissue, but the bulk of its substance is great enough to be formed of both. Binding tissues are all without sensation, but all nerves are sensitive. The tendon is not insensitive because it contains nerve but it is not as sensitive as nerve because it is not solely nerve. To the extent that it has the nature of binding tissue, the accuracy of sensation is blunted. The tendon arises from the tail [insertion] of the muscle. Attaching to its head, however, are both nerve and binding tissue and they are distributed to the whole muscle making it reasonable that the tendon is formed from both.

The way to learn this more distinctly is through dissection, for then you would see clearly that the origin which they call the head of the muscle is more sinewy [NEUROEIDES = nerve-like], the middle, more flesh-like, [375] is called the belly of the muscle, and thereafter it becomes more and more sinewy in proportion to the beginning until finally the lower end seems more sinewy than the head. The nerve, having reached it at its origin, is distributed in small subdivisions; these in turn dividing into others and again the latter divide into still others, until this division advances in such a degree as to end in membranous and very thin fibers. Continuing farther, in

turn, the latter join with each other and create sinews, larger in bulk than they were formerly, but smaller in number, until they become at the end of the muscle as great in number and size as are those found at the first origin. Since the tendon becomes much larger than the nerve running to the muscle, it is quite clear that it is not formed of nerve alone but appropriates something of the nature of the binding tissue, and this in no small part. For in many places it seems six times and in many places ten times as thick as the nerve [376] and then its constitution is suitable in kind and size to provide the function of both the nerve and the binding tissue. It binds the muscle to the subjacent bone to which it inserts, and in this way does not differ from the binding tissue. It is sensitive and is moved and in this way shares with nerve. It becomes greater than the nerve, being designed to move the bone. The whole tendon is implanted for the most part toward the end of the bone invested with cartilage, not indeed at its very end nor in its accustomed shape, but flattened out, and wound around the bone at its upper end, which is called the head. The tendon, attaching itself to the underlying bone, is pulled along by the contracting muscle, for the muscle needs some firm cord to move the bone and nothing would be more suitable for this than binding tissue. The nerve from the brain, being a path for the motive power, contributes its share by extending along and mixing together with the binding tissue and in this way the tendon comes from both. [377]

Chapter III

Every tendon is attached to bone, generally speaking, but not every muscle ends in a tendon. No tendon comes from the muscles moving the tongue. It is not necessary for the tongue to move bones; instead, it articulates sound, distinguishes juices, and assists in chewing and drinking. If it seems to anyone that the heart is somewhat similar, he must not have studied the substance of muscle carefully, or he would have recognized that they differ much both in thickness, moulding, texture, and hardness. Their actions, moreover, are not alike. The motion of the heart, being com-

pounded of the double and complex perpetual motion of diastole and systole, does not require voluntary impulse for its initiation. The motions of the muscles are not the same and would not arise without voluntary impulse. There are some binding tissue cords in the cavity of the heart, exactly like tendons, about whose purpose we speak elsewhere, the name binding tissue being used here in its general meaning. [378] The lips of the mouth, composed of a careful mixture of skin and muscle without bone, are moved, just as the eyes are moved, by voluntary impulse. The latter are moved by muscles but bone is not moved with them. The skin in the forehead, eyebrows, and the greatest part of the face is moved by impulse while the bones remain still. This skin is different from the eyes and lips because it has a thin layer of muscular nature stretched under it in place of muscle, but the eyes are moved by muscles and the composition of the lips is a mixture of skin with muscle. If you consider the entrance to the stomach, which the ancients called the esophagus [ORSOPHAGOS], to be muscle and to do the work of muscle in animals, this would be a muscle not ending in tendon nor operating bone. The muscle at the neck of the bladder receiving the urine has a substance exactly like muscle and performs the work of muscle, and so likewise with the perineum, whether it is fitting to call the latter a single muscle or [379] many attached together. Bones are not moved by them nor by the muscles running down to the testes and the penis.

In summary it can be said of all muscles that they are the organs of voluntary motion. On the one hand, pulling the skin at their own origin, they draw themselves together as those in the lips and the brow and those of the entire face. No tendon arises from these. On the other hand, all other muscles which move bones generally end in tendons to a greater or lesser extent. Some of the muscles which move something else have tendons and some do not. The muscles which move something other than bone are those of the eyes, of the tongue, of the testes and penis, and those of the pharynx. The muscles of the eyes have membranous but strong [380] apo-

neuroses attached to the sclera and choroid surrounding the nerve-like coat. The muscles of the penis and testes, not forming any aponeurosis, attach to the fleshy parts of their own organs. Some of the muscles of the pharynx and larynx give origin to indistinct aponeuroses, others to none at all.

One kind of motion may appear in one place, another in another. No motion exists that is not intrinsic to the tongue, for it moves up and down, forward and backward, unrolls, and moves around in a complete circle. There are four direct motions for the eyes, upward, downward, to the right and to the left and two other motions, rolling around in a circle. When the two muscles of the temple, by pulling, approximate the teeth to each other, they protrude in an arch, but during gaping, on the other hand, they slacken and are drawn in. The motion of the great muscle in the arm is sufficiently evident. When it bends the arm at [381] the elbow, it protrudes in an arch and pulls itself together, but in straightening of the elbow it slackens and is drawn in. The great muscle of the forearm has the same motions clearly evident. In bending down the fingers it protrudes into an arch and pulls together, but in extension of the fingers it is stretched out, slackened and drawn in. And so it happens with almost all the other muscles. Those in the thigh appear to have a twofold motion if you strip them of the skin, or indeed they are apparent without the skinning on account of their size. In lean muscular bodies the largest of the muscles when moving are seen clearly before they are stripped of their skin.

Some muscles have a peculiar motion because their shape is different. The muscle at the anus would acquire a motion appropriate for pouches closed by a pulling together (as by a purse string). The diaphragm is like this to some extent except that it has no hole made in it. You may observe the motion of this muscle clearly if, dividing the peritoneum, you draw aside the underlying viscera. But for observation of other muscles of the [382] thorax and the whole epigastrium, it is necessary only to raise the skin. What happens to the muscles of the epigastrium is the opposite of

what happens to those of the limbs and of the face. The latter when contracting protrude and bend into an arch but the former are drawn in when contracting and protrude in an arch when relaxing.

Chapter IV

Now, do the muscles (and this was the first thing examined at the beginning) have any types of motion which are seen after they are dissected into parts or before the body is denuded or are they much less numerous than they appear? Even setting aside other reasons, it would be as extraordinary, if all the muscles did not have a single motion, as if someone said that different arteries have different motions, for nature always seems to function similarly through the same organs. That six motions exist for all muscles, as some have said already, clearly has been refuted. None of the muscles in the arm and the leg has any third motion other than lengthening and shortening [383], just as each of the two temporal muscles evidently has two motions. Even if the muscles move the whole member in six directions, it does not cause doubt that a twofold motion exists in each of them. For, if only one muscle moved the whole member, it would be necessary that whatever motions the member has would be the same as the motions of the muscle. Since there are many more than just six muscles in each of the limbs, would it not be astonishing if different motions arose from the different muscles? I think the tongue has deceived those who declare these things because they suppose that it is a single muscle. If it were a single muscle, it would demonstrate that many motions belonged to one muscle. On the contrary, since not one but many muscles move the tongue, I think it is to be concluded that there are not many motions belonging to each muscle. It would be useless to have many muscles if it were possible for all motions to be accomplished by one. But, you may say, each of the [384] eyes goes through motions in four directions. True, my friends! And, what is more, there are four rectus muscles. There would be only one for each eye if it were in accord with nature for a muscle to move in all directions. Just as, if there were one mus-

turn, the latter join with each other and create sinews, larger in bulk than they were formerly, but smaller in number, until they become at the end of the muscle as great in number and size as are those found at the first origin. Since the tendon becomes much larger than the nerve running to the muscle, it is quite clear that it is not formed of nerve alone but appropriates something of the nature of the binding tissue, and this in no small part. For in many places it seems six times and in many places ten times as thick as the nerve [376] and then its constitution is suitable in kind and size to provide the function of both the nerve and the binding tissue. It binds the muscle to the subjacent bone to which it inserts, and in this way does not differ from the binding tissue. It is sensitive and is moved and in this way shares with nerve. It becomes greater than the nerve, being designed to move the bone. The whole tendon is implanted for the most part toward the end of the bone invested with cartilage, not indeed at its very end nor in its accustomed shape, but flattened out, and wound around the bone at its upper end, which is called the head. The tendon, attaching itself to the underlying bone, is pulled along by the contracting muscle, for the muscle needs some firm cord to move the bone and nothing would be more suitable for this than binding tissue. The nerve from the brain, being a path for the motive power, contributes its share by extending along and mixing together with the binding tissue and in this way the tendon comes from both. [377]

Chapter III

Every tendon is attached to bone, generally speaking, but not every muscle ends in a tendon. No tendon comes from the muscles moving the tongue. It is not necessary for the tongue to move bones; instead, it articulates sound, distinguishes juices, and assists in chewing and drinking. If it seems to anyone that the heart is somewhat similar, he must not have studied the substance of muscle carefully, or he would have recognized that they differ much both in thickness, moulding, texture, and hardness. Their actions, moreover, are not alike. The motion of the heart, being com-

pounded of the double and complex perpetual motion of diastole and systole, does not require voluntary impulse for its initiation. The motions of the muscles are not the same and would not arise without voluntary impulse. There are some binding tissue cords in the cavity of the heart, exactly like tendons, about whose purpose we speak elsewhere, the name binding tissue being used here in its general meaning. [378] The lips of the mouth, composed of a careful mixture of skin and muscle without bone, are moved, just as the eyes are moved, by voluntary impulse. The latter are moved by muscles but bone is not moved with them. The skin in the forehead, eyebrows, and the greatest part of the face is moved by impulse while the bones remain still. This skin is different from the eyes and lips because it has a thin layer of muscular nature stretched under it in place of muscle, but the eyes are moved by muscles and the composition of the lips is a mixture of skin with muscle. If you consider the entrance to the stomach, which the ancients called the esophagus [OISOPHAGOS], to be muscle and to do the work of muscle in animals, this would be a muscle not ending in tendon nor operating bone. The muscle at the neck of the bladder receiving the urine has a substance exactly like muscle and performs the work of muscle, and so likewise with the perineum, whether it is fitting to call the latter a single muscle or [379] many attached together. Bones are not moved by them nor by the muscles running down to the testes and the penis.

In summary it can be said of all muscles that they are the organs of voluntary motion. On the one hand, pulling the skin at their own origin, they draw themselves together as those in the lips and the brow and those of the entire face. No tendon arises from these. On the other hand, all other muscles which move bones generally end in tendons to a greater or lesser extent. Some of the muscles which move something else have tendons and some do not. The muscles which move something other than bone are those of the eyes, of the tongue, of the testes and penis, and those of the pharynx. The muscles of the eyes have membranous but strong [380] apo-

for just as common occurrences, considered by themselves, indicate some common function, and obscure whatever is peculiar to each, when the different occurrences make a display of the function peculiar to each of the muscles, then the truth becomes evident. The occurrences peculiar to each of the muscles are these: when the internal muscle is cut through, the part remains thereafter in the position of extension; if the external, it is flexed and cannot be extended. If, taking it with your own hands, you flex the extended part or extend the flexed, you will accomplish each of them easily but forthwith the part will return to the previous state. What is demonstrated by these things? That it is flexed by the internal muscle, and extended by the external. For this reason, if the external is wounded and loses its action while the internal remains active, the latter will bend the part since the muscle intended by nature to flex would be there, unwounded. If the internal [389] is cut across, the opposite takes place; the limb is extended and no longer can flex. For what reason does the part remain motionless in each position? Is it because the motions which follow one another in succession are abolished? The muscle meant by nature to flex, being sound, flexes the first time but cannot flex a second and a third because the member does not undertake to extend again. Flexion of the extended part alone is possible. The muscle intended by nature to extend, by the same logic, extends first and cannot a second or third time, because no muscle again undertakes to flex the part, for extension of the flexed only is possible. Under these conditions if you, mimicking the action lost by the wounded muscle, with your hands extend the flexed part, you will see that the motion intended by nature to flex has been preserved. For without you it will not be flexed spontaneously by the action of the muscle placed on the internal side when it pulls, since it will not be extended again by any muscle but will always require you to do it. Likewise, if you cut the internal muscle, the part will always remain extended without you. It will not be flexed by [390] any muscle but will need you to make this motion. From what has been said, there-

fore, it is clear that, as the work of the internal muscle is to flex, so the work of the external is to extend.

It should no longer be obscure that to pull and draw themselves together is the inherent function of the muscles whereas it is to lengthen and be relaxed when the antagonistic muscles contract and draw themselves together. You may confirm this from other not unimportant phenomena similar to those observed at the beginning. If you take in your hands the legs of a bird completely removed from the body, and attempt to pull its tendons with your own fingers, first the internal and then the external, on the one hand you will see the limb flexed and on the other extended. Also, if the leg preserves intact its attachment to the body of the animal, and you take each of the tendons or muscles you wish to pull, you will see in turn the part being flexed by the internal and extended by the external. If you wish to cut through a muscle either in [391] the dead or living animal, you will see clearly that of its two parts, one will be drawn upward and the other downward, each toward its own extremity, and you will recognize this effect at whatever part you cut across the whole muscle. So it is clear that every part of the muscle has the inherent motion of retracting to itself. For if you cut only the head of the muscle above, all the muscle belly is carried to the tail, but if the tail is cut, the muscle is drawn up to the head. And if you cut it at each end, you will see it round up and retract toward the middle from both ends. I believe that in each of the examples presented the material is explained with sufficient clarity.

Chapter VI

On account of the efforts of the physicians and philosophers who are attempting to cast doubt on all inquiry into activity, however, not only the above material but also everything else about to be presented lies before us. When any of the muscles or tendons placed internally on the limb have been scarred, [392] the part, having become flexed, is not again extended, or when any of those placed externally are scarred, the part, having become extended, is not again flexed. This is contrary to what

cle, in this instance it would show that four motions exist for each muscle, likewise, it shows that one motion would arise from each, since four is the number of muscles, and correspondingly, when the eyes turn about, *each of two muscles makes one motion.*

By your own words, however, they say, it is agreed that if not many, at least two motions are seen in each of the muscles. What then, is the logic in saying there is one? It is not surprising for each has one motion as its activity and the other incidentally. It is active when it draws the moving part toward it, but it is not active when it is dragged away to the opposite side by another muscle. On account of this, no moving part is furnished with one muscle only. If some muscle attaches above, another certainly attaches opposite below; if one from the right side, then certainly another from the left. For when each of the moving parts is drawn in opposite directions by the guiding reins [385] of the muscles, the latter are alternately in contraction and relaxation. The one contracting draws the part to itself, the one relaxed is drawn by the part. Because of this, both muscles are moved in both motions. The action of the moving muscle is to contract, not to follow. It does follow passively, however, just as any other part of the limb when it is inactive.

Shall we postpone our attempt to demonstrate that all the muscles have one inherent motion, or shall we first agree among ourselves on all the phenomena observed in them? The latter seems to me to be the best way to begin. Let us mention their manifestations one after another, therefore, in order not to neglect anything. First, let us take up one point which was mentioned in the earlier chapters, namely, that when the muscles have been cut across completely, any motion in the subjacent parts is destroyed, but when cut into, it is hindered. The amount of the damage follows the amount of the cut, more of the motion being destroyed in the greater incisions, and less in the smaller. [386] Let us grant that all these effects apply to the tendons also, for if you cut the latter entirely, you paralyze the motion of the whole part, but if you cut into them, you

damage them as much as you cut. If all the motions of a part were to be abolished when one muscle is cut, you establish, I think, that this one muscle is the producer of all the motions.

Again, if only one motion is abolished when one muscle is cut, you establish that the muscle cut produces the one motion. Since it happens that neither a single nor all motions are abolished, but always two, it would seem to be established that two motions arise from one muscle. On the other hand, when the muscle or tendon placed on the opposite side is cut, the same two motions are abolished and, dominated by the same logic, therefore, we say that the same two motions are governed or disabled by them both equally. Therefore, if one muscle is destroyed, either the motion of the one opposite is destroyed with it, or they are not designed by nature for the same performance, and each is responsible for its own motion only.

If either of these propositions is true, [387] we must of necessity attempt to demonstrate which one, after having first stated more clearly that if one of two motions alternating with each other is abolished, necessarily the remaining one will be abolished along with it. Let us suppose that the motion of extending the limb were destroyed. The part would be flexed first and remain thus thereafter, not having the power to extend again because it has been deprived of the extending motion. Moreover, since it can no longer be extended, it cannot again be flexed because it must be extended first before it can be flexed. In the same way, if the motion of flexing the part happens to be destroyed, first it is extended, then becoming motionless thereafter, it is no longer able to return to flexion which must precede if extension is to follow. It seems to be altogether true that the motions opposing and succeeding each other are destroyed together. It is right to inquire, therefore, whether two motions are produced by both muscles, or one by each, with the one remaining being destroyed with the first. [388]

Chapter V

How, then, will this distinction be made? By the different occurrences [SYMPTOMA],

toward itself. So you will find all the actions of the arms of wrestlers, archers, carpenters, and those doing all the other things, executed by the muscles. This now seems to me to be clear and no more discussion is necessary.

What has not yet been discussed and is not clear must, therefore, be mentioned at this time. Not all motions of the hand arise through action of the muscles and not all lack of motion through their inactivity. It is possible to discover movements in which all the muscles are inactive and absence of motion in which a great many are active. Let us speak first of the [397] movement. It will make our discourse clear to mention first two motions of the whole body which resemble each other but which do not arise in the same way. One of these is called lying down, the other falling down. It is evident that lying down takes place voluntarily, falling down involuntarily. Lying down is accomplished by the action of muscles, and for this reason is a voluntary act of the living being. Falling down is not an act but something that happens to one involuntarily and no muscle need to be acting. It is only necessary for all the muscles to be released from tension and the body, yielding to the weight, is carried downward in the direction toward which it was inclined. As falling differs from lying down, likewise bringing the arm down differs from letting it fall, for when it drops, drawn by the weight inherent in material bodies, all its muscles remain idle. When it is brought down, on the other hand, all the muscles in the axilla pull the humerus toward them. Thus we have discovered a third motion besides the two cited earlier. Of the latter, one, [398] in which they are active, represents a drawing together of the muscles on themselves, the other, in which they lie idle, being lengthened by their antagonistic muscles, takes place by some chance, and is not inherent in them.

The third motion now being brought forward resembles these latter in no way for in it no muscle shortens or lengthens. Does nothing move at all? When the whole limb is carried down by its weight, it is not to be admitted that the muscle remains motionless, being part of the limb, but it is moved bodily in this instance and is not length-

ened or shortened. What kind of motion is this? The same, evidently, as that of the bones. Not being shortened or lengthened it is carried about together with the limb as if it were some inanimate body which happened to be attached to it. Contraction is the power of a muscle as it would be of an instrument of the brain (*psyche*), lengthening would be not a power of an organ but simply a motion while the third motion just expounded does not belong to muscles alive but as inanimate and [399] completely motionless by themselves.

Passing over to the fourth motion, let us investigate the manner of it, for it seems to be quite opposite to the third. In the third manner of motion it was pointed out that the muscles remain idle while moving, but in the fourth it will be pointed out that they are active while appearing not to move in the least. We have in mind that the hand, having been raised up, is maintained in this position. We ask ourselves this: "Why is it not born down, brought downward by the weight?" We respond, thereupon, "Because the contraction of the muscles carrying it up persists." Until they are completely relaxed, the hand is not able to move back. The traction ceasing, however, if no other muscles contract and all remain inactive, it descends to that side where the weight pulls it. If some other muscle does contract, it is moved where the latter pulls. So, in keeping the arm extended, the traction of the muscles putting it there is maintained. Must one say that they are active and pull and do not move? [400] If you are too cautious to say this, you must say that they are not active. Would it not be absurd to agree that they are active in their inherent and most intimate activity and not to agree that they move? And yet, they do not appear to move. Why is it necessary to introduce contradictions when the unravelling of them would become most difficult and hard to interpret? Because, when difficulties are mentioned, we make a mistake if we lay stress upon contradictions. If, for this reason, we are not among those who, in order to prevent discovery, promote doubts, but rather are among those who, in order to investigate accurately, look about carefully in all directions, we must compromise all opposing views by leaving

takes place in wounds. In the latter conditions the part is drawn up in a direction opposite to the muscle wounded. That this is not opposed to the preceeding but greatly confirms it is apparent, for the scarring by its very nature makes everything contract. That which in the healthy muscle was caused by impulse now appears to come from the pathological process. On the one hand the motion is voluntary, caused by impulse, on the other involuntary, caused by a pathological condition. The affected parts cannot be pulled in the opposite direction by your own hands, as they could with wounds, for the scar, having replaced the muscle with a binding cord, holds against you. If it were possible for you to draw the member toward the opposite position with your hands, nothing would hinder it from being returned by the antagonistic muscles, since it would then be moved by the appropriate muscles in a natural motion. [393] The conditions caused by scars are mimicked by inflammations, for inflamed muscles and tendons pull the part toward themselves and frequently make it immobile. The induration following healed wounds no less than the above-mentioned maladies frequently immobilize it. All these conditions and those about to be mentioned no less seem to work together to prove the same point. In addition to the latter, however, many other problems are still before us to be solved.

If all the muscles have but one kind of motion, it might seem astonishing and almost impossible, that one part, such as the hand, would be extended at one time, flexed at another, or moved about from one side to the other, raised, lowered, or be turned backward toward the spine. It does not appear astonishing, however, when we know that to raise and lower the arm is the function of the muscles moving the shoulder joint; to extend and flex the forearm those at the elbow joint; to turn it to pronation or supination [394] those of the joint between the humerus and radius. In touching the spine, the motion comes from the same activity of the arm through the four joints moving together, that is, the lowering of the shoulder, flexing at the elbow, turning the forearm to pronation, and turning the wrist backward. All arise

by the functioning muscles but it is not fitting to say at this time which muscle performs what, for in the treatises "The Dissection of Muscles" and "The Purpose of the Parts" as well as in "The Anatomical Procedures", their great number and the motion of the parts brought about by each of them has been described.

The discussion which lies ahead of us also contributes to the problem already mentioned, namely, that it is not astonishing that, if one manner of motion exists in the muscles, the limb may change posture in many ways. Each muscle draws the part to which it is attached toward itself; it can pull either from the right to the left, or from left to the opposite, or one flexes, the other extends. When many muscles [395] act on many joints at the same time, how is it astonishing that much diversity arises in the postures of the limbs? Muscles inserting at the head of the humerus, I think, raise it; those inserting in the forearm on the outside of the elbow, extend the ulna; those which insert internally in the forearm and which cross it obliquely, move the radius to pronation; those in the forearm which insert on it externally, extend the wrist. Each of the fingers is flexed by the internal tendons and when each of the fingers has been flexed, the posture of the hand is especially like that of a boxer thrusting out his fist. If the humerus has been raised fittingly and the ulna has been extended exactly to supination, and if those muscles in the forearm attaching externally have bent the radius and the wrist back at the same time that the digits are extended, the posture of the whole arm would become the same as when extended by someone wishing to receive something. In the same way if you keep the other joints in position but change only the supination and place the hand exactly in the midposition between supination [396] and pronation, the entire posture you make will be that of the arm which is adopted especially by the archers when they shoot arrows, as Hippocrates has said. So also in each of the other postures of the whole arm it is not difficult to discover the position of each of the joints if you remember this one point, that each muscle, when it contracts, pulls the part to which it is attached

tions by the antagonistic muscles? If it did not happen thus, someone might equally well charge the power of the brain with seeming to command the muscles to lie in repose, whenever they must be moved by the antagonistic muscles. But if we agree upon this, we see immediately that it is contrary to what we said above. For if we say that the movement of the muscles is not by the psychic pull, [405] and that lack of movement is, we find that this contradicts many of the phenomena observed.

First and foremost, when the nerve running to the internal muscle has been cut, that muscle is seen to lengthen at once and to remain in this state thereafter. If indeed the shortening were inherent in its substance and the lengthening originated by command of the brain, it would be necessary for lengthening to be abolished sooner than shortening when the communications with the source [ARCHE] are cut away. The opposite, however, takes place. It shortens when the nerve is uncut; it lengthens under the opposite condition. It would be necessary, not only that the nerve of the cut muscle abolish the lengthening but also that the one not cut preserve both the lengthening and the shortening, if indeed the muscles obtain lengthening through the nerve and shortening through themselves.

What solution do we have of this difficulty? Here among these same peculiarities of things it is necessary to find the difference between the motion of the substance of the muscles [406] and the power making use of it. What is the difference? When the external muscle or tendon is cut, the part is flexed on the spot. Even should we not wish to flex it, it would be flexed by something, that is, and one must not neglect this, by the body of the internal muscles designed by nature to retract to themselves. If the flexing of the part is not from our volition, how could it be said that it arose from the power of the brain? In order to know what the proper motion of the power is, order a wounded man to attempt to flex completely the mutilated part and you will see it obviously bent. Then command him to discontinue the impulse of bending and you will see the mutilated part extend to the point to which

it was carried without impulse when it received the first flexion. From these phenomena, obviously, it is to be learned that the body of the muscle would never arrive by itself at exact and complete flexion if not urged by the power from the brain. It was in vain, someone will say perhaps, for the body of the muscles to have a constitution for shortening when it would be accomplished more completely [407] and better from the functioning of the brain. Whoever says this must be one of the lovers of difficulty and ambiguity, as they call themselves. Should I ask him gently if he believes that the part meant by nature to lengthen is the most suitable organ to have the power to contract, or the opposite? I cannot imagine how anyone could trump up an organ more unfit by nature for motion than if he made it disposed toward the opposite of the voluntary impulse. If the latter is unfit, then the opposite nerve is opposed spontaneously, then that which is disposed toward motion is most appropriate. Indeed, if the power of the brain urges the muscle to pull according to its intrinsic source, this preparation would be adapted for it, and this is how it is.

Chapter IX

Should someone inquire into this more reasonably and be puzzled as to why, speaking generally, we say that extreme shortening is the proper motion of the body of the muscle if, after complete lengthening, it shortens and after complete [408] shortening, it lengthens. Either, one must say that neither motion is proper to it but is brought about by some chance or, one must suppose that both are equally proper to it. Or again, must one suppose that it departs farthest from complete lengthening and least from complete shortening and for this reason that shortening is the more proper to it? Since there are two extreme positions, as someone might say, greatest lengthening and complete shortening, and since it is more proper for the body of the muscle to shorten than to lengthen, it would take up a position exactly intermediate between the two and thereafter would return to this position whenever released. But this does not take place, and instead,

nothing concealed. On the one hand, when the muscles are active we say that they move themselves; on the other hand, when they appear to move neither the whole limb of which they are a part nor themselves alone, we do not venture to agree that they move at all. What solution may one find of the difficulty? Shall we hypothesize contraction called tonic [TONIKOS=pulling], [401] or find something else better, or shall we decide nothing concerning this until we have examined it carefully and then speak up? This seems to me to be much better.

Chapter VIII

Let us do so then, and let the discussion proceed immediately as indicated above. Let us observe some inanimate object, either wood or stone, being dragged about by some force. Again, let us observe this same object pulled back contrariwise in the opposite direction by some other force and suppose that the first dragging force prevails by its might and for this reason the object follows it, but much less than if pulled back by no opposing force. Let us present a third situation for this object: where it is pulled in the opposite direction with equal force. Now, in the first situation the object made the one movement which the power of the moving force was capable of producing and it was necessary for it to proceed to the distance which the mover carried it. In the second situation, less distance was evident than in the first to the extent the other force dragged the moving object in the opposite direction. [402] In the third situation, where however much one motion drags forward, the other drags backward, the object is forced to remain in the same place. It does this, not as a completely motionless object which must remain thereafter in the same place, but because in the latter instance, it is not moved at all, whereas in the former, it is moved in two ways just as a swimmer striving against the current of a river is pulled in the opposite direction. This swimmer, if he has strength equal to the violence of the current, remains always in the same spot, not as if motionless but because he propels himself forward by his own effort as much as he is carried backward by the external force.

Since it is not wrong to explain an obscure point by numerous examples, let us suppose that some bird in the air seems to stay in the same place. Should it be said that it is motionless as if it happened to be hung suspended or that it is moved by its own upward motion to the same extent as carried downward by the weight of its body? The latter seems to me to be the truest. Should you deprive it of the control of the brain or the pull of the muscles, you would quickly see it born down to [403] earth. It is clear that the downward tendency, inherent in objects from their weight, is counterbalanced by the upward force of the power from the brain. In all similar situations, the object is carried alternately now downward, now upward, and, since the changes are rapid and sudden and the motions are carried out in the shortest intervals, it seems to remain in the same place, held in one spot thereafter. This is not the fitting place to make this clear, for in the book of physics "On Motion", these points are examined more according to custom. It is enough for the present to have disclosed that there is some form of activity which is called tonic, or if you wish to call it something else, it will not matter. It is better to know what it is than to think that the muscles are inactive when the arm is raised. Indeed these four are all of the different motions seen in the muscles. They are shortened, or lengthened, or are carried about or remain taut. The fourth difference is of the same [404] kind as the first, for both are activities of the muscle.

When a dead muscle, which has none of the influence of the brain [PSYCHIKOS], has been cut across entirely, you see it retract toward the ends. This would seem, not illogically, to be the work of the constitution of the muscular substance. If the substance of the muscle is intended by nature to retract to itself, what need is there of the psychic power to move it unless the power from the brain is useful for making the muscles give way to each other's motions? If each carried on perpetually what it is designed by nature to perform, nothing would prevent the body from being afflicted by the disease called tetanos. What is tetanos but that the parts are drawn back involuntarily in opposite direc-

tions by the antagonistic muscles? If it did not happen thus, someone might equally well charge the power of the brain with seeming to command the muscles to lie in repose, whenever they must be moved by the antagonistic muscles. But if we agree upon this, we see immediately that it is contrary to what we said above. For if we say that the movement of the muscles is not by the psychic pull, [405] and that lack of movement is, we find that this contradicts many of the phenomena observed.

First and foremost, when the nerve running to the internal muscle has been cut, that muscle is seen to lengthen at once and to remain in this state thereafter. If indeed the shortening were inherent in its substance and the lengthening originated by command of the brain, it would be necessary for lengthening to be abolished sooner than shortening when the communications with the source [ARCHE] are cut away. The opposite, however, takes place. It shortens when the nerve is uncut; it lengthens under the opposite condition. It would be necessary, not only that the nerve of the cut muscle abolish the lengthening but also that the one not cut preserve both the lengthening and the shortening, if indeed the muscles obtain lengthening through the nerve and shortening through themselves.

What solution do we have of this difficulty? Here among these same peculiarities of things it is necessary to find the difference between the motion of the substance of the muscles [406] and the power making use of it. What is the difference? When the external muscle or tendon is cut, the part is flexed on the spot. Even should we not wish to flex it, it would be flexed by something, that is, and one must not neglect this, by the body of the internal muscles designed by nature to retract to themselves. If the flexing of the part is not from our volition, how could it be said that it arose from the power of the brain? In order to know what the proper motion of the power is, order a wounded man to attempt to flex completely the mutilated part and you will see it obviously bent. Then command him to discontinue the impulse of bending and you will see the mutilated part extend to the point to which

it was carried without impulse when it received the first flexion. From these phenomena, obviously, it is to be learned that the body of the muscle would never arrive by itself at exact and complete flexion if not urged by the power from the brain. It was in vain, someone will say perhaps, for the body of the muscles to have a constitution for shortening when it would be accomplished more completely [407] and better from the functioning of the brain. Whoever says this must be one of the lovers of difficulty and ambiguity, as they call themselves. Should I ask him gently if he believes that the part meant by nature to lengthen is the most suitable organ to have the power to contract, or the opposite? I cannot imagine how anyone could trump up an organ more unfit by nature for motion than if he made it disposed toward the opposite of the voluntary impulse. If the latter is unfit, then the opposite nerve is opposed spontaneously, then that which is disposed toward motion is most appropriate. Indeed, if the power of the brain urges the muscle to pull according to its intrinsic source, this preparation would be adapted for it, and this is how it is.

Chapter IX

Should someone inquire into this more reasonably and be puzzled as to why, speaking generally, we say that extreme shortening is the proper motion of the body of the muscle if, after complete lengthening, it shortens and after complete [408] shortening, it lengthens. Either, one must say that neither motion is proper to it but is brought about by some chance or, one must suppose that both are equally proper to it. Or again, must one suppose that it departs farthest from complete lengthening and least from complete shortening and for this reason that shortening is the more proper to it? Since there are two extreme positions, as someone might say, greatest lengthening and complete shortening, and since it is more proper for the body of the muscle to shorten than to lengthen, it would take up a position exactly intermediate between the two and thereafter would return to this position whenever released. But this does not take place, and instead,

nothing concealed. On the one hand, when the muscles are active we say that they move themselves; on the other hand, when they appear to move neither the whole limb of which they are a part nor themselves alone, we do not venture to agree that they move at all. What solution may one find of the difficulty? Shall we hypothesize contraction called tonic [TONIKOS=pulling], [401] or find something else better, or shall we decide nothing concerning this until we have examined it carefully and then speak up? This seems to me to be much better.

Chapter VIII

Let us do so then, and let the discussion proceed immediately as indicated above. Let us observe some inanimate object, either wood or stone, being dragged about by some force. Again, let us observe this same object pulled back contrariwise in the opposite direction by some other force and suppose that the first dragging force prevails by its might and for this reason the object follows it, but much less than if pulled back by no opposing force. Let us present a third situation for this object: where it is pulled in the opposite direction with equal force. Now, in the first situation the object made the one movement which the power of the moving force was capable of producing and it was necessary for it to proceed to the distance which the mover carried it. In the second situation, less distance was evident than in the first to the extent the other force dragged the moving object in the opposite direction. [402] In the third situation, where however much one motion drags forward, the other drags backward, the object is forced to remain in the same place. It does this, not as a completely motionless object which must remain thereafter in the same place, but because in the latter instance, it is not moved at all, whereas in the former, it is moved in two ways just as a swimmer striving against the current of a river is pulled in the opposite direction. This swimmer, if he has strength equal to the violence of the current, remains always in the same spot, not as if motionless but because he propels himself forward by his own effort as much as he is carried backward by the external force.

Since it is not wrong to explain an obscure point by numerous examples, let us suppose that some bird in the air seems to stay in the same place. Should it be said that it is motionless as if it happened to be hung suspended or that it is moved by its own upward motion to the same extent as carried downward by the weight of its body? The latter seems to me to be the truest. Should you deprive it of the control of the brain or the pull of the muscles, you would quickly see it born down to [403] earth. It is clear that the downward tendency, inherent in objects from their weight, is counterbalanced by the upward force of the power from the brain. In all similar situations, the object is carried alternately now downward, now upward, and, since the changes are rapid and sudden and the motions are carried out in the shortest intervals, it seems to remain in the same place, held in one spot thereafter. This is not the fitting place to make this clear, for in the book of physics "On Motion", these points are examined more according to custom. It is enough for the present to have disclosed that there is some form of activity which is called tonic, or if you wish to call it something else, it will not matter. It is better to know what it is than to think that the muscles are inactive when the arm is raised. Indeed these four are all of the different motions seen in the muscles. They are shortened, or lengthened, or are carried about or remain taut. The fourth difference is of the same [404] kind as the first, for both are activities of the muscle.

When a dead muscle, which has none of the influence of the brain [PSYCHIKOS], has been cut across entirely, you see it retract toward the ends. This would seem, not illogically, to be the work of the constitution of the muscular substance. If the substance of the muscle is intended by nature to retract to itself, what need is there of the psychic power to move it unless the power from the brain is useful for making the muscles give way to each other's motions? If each carried on perpetually what it is designed by nature to perform, nothing would prevent the body from being afflicted by the disease called tetanos. What is tetanos but that the parts are drawn back involuntarily in opposite direc-

on the one hand, you cut one of the two things a little at a time but do not sever it completely, you will alter the articulation of the two bones definitely to one side of the middle position, but if you sever it completely, they will come nearly but not completely to the extreme position. For the extreme positions do not seem to arise except by drawing the things in the proper direction with the hands. [413]

The same manifestations are seen clearly with the muscles, the muscle being analogous to the thong, the brain to its movement by the hand. Without the hand, neither of the ropes can bring the articulation of the bone to an extreme position and without the impulse from the brain neither of the muscles will bring about either extreme flexion or complete extension of the part. If you deprive the muscles of the impulse from the brain, or the ropes of the hands, you will see arise the intermediate position of the bones. If you cut the external muscle you will see the part flexed beyond the middle position just as if you cut the external thong. So also when you cut the internal muscle, you will perceive that the part is extended beyond the middle position. What are the causes of these and all other conditions in the muscles? One principle especially is that the muscles have complete shortening in the extreme positions, just as in the example of the thongs. All the others [414] follow this.

Let us accept the principle on the spot, for one must take it not from some obscure hypothesis but from manifestations seen clearly in all the muscles. What is this principle? As has been said a little earlier, when the tendon has been cut from the head of the limb, the muscle shortens to an extent to which it shortens when the part is brought to complete flexion by deliberate choice. It was demonstrated clearly that the muscle seems disposed by nature to reach extreme shortening as a result of the properties of its substance. When it loses its attachment of the opposing bone, it is loosed from restraint and having become completely free, it shows its own nature. While the part is being pulled upon by the muscle arranged opposite, since they have the same nature in tending toward extreme contraction, each muscle is

prevented equally by the other from retracting itself. Thus it happens [415] that each of the antagonistic muscles in the limbs is half hindered from shortening, for if both are disposed by nature always to strive toward complete shortening, and both are attached to opposite parts of the head of one bone, it would be necessary that the part, receiving independent motions of equal force, should follow neither. To follow neither would be the same as to hold the position midway between the extremes, for each of the latter arises when one of the muscles holds sway, extension when the external, flexion when the internal. Motion of equal power arises from the substance of the muscles themselves when neither one has the voluntary pull allied with it; motion of unequal power when only one has sway. So that it would be necessary for the shortening of that muscle to prevail which would be aided by the power from the brain.

We have found the causes of three phenomena, from having tried out one principle which we have taken, not from some hypothesis of ours but from visible manifestations. Since the muscles appear to undergo extreme shortening [416] when they are released from the binding tissue which secures them to the head of the limb, it becomes clear to us that they are disposed by nature to shorten completely but are hindered from it by something else. When we sought what the hindrance might be, we found immediately that it was the binding tissue. When this is cut they shorten to the extreme, and this fact we make the first cause of their not shortening. For this reason we see the muscles hindered from shortening by the binding tissue not simply because it is binding tissue, but because it is connected to the head of the bone pulled in the opposite direction. For this reason also, we shall be furnished with the causes of the second phenomenon, that is, that the member takes the middle position, when none of the muscles is moved by the power from the brain. A third phenomenon in addition to these is that flexion or extension of the part occurs when volition prevails with one muscle only; for by this prevailing the other muscle is forced to extend itself with

the limb approaches complete flexion more nearly than extension. If this be granted and stated, and it should be accepted, (for it appears to be so), it seems to me that one must consider why, *after extreme flexion* of the limb has been caused by impulse, the muscle, whenever we set it free, appears to move but little and is *lengthened* to a very slight extent. It was not necessary for it to move at all if the nature of its substance [409] is disposed toward shortening. Let whatever arguments we shall supply in favor of this lie out in the open for contemplation by the lovers of truth, so that, if they appear to demonstrate correctly and are not to be controverted, we may say everything has been discovered. Or, if not quite everything, but the greatest part, then the things already investigated but still genuinely in doubt may be discovered at another time, one person finding one thing, another another.

In order that my discourse may be more clear, I need some example which not only will seem convincing to you but which you may set up for yourself if you desire. Take from whatever animal you wish two bones fastened together by a joint. Having twisted together several sinews into two thongs, either glue them down securely or bind them to those parts of the bones which I shall indicate. I urge you to glue or bind them on in the way that the muscles attach to the bones. Since the manner of the attachment for all muscles is double, it is not improper for them to be imitated in this respect by this example. One must now undertake to put into words clearly this double manner (of attachment), for someone might not [410] imitate it correctly if he had not understood it thoroughly, and it is most fitting for this to become the purpose of our discourse.

Of the bones attached to each other to form an articulation, one is moved about, while the other is placed over it like a sheath in the manner seen in the hinges of a door. Of necessity, therefore, the one remaining quiet has the hollow surface, the one moved, the arched surface. The hollow one is called the cup [KOTYLE] or the socket [GLENE], the arched one is the head [KEPHALOS] and knuckle [KONDYLOS]. When the socket is deeper, the knuckle is

more prominent, for nature provides a place as well adapted as for a hinge. Since the moving parts are so well constructed, the parts responsible for the motion should be much more skillfully constructed. The instruments of motion, the muscles, take origin from the bones lying above which have cups and they insert on the heads of the bones which lie below and which are about to be moved. Accordingly, when the muscles contract, the heads [411] are drawn up and the whole limb is brought up at the same time. Since one of them might have to move a larger and another a smaller bone, the size of the moving muscle is made in proportion to the bulk of the bone to be moved. Logically, some attach at the heads or condyles themselves of the overlying bones, others attach a little lower than these, near the cup or socket, but not too much so, for thus it would become entirely too small and unable to move the bone lying below.

Such is the nature of the bones articulating with other bones and the muscles moving them. You will imitate it exactly if you fasten the thong to one of the bones at the part from which the muscle would originate, and attach the remaining part to the head of the other bone, as the muscle was attached, giving attention to these two particulars: one, that the thickness of the thong be sufficient to move and support the underlying bone; the other, that the thongs not be pulled in the extreme position, but lie as if attached to nothing in the world. Of the [412] thongs occupying the places of antagonistic muscles intended to extend and flex the part, one of the two is completely free of tension at the time when the part is in an extreme position, the external being free when there is complete extension, the internal when there is flexion. After these preparations have been made, the articulation will move to extreme extension or flexion if one of the thongs is pulled by our hands. If these thongs are left to themselves, they will bring about a middle position of the articulation of the bones and there they would remain at rest for the future. It is necessary to give scrupulous attention to this same position for it is exactly midway between extreme extension and flexion. If,

on the one hand, you cut one of the two thongs a little at a time but do not sever it completely, you will alter the articulation of the two bones definitely to one side of the middle position, but if you sever it completely, they will come nearly but not completely to the extreme position. For the extreme positions do not seem to arise except by drawing the thongs in the proper direction with the hands. [413]

The same manifestations are seen clearly with the muscles, the muscle being analogous to the thong, the brain to its movement by the hand. Without the hand, neither of the ropes can bring the articulation of the bone to an extreme position and without the impulse from the brain neither of the muscles will bring about either extreme flexion or complete extension of the part. If you deprive the muscles of the impulse from the brain, or the ropes of the hands, you will see arise the intermediate position of the bones. If you cut the external muscle you will see the part flexed beyond the middle position just as if you cut the external thong. So also when you cut the internal muscle, you will perceive that the part is extended beyond the middle position. What are the causes of these and all other conditions in the muscles? One principle especially is that the muscles have complete shortening in the extreme positions, just as in the example of the thongs. All the others [414] follow this.

Let us accept the principle on the spot, for one must take it not from some obscure hypothesis but from manifestations seen clearly in all the muscles. What is this principle? As has been said a little earlier, when the tendon has been cut from the head of the limb, the muscle shortens to an extent to which it shortens when the part is brought to complete flexion by deliberate choice. It was demonstrated clearly that the muscle seems disposed by nature to reach extreme shortening as a result of the properties of its substance. When it loses its attachment of the opposing bone, it is loosed from restraint and having become completely free, it shows its own nature. While the part is being pulled upon by the muscle arranged opposite, since they have the same nature in tending toward extreme contraction, each muscle is

prevented equally by the other from retracting itself. Thus it happens [415] that each of the antagonistic muscles in the limbs is half hindered from shortening, for if both are disposed by nature always to strive toward complete shortening, and both are attached to opposite parts of the head of one bone, it would be necessary that the part, receiving independent motions of equal force, should follow neither. To follow neither would be the same as to hold the position midway between the extremes, for each of the latter arises when one of the muscles holds sway, extension when the external, flexion when the internal. Motion of equal power arises from the substance of the muscles themselves when neither one has the voluntary pull allied with it; motion of unequal power when only one has sway. So that it would be necessary for the shortening of that muscle to prevail which would be aided by the power from the brain.

We have found the causes of three phenomena, from having tried out one principle which we have taken, not from some hypothesis of ours but from visible manifestations. Since the muscles appear to undergo extreme shortening [416] when they are released from the binding tissue which secures them to the head of the limb, it becomes clear to us that they are disposed by nature to shorten completely but are hindered from it by something else. When we sought what the hindrance might be, we found immediately that it was the binding tissue. When this is cut they shorten to the extreme, and this fact we make the first cause of their not shortening. For this reason we see the muscles hindered from shortening by the binding tissue not simply because it is binding tissue, but because it is connected to the head of the bone pulled in the opposite direction. For this reason also, we shall be furnished with the causes of the second phenomenon, that is, that the member takes the middle position, when none of the muscles is moved by the power from the brain. A third phenomenon in addition to these is that flexion or extension of the part occurs when volition prevails with one muscle only; for by this prevailing the other muscle is forced to extend itself with

the entire limb. Now in addition to these, [417] let us state the causes of all the other phenomena, so that, if they agree with each other, we should trust to the arguments in favor of them, and if they should differ in one point, we should doubt all equally.

First let us consider the above-mentioned phenomenon that when the external muscle has been cut, the limb is flexed beyond the middle position, but not to the extreme. Perhaps it would seem equally logical for it to reach extreme shortening if no internal muscle pulled in the opposite direction. But he who judges thus would be forgetful of the weight of the limb which resists complete shortening of the muscle. In this regard events seem to take place in the same manner as with the thongs. If the external of these has been cut, the remaining one is not able to arrive at complete shortening, until the bone moved by it is detached. As long as there is articulation, it pulls the thong to itself. Whenever someone cuts across the internal muscle, the limb remains between the middle position [418] and complete extension, for the external muscle would be powerless to extend it without the impulse from the brain. And so, these phenomena agree with those stated above and with each other.

Chapter X

What Hippocrates wrote long ago concerning all the positions of the parts still seems to be true. But does it agree remarkably with the following? First, that we suffer pain if we flex a part completely or extend it extremely; second, that the position midway of these is free of pain; third, that we desire a quick change from the extreme positions; fourth, that we maintain the middle position longer without desiring change; fifth, that we even wish to change this sometimes; sixth, that all positions are hard for the extremely feeble to bear. The extreme positions logically are painful since one of the muscles operates to extend the other against its nature. The middle position [419] is justly agreeable since both muscles are resting not only from activity but also from excessive tension. Just as we need a change from a painful position quickly, we need a change from one not painful slowly. Why do we need a change at all from one not

painful? Because even in this position the muscles are under some tension, but less than in all other positions. We say that it is painless, not as if entirely without pain, but as if the pain were very small and, from its slight intensity, nearly insensible. We wish to change it when, having increased gradually, the pain becomes perceptible. That the muscles would have some tension in this position we have no need to explain, if we recall the previous discourse. We said that they are pulled by the member to which they are attached and for this reason, when freed of this tension by cutting the tendon, they readily adopt their natural shortening. No muscle will be without tension, not even in the middle position, but despising it as slight [420], we adopt it and avoid the others, not enduring them because excessive and irresistible. When we have become extremely feeble, as in gastric and cardiac syncope, we do not endure even the small tension of the middle position and for this reason, although we are able to move scarcely at all, nevertheless we move the parts from one side to the other wishing to find some painless position, but finally never being able to find one. Just so, if one of us had to carry some small stone suspended from his neck, being in good health, he could bear it without difficulty, but if he had become feeble, he would wish to reject it as a burden. In the same way if each muscle were vigorous, they would despise supporting an attached bone as one would a stone, not being aware of the slight addition to the weight, but when they are feeble, they are aware of it and carry it with difficulty, and hoping to shake off the load, pull themselves about from one position to the other. So all the manifestations in the muscles seem to agree [421] and seem to share in the common source, in which they are shown always tending of themselves toward complete shortening, but unable to reach this because they have the antagonistic muscles and the weight of the attached bones pulling against them.

BOOK TWO

Chapter I

Since the elementary principles of muscular motion have already been

pointed out, it is time for us to add the details which were omitted and thus complete our exposition. Then, if someone has absorbed all this information accurately, he will, if he wishes, be competent to carry on a discourse concerning muscle. Let us begin at the point where the first discussion ended, with the posture of the parts. Having first chosen the middle position we say that one of two conditions must exist in the muscles; one, mentioned above, [423] in which none of the antagonistic muscles are active and the other, about to be described, in which both are equally active. The first is present when we are at rest, as Hippocrates has said; the other, when we do not allow someone to extend or flex our limbs even if they use great force. The latter is what happens when the antagonistic muscles are in a state of activity called tonic, so that, if you should place the limb in a position midway of each side, there would be equal activity in both the muscles. When you move it to one of the extreme positions, however, either one muscle or the other is sufficient for such activity. It is clear that in each of the positions mentioned, the muscles employ tonic activity sometimes more and sometimes less, and thus the middle position relative to a particular action avoids either of the extremes. Now we say *not merely* that the middle position is without burden [*ANODUNOS* = painless], but that the muscles must be at rest in it. For, with tension in each of the muscles, the intermediate [424] position is as burdensome as the extremes. Since in the state of rest it may be either exactly in the middle position or not exactly so, the exact mean of all the extreme positions of the limb, not just the mean of each set of extremes alone, would be without sense of toil. As Hippocrates has said, none of the others would be strictly untiring.

Explanation of what has been said will become clear if we first distinguish the exact middle position from one not so. In this discussion the arm will be referred to particularly as a model. Therefore, there being four extreme positions in this limb, pronation, supination, extreme extension and flexion, the exact middle is the mean of all of these. It would not be exactly middle when only one of the two antith-

eses, either intermediate of full extension and flexion or of supination and pronation exists. Supination is the position of the hand when the hollow of this part is upward, the arch downward. [425] Pronation is the opposite of this. Midway of the two is when the hollow is inward, the arch outward, the little finger lying below the others; the ulna lying below the radius. This middle position can come about with the arm completely extended and completely flexed just as the middle position of the latter antagonists can exist with the hand supinated as well as pronated. The specific characteristic of the flexed position is that the ulna makes a right angle with the humerus and for this reason they call it the angular position.

Now the exact middle of the combination of both the above mentioned middle positions concerns us. Four other positions are all intermediate; they come not from the exact middle for the whole limb, but from one antagonism only, for each is midway of extension and flexion alone or of supination and pronation. Since each of them is double, linked in part to the extremes of the remaining antagonism, it is necessary that all four come about. [426] In each of them there is something common to all and proper to each. The common thing is for some one group of muscles to be fully active, while the other three are stretched incidentally, not being active. The thing proper to each is: of the pronated and angular, those muscles twisting about internal to the radius are active, all others being stretched passively; of the supinated and angular, those twisting about externally are active, all others being stretched passively; likewise also in the middle of pronation and supination with sharp extension only the extending muscles would be active and with flexion only the flexing muscles, all the others, idle, would be stretched.

Chapter II

For the discussion to be clear, it must first be known by which muscles, having what position and moving what articulation, these same four motions of the limb are executed. The BRACHION is the largest part of the whole arm. The boundaries of it below [427] are at the joint of the elbow;

"We call the elbow the part on which we prop ourselves," says Hippocrates. Above, likewise, it extends as far as the joint of the shoulder. The part of the arm next in size after the brachion is called the *PECHYS* [forearm]. It is bounded, where it is joined to the brachion, by the joint of the elbow; it is joined to the wrist at the latter joint. In the brachion there is one large rounded bone [humerus] named the same as the part. In the forearm there are two bones, one having the same name as the whole part, [*PECHYS* or ulna], the other is called *KERKIS* [radius]. They both articulate with the lower end of the humerus, the ulna with the middle of the condyle of the humerus; the radius, ending in a cup, surrounds the outer condyle and indeed, rotating on the latter as an axis, it guides the twistings of the hand. When it rotates inward the prone position of the hand follows, when outward, the supine position. Extension and flexion of the arm is the work of the joint of the ulna with the humerus. [428]

I do not know whether there exists such an exact fitting together of bones as this in any other joint. For, on the one hand, the lower end of the humerus, widening, is bounded by the condyles. The ulna, on the other hand, presents two crooked *APOPHYSES* [processes] opposite each other which make a hollow in between them resembling the letter sigma. In this hollow is embraced the middle part of the condyle of the humerus in a manner exactly like the parts of what we call a *TROCHILIA* [pulley]. When the hollow of the ulna is carried around the convexity of the humerus, extension and flexion of the whole limb take place. The brows of the middle hollow are responsible for the accurate maintenance of the joint and for the failure to be displaced to one side or the other, the processes of the ulna binding it tight. When the anterior process guides the motion, the limb is flexed, when the posterior, it is extended. The limit of flexion occurs when the anterior process seats against the humerus; of extension, when the posterior. Also, since the humerus [429] is arched and each of the processes of the ulna is elongated, there is more than ordinary danger of the bones coming

against each other and hindering the motion of the limb. Nature has scooped out the bone of the humerus on each side to the depth that the processes of the ulna would extend down into the hollows in extreme extension and flexion. Since the posterior process of the ulna is greater, the corresponding hollow of the humerus is deeper. The part of the bone of the humerus between the hollows becomes thin because of their depth. Nature has avoided penetrating it, thin as it is, in order that the joint might not be completely loose and unstable nor the motions of the muscles excessive. If the bone were pierced it would be possible to flex the arm backward and whatever motions we might undertake with the arm in continued extension would be greatly exaggerated, and the pull of both muscles would be quite painful. If the posterior muscles were shortened by the power of the brain more than they were intended by nature, the [430] anterior muscles would be stretched and be in danger of being ruptured. Such is the skill of nature in regard to the precision of this joint.

Chapter III

Let us discuss next how the arrangement of the muscles already mentioned is related to the movements of the joint. Two muscles have their origins in the anterior part of the arm and two in the posterior; their insertions are into the ulna through strong aponeuroses. The largest of them begins at the head of the humerus, the smallest much lower, and they all four run straight to the ulna and attach mainly at the same place as the foundation of the bony processes. The very posterior process of the elbow, which the Athenians call the *olekranon* and the Dorians the *KUBITOS*, arises at the same part as that to which the coronoid process is attached in front. These muscles, both those anterior and those posterior to the humerus, act on the ulna to produce extension and flexion. Four other muscles have their origin from the ulna on each side [431] of the most bent part of the elbow, two externally and two internally. All are oblique to the bone of the radius, and they attach, the larger at the lower part near the wrist joint, the smaller at the middle part. When these muscles pull toward their origins, the radius follows

th the result that the internal muscles pronate the arm, and the external supinate

Remembering that this is the nature of the muscles moving the elbow joint, we are now prepared to demonstrate that in the four variations of the positions not simply middle, one kind of muscle acts each time while all the rest are in repose and stretched. Let us examine the first position mentioned, that which we call right-angled and prone, in which it is only necessary to say that the internal muscles moving the radius are active while the external are passive and stretched. Concerning the muscles moving the ulna, however, there is need of further explanation, [432] for we might imagine that they have an exactly middle condition because the angular is a middle position, but this is not true. If the whole arm is in the angular position, then it must have a position midway of supination and pronation for the muscles to be in a middle condition. Since it does not have this condition, it is necessary for these and all other muscles to be displaced as much as the whole arm departs from the natural position. the extent to which the muscles are twisted around the curved parts of the bones determines, I think, the amount that they are pushed out and suffer. For, the exactly middle position, besides having no muscle either active or moved, would not have anything in the limb twisted about, and moreover, Hippocrates, the greatest of all authorities testifies to this. In all the other positions, more in some, less in others, the muscles are twisted, as well as the tendons and nerves and besides these the veins and arteries, some of all these will be external to the [433] member and some internal. The midposition of supination and pronation, therefore, protects them while either supination or pronation twists all these structures considerably. In pronation, about which we proposed to speak first, the muscles external to the ulna which cause supination are distorted, so that their heads are external to the member. the bellies in front, the insertions internal. If you twist the arm more forcibly still, you will see the greater muscle attaching to the end of the radius, twisting about the member so that those on the outside of the

part, those inside, those above and those below seem to be outside the head, the so-called belly above, the part beyond this inside, the insertion below, as if they were already bulged out and contracted. The muscles in the upper arm, by which we are able to extend and flex the limb as a whole are distorted much less than these, but the others in the [434] forearm participate in the distortion to some extent. The same phenomena occur in the supinated positions. In these positions, therefore, the muscles in the forearm toil to the limit, but those in the upper arm labor with them. When, assuming the position intermediate of supination and pronation, we extend or flex the limb completely, the muscles in the upper arm labor somewhat, those in the forearm labor with them. Thus only the exactly middle position, where nothing excessive in either antagonism occurs, is completely free of burden. All the other four, some less, some more, are quite burdensome. In each of them, on the contrary, you render the position less burdensome the more you move the member away from the extreme and toward the middle position, but it will not be completely burdenless until you reach the exactly middle position. It is evident from what has been said that in this middle position only are all muscles completely in repose, [435] and in all the others, some less, some more, there is some kind of activity in the muscles.

Chapter IV

Not even during sleep are all the muscles completely in repose. Only through drunkenness, weariness, or poor health are all the parts of the body completely relaxed and the muscles inclined toward the middle position, and entirely at rest. Someone asleep cannot have any part in the extreme positions, because these require strong, robust, and intense activity of the muscles. Ordinarily we sleep in positions which are intermediate between the extremes and exactly in the middle. For if you place the member in any of these positions, you rely on the muscles in tonic activity around it to maintain it, so that many times individuals may go to sleep either sitting up or walking about. Indeed, at first hearing this, I put no faith in it, but after being obliged to walk

"We call the elbow the part on which we prop ourselves," says Hippocrates. Above, likewise, it extends as far as the joint of the shoulder. The part of the arm next in size after the brachion is called the PECHYS [forearm]. It is bounded, where it is joined to the brachion, by the joint of the elbow; it is joined to the wrist at the latter joint. In the brachion there is one large rounded bone [humerus] named the same as the part. In the forearm there are two bones, one having the same name as the whole part, [PECHYS or ulna], the other is called KERKIS [radius]. They both articulate with the lower end of the humerus, the ulna with the middle of the condyle of the humerus; the radius, ending in a cup, surrounds the outer condyle and indeed, rotating on the latter as an axis, it guides the twistings of the hand. When it rotates inward the prone position of the hand follows, when outward, the supine position. Extension and flexion of the arm is the work of the joint of the ulna with the humerus. [428]

I do not know whether there exists such an exact fitting together of bones as this in any other joint. For, on the one hand, the lower end of the humerus, widening, is bounded by the condyles. The ulna, on the other hand, presents two crooked APOPHYSES [processes] opposite each other which make a hollow in between them resembling the letter sigma. In this hollow is embraced the middle part of the condyle of the humerus in a manner exactly like the parts of what we call a TROCHILIA [pulley]. When the hollow of the ulna is carried around the convexity of the humerus, extension and flexion of the whole limb take place. The brows of the middle hollow are responsible for the accurate maintenance of the joint and for the failure to be displaced to one side or the other, the processes of the ulna binding it tight. When the anterior process guides the motion, the limb is flexed, when the posterior, it is extended. The limit of flexion occurs when the anterior process seats against the humerus; of extension, when the posterior. Also, since the humerus [429] is arched and each of the processes of the ulna is elongated, there is more than ordinary danger of the bones coming

against each other and hindering the motion of the limb. Nature has scooped out the bone of the humerus on each side to the depth that the processes of the ulna would extend down into the hollows in extreme extension and flexion. Since the posterior process of the ulna is greater, the corresponding hollow of the humerus is deeper. The part of the bone of the humerus between the hollows becomes thin because of their depth. Nature has avoided penetrating it, thin as it is, in order that the joint might not be completely loose and unstable nor the motions of the muscles excessive. If the bone were pierced it would be possible to flex the arm backward and whatever motions we might undertake with the arm in continued extension would be greatly exaggerated, and the pull of both muscles would be quite painful. If the posterior muscles were shortened by the power of the brain more than they were intended by nature, the [430] anterior muscles would be stretched and be in danger of being ruptured. Such is the skill of nature in regard to the precision of this joint.

Chapter III

Let us discuss next how the arrangement of the muscles already mentioned is related to the movements of the joint. Two muscles have their origins in the anterior part of the arm and two in the posterior; their insertions are into the ulna through strong aponeuroses. The largest of them begins at the head of the humerus, the smallest much lower, and they all four run straight to the ulna and attach mainly at the same place as the foundation of the bony processes. The very posterior process of the elbow, which the Athenians call the olekranon and the Dorians the KVANTOS, arises at the same part as that to which the coronoid process is attached in front. These muscles, both those anterior and those posterior to the humerus, act on the ulna to produce extension and flexion. Four other muscles have their origin from the ulna on each side [431] of the most bent part of the elbow, two externally and two internally. All are oblique to the bone of the radius and they attach, the larger at the lower part near the wrist joint, the smaller at the middle part. When these muscles pull toward their origins, the radius follows

with the result that the internal muscles pronate the arm, and the external supinate it.

Remembering that this is the nature of the muscles moving the elbow joint, we are now prepared to demonstrate that in the four variations of the positions not simply middle, one kind of muscle acts each time while all the rest are in repose and stretched. Let us examine the first position mentioned, that which we call right-angled and prone, in which it is only necessary to say that the internal muscles moving the radius are active while the external are passive and stretched. Concerning the muscles moving the ulna, however, there is need of further explanation, [432] for we might imagine that they have an exactly middle condition because the angular is a middle position, but this is not true. If the whole arm is in the angular position, then it must have a position midway of supination and pronation for the muscles to be in a middle condition. Since it does not have this condition, it is necessary for these and all other muscles to be displaced as much as the whole arm departs from the natural position. the extent to which the muscles are twisted around the curved parts of the bones determines, I think, the amount that they are pushed out and suffer. For, the exactly middle position, besides having no muscle either active or moved, would not have anything in the limb twisted about, and moreover, Hippocrates, the greatest of all authorities testifies to this. In all the other positions, more in some, less in others, the muscles are twisted, as well as the tendons and nerves and besides these the veins and arteries, some of all these will be external to the [433] member and some internal. The midposition of supination and pronation, therefore, protects them while either supination or pronation twists all these structures considerably. In pronation, about which we proposed to speak first, the muscles external to the ulna which cause supination are distorted, so that their heads are external to the member, the bellies in front, the insertions internal. If you twist the arm more forcibly still, you will see the greater muscle attaching to the end of the radius, twisting about the member so that those on the outside of the

part, those inside, those above and those below seem to be outside the head, the so-called belly above, the part beyond this inside, the insertion below, as if they were already bulged out and contracted. The muscles in the upper arm, by which we are able to extend and flex the limb as a whole are distorted much less than these, but the others in the [434] forearm participate in the distortion to some extent. The same phenomena occur in the supinated positions. In these positions, therefore, the muscles in the forearm toil to the limit, but those in the upper arm labor with them. When, assuming the position intermediate of supination and pronation, we extend or flex the limb completely, the muscles in the upper arm labor somewhat, those in the forearm labor with them. Thus only the exactly middle position, where nothing excessive in either antagonism occurs, is completely free of burden. All the other four, some less, some more, are quite burdensome. In each of them, on the contrary, you render the position less burdensome the more you move the member away from the extreme and toward the middle position, but it will not be completely burdenless until you reach the exactly middle position. It is evident from what has been said that in this middle position only are all muscles completely in repose, [435] and in all the others, some less, some more, there is some kind of activity in the muscles.

Chapter IV

Not even during sleep are all the muscles completely in repose. Only through drunkenness, weariness, or poor health are all the parts of the body completely relaxed and the muscles inclined toward the middle position, and entirely at rest. Someone asleep cannot have any part in the extreme positions, because these require strong, robust, and intense activity of the muscles. Ordinarily we sleep in positions which are intermediate between the extremes and exactly in the middle. For if you place the member in any of these positions, you rely on the muscles in tonic activity around it to maintain it, so that many times individuals may go to sleep either sitting up or walking about. Indeed, at first hearing this, I put no faith in it, but after being obliged to walk

throughout the whole night, [436] I learned the truth by experience, and had to believe it. I walked nearly a whole stadion asleep and, absorbed in a dream, did not waken until I stumbled upon a stone. Indeed, the lack of a tendency of those asleep to walk farther is the result of their inability to happen upon a smooth path. Although this is believable only to someone who has experienced it, sitting up while asleep may be seen by everyone every day. Also, extremely few of those lying down have each of the limbs exactly in the middle position. Those who hold something in their hands while asleep demonstrate the tonic activity especially well, for their fingers often remain carefully flexed around a small object, a piece of gold, a stone, or a coin.

Is it not clear also what happens in dropping of the lower jaw? For it only separates from the upper if someone goes to sleep drunk, or very lazy, or extremely weary. And actual snoring, for the same reason, usually occurs from the slackening downward of the jaw in a man remaining [437] in a supine position. Indeed, this very remaining supine is a sign of being relaxed. Moreover, Hippocrates found fault with either lying supine and sleeping with the mouth open, but he approved of lying on either side. How much activity there is in those lying on their sides you would perceive best if you placed the body of a dead man in that position. It will not remain even a short time, but will immediately become either supine or prone because inevitably it would slip from its weight. Indeed lying supine and snoring with the mouth open are signs of slackness, drunkenness, or laxiness. For this reason, again, Hippocrates recommends putting all the parts in painless positions for operating on dislocations and fractures, and "For operating on the lower jaw," he says, "when the man gapes moderately." What the angular posture is to the arm, moderate gaping is to the lower jaw, for this is the middle position. The extreme positions of the lower jaw are with it most widely opened and with the teeth [438] set against each other. The former of these is performed by the muscles in the chin and the neck pulling downward; the latter is performed by the muscles inside the jaw,

those from the palate, those called temporal, and probably also the muscles at the sides of the lower jaw called masseters assist the action to some extent; but we discuss this elsewhere. Gaping moderately is the middle position when all the muscles enumerated are in repose. In those dying, moreover, the jaw assumes this position and with reason, for in them all the muscles are deprived of activity. Likewise, it is evident that when someone sleeps without gaping, the activity of the muscles raising the jaw is maintained. Many sleep with their arms or legs extended or flexed, thus preserving the tonic activity in their muscles.

But I speak at too great length, while I might have mentioned what is most readily at hand. For example, would anyone contend that no effort is contributed when the muscles guard against the outflow of the excretions? [439] Strong muscles are placed at the ends of their conduits like guardians at some gates, not allowing them to be evacuated before reasoning power commands. During sleep these muscles perform their task faultlessly. If one of the excretions is released involuntarily, it happens either that these muscles are paralyzed, or reason suffers as in phrenitis, or both reason and muscles are depressed, as in drunkenness; for surely, either the reason must not be in control, or the muscles be without power, or both be disabled at the same time.

Let us not be rash and deny that the brain is at rest during sleep unless we mean that rest is not complete stillness; so let us rather call it a cessation of intense application. If someone says this, they say well and we agree with them. For those sleeping are not entirely without sensation, although they sense with difficulty. Otherwise how would they hear someone calling, or arise when a light is brought in, or feel someone touching them? If you remind me that the drunkard who does not know where in the world he is, [440] and who sleeps more heavily than the torpor of Epimenides, was close to stupor before going to sleep, then I say it would be better for you to turn to watching some vigorous man asleep or someone awakening, since in them many of the activities of the brain are preserved.

Chapter V

The argument is unreliable indeed of those who say that all the activities of someone asleep and stupefied are natural [i.e., without benefit of the brain], as this is not entirely true. For example, why do they shift and move their limbs in many ways? Why do they utter sounds while sleeping? Do they say that these acts are natural? But we do not agree that they take place by intention, someone may say, for you maintain intentionally neither the continuous motion of your eyelids, nor the motions of all the parts when you speak publicly, use oratory, converse, nor, when you walk to Athens from Peiraeus, do you apply yourself to the activities of your legs in particular. Often while deep in thought people fail to notice that they have come to the end of their journey [441] and go past the place toward which they started in the beginning. Did the walking come about neither as the work of the brain nor by voluntary impulse? In like manner, it seems to me that walking while absorbed or while asleep involves the motion of the moving parts on the one hand and the tonic activity of the unmoving parts on the other. Consequently, what reason would you give for those awake often not paying attention to the activities of a part of the body, and why not apply this same reason to those sleeping and stupefied and, at the same time, why not wonder how much came about voluntarily? When unable to find the cause readily, would it not be rash to say that none of these acts occur voluntarily? If no truer criterion than this can be found for deciding whether the acts are by deliberate choice or by nature, why must we not demonstrate something else concerning them? It is more appropriate to become skeptical in these matters than be rashly dogmatic. Since we have a most obvious criterion for the voluntary acts, taking courage, let us give evidence not only for each example already mentioned, but also [442] show that respiration itself arises voluntarily, as far as it would seem to fall under the criterion.

What is it now by which we judge the voluntary acts? I propose to give you many, not one criterion, all agreeing with each

other. If, choosing deliberately, you can stop actions taking place and not perform them, they are voluntary. If, in addition to this, you have the power to execute them more quickly or more slowly or more often or more seldom is it not in manifold ways evident that the act is the subject of deliberate choice? Deliberate choice cannot stop nor initiate, nor make more frequent, nor more seldom, nor more rapid the motion of the arteries and the heart. For this reason, these acts appear not to be of the brain, but happen through nature. The power of reasoning makes the motion of the legs consistent with all these, for one can act to stop the motion happening, activate it again when quiet, and make it faster, and slower, and more seldom and more frequent. These same things occur in the case of the motions of respiration, an activity [443] of the diaphragm and muscles of the thorax, as we demonstrate in the work, "Concerning the Causes of Respiration", they are an activity of the brain, not of nature, since to move the muscles is an activity of the brain.

It is inappropriate to discard the things that are well known simply because we lack knowledge of their causes. Indeed, the criteria of the activities by deliberate choice obviously are known, but we overlook the cause in those instances in which we do not follow the individual acts closely. The stupid person, disbelieving what is clearly visible, the gullible one, being at a loss concerning the things readily displayed, and the one suspicious of the known because something is unknown, are among the lovers of doubt. Anyone would be not only suspicious, but also extremely stupid if he disregards the known because of the unknown. Now let us not willingly acknowledge ourselves to be without sense, nor admire the doubtful, nor be stupid, nor any other of these things, but, because it is right and is befitting moderate men, let us accept the obvious readily, and inquire [444] into the dubious at leisure. Although it is clear that volition dominates respiration, it is difficult to understand why we do not follow many other voluntary activities closely with our intelligence. Having established our obvious knowledge, let us now pass to an investigation of

the cause, without being drawn into it completely nor as yet pretending to discover the true cause, since the things already said may be more plausible. No one has found the cause, I maintain, but some writers reporting only the search for the difficulties, which I have just now finished discussing, assume that they have discovered the cause. And indeed we must accept them favorably, whether they find or whether they strive eagerly to find, but it is necessary, also, for us not to shrink from investigating the remainder.

Chapter VI

In our search for these causes, we shall take it as our general background, that frequently many men, after passing through some achievements, a little later forget them completely. Similarly, those beset with fear or through drunkenness or some such cause, remember nothing of what they went through while in these conditions. [445] It seems to me the reason is that they have not applied themselves attentively with all their mind [NOUS, not PSYCHE] to the experiences. For the imaginative part of the brain [PSYCHE], whatever it might be, is like this very remembering itself. If it should receive the impressions of objects clearly in these fantasies, it would preserve them always, and this is to remember. If it should receive them indistinctly and superficially, it would not preserve them and this is to forget. And for this reason, in anger and in deep meditation, drunkenness, phrenitis, fear, and very stubborn sufferings of the brain, none of them would remember their achievements at a later time. Indeed, is it extraordinary in those asleep, the brain operating indistinctly, for the impressions to become indistinct and for this reason not to be lasting? If those keeping watch or pondering some problem have almost all their attention directed toward their thoughts, scarcely having any of it concerned with their walking, is it extraordinary that the impression of the performance is received indistinctly and is forgotten forthwith, and that these individuals, therefore, do not remember whether the act was accomplished voluntarily [446]. Likewise, if we do not remember completely, we cannot re-

call accurately anything that happened, and therefore we do not know what the things were which we do not remember, because it is necessary to keep them in the memory first, in order to observe their quality afterward. At any rate, to me it does not appear extraordinary that, although breathing during sleep is voluntary, when we arise, we cannot say whether we breathed voluntarily, and it would be the same if those moving their feet and hands and uttering sounds while asleep should forget and say the motion of the limbs and the voice arose involuntarily.

Patients in delirium prattle, walk about, and perform all the voluntary motions, but when they recover from their PARANOIA, they remember nothing of what they have done. At any rate, for 13 days I saw someone in a delirium carry on as follows: He thought he lay sick in Athens, not in Rome. Continually calling his accustomed boy, he ordered him [447] to carry the necessary things to the gymnasium, and a little later, "Oh you," he said, "to the Ptolemaion, I say, for I wish to be free in it for a long time." And then sometime afterward he leaped up and, donning his clothes, would straightway have gone forth from the outer court door, but those within restrained him and prevented him from going out. "For what reason do you prevent me?" he demanded of them. They told him (for there was nothing to say but the truth) that he had had and was still having a fever. He replied to this altogether moderately for, he said, he knew that some of his fever remained, that this was something quite small and nothing suspicious to hinder him from bathing, for the whole fever affecting him had arisen from travel. "Do you not remember," he said turning to his boy, "how violently we traveled yesterday from Megara to Athens?" While he was speaking thus and doing these things, a massive hemorrhage through his nose overtook him and after this a sweat. He recovered forthwith but remembered nothing of the foregoing. Were not among his voluntary acts (for this is what we proposed to show from the beginning) [448] the standing up, speaking aloud, defecating or urinating (for the man accomplished all these things during those many days)? Or, is it indeed absurd (for if these acts are not voluntary,

no others are) for him not to remember them, when those sober do not remember what they performed in drunkenness?

If it is true that breathing arises voluntarily, how is it extraordinary that if we pay attention more carefully at one time, but more carelessly and lazily at another, we remember the activities occurring while we were intent, but otherwise we forget them? Also, since we consider that we have not accomplished what we may have forgotten completely, we do not remember if it was accomplished voluntarily. How the act of breathing may be controlled voluntarily wholly through the brain is shown by the foreign slave who had been made angry and resolved to die. Throwing himself to the ground and [449] holding his breath, he was motionless for a long time; later, rolling over slowly, he died. Even if it were impossible to hold the breath continuously, no one would deny that it is voluntary. Thus, it seems that some voluntary acts are free and some are subject to the exigencies of the body. The former we perform free of hindrance at all times, the latter only at certain times and to a limited extent. Thus, walking toward something, talking, or taking and receiving something are completely free; but defecating and urinating are responses to the urgencies of the body. Now someone may be silent for a whole year or a longer time if he wishes; but holding the feces or the urine is not carried out in a similar manner because no one can do so for a month, not even for a few days. There would be pressure, often with distress, or the weight of fullness or a stinging with such sharpness that [450] there is not time enough to reach the accustomed place. Breathing is the same as these but much more pressing with more immediate necessity, for there is danger of death without breathing. It is exceedingly painful to be choked and it is not extraordinary that holding the breath is extremely difficult. All people are zealous not to die, but should they be afflicted by a myriad evils, and wish to die, they would not hasten into this, unless they wished to go out painfully. Simply because we are able to remain continuously silent but are unable to hold our breath, however, no one should consider that only the speaking is a voluntary act and breathing an involun-

tary and natural one. I think I have demonstrated this clearly.

Chapter VII

What has been left incomplete in our discourse concerning the middle positions should be added next. Since the so-called angular posture of the arm, being precisely middle between full extension and flexion, is most free of burden, it seems likely that a similar condition would hold true for the legs, but this is not so. The painless position without burden in the latter members is in the interval between the middle position and full extension. The reason for this involves habit, for ordinarily our legs are extended because we hold the whole body up by them when we stand or walk. Also before we are active with them, they are molded in extension by swaddling clothes. Also while sleeping and reclining for other reasons, they are extended more often than flexed. We are distressed much more in extremes of flexion than extension. Many people cannot bring their legs entirely to extreme flexion without assisting with their hands. We are unaccustomed to making this part go through this action and only those flex easily who are adept in dancing or expert in wrestling and especially accustomed to flexing completely. This intermediate position approaching extension which is completely without burden, was caused by custom of the parts over a long period of time.

These two things, nature and habit, are to be considered in all the joints, [452] if you would find the intermediate and burdenless position. It seems that everywhere habit corresponds to nature and the intermediate burdenless position is rightly called newly acquired nature. In the legs, this same intermediate position without burden would be the middle of the motions taking place in the parts and not the middle of complete extension and flexion. For you will find that we withdraw from the position without burden toward extension as much as we depart from flexing to the uttermost. In general, therefore, you will discover the intermediate and burdenless position from examining the uttermost motions in all the joints. Thus, in the joint of the elbow it is the so-called angular

position, in the knee that closer to extension, in the spine that closer to flexion and for the joint of the wrist, the exactly straight. We can make the spine quite fully arched or flexed. We bend the head backward and forward from upright equally so that the [453] precisely straight position is exactly middle between these extreme motions, and is the most without burden. In the spine the intermediate position is not the straight but that slightly curved, for this motion predominates. We exert ourselves more in the region of the spine when standing upright than when sitting or lying down, for, in standing, the spine must be extended but in sitting or lying down it is not hindered from being flexed. If you examine this in all the joints you will find that they all make our exposition consistent within itself.

With the muscles not associated with joints, an intermediate condition would be without burden, as with the anus, the bladder, and the tongue. For, both closing the anus extremely tightly and dilating it to the utmost are burdensome; also, protruding the tongue to the greatest extent, or flexing it, or however many other motions are carried out excessively, are burdensome. It is easy, indeed, to discover the intermediate of the extremes for the muscles of the tongue, as well as what is burdenless. All men, at the time when they cease their life-long activities, maintain an intermediate and burdenless posture in all the parts [454], "having been compelled to this by a well-ordered nature," says Hippocrates. In the tongue all the muscles attach in pairs, above and below, at the right and at the left so that it is not extraordinary that it is moved in opposite directions by antagonists. From the facts at hand, however, it is not equally clear how the muscle of the anus, the bladder, and the diaphragm may be moved in opposite directions (for the single muscle in each of these is circular, no muscle apparently being antagonistic), but let us look into this.

Chapter VIII

The action of the muscle of the bladder and the anus is not to eliminate the excretions of the food but to retain them. Many have been mistaken straight off in this

very thing, believing that these muscles were created for the sake of expelling the excreta, because they have not been able to observe that after paralysis, elimination takes place involuntarily. When the muscle in the anus has been cut many times [455] excessively through wretched surgery, the feces flow by it involuntarily, as if, I think, the organs which prevent the flowing did not remain. This muscle is strictly not the primary organ of expulsion, but in order that what happens when it is cut or paralyzed may not occur continually throughout life, nature has placed it as a guard against the ill-timed exodus of the excreta. We turn our attention, therefore, not toward something to prevent the expulsion, but rather toward the structures accomplishing this activity.

What, therefore, are the organs of this expulsive activity? They are many as individuals but of two kinds, *those of the brain* [PSYCHE] and *those of nature* [PHYSIS], and, therefore, the organs of the brain always act voluntarily, *those of nature* involuntarily. The diaphragm and all the muscles of the epigastrium are organs of the brain. The whole system of the intestines and the stomach are organs of nature, but the activity of these has been written about in other books. Let us speak now concerning the muscles, since the present discussion is an explanation of their motion. [456] All the muscles in the epigastrium, when they pull actively, press into the organs of nature inside. These, if the diaphragm yields, go back up into the latter's place, giving way before the force of the muscles. If the diaphragm does the opposite, the contents of their cavities would be pressed out as if squeezed by two hands, outside by the muscles and inside by the diaphragm. The obliquity of the diaphragm aids this greatly, since it has one end at the cartilage in the breast lying above, the other behind at the lumbar spine. The compression of the excreta in the intestines takes place by the activity of the muscles on two sides, outside by those of the epigastrium, inside by the diaphragm. The obliquity of the diaphragm is the cause of the descent of the compressed. The muscle in the anus is idle during this time. The muscles in the abdomen are numerous, and all contract

during these emptyings; those in the hypochondrium contract more, those below less, contrary to what takes place in urination. For in the latter those below act more, [457] those in the hypochondrium less, both, not as organs of urination or defecation for this is extremely illogical, but, since the pull of the diaphragm must be as strong as the pull of the muscles in the abdomen, it would be impossible for one muscle by itself to compete with the many large ones. The danger in this is that if they overpowered the diaphragm everything would be forced into the cavity of the thorax. For this reason the muscles between the ribs contract, binding them together from all sides. The lax thorax easily yields to the pushing diaphragm, as it is possible to observe when the muscles in the abdomen contract, and especially the inferior ones, while all those inside the thorax relax. Almost the whole content of the abdomen, in these conditions, is pushed into the cavity of the thorax along with the diaphragm itself. In order that this may not happen and the act of defecation be abolished, the entire thorax is held securely fast on all sides. It is evident from all that has been said [458] that the muscles placed at the outlet for the feces are destined to shut them in. This is their proper action, and they cannot expel them except inadvertently when they cease acting. Just as opposing muscles promote opposite actions in all other regions, so it is here, for retention of the feces comes from the activity of the latter muscles, and expulsion from the muscles in the epigastrium and diaphragm.

Chapter IX

Which muscles in the diaphragm have analogy to the antagonistic muscles of other parts? The antagonistic muscles cannot be stated simply because first, as an organ for expulsion of feces, it has those retaining them, and second, especially, in another kind of antagonism, it has those of the epigastrium. As an organ of respiration the latter antagonism is in part true and in part not entirely true, for in expiration no muscle is wholly agent, since this action of the thorax, it seems, is more like the passive condition of falling [459] mentioned by

us earlier. *Blowing out* is a massive carrying out of the air caused by the activity of the intercostal muscles. All the muscles between the ribs inside [internal intercostals] are agents for blowing out. The former is like the action of the thorax in making someone lie down with respect to his whole body already mentioned, the latter is like the laying down of each of the parts. Inspiration is opposite to expiration, blowing out to violent inspiration (for it does not have a specific name). The diaphragm alone presides over the earlier antithesis, over the other antithesis the intercostals with the muscles in the thorax coming down from the scapula and the neck preside. Especially in need of this are flute players, trumpeters, and heralds when they are about to call out their monotonous cries, and, not least, those blowing into leather wine skins and other organs or, to speak simply, anyone who wishes particularly to make expanded and contracted changes in the thorax. Someone might rightly say that the external muscles of the thorax are [460] antagonistic to the internal intercostals. These things concerning the muscles of the thorax are pointed out not only in this treatise but also in the treatise "On the Causes of Respiration," and "On the Voice," and "On the Purpose of Respiration." But now indeed the continuity of the discussion is at an end.

The diaphragm has certain peculiarities different from the other muscles due to its situation and form. When it ceases to act and becomes more lax, its convexity is inclined toward the spine on the one hand and the stomach on the other, but much more easily toward the spine. In all of a man's positions except lying prone, the diaphragm is above and the spine below, so that logically it is inclined toward the latter because it is under pressure from the abdominal viscera in front, from the softest and most nimble of all the splanchna, the lungs, behind. [461] Its convexity inclines forward, however, in the prone position, and when the intercostal muscles are active, those in the paunch are in repose and it is evident that the abdomen under these circumstances raises itself. Gymnasts seek this position habitually after exercise. Just as the intercostal mus-

position, in the knee that closer to extension, in the spine that closer to flexion and for the joint of the wrist, the exactly straight. We can make the spine quite fully arched or flexed. We bend the head backward and forward from upright equally so that the [453] precisely straight position is exactly middle between these extreme motions, and is the most without burden. In the spine the intermediate position is not the straight but that slightly curved, for this motion predominates. We exert ourselves more in the region of the spine when standing upright than when sitting or lying down, for, in standing, the spine must be extended but in sitting or lying down it is not hindered from being flexed. If you examine this in all the joints you will find that they all make our exposition consistent within itself.

With the muscles not associated with joints, an intermediate condition would be without burden, as with the anus, the bladder, and the tongue. For, both closing the anus extremely tightly and dilating it to the utmost are burdensome; also, protruding the tongue to the greatest extent, or flexing it, or however many other motions are carried out excessively, are burdensome. It is easy, indeed, to discover the intermediate of the extremes for the muscles of the tongue, as well as what is burdenless. All men, at the time when they cease their life-long activities, maintain an intermediate and burdenless posture in all the parts [454], "having been compelled to this by a well-ordered nature," says Hippocrates. In the tongue all the muscles attach in pairs, above and below, at the right and at the left so that it is not extraordinary that it is moved in opposite directions by antagonists. From the facts at hand, however, it is not equally clear how the muscle of the anus, the bladder, and the diaphragm may be moved in opposite directions (for the single muscle in each of these is circular, no muscle apparently being antagonistic), but let us look into this.

Chapter VIII

The action of the muscle of the bladder and the anus is not to eliminate the excretions of the food but to retain them. Many have been mistaken straight off in this

very thing, believing that these muscles were created for the sake of expelling the excreta, because they have not been able to observe that after paralysis, elimination takes place involuntarily. When the muscle in the anus has been cut many times [455] excessively through wretched surgery, the feces flow by it involuntarily, as if, I think, the organs which prevent the flowing did not remain. This muscle is strictly not the primary organ of expulsion, but in order that what happens when it is cut or paralyzed may not occur continually throughout life, nature has placed it as a guard against the ill-timed exodus of the excreta. We turn our attention, therefore, not toward something to prevent the expulsion, but rather toward the structures accomplishing this activity.

What, therefore, are the organs of this expulsive activity? They are many as individuals but of two kinds, those of the brain [PSYCHE] and those of nature [PHYSIS], and, therefore, the organs of the brain always act voluntarily, those of nature involuntarily. The diaphragm and all the muscles of the epigastrium are organs of the brain. The whole system of the intestines and the stomach are organs of nature, but the activity of these has been written about in other books. Let us speak now concerning the muscles, since the present discussion is an explanation of their motion. [456] All the muscles in the epigastrium, when they pull actively, press into the organs of nature inside. These, if the diaphragm yields, go back up into the latter's place, giving way before the force of the muscles. If the diaphragm does the opposite, the contents of their cavities would be pressed out as if squeezed by two hands, outside by the muscles and inside by the diaphragm. The obliquity of the diaphragm aids this greatly, since it has one end at the cartilage in the breast lying above, the other behind at the lumbar spine. The compression of the excreta in the intestines takes place by the activity of the muscles on two sides, outside by those of the epigastrium, inside by the diaphragm. The obliquity of the diaphragm is the cause of the descent of the compressed. The muscle in the anus is idle during this time. The muscles in the abdomen are numerous, and all contract

during these emptyings; those in the hypochoondrium contract more, those below less, contrary to what takes place in urination. For in the latter those below act more, [457] those in the hypochoondrium less, both, not as organs of urination or defecation for this is extremely illogical, but, since the pull of the diaphragm must be as strong as the pull of the muscles in the abdomen, it would be impossible for one muscle by itself to compete with the many large ones. The danger in this is that if they overpowered the diaphragm everything would be forced into the cavity of the thorax. For this reason the muscles between the ribs contract, binding them together from all sides. The lax thorax easily yields to the pushing diaphragm, as it is possible to observe when the muscles in the abdomen contract, and especially the inferior ones, while all those inside the thorax relax. Almost the whole content of the abdomen, in these conditions, is pushed into the cavity of the thorax along with the diaphragm itself. In order that this may not happen and the act of defecation be abolished, the entire thorax is held securely fast on all sides. It is evident from all that has been said [458] that the muscles placed at the outlet for the feces are destined to shut them in. This is their proper action, and they cannot expel them except inadvertently when they cease acting. Just as opposing muscles promote opposite actions in all other regions, so it is here, for retention of the feces comes from the activity of the latter muscles, and expulsion from the muscles in the epigastrium and diaphragm.

Chapter IX

Which muscles in the diaphragm have analogy to the antagonistic muscles of other parts? The antagonistic muscles cannot be stated simply because first, as an organ for expulsion of feces, it has those retaining them, and second, especially, in another kind of antagonism, it has those of the epigastrium. As an organ of respiration the latter antagonism is in part true and in part not entirely true, for in expiration no muscle is wholly agent, since this action of the thorax, it seems, is more like the passive condition of falling [459] mentioned by

us earlier. Blowing out is a massive carrying out of the air caused by the activity of the intercostal muscles. All the muscles between the ribs inside [internal intercostals] are agents for blowing out. The former is like the action of the thorax in making someone lie down with respect to his whole body already mentioned, the latter is like the laying down of each of the parts. Inspiration is opposite to expiration, blowing out to violet inspiration (for it does not have a specific name). The diaphragm alone presides over the earlier antithesis, over the other antithesis the intercostals with the muscles in the thorax coming down from the scapula and the neck preside. Especially in need of this are flute players, trumpeters, and heralds when they are about to call out their monotonous cries, and, not least, those blowing into leather wine skins and other organs or, to speak simply, anyone who wishes particularly to make expanded and contracted changes in the thorax. Someone might rightly say that the external muscles of the thorax are [460] antagonistic to the internal intercostals. These things concerning the muscles of the thorax are pointed out not only in this treatise but also in the treatise "On the Causes of Respiration," and "On the Voice," and "On the Purpose of Respiration." But now indeed the continuity of the discussion is at an end.

The diaphragm has certain peculiarities different from the other muscles due to its situation and form. When it ceases to act and becomes more lax, its convexity is inclined toward the spine on the one hand and the stomach on the other, but much more easily toward the spine. In all of a man's positions except lying prone, the diaphragm is above and the spine below, so that logically it is inclined toward the latter because it is under pressure from the abdominal viscera in front, from the softest and most nimble of all the splanchna, the lungs, behind. [461] Its convexity inclines forward, however, in the prone position, and when the intercostal muscles are active, those in the paunch are in repose and it is evident that the abdomen under these circumstances raises itself. Gymnasts seek this position habitually after exercise. Just as the intercostal mus-

cles are active so also are those in the abdomen, during what they call holding the breath. For this it is necessary that the upper end of the larynx be closed, since if it is open when the muscles mentioned are active, there is blowing out. If again, with them, the muscles of the pharynx and larynx extend, there is not blowing out but the voice comes forth.

A double tension exists for all the muscles. The first is when, being active, they pull themselves together, the second is when they are extended by the antagonistic muscles. The first holds true for the diaphragm in non-violent inspirations. The other has a double origin, as has been said above, either when the muscles in the belly are active or only the intercostals alone. [462] In non-violent expirations which specifically we call expirations to distinguish them from blowings out, neither of them holds. But in all others, that condition which we say comes in the middle of the extreme motions, only in the case of the diaphragm is double. It inclines toward the spine in all positions but the prone, in which position only it inclines toward the stomach.

The intercostal muscles and those in the abdomen are forever curved out due to their form having been made like the underlying organs. When they are in repose, naturally they are so. When they are active they retract and become less convex while nearly all the other muscles, those which move the parts, are the opposite. The latter, being straight in repose, become convex when they are active. The reason for their difference is clear. For, since the substance of the bones, hard and rigid, is placed under some of them, and some hollow yielding space under the others, logically all those lying on the bones [463] during contraction gain as much in depth and width as they lose in length and hold prominent the whole bulk of their body. In those which conceal the softness of their background, the greater part of their bodies is hidden away during contraction. Indeed, it is not extraordinary, if nearly all the muscles in the limbs curve out when they are active, that those in the thorax and epigastrium only retract, for they alone have the yielding hollow space

underneath. Certainly when the stomach is gorged so much that it is painfully distended, they do not retract. For, what happens with the others at all times, happens in those of the epigastrium in gorging of the stomach due to the rigidity of the underlying background. The latter clearly is filled by engorgings, hydropsy or in whoever is fat. In those with the stomach empty, the muscles, before they become active, are curved in resemblance to the underlying organs, for they are pushed out according to the curving of the latter, but when they become active they retract for they easily compress [464] the underlying cavity. And now also the muscles in the thorax, attached in between the bony parts, before they are active, have a form similar to the whole ribs, being convex outward and concave inward. When they are active, compressing first and especially and the membrane lying under them called the pleura and through it the lungs which are soft and spongy, they give way inward to the extent that the yielding substance of the underlying organs permits.

Anyone knowing these generalities concerning the motion of muscles can discover everything else in individual parts.

DISCUSSION

The source of error which has caused the misunderstanding of Galen's comprehension of nerves and tendons stems from the early Latin translations. The able scholars of the Renaissance, because their knowledge of anatomy was greatly inferior to their knowledge of Greek, decided that the Greek word *SYNDESMOS* should be translated *ligamentum* in Latin regardless of the context. It has been the tradition through the succeeding centuries to Latinize the Greek, and for the most part modern translators have slavishly followed the Latin by translating the word *ligament*. In this treatise Galen, being an extraordinarily accurate anatomical observer, hoped to avoid this mistake by giving a detailed definition and explanation of his use of *SYNDESMOS*. It seems clear that he understood fibrous connective tissue to range from the delicate areolar tissue of the *entymysium* to the dense bands and sheets of ligaments and aponeuroses. He

even points out that the name SYNDESMOS follows the meaning. The derivation of the word is from SYN, meaning with, the DESMOS meaning something that binds. In a similar way, electron microscopists use desmosome for a binding body.

At the end of the first paragraph of the translation there is a key example of the subtlety of the shades of meaning in Greek and the stultifying influence of Latin translation. In Greek the SYNDESMOS "is a nerve-like substance associated with bone, etc." The Latin renders this "attached to bone," the significance of the entire passage is lost, and the interpretation as ligament is firmly established.

No less a historian of Medicine than Charles Singer, in discussing Galen's "false concepts," makes the following statement in the introduction to his translation of "On Anatomical Procedures": "Even greater difficulty arises from his theory of the nature of nerves. Galen saw that a nerve, NEURON, passes into each muscle and that it then divides. Knowing

that many muscles end in a whitish tendon, he thought that the branches of the nerves had reunited within the muscle to form this tendon, which he naturally also called NEURON." This undoubtedly refers to the second chapter of the present treatise, but it is a deliberately false interpretation, even to the statement that Galen called tendons nerves, which he certainly never did. He was much averse to loose ends in any description or explanation. He traced the nerves into the endomysium, and not having a microscope with which to see the motor end plates, it was logical, as he says, to carry them along with the connective tissue as it became condensed into the tendon.

LITERATURE CITED

- Kühn, C. G. 1821-1833 Galen, Opera omnia. Greek and Latin text. 20 volumes in 22. Cnobloch, Lipsiae., 4: 367-464.
- Singer, C. 1956 Galen on Anatomical Procedures, Translation of the Surviving Books. Oxford University Press, London and New York. xxvi + 289 pages.

Central Projections of Spinal Dorsal Roots in the Monkey¹

I. CERVICAL AND UPPER THORACIC DORSAL ROOTS

JOYCE E. SHRIVER,² BENNETT M. STEIN³ AND MALCOLM B. CARPENTER

Department of Anatomy, College of Physicians and Surgeons, Columbia University, New York, N.Y.

ABSTRACT A study of the central distribution of cervical and upper thoracic dorsal roots (DR) was made in 18 monkeys subjected to 31 dorsal rhizotomies. Degeneration was studied in multiple spinal and medullary sections stained by the Nauta technic.

Dorsal roots C2 through T7 project fibers to: (1) portions of laminae III and IV, (2) the intermediomedial nucleus, and (3) portions of laminae VII, VIII and IX. DR C5 through T1 project fibers to medial parts of lamina VI. DR fibers reach cell groups of lamina IX via different trajectories, one of which is dominant in the brachial enlargement. Fibers project to the spinal accessory nucleus from C2 through C5 DR, while portions of the dorsal nucleus receive fibers from C5 to T7 DR.

Ascending fibers in the fasciculus cuneatus: (1) arise from C1 through T7 DR, (2) exhibit only general segregation due to overlap, and (3) project somatotopically throughout the extent of the cuneate (CN) and accessory cuneate (ACN) nuclei. Fiber terminations in CN and ACN are: (1) similar for C1 through T1 DR, and (2) distinctive for T2 through T7 DR. The upper five cervical DR project fibers to: (1) the supraspinal nucleus, and (2) both the central cervical and intermediate nuclei. Cytological and degeneration studies suggest that the central cervical and intermediate nuclei constitute parts of the same cell column.

Although many studies of the central projections of spinal dorsal root fibers have been made, the majority of these investigations has utilized the Marchi method (Sherrington, 1893; Collier and Buzzard, '03; Ranson, Davenport and Doles, '32; Pass, '33; Corbin and Hinsey, '35; Ferraro and Barrera, '35b; Corbin, Lhamon and Petit, '37; Schimert, '39; Yee and Corbin, '39; Walker and Weaver, '42; Chang and Ruch, '47; Escobar, '48). More recent studies of dorsal root fibers (Torvik, '56; Liu, '56; Sprague, '58; Grant and Raxed, '58; Kerr, '61; Kuypers and Tuerk, '64; Sprague and Ha, '64; Hand, '66; Sterling and Kuypers, '67) employing silver staining methods have provided new data concerning: (1) the distribution of these fibers in the spinal gray, and (2) their mode and patterns of termination in medullary nuclei. Most investigations utilizing the Nauta staining method have been done on the cat and have been based upon section of a limited number of dorsal roots in restricted regions of the spinal cord. A notable exception is Liu's ('56) study of dorsal root

afferents to the dorsal and accessory cuneate nuclei in the cat.

The purpose of this study of spinal dorsal roots in the monkey was to determine: (1) the distribution of these fibers within the spinal cord, and (2) the projection and patterns of termination of ascending fibers in medullary relay nuclei.

Material from this study has been divided into two parts. Part I concerns the central projections of the cervical and upper thoracic (i.e., C1 through T7) dorsal roots; ascending branches of these dorsal roots project primarily upon the cuneate and accessory cuneate nuclei. Part II of this study (Carpenter, Stein and Shriver, '68) presents similar data concerning the lower thoracic, lumbosacral and coccygeal dorsal roots and includes a comparison of projections to the posterior column nuclei.

¹This study was supported by a research grant (NB-01538-09) from the Institute of Neurological Diseases and Blindness of the National Institutes of Health, Bethesda, Maryland.

²Postdoctoral Fellow in neuroanatomy supported by training grant 5T1-NB-5242-08 from the Institute of Neurological Diseases and Blindness.

³Associate in Neurosurgery, College of Physicians and Surgeons, Columbia University.

MATERIAL AND METHODS

In 18 rhesus monkeys single dorsal rhizotomies were done at different levels and on different sides. For economy of time, effort and material three or four different single dorsal roots at selected levels were sectioned in some animals. Table 1 indicates the single dorsal roots sectioned in individual animals. Although this study concerns only the cervical and upper thoracic dorsal roots, dorsal roots at other levels were sectioned in some animals (see Part II).

Surgical procedures were performed aseptically. Following rather extensive bilateral laminectomies, the dura was opened in the midline and the root to be sectioned was identified. Dorsal roots were sectioned with microsurgical scissors with the aid of the Zeiss operating microscope. Using various magnifications, it was possible to section the dorsal roots without traumatizing the spinal cord or interrupting radicular vessels. The proximal stump of the severed dorsal root was marked with a black silk suture. Following dorsal rhizotomies the dura was closed with 5-0 silk sutures, except in thoracic regions where the dural defect was covered with gelfoam.

In the thoracic region the narrow confines of the spinal canal made it difficult to close the dura and exposed portions of the spinal cord sometimes revealed evidence of trauma postoperatively. In order to avoid this, certain thoracic dorsal roots were sectioned within the dural sleeve following laminectomy. Dorsal and ventral roots were separated, and the dorsal root was cut without injury to radicular vessels.

In certain prior studies of dorsal root fibers (Liu, '56; Sprague, '58; Sprague and Ha, '64; Hand, '66) extradural section of the dorsal root was done in the intervertebral foramen. This technic was preferred by these authors because spinal cord injury frequently followed intraspinal dorsal rhizotomy. Experience from this study indicates that intralaminar dorsal rhizotomy in the monkey can be done using microsurgical technic without injury to the spinal cord or radicular vessels.

Animals were observed postoperatively in single cages for at least two weeks. Neurological examinations of each animal were made on the sixth postoperative day and prior to sacrifice. Animals were anesthetized and sacrificed by perfusion; each animal was perfused via the left ventricle

TABLE 1
Dorsal roots sectioned in eighteen monkeys

Animal Number	Spinal roots																			
	C1	C2	C3	C4	C5	C6	C7	C8	T1	T2	T3	T4	T5	T6	T7	T8	T10	T12	L1	L2
C-879					L					L										
C-912			R							L									R	
C-913*		R								L									R	
C-914					R			L												
C-915*							R								L					
C-916	R										L							L		
C-967						R						L								R
C-970*		R										L								
C-974					R															
C-978*			R																	
C-981		R		L																
C-1006		R		L																
C-1008	B									R										
C-1012					L													L		
C-1014				L				R												R
C-1017														L		R				
C-1024	L												R							
C-1025								L							R					

*In 18 animals 45 dorsal roots were sectioned individually on different sides and at different levels. Letters R, L and B refer to right, left and bilateral and indicate roots sectioned. Asterisks indicate that sections of the medulla were cut in horizontal planes, all others were cut transversely. Only observations on cervical and upper thoracic dorsal roots (C1 through T7) are reported here, data concerning all other dorsal roots are considered in Part II of this study.

the heart with a liter of normal saline followed by an equal volume of chilled 0% neutral formalin. The brain and entire spinal cord were removed *in toto*. After adequate fixation in 10% neutral formalin the brains were sectioned. The brain stems were cut in transverse and horizontal planes (see table 1). Levels of the spinal cord were determined by counting spinal roots under a dissecting microscope. Transverse blocks of the spinal cord were cut and placed in separate compartments of plastic boxes.

Blocks of the brain stem and spinal cord were sectioned at 20 μ on a freezing microtome. Multiple sections of the medulla and representative sections of the spinal cord above, below, and at the level of the rhizotomy were stained by the Laidlaw modification of the Nauta and Gyax ('54) technic. Representative sections of the medulla and numerous spinal levels also were stained with cresyl violet to facilitate identification of cell groups. Drawings of the spinal cord and brain stem sections and the resulting degeneration were made for all animals.

The lower brain stems of five animals were embedded in paraffin and sectioned serially at 15 μ in horizontal (3 animals) and transverse (2 animals) planes. Every ninth section was stained with cresyl violet and every tenth section was stained according to the Weil technic. These slides were projected and nuclear groups in the medulla were outlined in serial drawings. This control material facilitated the study of the medullary nuclei receiving ascending fibers from the spinal dorsal roots.

OBSERVATIONS

Normal anatomy. The cytoarchitectonic atlas of Rexed ('52, '54, '64) and his nomenclature for cell groups of the spinal cord have been used in describing the degeneration resulting from dorsal rhizotomy. While it is realized that these studies are based on the cat, there appears to be a fairly close general correspondence for the monkey. The use of Rexed's terminology also provides a basis for more precise description. There are several nuclear groups which deserve special attention and comment.

Evidence from the study of normal cytoarchitecture in the monkey indicated that lamina II corresponds exactly with the substantia gelatinosa as described by Rexed ('52) and as shown by the ultrastructural studies of Ralston ('65). These observations differed from those of Sprague and Ha ('64) and Szentágothai ('64) in the cat who regarded the substantia gelatinosa as composed of both laminae II and III. Observations in the monkey also indicated that laminae III and IV constituted the proper sensory nucleus as described by Rexed.

Although there are numerous descriptions of the lateral cervical nucleus in the cat (Rexed and Brodal, '51; Brodal and Rexed, '53; Morin and Catalano, '55; Ha and Liu, '66), there are few detailed descriptions of this nucleus in the primate (Ha and Morin, '64). Observations in several series of Nissl stained sections revealed a small linear collection of cells lateral to the posterior horn in the upper three cervical segments. These cells, appearing as the primate equivalent of the lateral cervical nucleus of the cat, were mainly medium sized, approximately equal to those in lamina IV. This nucleus in the monkey, compared with that in the cat, contained fewer cells which form a narrower band fairly close to the posterior horn. Cells consistently appeared most numerous at the C1 level, but a few cells usually were found at C2 and C3. No dorsal root fibers were observed to project to the lateral cervical nucleus in the monkey.

A small cell group in the medial part of lamina VII near the central gray, but slightly ventrolateral to the central canal, deserves comment. This cell group, found at all levels of the spinal cord, appears to correspond to the intermediomedial nucleus as described by Rexed. This nucleus received dorsal root afferents at all levels.

The central cervical nucleus (i.e., intermediate nucleus; Cajal, '09) constituted a column of relatively large cells in medial and central portions of lamina VII in the upper four cervical spinal segments. As described by Rexed ('54), the central cervical nucleus lies almost exactly lateral to the central canal. In the monkey this

nucleus was located closer to the central canal than in the cat and frequently extended into the rostral part of the C5 segment. Even though the borders of this nucleus were not sharply delimited, its large, star-shaped cells were distinctive (fig. 1). This nucleus received dorsal root fibers from certain cervical spinal roots and appeared to be directly continuous with the intermediate nucleus of the medulla.

In order to investigate the relationship between the central cervical nucleus and the intermediate nucleus, which has been denied by Rexed ('54), serial horizontal sections of the medulla and upper cervical segments were prepared in three animals. Observations in this material indicated that the intermediate nucleus was a long cell column extending from the caudal medulla rostrally beyond the caudal pole of the dorsal motor nucleus of the vagus. Throughout its extent cells of this nucleus were somewhat ventrolateral to the central canal, or ventral to the fourth ventricle. Rostral portions of the cell column were farther from the midline than caudal parts; the most rostral parts of the nucleus lay dorsolateral to the hypoglossal nucleus and lateral to the dorsal motor nucleus of the vagus nerve (fig. 2).

Cells of the intermediate nucleus of the medulla were heterogeneous in size and shape. In the caudal half of the nucleus large star-shaped cells predominated while rostrally smaller round or spindle-shaped cells formed the bulk of the nucleus (fig. 1). Observations suggested that the central cervical nucleus and the intermediate nucleus constituted parts of the same cell column; this cell column seemed to be partially interrupted in the region of the corticospinal decussation, but some large cells usually could be seen bridging this region.

The concept that the central cervical nucleus and the intermediate nucleus are parts of the same cell column is supported by the fact that: (1) cells of these nuclei share at least one common source of afferent fibers (i.e., fibers from the upper five cervical dorsal roots), and (2) dorsal root fibers terminate in extensive pericellular arborizations in all parts of the cell column.

Cervical dorsal roots

Each of the eight cervical dorsal roots was sectioned individually. Twenty-one cervical dorsal roots were sectioned in 16 different animals.

First cervical root. The first cervical dorsal root was sectioned unilaterally (C-916) and bilaterally (C-1008; fig. 3) and was found to be absent in four other animals (C-974, C-978, C-981 and C-1006) explored surgically. All degenerated fibers contained in the slender C1 root entered the most lateral part of the fasciculus cuneatus at this level and in the caudal medulla (fig. 7). No degenerated root fibers entered the spinal trigeminal tract or nucleus, but some fibers from the fasciculus cuneatus entered the spinal gray in the cervix region of the posterior horn and coursed ventromedially to terminate about cells of the central cervical nucleus. Very sparse degeneration was seen in parts of the anterior horn. A few degenerated fibers descended in the fasciculus cuneatus through the C2 level in rhesus C-1008, but none was seen in rhesus C-916. Moderate degeneration was present in the central cervical nucleus at C2 in both animals. All other cervical segments were free of degenerated fibers.

In transverse sections of the medulla ascending degeneration in the fasciculus cuneatus formed a small bundle between the lateral border of the cuneate nucleus and the medial border of the spinal trigeminal nucleus. Rostrally, ascending degeneration in the most lateral part of the fasciculus cuneatus formed a narrow band immediately dorsal to the spinal trigeminal tract and nucleus. At caudal medullary levels degenerated fibers entered the lateral border of the cuneate nucleus, swept ventromedially along the margin of this nucleus, and entered the intermediate nucleus. Some of these fibers traversed this nucleus in their projection to dorso-medial portions of the supraspinal nucleus (fig. 36). Degeneration in the intermediate nucleus was most profuse caudally, but extended through low olivary levels of the medulla.

Ascending root fibers passing to the accessory cuneate nucleus were more numerous than those terminating in the

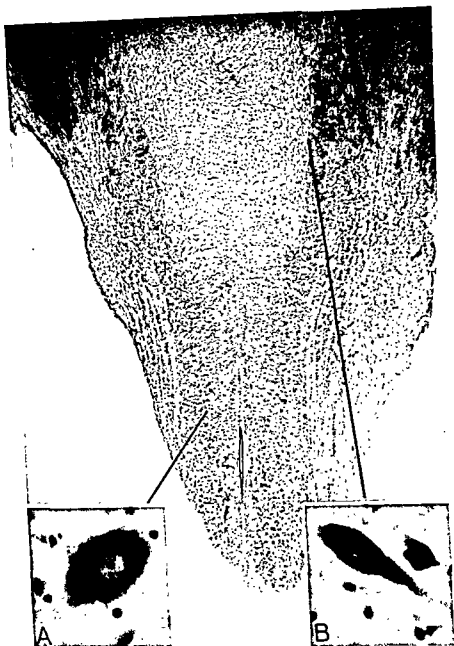


Fig 1 Horizontal brain stem section of rhesus C-972 demonstrating continuity of the intermediate and central cervical nuclei. This section corresponds to the most ventral section of the serial drawings of figure 2. Nissl $\times 14$. Insets A and B are photomicrographs of single cells in different parts of the cell column. Nissl $\times 500$.

nucleus was located closer to the central canal than in the cat and frequently extended into the rostral part of the C5 segment. Even though the borders of this nucleus were not sharply delimited, its large, star-shaped cells were distinctive (fig. 1). This nucleus received dorsal root fibers from certain cervical spinal roots and appeared to be directly continuous with the intermediate nucleus of the medulla.

In order to investigate the relationship between the central cervical nucleus and the intermediate nucleus, which has been denied by Rexed ('54), serial horizontal sections of the medulla and upper cervical segments were prepared in three animals. Observations in this material indicated that the intermediate nucleus was a long cell column extending from the caudal medulla rostrally beyond the caudal pole of the dorsal motor nucleus of the vagus. Throughout its extent cells of this nucleus were somewhat ventrolateral to the central canal, or ventral to the fourth ventricle. Rostral portions of the cell column were farther from the midline than caudal parts; the most rostral parts of the nucleus lay dorsolateral to the hypoglossal nucleus and lateral to the dorsal motor nucleus of the vagus nerve (fig. 2).

Cells of the intermediate nucleus of the medulla were heterogeneous in size and shape. In the caudal half of the nucleus large star-shaped cells predominated while rostrally smaller round or spindle-shaped cells formed the bulk of the nucleus (fig. 1). Observations suggested that the central cervical nucleus and the intermediate nucleus constituted parts of the same cell column; this cell column seemed to be partially interrupted in the region of the corticospinal decussation, but some large cells usually could be seen bridging this region.

The concept that the central cervical nucleus and the intermediate nucleus are parts of the same cell column is supported by the fact that: (1) cells of these nuclei share at least one common source of afferent fibers (i.e., fibers from the upper five cervical dorsal roots), and (2) dorsal root fibers terminate in extensive pericellular arborizations in all parts of the cell column.

Cervical dorsal roots

Each of the eight cervical dorsal roots was sectioned individually. Twenty-one cervical dorsal roots were sectioned in 16 different animals.

First cervical root. The first cervical dorsal root was sectioned unilaterally (C-916) and bilaterally (C-1008; fig. 3) and was found to be absent in four other animals (C-974, C-978, C-981 and C-1006) explored surgically. All degenerated fibers contained in the slender C1 root entered the most lateral part of the fasciculus cuneatus at this level and in the caudal medulla (fig. 7). No degenerated root fibers entered the spinal trigeminal tract or nucleus, but some fibers from the fasciculus cuneatus entered the spinal gray in the cervix region of the posterior horn and coursed ventromedially to terminate about cells of the central cervical nucleus. Very sparse degeneration was seen in parts of the anterior horn. A few degenerated fibers descended in the fasciculus cuneatus through the C2 level in rhesus C-1008, but none was seen in rhesus C-916. Moderate degeneration was present in the central cervical nucleus at C2 in both animals. All other cervical segments were free of degenerated fibers.

In transverse sections of the medulla ascending degeneration in the fasciculus cuneatus formed a small bundle between the lateral border of the cuneate nucleus and the medial border of the spinal trigeminal nucleus. Rostrally, ascending degeneration in the most lateral part of the fasciculus cuneatus formed a narrow band immediately dorsal to the spinal trigeminal tract and nucleus. At caudal medullary levels degenerated fibers entered the lateral border of the cuneate nucleus, swept ventromedially along the margin of this nucleus, and entered the intermediate nucleus. Some of these fibers traversed this nucleus in their projection to dorso-medial portions of the supraspinal nucleus (fig. 36). Degeneration in the intermediate nucleus was most profuse caudally, but extended through low olivary levels of the medulla.

Ascending root fibers passing to the accessory cuneate nucleus were more numerous than those terminating in the

cuneate nucleus. Caudally, degenerated fibers, which entered the dorsolateral border of the cuneate nucleus and swept ventromedially, appeared to be primarily fibers of passage. Degeneration, entering the lateral part of the nucleus in its middle and rostral thirds, terminated in a small region along the ventrolateral border of the nucleus (fig. 5). Additional small islands of degeneration were present in ventromedial and ventrocentral portions of the nucleus. The extreme oral pole of the cuneate nucleus was free of degeneration. Dorsal root fibers entering the medial part of the accessory cuneate nucleus in its middle and rostral thirds were distributed in a discrete wedge-shaped area in the most ventromedial portion of the nucleus (fig. 25). Degeneration in this wedge-shaped area diminished rostrally, but extended to the oral pole of the accessory cuneate nucleus.

Second cervical root. The second cervical dorsal root was sectioned in five monkeys (C-913, C-970, C-981, C-1006 and C-1024). Observations in these animals were similar, except that degeneration in rhesus C-1024 was more profuse, distributed more extensively, and extended farther caudally than in the other animals. At the level of the rhizotomy degenerated fibers entered the lateral part of the fasciculus cuneatus from which site part of the fibers traversed lamina II and terminated primarily in lateral regions of laminae III and IV (fig. 13). A bundle of degenerated fibers traversed central parts of laminae V and VI to arborize profusely about large cells of the central cervical nucleus (figs. 19, 20). In rhesus C-1024 a relatively large field of terminal degeneration was observed in the central portion of lamina VI. A contingent of degeneration passed to the intermediomedial nucleus. Groups of fibers (scattered and small in four monkeys and numerous in C-1024) coursed ventrally, both traversing and terminating, in medial and central parts of laminae VII and VIII. Relatively modest degeneration was seen in the ventromedial nucleus of lamina IX in rhesus C-913 and C-981, while in rhesus C-970 and C-1006 modest degeneration was seen mainly in the spinal accessory cell group. Approximately equal numbers of degenerated fibers were dis-

tributed to these cell groups of lamina IX in rhesus C-1024.

Descending C2 root fibers in the lateral part of the fasciculus cuneatus could be found at C3 (C-970 and C-981), and C4 (C-913, C-1006 and C-1024) spinal segments, but not at more caudal levels. Root fibers arborized extensively about cells of the central cervical nucleus at C3 and C4 levels in all animals and at the C5 level in one animal (C-1024). Less intense degeneration was present in laminae III, IV and IX at C3 and C4 segments in the same pattern as at C2. Degeneration extended caudally one segment in the intermediomedial nucleus and two to four segments in medial and central parts of lamina VII.

In the C1 segment the distribution and amount of ascending C2 root fibers in all portions of the spinal gray, except in laminae III and IV, was similar to that observed in the segment of root entry. Degenerated fibers in laminae III and IV were absent (three animals), scant and localized ventrolaterally (C-1006), and numerous and localized laterally (C-1024).

Ascending degeneration passing to medullary relay nuclei was studied in horizontal (C-913 and C-970) and transverse (C-1006 and C-1024) sections. Degeneration in the accessory cuneate nucleus was profuse and well localized throughout its rostrocaudal extent. Degenerated fascicles from the fasciculus cuneatus passed directly into the ventralmost part of the caudal pole of the accessory cuneate nucleus (figs. 26, 31). Degeneration in middle and rostral portions of the nucleus occupied a prominent wedge-shaped area in its ventral third. A narrow area in the ventralmost part of the nucleus was relatively free of degeneration. In the ventral third of the rostral pole of the nucleus, degeneration terminated in a circular area slightly removed from the most ventral and lateral borders of the nucleus.

Degenerated fibers from the fasciculus cuneatus entered the dorsolateral part of the cuneate nucleus and swept ventromedially, forming an oblique band along virtually its entire length (fig. 26). This degeneration was slightly removed from the most ventrolateral portion of the nucleus. Caudally, the majority of these

Abbreviations

ACN, accessory cuneate nucleus	NC, nucleus cuneatus
Ce, central cervical nucleus	NG, nucleus gracilis
CST, corticospinal tract	NI, nucleus intermedius
CST dec., corticospinal decussation	Nuc. V, spinal trigeminal nucleus
FC, fasciculus cuneatus	PH, posterior horn
FG, fasciculus gracilis	PRN, paramedian reticular nucleus
ICP, inferior cerebellar peduncle	RF, reticular formation
IO, inferior olivary complex	SF, solitary fasciculus
LCN, lateral cervical nucleus	SN, solitary nucleus
LRN, lateral reticular nucleus	Tr. V, spinal trigeminal tract
ML, medial lemniscus	X, dorsal motor nucleus of the vagus
MLF, medial longitudinal fasciculus	XII, hypoglossal nucleus

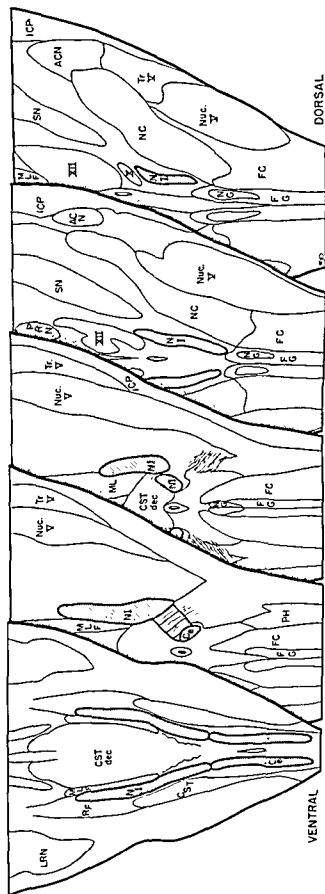


Fig 2 Rhesus C-972. Selected drawings from projected serial horizontal sections demonstrating the continuity and extent of the intermediate and central cervical nuclei. Abbreviations used here and in other figures are listed separately.

terminations were seen in all portions of the nucleus, but were most concentrated dorsomedially. In rhesus C-1024 degeneration in the supraspinal nucleus was more profuse than in other animals.

Two animals (C-1006 and C-1024) exhibited small, but definite, projections to certain other medullary nuclei. A few fibers from the ventrolateral part of the fasciculus cuneatus coursed through medial portions of the spinal trigeminal nucleus to terminate in ventrolateral parts of the magnocellular division of the nucleus. Degenerated fibers also were traced to the nucleus of Roller, the parvocellular reticular formation medial to the cuneate nucleus, the nucleus intercalatus and the peripheral ventral parts of the solitary nucleus. Degeneration seen in ventrolateral parts of the inferior vestibular nucleus and in cell group *x* in one animal (C-1024) appeared related to ascending degeneration in the posterior spinocerebellar tract.

Third cervical root. Since section of the third cervical dorsal root in two animals (C-912 and C-978) produced essentially the same pattern and amount of degeneration, a single description will be given. At the level of rhizotomy degeneration was similar to that described for the C2 dorsal root. Root fibers entered the most lateral part of the fasciculus cuneatus, traversed lamina II in small fascicles, and were distributed to cells throughout laminae III and IV (fig. 8). Fibers coursing through central parts of laminae V and VI projected profusely to the central cervical nucleus. From this region some fibers passed to the intermediomedial nucleus while other fibers projected into parts of laminae VII and VIII. Degeneration seen among cells of lamina IX was particularly prominent in the spinal accessory cell group (fig. 22), though not limited to this group.

At the C4 level degeneration descending in the lateral part of the fasciculus cuneatus terminated in lateral parts of laminae III and IV, while other fibers projected to the central cervical nucleus, as well as, the spinal accessory cell group of lamina IX. The amount of degeneration in these locations was less than at C3. No degeneration was detectable in the fasciculus cuneatus

at the C5 level (C-978), but sparse degeneration was seen in laminae III, IV and VII. Modest degeneration was seen in the intermediomedial nucleus and in what appeared to be the caudal part of the central cervical nucleus. No degeneration was seen in more caudal spinal segments.

At the second cervical segment spinal degeneration was similar to that described at C3. Degeneration in the central cervical nucleus was profuse while fibers passing to lamina IX surrounded primarily spinal accessory neurons. Ascending fibers in the fasciculus cuneatus formed a narrow band dorsomedial to the posterior horn. No sections of C1 were available for these animals.

Sections of the medulla were cut transversely (C-912) and horizontally (C-978). Degenerated fibers traversed and terminated in caudal portions of the cuneate nucleus. Fibers entering the lateral part of the cuneate nucleus in its middle third swept ventromedially in a gentle arc and terminated in a crescent-shaped area along the ventral and medial borders of the nucleus. Terminal degeneration was maximal ventrally. More moderate degeneration in the oral third of the nucleus was seen primarily in medial regions. The area of termination of C3 dorsal root fibers in the cuneate nucleus was slightly dorsal to that receiving C2 dorsal root fibers. Root fibers entered the caudal pole of the accessory cuneate nucleus and terminated in ventromedial portions of its caudal third. In ventral parts of the nucleus a bundle of degenerated fibers, coursing in the lateral half of the nucleus, projected to rostral parts of the nucleus, excluding the oral pole. Only modest degeneration was seen caudally in dorsolateral parts of the nucleus.

Collateral fibers from the fasciculus cuneatus projected ventromedially beyond the cuneate nucleus to the intermediate nucleus of the medulla. Although a considerable number of fibers surrounded elements of this long cell column, degeneration was less profuse and extensive than that associated with the C2 dorsal root. Degenerated fibers in the intermediate nucleus extended rostrally almost to the hypoglossal nucleus and caudally as far as the lower border of the corticospinal decus-

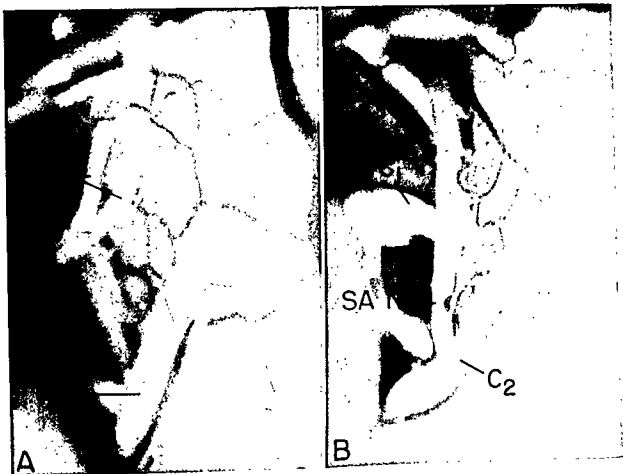


Fig. 3 Rhesus C-1008. Photographs of the first and second cervical dorsal roots taken through the operating microscope. In A, intact rootlets of the left first cervical root are seen. In B, the rootlets of the first cervical dorsal root have been sectioned. The spinal part of the spinal accessory nerve (SAN) can be seen coursing rostrally dorsal to the denticulate ligaments.

fibers appeared to merely traverse the nucleus, though scant terminations were sometimes observed dorsolaterally. In the middle third of the cuneate nucleus, terminal degeneration was chiefly in ventrolateral and ventromedial portions. Rostrally, terminations were localized primarily in the ventromedial part of the nucleus. Collateral fibers, traversing the cuneate nucleus in an oblique ventromedial direction, projected profusely to cells of the intermediate cell column (figs. 33, 34). Impressive pericellular arborizations were seen throughout this cell column (fig. 35). Degeneration about cells of this nucleus extended rostrally beyond the caudal poles of the hypoglossal and dorsal motor vagal nuclei; rostrally terminal degeneration was found about cells of the intermediate nucleus lateral to the dorsal motor nucleus of the vagus. Caudally degenerated fibers

were seen about cell groups of the nucleus lying among decussating corticospinal fibers; caudal to the corticospinal decussation virtually identical degeneration arborized about cells of the central cervical nucleus at the C1 level. Observations in these four animals demonstrated that collaterals from the C2 dorsal root project profusely to cells in all parts of the intermediate nucleus of the medulla and to the central cervical nucleus in the upper four cervical spinal segments. The amount and the extent of degeneration seen in these nuclei following C2 dorsal root section was more profuse than that associated with any other cervical dorsal root.

Fascicles of degeneration coursed from ventromedial portions of the cuneate nucleus and ventrolateral portions of the intermediate nucleus to enter the supraspinal nucleus throughout its length. Profuse

upraspinal nucleus. Terminations in the upraspinal nucleus were greatest dorsomedially.

Fifth cervical root. In four animals (C-179, C-914, C-974 and C-1014) the fifth cervical dorsal root was sectioned. Resulting degeneration was similar in these animals, but not identical. At the level of the rhizotomy most of the root fibers coursed medial to the posterior horn to enter the lateral part of the fasciculus cuneatus (figs. 4, 9). From the above location fascicles of root fibers traversed lamina II to arborize about cells in laminae III and IV. Degenerated fibers passed ventromedially through central parts of laminae V and VI and broke up into smaller fascicles in lamina VII. Some fibers appeared to terminate about cells in the central part of lamina VI. A small number of fibers in the medial part of lamina VII arborized about cells of the intermediomedial nucleus (fig. 9). In rhesus C-974 some cells in this part of lamina VII resembled those of the central cervical nucleus. A large number of fibers in central parts of lamina VII projected to ventral and lateral cell groups of lamina IX. Some of these fibers were distributed to the spinal accessory nucleus. A relatively small bundle of fibers entered the most medial part of lamina VII.

At the C6 level (fig. 4) degeneration was distributed similarly to that at C5, except in laminae III and IV where terminal degeneration was confined to a small ventrolateral region. Descending fibers in the fasciculus cuneatus moved medially away from the posterior horn to a position near the posterior intermediate septum. In diminishing quantities these fibers could be followed caudally in the fasciculus cuneatus to the T4 level (C-879, C-914 and C-1014), but only as far as T1 in rhesus C-974. In lower cervical segments degenerated fibers from the fasciculus cuneatus entered medial parts of lamina VI and central regions of lamina VII. In the upper four thoracic segments modest degeneration passed directly into the dorsal nucleus (fig. 4).

At the C4 level degenerated root fibers were distributed similar to that at C5 with two exceptions: (1) modest degeneration surrounded cells of the central cervical nucleus in all animals, and (2) virtually no degeneration was seen in laminae VIII or

IX in two animals (C-879 and C-914). In rostral cervical spinal segments much less degeneration was seen in cell groups of the posterior horn. Some fibers from the fasciculus cuneatus traversed medial parts of laminae V and VI to enter the central cervical nucleus, but the number of degenerated fibers in this nucleus was less than at the C4 level. At C3 and C2 spinal levels a moderate number of degenerated fibers were seen about cells of the spinal accessory nucleus. In all spinal segments rostral to the rhizotomy, fascicles of degenerated fibers streamed ventrally from the fasciculus cuneatus into lateral portions of medial lamina VI.

In the lower medulla ascending fibers from the C5 dorsal root formed a discrete band slightly lateral to the central part of the fasciculus cuneatus (fig. 11). Fibers given off from this bundle entered dorsolateral parts of the cuneate nucleus, swept ventromedially in a curved fashion, and formed a crescent-shaped area just ventral to the central region of the nucleus (figs. 4, 27). Degeneration in this position was seen throughout the cuneate nucleus, except for its oral pole. Fibers tended to be more ventrolateral in rostral areas. Throughout most of the nucleus a small group of fibers remained in the dorsolateral corner of the cuneate nucleus adjacent to the spinal trigeminal nucleus. In regions of the medulla caudal to the hypoglossal nucleus a moderate number of fibers passed ventromedially beyond the cuneate nucleus to enter the intermediate nucleus. Fibers arborizing about cells of this nucleus were most numerous in caudal regions. Some fibers projected beyond the intermediate nucleus to terminate about dorsomedial cells of the supraspinal nucleus.

A moderate number of degenerated fibers entered ventral parts of the accessory cuneate nucleus caudally, but larger numbers of fibers entered medial parts of the nucleus throughout most of its extent. These fibers arborized about cells in a wedge-shaped area just ventral to the central part of the nucleus (figs. 4, 27). In the rostral third of the nucleus a group of fibers from the main wedge-shaped area curved dorsally in a wing-like extension, slightly removed from the lateral border of the nucleus. Although terminal degeneration in this wedge-shaped pattern extended

sation. A small number of collateral fibers passed ventrally through and around cells of the intermediate nucleus to dorsomedial parts of the supraspinal nucleus.

Fourth cervical root. The fourth cervical dorsal root was sectioned in two animals (C-981 and C-1006). Only the spinal degeneration will be described in rhesus C-981 (since the medulla was not available for study) and only the medullary degeneration will be described in rhesus C-1006 (since the spinal cord exhibited some trauma).

Degeneration produced by this root section entered the lateral part of the fasciculus cuneatus and projected in small fascicles through lamina II to arborize about cells throughout laminae III and IV. Root fibers passing ventromedially through central portions of laminae V and VI projected: (1) profusely to cells of the central cervical nucleus, (2) to cells of the intermediomedial nucleus, and (3) to ventral cell groups in lamina IX. Ventromedial cell groups in lamina IX received most of these fibers, although a few fibers passed to cells of the spinal accessory cell group. At C5 descending branches of the C4 root were distributed in the same way as at C4, except that terminal degeneration in laminae III and IV was confined to lateral regions (fig. 14). Root fibers arborized about a discrete collection of large cells in the medial part of lamina VII that resembled the central cervical nucleus. At the C6 level descending degeneration in the fasciculus cuneatus was more medial while degeneration in the gray was present mainly in medial parts of lamina VII. In C7 and C8 spinal segments descending C4 dorsal root fibers were diminished and located medially near the posterior intermediate septum. A few fibers were present about large cells in the medial part of lamina VII at C8 and T1. No descending degeneration was evident in more caudal spinal segments.

In sections of the upper cervical cord ascending degeneration in the fasciculus cuneatus shifted dorsomedially. The distribution of C4 root fibers at C3 was similar to that described at the level of the dorsal rhizotomy, except that a larger number of degenerated fibers were present about cells of the spinal accessory nuclear group. Degeneration surrounding the central

cervical nucleus at these levels was impressive. At C2 degeneration was most extensive in laminae IV and VII, moderate in the central cervical nucleus, and scant in the anterior horn.

The medulla of C-1006 was studied in transverse sections. Caudally, degeneration was disposed in a lamina in the dorsal part of the lateral third of the fasciculus cuneatus. A few fibers coursed dorsolaterally for a short distance along the periphery of the fasciculus. Fibers from this bundle entered the lateral part of the cuneate nucleus and swept ventromedially forming a crescent-shaped area of degeneration in the dorsal part of the ventral third of the nucleus. Although a large number of these fibers merely traversed the nucleus, a locus of terminal degeneration was seen ventrolaterally. In middle portions of the cuneate nucleus degenerated fibers formed a discrete wedge-shaped area with the base lateral and the tapering apex curving ventromedially. This wedge-shaped area occupied the dorsal part of the ventral third of the nucleus. Rostrally, some fibers from the base of the wedge extended dorsolaterally for a short distance. Degeneration in the rostral pole of the nucleus was diminished compared with mid-cuneate levels.

A moderate amount of degeneration entered ventral portions of the accessory cuneate nucleus caudally, but a larger number of fibers entered medial parts of the nucleus throughout most of its extent. In middle portions of the nucleus these fibers arborized about cells in a wedge-shaped area (base directed laterally) in the dorsal part of its ventral third. Rostrally, fibers from the base of this wedge of degeneration moved medially, leaving a clear area laterally near the border of the accessory cuneate nucleus. This wedge-shaped configuration of degeneration gradually diminished rostrally but extended to the rostral pole of the nucleus.

In caudal parts of the medulla a moderate number of degenerated fibers coursed ventromedially beyond the cuneate nucleus to enter the intermediate nucleus. Terminations, gradually diminishing rostrally, were present in all, except the most rostral portions, of the intermediate nucleus. Some degenerated fibers traversed the intermediate nucleus, and fibers of the pyramidal decussation to terminate in the

raspinal nucleus. Terminations in the rapspinal nucleus were greatest dorsomedially.

Fifth cervical root. In four animals (C-9, C-914, C-974 and C-1014) the fifth cervical dorsal root was sectioned. Resulting degeneration was similar in these animals, but not identical. At the level of the rhizotomy most of the root fibers coursed medial to the posterior horn to enter the most lateral part of the fasciculus cuneatus (figs. 4, 9). From the above location fascicles of root fibers traversed lamina II and arborized about cells in laminae III and IV. Degenerated fibers passed ventromedially through central parts of laminae V and VI and broke up into smaller fascicles in lamina VII. Some fibers appeared to terminate about cells in the central part of lamina VI. A small number of fibers in the medial part of lamina VII arborized about cells of the *intermediomedial nucleus* (fig. 4). In rhesus C-974 some cells in this part of lamina VII resembled those of the central cervical nucleus. A large number of fibers in central parts of lamina VII projected to central and lateral cell groups of lamina X. Some of these fibers were distributed to the spinal accessory nucleus. A relatively small bundle of fibers entered the most medial part of lamina VIII.

At the C6 level (fig. 4) degeneration was distributed similarly to that at C5, except in laminae III and IV where terminal degeneration was confined to a small ventrolateral region. Descending fibers in the fasciculus cuneatus moved medially away from the posterior horn to a position near the posterior intermediate septum. In diminishing quantities these fibers could be followed caudally in the fasciculus cuneatus to the T4 level (C-879, C-914 and C-1014), but only as far as T1 in rhesus C-974. In lower cervical segments degenerated fibers from the fasciculus cuneatus entered medial parts of lamina VI and central regions of lamina VII. In the upper four thoracic segments modest degeneration passed directly into the dorsal nucleus (fig. 4).

At the C4 level degenerated root fibers were distributed similarly to that at C5 with two exceptions: (1) modest degeneration surrounded cells of the central cervical nucleus in all animals, and (2) virtually no degeneration was seen in laminae VIII or

IX in two animals (C-879 and C-914). In rostral cervical spinal segments much less degeneration was seen in cell groups of the posterior horn. Some fibers from the fasciculus cuneatus traversed medial parts of laminae V and VI to enter the central cervical nucleus, but the number of degenerated fibers in this nucleus was less than at the C4 level. At C3 and C2 spinal levels a moderate number of degenerated fibers were seen about cells of the spinal accessory nucleus. In all spinal segments rostral to the rhizotomy, fascicles of degenerated fibers streamed ventrally from the fasciculus cuneatus into lateral portions of medial lamina VI.

In the lower medulla ascending fibers from the C5 dorsal root formed a discrete band slightly lateral to the central part of the fasciculus cuneatus (fig. 11). Fibers given off from this bundle entered dorsolateral parts of the cuneate nucleus, swept ventromedially in a curved fashion, and formed a crescent-shaped area just ventral to the central region of the nucleus (figs. 4, 27). Degeneration in this position was seen throughout the cuneate nucleus, except for its oral pole. Fibers tended to be more ventrolateral in rostral areas. Throughout most of the nucleus a small group of fibers remained in the dorsolateral corner of the cuneate nucleus adjacent to the spinal trigeminal nucleus. In regions of the medulla caudal to the hypoglossal nucleus a moderate number of fibers passed ventromedially beyond the cuneate nucleus to enter the intermediate nucleus. Fibers arborizing about cells of this nucleus were most numerous in caudal regions. Some fibers projected beyond the intermediate nucleus to terminate about dorsomedial cells of the supraspinal nucleus.

A moderate number of degenerated fibers entered ventral parts of the accessory cuneate nucleus caudally, but larger numbers of fibers entered medial parts of the nucleus throughout most of its extent. These fibers arborized about cells in a wedge-shaped area just ventral to the central part of the nucleus (figs. 4, 27). In the rostral third of the nucleus a group of fibers from the main wedge-shaped area curved dorsally in a wing-like extension, slightly removed from the lateral border of the nucleus. Although terminal degeneration in this wedge-shaped pattern extended

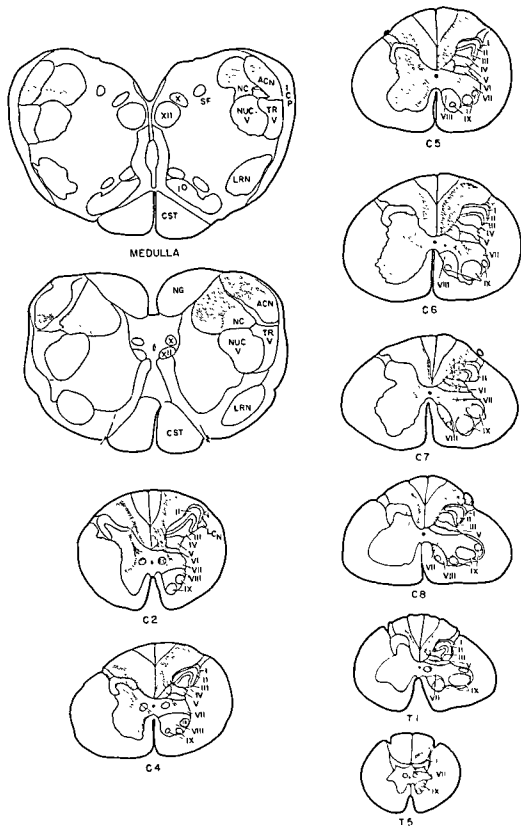


Fig. 4 Rhesus C-1014. Projected drawings showing the distribution of spinal and medullary degeneration resulting from section of dorsal roots C5 (left) and C8 (right). Roman numerals at spinal levels indicate laminae of Rexed.

Throughout most of the nucleus, only scant degeneration was seen in its oral pole. Dorsomedial regions of the nucleus were free of degeneration at all levels.

Sixth cervical root. The sixth cervical dorsal root was sectioned in two animals (C-967 and C-1012). At the level of the root section the majority of degenerated fibers projected medial to the posterior horn and entered the lateral part of the fasciculus cuneatus. From this site fibers passed in all fascicles into laminae III and IV. Centrally coursing fibers both traversed and arborized about cells in the medial parts of laminae V and VI. Fibers passing through these laminae entered lamina VII and projected almost exclusively to ventromedial cell groups of lamina IX. A small number of fibers projected to the intermediate nucleus and some of these fibers continued into the dorsomedial part of lamina VIII. Similar degeneration was seen in adjacent spinal segments (C7 and C8).

Descending degeneration, migrating into medial parts of the fasciculus cuneatus near the posterior intermediate septum at C8, continued caudally as far as T3. At C8 some degenerated fibers were seen in medial parts of laminae V, VI and VII. In the upper three thoracic segments degeneration was present in the dorsal nucleus and medial parts of lamina VII. Only questionable degeneration was seen in the dorsal nucleus at T4.

The number and distribution of ascending degenerated fibers in the spinal gray was more extensive in C-1012 than in C-967. Degeneration in the C4 and C3 segments of C-1012 was distributed similarly to that observed at the level of root section, but was less profuse. At C3 (C-967) and C2 (C-1012) levels a few fibers were scattered in parts of lamina VII and in parts of the ventral cervical nucleus. In all spinal segments rostral to the root section, fascicles of degenerated fibers streamed ventrally from the fasciculus cuneatus into lateral portions of medial lamina VI.

In medullary transverse sections degenerated fibers entering the dorsolateral part of the cuneate nucleus swept ventromedially in a crescent configuration (fig. 28). The most ventrolateral part of the nucleus and a large dorsomedial region was free of

degeneration. Fibers in the ventral part of the nucleus passed into a ventromedial area along the border of the nucleus. Thus degenerated fibers in the caudal half of the nucleus formed a half circle about a clear dorsomedial region of cuneate neurons. In rostral parts of the cuneate nucleus degenerated fibers appeared to end about cells in an oblique band extending from dorsolateral to ventromedial borders of the nucleus. Near the oral pole of the cuneate nucleus degeneration was seen only in ventromedial regions.

Posterior column fibers entered the accessory cuneate nucleus from its medial border and arborized about cells in a wedge-shaped area slightly ventral to the central part of the nucleus (fig. 28). These fibers occupied a larger area laterally but did not extend to the lateral margin of the nucleus. The position of these fibers was similar to that described for root fibers of C5 except that the wedge-shaped area was slightly more dorsal. In rostral parts of the nucleus the area of maximal degeneration was smaller and more dorsal. These findings suggested a partial overlap in the areas of termination of C5 and C6 dorsal root fibers in the accessory cuneate nucleus.

A few degenerated fibers from the C6 dorsal root projected to dorsomedial regions of the supraspinal nucleus (C-967) and caudal parts of the intermediate nucleus in both animals.

Seventh cervical root. The seventh cervical dorsal root was sectioned in rhesus C-915. At the level of rhizotomy root fibers projected medial to the posterior horn and entered the lateral part of the fasciculus cuneatus. Fascicles of degenerated fibers coursed through medial parts of lamina II to terminate about cells in all parts of laminae III and IV. Small fascicles of fibers from this region passed ventrally, both traversing and arborizing about cells in central portions of laminae V and VI. Fibers entering dorsocentral parts of lamina VII followed two principal projection routes to cells of the anterior horn. A small, distinct bundle of fibers passing ventromedially entered the intermediate nucleus and the area immediately ventral to it. Part of the fibers, bypassing these nuclei, projected into medial parts of

lamina VIII and reached the ventromedial cell group of lamina IX. A larger number of fibers in dorsocentral parts of lamina VII streamed ventrally through central parts of this lamina to enter lateral and ventrolateral cell groups of lamina IX. Most of these fibers appeared to end within the dendritic fields of large motor neurons. The pattern of distribution of root fibers in adjacent spinal segments (C8 and C6) was similar but degeneration was less profuse.

Descending degeneration in medial parts of the fasciculus cuneatus was followed caudally as far as T2; degeneration in this location probably continued beyond this level but was not detectable at T5. Most of these fibers terminated about cells in the dorsolateral part of the dorsal nucleus, though some fibers were scattered in adjacent parts of lamina VII.

Ascending degeneration in the fasciculus cuneatus occupied a broad band in the central part of the fasciculus. At the C3 level fibers projected from the fasciculus cuneatus into the lateral part of the medial lamina VI. A tiny amount of degeneration was seen about cells of the central cervical nucleus. Sections of more rostral cervical segments were not available for study.

Sections of the lower brain stem were cut horizontally. Fibers from the fasciculus cuneatus entered the dorsolateral surface of the cuneate nucleus in its caudal half. In successively more ventral sections these fibers occupied more medial areas and extended rostrally in the nucleus. Near central regions of the nucleus a large core area of terminal degeneration was oriented obliquely to the long axis of the nucleus (fig. 32). Degeneration in rostral regions extended nearly to the medial border of the nucleus, while caudally degeneration touched the lateral border of the nucleus. At these levels extreme rostral and caudal poles of the nucleus were free of degeneration, as were the most medial and lateral regions of the nucleus. In the ventral half of the nucleus the central core of terminal degeneration broke up into two linear bands partially connected by fascicles of degenerated fibers. One of these linear bands was along the medial margin of the rostral half of the nucleus and the other, extending the length of the nucleus, was slightly lateral to the central longitudinal axis of the nucleus. In the most ventral

regions of the cuneate nucleus terminal degeneration was present in both rostral and caudal poles of the nucleus.

Fibers from the fasciculus cuneatus directly entered the medial and caudal parts of the accessory cuneate nucleus where the majority of fibers terminated in a wedge-shaped central region (fig. 33). Centrally areas of terminal degeneration were found along the medial border of the nucleus. In the most ventral sections small number of fibers from the oral pole of the cuneate nucleus passed into the rostral regions of the accessory cuneate nucleus.

A very small number of degenerated fibers from the fasciculus cuneatus passed ventromedially beyond the cuneate nucleus to cells of the intermediate nucleus near the decussation of the corticospinal tract. These fibers were localized to the small region and did not arborize extensively about the individual cells. Rostral portions of the intermediate nucleus of the medulla were free of degeneration. No fibers from the C7 dorsal root were observed to enter the supraspinal nucleus.

Eighth cervical root. The eighth cervical dorsal root was sectioned in two animals (C-914 and C-1014).

At the level of the rhizotomy the bulk of degenerated root fibers arched medially to the posterior horn to enter the lateral part of the fasciculus cuneatus (fig. 4). From this location fibers traversed the substantia gelatinosa to enter laminae I and IV. Ventrally coursing degenerated fibers traversed central parts of laminae V and VI to enter lamina VII. Numerous small fascicles of degenerated fibers in lamina VII projected ventrolaterally to lateral cell groups of lamina IX. A distinct group of degenerated fibers passed into medial parts of lamina VII where they closely surrounded cells of the intermediomedial nucleus (fig. 17). Part of these medially coursing fibers descended ventrally in the medial part of lamina VIII to reach the ventromedial cell group of lamina IX. Fiber degeneration in the adjacent segments (fig. 23) was similar to that described for C8 except that degeneration in lamina IX was relatively modest and limited to the lateral cell group at T1.

Descending laterals of C8 dorsal root fibers, shifting into more medial parts of the fasciculus cuneatus at the T2 level

re followed caudally to the T6 level in C-4 and through the T8 level in C-1014. In the upper six (C-914) or nine (C-1014) thoracic segments fibers entering the spinal gray were distributed to dorsal parts of the dorsal nucleus (fig. 4). In the uppermost thoracic segments degeneration also was present in medial parts of lamina V, medial and central parts of lamina VI, and adjacent regions of lamina VII.

The number of degenerated ascending fibers from the C8 dorsal root was greater than that associated with any other cervical dorsal root and these fibers occupied a larger area in the fasciculus cuneatus (figs. 4, 11). In the C6 and C5 segments (C-1014) degeneration was distributed in a pattern similar to that observed at the level of root entry but fewer fibers were present, especially in lamina IX. At C4 and all more rostral cervical segments, degenerated fibers, entering the spinal gray from the fasciculus cuneatus, were limited virtually to medial lamina VI (fig. 21).

In transverse sections of the caudal cuneate nucleus degenerated fibers terminated in an oval or circular area in the dorsocentral region of the nucleus immediately ventral to the fasciculus cuneatus. Terminal degeneration in this region of the nucleus persisted throughout the caudal half of the nucleus with only a few fibers passing into the dorsomedial regions. In the middle third of the nucleus the main area of terminal degeneration shifted slightly ventrally, leaving dorsomedial, ventromedial and lateral areas free of terminal degeneration. Rostrally terminal degeneration occupied an oval area in the dorsomedial part of the nucleus (figs. 4, 29), but removed from the borders of the nucleus. Regions of terminal degeneration in the cuneate nucleus associated with the C8 dorsal root were more extensive than those seen with any other dorsal root.

Dorsal root fibers entering the accessory cuneate nucleus projected laterally from the fasciculus cuneatus. These fibers entered dorsomedial parts of the nucleus throughout most of its length and occupied approximately the dorsal third of the nucleus (figs. 4, 29), except rostrally and caudally where degeneration was diminished. Throughout levels of maximal degeneration in the middle third of the accessory cuneate nucleus degeneration

was always minimal or absent along the dorsolateral border of the nucleus (fig. 6). Near the oral pole of the nucleus terminal degeneration was found mainly in dorsocentral regions. No C8 root fibers projected to the intermediate or supraspinal nuclei.

Thoracic dorsal roots

Each of the upper seven thoracic dorsal roots was sectioned individually in different monkeys. The first, second and seventh thoracic dorsal roots were sectioned in two different animals.

First thoracic root. In two animals (C-912 and C-1025) the first thoracic dorsal root was sectioned. The distribution of degenerated fibers in these monkeys differed at certain levels, while the amount of degeneration differed at all levels, being much more profuse in rhesus C-1025. Attention will be directed to notable individual variations in the distribution. At the level of rhizotomy, degenerated fibers from the root entry zone mainly passed into the lateral part of the fasciculus cuneatus, from which location part of the fibers traversed medial portions of the substantia gelatinosa to enter the medial two-thirds of laminae III and IV. Fewer fibers coursed from the zone of Lissauer along the lateral border of the substantia gelatinosa to terminate in a small ventrolateral part of lamina III and to a lesser extent in lamina IV. Degenerated fibers traversed medial and central parts of lamina V to enter central portions of laminae VI and VII. Modest degeneration was seen about cells of the dorsal nucleus in rhesus C-912, but this nucleus was not apparent in our sections in rhesus C-1025. Degenerated fibers from this locus in central parts of laminae VI and VII followed two trajectories. A smaller number of fibers projected ventromedially to the intermediomedial nucleus. Some fibers traversing this nucleus streamed ventrally along the medial border of lamina VIII to enter the ventromedial cell group of lamina IX. Numerous fibers, forming the other trajectory, both terminated in, and coursed ventrally through, medial and central parts of lamina VII to terminate in portions of all lateral cell groups of lamina IX.

In the adjacent rostral segment (C8) the amount and distribution of degeneration was similar to that at T1, except that

degeneration was present throughout laminae III and IV and present in the ventrolateral part of lamina II in both animals. However, fewer fibers terminated in the medial third of laminae III and IV in rhesus C-1025. In the adjacent caudal segment (T2) the amount of degeneration in the spinal gray was decreased, especially in laminae VII and IX. The distribution of fibers was similar to that at T1, with the following exception: degeneration was localized sharply to the medial half of laminae III and IV, although a small island of degeneration persisted in ventrolateral parts of these laminae.

Descending degeneration in the lateral part of the fasciculus cuneatus shifted to more medial parts of the fasciculus at caudal levels; in diminishing numbers these fibers descended to the T9 level. Fibers given off from this bundle projected without localization to portions of the dorsal nucleus as far caudally as T9, and at some levels scattered degeneration also was seen in parts of lamina VII. In one animal (C-1025) diminished and scattered degeneration was present in laminae III, IV and medial and central parts of V through the T4 segment.

Ascending fibers from the T1 dorsal root shifted to medial parts of the fasciculus cuneatus adjacent to the posterior intermediate and posterior median septa. Some of the dorsal fibers extended laterally along the periphery of the fasciculus cuneatus for a short distance. This lamina of ascending T1 dorsal root fibers was extensive though narrower than that formed by fibers of the C8 dorsal root. No sections of the C7 through C5 segments were available for rhesus C-912. In the C7 and C6 segments in rhesus C-1025, degeneration terminating in the spinal gray was considerably decreased but distributed in a pattern similar to that described for the C8 segment. In the C5 segment degenerated fibers projected to: (1) the medial half of laminae III and IV, (2) medial parts of lamina V, (3) medial and central parts of lamina VI, and (4) dorsocentral parts of lamina VII. We were unable to explain this extensive distribution of T1 fibers in laminae III and IV at this level. At C4 and more rostral cervical segments, some fibers were given off from ventromedial parts of the fasciculus cuneatus to the medial subdivi-

sion of lamina VI, but these fibers were not as numerous as those associated with the C8 dorsal root.

In transverse medullary sections, degenerated fibers from the medial part of the fasciculus cuneatus entered dorsomedial parts of the cuneate nucleus caudally. At caudal levels terminal degeneration was seen in a crescent-shaped area in the dorsomedial part of the cuneate nucleus partially surrounding a large circular cell mass. Some of the degenerated fibers extended into ventromedial parts of the nucleus, leaving the dorsal and medial borders of the nucleus free of degeneration. In central parts of the nucleus (fig. 5) terminal degeneration was seen in an inverted "U" shaped formation in the dorsomedial part of the nucleus. The open part of the "U" was directed ventrolaterally and a clear zone separated the degeneration from the borders of the nucleus, except dorsolaterally where fibers were entering from the fasciculus cuneatus. A small number of fibers from the medial arm of the "U" projected dorsolaterally to virtually encircle the central cell mass. The latter fibers were especially prominent in rhesus C-1025. The above pattern persisted throughout most of the nucleus but near the oral pole terminal degeneration was concentrated in a smaller dorsomedial region slightly removed from the borders of the nucleus.

Fibers entering the accessory cuneate nucleus arched laterally into dorsomedial parts of the nucleus. While terminal degeneration was greatest dorsomedially, it also was seen about some cells in lateral parts of the nucleus rostrally. The distribution of terminal degeneration was comma-shaped with the tail directed laterally and ventrally (fig. 6). The most dorsal margin of the nucleus was free of degenerated fibers as was most of the ventral two-thirds of the nucleus. In extreme rostral parts of the nucleus reduced amounts of degeneration were seen in dorsocentral regions in C-912 and in dorsal and lateral regions in C-1025. Although these fibers were distributed in a pattern similar to that of the C8 dorsal root they were less numerous and extended further ventrally in lateral parts of the nucleus. No T1 dorsal root fibers projected to other medullary relay nuclei.

Second thoracic root. The second thoracic dorsal root was sectioned in two animals (C-913 and C-1008). In sections of the T2 segment degeneration was present in the lateral part of the fasciculus cuneatus; part of these fibers traversed, or curved around the medial border of, the substantia gelatinosa to enter laminae III and IV (fig. 10). A smaller number of fibers from the lateral part of the zone of Lissauer coursed through lateral parts of the posterior horn to terminate in a small island of cells in the ventrolateral parts of laminae III and IV (fig. 15). Degenerated fibers destined for the ventromedial cell group of lamina IX followed two main routes: some ventrally coursing fibers traversed central parts of laminae V, VI, VII and VIII, while a greater number of fibers passed through the dorsal nucleus and coursed ventrally along the medial border of lamina VIII. In the dorsal nucleus degeneration was profuse, but not all cells were surrounded by root fibers. A modicum of degeneration was present in the intermediomedial nucleus.

Degeneration in sections of the T1 spinal segment was distributed similar to that of the T2 segment, except that degeneration in the dorsal nucleus (C-913; fig. 16) and lamina IX (C-1008) was more profuse. Similarly distributed, but more modest degeneration, at T3 was seen in laminae III and IV (C-1008) and in laminae VII, VIII and IX. The extent of the descending degeneration from the T2 dorsal root could not be accurately determined in rhesus C-913. In rhesus C-1008 descending degeneration from the T2 dorsal root was present in the lateral part of the fasciculus cuneatus through T6. The dorsal nucleus, and all laminae which received degeneration at the level of root section, except lamina IX, exhibited some degeneration at T4 and T5 levels; the amount of degeneration was reduced at these levels. At the T6 level, degeneration was limited to dorsal portions of the dorsal nucleus.

Fibers from the T2 dorsal root ascended in the dorsomedial portion of the fasciculus cuneatus. The extent and distribution of T2 dorsal root degeneration in the spinal gray of the lower cervical cord could not be determined in rhesus C-1008 because of trauma to the lateral funiculus. At C8 in rhesus C-913 scant degeneration was

present in lateral portions of laminae III and IV and in medial and central portions of laminae V, VI and VII. No sections of the C7 through C5 spinal segments were available; degeneration at C4 and in more rostral cervical segments was confined to the fasciculus cuneatus.

Sections of the lower brain stem were cut horizontally (C-913) and transversely (C-1008). Observations in these two animals were similar in that relatively modest degeneration was found mainly in dorso-medial parts of the cuneate nucleus. In rhesus C-913 the bulk of this degeneration was in the caudal two-thirds of the nucleus, while in rhesus C-1008 degeneration in this location was found predominantly in the rostral two-thirds of the nucleus. In both animals degenerated fibers extended ventrally along the medial border of the cuneate nucleus, and a few fibers arched laterally along the dorsal border of the nucleus. Degenerated fibers in the accessory cuneate nucleus were distributed along the lateral border of the nucleus (fig. 30). Rostrally degeneration was most abundant dorsally; smaller amounts of degeneration coursed ventrally along the lateral border of the nucleus.

Third thoracic root. After section of the T3 dorsal root in rhesus C-967 the majority of degenerated fibers at this level passed into lateral parts of the fasciculus cuneatus. Degeneration entered the spinal gray by traversing the substantia gelatinosa and by curving along its medial border. Degeneration was seen in laminae III and IV, central portions of lamina V, and in the dorsal and intermediomedial nuclei. Degeneration in the dorsal nucleus was scattered. From the area of the dorsal nucleus degenerated fibers coursed ventrally in medial portions of laminae VII and VIII to the ventromedial cell groups in lamina IX. Many of these medial fibers curved along the border of the anterior horn to supply cells in medial, central and lateral portions of lamina IX. Degeneration in adjacent thoracic segments, T2 and T4, was essentially the same as at the T3 level though less abundant.

Descending degeneration consisted of a small bundle of fibers in lateral parts of the fasciculus cuneatus that could be traced as far as T5; degeneration in the dorsal

degeneration was present throughout laminae III and IV and present in the ventrolateral part of lamina II in both animals. However, fewer fibers terminated in the medial third of laminae III and IV in rhesus C-1025. In the adjacent caudal segment (T2) the amount of degeneration in the spinal gray was decreased, especially in laminae VII and IX. The distribution of fibers was similar to that at T1, with the following exception: degeneration was localized sharply to the medial half of laminae III and IV, although a small island of degeneration persisted in ventrolateral parts of these laminae.

Descending degeneration in the lateral part of the fasciculus cuneatus shifted to more medial parts of the fasciculus at caudal levels; in diminishing numbers these fibers descended to the T9 level. Fibers given off from this bundle projected without localization to portions of the dorsal nucleus as far caudally as T9, and at some levels scattered degeneration also was seen in parts of lamina VII. In one animal (C-1025) diminished and scattered degeneration was present in laminae III, IV and medial and central parts of V through the T4 segment.

Ascending fibers from the T1 dorsal root shifted to medial parts of the fasciculus cuneatus adjacent to the posterior intermediate and posterior median septa. Some of the dorsal fibers extended laterally along the periphery of the fasciculus cuneatus for a short distance. This lamina of ascending T1 dorsal root fibers was extensive though narrower than that formed by fibers of the C8 dorsal root. No sections of the C7 through C5 segments were available for rhesus C-912. In the C7 and C6 segments in rhesus C-1025, degeneration terminating in the spinal gray was considerably decreased but distributed in a pattern similar to that described for the C8 segment. In the C5 segment degenerated fibers projected to: (1) the medial half of laminae III and IV, (2) medial parts of lamina V, (3) medial and central parts of lamina VI, and (4) dorsocentral parts of lamina VII. We were unable to explain this extensive distribution of T1 fibers in laminae III and IV at this level. At C4 and more rostral cervical segments, some fibers were given off from ventromedial parts of the fasciculus cuneatus to the medial subdivi-

sion of lamina VI, but these fibers were not as numerous as those associated with the C8 dorsal root.

In transverse medullary sections, degenerated fibers from the medial part of the fasciculus cuneatus entered dorsomedial parts of the cuneate nucleus caudally. At caudal levels terminal degeneration was seen in a crescent-shaped area in the dorsomedial part of the cuneate nucleus, partially surrounding a large circular cell mass. Some of the degenerated fibers extended into ventromedial parts of the nucleus, leaving the dorsal and medial borders of the nucleus free of degeneration. In central parts of the nucleus (fig. 5) terminal degeneration was seen in an inverted "U" shaped formation in the dorsomedial part of the nucleus. The open part of the "U" was directed ventrolaterally and a clear zone separated the degeneration from the borders of the nucleus, except dorsolaterally where fibers were entering from the fasciculus cuneatus. A small number of fibers from the medial arm of the "U" projected dorsolaterally to virtually encircle the central cell mass. The latter fibers were especially prominent in rhesus C-1025. The above pattern persisted throughout most of the nucleus but near the oral pole terminal degeneration was concentrated in a smaller dorsomedial region slightly removed from the borders of the nucleus.

Fibers entering the accessory cuneate nucleus arched laterally into dorsomedial parts of the nucleus. While terminal degeneration was greatest dorsomedially, it also was seen about some cells in lateral parts of the nucleus rostrally. The distribution of terminal degeneration was comma-shaped with the tail directed laterally and ventrally (fig. 6). The most dorsal margin of the nucleus was free of degenerated fibers, as was most of the ventral two-thirds of the nucleus. In extreme rostral parts of the nucleus reduced amounts of degeneration were seen in dorsocentral regions in C-912 and in dorsal and lateral regions in C-1025. Although these fibers were distributed in a pattern similar to that of the C8 dorsal root, they were less numerous and extended further ventrally in lateral parts of the nucleus. No T1 dorsal root fibers projected to other medullary relay nuclei.

Descending degeneration exhibited a stable attenuation between the T6 and T7 segments but was traced through the T11 segment. This degeneration consisted of a narrow, progressively diminishing, lamina of fibers in the lateral part of the fasciculus cuneatus, and a modicum of fibers in the dorsal nucleus. Degeneration in caudal portions of the dorsal nucleus was scant.

Ascending degeneration in the fasciculus cuneatus moved progressively dorsomedially in upper thoracic segments. At T1 and C8 levels, these fibers occupied portions of the fasciculus cuneatus adjacent to the posterior intermediate and posterior median septa. Some of the most dorsal fibers extended laterally along the periphery of the fasciculus cuneatus. In the C7 and all more rostral cervical segments, ascending degeneration in the fasciculus cuneatus formed a discrete, narrow lamina along the entire length of the posterior intermediate septum and extended laterally for a short distance along the dorsal border of the fasciculus. In the T3 segment, scant degeneration was present in laminae III and IV, and medial parts of laminae VII and VIII. The dorsal nucleus exhibited degeneration through the T2 segment.

In transverse sections of the medulla degenerated fibers formed a very narrow, discrete lamina along the entire medial part of the fasciculus cuneatus. Some fibers coursed ventrolaterally along the periphery of the fasciculus. Caudally, a few fibers terminated in medial parts of the cuneate nucleus. At mid-cuneate levels, degeneration extended along the entire medial portion of the nucleus. Degeneration filled the apex of the nucleus dorsally but was slightly removed from the medial border of the nucleus. Ventrally a few fibers appeared to terminate within the dorsolateral border of the nucleus gracilis. In its rostral third, degeneration terminated along the medial border of the cuneate nucleus with the greatest concentration of fibers dorsomedial. No degeneration was apparent in the rostral pole of the cuneate nucleus.

In caudal portions of the accessory cuneate nucleus, degeneration terminated dorsolaterally. Proceeding rostrally, some fibers from this dorsolateral area extended ventrally so that two areas of termination

could be distinguished in middle portions of the nucleus: (1) a larger dorsolateral area, and (2) a smaller ventrolateral area. Rostrally, degeneration was limited to a small ventrolateral area in the accessory cuneate nucleus.

Sixth thoracic root. Section of the sixth thoracic dorsal root in rhesus C-1017 produced degeneration in the lateral part of the fasciculus cuneatus adjacent to the posterior horn, and in the zone of Lissauer. Fascicles of degenerated fibers from the fasciculus cuneatus entered the spinal gray by coursing through, or curving around, medial portions of the substantia gelatinosa. Fibers terminated throughout laminae III and IV, but were most concentrated medially. Other fascicles of degeneration traversed medial parts of laminae III and IV and central parts of lamina V to enter the dorsal nucleus. Profuse pericellular arborizations were observed throughout the dorsal nucleus, but were most abundant medially. Some fibers merely traversing the dorsal nucleus or adjacent portions of lamina VII, were distributed in three main directions. Numerous fibers emerged from the ventromedial border of the dorsal nucleus and after traversing and terminating in the intermediomedial nucleus and adjacent parts of lamina VII, coursed ventrally along the medial borders of laminae VII and VIII to enter lamina IX. Some of these fibers following the curvature of the anterior horn were distributed throughout the ventromedial cell group and to portions of the lateromedial cell group. Other fibers issuing from the dorsal nucleus coursed ventrolaterally to terminate along the lateral border of lamina VIII; a few of these fibers reached the lateromedial cell group of lamina IX. Few fibers passed ventrally through central portions of laminae VII and VIII.

In the T7 segment degenerated fibers were markedly decreased in number, but their distribution in the spinal gray was similar to that at T6, except that degeneration in the dorsal nucleus was primarily dorsolateral. Descending degeneration in the lateral part of the posterior funiculus formed a narrow, progressively diminishing, lamina which extended caudally through the T12 segment. These fibers primarily projected to dorsolateral parts of the dorsal nucleus through the L2 level.

nucleus was modest at T5 and minute at T7.

Ascending degeneration shifted to dorso-medial parts of the fasciculus cuneatus near the posterior intermediate septum. Spinal terminations observed rostral to the T2 segment were not reliable due to cord trauma.

In transverse sections of the caudal medulla degenerated fibers entered dorso-medial parts of the cuneate nucleus; at mid-cuneate levels, this dorsomedial degeneration was greater and some fibers coursed toward ventromedial regions of the nucleus. Degeneration in the cuneate nucleus was most abundant in dorsal regions rostrally. A small contingent of degenerated fibers passed along the lateral border of the cuneate nucleus throughout its rostrocaudal extent and terminated in a small ventrolateral area. Fibers from the fasciculus cuneatus entered dorsolateral parts of the accessory cuneate nucleus where they terminated in a crescent-shaped area. No degeneration was observed in other medullary nuclei.

Fourth thoracic root. In rhesus C-970 the fourth thoracic dorsal root was sectioned. At the level of the root section the distribution and amount of degeneration in the fasciculus cuneatus, the posterior horn and the anterior horn (fig. 24) was similar to that described after section of the T3 dorsal root. Degeneration in the T3 segment was like that at T4, but much more modest degeneration was seen in the T5 segment. Caudal to T5 degenerated dorsal root fibers were present in the posterior funiculus and dorsal nucleus through the T9 segment. The amount of degeneration in the dorsal nucleus was small and never distributed throughout the nucleus.

Fibers from the T4 dorsal root ascended in the dorsomedial part of the fasciculus cuneatus near the posterior intermediate septum. At T2 diminished degeneration was present primarily in the dorsal nucleus and adjacent parts of lamina VII. Degeneration at C8 was confined to the fasciculus cuneatus.

In horizontal sections of the medulla ascending fibers entering the dorsomedial aspect of the cuneate nucleus extended nearly the entire length of the nucleus; terminations were most numerous in the caudal two-thirds of the nucleus. More

ventral portions of the cuneate nucleus contained small amounts of degeneration in medial and caudal regions. Small patches of degeneration occupied lateral portions of the cuneate nucleus, especially in its middle third.

Dorsal root fibers primarily reached the accessory cuneate nucleus by passing rostral to the cuneate nucleus. Terminal degeneration was localized to a small lateral area of the nucleus. No degeneration was present in other medullary nuclei.

Fifth thoracic root. Section of the fifth thoracic dorsal root in rhesus C-1024 produced degeneration in the root entry zone, the lateral part of the fasciculus cuneatus and lateral portions of the zone of Lissauer. Degenerated fibers from the fasciculus cuneatus entered the spinal gray in large fascicles by coursing through, or curving around, the ventromedial portion of lamina II. A small number of fine fibers passed from the zone of Lissauer through dorsal parts of lamina II into laminae III and IV. Terminations were noted throughout laminae III and IV, but were scant ventrolaterally. Degenerated fibers traversed the central part of lamina V to reach the intermediomedial and dorsal nuclei (fig. 18), where profuse pericellular arborizations were observed. Other fibers passing through the dorsal nucleus were distributed in three trajectories. Numerous fibers, emerging from the ventral surface of the dorsal nucleus, coursed ventrally along the medial borders of laminae VII and VIII and entered lamina IX. Some of these fibers following the curvature of the anterior horn were distributed to all portions of the ventromedial cell group. A scant number of fibers coursed through central parts of laminae VII and VIII to reach the lateromedial cell group of lamina IX. Finally, a few fibers passed from the lateral part of the dorsal nucleus ventrally along the lateral border of the anterior horn.

The distribution and amount of degeneration in the T4 spinal segment was similar to that in the T5 segment, except that fewer fibers were seen in medial parts of laminae VII and VIII, and in lamina IX. Degeneration in the adjacent caudal segment (T6) was similar to that described for the segment of root section, but the number of degenerated fibers was reduced.

number of cell groups within the medial border of the nucleus cuneatus and within the lateral border of the nucleus gracilis. The bulk of degeneration in the posterior column nuclei was seen dorsally in a junctional zone between the caudal two-thirds of the nucleus cuneatus and the middle third of the nucleus gracilis. Dorsally, degenerated fibers projected from the common border between the nuclei gracilis and cuneatus into the lateral parts of the accessory cuneate nucleus.

DISCUSSION

This study provides data for the rhesus monkey concerning the distribution and termination of cervical and upper thoracic dorsal root fibers within the spinal cord and certain medullary nuclei. Observations consider the distribution of dorsal root fibers within the spinal gray, ascending and descending dorsal root projections in the posterior funiculus, and projections of dorsal root fibers to the cuneate, the accessory cuneate, the intermediate and the supraspinal nuclei of the medulla. Comparisons of these observations with similar data for the lower thoracic, lumbosacral and coccygeal dorsal roots are made in Part II of this study (Carpenter, Stein and Shriver, '68).

Spinal projections

Fiber projections to the spinal gray. The local distribution of degenerated fibers from all cervical and the upper seven thoracic dorsal roots in the monkey appears similar to that described in the cat following section of selected individual dorsal roots (Sprague and Ha, '64; Sterling and Kuypers, '67). At the level of rhizotomy degenerated fibers occupy the root entry zone and the most lateral part of the posterior funiculus. From this site dorsal root fibers enter the posterior horn by traversing the medial portions of, or by coursing medially around, laminae II through IV. While numerous degenerated fibers terminate in laminae III and IV, relatively few appear to end in lamina II (Anderson, '60; Ralston, '65; Sterling and Kuypers, '67). Other authors (Szentágothai, '64; Sprague and Ha, '64) described dorsal root fibers that project to lamina IV and then recurve dorsolaterally to enter in

radial fashion the entire depth of laminae II and III. Many degenerated fibers traverse lamina IV to course ventrally into laminae V and VI, where they terminate, especially in central and medial regions. A paucity of degeneration in lateral portions of laminae V and VI is notable both in the cat and monkey. From central portions of lamina VI, degenerated fibers stream ventrally through portions of laminae VII and VIII to reach cell groups in lamina IX. A smaller number of fibers consistently project ventromedially to terminate in a nuclear group that seems to correspond to the intermediomedial nucleus of Rexed ('52, '54).

The density of degenerated dorsal root fibers in the spinal cord is greatest at the level of the cut root (fig. 4), an observation in accord with virtually all authors. With certain exceptions, degeneration in spinal segments above and below the rhizotomy is distributed similarly in the spinal gray, but in reduced amounts.

The distribution of dorsal root afferents to the spinal gray at the level of the rhizotomy and in adjacent spinal segments can be discussed systematically with respect to the laminae of Rexed. While a moderate number of dorsal root afferents project to lamina I, especially its medial part, projections to other laminae are more impressive.

Laminae II through IV. As mentioned previously recent observations concerning dorsal root projections to lamina II are not consistent. The extent to which this may be due to differences in terminology is difficult to resolve, but based on the criteria of Rexed ('52, '54, '64), very few dorsal root fibers appear to terminate in this lamina (Anderson, '60; Ralston, '65; Sterling and Kuypers, '67). There is almost universal agreement that dorsal root fibers project profusely to laminae III and IV (i.e., nucleus proprius).

Several investigators have reported a localization of dorsal root terminations within different parts of the laminae of the posterior horn. Szentágothai and Kiss ('49) and Szentágothai ('64) reported that collaterals of large caliber dorsal root afferents exhibit a marked somatotopic projection of dorsal cutaneous regions upon the lateral, and of ventral cutaneous regions upon the

Degeneration one and two segments above the root section was slightly decreased and considerably decreased, respectively, but distributed similar to that in the T6 segment. In the dorsal nucleus, progressively diminishing amounts of degeneration were distributed, without precise localization, through the T2 level. The disposition of the narrow, discrete lamina of ascending degenerated fibers in the fasciculus cuneatus was very similar to that described for the T5 dorsal root.

In transverse sections of the caudal medulla, the majority of degenerated fibers formed a narrow lamina along the medial border of the fasciculus cuneatus; a few fibers extended along the lateral border of the fasciculus gracilis. Caudally, scant degeneration was present in the medial border of the cuneate nucleus and in the ventrolateral border of the nucleus gracilis. At mid-cuneate levels, terminal degeneration was maximal in the medial border of the dorsal two-thirds of the cuneate nucleus; some fibers terminated in adjacent lateral portions of the nucleus gracilis. Fewer fibers extended into ventral parts of these nuclei. Rostrally, degeneration in the medial border of the cuneate nucleus was most abundant dorsally. No degenerated fibers were apparent in the rostral pole of the cuneate nucleus. Throughout the extent of the accessory cuneate nucleus, a modicum of degeneration terminated in a small cluster of neurons in its lateral border. This area of degeneration was dorsal in caudal parts of the nucleus, but shifted ventrally farther rostrally.

Seventh thoracic root. The seventh thoracic dorsal root was sectioned in two monkeys (C-915 and C-1025). At the level of root section degenerated fibers were located in the lateral part of the posterior funiculus and portions of the zone of Lissauer (fig. 12). Degenerated fibers entered the spinal gray by traversing medial portions of lamina II and terminated primarily in medial and central portions of laminae III and IV; sparse degeneration was seen ventrolaterally in these laminae. Degenerated fibers traversed the central part of lamina V to enter the dorsal nucleus where degeneration was noted throughout. Some fibers merely traversed the dorsal nucleus

and coursed in three main directions. Numerous fibers emerged from the ventromedial border of the dorsal nucleus and, after sending a small projection to the intermediomedial nucleus, coursed ventrally along the medial borders of laminae VII and VIII to enter lamina IX. These fibers followed the curvature of the anterior horn and were distributed to the ventromedial cell group. Fewer fibers issuing from the ventrolateral surface of the dorsal nucleus coursed: (1) ventrally through central portions of laminae VII and VIII to reach the lateromedial cell group of lamina IX, or (2) ventrolaterally to terminate along the lateral border of lamina VIII.

In the T8 segment degeneration was considerably decreased, but fibers were distributed in laminae III, IV and V as at T7. Degeneration in the dorsal nucleus was concentrated in dorsal regions. At this level fibers coursed through central parts of laminae VII and VIII, but few reached cell groups of lamina IX. Degenerated descending fibers in the lateral part of the posterior funiculus passed primarily to the dorsal nucleus at levels as far caudally as L1. These fibers were distributed mainly to ventral and lateral portions of the nucleus.

In the segment above the root section (i.e., T6) degeneration was reduced but distributed similar to that in the T7 segment. In segments T5 to T2 ascending fibers were distributed to the dorsal nucleus without precise localization.

Ascending degeneration in the fasciculus cuneatus moved progressively dorso-medially in upper thoracic segments, forming a narrow lamina adjacent to the posterior intermediate and posterior medial septa. Dorsolaterally some fibers extended along the margin of the fasciculus cuneatus for a short distance. In C7 and all more rostral cervical segments, degenerated fibers formed a narrow, discrete lamina along the entire length of the posterior intermediate septum. Some fibers were located in the most medial portion of the fasciculus cuneatus while others were in the most lateral part of the fasciculus gracilis.

In horizontal (C-915) and transverse (C-1025) sections of the medulla ascending T7 dorsal root fibers supplied a modes

Studies of Escobar ('48) in the cat indicated that the C1 dorsal root projects no fibers to the substantia gelatinosa at that level. Fibers from C2 and C3 dorsal roots were reported to enter the substantia gelatinosa via Lissauer's tract in these segments. Torvik ('56) found that the C2 and C3 dorsal roots projected fibers into the substantia gelatinosa and the nucleus proprius at these levels, but none entered the posterior horn at C1. On the other hand, descending trigeminal fibers projected into the posterior horn at C1 while a few fibers, localized to dorsomedial parts of the posterior horn, were found at C2 levels. More recent studies in the cat (Kerr, '61) indicated that trigeminal fibers form a major afferent component of the posterior horn at C1 and fibers from the first three cervical dorsal roots also end there. Trigeminal fibers were dorsomedial while dorsal root fibers were found ventrolateral.

Although the C1 dorsal root is frequently absent in the monkey (Sherrington, 1898; Howell and Straus, '33; Corbin, Lhamon and Petit, '37; Thomas and Combs, '65), no fibers from this root were seen to enter the head of the posterior horn in the present study. Fibers from the C2 dorsal root terminated primarily in lateral portions of laminae III and IV, while C3 fibers terminated in all parts of these laminae at the C2 level. In two animals a small number of C2 root fibers were seen in ventrolateral (C-1006) or lateral (C-1024) parts of laminae III and IV at the C1 level. In horizontal sections of the C1 segment in two other animals with C2 dorsal rhizotomies only scant degeneration was seen in the head of the posterior horn. These observations suggest that very few dorsal root fibers from the upper cervical segments enter the posterior horn at C1.

Lamina V and VI. The pattern of dorsal root degeneration in the neck (lamina V) and base (lamina VI) of the posterior horn as observed in the cat (Sprague and Ha, '64; Sterling and Kuypers, '67) is strikingly similar to that noted in the monkey. Fascicles of degenerated dorsal root fibers course ventrally through lamina IV into laminae V and VI where they form a large terminal field, primarily in central and medial regions. In all segments, lateral parts of laminae V and VI are nearly free of terminal degeneration.

According to Sterling and Kuypers ('67), dorsal root fibers terminate profusely in laminae V and VI, but, unlike those in laminae III and IV, they do not terminate somatotopically. Observations in the present study indicate that fibers from C5 to T1 dorsal roots terminate in central and medial portions of lamina VI throughout the entire cervical spinal cord. Fibers from the more caudal of these roots project predominantly to more medial areas, while those from the more rostral roots project to more lateral areas. Fibers from C8 dorsal root are the most numerous and fill nearly the entire medial part of lamina VI at all cervical levels (figs. 4, 21). The cells in the medial part of lamina VI at high cervical levels seem to merge almost imperceptibly with cells in the caudal part of the cuneate nucleus. This finding, not noted by previous authors, suggests a unique relationship between dorsal root fibers of the brachial enlargement and cells of the medial part of lamina VI.

Laminae VII and VIII. Degenerated upper cervical dorsal root fibers course ventrally through medial and central portions of laminae VII and VIII to reach motor neurons of lamina IX. The number of terminal ramifications in laminae VII and VIII appeared to be considerably less than in the posterior horn. The pattern of distribution of dorsal root degeneration in laminae VII and VIII in the enlargement confirms the findings of Sprague and Ha ('64) and Sterling and Kuypers ('67). The C5 to T1 dorsal root projections to lamina VIII in segments through the brachial enlargement, where this lamina is restricted to the medial portion of the anterior horn, are chiefly to its dorsal part. Few fibers coursing ventrally in the medial part of lamina VIII reach the medial cell groups of lamina IX. At these levels a larger number of fibers coursing ventrally through medial and central portions of lamina VII reach the more laterally situated cell groups of lamina IX. The majority of degenerated T2 to T7 dorsal root fibers coursed ventrally along the medial borders of laminae VII and VIII to enter lamina IX (fig. 24). Few of these fibers coursed ventrally in central portions or along the lateral borders of these laminae to enter lamina IX.

Four nuclei can be distinguished within lamina VII at certain spinal levels: (1) the

medial halves of laminae II and III. After single rhizotomies of selected lumbosacral dorsal roots, Sprague and Ha ('64) noted the "synaptic compartments of arborization" described by the above authors, as well as a similar compartmentalization of the plexus in lamina IV, not previously described. Comparisons of the distribution of degenerated root fibers at the level of section with segments above and below revealed different parts of laminae II, III and IV to be free of degeneration. In spite of some variation in the terminal fields associated with different lumbosacral roots, in all cases ascending and descending dorsal root fibers showed a marked tendency to send collaterals into medial, or more frequently, lateral parts of laminae II, III and IV of segments adjacent to the cut root. Sterling and Kuypers ('67) reported a somatotopically organized distribution of C5 to T1 dorsal root fibers in laminae III and IV of the brachial enlargement in the cat. They found that caudal roots, supplying primarily distal and postaxial portions of the limb (Hekmatpanah, '61), terminated medially, and more rostral roots, supplying primarily proximal and preaxial portions of the limb, terminated laterally. These observations regarding a somatotopic organization within laminae of the posterior horn are supported by physiological data. Micro-electrode studies of the lumbosacral enlargement in the cat (Wall, '60) suggest that medial portions of the laminae are related to peripheral parts of the leg and lateral portions are related to more proximal parts. Portions of the posterior horn ventral to the substantia gelatinosa could be divided into a dorsal lamina containing cells responding to light touch and a ventral lamina of cells monopolized by proprioceptive afferents.

According to certain authors (Szentágothai and Kiss, '49; Szentágothai, '64; Sprague and Ha, '64), arborizations of collaterals of dorsal root fibers divide laminae II, III and IV into a series of radially oriented "synaptic compartments" or "lobuli." On the basis of studies of brachial spinal cord segments in all three planes with a variety of staining methods, Sterling and Kuypers ('67) have concluded that: (1) the dendritic orientation in laminae I-III is predominantly longitudinal, while

that in lamina IV is radial, (2) some dorsal root fibers from Lissauer's tract pass radially into laminae I-III, or recurve from below into laminae III-IV, and (3) the majority of dorsal root afferents to laminae I, III and IV course longitudinally in these laminae after separating from the bundles penetrating the posterior horn. These authors suggested that the posterior horn of the brachial spinal cord consists of longitudinal "slabs" of cells extending throughout this portion of the cord in which progressively more medial portions of the laminae are related to progressively more distal and postaxial portions of the limb.

In the present study dorsal root fibers from C2 to C4 terminated in parts of laminae III and IV one segment above and below the rhizotomy. The dispersion of dorsal root fibers to parts of these laminae was greater for lower cervical dorsal roots (i.e., C5 to C8) in that it extended two or three segments above and below the rhizotomy. Dorsal root fibers from C2 were consistently localized in their terminations to the lateral parts of laminae III and IV at the root entry level and in the adjacent rostral and caudal segments (fig. 13). In other upper cervical segments (i.e., C3, C4 and C5) dorsal root fibers in the segment below their entrance occupied lateral portions of these laminae (fig. 14), but in immediately rostral segments fibers usually were distributed throughout. In all remaining cervical and thoracic segments, dorsal root fibers at their level of entrance and in adjacent segments were distributed to all parts of laminae III and IV, though thoracic dorsal root degeneration frequently was most abundant medially.

The posterior horn in the upper cervical region (i.e., C1 to C3) merits special consideration, because portions of it constitute the nucleus caudalis of the spinal trigeminal nucleus. According to Olszewski ('50) and Torvik ('56), the nucleus caudalis has the same fundamental cellular arrangement as the head of the posterior horn. Following section of the upper three cervical dorsal roots in the cat (Ranson, Davenport and Doles, '32), degenerated fibers were scattered in the posterior horn at C2 and C3, but little degeneration was seen at C1. Very few fibers entered the substantia gelatinosa in any of these spinal segments.

e VII and VIII. Based upon these authors' diagrammatic representation of this fiber distribution, this area of termination appears to correspond to the intermediomedial nucleus and the area immediately ventral to it—the same areas which receive dorsal root afferents in the monkey. Fibers projecting to the intermediomedial nucleus were seen at the level of the rhizotomy and in adjacent spinal segment (figs. 4, 17).

Lamina IX. In the present study all dorsal roots, except the first cervical, projected fibers to motor neurons of the anterior horn at the level of root entry and in adjacent spinal segments. The projection from C1 is inconsistent, very sparse, and only at the level of entrance. These findings are similar to those of Yee and Corbin ('39), Liu ('56), Kerr ('61) and Dunn and Matzke ('67) with respect to the C1 dorsal root. In all animals the amount of degeneration in lamina IX was greatest in the segment of dorsal rhizotomy. Previous observations (Sprague and Ha, '64; Sterling and Kuypers, '67) indicating that the number of degenerated fibers in cell groups of lamina IX diminish sharply immediately rostral and caudal to the cut root are corroborated. The finding of Sterling and Kuypers ('67) that the C7 and C8 dorsal roots seem to be distributed more profusely to motor neurons in segments below these roots than to those above was not observed in the monkey.

Dorsal roots of C2 through C5 projected fibers to the spinal accessory nucleus in the upper cervical cord. These findings are similar to those of Escolar ('48) and Liu ('56) indicating that C2 and C3 dorsal roots project to the spinal accessory nucleus, but differ from those of Corbin, Lhamon and Petit ('37) who found no projection from C2 to the spinal accessory nucleus. In the monkey the C3 dorsal root contributed the greatest number of fibers to the spinal accessory nucleus (fig. 22). Quantitative estimates of individual dorsal root projections to this nucleus were not reported to the other investigators. A dorsal root projection from C1 to the spinal accessory nucleus, as reported by Escolar ('48) and Liu ('56) was not consistently observed in the monkey.

Projections in the posterior funiculus. The cross-sectional configuration of

the posterior columns varies at different levels of the spinal cord and the precise limits of the fasciculi gracilis and cuneatus are difficult to determine especially in the mid-thoracic region. In the strict sense the fasciculus cuneatus should be defined as consisting of posterior column fibers terminating in the nucleus cuneatus, but it should be noted that all dorsal roots projecting fibers to the cuneate nucleus also project to the accessory cuneate nucleus. The principal spinal projections to these nuclei come from the cervical and upper seven thoracic dorsal roots.

Dorsal root fibers enter the lateral part of the fasciculus cuneatus where they divide into long ascending and short descending branches. At successively higher levels ascending fibers shift to more medial parts of the fasciculus cuneatus as in classical descriptions (figs. 4, 11). Ascending dorsal root fibers from the upper thoracic segments form relatively narrow bands of degeneration in medial portions of the fasciculus cuneatus. The dorsal part of this band of degeneration extends laterally at the surface of the spinal cord for approximately half the width of the fasciculus cuneatus. Ascending fibers from the T2 through T7 dorsal roots form discrete, very narrow laminae along the entire length of the posterior intermediate septum. The T7 fibers are located in the most medial portion of the fasciculus cuneatus and in the most lateral part of the fasciculus gracilis, while the majority of T2 through T6 fibers are in medial portions of the fasciculus cuneatus, especially dorsomedially.

Ascending fibers from brachial dorsal roots (i.e., C5 through T1) occupy the largest portions of the fasciculus cuneatus. These dorsal roots contribute the greatest number of ascending fibers but also demonstrate considerable overlap. The T1 dorsal root fibers occupy a large medial part of the fasciculus cuneatus, overlapping the area containing fibers from all more caudal thoracic dorsal roots. The number of ascending fibers from the C8 dorsal root is greater than that of any other cervical root. Ascending degeneration in the fasciculus cuneatus from the upper four cervical dorsal roots is relatively small, occupies lateral parts of the fasciculus and exhibits overlapping features de-

central cervical nucleus at C1 through C4, (2) the dorsal nucleus of Clarke and the intermediolateral nucleus at T1 through L3, and (3) the intermediomedial nucleus at all spinal levels. All of these nuclei, except the intermediolateral nucleus, receive afferents from specific dorsal roots. Afferent fibers to the central cervical nucleus are derived chiefly from the upper five cervical dorsal roots. Because of the relationship of this nucleus to the intermediate nucleus of the medulla, it will be discussed with the medullary relay nuclei.

Pass ('33), Liu ('56) and Grant and Rexed ('58) have published detailed accounts of degeneration in the dorsal nucleus following dorsal rhizotomies in the cat. Present findings corroborate those of Liu ('56) indicating afferent projections to the dorsal nucleus from all, except the upper four cervical dorsal roots, and differ from those of Pass ('33) and Grant and Rexed ('58) which indicated that the cervical and first thoracic dorsal roots project no fibers to the dorsal nucleus. In accordance with earlier observations in the cat (Pass, '33; Schimert, '39; Liu, '56; Grant and Rexed, '58) and dog (Szentágothai and Albert, '55), the present experiments indicate that dorsal root collaterals project only to the ipsilateral dorsal nucleus. In the cat (Liu, '56; Grant and Rexed, '58) and monkey, dorsal root collaterals from the posterior funiculus penetrate the medial aspect of the posterior horn and enter the dorsal nucleus directly, without passing through other parts of the posterior horn.

At the level of root section degeneration in the dorsal nucleus is profuse, but not all cells are surrounded by root fibers. In segments rostral and caudal to the cut root, degeneration in the dorsal nucleus is diminished and distributed to only part of the nucleus. Although the dorsal root collaterals exhibit an asymmetrical and differential distribution within the dorsal nucleus, no unequivocal and consistent pattern of localized terminations for different dorsal roots is apparent. These findings differ from those of Liu ('56) indicating that C5 to T5 dorsal root degeneration is distributed throughout the dorsal nucleus, and from those of Grant and Rexed ('58) who indicated that ascending degenerated fibers from T2 to T8 dorsal roots project

throughout the cross-section of the nucleus in the more rostral segments. In general, descending collaterals of dorsal roots are most often localized to lateral parts of the dorsal nucleus.

The C5 through T7 dorsal roots have an extensive projection to the dorsal nucleus in the monkey, with a single dorsal root distributing fibers in four to ten segments. The projections of the lower four cervical dorsal roots to the dorsal nucleus in the monkey differ from those of the upper seven thoracic dorsal roots in that there are: (1) considerably fewer fibers, and (2) pericellular arborizations are infrequent or absent. Previous investigators who have reported relatively extensive projections from individual dorsal roots to the dorsal nucleus in the cat include Liu ('56) who indicated a two to nine segment distribution of fibers from C5 to T5 dorsal roots, and Grant and Rexed ('58) who indicated a two to six segment distribution of fibers from T2 to T7 dorsal roots. Considerable overlap in the central distribution of different dorsal root fibers to the dorsal nucleus was observed in the monkey, in agreement with findings in the cat (Liu, '56; Grant and Rexed, '58).

After all dorsal rhizotomies in this series, a contingent of degeneration terminates in a small group of cells in the medial part of lamina VII ventrolateral to the central canal (figs. 4, 9, 17). This nucleus appears to correspond with the intermediomedial nucleus of Rexed ('52, '54). Some fibers coursed through, or adjacent to, this nucleus to terminate in areas immediately ventral to it. Fibers projecting to the intermediomedial nucleus course ventromedially from an area of concentrated degeneration which is the central cervical nucleus in the upper four cervical segments, the central portion of lamina VI in the brachial enlargement and the dorsal nucleus in the thoracic segments. In accordance with these observations Schimert ('39) and Sprague and Ha ('64) traced collaterals of dorsal root fibers to the intermediomedial nucleus in the cat. After C5 to T1 dorsal rhizotomies in the cat, Sterling and Kuypers ('67) reported irregular "bursts" of terminal degeneration distributed to a group of cells occupying the medial parts of the junction between lami-

ae VII and VIII. Based upon these authors' diagrammatic representation of this per distribution, this area of termination appears to correspond to the intermediomedial nucleus and the area immediately ventral to it—the same areas which receive dorsal root afferents in the monkey. Fibers projecting to the intermediomedial nucleus were seen at the level of the rhizotomy and in adjacent spinal segment (figs. 4, 17).

Lamina IX. In the present study all dorsal roots, except the first cervical, projected fibers to motor neurons of the anterior horn at the level of root entry and in adjacent spinal segments. The projection from C1 is inconsistent, very sparse, and only at the level of entrance. These findings are similar to those of Yee and Corbin ('39), Liu ('56), Kerr ('61) and Dunn and Matzke ('67) with respect to the C1 dorsal root. In all animals the amount of degeneration in lamina IX was greatest in the segment of dorsal rhizotomy. Previous observations (Sprague and Ha, '64; Sterling and Kuypers, '67) indicating that the number of degenerated fibers in cell groups of lamina IX diminish sharply immediately rostral and caudal to the cut root are corroborated. The finding of Sterling and Kuypers ('67) that the C7 and C8 dorsal roots seem to be distributed more profusely to motor neurons in segments below these roots than to those above was not observed in the monkey.

Dorsal roots of C2 through C5 projected fibers to the spinal accessory nucleus in the upper cervical cord. These findings are similar to those of Escobar ('48) and Liu ('56) indicating that C2 and C3 dorsal roots project to the spinal accessory nucleus, but differ from those of Corbin, Lhamon and Petit ('37) who found no projection from C2 to the spinal accessory nucleus. In the monkey the C3 dorsal root contributed the greatest number of fibers to the spinal accessory nucleus (fig. 22). Quantitative estimates of individual dorsal root projections to this nucleus were not reported to the other investigators. A dorsal root projection from C1 to the spinal accessory nucleus, as reported by Escobar ('48) and Liu ('56) was not consistently observed in the monkey.

Projections in the posterior funiculus. The cross-sectional configuration of

the posterior columns varies at different levels of the spinal cord and the precise limits of the fasciculi gracilis and cuneatus are difficult to determine especially in the mid-thoracic region. In the strict sense the fasciculus cuneatus should be defined as consisting of posterior column fibers terminating in the nucleus cuneatus, but it should be noted that all dorsal roots projecting fibers to the cuneate nucleus also project to the accessory cuneate nucleus. The principal spinal projections to these nuclei come from the cervical and upper seven thoracic dorsal roots.

Dorsal root fibers enter the lateral part of the fasciculus cuneatus where they divide into long ascending and short descending branches. At successively higher levels ascending fibers shift to more medial parts of the fasciculus cuneatus as in classical descriptions (figs. 4, 11). Ascending dorsal root fibers from the upper thoracic segments form relatively narrow bands of degeneration in medial portions of the fasciculus cuneatus. The dorsal part of this band of degeneration extends laterally at the surface of the spinal cord for approximately half the width of the fasciculus cuneatus. Ascending fibers from the T2 through T7 dorsal roots form discrete, very narrow laminae along the entire length of the posterior intermediate septum. The T7 fibers are located in the most medial portion of the fasciculus cuneatus and in the most lateral part of the fasciculus gracilis, while the majority of T2 through T6 fibers are in medial portions of the fasciculus cuneatus, especially dorsomedially.

Ascending fibers from brachial dorsal roots (i.e., C5 through T1) occupy the largest portions of the fasciculus cuneatus. These dorsal roots contribute the greatest number of ascending fibers but also demonstrate considerable overlap. The T1 dorsal root fibers occupy a large medial part of the fasciculus cuneatus, overlapping the area containing fibers from all more caudal thoracic dorsal roots. The number of ascending fibers from the C8 dorsal root is greater than that of any other cervical root. Ascending degeneration in the fasciculus cuneatus from the upper four cervical dorsal roots is relatively small, occupies lateral parts of the fasciculus and exhibits overlapping features de-

central cervical nucleus at C1 through C4, (2) the dorsal nucleus of Clarke and the intermediolateral nucleus at T1 through L3, and (3) the intermediomedial nucleus at all spinal levels. All of these nuclei, except the intermediolateral nucleus, receive afferents from specific dorsal roots. Afferent fibers to the central cervical nucleus are derived chiefly from the upper five cervical dorsal roots. Because of the relationship of this nucleus to the intermediate nucleus of the medulla, it will be discussed with the medullary relay nuclei.

Pass ('33), Liu ('56) and Grant and Rexed ('58) have published detailed accounts of degeneration in the dorsal nucleus following dorsal rhizotomies in the cat. Present findings corroborate those of Liu ('56) indicating afferent projections to the dorsal nucleus from all, except the upper four cervical dorsal roots, and differ from those of Pass ('33) and Grant and Rexed ('58) which indicated that the cervical and first thoracic dorsal roots project no fibers to the dorsal nucleus. In accordance with earlier observations in the cat (Pass, '33; Schimert, '39; Liu, '56; Grant and Rexed, '58) and dog (Szentágothai and Albert, '55), the present experiments indicate that dorsal root collaterals project only to the ipsilateral dorsal nucleus. In the cat (Liu, '56; Grant and Rexed, '58) and monkey, dorsal root collaterals from the posterior funiculus penetrate the medial aspect of the posterior horn and enter the dorsal nucleus directly, without passing through other parts of the posterior horn.

At the level of root section degeneration in the dorsal nucleus is profuse, but not all cells are surrounded by root fibers. In segments rostral and caudal to the cut root, degeneration in the dorsal nucleus is diminished and distributed to only part of the nucleus. Although the dorsal root collaterals exhibit an asymmetrical and differential distribution within the dorsal nucleus, no unequivocal and consistent pattern of localized terminations for different dorsal roots is apparent. These findings differ from those of Liu ('56) indicating that C5 to T5 dorsal root degeneration is distributed throughout the dorsal nucleus, and from those of Grant and Rexed ('58) who indicated that ascending degenerated fibers from T2 to T8 dorsal roots project

throughout the cross-section of the nucleus in the more rostral segments. In general, descending collaterals of dorsal roots are most often localized to lateral parts of the dorsal nucleus.

The C5 through T7 dorsal roots have an extensive projection to the dorsal nucleus in the monkey, with a single dorsal root distributing fibers in four to ten segments. The projections of the lower four cervical dorsal roots to the dorsal nucleus in the monkey differ from those of the upper seven thoracic dorsal roots in that they are: (1) considerably fewer fibers, and (2) pericellular arborizations are infrequent or absent. Previous investigators who have reported relatively extensive projections from individual dorsal roots to the dorsal nucleus in the cat include Liu ('56) who indicated a two to nine segment distribution of fibers from C5 to T5 dorsal roots, and Grant and Rexed ('58) who indicated a two to six segment distribution of fibers from T2 to T7 dorsal roots. Considerable overlap in the central distribution of different dorsal root fibers to the dorsal nucleus was observed in the monkey, in agreement with findings in the cat (Liu, '56; Grant and Rexed, '58).

After all dorsal rhizotomies in this series a contingent of degeneration terminates in a small group of cells in the medial part of lamina VII ventrolateral to the central canal (figs. 4, 9, 17). This nucleus appears to correspond with the intermediomedial nucleus of Rexed ('52, '54). Some fibers coursed through, or adjacent to, this nucleus to terminate in areas immediately ventral to it. Fibers projecting to the intermediomedial nucleus course ventromedially from an area of concentrated degeneration which is the central cervical nucleus in the upper four cervical segments, the central portion of lamina VII in the brachial enlargement and the dorsal nucleus in the thoracic segments. In accordance with these observations Schimert ('39) and Sprague and Ha ('64) traced collaterals of dorsal root fibers to the intermediomedial nucleus in the cat. After C5 to T1 dorsal rhizotomies in the cat, Sterlin and Kuypers ('67) reported irregular "bursts" of terminal degeneration distributed to a group of cells occupying the medial parts of the junction between lam

small number of fibers to this nucleus. Dorsal root projections to the cuneate nucleus have been reported from levels as low as T8 in the rhesus monkey (Walker and Weaver, '42) and from levels as caudal as T12 (Kuypers and Tuerk, '64) and S1 (Hand, '66) in the cat.

Following a multiple section of the upper three cervical dorsal roots in the rat, Torvik ('56) observed a small, sharply circumscribed area of degeneration in the lateral part of the cuneate nucleus. Escobar ('48) individually sectioned the upper three cervical dorsal roots in the cat and reported a somatotopic arrangement of degeneration in the cuneate nucleus, in which C1 fibers were located most superiorly and laterally while C2 and C3 fibers were located laterally at all levels. Fibers from C3 were found dorsal to those of C2.

The most detailed analysis of dorsal root projections to the cuneate nucleus in the cat using the Nauta technic was made by Kuypers and Tuerk ('64). Dorsal rhizotomies included C2 and C3 (multiple section), C7 and C8 (multiple section) and T12. While the number of dorsal roots sectioned was small and no overall pattern of termination in the cuneate nucleus was established, certain data seem significant. These authors found degeneration from C2 and C3 dorsal roots in caudal parts of the nucleus cuneatus was dense ventrolaterally and diffuse in the base of the nucleus; in rostral parts of the nucleus degeneration was diffuse. Ascending degeneration from C7 and C8 dorsal roots was dense in dorso-medial parts of the nucleus and diffuse in basal regions caudally; rostrally degeneration from these roots seemed widespread. These authors indicated overlapping projections from these different dorsal roots in rostral parts of the cuneate nucleus. Ascending fibers from T12 dorsal root were distributed to cells in a transitional area between the nuclei gracilis and cuneatus; additional degeneration projected diffusely to basal parts of the cuneate nucleus rostrally. While limited, these observations suggested a dual pattern of fiber termination in the nucleus cuneatus not seen in our material.

On the basis of single dorsal rhizotomies and cordotomies at various levels Walker and Weaver ('42) reported a topical lamina-

nar pattern of fiber termination in the mediolateral and rostrocaudal dimensions of the cuneate nucleus of the monkey. Ascending fibers from T1 through T7 projected to medial and caudal regions of the cuneate nucleus; all cervical dorsal roots projected fibers to lateral and rostral parts of the nucleus. These authors noted that fibers passing to the cuneate nucleus seemed to be derived from basal parts of the fasciculus cuneatus while fibers entering the accessory cuneate nucleus were located more dorsally in the fasciculus.

Data concerning the termination of fibers from the upper three cervical dorsal roots in the cuneate nucleus heretofore have been fragmentary. Fibers from these cervical dorsal roots terminate in the most ventrolateral part of the nucleus at different rostrocaudal levels. Fibers of the C1 dorsal root are located most ventrolaterally in the rostral two-thirds of the nucleus. Fibers of the C2 dorsal root occupy the ventrolateral border of the caudal third of the nucleus, but at more rostral levels form a band medial to the C1 fibers. In the caudal pole of the cuneate nucleus fibers of the C3 dorsal root occupy the ventrolateral border of the nucleus, but at more rostral levels form a band medial to the fibers of C2. This pattern of somatotopic termination of upper cervical dorsal root fibers in the nucleus cuneatus appears more specific than in any previous study.

Ascending dorsal root fibers from C4 through C7 are distributed in crescent-shaped bands in progressively more dorso-medial parts of the cuneate nucleus; the hilus of these serial crescents is directed dorsomedially. Fibers of the C8 dorsal root terminate in a large circular or oval cell mass in the dorsal and central parts of the nucleus. Root fibers from T1 terminate in a large inverted "U" shaped area with the open part directed ventrolaterally. The T1 terminal zone caps the region receiving fibers from C8. Upper thoracic dorsal root fibers terminate in narrow, overlapping crescent-shaped bands oriented along the dorsomedial border of the cuneate nucleus. Fibers from all of these dorsal roots terminate throughout the length of the nucleus (fig. 5).

In the monkey the number of ascending dorsal root fibers projecting to the cuneate nucleus and the areas of their laminar

scribed for other root fibers. The smallest contribution of ascending fibers to the fasciculus cuneatus is from C1. These fibers form a narrow band in the lateral part of the fasciculus immediately dorsal to the nucleus caudalis of the spinal trigeminal complex.

According to classical descriptions descending branches of cervical and thoracic dorsal roots form the small compact fasciculus interfascicularis, or comma tract of Schultze, situated in or near the posterior intermediate septum (Flechsig, 1876; Schultze, 1883). In the monkey descending fibers from cervical and upper thoracic dorsal roots form bands in the posterior funiculus, lateral and parallel to, but at varying distances from the posterior intermediate septum, rather than forming a compact bundle in the septum's middle portion. Descending fibers tend to mimic the position of the ascending fibers, except they do not migrate as far dorsomedially, and there is a greater concentration of fibers in ventromedial parts of the bundle close to the spinal gray. At successive caudal levels there is a gradual reduction in the number of fibers and those in ventromedial locations are the last to disappear. The number and length of the descending fibers in the posterior funiculus varies according to the dorsal root. Fibers from the upper three cervical roots descend from one to two segments, those from C4 through T1 dorsal roots descend from three to eight segments, and those from T2 through T7 dorsal roots extend caudally from two to six segments. Pass ('33) traced degeneration in the posterior funiculus from C6 and C7 dorsal roots caudally for about four segments; similar fibers could be followed caudally for five segments in the present study.

The present findings are in accord with those of Papez ('29), Ranson, Davenport and Doles ('32) and Corbin and Hinsey ('35) indicating that fibers from the upper three cervical dorsal roots do not descend more than two segments, but differ from those of van Gehuchten ('01), Corbin, Lhamon and Petit ('37), Yee and Corbin ('39) and Liu ('56) who reported that fibers of C1 and C2 dorsal roots extend caudally for three segments, and those of C3 for three or four segments. Observations

demonstrating that fibers from C4 and dorsal roots extend caudally for four or five segments (Yee and Corbin, '39; Liu, '56) were confirmed in the monkey.

The amount, extent, and location of ascending fibers from a single dorsal root showed regional variations in the monkey's spinal gray. Earlier investigators did not indicate the extent of the distribution of these fibers in the spinal gray. After sectioning dorsal roots of the brachial plexus, Sterling and Kuypers ('67) reported many degenerated fibers from a single dorsal root distributed to laminae III-VI throughout the brachial cord. In the monkey, some fibers from C5 through T1 dorsal roots supplied certain of these laminae throughout the brachial enlargement, but not all of these roots supplied all of the laminae throughout this region.

Medullary projections

Nucleus cuneatus. The nucleus cuneatus exhibits regional differences in its cytoarchitecture, position and shape (Ferraro and Barrera, '35a; Meesen and Olszewski, '49; Olszewski and Baxter, '54). In Nissl and Golgi stained sections Kuypers and Tuerk ('64) reported rostrocaudal and dorsoventral variations in the cellular and dendritic architecture of this nucleus in the cat. Dorsal areas of the cuneate nucleus contained clusters of round cells with many bushy dendrites, while basal areas contained triangular, multipolar and fusiform cells with long, sparsely radiating dendrites. These authors indicated that the mode of distribution of dorsal root fibers in the cuneate nucleus is related to certain features of the nuclear organization. Round cell clusters with multiple bushy dendrites, considered to receive afferents principally from distal parts of the extremities, were thought to be related to small cutaneous receptive fields. Triangular and multipolar cells with sparsely radiating dendrites, considered to receive afferents primarily from proximal parts of the extremities and trunk, were regarded as being related to larger cutaneous fields.

All dorsal roots studied in this series (C through T7) projected fibers to specific parts of the cuneate nucleus (fig. 5). In addition, dorsal roots T8 through L1 (Carpenter, Stein and Shriver, '68), project

all number of fibers to this nucleus. Dorsal root projections to the cuneate nucleus have been reported from levels as low as T8 in the rhesus monkey (Walker and Weaver, '42) and from levels as caudal as T12 (Kuypers and Tuerk, '64) and S1 (Land, '66) in the cat.

Following a multiple section of the upper three cervical dorsal roots in the rat, Torvik (56) observed a small, sharply circumscribed area of degeneration in the lateral part of the cuneate nucleus. Escobar ('48) individually sectioned the upper three cervical dorsal roots in the cat and reported a somatotopic arrangement of degeneration in the cuneate nucleus, in which C1 fibers were located most superiorly and laterally while C2 and C3 fibers were located laterally at all levels. Fibers from C3 were found dorsal to those of C2.

The most detailed analysis of dorsal root projections to the cuneate nucleus in the cat using the Nauta technic was made by Kuypers and Tuerk ('64). Dorsal rhizotomies included C2 and C3 (multiple section), C7 and C8 (multiple section) and T12. While the number of dorsal roots sectioned was small and no overall pattern of termination in the cuneate nucleus was established, certain data seem significant. These authors found degeneration from C2 and C3 dorsal roots in caudal parts of the nucleus cuneatus was dense ventrolaterally and diffuse in the base of the nucleus; in rostral parts of the nucleus degeneration was diffuse. Ascending degeneration from C7 and C8 dorsal roots was dense in dorsomedial parts of the nucleus and diffuse in basal regions caudally; rostrally degeneration from these roots seemed widespread. These authors indicated overlapping projections from these different dorsal roots in rostral parts of the cuneate nucleus. Ascending fibers from T12 dorsal root were distributed to cells in a transitional area between the nuclei gracilis and cuneatus; additional degeneration projected diffusely to basal parts of the cuneate nucleus rostrally. While limited, these observations suggested a dual pattern of fiber termination in the nucleus cuneatus not seen in our material.

nar pattern of fiber termination in the mediolateral and rostrocaudal dimensions of the cuneate nucleus of the monkey. Ascending fibers from T1 through T7 projected to medial and caudal regions of the cuneate nucleus; all cervical dorsal roots projected fibers to lateral and rostral parts of the nucleus. These authors noted that fibers passing to the cuneate nucleus seemed to be derived from basal parts of the fasciculus cuneatus while fibers entering the accessory cuneate nucleus were located more dorsally in the fasciculus.

Data concerning the termination of fibers from the upper three cervical dorsal roots in the cuneate nucleus heretofore have been fragmentary. Fibers from these cervical dorsal roots terminate in the most ventrolateral part of the nucleus at different rostrocaudal levels. Fibers of the C1 dorsal root are located most ventrolaterally in the rostral two-thirds of the nucleus. Fibers of the C2 dorsal root occupy the ventrolateral border of the caudal third of the nucleus, but at more rostral levels form a band medial to the C1 fibers. In the caudal pole of the cuneate nucleus fibers of the C3 dorsal root occupy the ventrolateral border of the nucleus, but at more rostral levels form a band medial to the fibers of C2. This pattern of somatotopic termination of upper cervical dorsal root fibers in the nucleus cuneatus appears more specific than in any previous study.

Ascending dorsal root fibers from C4 through C7 are distributed in crescent-shaped bands in progressively more dorsomedial parts of the cuneate nucleus; the hilus of these serial crescents is directed dorsomedially. Fibers of the C8 dorsal root terminate in a large circular or oval cell mass in the dorsal and central parts of the nucleus. Root fibers from T1 terminate in a large inverted "U" shaped area with the open part directed ventrolaterally. The T1 terminal zone caps the region receiving fibers from C8. Upper thoracic dorsal root fibers terminate in narrow, overlapping crescent-shaped bands oriented along the dorsomedial border of the cuneate nucleus. Fibers from all of these dorsal roots terminate throughout the length of the nucleus (fig. 5).

In the monkey the number of ascending dorsal root fibers projecting to the cuneate nucleus and the areas of their laminar

* On the basis of single dorsal rhizotomies and cordotomies at various levels Walker and Weaver ('42) reported a topical lami-

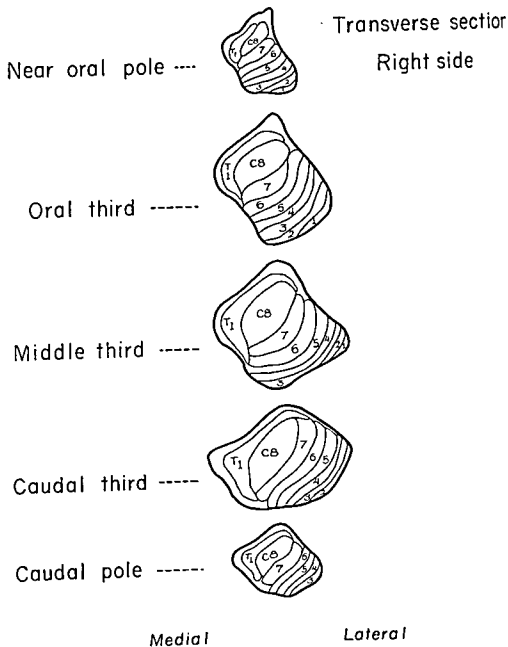


Fig. 5 Schematic diagram of the terminal zones in the cuneate nucleus receiving fibers from dorsal roots C1 through T1. The zone for each root shows the principal area of fiber termination but not the extent of overlap. Fibers from dorsal roots T2 through T7 terminate in overlapping fashion mainly along the dorsomedial border of the nucleus.

termination are roughly related to the size of the dorsal root. The largest areas of terminal degeneration in the cuneate nucleus are those related to dorsal roots C5 through T1. In absolute size the areas of termination of C7, C8 and T1 dorsal root fibers are the largest. While C1 through T1 dorsal root fibers projecting to the cuneate nucleus terminate in exclusive and overlapping zones, the degree of overlap of

adjacent dorsal roots appears less than the accessory cuneate nucleus. Overlap dorsal root fibers in the cuneate nucleus primarily within the territory of the highest root. The present study does not provide detailed information concerning the manner in which fibers from C1 through T7 dorsal roots terminate in the cuneate nucleus. Fibers from the thoracic dorsal roots are modest in

appear to have almost entirely overlapping terminations in dorsomedial parts of nucleus.

Accessory cuneate nucleus. The accessory cuneate nucleus is considered to be medullary equivalent of the dorsal nucleus of Clarke (Hollis, 1884; Blumenthal, 1891; Sherrington, 1893; Pass, '33; Odell, '41). These nuclei share the following anatomical and functional characteristics: (1) cells are morphologically similar to the eccentric nuclei, (2) afferent fibers are derived from dorsal roots, (3) both nuclei give rise to uncrossed cerebellar afferent fibers, and (4) both nuclei relay impulses from muscle spindles, type II muscle afferents, and cutaneous afferents to the cerebellum (Oscarsson, '65). Although impulses from Golgi tendon organs are relayed via the dorsal nucleus, this has not been established for the accessory cuneate nucleus.

Dorsal roots C1 through T7 project fibers to the accessory cuneate nucleus (fig. 6). Previous investigations in the rhesus monkey have reported ascending dorsal root projections to the accessory cuneate nucleus from levels as caudal as T4 (Ferraro and Barrera, '35b) and T8 (Walker and Weaver, '42). In the cat (Liu, '56) T5 was the most caudal dorsal root reported to contribute fibers to this nucleus, but dorsal roots T6 through T9 were not sectioned in this study. Hand ('66) observed some degeneration from lumbar and S1 dorsal roots projecting to the rostral part of the accessory cuneate nucleus. Classically, the neocerebellar tract is considered to be related primarily to the upper extremity and neck, while the posterior spinocerebellar tract is considered to be related primarily to the lower extremity and trunk (Oscarsson, '65). The present study indicates that C5 through T7 dorsal roots project to both the accessory cuneate and dorsal nuclei, while C1 through C4 dorsal roots supply only the accessory cuneate nucleus. Since dorsal roots conveying afferents from the upper extremity and upper trunk have central projections to both of these nuclei, dual pathways exist for the conduction of impulses to the cerebellum.

Previous investigators have reported projections to the accessory cuneate nucleus after section of selected cervical dorsal

roots in the marmoset monkey (Dunn and Matzke, '67), cat (Ranson, Davenport and Doles, '32; Pass, '33; Escobar, '48), and rabbit (Yee and Corbin, '39). None of these studies indicated the pattern or extent of the dorsal root projection.

According to Torvik's ('56) studies in the rat fibers from the upper three cervical dorsal roots terminate in the most ventral and lateral parts of the accessory cuneate nucleus. In the only detailed study of dorsal root projections to the accessory cuneate nucleus in the cat (Liu, '56), dorsal root fibers from spinal segments C1 through T5 were found to terminate in oblique, overlapping spiral laminae. Fibers from the C7 dorsal root terminated in the central core of the nucleus about which oblique laminae from other roots were arranged. Dorsal root fibers from T5 through C8 were found dorsal to the central core with T5 fibers most rostral and lateral, and C8 fibers most caudal and medial. Spiral laminae ventral to the central core were formed by dorsal root fibers from the upper six cervical segments with fibers from C6 most rostral and medial and fibers from C1 most caudal and lateral. Our interpretation of these observations, presented in a schematic reconstruction, suggests that medial and lateral as indicated in Liu's ('56) figure 8 are reversed.

Observations concerning the laminar termination of ascending dorsal root fibers in the accessory cuneate nucleus in the monkey have been based upon Marchi stained material. Sherrington (1893) found that C2 dorsal root fibers were distributed primarily to dorsal and lateral regions of the accessory cuneate nucleus. The arrangement described by Ferraro and Barrera ('35b) indicated that fibers from high cervical dorsal roots appeared to end in ventral and lateral parts of the nucleus, while those from lower cervical and upper thoracic dorsal roots appeared to end in dorsomedial regions of the accessory cuneate nucleus. Walker and Weaver ('42) reported similar findings except that fibers from C1 through C8 appeared to end in lateral regions of the nucleus while those of T1 through T8 passed to more medial locations. The latter authors indicated that while all of these dorsal roots projected fibers to both the cuneate and accessory cuneate nuclei, fibers passing to the acces-

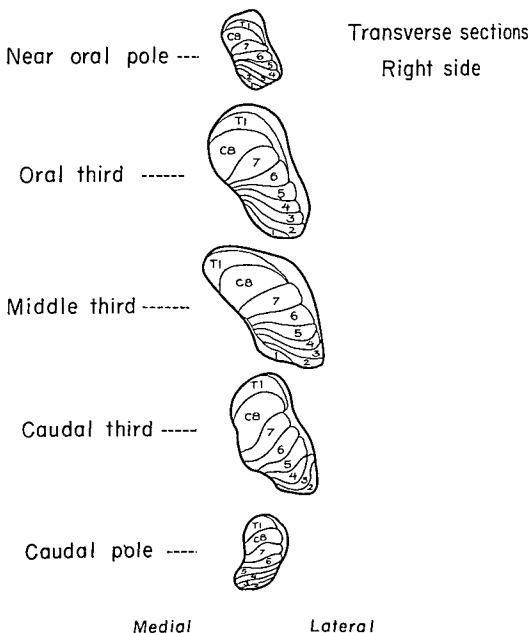


Fig. 6 Schematic diagram of the terminal zones in the accessory cuneate nucleus receiving fibers from dorsal roots C1 through T1. The zone for each root shows the principal area of fiber termination but not the extent of overlap. Fibers from dorsal roots T2 through T7 terminate in overlapping fashion mainly along the lateral border of the accessory cuneate nucleus.

sory cuneate nucleus were more numerous and more heavily myelinated. None of these authors specifically mentioned differences in the rostrocaudal distribution of various dorsal root fibers within the accessory cuneate nucleus.

In spite of specific differences, the laminar pattern of topical termination of dorsal root fibers in the accessory cuneate nucleus described by Liu ('56) appears to

correspond more with the current observations than prior studies done in the monkey. While prior observations made in the monkey are in general true, they lack significant details provided by silver staining methods. In the monkey the central region of the nucleus is the area of termination of fibers from C5 through C8 dorsal roots. Other differences in the pattern of laminar termination noted in the current

dy concern the rostrocaudal disposition fibers from the upper three cervical dorsal roots.

Although a C1 dorsal root is not present in every monkey, when present, fibers of this root do not project to the caudal third of the nucleus; fibers from this root are distributed only to ventromedial regions of the rostral two-thirds of the accessory cuneate nucleus. Fibers from C2 and C3 dorsal roots project to ventromedial regions of the nucleus throughout its extent. Liu ('56) found fibers from C1 dorsal root localized to the caudal pole of the accessory cuneate nucleus while fibers from C2 and C3 projected to ventrolateral regions of the caudal half of the nucleus (fig. 6). Dorsal root projections from C8 appear more extensive in the monkey than in the cat, and in the monkey they project throughout dorsomedial regions of the nucleus. In the cat fibers of C8 were described as terminating only in dorsocaudal regions of the nucleus. Dorsal root fibers from T1 terminate dorsomedial to those of C8 and appear to cap the dorsomedial pole of the nucleus. The laminar terminations of dorsal root fibers T2 through T7 were not plotted in the present study, but it was evident that fibers from these roots projected primarily to the lateral surface of the accessory cuneate nucleus.

Findings in the monkey related to ascending dorsal root fibers terminating in the accessory cuneate nucleus (fig. 6) suggest that: (1) the number of fibers projected to this nucleus is related to the size of the dorsal root, (2) fibers from all cervical and the first thoracic dorsal roots terminate in an orderly sequence in both exclusive and overlapping zones, and (3) fibers from upper thoracic dorsal roots (i.e., T2 through T7) are less numerous, terminate in smaller regions of the nucleus and exhibit a higher degree of overlap. While data are not precise with respect to overlapping terminations in this nucleus, fibers from C1 through T1 dorsal roots partially overlap only the territory of the next highest root. Comparisons of these results with those of Liu ('56) indicate that the degree of overlapping projections in the monkey is much less than in the cat.

When the patterns of dorsal root terminations in the accessory cuneate and cuneate

nuclei are compared, pertinent similarities and differences are evident. The patterns of termination of C1 through T1 dorsal root fibers in these nuclei are remarkably similar. The C5 through C8 fibers terminated in the central core region about which fibers from the other dorsal roots are arranged in oblique laminae. The laminar pattern of termination of these dorsal roots is such that fibers from the highest root are ventrolateral and those from the lowest root are dorsomedial. All of these dorsal roots, except C1 and C2, terminate throughout the rostrocaudal extent of both nuclei.

The patterns of termination of T2 through T7 dorsal root fibers in these nuclei are different. Fibers from T2 through T7 dorsal roots terminate primarily in dorsomedial parts of the cuneate nucleus; in the accessory cuneate nucleus fibers from these roots terminate in lateral regions. Dorsal roots T5, T6 and T7 project fibers within both the medial border of the cuneate nucleus and the lateral border of the nucleus gracilis.

Central cervical and intermediate nuclei. Several authors have provided anatomical descriptions of the intermediate nucleus in the upper cervical spinal cord and in the medulla of the cat (Cajal, '09; Papez, '29; Ranson, Davenport and Doles, '32; Rexed, '54) and the rat (Torvik, '56). These nuclei also are mentioned in studies of the cervical dorsal roots in the rabbit (Yee and Corbin, '39), cat (Kerr, '61) and monkey (Corbin, Lhamon and Petit, '37). The present study provides a description of these nuclei in the rhesus monkey. According to Torvik ('56), the intermediate nucleus in the upper cervical spinal cord (Cajal, '09) probably is identical with the central cervical nucleus of Rexed ('54). Most authors (Papez, '29; Ranson, Davenport and Doles, '32; Corbin, Lhamon and Petit, '37; Torvik, '56) indicate that the intermediate nucleus of the medulla is the rostral continuation of the intermediate, or central cervical, nucleus of the spinal cord. Rexed ('54), however, is firm in his belief that the central cervical nucleus is not directly continuous with any cell column in the medulla.

The present study indicates that the central cervical and intermediate nuclei are parts of the same cell column (figs. 1, 2),

within which cytological variations are seen. As Torvik ('56) indicated, cells at spinal levels and in caudal parts of the medulla are larger than those in more rostral regions. There has been little agreement concerning the rostral extent of this cell column. Corbin, Lhamon and Petit ('37) could not distinguish the intermediate nucleus at caudal levels of the hypoglossal nucleus in the monkey, and concluded that cells of the nucleus do not extend as far rostrally in the monkey as in the cat and rabbit. According to Torvik ('56) the rostral part of the intermediate nucleus lies slightly above the level of the caudal limit of the hypoglossal nucleus. Papez ('29) and Ranson, Davenport and Doles ('32) considered the oral part of the intermediate nucleus to lie along the lateral border of the hypoglossal nucleus and to virtually merge with the nucleus intercalatus. The present study indicates that the most rostral part of the intermediate nucleus in the monkey extends slightly beyond the caudal pole of the dorsal motor nucleus of the vagus. Although the rostral part of the nucleus is small, it is distinct and separate from the nucleus intercalatus. In normal material the intermediate nucleus does not stand out as an impressive cell column, but following section of the C2 dorsal root, extensive arborizations about cells of the nucleus outline the borders of the cell column in an impressive way (figs. 33, 34). The thesis that the central cervical nucleus and intermediate nucleus of the medulla constitute a single cell column is based upon: (1) anatomical evidence of a continuous aggregation of cells in corresponding locations in the upper cervical spinal cord and lower medulla, (2) the observation that cells in various parts of this column share at least one common source of afferent fibers, and (3) the finding that dorsal root fibers in all parts of the cell column terminate in similar profuse pericellular arborizations. The manner in which dorsal root fibers terminate upon cells in these nuclei (fig. 35) resembles that seen in the dorsal nucleus (Szentágothai and Albert, '55).

The present observations confirm that single or multiple section of the upper three cervical dorsal roots produces profuse degeneration in the central cervical

nucleus (Ranson, Davenport and '32; Corbin and Hinsey, '35; Corbin, Lhamon and Petit, '37; Yee and Corbin, '39; Escobar, '48; Torvik, '56). Maximal degeneration in this nucleus has been found at the level of the sectioned dorsal root. Current data also are consistent with the observations of Corbin and Hinsey ('35) and those of Yee and Corbin ('39) that C1 and C5 dorsal roots project fibers throughout the rostrocaudal extent of the central cervical nucleus. All of the upper five cervical dorsal roots, except C1, project fibers to all parts of the central cervical nucleus and to portions of the intermediate nucleus of the medulla. Dorsal root fibers from C1 project to the central cervical nucleus in the upper two cervical segments and contribute modestly to caudal parts of the intermediate nucleus of the medulla. Profuse degeneration from the C2 dorsal root projects to all parts of the central cervical and intermediate nuclei. Dorsal roots C3 through C5 contribute fibers to the central cervical nucleus at spinal levels and to all, except the most rostral, parts of the intermediate nucleus. Ascending fibers from these dorsal roots extend rostrally to levels slightly caudal to the hypoglossal nucleus. The upper five cervical dorsal roots all have extensive overlapping projections to the central cervical and intermediate nuclei with the C2 dorsal root having the most extensive distribution. The overlapping nature of dorsal root projections to the central cervical nucleus has been demonstrated by Schimert ('39) and Kerr ('61).

Dorsal root projections to the intermediate nucleus of the medulla have been described only from the upper three cervical roots (Ranson, Davenport and Doles, '32; Corbin, Lhamon and Petit, '37; Yee and Corbin, '39). The present findings differ from those of Yee and Corbin ('39) who found that the C1 dorsal root projects the greatest number of fibers to the intermediate nucleus in the rabbit.

Hypotheses concerning the functional significance of the intermediate nucleus seem to have been based mainly upon anatomical considerations. Papez ('29) suggested that the intermediate nucleus was associated with the hypoglossal nucleus and received muscle afferents from the

lingue via a reflexo-motor bundle from C1 dorsal root (i.e., descendens hypoglossi). Ranson, Davenport and Doles ('32) considered that this nucleus might be involved in tonic neck and righting reflexes, but admitted that the bulbar portion of the nucleus could not be essential since the tonic neck reflex can still be obtained after transection of the spinal cord above the level of the C1 dorsal root. Rexed ('54) suggested that the central cervical nucleus might be a caudal continuation of the hypoglossal nucleus. He postulated that fibers from this nucleus might exit with the ventral roots of C1 through C3 (or C4), join the hypoglossal nerve to form the descending ramus, and innervate muscles attached to the hyoid bone.

Evidence from the present study suggests that the central cervical and intermediate nuclei may constitute an important relay nucleus in an ascending pathway. Extensive cerebellar cortical ablations in two monkeys have not provided data indicating that fibers of this nucleus project to the cerebellum, but these experiments cannot be regarded as conclusive.

Supraspinal nucleus. Throughout levels of the pyramidal decussation, scattered neurons of the ventromedial nuclear group of the anterior gray horn extend rostrally into the medulla. These neurons, termed the supraspinal nucleus (Jacobsohn, '09; Olszewski and Baxter, '54) connect spinal and medullary (hypoglossal nucleus) portions of the general somatic efferent cell column. The supraspinal nucleus is considered to give rise to the C1 ventral root fibers.

In the monkey, the upper five cervical dorsal roots project fibers to the supraspinal nucleus. Within the nucleus most fibers terminate dorsomedially. The first two dorsal roots contribute the greatest number of fibers to the supraspinal nucleus; projections from the remaining cervical dorsal roots progressively decrease in a caudal sequence. Although numerous investigators have observed dorsal root projections to the ventromedial portion of the anterior horn at the C1 level, projections to its rostral continuation, the supraspinal nucleus, have not been reported.

Other medullary nuclei. Several authors have reported that ascending fibers

from upper cervical dorsal roots project to: (1) nucleus and tractus solitarius (Ranson, Davenport and Doles, '32; Corbin and Hinsey, '35; Yee and Corbin, '39; Liu, '56; Torvik, '56), (2) the inferior vestibular nucleus (Corbin and Hinsey, '35; Yee and Corbin, '39; Escobar, '48; Dunn and Matzke, '67), (3) the commissural nucleus of the vagus (Schwartz, Roulhac, Lam and O'Leary, '51; Torvik, '56), and (4) the nucleus intercalatus and the nucleus of Roller (Torvik, '56).

In the monkey a few ascending fibers from the C2 dorsal root projected to parts of the nucleus solitarius in two animals (C-1006 and C-1024). In these animals small, but definite, projections from the fasciculus cuneatus entered the magnocellular part of the spinal trigeminal nucleus, the nucleus of Roller, the nucleus intercalatus and the parvocellular reticular formation. One other animal (C-912) had minimal degeneration in the nucleus intercalatus associated with a C3 dorsal rhizotomy. These observations with respect to the nucleus solitarius differ from those of Corbin, Lhamon and Petit ('37), Schwartz, Roulhac, Lam and O'Leary ('51) and Kerr ('61).

One point which might account for the above discrepancies relative to the inferior vestibular nucleus concerns cell group x (Brodal and Pompeiano, '57), a small aggregation of cells lateral to the caudal part of the inferior vestibular nucleus and rostral to the accessory cuneate nucleus. This cell group has been considered by some as part of the inferior vestibular nucleus, although it does not receive primary vestibular fibers (Walberg, Bowsher and Brodal, '58). Spinovestibular afferents to this nucleus course with fibers of the posterior spinocerebellar tract. No degenerated fibers projecting to this nuclear group were found following C6 through C8 dorsal rhizotomies or cord lesions restricted to the posterior columns at C2 and C4 (Pompeiano and Brodal, '57). Observations in this study indicate that inadvertent trauma to the posterior spinocerebellar tract invariably resulted in degeneration projecting to cell group x. The extent of the degeneration in this nucleus seemed proportional to that in the posterior spinocerebellar tract. However,

within which cytological variations are seen. As Torvik ('56) indicated, cells at spinal levels and in caudal parts of the medulla are larger than those in more rostral regions. There has been little agreement concerning the rostral extent of this cell column. Corbin, Lhamon and Petit ('37) could not distinguish the intermediate nucleus at caudal levels of the hypoglossal nucleus in the monkey, and concluded that cells of the nucleus do not extend as far rostrally in the monkey as in the cat and rabbit. According to Torvik ('56) the rostral part of the intermediate nucleus lies slightly above the level of the caudal limit of the hypoglossal nucleus. Papez ('29) and Ranson, Davenport and Doles ('32) considered the oral part of the intermediate nucleus to lie along the lateral border of the hypoglossal nucleus and to virtually merge with the nucleus intercalatus. The present study indicates that the most rostral part of the intermediate nucleus in the monkey extends slightly beyond the caudal pole of the dorsal motor nucleus of the vagus. Although the rostral part of the nucleus is small, it is distinct and separate from the nucleus intercalatus. In normal material the intermediate nucleus does not stand out as an impressive cell column, but following section of the C2 dorsal root, extensive arborizations about cells of the nucleus outline the borders of the cell column in an impressive way (figs. 33, 34). The thesis that the central cervical nucleus and intermediate nucleus of the medulla constitute a single cell column is based upon: (1) anatomical evidence of a continuous aggregation of cells in corresponding locations in the upper cervical spinal cord and lower medulla, (2) the observation that cells in various parts of this column share at least one common source of afferent fibers, and (3) the finding that dorsal root fibers in all parts of the cell column terminate in similar profuse pericellular arborizations. The manner in which dorsal root fibers terminate upon cells in these nuclei (fig. 35) resembles that seen in the dorsal nucleus (Szentágothai and Albert, '55).

The present observations confirm that single or multiple section of the upper three cervical dorsal roots produces profuse degeneration in the central cervical

nucleus (Ranson, Davenport and Doles '32; Corbin and Hinsey, '35; Corbin, Lhamon and Petit, '37; Yee and Corbin '39; Escobar, '48; Torvik, '56). Maximal degeneration in this nucleus has been found at the level of the sectioned dorsal root. Current data also are consistent with the observations of Corbin and Hinsey ('35) and those of Yee and Corbin ('39) that C1 and C5 dorsal roots project fibers throughout the rostrocaudal extent of the central cervical nucleus. All of the upper five cervical dorsal roots, except C1, project fibers to all parts of the central cervical nucleus and to portions of the intermediate nucleus of the medulla. Dorsal root fibers from C1 project to the central cervical nucleus in the upper two cervical segments and contribute modestly to caudal parts of the intermediate nucleus of the medulla. Profuse degeneration from the C2 dorsal root projects to all parts of the central cervical and intermediate nuclei. Dorsal roots C3 through C5 contribute fibers to the central cervical nucleus at all spinal levels and to all, except the most rostral, parts of the intermediate nucleus. Ascending fibers from these dorsal roots extend rostrally to levels slightly caudal to the hypoglossal nucleus. The upper five cervical dorsal roots all have extensive overlapping projections to the central cervical and intermediate nuclei with the C2 dorsal root having the most extensive distribution. The overlapping nature of dorsal root projections to the central cervical nucleus has been demonstrated by Schimert ('39) and Kerr ('61).

Dorsal root projections to the intermediate nucleus of the medulla have been described only from the upper three cervical roots (Ranson, Davenport and Doles, '32; Corbin, Lhamon and Petit, '37; Yee and Corbin, '39). The present findings differ from those of Yee and Corbin ('39) who found that the C1 dorsal root projects the greatest number of fibers to the intermediate nucleus in the rabbit.

Hypotheses concerning the functional significance of the intermediate nucleus seem to have been based mainly upon anatomical considerations. Papez ('29) suggested that the intermediate nucleus was associated with the hypoglossal nucleus and received muscle afferents from the

its projecting to the cuneate and accessory cuneate nuclei terminate in smaller regions of the nuclei, exhibit greater overlap and are distinctive in that these fibers terminate primarily in dorsomedial parts of the cuneate nucleus and in lateral parts of the accessory cuneate nucleus.

15. Cytological and degeneration studies suggest that the central cervical nucleus and the intermediate nucleus of the medulla: (a) constitute parts of the same cell column, and (b) receive fibers from the upper five cervical dorsal roots which overlap in large regions of the cell column and terminate in rich pericellular arborizations. Afferent fibers to all parts of this cell column are derived from the C2 dorsal root.

16. The upper five cervical dorsal roots project fibers to the supraspinal nucleus, primarily to the dorsomedial part. The greatest number of fibers terminating in this nucleus are derived from the C1 and C2 dorsal roots.

LITERATURE CITED

- Anderson, F. D. 1960 Distribution of dorsal root fibers in the cat spinal cord. *Anat. Rec.*, 136: 154.
- Blumenau, L. 1891 Ueber den äusseren Kern des Keilstranges im verlängerten Mark. *Neur. Zentr.*, 10: 226-232.
- Brodal, A. 1941 Die Verbindungen des Nucleus cuneatus externus mit dem Kleinhirn beim Kaninchen und bei der Katze. Experimentelle Untersuchungen. *Z. ges. Neur. u. Psychiat.*, 171: 187-199.
- Brodal, A., and O. Pompeiano. 1957 The vestibular nuclei in the cat. *J. Anat.*, 91: 438-454.
- Brodal, A., and B. Rexed. 1953 Spinal afferents to the lateral cervical nucleus in the cat. An experimental study. *J. Comp. Neur.*, 98: 179-212.
- Cajal, S. Ramón Y. 1909 Histologie du système nerveux de l'homme et des vertébrés. Maloine, Paris, 2 vol. I.
- Carpenter, M. B., B. M. Stein and J. E. Shriver. 1968 Central projections of spinal dorsal roots in the monkey II. Lower thoracic, lumbosacral and coccygeal dorsal roots. *Am. J. Anat.*, 123: 75-118.
- Chang, H. T., and T. C. Ruch. 1947 Organization of the dorsal columns of the spinal cord and their nuclei in the spider monkey. *J. Anat.*, 81: 140-149.
- Collier, J., and E. F. Buzzard. 1903 The degenerations resulting from lesions of posterior nerve roots and from transverse lesions of the spinal cord in man. A study of twenty cases. *Brain*, 26: 559-591.
- Corbin, K. B., and J. C. Hinsey. 1935 Intramedullary course of the dorsal root fibers of each of the first four cervical nerves. *J. Comp. Neur.*, 63: 119-126.
- Corbin, K. B., W. T. Lhamon and D. W. Pettit. 1937 Peripheral and central connections of the upper cervical dorsal root ganglia in the Rhesus monkey. *J. Comp. Neur.*, 66: 405-414.
- Dunn, J., and H. Matzke. 1967 Central distribution of the dorsal root of the first cervical nerve of the marmoset monkey. *Anat. Rec.*, 157: 357.
- Escolar, J. 1948 The afferent connections of the 1st, 2nd, and 3rd cervical nerves in the cat. An analysis by Marchi and Rasdolsky methods. *J. Comp. Neur.*, 89: 79-92.
- Ferraro, A., and S. E. Barrera. 1935a The nuclei of the posterior funiculi in *Macacus rhesus*. An anatomical and experimental investigation. *Arch. Neur. Psychiat.*, 33: 262-275.
- . 1935b Posterior column fibers and their termination in *Macacus rhesus*. *J. Comp. Neur.*, 62: 507-530.
- Flechsig, P. 1876 Die Leitungsbahnen im Gehirn und Rückenmark des Menschen auf Grund entwicklungs geschichtlicher Untersuchungen. Engelmann, Leipzig.
- Gehuchten, A. van. 1901 Recherches sur la terminaison centrale des nerfs sensibles périphériques. IV. La racine postérieure des deux premiers nerfs cervicaux. *Le Névraque*, T. 2, pp. 227-256.
- Grant, G., and B. Rexed. 1958 Dorsal spinal root afferents to Clarke's column. *Brain*, 81: 567-576.
- Ha, H., and C. N. Liu. 1966 Organization of the spino-cervico-thalamic system. *J. Comp. Neur.*, 127: 445-470.
- Ha, H., and F. Morin. 1964 Comparative anatomical observations of the cervical nucleus, nucleus cervicalis lateralis, of some primates. *Anat. Rec.*, 148: 374-375.
- Hand, P. J. 1966 Lumbosacral dorsal root terminations in the nucleus gracilis of the cat. Some observations on terminal degeneration in other medullary sensory nuclei. *J. Comp. Neur.*, 126: 137-156.
- Hekmatpanah, J. 1961 Organization of tactile dermatomes, C1 through L4, in cat. *J. Neurophysiol.*, 24: 129-140.
- Hollis, W. A. 1884 Researches into the histology of the central gray substance of the spinal cord and medulla oblongata. *J. Anat. & Physiol.*, 18: 62-65.
- Howell, A. B., and W. L. Straus, Jr. 1933 The spinal nerves. In: *The Anatomy of the Rhesus Monkey*, C. G. Hartman and W. L. Straus, Jr. (Eds.), Hafner Publ. Co., New York, Chap. 16, 307-327.
- Jacobsohn, L. 1909 Ueber die Kerne des menschlichen Hirnstammes (der Medulla oblongata, des Pons und des Pedunculus). *Neur. Zbl.*, 28: 674-679.
- Kerr, F. W. L. 1961 Structural relation of the trigeminal spinal tract to upper cervical roots and the solitary nucleus in the cat. *Exptl. Neur.*, 4: 134-148.
- Kuypers, H. G. J. M., and J. D. Tuerk. 1964 The distribution of the cortical fibers within the nuclei cuneatus and gracilis in the cat. *J. Anat.*, 98: 143-162.
- Liu, C. N. 1956 Afferent nerves to Clarke's and the lateral cuneate nuclei in the cat. *Arch. Neur. Psychiat.*, 75: 67-77.
- Meesen, H., and J. Olszewski. 1949 A Cytoarchitectonic Atlas of the Rhombencephalon of the Rabbit. S. Karger, Basel.
- Morin, F., and J. V. Catalano. 1955 Central connections of a cervical nucleus (nucleus cervicalis lateralis of the cat). *J. Comp. Neur.*, 103: 17-32.
- Nauta, W. J. H., and P. A. Gyax. 1954 Silver impregnation of degenerating axons in the central nervous system. A modified technique. *Stain Tech.*, 29: 91-93.
- Olszewski, J. 1950 On the anatomical and functional organization of the trigeminal nucleus. *J. Comp. Neur.*, 92: 401-413.

in some animals small amounts of terminal degeneration were present in cell group x, even though none was detectable in the posterior spinocerebellar tract or in the inferior cerebellar peduncle.

CONCLUSIONS

The following conclusions were drawn from this study:

1. Degeneration in the spinal cord is most profuse at the level of dorsal rhizotomy and progressively diminishes in segments rostral and caudal to the sectioned root; progressive diminution of degeneration is greatest in the anterior horn.

2. At the level of dorsal rhizotomy, profuse terminal degeneration is present in laminae III and IV, central and medial portions of laminae V and VI, and among certain cell groups of lamina IX. Fewer fibers appear to terminate in laminae VII and VIII.

3. No dorsal root fibers from C1 project into the head of the posterior horn in the upper cervical region and fibers passing to the anterior horn are sparse.

4. Terminal fibers from dorsal roots C2 through C5 are localized to particular portions of laminae III and IV in a manner suggesting a somatotopic arrangement.

5. Fibers from dorsal roots of the brachial enlargement project to central and medial parts of lamina VI from four (C5) to eight (T1) segments rostral to their entry.

6. Cervical and upper thoracic dorsal roots project fibers to cell groups of lamina IX by distinctive pathways through either medial, or central, parts of laminae VII and VIII. At different levels the number of fibers following these pathways varies so that the greatest number of fibers from: (a) C5 through T1 dorsal roots course through central parts of lamina VII, (b) T2 through T7 dorsal roots project via medial parts of laminae VII and VIII, and (c) C2 through C4 dorsal roots project through both medial and central parts of laminae VII and VIII.

7. Cell groups of the spinal accessory nucleus in the upper cervical cord receive fibers from C2 through C5 dorsal roots with C3 contributing the greatest number of fibers.

8. Overlapping projections to the dors nucleus are derived from C5 through T1 dorsal roots; single dorsal roots distribute fibers to this cell column in four to five spinal segments, with the most profuse degeneration: (a) derived from thoracic dorsal roots, and (b) terminating in the cell column nearest the sectioned root.

9. A small, but distinct, bundle of fibers from all cervical and all upper thoracic dorsal roots terminate in the intermediate medial nucleus and the area ventral to it at the level of root entrance, and in adjacent spinal segments.

10. Ascending fibers in the fasciculus cuneatus in the monkey: (a) arise from the cervical and upper seven thoracic dorsal roots, and (b) exhibit only a general segregation because of extensive overlap. Dorsal roots of the brachial enlargement contribute the largest number of fibers.

11. Descending collaterals of cervical and upper thoracic dorsal roots form discrete bands in the posterior funiculus, lateral and parallel to, but at varying distances from the posterior intermediate septum. These bands resemble those of ascending fibers of the same root, except that they do not migrate as far dorsomedially, have a greater concentration of fibers in ventromedial locations, and are smaller.

12. Ascending branches of fibers from all cervical and the upper seven thoracic dorsal roots project somatotopically to both the cuneate and accessory cuneate nuclei. The pattern of termination of fibers from C1 through T1 dorsal roots in these nuclei is similar in that fibers from: (a) C5 through C8 terminate in a central core region about which other dorsal root fibers terminate in oblique serial laminae, (b) rostral roots terminate in ventrolateral regions, while those from caudal roots end in dorsomedial regions, and (c) all of these roots, except C1 and C2, terminate throughout the rostrocaudal extent of both nuclei.

13. Ascending fibers from C1 through T1 dorsal roots projecting to the cuneate and accessory cuneate nuclei terminate in both exclusive and overlapping zones; fiber from one dorsal root partially overlap the territory of the next highest root.

14. Fibers from T2 through T7 dorsal

ots projecting to the cuneate and accessory cuneate nuclei terminate in smaller regions of the nuclei, exhibit greater overlap and are distinctive in that these fibers terminate primarily in dorsomedial parts of the cuneate nucleus and in lateral parts of the accessory cuneate nucleus.

15. Cytological and degeneration studies suggest that the central cervical nucleus and the intermediate nucleus of the medulla: (a) constitute parts of the same cell column, and (b) receive fibers from the upper five cervical dorsal roots which overlap in large regions of the cell column and terminate in rich pericellular arborizations. Afferent fibers to all parts of this cell column are derived from the C2 dorsal root.

16. The upper five cervical dorsal roots project fibers to the supraspinal nucleus, primarily to the dorsomedial part. The greatest number of fibers terminating in this nucleus are derived from the C1 and C2 dorsal roots.

LITERATURE CITED

- Anderson, F. D. 1960 Distribution of dorsal root fibers in the cat spinal cord. *Anat. Rec.*, 136: 154.
- Aluminau, L. 1891 Ueber den äusseren Kern des Keilstranges im verlängerten Mark. *Neur. Zentr.*, 10: 226-232.
- Brodal, A. 1941 Die Verbindungen des Nucleus cuneatus externus mit dem Kleinhirn beim Kaninchen und bei der Katze. *Experimentelle Untersuchungen. Z. ges. Neur. u. Psychiat.*, 171: 167-199.
- Brodal, A., and O. Pompeiano. 1957 The vestibular nuclei in the cat. *J. Anat.*, 91: 438-454.
- Brodal, A., and B. Rexed. 1953 Spinal afferents to the lateral cervical nucleus in the cat. An experimental study. *J. Comp. Neur.*, 98: 179-212.
- Cajal, S. Ramón y. 1909 Histologie du système nerveux de l'homme et des vertébrés. Maloine, Paris, vol. I.
- Carpenter, M. B., B. M. Stein and J. E. Shriver. 1968 Central projections of spinal dorsal roots in the monkey II. Lower thoracic, lumbosacral and coccygeal dorsal roots. *Am. J. Anat.*, 123: 75-118.
- Chang, H. T., and T. C. Ruch. 1947 Organization of the dorsal columns of the spinal cord and their nuclei in the spider monkey. *J. Anat.*, 81: 140-149.
- Collier, J., and E. F. Buzzard. 1903 The degenerations resulting from lesions of posterior nerve roots and from transverse lesions of the spinal cord in man. A study of twenty cases. *Brain*, 26: 559-591.
- Corbin, K. B., and J. C. Hinsey. 1935 Intramedullary course of the dorsal root fibers of each of the first four cervical nerves. *J. Comp. Neur.*, 63: 119-126.
- Corbin, K. B., W. T. Lhamon and D. W. Pettit. 1937 Peripheral and central connections of the upper cervical dorsal root ganglia in the Rhesus monkey. *J. Comp. Neur.*, 66: 405-414.
- Dunn, J., and H. Matzke. 1967 Central distribution of the dorsal root of the first cervical nerve of the marmoset monkey. *Anat. Rec.*, 157: 357.
- Escobar, J. 1948 The afferent connections of the 1st, 2nd, and 3rd cervical nerves in the cat. An analysis by Marchi and Rasdolsky methods. *J. Comp. Neur.*, 89: 79-92.
- Ferraro, A., and S. E. Barrera. 1935a The nuclei of the posterior funiculi in *Macacus rhesus*. An anatomical and experimental investigation. *Arch. Neur. Psychiat.*, 33: 262-275.
- . 1935b Posterior column fibers and their termination in *Macacus rhesus*. *J. Comp. Neur.*, 62: 507-530.
- Flechsig, P. 1876 Die Leitungsbahnen im Gehirn und Rückenmark des Menschen auf Grund entwicklungsgeschichtlicher Untersuchungen. Engelmann, Leipzig.
- Gehuchten, A. van. 1901 Recherches sur la terminaison centrale des nerfs sensibles périphériques. IV. La racine postérieure des deux premiers nerfs cervicaux. *Le Névralg.*, T. 2, pp. 227-256.
- Grant, G., and B. Rexed. 1958 Dorsal spinal root afferents to Clarke's column. *Brain*, 81: 567-576.
- Ha, H., and C. N. Liu. 1966 Organization of the spino-cervico-thalamic system. *J. Comp. Neur.*, 127: 445-470.
- Ha, H., and F. Morin. 1964 Comparative anatomical observations of the cervical nucleus, nucleus cervicalis lateralis, of some primates. *Anat. Rec.*, 148: 374-375.
- Hand, P. J. 1966 Lumbosacral dorsal root terminations in the nucleus gracilis of the cat. Some observations on terminal degeneration in other medullary sensory nuclei. *J. Comp. Neur.*, 126: 137-156.
- Hekmatpanah, J. 1961 Organization of tactile dermatomes, C1 through L4, in cat. *J. Neurophysiol.*, 24: 129-140.
- Hollis, W. A. 1884 Researches into the histology of the central gray substance of the spinal cord and medulla oblongata. *J. Anat. & Physiol.*, 18: 62-65.
- Howell, A. B., and W. L. Straus, Jr. 1933 The spinal nerves. In: *The Anatomy of the Rhesus Monkey*, C. G. Hartman and W. L. Straus, Jr. (Eds.), Hafner Publ. Co., New York, Chap. 16, 307-327.
- Jacobsohn, L. 1909 Ueber die Kerne des menschlichen Hirnstammes (der Medulla oblongata, des Pons und des Pedunculus). *Neur. Zbl.*, 28: 674-679.
- Kerr, F. W. L. 1961 Structural relation of the trigeminal spinal tract to upper cervical roots and the solitary nucleus in the cat. *Exptl. Neur.*, 4: 134-148.
- Kuypers, H. G. J. M., and J. D. Tuerk. 1964 The distribution of the cortical fibres within the nuclei cuneatus and gracilis in the cat. *J. Anat.*, 98: 143-162.
- Liu, C. N. 1956 Afferent nerves to Clarke's and the lateral cuneate nuclei in the cat. *Arch. Neur. Psychiat.*, 75: 67-77.
- Meessen, H., and J. Oliszewski. 1949 A Cytoarchitectonic Atlas of the Rhombencephalon of the Rabbit. S. Karger, Basel.
- Morin, F., and J. V. Catalano. 1955 Central connections of a cervical nucleus (nucleus cervicalis lateralis of the cat). *J. Comp. Neur.*, 103: 17-32.
- Nauta, W. J. H., and P. A. Gyax. 1954 Silver impregnation of degenerating axons in the central nervous system: A modified technique. *Stain Tech.*, 29: 91-93.
- Oliszewski, J. 1950 On the anatomical and functional organization of the trigeminal nucleus. *J. Comp. Neur.*, 92: 401-413.

in some animals small amounts of terminal degeneration were present in cell group x, even though none was detectable in the posterior spinocerebellar tract or in the inferior cerebellar peduncle.

CONCLUSIONS

The following conclusions were drawn from this study:

1. Degeneration in the spinal cord is most profuse at the level of dorsal rhizotomy and progressively diminishes in segments rostral and caudal to the sectioned root; progressive diminution of degeneration is greatest in the anterior horn.

2. At the level of dorsal rhizotomy, profuse terminal degeneration is present in laminae III and IV, central and medial portions of laminae V and VI, and among certain cell groups of lamina IX. Fewer fibers appear to terminate in laminae VII and VIII.

3. No dorsal root fibers from C1 project into the head of the posterior horn in the upper cervical region and fibers passing to the anterior horn are sparse.

4. Terminal fibers from dorsal roots C2 through C5 are localized to particular portions of laminae III and IV in a manner suggesting a somatotopic arrangement.

5. Fibers from dorsal roots of the brachial enlargement project to central and medial parts of lamina VI from four (C5) to eight (T1) segments rostral to their entry.

6. Cervical and upper thoracic dorsal roots project fibers to cell groups of lamina IX by distinctive pathways through either medial, or central, parts of laminae VII and VIII. At different levels the number of fibers following these pathways varies so that the greatest number of fibers from: (a) C5 through T1 dorsal roots course through central parts of lamina VII, (b) T2 through T7 dorsal roots project via medial parts of laminae VII and VIII, and (c) C2 through C4 dorsal roots project through both medial and central parts of laminae VII and VIII.

7. Cell groups of the spinal accessory nucleus in the upper cervical cord receive fibers from C2 through C5 dorsal roots with C3 contributing the greatest number of fibers.

8. Overlapping projections to the dorsal nucleus are derived from C5 through T1 dorsal roots; single dorsal roots distribute fibers to this cell column in four to ten spinal segments, with the most profuse degeneration: (a) derived from C5 through T1 dorsal roots, and (b) terminating in the cell column nearest the sectioned root.

9. A small, but distinct, bundle of fiber from all cervical and all upper thoracic dorsal roots terminate in the intermediate medial nucleus and the area ventral to it at the level of root entrance, and in adjacent spinal segments.

10. Ascending fibers in the fasciculus cuneatus in the monkey: (a) arise from cervical and upper seven thoracic dorsal roots, and (b) exhibit only a general segregation because of extensive overlap. Dorsal roots of the brachial enlargement contribute the largest number of fibers.

11. Descending collaterals of cervical and upper thoracic dorsal roots form discrete bands in the posterior funiculus, dorsal and parallel to, but at varying distances from the posterior intermediate sulcus. These bands resemble those of ascending fibers of the same root, except that they do not migrate as far dorsomedially, have a greater concentration of fibers in ventromedial locations, and are smaller.

12. Ascending branches of fibers from all cervical and the upper seven thoracic dorsal roots project somatotopically to the cuneate and accessory cuneate nuclei. The pattern of termination of fibers from C1 through T1 dorsal roots in these nuclei is similar in that fibers from: (a) C2 through C8 terminate in a central region about which other dorsal root fibers terminate in oblique serial laminae rostral roots terminate in ventrolateral regions, while those from caudal roots terminate in dorsomedial regions, and (c) all these roots, except C1 and C2, terminate throughout the rostrocaudal extent of the nuclei.

13. Ascending fibers from C1 through dorsal roots projecting to the cuneate and accessory cuneate nuclei terminate in exclusive and overlapping zones; fibers from one dorsal root partially overlap territory of the next highest root.

14. Fibers from T2 through T7 d

- Olszewski, J., and D. Baxter 1954 Cytoarchitecture of the Human Brain Stem. S. Karger, Basel.
- Oscarsson, O. 1965 Functional organization of the spino- and cuneocerebellar tracts. *Physiol. Rev.*, 45: 495-522.
- Papez, J. W. 1929 *Comparative Neurology*. Thomas Y. Crowell Co., New York.
- Pass, I. J. 1933 Anatomic and functional relationship of nuc. dorsalis (Clarke's column). *Arch. Neur. Psychiat.*, 30: 1025-1045.
- Pompeiano, O., and A. Brodal 1957 Spino-vestibular fibers in the cat. An experimental study. *J. Comp. Neur.*, 108: 353-382.
- Ralston, H. J. III 1965 The organization of the substantia gelatinosa Rolandi in the cat lumbosacral spinal cord. *Z. Zellforsch.*, 67: 1-23.
- Ranson, S. W., H. K. Davenport and E. A. Doles 1932 Intramedullary course of the dorsal root fibers of the first three cervical nerves. *J. Comp. Neur.*, 54: 1-12.
- Rexed, B. 1952 The cytoarchitectonic organization of the spinal cord in the cat. *J. Comp. Neur.*, 96: 415-496.
- 1954 A cytoarchitectonic atlas of the spinal cord in the cat. *J. Comp. Neur.*, 100: 297-400.
- 1964 Some aspects of the cytoarchitectonics and synaptology of the spinal cord. In: *Organization of the Spinal Cord*, J. C. Eccles and J. P. Schädé (Eds.). Vol. 11, *Progress in Brain Research*. Elsevier, Amsterdam, pp. 58-90.
- Rexed, B., and A. Brodal 1951 The nucleus cervicalis lateralis. A spinocerebellar relay nucleus. *J. Neurophysiol.*, 14: 399-407.
- Schmiedt, J. 1939 Das Verhalten der Hinterwurzelkollateralen in Rückenmark. *Z. Anat. Entwicklsgesch.*, 109: 665-687.
- Schultze, F. 1883 Beitrag zur Lehre von der secondären Degeneration im Rückenmark des Menschen nebst Bemerkungen über die Anatomie der Tabes. *Arch. Psychiat. Nervenkr.*, 14: 359-390.
- Schwartz, H. G., G. E. Roulhac, R. L. Lam and J. L. O'Leary 1951 Organization of the fasciculus solitarius in man. *J. Comp. Neur.*, 94: 221-238.
- Sherrington, C. S. 1893 Note on the spinal portion of some ascending degenerations. *J. Physiol. (London)*, 14: 255-302.
- 1898 Experiments in examination of the peripheral distribution of the fibres of the posterior roots of some spinal nerves. Part II. *Phil. Trans. Roy. Soc. London, Ser. B*, 190: 45-185.
- Sprague, J. M. 1958 The distribution of dorsal root fibres on motor cells in the lumbosacral spinal cord of the cat, and the site of excitatory and inhibitory terminals in monosynaptic pathways. *Proc. Roy. Soc. B.*, 149: 534-556.
- Sprague, J. M., and H. Ha 1964 The terminal field of dorsal root fibers in the lumbosacral spinal cord of the cat, and the dendritic organization of the motor nuclei. In: *Organization of the Spinal Cord*, J. C. Eccles and J. P. Schädé (Eds.). Vol. 11, *Progress in Brain Research*. Elsevier, Amsterdam, pp. 120-15.
- Sterling, P., and H. G. J. M. Kuypers 1967 Anatomical organization of the brachial spinal cord of the cat. The distribution of dorsal root fibers. *Brain Research*, 4: 1-15.
- Szentágothai, J. 1964 Neuronal and synaptic arrangement in the substantia gelatinosa Rolandi. *Comp. Neur.*, 122: 219-240.
- Szentágothai, J., and A. Albert 1955 The synaptology of Clarke's column. *Acta morphol. (Budapest)*, 5: 43-52.
- Szentágothai, J., and T. Kiss 1949 Projection dermatomes in the substantia gelatinosa. *Arch. Neur. Psychiat.*, 62: 734-744.
- Thomas, C. E., and C. M. Combs 1965 Spinal cord segments. B. Gross structure in the monkey. *Anat. Anat.*, 116: 205-216.
- Torvik, A. 1956 Afferent connections to the sensory trigeminal nuclei, the nucleus of the solitary and adjacent structures. An experimental study in the rat. *J. Comp. Neur.*, 106: 51-142.
- Walberg, F., D. Bowsher and A. Brodal 1958 Termination of primary vestibular fibers in vestibular nuclei in the cat. An experimental study with silver methods. *J. Comp. Neur.*, 110: 391-407.
- Walker, A. E., and T. A. Weaver, Jr. 1942 The organization and termination of the fibers of the posterior columns in *Macaca mulatta*. *J. Comp. Neur.*, 76: 145-158.
- Wall, P. D. 1960 Cord cells responding to mechanical damage, and temperature of skin. *J. Neurophysiol.*, 23: 197-210.
- Yee, J., and K. B. Corbin 1939 The intramedullary course of the upper five cervical dorsal root fibers in the rabbit. *J. Comp. Neur.*, 70: 297-304.

VENTRAL DORSAL ROOT PROJECTIONS I
 by E. Shriver, Bennett M. Stein and Malcolm B. Carpenter

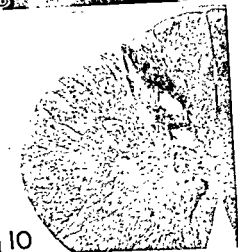
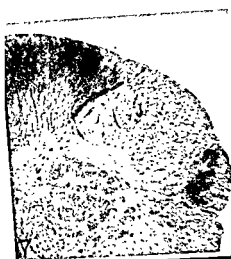


PLATE 1

EXPLANATION OF FIGURES

- 7 Rhesus C-1008. Photomicrograph of degeneration following section of the C1 dorsal root on the right. Degeneration is present dorsal to the head of the posterior horn at C1. Nauta-Gygax. $\times 15$.
- 8 Rhesus C-978. Photomicrograph of degeneration in root entry zone following section of the C3 dorsal root on the right. Note degeneration in the central part of laminae III and IV and fibers coursing ventrally through lamina V into the central cervical nucleus. Nauta-Gygax. $\times 16$.
- 9 Rhesus C-1014. Photomicrograph of degeneration at C5 following section of the dorsal root at that level. Note fibers passing medially to the intermedio-medial nucleus ventrolateral to the central canal. Nauta-Gygax. $\times 21$.
- 10 Rhesus C-913. Photomicrograph of degeneration at T2 following section of the dorsal root at that level. Root fibers enter laminae III and IV mainly by coursing through medial parts of lamina II. Nauta-Gygax. $\times 16$.
- 11 Rhesus C-1014. Photomicrograph of ascending degeneration in the fasciculi cuneatus resulting from section of dorsal roots C5 (left) and C8 (right). Less intense degeneration in the fasciculi gracilis resulted from section of dorsal roots L6 (left) and Co1 (right). Nauta-Gygax. $\times 13$.
- 12 Rhesus C-1025. Photomicrograph of degeneration at T7 following section of the dorsal root at that level. Degeneration is present in the fasciculus cuneatus, laminae III and IV and in the dorsal nucleus. Nauta-Gygax. $\times 64$.

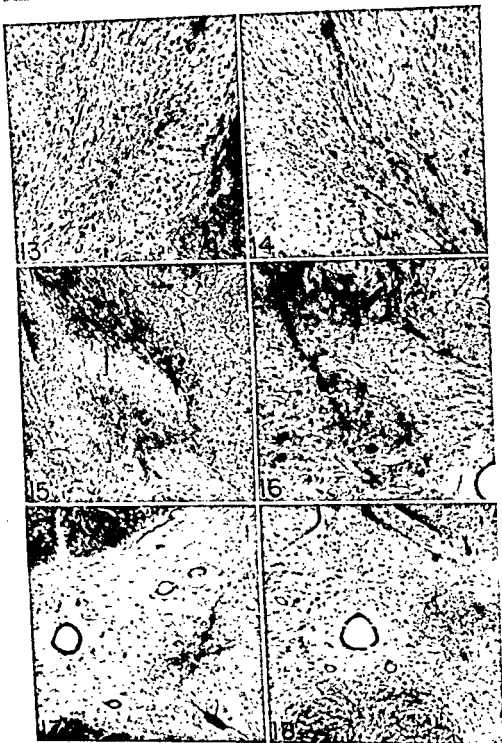


PLATE 2

EXPLANATION OF FIGURES

- 13 Rhesus C-981. Photomicrograph of terminal degeneration localized to the lateral parts of laminae III and IV on the right side at C2 following section of the dorsal root at that level. Nauta-Gygax. $\times 95$.
- 14 Rhesus C-981. Photomicrograph of terminal degeneration localized to the lateral parts of laminae III and IV on the left side at C5 following section of the C4 dorsal root. Nauta-Gygax. $\times 105$.
- 15 Rhesus C-913. Photomicrograph of terminal degeneration in laminae III and IV on the left side at T2 following section of the dorsal root at that level. Nauta-Gygax. $\times 50$.
- 16 Rhesus C-913. Photomicrograph of degenerated fibers from the T2 dorsal root projecting to the dorsal nucleus at T3 on the left. Nauta-Gygax. $\times 95$.
- 17 Rhesus C-1014. Photomicrograph of C8 dorsal root fibers projecting to the intermediomedial nucleus at C7 on the right side. Nauta-Gygax. $\times 95$.
- 18 Rhesus C-1024. Photomicrograph of T5 dorsal root fibers projecting to the dorsal nucleus at the level of root section. Nauta-Gygax. $\times 95$.

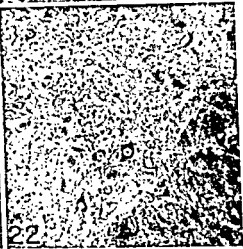
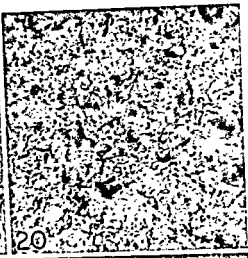
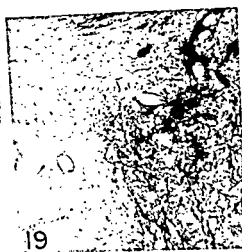


PLATE 3

EXPLANATION OF FIGURES

- 19 Rhesus C-1006. Photomicrograph of fibers from the C2 dorsal root arborizing about cells of the central cervical nucleus at the C2 level. Nauta-Gygax. $\times 100$.
- 20 Rhesus C-913. Photomicrograph of fibers from the C2 dorsal root arborizing about cells of the central cervical nucleus at the level of root section. Nauta-Gygax. $\times 240$.
- 21 Rhesus C-1014. Photomicrograph of C8 dorsal root fibers passing from the fasciculus cuneatus into the medial part of lamina VI at C5. Nauta-Gygax. $\times 50$.
- 22 Rhesus C-978. Photomicrograph of C3 dorsal root fibers passing to the spinal accessory cell group of lamina IX at the C3 level. Nauta-Gygax. $\times 125$.
- 23 Rhesus C-1014. Photomicrograph of C8 dorsal root fibers on the right projecting into motor cell groups of lamina IX at the C7 level. Nauta-Gygax. $\times 240$.
- 24 Rhesus C-970. Photomicrograph of T4 dorsal root fibers on the left projecting ventrally through the medial parts of laminae VII and VIII to cell groups of lamina IX at T4. Nauta-Gygax. $\times 100$.

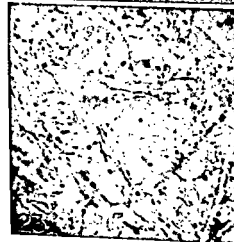
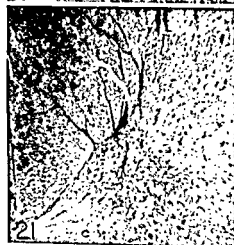
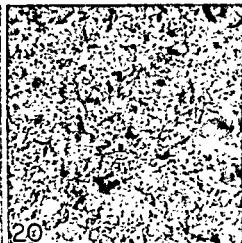


PLATE 4

EXPLANATION OF FIGURES

- 25 Rhesus C-1008. Photomicrograph of degenerated fibers from the C1 dorsal root terminating in the most ventral part of the accessory cuneate nucleus. Nauta-Gygax. $\times 40$.
- 26 Rhesus C-1006. Photomicrograph of degenerated fibers from the C2 dorsal root terminating in ventral portions of both the cuneate and accessory cuneate nuclei. Nauta-Gygax. $\times 16$.
- 27 Rhesus C-974. Photomicrograph of degenerated C5 dorsal root fibers terminating in localized zones of the cuneate and accessory cuneate nuclei. Nauta-Gygax. $\times 16$.
- 28 Rhesus C-967. Photomicrograph of degenerated C6 dorsal root fibers terminating in localized zones of the cuneate and accessory cuneate nuclei. Nauta-Gygax. $\times 13$.
- 29 Rhesus C-1014. Photomicrograph of C8 dorsal root fibers terminating in localized zones of the cuneate and accessory cuneate nuclei. Nauta-Gygax. $\times 16$.
- 30 Rhesus C-913. Photomicrograph of a horizontal brain stem section showing terminal degeneration from the T2 dorsal root in the lateral part of the left accessory cuneate nucleus. Nauta-Gygax. $\times 50$.

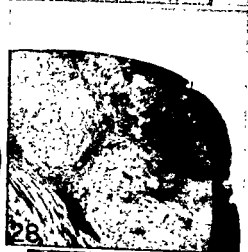
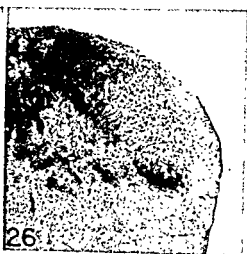


PLATE 4

EXPLANATION OF FIGURES

- 25 Rhesus C-1008. Photomicrograph of degenerated fibers from the C1 dorsal root terminating in the most ventral part of the accessory cuneate nucleus. Nauta-Gygax. $\times 40$.
- 26 Rhesus C-1006. Photomicrograph of degenerated fibers from the C2 dorsal root terminating in ventral portions of both the cuneate and accessory cuneate nuclei. Nauta-Gygax. $\times 16$.
- 27 Rhesus C-974. Photomicrograph of degenerated C5 dorsal root fibers terminating in localized zones of the cuneate and accessory cuneate nuclei. Nauta-Gygax. $\times 16$.
- 28 Rhesus C-967. Photomicrograph of degenerated C6 dorsal root fibers terminating in localized zones of the cuneate and accessory cuneate nuclei. Nauta-Gygax. $\times 13$.
- 29 Rhesus C-1014. Photomicrograph of C8 dorsal root fibers terminating in localized zones of the cuneate and accessory cuneate nuclei. Nauta-Gygax. $\times 16$.
- 30 Rhesus C-913. Photomicrograph of a horizontal brain stem section showing terminal degeneration from the T2 dorsal root in the lateral part of the left accessory cuneate nucleus. Nauta-Gygax. $\times 50$.

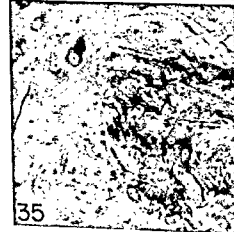


PLATE 5

EXPLANATION OF FIGURES

- 31 Rhesus C-913. Photomicrograph of horizontal brain stem section showing ascending fibers from the C2 dorsal root projecting profusely to the accessory cuneate nucleus and giving off small fascicles to the cuneate nucleus. Nauta-Gygax. $\times 15$.
- 32 Rhesus C-915. Photomicrograph of a horizontal brain stem section showing terminal degeneration from the C7 dorsal root in the central part of the cuneate nucleus. Nauta-Gygax. $\times 14$.
- 33-34 Rhesus C-970. Photomicrographs of C2 dorsal root fibers arborizing about clusters of cells in the intermediate nucleus of the medulla. Nauta-Gygax. $\times 40$, $\times 100$
- 35 Rhesus C-970. Photomicrograph of terminal degeneration from the C2 dorsal root in the rostral part of the intermediate nucleus. A few cells of the dorsal motor nucleus of the vagus nerve can be seen in the upper left. Nauta-Gygax. $\times 260$.
- 36 Rhesus C-1008. Photomicrograph of degenerated C1 dorsal root fibers projecting into the region of the supraspinal nucleus. Nauta-Gygax. $\times 240$.

Central Projections of Spinal Dorsal Roots in the Monkey¹

II. LOWER THORACIC, LUMBOSACRAL AND COCCYGEAL DORSAL ROOTS

MALCOLM B. CARPENTER, BENNETT M. STEIN² AND JOYCE E. SHRIVER¹
Department of Anatomy, College of Physicians and Surgeons, Columbia University, New York, N.Y.

ABSTRACT A study of the central distribution of lower thoracic, lumbosacral and coccygeal dorsal roots (DR) was made in 11 monkeys. Degeneration resulting from 17 individual dorsal rhizotomies was studied in multiple spinal and medullary sections stained by the Nauta technic.

At the rhizotomy level all DR project fibers to: (1) portions of laminae III and IV, (2) the intermediomedial nucleus, and (3) portions of laminae VII, VIII and IX. Lower thoracic, lumbar and the first sacral (S1) DR project in overlapping fashion to particular portions of Clarke's column, ascending and descending fibers terminate in a spatially organized manner. Lower lumbar DR project to medial lamina VI throughout the lumbar enlargement. DR fibers reach cell groups of lamina IX via two trajectories, one of which is dominant in the lumbar enlargement.

Ascending DR fibers in the fasciculus gracilis. (1) arise caudal to T7, (2) exhibit only general segregation due to overlap, and (3) project in an overlapping somatotopic fashion throughout the rostrocaudal extent of the nucleus gracilis. Zones of the nucleus gracilis receiving fibers are organized, so that (1) DR of the lumbar enlargement project to a central core region, (2) lower thoracic and upper lumbar DR project to narrow oblique laminae lateral to the core, and (3) S1 and Co1 DR project to crescent-shaped dorsomedial regions. Less autonomous terminal representation of DR fibers was found in the nucleus gracilis than in other posterior column nuclei.

As emphasized in Part I of this study (Shriver, Stein and Carpenter, '68), most previous anatomical investigations of the central projections of dorsal root fibers have been based upon the Marchi method and section of a limited number of dorsal roots in restricted regions of the spinal cord. Studies of the projections of certain lower thoracic, lumbosacral and coccygeal dorsal roots, done in the cat and dog (Szentágothai and Albert, '55; Liu, '56; Grant and Rexed, '58; Szentágothai, '64; Sprague and Ha, '64; Kuypers and Tuerk, '64; Hand, '66), have utilized silver staining methods. Investigations in the monkey (Ferraro and Barrera, '34, '35; Walker and Weaver, '42; Chang and Ruch, '47), based upon partial cordotomies and selective dorsal root sections, have used the Marchi method. Although Marchi studies have contributed little information concerning projections of dorsal root fibers within the spinal gray, they have provided information concerning the somatotopic organization of ascending fibers in the posterior columns

and in the nucleus gracilis. Studies using silver staining methods have provided important details concerning the distribution of dorsal root fibers in the spinal gray (Szentágothai and Albert, '55; Liu, '56; Grant and Rexed, '58; Szentágothai, '64; Sprague and Ha, '64) and information regarding termination of fibers in the nucleus gracilis (Kuypers and Tuerk, '64; Hand, '66). Recent anatomical (Kuypers and Tuerk, '64; Hand, '66) and physiological (Kuhn, '49; Gordon and Paine, '60; Perl, Whitlock and Gentry, '62; McComas, '63; Winter, '65) studies suggest that dorsal root fibers may terminate in a dual fashion in different parts of the nucleus gracilis, which has been interpreted to suggest rostrocaudal differences in the size of the receptor fields and/or differences in modal-

¹This investigation was supported by grant NB-01538-09 from the Institute of Neurological Diseases and Blindness of the National Institutes of Health, Bethesda, Maryland.

²Associate Neurosurgeon, Department of Neurological Surgery.

³Postdoctoral Fellow in neuroanatomy supported by training grant 5T1-NB 5242-08 from the Institute of Neurological Diseases and Blindness.

the intermediolateral cell group. Fibers passed from lamina VII ventrally into medial parts of lamina VIII and followed the border of the spinal gray into lamina IX. Within lamina IX degeneration was maximal about cells of the ventromedial group. Only a few fibers traversing central parts of laminae VII and VIII reached cells of the lateromedial cell group of lamina IX.

At the T9 spinal segment a marked reduction in the quantity of degeneration was observed. In rhesus C-970 degeneration in laminae III and IV was seen in lateral regions, while degeneration was present in medial parts of these laminae in rhesus C-1017. Slight differences were noted in the location of degeneration in the dorsal nucleus. In rhesus C-970 it was present in lateral portions, but in C-1017 it occupied dorsal regions of the nucleus. Only relatively sparse degeneration was seen in laminae VIII and IX.

At the T7 spinal segment reduced degeneration similar to that present at the T9 level was observed. This degeneration was principally in the central and medial portions of laminae III and IV, dorsolateral portions of the dorsal nucleus, and adjacent portions of lamina VII. Degeneration was sparse in the medial part of lamina VIII and in lamina IX.

Descending degeneration from the T8 dorsal root in both animals formed a narrow band in the lateral third of the posterior column separated from the posterior horn by a zone of normal fibers. This degeneration was traced as far caudally as T12 (C-970) and L2 (C-1017). Fibers given off in lower thoracic segments in rhesus C-970 were confined principally to parts of lamina VII and the dorsal nucleus; degeneration was maximal in lateral portions of the dorsal nucleus caudal to T10 in both animals.

Similar ascending degeneration in both animals occupied progressively more medial parts of the posterior column. At the T4 level the ventromedial portion of the band of ascending degeneration was present in the lateral part of the fasciculus gracilis, while the dorsolateral portion was located in medial parts of the fasciculus cuneatus (fig. 13). A gradual shift of the degeneration occurred rostrally so that at C8 only a tiny amount of the degeneration

was present in the dorsomedial part of the fasciculus cuneatus and the majority of the degeneration occupied the lateral border of the fasciculus gracilis. Thus, ascending degeneration was present in different locations on both sides of the posterior intermediate septum in upper thoracic segments. Ascending degeneration within the spinal gray rostral to T7 was confined to the dorsal nucleus and the adjacent portions of lamina VII. Degeneration within the dorsal nucleus, primarily the dorsolateral part, was seen as far rostrally as T5 (C-970) and T2 (C-1017).

Sections of the medulla were cut horizontally (C-970) and transversely (C-999 and C-1017). Posterior column degeneration in the three animals was contained in lateral portions of the fasciculus gracilis at caudal medullary levels. Relatively few fibers appeared to terminate in ventral parts of the nucleus gracilis at this level. In sections through mid- and rostral parts of the nucleus gracilis moderate amounts of terminal degeneration were seen within the lateral border of the nucleus (fig. 31). Initially these degenerated fibers occupied nearly the entire lateral border of the nucleus, but further rostrally they were confined to a smaller, more dorsal region (fig. 5). Fiber terminations were greatest in the rostral third of the nucleus gracilis. A small, but distinct, number of fibers entered the most medial part of the nucleus cuneatus in those regions where the nuclei gracilis and cuneatus have a common border. Rostrally degenerated fibers tended to invade more dorsal portions of the medial border of the cuneate nucleus.

In rhesus C-999 moderate degeneration was seen in cell group x and in portions of the inferior vestibular nucleus (Brodal and Pompeiano, '57). Degeneration in these nuclei appeared to be related to ascending degeneration of spinovestibular fibers (Pompeiano and Brodal, '57) which course in association with fibers of the posterior spinocerebellar tract.

Ninth thoracic root. In rhesus C-999 the ninth thoracic dorsal root was sectioned, but this operation, like that on the opposite side at T8, was complicated by unintentional injury to the lateral and anterior funiculi of the spinal cord.

ity segregation. In view of these data which are difficult to reconcile with classical concepts, further information concerning the termination of dorsal root fibers in the nucleus gracilis seems needed.

Material presented in this report is a continuation of Part I of a study of the central projections of dorsal root fibers in the monkey. In Part II anatomical data concerning lower thoracic, lumbosacral and coccygeal dorsal root projections are presented. Attempts have been made to compare observations in the two parts of this study, and to correlate certain anatomical and physiological data.

MATERIAL AND METHODS

In 11 rhesus monkeys single dorsal rhizotomies were done at different levels and on different sides. As reported in Part I, three or four different dorsal roots at selected levels were sometimes sectioned in individual animals to conserve time, effort and material. Table 1 supplements similar data contained in Part I of this study. Some of the animals were used in both parts of this study. Dorsal roots sectioned included four lower thoracic (i.e., T8, T9, T10 and T12), all seven lumbar, and the first sacral and coccygeal. A total of 17 dorsal rhizotomies were done at the levels mentioned.

The operative procedures, histological techniques and methods of study used here were the same as those described in Part I of this study.

OBSERVATIONS

Lower thoracic dorsal roots

Four lower thoracic dorsal roots (i.e., T8, T9, T10 and T12) were sectioned individually in five monkeys.

Eighth thoracic dorsal root. The eighth thoracic dorsal root was sectioned in three animals (C-970, C-999 and C-1017). In one animal (C-999) dorsal rhizotomy was complicated by bilateral injury to the anterior and lateral funiculi which precluded evaluation of the degeneration within the spinal gray. Spinal and medullary degeneration in the other two animals was similar but not identical.

Degenerated fibers from the root en zone projected into the most lateral portion of the posterior column and into the zone of Lissauer. Fibers in ventromedial parts of the fasciculus gracilis approached the posterior median septum. Degenerated fibers coursed obliquely through medial portions of lamina II and arborized profusely about cells in medial and central parts of laminae III and IV (fig. 7). Relatively sparse degeneration was seen in lamina V. In rhesus C-970 diffuse degeneration was present in all parts of the dorsal nucleus, but in rhesus C-1017 degeneration in the dorsal nucleus was found mainly in ventrolateral regions. A small amount of degeneration was seen in portions of lamina VII lateral to the dorsal nucleus, and an island of degeneration was noted within the intermediomedial nucleus. No degeneration was present

TABLE 1
Dorsal roots sectioned in eleven monkeys

Animal Number	Spinal roots																			
	C1	C2	C3	C5	C6	C7	C8	T1	T2	T4	T6	T7	T8	T9	T10	T12	L1	L2	L3	L4
C-912			R					L									R			L
C-913*		R						L	L									R		
C-914				R				L											R	L
C-915*						R						L								
C-916		R													L					R
C-970*		R								L			R	L						
C-999																			R	
C-1011					L														R	
C-1012							R								L				R	
C-1014				L							L			R						L
C-1017												R								R

*In 11 animals 32 dorsal roots were sectioned individually on different sides and at different levels. Some of the observations on these animals were reported in Part I of this study. Letters R and L refer to right and left sides and indicate roots sectioned. Asterisks indicate that sections of the medulla were cut in horizontal planes.

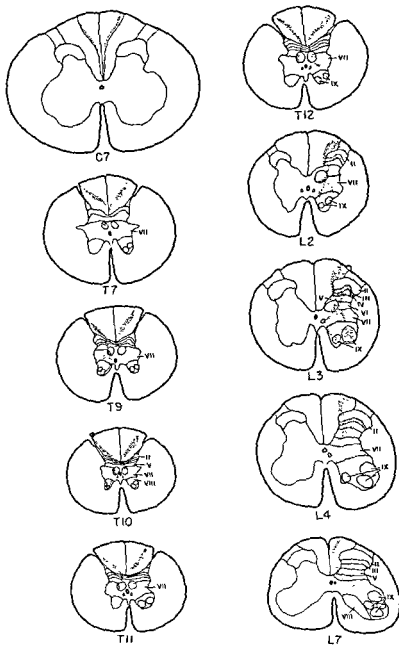


Fig 1 Drawings of the central distribution of degenerated fibers at spinal levels following section of T10 (left) and L3 (right) dorsal roots. Projected spinal cord sections of rhesus C-916 (T10) and C-914 (L3) were used in preparing these drawings.

Ascending degeneration, resulting from trauma, was present in both posterior spinocerebellar tracts. At the level of rhizotomy a moderate number of degenerated fibers from the root entry zone occupied a band along the lateral aspect of the posterior column. From this region degenerated fibers coursed obliquely through and around the medial portion of lamina II. Extensive degeneration was seen throughout the spinal gray except in lamina II. Because of these complicating features no description of degeneration within the spinal gray will be given.

In the posterior column, where no trauma was evident, descending degeneration from the T9 dorsal rhizotomy formed a narrow band in the lateral third of the posterior column, separated from the posterior horn by a narrow band of normal fibers. This degeneration was traced caudally as far as the L1 level. Ascending degeneration, localized to a diagonal band in the lateral portion of the fasciculus gracilis, shifted progressively medial at rostral spinal levels. In upper thoracic and cervical segments the most peripheral portion of this degenerated band occupied the dorsomedial border of the fasciculus cuneatus. As this band of degeneration extended ventromedially it crossed the posterior intermediate septum and lay along the lateral border of the fasciculus gracilis; the most ventral fibers were adjacent to the posterior median septum. A smaller proportion of the ascending degeneration was within the fasciculus cuneatus than following T8 dorsal rhizotomy (C-970, C-999 and C-1017).

Sections of the medulla were cut transversely. Degeneration from the T9 dorsal rhizotomy was located primarily within the gracile nucleus, but a few fibers projected to the medial parts of the cuneate nucleus. Extensive degeneration which appeared to originate from the posterior spinocerebellar tract was observed to project into cell group x (Brodal and Pompeiano, '57; Pompeiano and Brodal, '57).

Degeneration within the fasciculus gracilis was located laterally in sections through caudal portions of the nucleus gracilis. This portion of the nucleus remained relatively free of preterminal degeneration except for a small area

ventrolaterally. In mid-portions of the nucleus degeneration was located in a band along the dorsolateral border of the nucleus. In ventral portions of the nucleus this band lay medial to, and somewhat removed from, the lateral border of the nucleus. In the rostral portions of the nucleus gracilis degeneration diminished in amount, and although located predominantly in the dorsolateral portions of the nucleus, was not restricted to this area. Small amounts of degeneration were scattered throughout the central portion of the nucleus.

The pattern of degeneration seen in the nucleus gracilis was similar to that seen after T8 dorsal rhizotomy except that it was slightly more profuse and extended into somewhat more ventromedial portions of the nucleus.

Tenth thoracic root. In rhesus C-91 section of the tenth thoracic dorsal root produced a relatively narrow band of degenerated fibers along the entire lateral border of the fasciculus gracilis adjacent to the posterior horn (fig. 1). Part of the fibers projected to medial parts of laminae III and IV by coursing medially through parts of lamina II. Other fibers from the fasciculus gracilis passed directly ventrolateral parts of the dorsal nucleus. Relatively few degenerated fibers were seen in lamina V or in portions of lamina VII removed from the dorsal nucleus. A few fibers were given off to the intermediate medial nucleus, but the major portion of the degeneration from lamina VII projected ventrally into medial parts of lamina VIII. Fibers coursing through the medial part of lamina VIII followed the curve of the anterior horn and terminated primarily in the ventromedial cell group lamina IX. Relatively sparse degeneration in central parts of laminae VII and VI projected towards the lateromedial cell group of lamina IX.

In adjacent thoracic segments, T11 at T9, oblique narrow bands of degeneration in the fasciculus gracilis were removed slightly from the medial surface of the posterior horn. The only degeneration in the spinal gray at T11 was in the lateral part of the dorsal nucleus. In the T9 spinal segment a moderate reduction in the amount of degeneration was observed

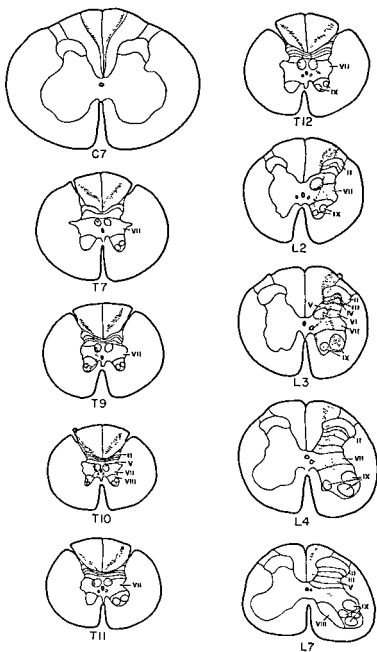


Fig. 1. Drawings of the central distribution of degenerated fibers at spinal levels following section of T10 (left) and L3 (right) dorsal roots. Projected spinal cord sections of rhesus C-916 (T10) and C-914 (L3) were used in preparing these drawings.

the spinal gray. This degeneration was found throughout laminae III and IV, in the ventral part of the dorsal nucleus and in adjacent central parts of lamina VII. Only sparse degeneration was present in medial parts of lamina VIII and virtually no degeneration was seen in lamina IX. (fig. 1).

Descending root fibers of T10 passed caudally in lateral parts of the fasciculus gracilis as far as the L1 spinal segment. At T12 and L1 spinal segments fibers entering the spinal gray projected exclusively into lateral parts of the dorsal nucleus.

Ascending T10 root fibers shifted to more medial portions of the fasciculus gracilis at higher levels, and where a well defined fasciculus cuneatus was present, they formed a narrow band medial, parallel and close to the posterior intermediate septum (fig. 14). These fibers ascended in this position to medullary levels. Collateral fibers were given off exclusively to dorsomedial parts of the dorsal nucleus in T8 and T7 spinal segments.

In transverse sections of the medulla ascending fibers from T10 were oriented along the lateral border of the nucleus gracilis with fewer fibers in the most dorsal and the most ventral regions (fig. 2). Very few of these fibers appeared to terminate about cells in ventrocaudal parts of the nucleus. In mid- and rostral portions of the nucleus most of the degenerated fibers terminated about small clusters of cells along the ventrolateral border of the nucleus gracilis near its common border with the cuneate nucleus. A few fibers seemed to extend into the dorsal apex of the nucleus cuneatus, but these were less numerous than those seen with rhizotomies at T8 or T9. In rostral parts of the nucleus gracilis, near the area postrema, degeneration was limited to cells in the dorsolateral part of the nucleus. No degeneration was seen in other medullary relay nuclei.

Twelfth thoracic root. The twelfth thoracic dorsal root was sectioned in rhesus C-1012. At the level of rhizotomy a narrow band of degenerated fibers from the root entry zone entered the lateral portions of the fasciculus gracilis. From this region fibers passed both through and around the medial portion of lamina II to

enter medial portions of laminae III and IV (fig. 8). Modest terminal degeneration as fibers of passage were located in the central portion of lamina V. From this region degenerated fibers projected to the central portion of lamina VII where they were especially prominent adjacent to the dorsal nucleus. From this site fibers passed in the dorsal nucleus, medial portions of lamina VIII, and to cell groups in lamina IX.

Degeneration within the dorsal nucleus was located principally in the ventrolateral parts of the nucleus (fig. 8). Small fascicles of degeneration projected to the intermediate medial nucleus located ventromedial to the dorsal nucleus. Fibers traversing lamina VII projected ventrally into lamina VIII which at the T12 level extends a broad band across the anterior horn. The most concentrated bundle of fibers passed into the medial part of lamina VIII, coursed along the medial and ventral margin of the anterior horn distributing fibers to both ventromedial and lateromedial groups in lamina IX. Smaller, somewhat diffuse, fascicles of fibers coursed ventrolaterally in central parts of lamina VI to reach the lateromedial cell group in lamina IX.

At the L1 level degeneration in the posterior column consisted of a narrow band slightly dorsomedial to the posterior horn. Virtually no degeneration was present in laminae III and IV, but moderate degeneration was seen in ventrolateral parts of the dorsal nucleus, surrounding portions of lamina VII and the dorsomedial part of lamina VIII. No descending degeneration was present in the posterior column at L2, but a few fibers were within lateral parts of the dorsal nucleus. No degeneration was detectable in caudal spinal segments.

At the T11 level, ascending degeneration in the posterior column had shifted rostrally and was separated from the posterior horn by a band of normal fibers. Degenerated fibers could be seen entering the spinal gray through medial portions of laminae III and IV; these fibers were distributed to medial parts of these laminae except for a lateral island of degeneration. The amount of degeneration was considerably less than at T12. Fibers projected

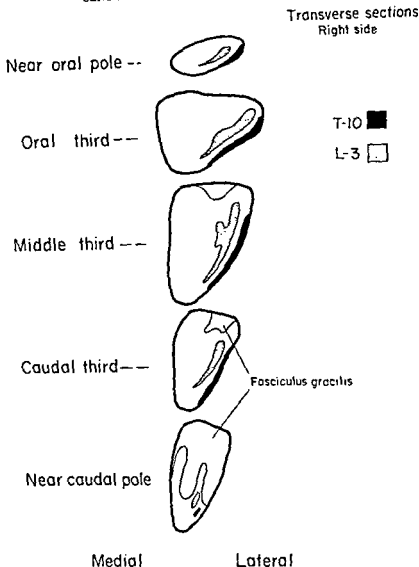


Fig. 2 Diagram of the principal zones of termination in the nucleus gracilis of ascending dorsal root fibers from T10 and L3. Because of the extensive overlap of fibers from certain dorsal roots, four separate drawings (also figs. 4, 5, 6) have been made of the terminal zones in the nucleus gracilis.

entrally passed mainly to ventrolateral parts of the dorsal nucleus. Rostral to this level the principal degeneration in the spinal gray was in the dorsal nucleus, but minimal, scattered degeneration was evident in laminae III and IV, as high as T10. Degenerated T12 dorsal root fibers projected to parts of the dorsal nucleus as far rostrally as T4. In spinal segments L2 to T10 degeneration in the dorsal nucleus

was greatest in ventrolateral regions; from T9 to T4 it was greatest in dorsal parts of the nucleus.

Ascending degeneration in the posterior column shifted medially at higher levels. In upper thoracic spinal segments where the fasciculi cuneatus and gracilis were clearly separated, fibers from the T12 dorsal root formed a narrow band along the lateral border of the fasciculus gracilis;

the spinal gray. This degeneration was found throughout laminae III and IV, in the ventral part of the dorsal nucleus and in adjacent central parts of lamina VII. Only sparse degeneration was present in medial parts of lamina VIII and virtually no degeneration was seen in lamina IX. (fig. 1).

Descending root fibers of T10 passed caudally in lateral parts of the fasciculus gracilis as far as the L1 spinal segment. At T12 and L1 spinal segments fibers entering the spinal gray projected exclusively into lateral parts of the dorsal nucleus.

Ascending T10 root fibers shifted to more medial portions of the fasciculus gracilis at higher levels, and where a well defined fasciculus cuneatus was present, they formed a narrow band medial, parallel and close to the posterior intermediate septum (fig. 14). These fibers ascended in this position to medullary levels. Collateral fibers were given off exclusively to dorsomedial parts of the dorsal nucleus in T8 and T7 spinal segments.

In transverse sections of the medulla ascending fibers from T10 were oriented along the lateral border of the nucleus gracilis with fewer fibers in the most dorsal and the most ventral regions (fig. 2). Very few of these fibers appeared to terminate about cells in ventrocaudal parts of the nucleus. In mid- and rostral portions of the nucleus most of the degenerated fibers terminated about small clusters of cells along the ventrolateral border of the nucleus gracilis near its common border with the cuneate nucleus. A few fibers seemed to extend into the dorsal apex of the nucleus cuneatus, but these were less numerous than those seen with rhizotomies at T8 or T9. In rostral parts of the nucleus gracilis, near the area postrema, degeneration was limited to cells in the dorsolateral part of the nucleus. No degeneration was seen in other medullary relay nuclei.

Twelfth thoracic root. The twelfth thoracic dorsal root was sectioned in rhesus C-1012. At the level of rhizotomy a narrow band of degenerated fibers from the root entry zone entered the lateral portions of the fasciculus gracilis. From this region fibers passed both through and around the medial portion of lamina II to

enter medial portions of laminae III and IV (fig. 8). Modest terminal degeneration and fibers of passage were located in the central portion of lamina V. From this region degenerated fibers projected to the central portion of lamina VII where they were especially prominent adjacent to the dorsal nucleus. From this site fibers passed into the dorsal nucleus, medial portions of lamina VIII, and to cell groups in lamina IX.

Degeneration within the dorsal nucleus was located principally in the ventrolateral parts of the nucleus (fig. 8). Small fascicles of degeneration projected to the intermediomedial nucleus located ventromedial to the dorsal nucleus. Fibers traversing lamina VII projected ventrally into lamina VIII which at the T12 level extends as a broad band across the anterior horn. The most concentrated bundle of fibers passed into the medial part of lamina VIII and coursed along the medial and ventral margin of the anterior horn distributing fibers to both ventromedial and lateromedial cell groups in lamina IX. Smaller, somewhat diffuse, fascicles of fibers coursed ventrolaterally in central parts of lamina VIII to reach the lateromedial cell group in lamina IX.

At the L1 level degeneration in the posterior column consisted of a narrow band slightly dorsomedial to the posterior horn. Virtually no degeneration was present in laminae III and IV, but modest degeneration was seen in ventrolateral parts of the dorsal nucleus, surrounding portions of lamina VII and the dorsomedial part of lamina VIII. No descending degeneration was present in the posterior column at L2, but a few fibers were seen within lateral parts of the dorsal nucleus. No degeneration was detectable in more caudal spinal segments.

At the T11 level, ascending degeneration in the posterior column had shifted medially and was separated from the posterior horn by a band of normal fibers. Degenerated fibers could be seen entering the spinal gray through medial portions of laminae III and IV; these fibers were distributed to medial parts of these laminae except for a lateral island of degeneration. The amount of degeneration was considerably less than at T12. Fibers projecting

Second lumbar root. The second lumbar dorsal root was sectioned in rhesus C-3. At the level of rhizotomy degeneration on the root entry zone passed medially to the lateral part of the fasciculus gracilis dorsomedial to the posterior horn. From this region degenerated fibers coursed through and around the medial portion of lamina II and terminated profusely about cells in the medial portions of laminae III and IV. A modest number of fibers of passage was observed in the central portion of lamina V. These fibers projected into the ventrolateral portion of the dorsal nucleus and adjacent portions of lamina VII. Degenerated fibers reached the anterior horn by two routes. The major degeneration coursed medially through lamina VII, giving off a few fascicles to the intermediomedial nucleus and curving ventrally through the medial portion of lamina VIII to terminate sparsely about both ventromedial and centromedial cell groups of lamina IX. A smaller amount of degeneration reached lamina IX through the central portions of laminae VII and VIII.

At the L3 spinal segment markedly reduced degeneration was confined to the medial portions of laminae III and IV. No dorsal nucleus was present in our sections of this level. No descending degeneration was observed in the fasciculus gracilis at L3 or in the spinal gray caudal to L3, presumably because of oversuppression of differential staining. Descending degeneration in the spinal gray at the L4 spinal level was meager and predominantly confined to parts of laminae III, IV and VII; very sparse degeneration occupied lamina IX.

At the L1 spinal segment modestly reduced degeneration was located predominantly in the medial portions of laminae III and IV and in ventrolateral portions of the dorsal nucleus. Only sparse, scattered degeneration was present in laminae VII and VIII.

Degeneration ascending in the fasciculus gracilis shifted progressively medial throughout lower thoracic segments. At levels with a well defined fasciculus cuneatus, degeneration occupied a spindle-shaped area in the lateral third of the fasciculus gracilis slightly medial to the region occupied by degeneration from the

L1 dorsal root. Degeneration in the spinal gray rostral to the L1 segment extended to T7 and was confined to the dorsal nucleus. At the T12 and T11 segments degeneration in the dorsal nucleus was ventrolateral, but it shifted to lateral regions of the nucleus at T10. At the T7 level only scattered sparse degeneration was present in the nucleus.

In horizontal sections of the medulla degeneration was confined to the nucleus gracilis. Fibers from the fasciculus gracilis formed a small band of degeneration in the caudocentral portion of the nucleus gracilis. This band of degenerated fibers extended rostrally in dorsolateral parts of the nucleus for most of its length. A secondary smaller group of fibers, branching off from the main band, passed more medially in the middle third of the nucleus. Degenerated fibers of passage and occasional terminal fibers occupied the central portions of the nucleus gracilis between these lateral and medial bands. Only scant degeneration was scattered in the most ventral portions of the nucleus (fig. 6). No degeneration was seen in other medullary relay nuclei.

Third lumbar root. In rhesus C-914 the third lumbar dorsal root was sectioned. At the level of the rhizotomy degenerated fibers entered the lateral part of the fasciculus gracilis and were concentrated in an area dorsal to the posterior horn (figs. 1, 16). Root fibers traversing and coursing around medial parts of lamina II arborized about cells in all parts of laminae III and IV. Relatively sparse degeneration was seen in laminae V and VI centrally. Degeneration was scattered throughout lamina VII but was maximal in the central and medial regions adjacent to the dorsal nucleus. Within the dorsal nucleus degeneration was located principally in lateral portions. A small fascicle of fibers from lamina VII ended in the intermediomedial nucleus, while a concentrated bundle of fibers curved ventrally through the medial portion of lamina VIII to terminate in the ventromedial cell group of lamina IX. More diffuse groups of degenerated fibers traversed central portions of laminae VII and VIII to terminate predominantly about the centromedial cell group of lamina IX.

At the L4 spinal segment a marked

dorsolaterally a few of these fibers seemed to be present in the medial part of the fasciculus cuneatus. At cervical levels ascending degeneration was confined to the lateral margin of the fasciculus gracilis.

In transverse medullary sections modest amounts of degeneration formed a narrow band paralleling the lateral border of the nucleus gracilis. In caudal portions of the nucleus gracilis the major degeneration lay within the fasciculus gracilis; only a few terminal fibers were seen about the ventrolateral cells of the nucleus. The most profuse terminal degeneration was observed in mid-portions of the nucleus gracilis, where fibers formed an oblique band just inside the lateral border of the nucleus (fig. 6). At more rostral levels through the nucleus gracilis, terminal degeneration diminished gradually especially in dorsolateral and ventromedial regions, although the basic pattern of the degeneration and its orientation persisted into the most oral parts of the nucleus. No degeneration was observed in other medullary relay nuclei.

Lumbar dorsal roots

All seven lumbar dorsal roots were sectioned individually in seven animals. The L4 dorsal root was sectioned in two animals.

First lumbar root. The first lumbar dorsal root was sectioned in rhesus C-912. At the level of root section, degeneration from the root entry zone was distributed along nearly the entire lateral part of the fasciculus gracilis. Fascicles of degenerated fibers traversed medial portions of lamina II and terminated in medial and central parts of laminae III and IV. Other fascicles of degenerated fibers coursed through medial parts of lamina V to enter medial lamina VII (fig. 25). Part of these fibers passed into ventrolateral portions of the dorsal nucleus where they arborized about individual cells; a smaller group of fibers, projecting ventrally, terminated in the intermedio-medial nucleus. The principal ventrally projecting fibers entered medial parts of lamina VIII and terminated about ventromedial cells of lamina IX. A few of these fibers followed the peripheral border of the anterior horn and entered the lateromedial

cell group of lamina IX. A small, more loosely organized, group of fibers passed ventrolaterally through central parts of laminae VII and VIII towards the lateromedial cell group of IX.

Relatively modest descending degeneration from the L1 dorsal root occupied lateral portions of the fasciculus gracilis medial to normal fibers from the root entry zone. The distribution of descending degeneration in the L2 spinal gray was similar to that described at L1, except the number of fibers was considerably reduced and degeneration was scattered unevenly throughout the dorsal nucleus. Evaluation of descending L1 degeneration at more caudal spinal levels was complicated by extraneous degeneration in the L3 dorsal root zone.

Ascending L1 dorsal root degeneration occupied progressively more medial parts of the fasciculus gracilis in thoracic spinal segments. At upper thoracic and all cervical spinal levels these fibers formed a narrow band along the lateral border of the fasciculus gracilis. Degeneration in the spinal gray at T12 was similar to that at the rhizotomy level except for more modest degeneration in the anterior horn. In T10, T9 and T8 spinal segments degeneration in the spinal gray was confined to the dorsal nucleus; these fibers were distributed diffusely throughout the nucleus.

In transverse sections of the medulla degenerated dorsal root fibers formed a narrow band in the lateral portion of the nucleus gracilis throughout its rostrocaudal extent. Caudally, degeneration was maximal dorsally in the lateral part of the nucleus, excluding only the most lateral border. In middle portions of the nucleus degeneration was most abundant in the dorsal two-thirds of this lateral portion, again excluding the lateral border. However, some fibers extended ventrally along the lateral nuclear border. Rostrally terminal degeneration occupied the entire dorsoventral extent of the lateral portion of the nucleus. In sections near the oral pole of the nucleus only modest degeneration was seen near the lateral border (fig. 4). A few fibers from the main band of degeneration appeared to pass laterally and to reach the most medial border of the cuneate nucleus.

the posterior median septum close to the posterior gray commissure. Degeneration in the spinal gray was greatly reduced at the L5 level; a few fibers arched ventrally to enter medial parts of the posterior horn but little degeneration was seen in laminae II and IV. These fibers, entering through medial parts of lamina V, mainly terminated about clusters of cells in central lamina VI. Fibers traversing the above laminae projected ventrally in central parts of lamina VII; only a few fibers reached cell groups of lamina IX. At L6, L7 and S1 levels the principal degeneration was present in central and medial parts of laminae V and VI; fibers projected to these locations directly from the posterior column. Scattered degeneration was seen in lamina IV at L6, and in dorsal parts of lamina VII, at L6, L7 and S1; no degenerated fibers were seen in lamina IX in these spinal segments. More caudal spinal segments were not available in rhesus C-1011.

Immediately rostral to the rhizotomy (i.e., L3) degenerated fibers were seen throughout lamina I and profusely in all parts of laminae III and IV. Similar profuse degeneration passed through lamina V into central parts of lamina VI. From this locus in lamina VI fibers pursued two courses: (1) ventromedially, through medial parts of laminae VII and VIII to lamina IX, and (2) ventrolaterally, through central parts of laminae VII and VIII to terminate about centromedial cell groups of lamina IX. A few fibers terminated about large cells of the dorsal nucleus in medial lamina VII. At the L2 level, moderate degeneration was present in laminae III and IV, but the principal degeneration was distributed to all parts of the dorsal nucleus (figs. 19, 20). In successively more rostral spinal segments, the degeneration in the spinal gray was seen only in the ipsilateral dorsal nucleus. Degeneration in the dorsal nucleus extended as high as T8. At L1 and T12 degeneration in this nucleus was mainly in lateral regions, but at higher levels it shifted to dorsal portions of the nucleus.

Ascending fibers in the fasciculus gracilis formed a relatively broad band in upper lumbar spinal segments which was displaced progressively medially by entering

normal fibers. In lower thoracic segments the band appeared narrower in the lateral half of the fasciculus but did not extend ventromedially to the spinal gray. In upper thoracic and cervical spinal segments ascending degeneration in the lateral part of the fasciculus gracilis was less concentrated and did not form as discrete a band as at lower levels.

In transverse medullary sections caudal cell groups of the nucleus gracilis were interlaced with degenerated fibers concentrated in the lateral third of the fasciculus gracilis, but removed from the lateral border. Only sparse degeneration was seen about central cell groups at this level. In middle portions of the nucleus degeneration, prominent in central and lateral parts of the nucleus, extended dorsally (fig. 4). Less degeneration was evident in ventromedial regions. Rostrally the principal terminal degeneration was seen in an irregularly shaped area in dorsolateral portions of the nucleus gracilis, but scattered islands of degeneration were present in central regions (fig. 32). Degeneration, seen in the oral pole of the nucleus, was scattered in central and lateral regions.

Fifth lumbar root. The fifth lumbar dorsal root was sectioned in rhesus C-1012. At the level of dorsal rhizotomy degenerated fibers occupied the root entry zone and lateral portions of the fasciculus gracilis dorsal to the posterior horn. Degenerated fibers coursed through and around the medial portion of lamina II to terminate in the central and medial parts of laminae III and IV. Ventrally coursing fascicles of fibers traversed central and medial parts of lamina V. Part of the fibers coursing from this lamina arborized about cells in the medial part of lamina VI, while others entered lamina VII. The majority of fibers from this area coursed ventrally through central portions of lamina VII to terminate in the ventral and ventrolateral cell groups of lamina IX. A small bundle of fibers coursing through medial parts of lamina VII projected to the intermediomedial nucleus and into medial parts of lamina VIII. A few of these fibers entered medial cell groups of lamina IX.

At the L6 level the band of degeneration in the fasciculus gracilis had moved ventromedially to occupy the central por-

reduction in the amount of degeneration occurred, so that only sparse and scattered degeneration was seen in parts of laminae III, IV, V, VI and VII. More degeneration was seen in medial parts of laminae III and IV at L2 and fibers passing through lamina V projected to ventrolateral parts of the dorsal nucleus and adjacent areas of lamina VII. Only a few scattered fibers were seen in laminae VIII and IX (fig. 1).

Descending branches of the L3 dorsal root shifted to more medial and dorsal parts of the fasciculus gracilis caudal to the rhizotomy. These fibers were traced as far as L7 in the fasciculus gracilis. A modest number of fibers were given off in lower lumbar segments primarily to medial parts of laminae VI and VII (figs. 24, 26).

Ascending degeneration from the L3 dorsal rhizotomy occupied an oblique band in the lateral half of the fasciculus gracilis that migrated medially at successively rostral levels. Fibers were given off to the dorsal nucleus and adjacent areas of lamina VII from L2 to T10 spinal segments. The location of degeneration within the dorsal nucleus changed as follows: (1) at L2 and L1 it was ventrolateral, (2) at T12 it was dorsolateral, and (3) at T10 it was dorsomedial. In upper thoracic and cervical spinal segments ascending degeneration formed a narrow band just medial to the posterior intermediate septum. More degenerated fibers were seen dorsally than ventrally, but none of the degenerated fibers reached the dorsal margin of the spinal cord.

In transverse sections of the lower medulla L3 root fibers continued to occupy a small dorsolateral part in the fasciculus gracilis; few fibers terminated in caudal parts of the nucleus gracilis. In the middle third of the nucleus degenerated fibers were most concentrated laterally near fibers of the fasciculus gracilis but scattered degenerated fibers began to appear in more medial parts of the nucleus. In the rostral third of the nucleus gracilis terminal degeneration was seen dorsally just inside the lateral border. Although the area containing terminal degeneration varied slightly from section to section, maximal degeneration persisted to the oral pole in a slightly curved band medial to, and separated from, the lateral border of the

nucleus (fig. 2). At these levels all other parts of the nucleus were free of degeneration.

Fourth lumbar root. The fourth lumbar dorsal root was sectioned in two animals (C-915 and C1011) but spinal trauma in rhesus C-915 caudal to the rhizotomy resulted in extraneous spinal degeneration. Only the reliable observations in rhesus C-1011 will be reported.

At the level of rhizotomy degenerated fibers entered the dorsolateral part of the fasciculus gracilis dorsal to the posterior horn. From this region a large number of root fibers passed through medial portions of laminae I and II to enter central and medial parts of laminae III and IV. Modest terminal degeneration was seen about cells in central and medial parts of lamina I, but no similar degeneration was seen in underlying parts of lamina II. Although terminal degeneration was seen in central and medial parts of laminae III and IV, the most medial portions of these laminae were free of degenerated fibers (fig. 9). A small number of fibers entered ventrolateral parts of lamina II from the zone of Lissauer. These fibers terminated in lateral parts of laminae II through IV. A relatively clear zone was present in the lateral half of laminae III and IV which did not receive fibers from fascicles entering either medially or laterally. Ventrally projecting fibers passed through central parts of laminae V and VI into dorsal parts of lamina VII. A number of these fibers terminated in central parts of lamina VI. From the large collection of degenerated fibers in lamina VII, a small, distinct bundle projected ventromedially to the intermediomedial nucleus, and continued ventrally into the dorsomedial part of lamina VIII (fig. 23). None of these fibers could be traced into cell groups of lamina IX. Fibers projecting to cell groups of lamina IX coursed through central parts of lamina VII in numerous small fascicles.

Descending branches of dorsal root fibers shifted to central regions of the fasciculus gracilis caudal to the rhizotomy; these fibers appeared diffuse and scattered at L5, but at the L6 level formed a relatively thin band in the medial part of the fasciculus. At the S1 level a small number of descending fibers were localized near

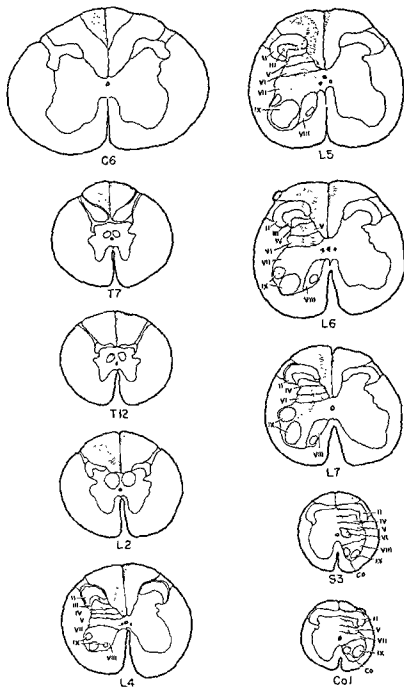


Fig. 3 Drawings of the central distribution of degenerated fibers at spinal levels following section of L6 (left) and Co1 (right) dorsal roots in rhesus C-1014.

tion of the fasciculus gracilis, leaving a band of normal fibers adjacent to the posterior horn. Root fibers entered the spinal gray at L6 chiefly through the medial portion of lamina V and were distributed primarily to medial parts of lamina VI. Smaller amounts of degeneration were scattered in central regions of lamina VII. No degeneration was observed in the intermediomedial nucleus at this level. Progressively diminishing amounts of descending degeneration were present in similar locations in the fasciculus gracilis and spinal gray as far caudally as S1.

At the L4 spinal segment the amount of degeneration in the spinal gray nearly equalled that observed at L5. This degeneration was distributed profusely throughout laminae III and IV, about the central cell clusters of lamina VI, and in central portions of lamina VII. Although a significant number of degenerated fibers traversed central portions of laminae VII and VIII, the number of degenerated fibers terminating in cell groups of lamina IX was less than at L5. A small amount of degeneration entered the intermediomedial nucleus while only sparse degeneration was present in the medial portion of lamina VIII. At the L3 spinal segment the greatest reduction in the amount of degeneration occurred within laminae III, IV and IX. Maximum degeneration persisted in the medial portion of lamina VI and adjacent portion of lamina VII. At the L2 spinal level and above, degeneration in the spinal gray was virtually limited to the dorsal nucleus; degeneration in this nucleus was seen rostrally as far as T7. At L2, L1 and T12 spinal segments profuse degeneration occupied virtually the entire cross-sectional area of the dorsal nucleus, but in more rostral segments degeneration was localized to dorsomedial portions of the nucleus.

Ascending L5 dorsal root fibers in the fasciculus gracilis occupied a broad band which progressively shifted medially. At the L1 level this band of degeneration occupied nearly the medial half of the fasciculus gracilis except for a dorsomedial wedge of normal fibers. At levels where a well defined fasciculus cuneatus was present, only the above-mentioned dorsomedial wedge and the lateral border of the

fasciculus gracilis were devoid of ascending degeneration.

In transverse sections through the caudal pole of the nucleus gracilis a few arborizations were noted about cells in the ventromedial part of the nucleus. In the caudal third of the nucleus gracilis degeneration occupied an irregular central area which extended into ventromedial regions in middle portions of the nucleus; degeneration was most profuse centrally and ventrally (figs. 5, 33). Only extreme dorsomedial and lateral portions of the nucleus were free of degeneration. At rostral level the major area of degeneration shifted dorsomedially. In the oral pole of the nucleus degeneration was dorsomedial. The impressive feature of terminal degeneration from the L5 dorsal rhizotomy within the nucleus gracilis was its diffuse distribution within the central core of the nucleus.

Sixth lumbar root. The sixth lumbar dorsal root was sectioned in two animals (C-916 and C-1014). Observations in these animals were remarkably similar. At the level of the dorsal rhizotomy degenerated root fibers were most numerous in the lateral part of the fasciculus gracilis immediately dorsal to the posterior horn (fig. 3). Fibers from this area coursed through medial parts of laminae I and II, as well as around the medial border of these laminae, to enter laminae III and IV. A moderate number of fibers terminated in medial parts of lamina I, while no fibers appeared to end in lamina II. In laminae III and IV terminal degeneration was maximal in medial and central regions. From lamina IV fibers projected ventrally through central parts of laminae V and VI to medial parts of lamina VII. Terminal arborizations were seen about clusters of cells in medial parts of lamina VI. A small, distinct bundle of fibers projected medially to the intermediomedial nucleus. Fibers bypassing this nucleus projected ventrally in the most medial part of lamina VIII; a few of these fibers ended upon cells of the central-medial cell group of lamina IX. A larger number of fibers radiated through central parts of lamina VII to enter large ventral and lateral cell groups of lamina IX.

At the L7 level descending degenerated fibers in the fasciculus gracilis had moved

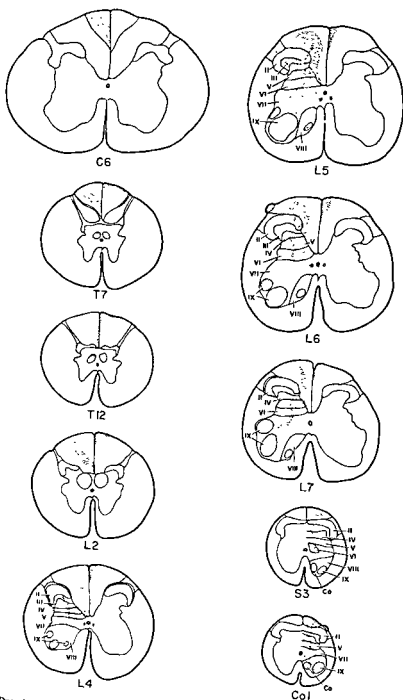


Fig 3 Drawings of the central distribution of degenerated fibers at spinal levels following section of L6 (left) and Col (right) dorsal roots in rhesus C-1014.

nearer the midline where they formed a narrow band extending from the dorsal border of the cord to the posterior gray commissure. Relatively sparse degeneration was present in medial parts of laminae III and IV. The most impressive degeneration was in medial and central parts of lamina VI; fibers projected to this location directly from the fasciculus gracilis by traversing medial parts of lamina V (fig. 27). A modest number of fibers, bypassing cells of lamina VI, radiated through central parts of lamina VII; part of these fibers terminated in the dendritic fields of cells in ventral and lateral regions of lamina IX (fig. 3).

At the S1 level descending degenerated fibers from the fasciculus gracilis swept ventrally through extreme medial parts of the posterior horn into medial parts of laminae V, VI and VII. In rhesus C-1014 a small number of these fibers entered lateral cell groups of lamina IX. In rhesus C-916 observations were similar, except that a distinct bundle of fibers, traversing medial parts of lamina VIII, projected to the oral pole of the commissural nucleus within this lamina. More caudal spinal sections were not available in this animal, but it seemed likely that descending degeneration extended further caudally.

At the L5 level ascending fibers from the L6 dorsal root shifted to central parts of the fasciculus gracilis where they formed a slightly curved broad band. Fewer fibers traversed laminae I and II and terminal degeneration in laminae III and IV was less than at L6. In rhesus C-916 degeneration was seen in lateral parts of laminae III and IV, while in rhesus C-1014 a larger number of fibers occupied only medial portions of these laminae. In both animals the most profuse degeneration was seen in medial parts of laminae V and VI; fibers entered these laminae directly from the fasciculus gracilis. Relatively modest degeneration passed through central parts of lamina VII to reach internal portions of lateral cell groups of lamina IX. At successively rostral spinal levels, progressively diminished degeneration within the spinal gray was seen in all locations except for medial portions of laminae V and VI which continued to receive direct fibers from the fasciculus gracilis as far rostrally as L3.

Persistent degeneration in medial parts of lamina VI was characterized by arborizations about clusters of large cells (fig. 2). At the L3 level medial parts of lamina VI appeared to merge with the dorsal nucleus. Rostral to L3 degeneration within the spinal gray was confined to portions of the dorsal nucleus. Degeneration within caudal parts of the dorsal nucleus (L3-L2) was distributed throughout its entire cross-sectional area (fig. 22). Ascending fibers in the fasciculus gracilis projected to portions of the dorsal nucleus as far rostrally as T9 (C-916) and T7 (C-1014). In these lower thoracic segments degeneration within the dorsal nucleus was localized to small dorsomedial regions (fig. 21).

Ascending dorsal root fibers formed an actively broad, obliquely oriented bundle in central parts of the fasciculus gracilis throughout the lumbar segments. In lower thoracic segments ascending fibers from the L6 dorsal root shifted to more medial and dorsal parts of the fasciculus gracilis, but still left a small wedge of more medial fibers in the most dorsomedial part of the fasciculus. This pattern persisted with minor variations throughout upper thoracic and cervical segments, but at these levels degenerated fibers seemed to occupy a smaller area (figs. 3, 18).

In caudal transverse medullary sections L6 dorsal root fibers were concentrated in medial parts of the fasciculus gracilis. When cell groups of the nucleus gracilis appeared, degenerated fibers shifted ventromedially and some fibers terminated about ventromedial cell clusters. As the nucleus gracilis enlarged in its middle third degenerated terminal fibers were distributed over a large area comprising nearly the medial two-thirds of the nucleus (figs. 4, 34, 36). Terminal degeneration was maximal in central and ventral regions of this part of the nucleus. In the rostral third of the nucleus profuse degeneration still occupied ventromedial parts, but it did not extend to either the medial or ventral borders of the nucleus. Scattered terminal degeneration was seen in central and ventral parts of the nucleus near its oral pole. Terminal degeneration in the nucleus gracilis was maximal in ventromedial regions of the middle and rostral parts of the nucleus. No L6 dorsal root fibers

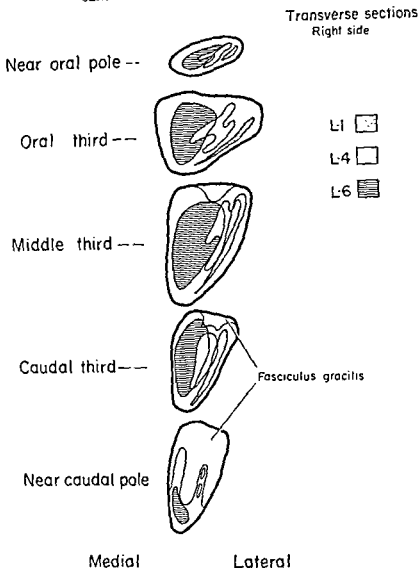


Fig 4 Diagram of the principal zones of termination in the nucleus gracilis of ascending dorsal root fibers from L1, L4 and L6.

passed to other medullary relay nuclei.

Seventh lumbar root. Section of the seventh lumbar dorsal root (C-914) produced degeneration, at the level of section, in the medial root entry zone and in the lateral two-thirds of the fasciculus gracilis dorsal and medial to the posterior horn (fig. 10). Fascicles of degeneration traversed and coursed around medial parts of lamina II in their projection to predominantly lateral cell groups of laminae III

and IV. Other degenerated fascicles coursing around laminae II, III and IV entered medial parts of lamina V directly. Part of these fibers terminated in medial parts of laminae V and VI, while others, in passage, entered dorsocentral regions of lamina VII. The majority of degenerated fibers in this location coursed ventrolaterally through central parts of lamina VII and entered ventral and ventrolateral cell groups in lamina IX. A smaller bundle of fibers

passed ventromedially to the intermedio-medial nucleus and medial portions of lamina VIII. A few of these fibers reached centromedial cell groups of lamina IX.

A marked reduction in the amount of degeneration in the spinal gray was evident in the L6 segment. The most impressive degeneration at this level was seen in medial parts of laminae V and VI; fibers in this region appeared to enter the gray directly from the posterior columns. Degeneration in laminae III and IV was modest in amount and scattered, except for a discrete island of terminal fibers in the lateral part of lamina III. Relatively scant degeneration was seen in laminae VII and IX. Similarly distributed degeneration was seen in the spinal gray at L5; the most profuse degeneration continued to be present in medial parts of laminae V and VI. At L4 degeneration within the spinal gray was seen only in medial portions of lamina VI. No sections of the spinal cord caudal to the L7 segment were available for study.

In their ascending course dorsal root fibers of L7 shifted rapidly to medial portions of the fasciculus gracilis, where they formed a relatively narrow band extending from the periphery of the cord to the posterior gray commissure. This band of fibers was widest dorsally and tapered ventrally where it was adjacent to the posterior median septum. None of these ascending fibers extended into the most dorsomedial part of the fasciculus gracilis; a clear triangular area in this location was devoid of degenerated fibers (figs. 15, 16). This pattern within the fasciculus gracilis persisted with slight variation until the L1 segment. At this level the degenerated fibers shifted dorsally, forming a dorsomedial diagonal band adjacent and lateral to a wedge-shaped area of normal fibers in the most dorsomedial part of the fasciculus gracilis. At T12 and higher levels of the spinal cord, these fibers formed a "boomerang-shaped" configuration with one arm parallel to the posterior median septum and the other arm following the curvature of the spinal cord. These degenerated fibers were separated from the posterior median septum and the dorsal margin of the cord by a narrow zone of normal fibers. This basic "boomerang" configuration of

ascending degeneration in the fasciculus gracilis persisted with minor variation throughout thoracic and cervical segments.

As previously described, ascending fibers from the fasciculus gracilis enter lamina V and projected to cells in medial parts of laminae V and VI throughout the lumbar enlargement. At the L3 level and above, similar fibers projecting to the dorsal nucleus constituted the only degenerated fibers from the L7 root distributed to the spinal gray. Root fibers passing to the dorsal nucleus terminated in different locations at various levels. At L3 and L4 relatively profuse degeneration was seen in lateral and ventrolateral portions of the nucleus while at T12 and T10 degenerated fibers occupied only dorsal portions of the nucleus.

In transverse medullary sections, L7 dorsal root fibers ascending in the fasciculus gracilis retained their basic "boomerang" configuration, although this pattern was not so sharp due to scattering of fibers. At caudal medullary levels degenerated fibers in the fasciculus gracilis were dorsal and medial to the principal cell groups of the nucleus gracilis. A number of terminal fibers were seen in medial parts of the nucleus caudally. At levels where most of the fibers of the fasciculus gracilis had disappeared, terminal degeneration was scattered throughout the medial half of the nucleus; more concentrated degeneration was seen in dorsomedial areas removed from the margins of the nucleus (fig. 5). Through rostral parts of the nucleus gracilis terminal degeneration was profuse and localized to dorsocentral areas. Surrounding regions of the nucleus were free of degeneration except for scattered terminations ventromedially. Near the oral pole of the nucleus gracilis the area containing terminal degeneration extended obliquely from the dorsocentral region to the most ventromedial area. At this level the lateral third of the nucleus and the extreme dorsomedial area were entirely devoid of degeneration.

First sacral root. In rhesus C-912 the first sacral dorsal root was sectioned. At the rhizotomy level degeneration occupied the lateral third of the fasciculus gracilis dorsal to the posterior horn. From the latter

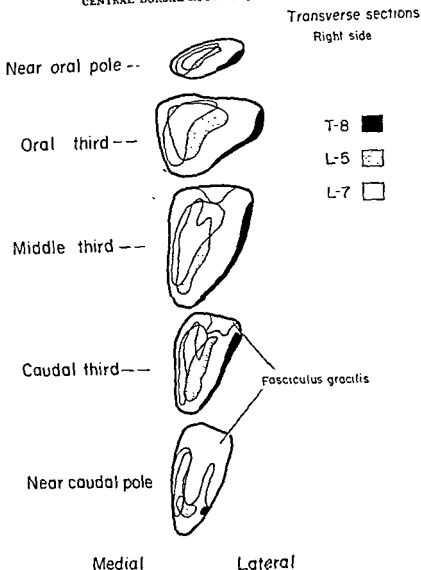


Fig. 5 Diagram of the principal zones of termination in the nucleus gracilis of ascending dorsal root fibers from T8, L5 and L7. Fibers from dorsal roots of the lumbar enlargement (fig. 4) project to irregular shaped areas in the central core of the nucleus

region fascicles of degeneration traversed medial portions of lamina II to terminate primarily in medial and central portions of laminae III and IV (fig. 11). A smaller number of fibers projected into the medial and central portions of laminae V and VI, where some of these fibers appeared to terminate. A modest number of degenerated fibers coursed ventrally through medial portions of lamina VII, giving off

fibers to the intermediomedial nucleus, and continuing ventrally in medial parts of lamina VIII. Fibers with this course entered mainly the ventromedial cell group of lamina IX. Smaller fascicles of degenerated fibers traversed central parts of lamina VII in passage toward ventral and lateral cell groups of lamina IX, but few of these fibers reached these cell groups.

passed ventromedially to the intermediomedial nucleus and medial portions of lamina VIII. A few of these fibers reached centromedial cell groups of lamina IX.

A marked reduction in the amount of degeneration in the spinal gray was evident in the L6 segment. The most impressive degeneration at this level was seen in medial parts of laminae V and VI; fibers in this region appeared to enter the gray directly from the posterior columns. Degeneration in laminae III and IV was modest in amount and scattered, except for a discrete island of terminal fibers in the lateral part of lamina III. Relatively scant degeneration was seen in laminae VII and IX. Similarly distributed degeneration was seen in the spinal gray at L5; the most profuse degeneration continued to be present in medial parts of laminae V and VI. At L4 degeneration within the spinal gray was seen only in medial portions of lamina VI. No sections of the spinal cord caudal to the L7 segment were available for study.

In their ascending course dorsal root fibers of L7 shifted rapidly to medial portions of the fasciculus gracilis, where they formed a relatively narrow band extending from the periphery of the cord to the posterior gray commissure. This band of fibers was widest dorsally and tapered ventrally where it was adjacent to the posterior median septum. None of these ascending fibers extended into the most dorsomedial part of the fasciculus gracilis; a clear triangular area in this location was devoid of degenerated fibers (figs. 15, 16). This pattern within the fasciculus gracilis persisted with slight variation until the L1 segment. At this level the degenerated fibers shifted dorsally, forming a dorsomedial diagonal band adjacent and lateral to a wedge-shaped area of normal fibers in the most dorsomedial part of the fasciculus gracilis. At T12 and higher levels of the spinal cord, these fibers formed a "boomerang-shaped" configuration with one arm parallel to the posterior median septum and the other arm following the curvature of the spinal cord. These degenerated fibers were separated from the posterior median septum and the dorsal margin of the cord by a narrow zone of normal fibers. This basic "boomerang" configuration of

ascending degeneration in the fasciculus gracilis persisted with minor variations throughout thoracic and cervical segments.

As previously described, ascending fibers from the fasciculus gracilis entered lamina V and projected to cells in medial parts of laminae V and VI throughout the lumbar enlargement. At the L3 level and above, similar fibers projecting to the dorsal nucleus constituted the only degenerated fibers from the L7 root distributed in the spinal gray. Root fibers passing to the dorsal nucleus terminated in different locations at various levels. At L3 and L4 relatively profuse degeneration was seen in lateral and ventrolateral portions of the nucleus while at T12 and T10 degenerated fibers occupied only dorsal portions of the nucleus.

In transverse medullary sections, L7 dorsal root fibers ascending in the fasciculus gracilis retained their basic "boomerang" configuration, although this pattern was not so sharp due to scattering of fibers. At caudal medullary levels degenerated fibers in the fasciculus gracilis were dorsal and medial to the principal cell groups of the nucleus gracilis. A number of terminal fibers were seen in medial parts of the nucleus caudally. At levels where most of the fibers of the fasciculus gracilis had disappeared, terminal degeneration was scattered throughout the medial half of the nucleus; more concentrated degeneration was seen in dorsomedial areas removed from the margins of the nucleus (fig. 5). Through rostral parts of the nucleus gracilis terminal degeneration was profuse and localized to dorsocentral areas. Surrounding regions of the nucleus were free of degeneration except for scattered terminations ventromedially. Near the oral pole of the nucleus gracilis the area containing terminal degeneration extended obliquely from the dorsocentral region to the most ventromedial area. At this level the lateral third of the nucleus and the extreme dorsomedial area were entirely devoid of degeneration.

First sacral root. In rhesus C-912 the first sacral dorsal root was sectioned. At the rhizotomy level degeneration occupied the lateral third of the fasciculus gracilis dorsal to the posterior horn. From the latter

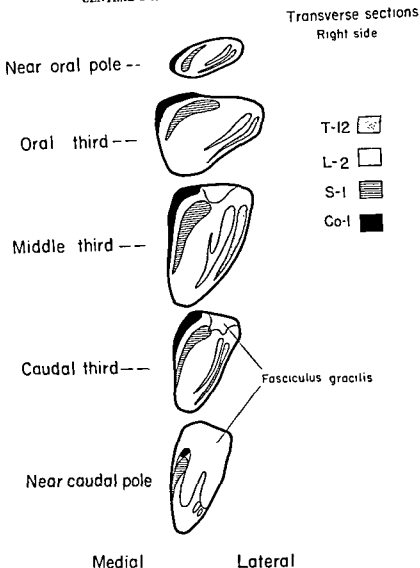


Fig. 6 Diagram of the principal zones of termination in the nucleus gracilis of ascending dorsal root fibers from T12, L2, S1 and Co1. Lower thoracic and upper lumbar roots project fibers to narrow oblique laminae lateral to the core regions (figs. 2, 4), while sacral and coccygeal dorsal roots project fibers to crescent-shaped laminae in dorsomedial parts of the nucleus.

ventrally in medial lamina V to be distributed in a triangular area in central lamina VII (fig. 12). The apex of this triangular area was directed dorsally. Cells in this part of lamina VII were large and intimately surrounded by degenerated fibers. Fibers projecting ventrally from

lamina VII traversed medial parts of lamina VIII and arborized about cells of the commissural nucleus within this lamina (figs. 29, 30). Very few dorsal root fibers entered ventromedial cell groups of lamina IX, although small bundles of fibers passed ventrolaterally through cen-

At the S2 level descending degeneration still occupied the lateral third of the fasciculus gracilis, and degenerated fibers entered the posterior horn in the same manner as described at S1. Reduced amounts of degeneration in the spinal gray were distributed to medial and lateral parts of laminae III and IV, central portions of laminae V and VI, and dorsal parts of lamina VII. A small number of fibers from lamina VII reached cell groups in lamina IX. In the S3 spinal segment traces of descending degeneration were seen in the lateral part of the fasciculus gracilis but little degeneration was seen in the spinal gray.

Rostral to the dorsal rhizotomy (i.e., L7) reduced amounts of degeneration were seen in medial parts of laminae III and IV. Fibers entering medial parts of lamina V directly from the posterior column projected into medial lamina VI where some of these fibers terminated. Fibers entering dorsal parts of lamina VII projected to the intermediomedial nucleus and into medial parts of lamina VIII. Part of these fibers entered ventromedial cell groups of lamina IX.

No sections of spinal segments L6 through L4 were available for study. At the L3 level sparse degeneration was seen in medial parts of laminae III, IV and VII. In more rostral spinal segments degeneration in the spinal gray was confined to the dorsal nucleus. At L2 degeneration was localized to the dorsomedial part of the dorsal nucleus, while at L1 and T12 only sparse scattered degeneration was seen within this nucleus.

Ascending degeneration in the fasciculus gracilis at the L7 level formed a narrow, oblique band, contiguous ventrally with the posterior median septum, but separated from it dorsally. The largest amount of degeneration, located dorsally, extended laterally for a short distance along the dorsal border of the spinal cord. A small dorsomedial wedge of normal fibers separated degenerated fibers from the dorsal part of the posterior median septum. At upper lumbar levels the degenerated fibers shifted dorsally and laterally, forming a narrow, oblique band adjacent to a small dorsomedial wedge of normal fibers (fig. 7). As this band of fibers ascended maximal degeneration appeared to be dorsolat-

eral. From the T9 level rostrally ascending degeneration formed a "boomerang-shaped" configuration, similar to that described for L7, except that the arms parallel to the posterior median septum were shorter and the lateral arm extended along nearly the entire dorsal border of the fasciculus gracilis. A small wedge of normal fibers always remained in the dorsomedial part of the fasciculus. In certain regions a modest number of degenerated fibers appeared within the concavity of the "boomerang," giving a somewhat diffuse pattern to the ascending degeneration.

Ascending degeneration from the S1 dorsal root was studied in transverse sections of the medulla. Degenerated fibers occupied dorsocentral parts of the fasciculus gracilis in the lower medulla, where they were arranged in a less pronounced "boomerang" configuration. Near the middle third of the nucleus fibers passed ventromedially to terminate about cells in a "comma-shaped" area in the medial part of the nucleus gracilis. The most ventral projections at this level surrounded cells along the medial border of the nucleus. In more rostral parts of the nucleus several distinct and separate groups of fibers passed ventromedially in small bands that coursed between and around certain cell groups. Terminal degeneration was seen about cells in the medial two-thirds of the nucleus dorsally, but at most levels several groups of cells were completely free of degeneration (figs. 6, 35). A large oblique band on the lateral border of the nucleus was devoid of degeneration. Near the oral pole of the nucleus the amount of degeneration diminished, but that present persisted in a ventromedial location; at these levels the degeneration did not extend to either the medial or ventral borders of the nucleus.

First coccygeal root. The first coccygeal dorsal root was sectioned in rhesus C-1014. At the level of the rhizotomy dorsal root fibers were scattered throughout the fasciculus gracilis, but with the greatest number of fibers in lateral regions (fig. 3). These fibers entered the spinal gray medially at a considerable distance from the apex of the posterior horn, and terminated about cells in medial portions of laminae III and IV. Degenerated fibers projected

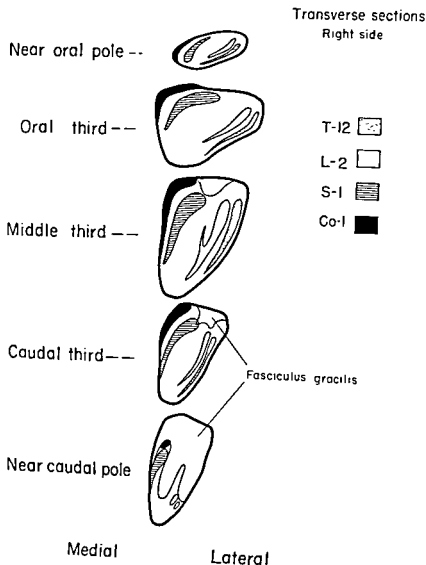


Fig. 6 Diagram of the principal zones of termination in the nucleus gracilis of ascending dorsal root fibers from T12, L2, S1 and Co1. Lower thoracic and upper lumbar roots project fibers to narrow oblique laminae lateral to the core regions (figs. 2, 4), while sacral and coccygeal dorsal roots project fibers to crescent-shaped laminae in dorsomedial parts of the nucleus

ventrally in medial lamina V to be distributed in a triangular area in central lamina VII (fig. 12). The apex of this triangular area was directed dorsally. Cells in this part of lamina VII were large and intimately surrounded by degenerated fibers. Fibers projecting ventrally from

lamina VII traversed medial parts of lamina VIII and arborized about cells of the commissural nucleus within this lamina (figs. 29, 30). Very few dorsal root fibers entered ventromedial cell groups of lamina IX, although small bundles of fibers passed ventrolaterally through cen-

tral parts of lamina VIII in the direction of this cell group. No spinal sections caudal to Co1 were available for study.

At the S3 level diffuse degeneration in the fasciculus gracilis was maximal in medial and dorsal regions. A small number of fibers from the fasciculus gracilis entered medial parts of the posterior horn to terminate in medial portions of laminae III and IV, as well as dorsomedial parts of lamina VII. Little degeneration was present in lamina VIII and none was seen in lamina IX. At the S2 level degeneration was similar in distribution but reduced in amount. No degeneration was seen in the spinal gray at S1 or in more rostral spinal sections.

Ascending degeneration in the fascicu-

confined to a small dorsomedial region, at and above the S1 level. These ascending fibers formed a narrow triangular area, with the long side against the posterior median septum, throughout most of the lumbar segments. At the second lumbar segment the bundle of degenerated fibers in the fasciculus gracilis shifted dorsally to occupy a less perfectly shaped triangle in which the long side conformed to the dorsal margin of the spinal cord. At mid-thoracic levels ascending fibers from Co1 formed a narrow band extending over nearly the entire dorsal surface of the fasciculus gracilis (figs. 3, 18); this pattern of fiber disposition persisted into lower cervical segments. In cervical segments C6 through C3, degenerated Co1 dorsal root fibers formed an inverted "L"-shaped pattern in the dorsomedial part of the fasciculus gracilis with the base of the "L" elongated. In the highest cervical segments these ascending fibers formed a thin band along the dorsal margin of the fasciculus gracilis.

Medullary degeneration resulting from section of the Co1 dorsal root was confined to dorsomedial parts of the nucleus gracilis. As ascending fibers entered the nucleus gracilis they were distributed to medial regions and along the dorsal border of the nucleus, in a "boomerang" configuration (fig. 36). Degeneration in this location was seen throughout the nucleus gracilis but was greatest in its middle third (fig. 6).

DISCUSSION

Part II of this study provides data for: rhesus monkey concerning the distribution and termination of low thoracic, lumbosacral and coccygeal dorsal root fibers. Observations reported here concern the distribution of dorsal root fibers in the spinal gray, ascending and descending dorsal root fibers in the posterior funiculus and the pattern of termination of ascending fibers in the nucleus gracilis. The data together with those from Part I of the study permit certain comparisons regarding ascending fibers passing to medullary relay nuclei.

Spinal projections

Fiber projections to the spinal gray

The spinal distribution of lower thoracic, lumbosacral and coccygeal dorsal root fibers in the monkey are similar to those of the cervical and upper thoracic dorsal roots, except for certain local differences. In lower thoracic spinal segments a small number of dorsal root fibers mainly enter more medial regions of the posterior horn. This appears to be due to the fact that laminae II through V extend across the midline and fuse with corresponding laminae of the opposite side. The number of degenerated fibers in the zone of Lissauer appears relatively greater and more evenly distributed in lower thoracic segments probably because this zone is so narrow. In these spinal segments dorsal root fibers are very nearly confined to their segmental entry except for fibers passing to the dorsal nucleus. This may be due to the long rostrocaudal extent of thoracic spinal segments (Thomas and Combs, '65).

Observations concerning the upper three lumbar dorsal roots are similar to those of the lower thoracic segments except that the number of root fibers is greater and moderate numbers of fibers are distributed to portions of the spinal gray in adjacent spinal segments in locations other than the dorsal nucleus.

Lower lumbar spinal segments (i.e., L1 to L7) are characterized by larger dorsal roots, more extensive spinal gray, enlarged and broader laminae in the posterior horn that are not fused across the midline, and well developed cell groups in lamina IX especially in ventral and lateral regions.

eneration in the zone of Lissauer is less concentrated than in lower thoracic and upper lumbar segments and some fibers in this zone enter lateral parts of the posterior horn. Dorsal root fibers in the spinal gray are most abundant in the segment of entry, but are more widely distributed in the gray of adjacent spinal segments than other lumbar, or thoracic, dorsal roots. The distribution of dorsal root fibers in the two segments rostral to a zotomy is greater than in adjacent caudal segments. In adjacent segments root fibers project most abundantly to cell groups of the posterior horn.

The configuration and laminar organization of the spinal gray at S1 in the monkey differs from that in the cat (Rexed, '52, 1). The S1 spinal segment in the monkey resembles S3 in the cat in that laminae III, IV, and V of the posterior horn extend in continuity across the midline as in most of the thoracic segments. However, laminae VI, VII, VIII and IX at S1 are similar in the cat and monkey. At this level where the lumbosacral enlargement is disappearing, fibers of the fasciculus gracilis form a flattened, horizontal wedge overlying the dorsomedial part of the posterior horn. Fibers entering the gray traverse medial parts of laminae I, II and III and terminate largely in medial parts of laminae III and IV. The distribution of S1 dorsal root fibers in certain respects resembles that of thoracic dorsal roots.

Coccygeal spinal segments in the monkey, though smaller, resemble sacral segments in laminar organization, except that there is no lamina VI, cell groups of lamina X are smaller, and the commissural nucleus develops in the medial part of lamina VIII. Dorsal root fibers at this level enter the gray dorsally near the midline at a considerable distance from the apex of the posterior horn. Dorsal root fibers passing into the spinal gray of the two adjacent rostral segments are distributed principally to laminae of the posterior horn. A systematic discussion of the distribution of lower thoracic, lumbosacral and coccygeal dorsal root fibers in the spinal gray must be made with respect to the laminae of Rexed.

Laminae I and II. Observations concerning laminae I and II in the lower

thoracic, lumbosacral and coccygeal spinal segments are essentially the same as in cervical and upper thoracic segments of the spinal cord. A small number of dorsal root fibers end in medial parts of lamina I. These fibers are inconspicuous in lower thoracic and upper lumbar segments where this lamina is small.

As discussed in Part I of this study, most of the dorsal root fibers seen in lamina II are in passage to deeper laminae of the posterior horn. While the largest number of the dorsal root fibers pass through medial parts of lamina II, there are some which curve around its medial border. Fibers entering in thoracic (fig. 8), upper lumbar, and sacrococcygeal (figs. 11, 12) segments where laminae II through V are fused across the midline seem to traverse more medial parts of lamina II than do fibers in the lumbar enlargement (fig. 10). A modest number of fibers course from the zone of Lissauer through, and to, small lateral parts of lamina II, but this is not constant. These observations are the same as those of Anderson ('60), Ralston ('65), Stein and Carpenter ('65) and Sterling and Kuypers ('67) which indicate that few dorsal root fibers terminate in lamina II.

Using more sophisticated techniques Ralston ('65) has demonstrated that the substantia gelatinosa corresponds only to lamina II and that the afferent inputs to laminae II and III differ significantly. From these studies it was concluded that lamina III receives a major projection of dorsal root collaterals, while the substantia gelatinosa receives very few. According to Szentágothai ('64), the substantia gelatinosa is essentially a closed system in which cells are interconnected with each other either by axons running within the substantia gelatinosa or passing via the zone of Lissauer to re-enter the substantia gelatinosa in neighboring segments. This paucity of terminal degeneration in lamina II following dorsal rhizotomy has suggested that the cells of the substantia gelatinosa may be excited polysynaptically via interneurons in deeper portions of the posterior horn. There appears to be little evidence that cells of lamina II are activated monosynaptically. In addition to the fibers projected to the spinal gray, fine

fibers from the root entry zone project into the zone of Lissauer. These small fascicles, located mainly in medial portions of the zone of Lissauer, are distributed to a number of segments both caudal and rostral to the root entry zone (Ranson, '13, '14; Earle, '52).

Laminae III and IV. While it is widely acknowledged that dorsal root fibers at all levels project profusely to laminae III and IV (i.e., the nucleus proprius), there are differences of opinion concerning localization of dorsal root terminals in these laminae. As discussed in Part I of this study, Szentágothai and Kiss ('49) consider medial parts of laminae II and III to be related to ventral cutaneous regions, and lateral parts of these laminae to be associated with dorsal cutaneous regions. Studies of dorsal root fibers entering the brachial enlargement of the cord in the cat (Sterling and Kuypers, '67) suggest a differential distribution of fibers in laminae III and IV in which: (1) more rostral roots supplying proximal parts of a limb, or preaxial regions, project preferentially to lateral parts of these laminae, and (2) caudal roots supplying distal parts of a limb, or postaxial regions, project to medial parts of these laminae. Physiological data (Wall, '60, '67) indicate that this type of localization is present also in the lumbar enlargement of the cat. In the most extensive anatomical study (Sprague and Ha, '64) of lumbar dorsal roots in the cat, these authors noted variations in the terminal fields of lumbosacral dorsal roots in laminae III and IV at levels above and below dorsal rhizotomies. This finding and those of Szentágothai and Kiss ('49) and Szentágothai ('64) have supported the thesis of radially oriented "synaptic compartments" or "lobuli" within these laminae. The variations in patterns of localization within these laminae have made it difficult to postulate a general scheme. Data in the monkey are similar to those reported for the cat.

In the monkey lower thoracic, upper lumbar and sacrococcygeal dorsal root fibers enter the posterior horn more medially than do the dorsal root fibers of the lumbar enlargement. Fibers from these roots radiate into medial and central parts

of laminae III and IV (figs. 7, 8, 11). Degeneration is seen in lateral portions of these laminae, it usually is modest in amount. In segments above and below the dorsal rhizotomy, fibers enter even more medial regions of the posterior horn and are distributed in essentially the same pattern as at the rhizotomy level, but in reduced amounts.

Observations concerning fibers of dorsal roots of the lumbar enlargement are similar in that the greatest concentration of terminal fibers at the level of root section is seen in medial and central parts of laminae III and IV (fig. 9). However, degeneration in these laminae rostral and caudal to the rhizotomies sometimes revealed a different pattern of localization. In only one animal (C-914) with an L7 dorsal rhizotomy was degeneration in laminae III and IV seen predominantly in lateral regions at levels of the root section. Adjacent rostral spinal segments in this animal revealed less degeneration in these laminae distributed in "synaptic compartments" as described by Sprague and Ha ('64). Data available from this study suggest that the pattern of distribution of dorsal root fibers in laminae III and IV of the lumbar enlargement in the monkey probably is similar to that described by Sterling and Kuypers ('67) for the brachial enlargement of the cat. Precise confirmation of these data would seem to require staining of virtually serial sections through several segments of the spinal cord, a procedure not done in the current study. Further, some of the variations seen in our material undoubtedly are the result of comparing patterns of degeneration at different locations within various spinal segments. The establishment of precise patterns of localization of terminal degeneration in these laminae would seem to require a detailed study of the fibers of each dorsal root in several animals. Even when this is done (Sprague and Ha, '64), it is difficult to generalize broadly on the patterns of localizations in laminae III and IV. It is apparent from the present investigation that more detailed studies of the distribution of dorsal root fibers in these laminae are necessary.

Laminae V and VI. While lamina V is present at all spinal levels, lamina VI is

found only in the brachial and lumbar enlargements and in upper cervical segments. Dorsal root fibers enter central and medial parts of lamina V almost exclusively from lamina IV, except in the spinal enlargements. In lower thoracic and upper lumbar segments, dorsal root fibers traversing central and medial regions of lamina V appear to be mainly fibers of passage which project ventrally into laminae VII, VIII and IX. Virtually no degenerated fibers are present in lateral parts of lamina V.

In the cord enlargements a considerable number of dorsal root fibers appear to terminate in medial parts of laminae V and VI. According to Sterling and Kuypers ('67), fibers from a single dorsal root of the brachial enlargement of the cat are distributed to parts of these laminae throughout the brachial cord. However, there is no evident topical distribution of fibers within laminae V and VI. A slightly different arrangement is present in the brachial enlargement in the monkey (Shriver, Stein and Carpenter, '68) in that brachial dorsal roots project fibers to medial and central parts of lamina VI which is maximal in segments rostral to their entry, and present in lesser amounts for variable distances in more caudal segments.

In the lumbar enlargement root fibers enter laminae V and VI from lamina IV, while other fibers enter lamina V directly from the posterior funiculus. Fibers entering lamina V directly are seen at the level of the rhizotomy but frequently these are more impressive in adjacent spinal segments. These fibers, like those at the level of the root section, appear mainly to arborize about individual cells, but some fibers are in passage to more ventral laminae. Fibers enter laminae V and VI at all levels above the cut root until the L3 level is reached and the dorsal nucleus is evident. At the L3 level and above most of the entering fibers seem to merely traverse medial parts of lamina V en route to cells of the dorsal nucleus. Degenerated fibers and cells in the medial part of laminae VI seem to merge imperceptibly into the caudal pole of Clarke's column at L3. The relationship between cells of the medial part of lamina VI at this level to the dorsal nucleus resembles a similar relationship of medial

lamina VI in the upper cervical cord to the caudal cuneate nucleus (Shriver, Stein and Carpenter, '68).

Dorsal roots of the lumbar enlargement also contribute fibers to medial parts of laminae V and VI at levels below the rhizotomy. Fibers descending in the fasciculus gracilis project to these laminae as far caudally as S1. Medial parts of laminae V and VI appear to be the principal regions of termination of fibers descending in the fasciculus gracilis from dorsal roots of the lumbar enlargement (figs. 26, 27, 28).

According to Sprague and Ha's ('64) analysis and correlation of anatomical and physiological findings (Eccles, Eccles and Lundberg, '60), dorsal root fibers terminating in laminae V and VI are group Ia and Ib muscle afferents, group III muscle afferents, and some cutaneous fibers. Recent physiological studies (Wall, '67) of the laminar organization of the posterior horn in the cat indicate that cells in laminae IV, V and VI all respond to cutaneous stimulation but only cells of lamina VI respond to joint movement. Cells of lamina IV differ from those of lamina V in that receptive cutaneous fields are smaller. Cells of lamina V are described as responding as if impulses from lamina IV converge upon them. These observations suggest that dorsal root afferents projecting to laminae V and VI may be concerned with the integration of impulses from more than one type of peripheral receptor.

Laminae VII and VIII. Although laminae VII and VIII are recognized at all spinal levels, the configurations of these laminae show variations at different levels. Lamina VII has a much greater extent in the cord enlargements, where its lateral part extends into the anterior horn. Conversely, lamina VIII is reduced greatly in the cord enlargements where it occupies only the medial part of the anterior horn.

The distribution of dorsal root fibers in laminae VII and VIII appears different in the lower thoracic and upper lumbar regions than in the lumbar enlargement. While the distribution of dorsal root fibers in sacral and coccygeal segments is similar to that of the thoracic cord, there are certain distinctive features.

In the lower thoracic and upper lumbar spinal segments (i.e., T8 to L2), dorsal root

fibers from the root entry zone project into the zone of Lissauer. These small fascicles, located mainly in medial portions of the zone of Lissauer, are distributed to a number of segments both caudal and rostral to the root entry zone (Ranson, '13, '14; Earle, '52).

Laminae III and IV. While it is widely acknowledged that dorsal root fibers at all levels project profusely to laminae III and IV (i.e., the nucleus proprius), there are differences of opinion concerning localization of dorsal root terminals in these laminae. As discussed in Part I of this study, Szentágothai and Kiss ('49) consider medial parts of laminae II and III to be related to ventral cutaneous regions, and lateral parts of these laminae to be associated with dorsal cutaneous regions. Studies of dorsal root fibers entering the brachial enlargement of the cord in the cat (Sterling and Kuypers, '67) suggest a differential distribution of fibers in laminae III and IV in which: (1) more rostral roots supplying proximal parts of a limb, or preaxial regions, project preferentially to lateral parts of these laminae, and (2) caudal roots supplying distal parts of a limb, or postaxial regions, project to medial parts of these laminae. Physiological data (Wall, '60, '67) indicate that this type of localization is present also in the lumbar enlargement of the cat. In the most extensive anatomical study (Sprague and Ha, '64) of lumbar dorsal roots in the cat, these authors noted variations in the terminal fields of lumbosacral dorsal roots in laminae III and IV at levels above and below dorsal rhizotomies. This finding and those of Szentágothai and Kiss ('49) and Szentágothai ('64) have supported the thesis of radially oriented "synaptic compartments" or "lobuli" within these laminae. The variations in patterns of localization within these laminae have made it difficult to postulate a general scheme. Data in the monkey are similar to those reported for the cat.

In the monkey lower thoracic, upper lumbar and sacrococcygeal dorsal root fibers enter the posterior horn more medially than do the dorsal root fibers of the lumbar enlargement. Fibers from these roots radiate into medial and central parts

of laminae III and IV (figs. 7, 8, 11). Degeneration is seen in lateral portions of these laminae, it usually is modest in amount. In segments above and below the dorsal rhizotomy, fibers enter even more medial regions of the posterior horn and are distributed in essentially the same pattern as at the rhizotomy level, but in reduced amounts.

Observations concerning fibers of dorsal roots of the lumbar enlargement are similar in that the greatest concentration of terminal fibers at the level of root section is seen in medial and central parts of laminae III and IV (fig. 9). However, degeneration in these laminae rostral and caudal to the rhizotomies sometimes revealed a different pattern of localization. In only one animal (C-914) with an L7 dorsal rhizotomy degeneration in laminae III and IV was seen predominantly in lateral regions at levels of the root section. Adjacent rostral spinal segments in this animal revealed less degeneration in these laminae distributed in "synaptic compartments" as described by Sprague and Ha ('64). Data available from this study suggest that the pattern of distribution of dorsal root fibers in laminae III and IV of the lumbar enlargement in the monkey probably is similar to that described by Sterling and Kuypers ('67) for the brachial enlargement of the cat. Precise confirmation of these data would seem to require staining of virtually serial sections through several segments of the spinal cord, a procedure not done in the current study. Further, some of the variations seen in our material undoubtedly are the result of comparing patterns of degeneration at different locations within various spinal segments. The establishment of precise patterns of localization of terminal degeneration in these laminae would seem to require a detailed study of the fibers of each dorsal root in several animals. Even when this is done (Sprague and Ha, '64), it is difficult to generalize broadly on the patterns of localization in laminae III and IV. It is apparent from the present investigation that more detailed studies of the distribution of dorsal root fibers in these laminae are necessary.

Laminae V and VI. While lamina V is present at all spinal levels, lamina VI is

is nucleus varies. Most authors indicate that following section of a single dorsal root, degeneration projecting to the dorsal nucleus extends in a span of six or seven segments. Liu ('56) reported the most extensive study of dorsal root projections to the dorsal nucleus. According to this author, the T10 dorsal root projected fibers to the dorsal nucleus as far rostral as T3 and as far caudal as L1. The distribution of dorsal root fibers from different segments indicated that those concerned with the trunk were found in all regions of the nucleus, while those roots conveying afferents from the tail, hindlimb and forelimb were confined to specific regions.

The distribution of fibers from a single dorsal root in the monkey to cells of the dorsal nucleus at various levels seems even greater than in the cat. Lower thoracic and upper lumbar (i.e., T8 through L2) dorsal roots contribute fibers to cells of the dorsal nucleus three to eight segments above the level of the rhizotomy and one to four segments below. Dorsal roots of the lumbar enlargement (i.e., L3 to L7) project only ascending fibers to the dorsal nucleus. Although these fibers ascend in the posterior columns for variable distances caudal to the column of Clarke, they all contribute fibers to approximately the same portions of this cell column, namely, that part of the cell column between L3 and T7 segments. While dorsal root fibers from the lumbar enlargement overlap those from upper lumbar and lower thoracic segments, their terminations are restricted to definite portions of Clarke's column. The first sacral dorsal root projects fibers to more restricted caudal parts of Clarke's column. Coccygeal roots do not appear to project fibers to the dorsal nucleus in the monkey, although they have been described in the cat (Liu, '56) as projecting fibers to the dorsal nucleus at the L4 level. Data in the monkey support the observations of Liu ('56) that dorsal root fibers from different parts of the body project to the cells of the dorsal nucleus at particular spinal levels.

There is evidence that dorsal root fibers from various spinal levels project to different parts of the dorsal nucleus. Szentágothai and Albert ('55) noted that in the dog sacral dorsal rhizotomies produced degen-

eration in the medial part of Clarke's column, while degeneration resulting from lumbar rhizotomies occupied lateral parts of Clarke's column. In the cat Grant and Rexed ('58) found that fibers from sacral dorsal roots were distributed throughout the cross-sectional area of the dorsal nucleus in the four caudal segments containing this nucleus, while more rostral fibers terminated in medial or dorsomedial parts of the column. Lumbar dorsal roots projected fibers to lateral parts of the cell column caudally and to dorsomedial regions of the cell column rostrally. In intermediate regions of the cell column fibers seemed distributed throughout the cross-sectional area of the nucleus.

Dorsal root fibers in lower thoracic and upper lumbar segments of the monkey enter the dorsal nucleus by coursing along its lateral and ventral borders. While at some levels dorsal root fibers are distributed throughout the dorsal nucleus at the level of rhizotomy (e.g., T8, L2 and L3), most of these fibers project to ventrolateral parts of the nucleus (figs. 8, 25). Degenerated fibers from these dorsal roots terminating in the dorsal nucleus at more rostral levels also are localized to parts of the cell group. In the two or three adjacent rostral spinal segments terminal degeneration usually is localized to ventrolateral parts of the nucleus, but further rostrally terminal degeneration occupies small dorsal parts of the nucleus. This change in the intranuclear distribution of fibers appeared related to the fact that at more rostral levels fibers enter the dorsal nucleus directly from the posterior column. Branches of dorsal roots projecting fibers to cells of the dorsal nucleus caudal to the level of the rhizotomy consistently terminate in lateral parts of the nucleus.

Dorsal root fibers of lumbar segments caudal to L4 ascend in the posterior column and enter the column of Clarke by passing ventrally through medial parts of lamina V. It is also possible that some dorsal root fibers entering the medial part of lamina VI throughout the lumbar enlargement may reach the dorsal nucleus by passing rostrally through this lamina. Fibers from all dorsal roots of the lumbar enlargement project profusely throughout the cross-sectional area of the dorsal nucleus

fibers traverse medial parts of laminae III, IV and V and enter portions of lamina VII lateral to the dorsal nucleus. Part of these fibers pass directly to cells of the dorsal nucleus, while others project to the intermediomedial nucleus. Fibers passing through, and adjacent to, the intermediomedial nucleus enter the medial part of lamina VIII, course ventrally along the medial border of the anterior horn, and follow the curve of the spinal gray into ventral and lateral parts of the anterior horn. Fascicles of fibers following this path project to ventromedial and lateromedial cell groups of lamina IX. A smaller and variable number of fibers pass ventrolaterally through central parts of laminae VII and VIII to reach the lateromedial cell group of lamina IX.

Beginning at the L3 level and extending through L7, quantitative changes are seen in the distribution of fibers in laminae VII and VIII. From the region of concentrated fibers in dorsal and central parts of lamina VII, one small bundle of fibers projects ventromedially toward the intermediomedial nucleus (figs. 23, 24). Some fibers with this course terminate in the latter nucleus while others bypass it and enter the dorsomedial part of lamina VIII. The above fibers follow the pattern of distribution previously described for lower thoracic and upper lumbar segments. The major difference in the lumbar enlargement is that fewer fibers projecting in this manner reach cell groups of lamina IX; fibers pursuing this course project mainly to ventromedial and centromedial cell groups. The major fiber projection from dorsal and central parts of lamina VII in the lumbar enlargement consists of numerous small radiating fascicles which stream ventrolaterally through central regions of lamina VII and enter large cell groups of lamina IX located ventrally and laterally (fig. 23). In spinal segments caudal to the rhizotomies greatly reduced amounts of degeneration are seen passing ventrally in lamina VII and only a few of these reach cell groups in lamina IX. Rostral to the rhizotomies more degenerated fibers projecting through central parts of lamina VII reach cell groups of lamina IX.

While data regarding sacral and coccygeal roots in this study are limited, availa-

ble evidence indicates that the majority of these dorsal root fibers course through medial parts of laminae VII and VIII. Sacral dorsal root fibers reach ventromedial cell groups of lamina IX while coccygeal roots project to cells of the dorsomedial nucleus (figs. 29, 30). A small number of diffuse and scattered fibers pass ventrally through central parts of laminae VII and VIII at S1 and Co1, but few of the fibers reach cell groups of lamina IX.

Thus fibers entering lamina VII appear to project to cell groups of lamina I through lamina VIII, and (2) one ventromedially through the medial part of lamina VIII, and (3) one ventrolaterally through central parts of lamina VII. Dorsal root collaterals follow both of these pathways at all spinal levels, but the ventromedial projection is the major one in thoracic and upper lumbar segments while the projection through central parts of lamina VII is predominant in the spinal cord enlargements. These findings are in agreement with those of Sprague and Lund ('64), Sterling and Kuypers ('67), and our own observations concerning rostral projections of the spinal cord (Shriver, Stein and Carpenter, '68).

At levels studied here, three distinct cell groups can be identified within lamina VII: (1) the dorsal nucleus, (2) the intermediomedial nucleus, and (3) the interneuronal lateral nucleus. The interneuronal nucleus in thoracolumbar and sacral segments does not receive dorsal root afferents. The intermediomedial nucleus receives a constant small projection at the level of root entrance in all spinal segments (Schimert, '39; Sprague and Haase, '58; Sterling and Kuypers, '67; Shriver, Stein and Carpenter, '68). While the significance of dorsal root projections to the intermediomedial nucleus is not apparent, the constancy of this termination at all spinal levels suggests that its cells are interneurons of importance.

Data concerning the extensive distribution of fibers from a single dorsal root to the dorsal nucleus of Clarke have been reported by Pass ('33), Szentágothai and Albert ('55), Liu ('56) and Grant and Rexed ('58) for the cat and dog. The distance above and below the level of the rhizotomy at which degeneration has been found is

21), there is no clearcut lateral boundary of this fasciculus in the mid-thoracic region. Thus in the strict sense the fasciculus gracilis should consist only of posterior column fibers terminating in the nucleus gracilis. Our data indicate that a few fibers from all lower thoracic and the L1 dorsal root project to the cuneate nucleus, although the bulk of these fibers terminates in the nucleus gracilis. Ascending dorsal root fibers from lower thoracic and upper lumbar dorsal roots form oblique narrow bands in the fasciculus gracilis with fibers from thoracic segments most lateral (figs. 1, 13, 14). Central lumbar dorsal roots (L4, L5 and L6) contribute larger numbers of fibers to the fasciculus gracilis which occupy larger areas (figs. 3, 18). While all ascending dorsal root fibers overlap those from adjacent segments, the overlap of central lumbar fibers appears greatest. Ascending fibers from the most caudal dorsal roots (i.e., L7, S1 and Co1) initially occupy more medial regions of the fasciculus gracilis (figs. 15, 16, 17), but in upper thoracic segments, these fibers spread out over the dorsal surface of the fasciculus (figs. 3, 18). At cervical levels fibers from these caudal roots assume a curved configuration in which fibers are present medially near the raphe and extend dorsally along the surface of the fasciculus. The manner in which fibers from caudal roots are organized in the rhesus monkey is remarkably similar to that described in the spider monkey (Chang and Ruch, '47).

The number of fibers contributed to the fasciculus gracilis and the area which they occupy appears related to the size of the dorsal root. The physiological implication of these findings is that the lower lumbar roots (L4, L5, L6 and L7) probably convey sensation from the most important cutaneous areas. This view appears consistent with the conclusions of Mott and Sherrington (1895).

Dichotomizing descending branches of dorsal root fibers in the posterior columns have been described as relatively small compact bundles. Fibers from thoracic and lumbar dorsal roots are said to form an oval bundle adjacent to the posterior median septum (Flechsig, 1876), while similar fibers from sacral roots descend

an extreme dorsomedial part of the fasciculus gracilis (Gombault and Philippe, 1894). The extent of these descending fibers varies with different spinal roots. In the cat Liu ('56) found descending fibers, irregularly distributed in the posterior funiculus, extending four to six segments caudal to the level of entrance. In one human case (Collier and Buzzard, '03) fibers from the L3 dorsal root descended eight segments in the posterior columns.

Observations concerning descending branches of dorsal root fibers in the monkey indicate that these fibers are arranged in oblique bands within various parts of the fasciculus gracilis and do not form small compact bundles. The organization of these narrow bands resembles that of ascending fibers in the posterior columns, although descending bands undergo a relatively rapid attenuation and dissolution with increasing distance from the sectioned dorsal root, as fibers are given off to the spinal gray. Fibers from lower thoracic and upper lumbar roots occupy the lateral third of the fasciculus gracilis while fibers from lower lumbar roots are in more medial parts of the fasciculus gracilis. In most instances these fibers projected caudally two to four spinal segments. Descending fibers from lower thoracic and the upper three lumbar dorsal roots project to lateral parts of the dorsal nucleus and adjacent portions of lamina VII. More caudal lumbar dorsal roots project fibers into the medial part of lamina VI and adjacent parts of lamina VII.

Medullary projections

Dorsal root projections to the nucleus gracilis. According to Ferraro and Barrera ('35) and Walker and Weaver ('42), ascending dorsal root fibers projecting to the nucleus gracilis are somatotopically organized. Fibers from sacral dorsal roots were found to terminate in caudal and medial parts of the nucleus gracilis, while lumbar dorsal root fibers projected to slightly more rostral and lateral parts of the nucleus. Lower thoracic roots were described as terminating in the most rostral and lateral parts of the nucleus gracilis. The limited number of dorsal rhizotomies

at L3 and L2 (figs. 19, 20, 22); at L1 and in lower thoracic segments terminal degeneration within the dorsal nucleus is consistently and discretely localized to dorso-medial regions (fig. 21). These observations are similar to those of Grant and Rexed ('58) and support the thesis that dorsal root afferents to the dorsal nucleus terminate in an overlapping but spatially organized topical manner. There is abundant physiological evidence that group Ia and Ib afferents from stretch receptors terminate upon cells of this nucleus which in turn conveys impulses to the cerebellum via the posterior spinocerebellar tract (Lloyd and McIntyre, '50; Oscarsson, '65).

Lamina IX. Collaterals of lower thoracic, lumbosacral and coccygeal dorsal roots have a more restricted segmental distribution in cell groups of lamina IX, than similar collaterals in laminae of the posterior horn or in lamina VII. In lower thoracic and upper lumbar segments collaterals of dorsal root fibers reaching lamina IX are virtually restricted to the segment of entry. In the lumbar enlargement the number of dorsal root collaterals reaching cell groups of lamina IX is greater and these fibers are distributed to this lamina not only at the level of root entry but in the two adjacent spinal segments above and below. Fibers passing to adjacent spinal segments are modest in number, but definite. The two pathways by which dorsal root fibers reach cell groups of lamina IX have been discussed in relationship to laminae VII and VIII. These observations for the lumbar enlargement are similar to those of Spargue and Ha ('64), but these authors made no comparisons between thoracic and lumbar levels. Sacral and coccygeal dorsal root fibers conform to the pattern described for the lower thoracic dorsal roots in that collaterals pass mainly to medial cell groups of lamina IX via the medial part of lamina VIII.

According to Sprague ('58), lumbar dorsal root collaterals in the cat establish both axosomatic and axodendritic contacts with motor neurons in their segment of entry, but in adjacent segments connections are primarily axodendritic. In the present study most dorsal root collaterals appeared to terminate in the dendritic fields of motor

neurons, an observation which might be due only to longer postoperative survival of our animals. In this connection it is of interest that Golgi studies of motor axons and interneurons of the anterior horn (Sprague and Ha, '64) indicate that dendrites of motor neurons extend beyond the limits of Rexed's lamina IX into adjacent portions of laminae VII and VIII.

Projections in the posterior funiculus. Classic descriptions of ascending fibers in the posterior columns in the rhesus monkey have been based upon the study of Marchi degeneration following selective dorsal root section and various types of cordotomies (Ferraro and Barrera '35; Walker and Weaver, '42). The most detailed study (Walker and Weaver, '42) included data from eight dorsal rhizotomies and 16 cordotomies; only six dorsal roots were sectioned caudal to T8. All authors have reported an oblique laminar arrangement of ascending fibers in the fasciculus gracilis in which lower thoracic fibers were most lateral and sacral fibers most dorsomedial. Composite diagrams illustrating the somatotopic arrangement of ascending fibers in the posterior columns show quantitative differences in the number of ascending fibers and in the areas they occupy for different dorsal rhizotomies. These authors emphasized that ascending fibers from adjacent dorsal roots exhibit extensive overlap in the posterior columns. Intermingling of ascending dorsal root fibers was especially pronounced for lumbar and sacral root fibers in cervical spinal segments. Observations concerning the organization of the posterior columns in the spider monkey (Chang and Ruch, '47) based upon complete and partial transections of the spinal cord, indicated that fibers ascending from coccygeal regions initially occupy dorsomedial parts of the fasciculus gracilis but at thoracic levels form a band or cap along the dorsal margin of the fasciculus gracilis.

The current study based upon more extensive data in the monkey confirms prior investigations and reconciles certain minor differences. Dorsal roots from the five lowest thoracic segments (T8 through T12) and all more caudal spinal segments project fibers rostrally in the fasciculus gracilis. As noted by Walker and Weaver

at" region in that they receive the principal projections from the cerebral cortex. The concept that neurons in various rostrocaudal parts of the nucleus gracilis exhibit differences with respect to: (1) size of their peripheral field, and (2) the sensory modality they relay to higher levels of the cortex, is difficult to reconcile with the observations of Mountcastle and Powell (59) and Poggio and Mountcastle (60) concerning tactile sense and kinesthesia. These authors conclude that: "the ventrobasal complex of the thalamus is the site of thalamic transfer of the medial lemniscus component of the somatic afferent system, a component defined as comprising those fibers whose cells of origin lie within the dorsal column nuclei." Each neuron of the ventrobasal complex: (1) is related to restricted, specific and unchanging receptive fields on the contralateral side of the body, and (2) can be activated by either superficial mechanical stimulation of the skin or mechanical alteration of deep structures (especially joint rotation), but only by one of these. These neurons, regarded as modality specific, are thought to contribute almost exclusively to perception of tactile sense and kinesthesia. These findings strongly suggest that the somatotopic organization for specific modalities, conveyed to the thalamus via the posterior columns and the medial lemniscus, must be maintained at the only known synaptic junction of this system, the nuclei gracilis and cuneatus. Mountcastle and Powell (59) clearly state: "At each level elements devoted to this submodality (i.e., kinesthesia) are intermingled with those of others (i.e., tactile sense) in a single and mutual somatotopic pattern."

The physiological studies of Kruger, Siminoff and Witkovsky (61), based upon single neuron analysis of dorsal column nuclei in the cat, provide no clear suggestion of a rostro-caudal differentiation either in terms of somatotopy or modality segregation. It was further clear from this study that the entire body was represented at all rostrocaudal levels explored in detail. The evidence provided by these authors appears to substantiate the findings of Mountcastle and his colleagues and data available from the present investigation.

Observations in the current study con-

cerning the somatotopic termination of ascending dorsal root fibers in the nucleus gracilis appear to support the studies of Mountcastle and his colleagues. The somatotopic termination of dorsal root fibers in the nucleus gracilis, while very irregular for certain dorsal roots, seems to extend throughout the nucleus. It is characterized by relatively regular zones of termination for dorsal root fibers related to the lower thoracic, upper lumbar and sacral segments, relatively irregular and larger zones of termination for fibers from the lumbar enlargement, and a high degree of overlapping terminations, especially for the lower lumbar roots (figs. 2, 4, 5, 6). The area of the terminal zones for fibers from different dorsal roots varies. Terminal zones for the lower thoracic and upper lumbar dorsal root fibers, arranged parallel to the lateral border of the nucleus gracilis, are relatively small (fig. 31). The terminal zone for root fibers of Co1, located dorsomedial throughout most of the nucleus, also is relatively small (fig. 36). The lower lumbar dorsal roots terminate in overlapping, irregularly shaped zones in the central region of the nucleus (figs. 4, 5, 34). The S1 dorsal root terminal zone is fairly large, located dorsomedially, and overlaps portions of the central part of the nucleus (fig. 35). The largest terminal zones in the nucleus gracilis are those related to the lower four lumbar dorsal roots.

Attempts to determine the somatotopic termination of dorsal root fibers in the nucleus gracilis are much more difficult than similar studies for the nucleus cuneatus, because: (1) the nucleus gracilis has a greater rostrocaudal extent, (2) the fibers of the fasciculus gracilis are intermingled with irregularly shaped cell groups for long distances, and (3) there is greater difficulty in establishing whether degeneration is terminal or in passage. While there probably are some areas within the nucleus gracilis that receive exclusively the ascending fibers from particular dorsal roots, such exclusive areas are much smaller than those in the nucleus cuneatus.

Comparison of dorsal root projections to the medullary relay nuclei. A comparison of dorsal root projections to different medullary relay nuclei in the monkey

precluded a more detailed analysis of terminations in this relay nucleus.

Recent studies (Hand, '66) of lumbosacral dorsal root terminations in the nucleus gracilis of the cat employing silver staining methods have demonstrated a different organization. This author relates his observations to cytologically distinct subdivisions of the nucleus gracilis. Three cytologically distinct regions of the nucleus gracilis have been recognized (Cajal, '09; Taber, '61; Kuypers and Tuerk, '64): (1) a reticular region rostral to the obex characterized by a loose organization of cells, (2) a "cell nest" region caudal to the obex characterized by cell clusters, and (3) a caudal region of the nucleus characterized by fewer cells occurring singly or in small clusters. Although a definite somatotopic lamination was found in the nucleus gracilis, generally similar to that reported by Ferraro and Barrera ('35) and Walker and Weaver ('42), this lamination was found chiefly in the "cell nest" region and was not demonstrable in the reticular region where terminal degeneration was diffuse with impressive intersegmental overlap. In the "cell nest" region, dorsal root fibers related to more distal parts of the body terminated more dorsally than those related to proximal parts of the body. Of special interest was the observation that the density and extent of degeneration in the nucleus gracilis did not appear to be related to the size of the peripheral dermatome, but to its proximal or distal position on the body surface. It has been suggested that this finding may be related to the greater density of cutaneous receptors in more distal dermatomes.

Physiological studies in the cat suggest that neurons in the nucleus gracilis exhibit rostrocaudal differences with respect to: (1) the size of peripheral receptive fields which supply afferent input (Gordon and Paine, '60; McComas, '63), and (2) segregation of sensory modality (Kuhn, '49; Perl, Whitlock and Gentry, '62; Gordon and Jukes, '64; Winter, '65). Rostral portions of the nucleus (i.e., reticular region) are said to be related to deep pressure and joint movement, while the "cell nest" and caudal regions of the nucleus are related to hair and skin receptors.

Anatomical studies (Kuypers and Tuerk,

'64) of the nuclei cuneatus and gracilis in the cat provide information concerning dendritic architecture, dorsal root terminations, and cells contributing fibers to the medial lemniscus. Cell clusters in the nucleus gracilis are said to consist of large round cells arranged in a circular fashion which possess densely packed dendritic trees composed of many bushy dendrites. Cells in rostral and caudal parts of the nucleus gracilis appear to be triangular in shape, smaller, and possess long radiating dendrites. Dorsal root fibers from L6, L7 and S1 distributed fibers to both rostral and caudal parts of the nucleus gracilis. Caudally fibers were distributed to cell clusters in medial parts of the nucleus. Rostral fibers were distributed more diffusely. These authors postulated that regions of the nucleus gracilis having cells with small densely packed dendritic trees probably maintain small receptive fields, while those regions of the nucleus characterized by cells with radiating dendrites maintain larger receptive fields. Their anatomical findings were considered to correlate closely with the physiological observations of Gordon and Paine ('60). These data have been interpreted (Kuypers and Tuerk '64) as suggesting that the cell clusters of the nucleus gracilis possess a greater spatial resolving power than the regions containing smaller cells with long radiating dendrites. Cell clusters in the so-called "cell nest" region were considered to be related to small receptive fields that convey impulses largely from hair receptors (Perl, Whitlock and Gentry, '62). Cells in the rostral part of the nucleus gracilis with radiating dendrites were considered to respond to proprioceptive stimuli (Kuhn '49).

Following section of the medial lemniscus in the upper midbrain of kittens Kuypers and Tuerk ('64) reported chronic retrograde cell changes mainly in the cell clusters of the "cell nest" region of the nucleus gracilis. While these data were not interpreted to mean that cells in the rostral part of the nucleus gracilis do not contribute fibers to the medial lemniscus, they supported the thesis that rostrally located cells at least react differently to axonal interruption. These rostral cells of the nucleus gracilis also differ from those of the "cell

rhizotomy and progressively diminishes at increasing distances from the sectioned root; progressive diminution of degeneration is greatest in the anterior horn and in the segments caudal to the dorsal rhizotomy.

2. Lower thoracic and upper lumbar dorsal roots distribute fibers within the spinal gray, which are virtually limited to one segment above and below root entry, except for fibers projecting to the dorsal nucleus.

3. Dorsal roots of the lumbar enlargement distribute fibers within certain parts of the spinal gray at the level of rhizotomy and in the two adjacent spinal segments above and below, except for fibers projecting to medial parts of lamina VI and the dorsal nucleus. The first coccygeal dorsal root distributes fibers in the spinal gray in the segment of entry and in the two adjacent rostral spinal segments.

4. Lower thoracic, lumbar and sacrococcygeal dorsal roots project fibers to medial and central parts of laminae III and IV at the level of the rhizotomy; lower thoracic, upper lumbar and sacrococcygeal dorsal root fibers terminate in more medial regions of these laminae than do fibers of dorsal roots in the lumbar enlargement.

5. Dorsal root fibers of the lumbar enlargement project fibers to cells in the medial part of lamina VI throughout all levels of the lumbar enlargement.

6. Dorsal root fibers from lower thoracic, lumbar and sacral segments project to the dorsal nucleus; fibers from lower thoracic and upper lumbar dorsal roots reach portions of the dorsal nucleus three to eight segments above the rhizotomy level and one to four segments below it. Dorsal root fibers from the lumbar enlargement project to portions of Clarke's column caudal to T7 with the most profuse terminations at the L2 and L3 levels.

7. Dorsal root fibers projecting to portions of the dorsal nucleus above the level of rhizotomy change their disposition at various levels, but ultimately become localized to dorsomedial parts of the nucleus; descending fibers from these roots terminate in lateral parts of the dorsal nucleus at nearly all levels.

8. Fibers from lower thoracic, lumbar, sacral and coccygeal dorsal roots project to

the intermediomedial nucleus, usually maximally, at the segment of entry.

9. Fibers from lower thoracic, lumbar, and sacral dorsal roots project to cell groups of lamina IX by two pathways: (a) via medial parts of lamina VIII, and (b) via central parts of lamina VII. Lower thoracic, upper lumbar and sacral dorsal root fibers reach cell groups of lamina IX primarily via medial parts of lamina VIII, while dorsal root fibers of the lumbar enlargement mainly traverse central parts of lamina VII.

10. Ascending fibers in the fasciculus gracilis arise from the dorsal roots of T8 and all more caudal spinal segments; fibers issuing from dorsal roots of the lumbar enlargement contribute the largest number of fibers.

11. Ascending dorsal root fibers in the fasciculus gracilis exhibit only a general segregation because of extensive overlap; fibers from rostral spinal segments are lateral and those from caudal segments are medial.

12. Descending collaterals of dorsal root fibers, arranged in oblique bands in parts of the fasciculus gracilis comparable to that of ascending fibers of the same dorsal root, project caudally for two to four spinal segments, and enter: (a) lateral portions of the dorsal nucleus in lower thoracic or upper lumbar segments, or (b) medial parts of lamina VI throughout the lumbar enlargement.

13. Ascending collaterals of lower thoracic, lumbar, sacral and coccygeal dorsal roots project in a somatotopic and overlapping fashion throughout the rostrocaudal extent of the nucleus gracilis. Zones of the nucleus gracilis receiving terminal dorsal root fibers are organized, so that: (a) roots of the lumbar enlargement project to irregular shaped areas in the central core region of the nucleus, (b) lower thoracic and upper lumbar roots project in serial fashion to narrow oblique laminae lateral to the central core region, and (c) sacral and coccygeal dorsal roots project in serial fashion to crescent-shaped laminae in dorsomedial parts of the nucleus.

14. The areas of the terminal projection zones of dorsal root fibers in the nucleus gracilis: (a) are related to the size of the dorsal root and the number of ascending

reveals both similar and unique features. Fibers from all cervical and the upper seven thoracic dorsal roots project in a somatotopic fashion upon portions of the cuneate and accessory cuneate nuclei. Fibers from lower thoracic, lumbar, sacral and coccygeal dorsal roots project somatotopically upon portions of the nucleus gracilis. In addition a few fibers from the lower thoracic and the first lumbar dorsal roots appear to project within the medial border of the nucleus cuneatus. No fibers from dorsal roots caudal to T7 project fibers to the accessory cuneate nucleus.

In Part I (Shriver, Stein and Carpenter, '68) of this study comparisons were made of dorsal root projections to the cuneate and accessory cuneate nuclei. Briefly, this comparison indicated that the patterns of terminations of C1 to T1 dorsal root fibers in these nuclei was remarkably similar, in that: (1) fibers from C5 to C8 terminated in a central core region, while fibers from other dorsal roots were arranged in oblique laminae about this core, and (2) fibers from the most rostral root (i.e., C1) terminated ventrolaterally, while those from T1 ended dorsomedially. Ascending dorsal root fibers projecting to these nuclei terminated in relatively discrete, but overlapping areas; fibers from one dorsal root mainly overlapped part of the territory of the next highest root.

Ascending fibers from the lower four lumbar dorsal roots terminate in a central core region comparable to that described for the cuneate and accessory cuneate nuclei. The zones of termination of these fibers in the nucleus gracilis are characterized by their large size, irregular configurations and extensive overlap. Fibers projecting to the central core region in the cuneate nucleus terminate in relatively regular wedge-shaped areas that have a consistent patterned overlap. In both the nuclei gracilis and cuneatus the area of the terminal zones bears a definite relationship to the size of the dorsal root and the number of ascending fibers in the posterior columns.

Dorsal root fibers terminating in laminae surrounding the central core region in the nucleus gracilis form narrower, more regularly shaped, primarily vertically-oriented laminar zones which overlap each other in

a lateral to medial sequence. Fibers of dorsal roots rostral to the lumbar segment terminate lateral to the central region, while fibers from roots caudal to the enlargement terminate dorsomedial to the core region. In the cuneate and accessory cuneate nuclei the laminar arrangement of the terminal zones of all cervical and the first thoracic dorsal roots is more nearly horizontal. Fibers of the first thoracic dorsal root terminate most dorsomedially, while those from other dorsal roots terminate more laterally. This difference in orientation of terminal laminar zones seen in these medullary relay nuclei may be due to the lateral shift and external rotation of the alar plate of the myelencephalon which occurs with the development of the fourth ventricle. Thoracic dorsal roots caudal to T1 form the narrowest terminal laminae in all three of the medullary relay nuclei. Upper thoracic dorsal root fibers terminate in lateral parts of the accessory cuneate nucleus, and in dorsomedial parts of the cuneate nucleus. Lower thoracic dorsal root fibers terminate in lateral parts of the nucleus gracilis.

Comparisons of the laminar terminations in the medullary relay nuclei indicate that fibers of nearly all dorsal roots studied project throughout the rostrocaudal extent of their respective medullary relay nuclei. The degree of overlapping fiber terminations in the central core region is much greater in the nucleus gracilis than in the cuneate or accessory cuneate nuclei. This suggests that in the cuneate and accessory cuneate nuclei there is a higher degree of autonomous terminal representation of individual dorsal root fibers than in the gracile nucleus. Further this pattern of autonomous and overlapping terminal zones, clearly demonstrated in the cuneate and accessory cuneate nuclei, applies to all cervical and the first thoracic dorsal roots. Fibers from all more caudal dorsal roots including those from the lumbar enlargement, appear to have predominantly overlapping terminal projections in their respective medullary relay nuclei.

CONCLUSIONS

The following conclusions were drawn from this study:

1. In the monkey spinal degeneration is most profuse at the level of the dorsal

- vague, J. M., and H. Ha. 1964 The terminal fields of dorsal root fibers in the lumbosacral spinal cord of the cat, and the dendritic organization of the motor nuclei. In: *Organization of the Spinal Cord*, Eds., J. C. Eccles and J. P. Schadé, vol. 11. Progress in Brain Research. Elsevier, Amsterdam, pp. 120-154.
- Fin, B. M., and M. B. Carpenter. 1965 Effects of dorsal rhizotomy upon subthalamic dyskinesia in the monkey. *Arch. Neur.*, 13: 567-583.
- Frieling, P., and H. G. J. M. Kuypers. 1967 Anatomical organization of the brachial spinal cord of the cat. I. The distribution of dorsal root fibers. *Brain Research*, 4: 1-15.
- Gratáwohl, J. 1964 Neuronal and synaptic arrangement in the substantia gelatinosa Rolandi. *J. Comp. Neur.*, 122: 219-240.
- Gratáwohl, J., and A. Albert. 1955 The synapology of Clarke's column. *Acta Morphol. (Budapest)*, 5: 43-52.
- Gratáwohl, J., and T. Kiss. 1949 Projection of dermatomes in the substantia gelatinosa. *Arch. Neur. Psychiat.*, 62: 734-744.
- Taber, E. 1961 The cytoarchitecture of the brain stem of the cat. I. Brain stem nuclei of cat. *J. Comp. Neur.*, 116: 27-70.
- Thomas, C. E., and C. M. Combs. 1965 Spinal cord segments. B. Gross structure in the monkey. *Am. J. Anat.*, 116: 205-216.
- Walker, A. E., and T. A. Weaver, Jr. 1942 The topical organization and termination of the fibers of the posterior columns in *Macaca mulatta*. *J. Comp. Neur.*, 76: 145-158.
- Wall, P. D. 1960 Cord cells responding to touch, damage, and temperature of skin. *J. Neurophysiol.*, 23: 197-210.
- . 1967 The laminar organization of dorsal horn and effects of descending impulses. *J. Physiol.*, 188: 403-423.
- Winter, D. L. 1965 N. Gracilis of cat. Functional organization and corticofugal effects. *J. Neurophysiol.*, 28: 48-70.

fibers in the fasciculus gracilis, and (b) are arranged in an overlapping lateral (rostral dorsal root) to medial (caudal dorsal root) sequence.

15. The degree of overlapping terminations of dorsal root fibers in the nucleus gracilis is more extensive and irregular than in the cuneate or accessory cuneate nuclei, and suggests that there is less autonomous terminal representation of individual dorsal root fibers in the nucleus gracilis.

LITERATURE CITED

- Anderson, F. D. 1960 Distribution of dorsal root fibers in the cat spinal cord. *Anat. Rec.*, 136: 154.
- Brodal, A., and O. Pompeiano 1957 The vestibular nuclei in the cat. *J. Anat.*, 91: 438-454.
- Cajal, S. Ramón Y. 1909 *Histologie du Système nerveux de l'homme et des vertébrés*. Maloine, Paris, Vol. I.
- Chang, H. T., and T. C. Ruch 1947 Organization of the dorsal columns of the spinal cord and their nuclei in the spider monkey. *J. Anat.*, 81: 140-149.
- Collier, J., and E. F. Buzzard 1903 The degenerations resulting from lesions of posterior nerve roots and from transverse lesions of the spinal cord in man. A study of twenty cases. *Brain*, 26: 559-591.
- Earle, K. M. 1952 Tract of Lissauer and its possible relation to the pain pathway. *J. Comp. Neur.*, 96: 93-111.
- Eccles, J. C., R. M. Eccles and A. Lundberg 1960 Types of neurones in and around the intermediate nucleus of the lumbosacral cord. *J. Physiol.*, 154: 89-114.
- Ferraro, A., and S. E. Barrera 1934 Effects of experimental lesions of the posterior columns in *Macacus rhesus* monkeys. *Brain*, 57: 307-332.
- 1935 Posterior column fibers and their terminations in *Macacus rhesus*. *J. Comp. Neur.*, 62: 507-530.
- Flechsig, P. 1876 *Die Leitungsbahnen im Gehirn und Rückenmark des Menschen auf Grund entwicklungsgeschichtlicher Untersuchungen*. Engelmann, Leipzig.
- Gombault, A., and Philippe 1894 Contribution à l'étude des lésions systématisées dans les cordons blancs de la moelle épinière. *Arch. Med. exp.*, 6: 365-424; 538-582.
- Gordon, G., and M. G. M. Jukes 1964 Dual organization of the exteroceptive components of the cat's gracile nucleus. *J. Physiol.*, 173: 263-290.
- Gordon, G., and P. H. Paine 1960 Functional organization in nucleus gracilis of the cat. *J. Physiol.*, 153: 331-349.
- Grant, G., and B. Rexed 1958 Dorsal spinal root afferents to Clarke's column. *Brain*, 81: 567-576.
- Hand, P. J. 1966 Lumbosacral dorsal root terminations in the nucleus gracilis of the cat. Some observations on terminal degeneration in other medullary sensory nuclei. *J. Comp. Neur.*, 126: 137-156.
- Kruger, L., R. Siminoff and P. Witkovsky 1961 Single neuron analysis of dorsal column nuclei and spinal nucleus of trigeminal in cat. *J. Neurophysiol.*, 24: 333-349.
- Kuhn, R. 1949 Topographical pattern of cutaneous sensibility in the dorsal column nuclei of the Trans. A.N.A., 74: 227-230.
- Kuypers, H. G. J. M., and J. D. Tuerk 1964 Contribution of the cortical fibers within the nucleus gracilis and gracilis in the cat. *J. Anat. (London)*, 143-162.
- Liu, C. N. 1956 Afferent nerves to Clarke's and lateral cuneate nuclei in the cat. *Arch. Neurol. Psychiat.*, 75: 67-77.
- Lloyd, D. P. C., and A. K. McIntyre 1950 Dorsal column conduction of group I muscle afferent impulses and their relay through Clarke's column. *Neurophysiol.*, 13: 39-54.
- McComas, A. J. 1963 Responses of the rat dorsal column system to mechanical stimulation of the paw. *J. Physiol.*, 166: 435-448.
- Mott, F. W., and C. S. Sherrington 1895 Experiments upon the influence of sensory nerves upon movement and nutrition of the limbs. *Proc. Roy. Soc.*, 5: 481-488.
- Mountcastle, V. B., and T. P. S. Powell 1959 Central nervous mechanisms subserving position sense and kinesthesia. *Bull. Johns Hopkins Hosp.*, 11: 173-200.
- Oscarsson, O. 1965 Functional organization of spinocerebellar and cuneocerebellar tracts. *Physiol. Rev.*, 45: 495-522.
- Pass, I. J. 1933 Anatomic and functional relationship of nuc. dorsalis (Clarke's column). *Arch. Neurol. Psychiat.*, 30: 1025-1045.
- Perl, E. R., D. G. Whitlock and J. R. Gentry 1967 Cutaneous projection to second-order neurons of the dorsal column system. *J. Neurophysiol.*, 25: 337-353.
- Poggio, G. F., and V. B. Mountcastle 1960 A functional contributions of the lemniscal spinothalamic systems to somatic sensibility. *J. Johns Hopkins Hosp.*, 106: 266-316.
- Pompeiano, O., and A. Brodal 1957 Spino-cuneate fibers in the cat. An experimental study. *J. Comp. Neur.*, 108: 353-382.
- Ralston, H. J. III 1965 The organization of the stantia gelatinosa Rolandi in the cat lumbosacral spinal cord. *Z. Zellforsch.*, 67: 1-23.
- Ranson, S. W. 1913 The course within the spinal cord of non-medullated fibers of the dorsal roots: a study of Lissauer's tract in the cat. *J. Comp. Neur.*, 23: 259-281.
- 1914 An experimental study of Lissauer's tract and the dorsal roots. *J. Comp. Neur.*, 24: 531-545.
- Rexed, B. 1952 The cytoarchitectonic organization of the spinal cord in the cat. *J. Comp. Neur.*, 96: 415-496.
- 1954 A cytoarchitectonic atlas of the spinal cord in the cat. *J. Comp. Neur.*, 100: 297-400.
- Schmiedt, J. 1939 Das Verhalten der Hinterwurzel kollateralen im Rückenmark. *Z. Anat. Entwickl.-gesch.*, 109: 665-687.
- Shriver, J. E., B. M. Stein and M. B. Carpenter 1968 Central projections of spinal dorsal roots in the monkey. I. Cervical and upper thoracic dorsal roots. *Am. J. Anat.*, 123: 27-74.
- Sprague, J. M. 1958 The distribution of dorsal root fibres on motor cells in the lumbosacral spinal cord of the cat, and the site of excitatory and inhibitory terminations in monosynaptic pathways. *Proc. Roy. Soc. B*, 149: 534-556.



PLATE 1

EXPLANATION OF FIGURES

- 7 Rhesus C-1017. Photomicrograph of degeneration at level of root entry following section of the right T8 dorsal root. Note degeneration in medial and central parts of laminae III and IV and in the dorsal nucleus. Nauta-Gygax. $\times 65$.
- 8 Rhesus C-1012. Photomicrograph of degeneration at T12 following section of the left dorsal root at that level. Note fascicles of degeneration coursing through, and curving around, the medial portion of lamina II to enter medial parts of laminae III and IV and the ventrolateral portion of the dorsal nucleus. Nauta-Gygax. $\times 65$.
- 9 Rhesus C-1011. Photomicrograph of degeneration at L4 following right dorsal rhizotomy at that level. Degeneration is present in medial and central parts of laminae III and IV and lateral parts of laminae II through IV. Note the relatively clear zones in the most medial portions, and the lateral half, of laminae III and IV. Nauta-Gygax. $\times 65$.
- 10 Rhesus C-914. Photomicrograph of degeneration at L7 following section of the left dorsal root at that level. Note degeneration in the lateral two-thirds of the fasciculus gracilis dorsal and medial to the posterior horn. Nauta-Gygax. $\times 37$.
- 11 Rhesus C-912. Photomicrograph of degeneration at the level of root entry following left S1 dorsal rhizotomy. Root fibers enter medial and central portions of laminae III and IV mainly by coursing through medial parts of lamina II. Nauta-Gygax. $\times 42$.
- 12 Rhesus C-1014. Photomicrograph of degeneration at Co1 following section of the right dorsal root at that level. Note the medial position of fascicles of fibers entering the spinal gray and the large triangular area of degeneration in central lamina VII. Nauta-Gygax. $\times 33$.

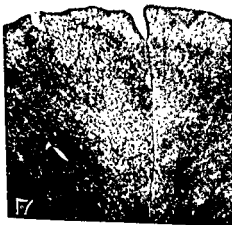
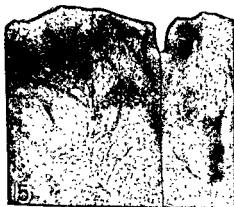


PLATE 2

EXPLANATION OF FIGURES

- 13 Rhesus C-1017. Photomicrograph of degeneration at the T2 level following section of the right T8 dorsal root. The ventromedial portion of the band of ascending degeneration is present in the lateral part of the fasciculus gracilis, while the dorsolateral portion is located in medial parts of the fasciculus cuneatus. Nauta-Gygax. $\times 65$.
- 14 Rhesus C-916. Photomicrograph of degeneration at the T2 level following section of the left T10 dorsal root. These ascending fibers form a narrow band in the fasciculus gracilis medial, parallel and close to the posterior intermediate septum. Nauta-Gygax. $\times 65$.
- 15-16 Rhesus C-914. Photomicrographs of ascending degeneration in medial portions of the fasciculus gracilis at the L5 (fig. 15) and the L3 (fig. 16) levels following left L7 dorsal rhizotomy. In figure 16 degenerated dorsal root fibers can be seen entering the dorsolateral part of the fasciculus gracilis following right L3 dorsal rhizotomy. Nauta-Gygax. $\times 37, \times 33$.
- 17 Rhesus C-912. Photomicrograph of degeneration in medial parts of the fasciculus gracilis at the T12 level after section of the left S1 dorsal root. Note that this crescent-shaped band of ascending fibers is contiguous with the posterior median septum ventrally, but separated from it dorsally by a small medial wedge of normal fibers. Nauta-Gygax. $\times 68$.
- 18 Rhesus C-1014. Photomicrograph of ascending degeneration in the fasciculus gracilis at the T3 level resulting from section of dorsal roots L6 (left) and Co1 (right). The large band of degeneration in medial parts of the fasciculus cuneatus resulted from section of the right C8 dorsal root. Drawings in figure 3 show both ascending and descending degeneration in the posterior columns resulting from sections of these roots. Nauta-Gygax. $\times 40$.

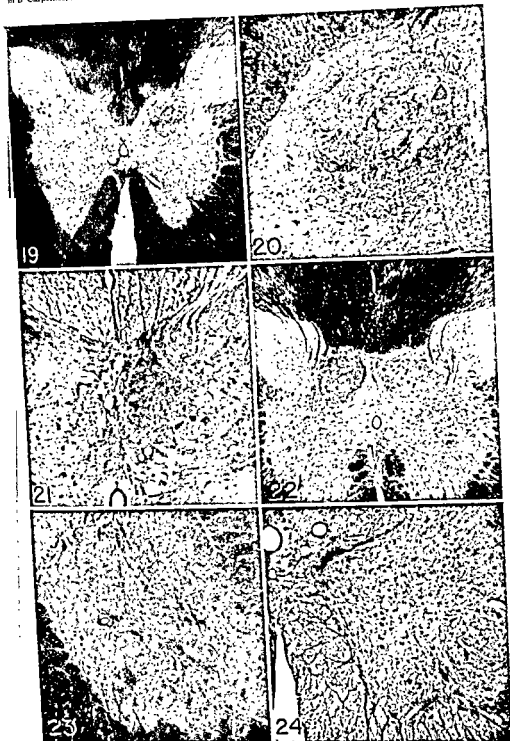


PLATE 3

EXPLANATION OF FIGURES

- 19-20 Rhesus C-1011. Photomicrographs of terminal degeneration in the dorsal nucleus at the L2 level following section of the right L4 dorsal root. Note that the degeneration is distributed widely to virtually all parts of the dorsal nucleus. Nauta-Gygax. $\times 30$, $\times 100$.
- 21 Rhesus C-916. Photomicrograph of right degenerated L6 dorsal root fibers terminating within a small dorsomedial region of the dorsal nucleus at the L1 level. Nauta-Gygax. $\times 95$.
- 22 Rhesus C-1014. Photomicrograph of degenerated fibers from the left L6 dorsal root terminating throughout the entire cross-sectional area of the dorsal nucleus at the L2 level. Nauta-Gygax. $\times 45$.
- 23 Rhesus C-1011. Photomicrograph of L4 dorsal root fibers on the right projecting ventromedially to the intermediomedial nucleus and the dorsomedial part of lamina VIII and ventrally through central parts of lamina VII to cell groups of lamina IX at L4. Nauta-Gygax. $\times 50$.
- 24 Rhesus C-914. Photomicrograph of L3 dorsal root degeneration on the right projecting to the intermediomedial nucleus and into the most medial part of lamina VIII at L5. Nauta-Gygax. $\times 35$.

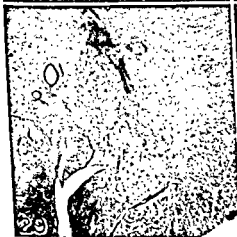
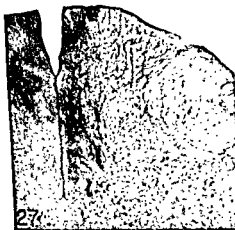
TRIAL DORSAL ROOT PROJECTIONS II
John B. Carpenter, Bennett M. Stein and Joyce E. Shriver

PLATE 4

EXPLANATION OF FIGURES

- 25 Rhesus C-912. Photomicrograph of right L1 dorsal root fibers projecting into laminae III and IV, and directly and profusely to cells of the dorsal nucleus at the level of root section. Nauta-Gygax. $\times 30$.
- 26 Rhesus C-914. Photomicrograph of descending L3 dorsal root fibers projecting to medial parts of lamina VI at L5 on the right side. Nauta-Gygax. $\times 165$.
- 27-28 Rhesus C-916. Photomicrographs of right L6 dorsal root fibers projecting from the fasciculus gracilis into medial and central parts of lamina VI at L7 (fig. 27) and L3 (fig. 28) levels. Nauta-Gygax. $\times 40, \times 100$.
- 29-30 Rhesus C-1014. Photomicrographs of right C6 dorsal root fibers passing ventrally from lamina VII through medial parts of lamina VIII to the commissural nucleus within this lamina. In figure 30 these fibers are seen closely surrounding cells of this nucleus. Nauta-Gygax. $\times 68, \times 165$.

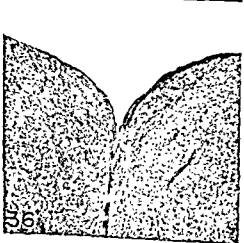
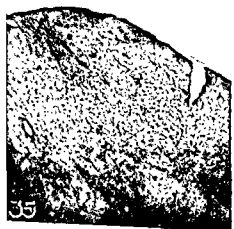
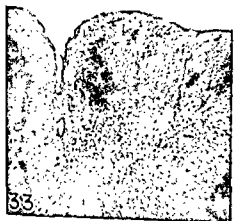
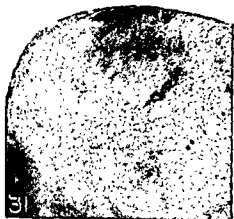


PLATE 5

EXPLANATION OF FIGURES

- 31 Rhesus C-1017. Photomicrograph of degenerated fibers from the right T8 dorsal root terminating in the lateral border of the nucleus gracilis. Nauta-Gygax, $\times 30$.
- 32 Rhesus C-1011. Photomicrograph of right degenerated L4 dorsal root fibers terminating rather diffusely in dorsolateral portions of the nucleus gracilis. Nauta-Gygax, $\times 35$.
- 33 Rhesus C-1012. Photomicrograph of right degenerated L5 dorsal root fibers terminating ventrally and centrally in middle portions of the nucleus gracilis. Nauta-Gygax, $\times 30$.
- 34 Rhesus C-1014. Photomicrograph of left L6 dorsal root fibers terminating in irregular shaped central portions of the nucleus gracilis. (See fig. 36). Nauta-Gygax, $\times 30$.
- 35 Rhesus C-912. Photomicrograph of left S1 dorsal root fibers terminating in a crescent-shaped area in the dorsomedial portion of the nucleus gracilis. Nauta-Gygax, $\times 70$.
- 36 Rhesus C-1014. Photomicrograph of L6 (left) and Co1 (right) dorsal root fibers terminating in portions of the nuclei gracilis. Nauta-Gygax, $\times 30$.

Subcutaneous Implantation of Autogenous Rat Molars¹

JAMES T. IRVING AND JAMES A. BOND²
Forsyth Dental Center, Boston, Massachusetts

TRACT Maxillary molars were extracted, and decalcified or devitalized prior to subcutaneous implantation in the same animals. All molar implants attracted large numbers of osteocytes during the first week of implantation. After two weeks small basophilic mononuclear cells appeared which penetrated the dentinal tubules of decalcified molars and were associated with considerable resorption of dentin and predentin. Giant cells were not usually observed near decalcified molars, but large numbers of them were attracted to FDNB treated molars. Giant cells appeared in moderate numbers around devitalized molars and were associated with resorption of intact root surfaces after 56 days. The significance of these results is discussed.

Method for studying bone resorption around subcutaneously implanted, autogenously standardized environments was described by Irving and Bond (1963). They implanted, subcutaneously, pieces of autogenous rat scapulae and observed the cellular response. Multinucleated giant cells rapidly accumulated around the bone implants and were associated with extensive resorption. The response was the same for bone implants which were either decalcified, or treated by repeated freezing and thawing. On the other hand, rachitic osteoids did not attract giant cells until it had been calcified after implantation. The results were similar, in most respects, to those of Irving and Handelman (1963) who included that the subcutaneous implantation of autogenous bone was a valid method for the study of osteoclasts.

Irving and Migliore (1965) conducted a study of implants of chemically treated autogenous collagen and sought to determine what influence the chemical and physical nature of the treatment has on the cellular response. Giant cells were not observed around collagen implants which were not chemically treated, and several different kinds of chemical treatment had no effect on the cellular response. On the other hand, a giant cell response was observed around collagen which was treated prior to implantation with 1-fluoro-2,4-dinitrobenzene (FDNB). The untreated bone implants did not elicit a giant cell response which was enhanced in bone treated with FDNB.

These findings showed that there is a high degree of specificity of the chemical changes induced in both isolated collagen and bone, which govern the appearance of giant cells.

Since teeth, under most circumstances, do not readily resorb, it appeared of interest to study the tissue reaction to implanted molars and to relate the findings to resorption of bone implants. The present study was designed to utilize the subcutaneous environment (Irving and Handelman, 1963) for the implantation of autogenous rat molars.

METHODS AND MATERIALS

Holtzman strain 23 day old male albino rats (65-70 gm) were used in the study. Thirty to sixty animals were used in each experiment, with 4-6 animals for each implantation period.

Surgical procedures. Maxillary first molars were extracted under ether anesthesia, placed in test tubes, and treated as follows.

Preparation of molars for implantation

Group I. Devitalized molar implants. Extracted molars were scraped free of food debris and adherent alveolar bone, then placed in an aqueous antibiotic solu-

¹This work was supported by U.S. Public Health grant DE-1592, National Institute of Dental Research.

²A Postdoctoral Research Fellow in Orthodontics supported by the National Institute of Dental Research while this work was in progress.

The Subcutaneous Implantation of Autogenous Rat Molars¹

JAMES T. IRVING AND JAMES A. BOND²

Forsyth Dental Center, Boston, Massachusetts

ABSTRACT Maxillary molars were extracted, and decalcified or devitalized prior to subcutaneous implantation in the same animals. All molar implants attracted large numbers of leukocytes during the first week of implantation. After two weeks small basophilic mononuclear cells appeared which penetrated the dentinal tubules of decalcified molars and were associated with considerable resorption of dentin and predentin. Giant cells were not usually observed near decalcified molars, but large numbers of them were attracted to FDNB treated molars. Giant cells appeared in moderate numbers around devitalized molars and were associated with resorption of intact root surfaces after 56 days. The significance of these results is discussed.

A method for studying bone resorption under relatively standardized environmental conditions was described by Irving and Handelman ('63). They implanted, subcutaneously, pieces of autogenous rat scapulae and observed the cellular response. Large multinucleated giant cells rapidly aggregated around the bone implants and were associated with extensive resorption. The response was the same for bone implants which were either decalcified, or devitalized by repeated freezing and thawing. On the other hand, rachitic osteoid did not attract giant cells until it has become calcified after implantation. The giant cells were similar, in most respects, to osteoclasts, and Irving and Handelman ('63) concluded that the subcutaneous implantation of autogenous bone was a valid model for the study of osteoclasts.

Irving and Migliore ('65) conducted a study using implants of chemically treated and untreated autogenous collagen and bone to determine what influence the chemical and physical nature of the implant has on the cellular response. Giant cells were not observed around collagen implants which were not chemically treated, and several different kinds of chemical treatment had no effect on the cellular response. On the other hand, a strong giant cell response was observed when collagen was treated prior to implantation with 1-fluoro-2,4-dinitrobenzene (FDNB). The untreated bone implants showed a mild giant cell response which was enhanced in bone treated with FDNB.

These findings showed that there is a high degree of specificity of the chemical changes induced in both isolated collagen and bone, which govern the appearance of giant cells.

Since teeth, under most circumstances, do not readily resorb, it appeared of interest to study the tissue reaction to implanted molars and to relate the findings to resorption of bone implants. The present study was designed to utilize the subcutaneous environment (Irving and Handelman, '63) for the implantation of autogenous rat molars.

METHODS AND MATERIALS

Holtzman strain 23 day old male albino rats (65-70 gm) were used in the study. Thirty to sixty animals were used in each experiment, with 4-6 animals for each implantation period.

Surgical procedures. Maxillary first molars were extracted under ether anesthesia, placed in test tubes, and treated as follows.

Preparation of molars for implantation

Group I. Devitalized molar implants. Extracted molars were scraped free of food debris and adherent alveolar bone, then placed in an aqueous antibiotic solu-

¹This work was supported by U.S. Public Health grant DE-1592, National Institute of Dental Research.

²A Postdoctoral Research Fellow in Orthodontics supported by the National Institute of Dental Research while this work was in progress.

TABLE 1

Group 1 Devitalized molar implants

Number of animals	Treatment prior to implantation	Implantation periods
56	Freeze-thaw	2, 7, 14, 21, 28, 56, 84, 112, 140 days

Group 2 Decalcified molar implants

63	Decalcification	Hourly intervals from 1-24 hours and 1, 2, 3, 4, 5, 6, 7, 14, 28, 56 days
8	Decalcification and FDNB treatment	14 days
24	Decalcification	4, 14, 35, 56 days followed by acid phosphatase determination.

RESULTS

One of the implantation sites became necrotic, and most of the molars were recovered in highly vascular connective tissue capsules.

Reference molars. Reference sections of molars which were either devitalized or decalcified, but not implanted, were judged to be nonvital by the torn and disrupted appearance of all pulpal cells when compared with molars whose cells were fixed prior to decalcification.

Implanted molars. Histological examination of devitalized (Group I) and decalcified (Group II) molar implants revealed a marked difference in the tissue response.

Group I. The initial tissue response to the devitalized molar implants was the presence of large numbers of inflammatory cells, primarily neutrophils and eosinophils, which surrounded each tooth, and invaded the pulp chambers through the root canals. On rare occasions, leukocytes penetrated and dentinal tubules as far as the predentin layer (fig. 1).

After 14 days the leukocytes decreased in numbers and were replaced with small, basophilic mononuclear cells, which also invaded the capsules and pulp cavities. They were also occasionally seen within the tubules of the predentin layer. Unlike the leukocytes, the basophilic mononuclear cells were associated with mild resorption of predentin and dentin as evidenced by the scalloping of these usually smooth surfaces (fig. 2).

In most cases a decrease in cell numbers in the coronal pulp cavity was observed after 28 days, while multinucleated giant cells began to appear in significant numbers around fragmented or damaged roots. Little, if any, cellular activity was evident near intact roots or crown dentin surfaces at this stage. Deposition of an osteoid type of substance occurred in the pulp horns of some of the implants (fig. 3).

After 56 days moderate resorption of intact root surfaces by giant cells was evident (fig. 4).

Group II. The primary response to decalcified molar implants during the first week was very similar to that of the devitalized molar implants, but more invasive. After three hours of implantation, leukocytes surrounded the molars and invaded the pulp cavities by way of the root canals. Six hours later, these cells were observed penetrating deeply into the dentinal tubules. Penetration of the tubules was not restricted to the predentin layer (fig. 5).

After 14 days, the leukocytes decreased in numbers and were replaced with large numbers of small basophilic mononuclear cells which also invaded the pulp cavities. These cells aggregated on pulpal and external dentin surfaces (former dentoenamel junction) and penetrated deeply into the dentinal tubules (fig. 6). After penetration, the nuclei of the mononuclear cells became indistinguishable from the cytoplasm and the elongated cells

tion, and frozen. The antibiotic solution consisted of 100 $\mu\text{gm/ml}$ streptomycin, 100 units/ml penicillin, and 100 $\mu\text{gm/ml}$ mycostatin in 500 ml sterile distilled water (Goldhaber, '58). The antibiotic solution was used to eliminate bacterial contamination carried on the teeth from the oral cavity. Molars were devitalized by repeated slow freezing and thawing, which consisted of one hour at 1°C , four hours at -4°C , four hours at -60°C (dry ice-acetone bath) followed by a one hour thaw period at room temperature. This procedure was repeated four times. Destruction of vital tissue structures resulted from the formation of large ice crystals within the cells, and from the subsequent thaw. Following devitalization, teeth were implanted directly from the antibiotic solution.

Group II. Decalcified molar implants. After extraction, molars were placed in 5% EDTA solution pH 7.0 for decalcification. After one day of immersion, food debris and alveolar bone remnants were scraped from the teeth. They were then decalcified for a period of 14 days in frequently changed EDTA solution, and thoroughly rinsed for two days in refrigerated distilled water. Decalcification with EDTA also devitalized the teeth and destroyed residual oral bacteria. Decalcified reference molars which were not implanted, were prepared for histological section and stained with hematoxylin and eosin. The method of von Kossa was used to determine the completeness of decalcification.

Implantation and histological examination. Implantation of treated molars was accomplished under ether anesthesia. The shaved hindquarters of the donor rat were painted with dilute tincture of iodine and a small incision was made. The molar was placed aseptically under the skin.

Molars were implanted for periods ranging from one hour to 140 days. At the end of the appropriate period the animals were sacrificed with chloroform, the implants recovered in their connective tissue capsules and immediately fixed in neutral formal-saline solution for 24 hours. The devitalized molar implants were then decalcified in formic acid-sodium citrate solution, and prepared for histological section. The decalcified molar implants

occasionally exhibited recalcification after implantation and required redecalcification in formic acid-sodium citrate solution for 24 hours prior to sectioning. The majority of decalcified molar implants, however, were imbedded after fixation. Staining was done with hematoxylin and eosin.

A majority of decalcified molars were implanted without further treatment, as were processed afterward as previously described. Three other groups of decalcified molars were treated by different techniques which will now be explained.

Molars treated with 1-fluoro-2,4-dinitrobenzene (FDNB). In order to make histological comparisons with FDNB-treated bone implants (Irving and Migliore, '65) a group of decalcified rat molars were treated with FDNB before implantation (Sanger, '45). Treatment was restricted to decalcified molars since the reaction is not complete in undecalcified specimens.

All FDNB-treated molars were implanted for 14 days, the period of maximum giant cell formation in bone implants. After recovery, implants were fixed in neutral formal-saline solution, prepared for histological section, and stained with hematoxylin and eosin.

A summary of the treatment of the two groups of rats is given in table 1.

Acid phosphatase determination. Molars in this group were extracted, decalcified, and implanted for periods of 4-140 days. After recovery, they were fixed in refrigerated Baker's formal-calcium solution pH 7.2 for 24 hours followed by at least 24 hours in a refrigerated solution of 0.88 M sucrose and 1% gum acacia (Holt, '59). Cryostat sections 8μ thick were made at -20°C and air dried. The acid phosphatase method of Barka and Anderson ('62) was then used. Air dried cryostat sections were incubated in the test solution at 25°C for periods of time ranging from ten minutes to two hours. Sixty minutes at 25°C was considered to produce optimal color. Decalcified reference molars, boiled reference molars, and liver sections in solutions, with and without substrate, were processed simultaneously as controls.

resorptive activity of the giant cells in molars was considerably less than that observed in bone.

The invasion of decalcified and vitalized molar implants by basophilic mononuclear cells was of considerable significance, in that these cells were associated with resorption of dentin and dentin. Similar cells were also observed in various tissue implants of Irving and Handelman ('62) and Irving and Migliore ('65), but were not related to resorption because of the presence of multinucleated giant cells and the irregular structure of the implanted tissues. The virtual absence of giant cells and the original smoothness and regularity of decalcified dentin and dentin surfaces allowed the formation of resorption lacunae associated with the basophilic mononuclear cells to be clearly demonstrated. Predentin resorption in calcified and devitalized molars was of interest in that this tissue has been regarded as immune to resorption (Cabrini, Maisto and Manfredi, '57).

Although resorption of dentin by mononuclear cells was observed in all molars (except those treated with FDNB) it was most extensive in decalcified molars and was often related to penetration of the dentinal tubules by these cells. As with the receding leukocytes, penetration of the dentinal tubules by the mononuclear cells appeared to be an active process. This was suggested by the extension of long aciculated cytoplasmic processes that often appeared to seek out dentinal tubules, which the processes entered before the nuclei.

The mechanism of dentin resorption could not be determined. However, extracellular enzyme secretion or phagocytosis were given serious consideration in view of the presence of acid phosphatase in discrete "lysosome-like" cytoplasmic bodies in the basophilic mononuclear cells. Acid phosphatase is a hydrolase which has been associated with lysosomes by DeDuve ('59). According to Barka ('62), phagocytic, secretory, and absorptive cells display the greatest acid phosphatase activity. This enzyme is found in high concentrations in multinucleated giant cells (Cabrini et al., '62) and has been associated with bone resorption (Suzi, Goldhaber, and Jennings,

'66). The presence of high concentrations of acid phosphatase, localized in cytoplasmic particles, would seem to be evidence of the resorptive capability of these cells.

The results of this study showed that the cellular responses to decalcified molars closely resembled that to implanted collagen (Irving and Migliore, '65) while the response to devitalized molar implants resembled that to bone implants. Although resorption of molars by mononuclear cells and multinucleated giant cells was significant, resorption of similar bone implants was more extensive and occurred more rapidly.

The cellular responses observed in this study closely resembled those reported by Langeland ('57) and Orban ('40) in studies of pulpal inflammation and dentin resorption in human teeth. For this reason the use of subcutaneous autogenous molar implants is suggested as a model for the experimental study of tooth resorption.

ACKNOWLEDGEMENTS

The writers are indebted to Mr. John D. Heeley and to Miss Brenda H. Dance for technical assistance.

LITERATURE CITED

- Barka, T. 1962 Cellular localization of acid phosphatase activity. *J. Histochem. Cytochem.*, 10: 231-232.
- Barka, T., and P. J. Anderson 1962 Histochemical methods for acid phosphatase using hexazonium pararosanilin as coupler. *J. Histochem. Cytochem.*, 10: 741-753.
- Cabrini, R. L., O. A. Maisto and E. E. Manfredi 1957 Internal resorption of dentin. *Oral Surg., Oral Med. and Oral Pathol.*, 10: 90-96.
- Cabrini, R. L., F. Schajowicz and C. Merea 1962 Histochemical behavior of the giant cell of foreign body granulomata as compared with the osteoclast. *Experientia*, 18: 322-323.
- DeDuve, C. 1959 Lysosomes, a new group of cytoplasmic particles. In: *Subcellular Particles*. J. Hayashi, ed. Roland Press, New York, 128-159.
- Holt, S. J., and R. M. Hicks 1961 The localization of acid phosphatase in rat liver cells as revealed by combined cytochemical staining and electron microscopy. *J. Biophys. and Biochem. Cytol.*, 11: 47-66.
- Irving, J. T. and C. S. Handelman 1963 Bone destruction by multinucleated giant cells. In: *Mechanisms of Hard Tissue Destruction*. R. F. Sognnaes, ed. Amer. Assoc. Adv. Sci., Washington, D.C., 515-530.
- Irving, J. T., and S. A. Migliore 1965 Connective tissue responses to altered collagen and bone implants. *Am. J. Anat.*, 117: 151-158.

appeared as long, thin basophilic lines in the dentinal tubules (fig. 7).

The basophilic mononuclear cells were associated with considerable resorption of predentin and dentin after 28 days of implantation. Those which remained on the surface were associated with surface resorption, while the penetrative cells were found in large "pockets" of dentin resorption (fig. 8). Giant cells were usually not observed in these 28 day molar implants.

After 56 days of implantation, all decalcified molars exhibited a "moth-eaten" appearance caused by coalescence of dentinal tubules by resorption associated with the mononuclear cells (fig. 9).

Infrequently a few multinucleated giant cells were associated with mild dentin resorption after 84-140 days of implantation.

FDNB treated decalcified molar implants. Large numbers of multinucleated giant cells were observed around 14 day FDNB-treated molar implants. Most of the giant cells aggregated around the outer root surfaces, where they appeared to engulf particles of cementum and periodontal remnants (fig. 10). Other giant cells were found in the pulp chambers, and occasionally within well-defined resorption lacunae in the coronal dentin (fig. 11). Penetrative mononuclear cells were rarely observed in the dentinal tubules and were markedly reduced in numbers in the pulp cavities and capsules.

Acid phosphatase determination. The leukocytes observed during the first week of implantation gave a moderately positive test for acid phosphatase. The penetrative mononuclear cells were, on the other hand, strongly positive, and the enzyme seemed to be concentrated within discrete bodies in the cytoplasm, possible lysosomes (fig. 12).

DISCUSSION

The appearance of numerous leukocytes in the primary response to all molar implants seemed to be a localized acute inflammatory reaction unrelated to the specific implanted tissue. A similar response was also stimulated by implanted autogenous bone (Irving and Handelman, '63), and FDNB-treated collagen (Irving and Migliore, '65). Infiltration of the pulp

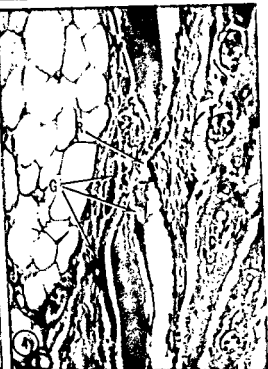
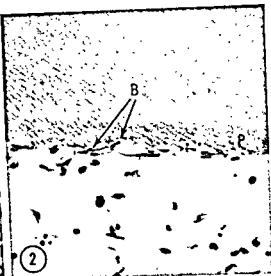
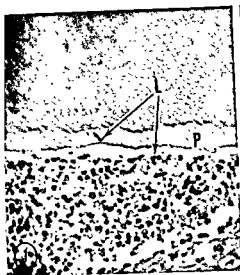
cavities and penetration of the dentinal tubules by the leukocytes appeared to be an active process. Orban ('40) called attention to the ability of leukocytes to change shape as they pass through capillary walls. He concluded, as do the present authors, that these cells actively elongate and enter the dentinal tubules. The fate of the leukocytes was presumably degenerative. Although lytic enzymes may have been released from these cells, there was no evidence of resultant dentin resorption after their disappearance.

The secondary cellular response which appeared after 14 days also contained a "non-specific" component. The appearance of basophilic mononuclear cells, fibroblasts, and capillary networks was noted in all molar implants, as well as implants in bone (Irving and Handelman, '63) (Irving and Migliore, '65) and collagen (Irving and Migliore, '65).

On the other hand, the appearance of giant cells in the secondary response seemed to be mediated by the nature of the implanted tissue. Giant cells were rarely seen around decalcified molar implants whereas decalcified bone implants were rapidly attacked by giant cells. Apparently a giant cell-stimulating factor present in decalcified bone matrix is absent or present in reduced amounts, in the dentin matrix.

As with bone implants, treatment with FDNB resulted in the appearance of large numbers of resorptive multinucleated giant cells around decalcified molar implants. FDNB reacts with the epsilon amino groups of lysine or hydroxylysine in collagen. The presence of nitro groups in the para position seems to be the chemical configuration responsible for giant cell stimulation when this reagent combines with collagen (Irving and Migliore, '65).

Unlike the decalcified molars, devitalized molars did eventually attract giant cells, but they were fewer in numbers and appeared more slowly. At first the giant cells were attracted only to fragmented roots, a "tropic effect" observed with the sharp ends of bone implants (Irving and Handelman, '63). After most dentin fragments were resorbed, giant cells were associated with gradual resorption of intact root and crown dentin (after 56 days). The

PLANTATION OF RAT MOLARS
by T. Irving and James A. Bond

Langeland, K. 1957 Tissue Changes in the Dental Pulp. Oslo University Press, Oslo, Norway, 35-114.

Masterton, J. B. 1965 Internal resorption of the dentin. *Brit. Dent. J.*, 118: 241-249.

Orban, B. 1940 Migration of leukocytes into the dentinal tubules. *J. Amer. Dent. Assoc.*, 27: 239-250.

Sanger, F. 1945 The free amino groups of ins... *Biochem. J.*, 32: 542-551.

Suzi, F. R., P. Goldhaber and J. M. Jennings 1961 Histochemical and biochemical study of acid phosphatase in resorbing bone in culture. *Am. J. Phys.* 211: 959-962.

PLATE 1

EXPLANATION OF FIGURES

- 1 Cellular response around devitalized molar, removed after seven days of implantation. Massive invasion of leukocytes (L) in the pulp chamber with minimal penetration of tubules of the predentin (P) layer. $\times 440$.
- 2 Cellular response around devitalized molar, removed after 14 days of implantation. Basophilic, ovoid mononuclear cells (B) have replaced the leukocytes in the pulp chamber and are associated with resorption lacunae in the predentin (P). $\times 440$.
- 3 Deposition of an "osteoid-like" material (a) in the pulp horn of a devitalized molar, removed after 28 days of implantation. Formative cell layer (b). $\times 270$.
- 4 Area of resorption (R) of root dentin (D) in devitalized molar, removed after 56 days of implantation. Multinucleated giant cells (G). Connective tissue capsule (C). $\times 440$.

LANTATION OF RAT MOLARS
 ers T. Irving and James A. Bond

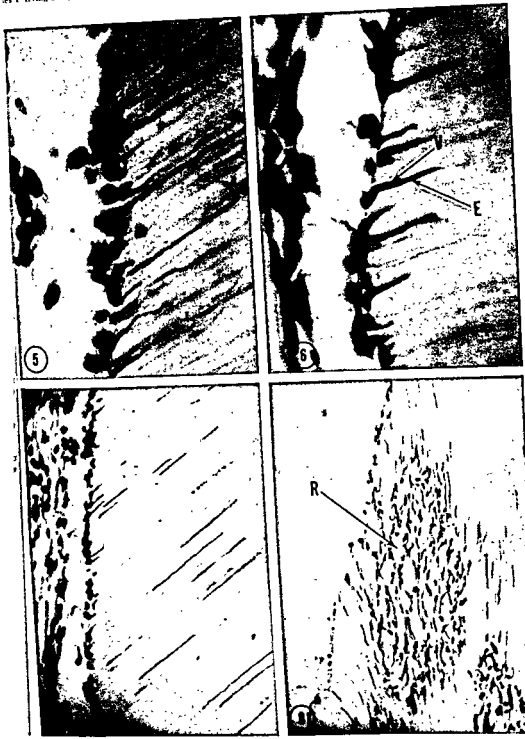


PLATE 2

EXPLANATION OF FIGURES

- 5 Aggregation of leukocytes along the pulpal dentin wall of a decalcified molar removed after 18 hours of implantation. Note the extensive cellular penetration of the dentinal tubules. $\times 970$.
- 6 Penetration of dentinal tubules by basophilic mononuclear cells in decalcified molar removed after 14 days of implantation. Cytoplasmic extension (E) containing a vacuole (V). $\times 970$.
- 7 Deep penetration of dentinal tubules by basophilic mononuclear cells in decalcified molar, removed after 14 days of implantation. $\times 440$.
- 8 Centralized area of dentin resorption (R) in the cusp of a decalcified molar removed after 28 days of implantation. Note the presence of basophilic mononuclear cells in the resorption cavity and in the dentinal tubules. $\times 270$.

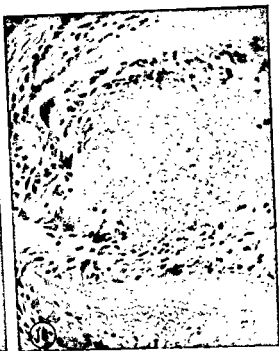
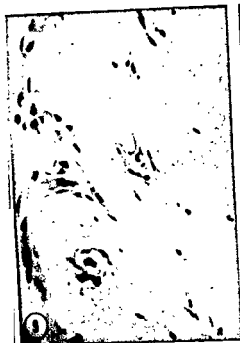
LANTATION OF RAT MOLARS
es T. Irving and James A. Bond

PLATE 3

EXPLANATION OF FIGURES

- 9 Cross-section view of dentinal tubules in decalcified molar removed after 56 days of implantation. "Moth-eaten" appearance produced by resorption of dentin between adjacent dentinal tubules containing basophilic mononuclear cells. $\times 440$.
- 10 Aggregation of numerous multinucleated giant cells around the root apex of an FDNB treated decalcified molar removed after 14 days of implantation. $\times 440$.
- 11 Cellular response in pulp chamber of FDNB treated decalcified molar removed after 14 days of implantation. Note the presence of large numbers of multinucleated giant cells and area of dentin resorption (R). $\times 270$.
- 12 Positive acid phosphatase reaction (Barka and Anderson, '62) in two basophilic mononuclear cells. Cryostat section of decalcified molar removed after 14 days of implantation. Numerous acid phosphatase positive "lysosome-like" bodies are present within the cytoplasmic extensions in the dentinal tubules. $\times 970$.

PLANTATION OF RAT MOLARS

T. Irving and James A. Bond



Development of the Gonads in the Female Japanese Quail¹

J. V. KANNANKERIL² AND L. V. DOMM

Department of Anatomy, Loyola University Stritch School of Medicine,
706 So. Wolcott Avenue, Chicago, Illinois

ABSTRACT The germ cells in the Japanese quail, appear in the gonadal area between two to two and one half days incubation with a preferential distribution favoring the left gonad. Proliferation of the primary or medullary cords from the germinal epithelium was observed between four and five and one half days. The secondary or cortical cords were found to proliferate in the left gonad on the sixth day. The right gonad revealed neither cortical cords nor cortex in any of the cases studied. It began to involute around eighth day and reached its minimum size by seven to ten days after hatching. In the adult it was composed of loose, or occasionally cord-like, epithelial cells, sparsely scattered "fat laden" cells, masses of lymphocytes and fibrous connective tissue, the latter predominating in older stages. Germ cells either disappeared or could no longer be recognized in the right gonad by four days after hatching. In the left ovary oögonia began to show meiotic changes by the eleventh day and primary follicles were present on the day of hatching. Ovulation was observed as early as 45 days after hatching. In female embryos the right Mullerian duct underwent atrophy and became a rudimentary cloacal remnant between eight and 14 days. In males complete atrophy of both left and right Mullerian ducts occurred between seven and 13 days. The mesonephric ducts persisted in females and were demonstrable throughout post-hatch period as thread-like structures.

Although the Japanese quail, *Coturnix japonica* Temminck and Schlegel, was first introduced into North America for the purpose of providing game, the attempts both earlier (Philips, '28) and more recently (Cottam and Stanford, '59) have apparently failed to establish it as a successful fauna in this country. However,

Padgett and Ivey ('59) pointed out, *Coturnix* has become an ideal laboratory animal because of its hardiness, ease of handling, precociousness and great laying capacity. Our principal interest in this bird up to now has been to study the effects of bilateral ovariectomy with particular reference to its effects on the rudimentary right gonad. In order to interpret the changes observed following unilateral ovariectomy, it became necessary to know something of the embryonic development of the right gonad in the female and its subsequent involution. Since we found no pertinent literature on the subject, we decided to investigate this problem.

MATERIALS AND METHODS

Quail eggs³ were incubated at 100°F and the embryos sacrificed at one half day intervals throughout the incubation period of 16 to 17 days. A number of specimens

for each age group were examined grossly in order to gain some information as to the variability in normal development. The typical embryos of each group were then compared with the stages reported by Padgett and Ivey ('60). Postembryonic birds were sacrificed at one day intervals for the first ten days, at two day intervals for the next ten, then at five day intervals up to maturity (45 to 60 days) and at random thereafter up to three and one half years. The number of specimens studied for each stage is shown in table 1.

Specimens were fixed in Bouin's and Zenker's fluids and in Bensley's acetic-osmic-bichromate mixture which was

¹This investigation was supported in part by NIH Research grants AM-03895 and AM-09926, an NIH General Research Support Grant, and an Institutional Grant from the American Cancer Society.

²The study was carried out in partial fulfillment of the requirements for the degree of Doctor of Philosophy in Anatomy, Loyola University Stritch School of Medicine, during the tenure of a Graduate Student Teaching Assistantship. The senior author subsequently was supported by a Medical Student Research Fellowship in Anatomy and currently is a Research Associate in the Department of Anatomy, Loyola University Stritch School of Medicine.

³The initial stock of eggs and birds were purchased from the Antelope Valley Farm, Lincoln, Nebraska. Gifts of young stock were also received from Dr. A. V. Nalbandov, Department of Animal Physiology, University of Illinois, Urbana; Dr. R. K. Meyer, Department of Zoology, University of Wisconsin, Madison; and young stock and fertile eggs through the courtesy of Dr. J. R. Howes, Department of Poultry Science, Auburn University, Auburn, Alabama. These gifts are gratefully acknowledged. The birds are now reared in our own laboratory.

elongated, narrow, light-colored bodies along the medial-ventral side of the mesonephric ridges extending from behind the coelomic end of the Wolffian body to about 2 mm caudally. They are composed of a germinal epithelium of two to three layers and an underlying tissue of loosely arranged mesenchymal cells (fig. 2). A lateral asymmetry as concerns the number of germ cells and the size of the gonads is already evident at this time. Among the ten embryos examined, seven showed a somewhat larger left (30 to 60 μ in thickness) than right (25 to 55 μ) gonad and the germ cells were distributed in approximately a 5:2 ratio between left and right.

In the remaining embryos both gonads were approximately the same size, however, distribution of the germ cells showed a 4:3 ratio in favor of the left gonad. By the fourth day of incubation bud-like projections from the germinal epithelium were noticeable, indicating the beginning proliferation of the first or primary set of sex cords. This proliferation was active by four and one half days and had practically terminated by five and one half days (fig. 3). The mesenchyme cells appear to distribute themselves between the sex cords, to form the connective tissue stroma rather than contributing to the formation of the cords themselves. The cords consist mainly of epithelial cells with a few germ cells embedded in them. When proliferation is complete, a layer of connective tissue stroma appears under the epithelium representing the primary tunica albuginea.

In general, the PGCs up to this time (5 to 6 days) have retained their original size and shape. A few of them, however, are somewhat smaller and this is apparently the result of mitotic division. One noticeable change at this time is the disappearance of the cytoplasmic fat globules. The size of the germ cells, however, remains the most significant identifying characteristic during this period.

Sex differentiation and development of gonads to time of hatching. The period of development from sex differentiation to the time of hatching may be arbitrarily be divided, for convenience of description, into two stages: (1) from six to nine days of incubation when most of the cortical cords

are formed and (2) from ten days to hatching when differentiation of the germ cells and involution of the right gonad in females appear to be the most important events.

From six to nine days of incubation. Proliferation of the primary or medullary cords is terminated by five and one half to six days, at which time a definite determination of sex can be made. In addition to the fact that the left gonad in females is larger than the right, the germinal epithelium of the left is also much thicker (3 to 5 cells or 25 to 30 μ). In the right gonad on the other hand, the epithelium has diminished to little more than a single layer of cells (fig. 4). In male embryos, as the first proliferation comes to an end, both right and left gonads acquire an epithelium similar to that of the right in females, i.e., a single layer of cuboidal cells.

Sex differentiation is further evident when the cortical cords, or cords of second proliferation begin to appear as bud-like projections from the epithelium of the left gonad of females starting on the sixth day of incubation. This proliferation becomes very pronounced during the succeeding days, especially between seven and nine days. Although a sporadic division of germ cells was noticed in earlier stages, it is during the height of cortical proliferation that the active phase of mitotic division of these cells was seen. The resulting daughter cells are smaller and show no trace of cytoplasmic fat depositions. Unlike the medullary cords, the cortical cords consist mainly of germ cells and a few somatic cells derived from the germinal epithelium.

In none of the 25 embryos examined between six and nine days of incubation did we find any trace of a cortex or proliferation of cortical cords in the rudimentary right gonad. As mentioned earlier, the epithelium of this gonad is already a thin, single layered, structure by six days of incubation.

The medulla of both left and right gonads in females continued to increase in size during the period of cortical proliferation. At seven days of incubation the medulla of the left had reached a thickness of 170 to 190 and the right 130 to 150 μ .

TABLE 1

Specimens employed in microscopic study of gonads¹

Embryonic period		Postembryonic period	
Age of embryos in days	Number of spec- imens examined	Age of birds in days	Number of spec- imens examined
0-1	4	1-2	2
1-2	6	2-3	4
2-3	12	3-4	4
3-4	10	4-5	3
4-5	10	5-6	1
5-6	9	6-7	2
6-7	8	7-8	2
7-8	8	8-9	2
8-9	9	9-10	4
9-10	5	10-12	3
10-11	2	12-14	2
11-12	6	14-16	4
12-13	2	16-18	3
13-14	7	18-20	2
14-15	3	20-25	6
15-16	2	25-30	2
16-17 ²	5	30-35	3
		35-40	1
		40-50	5
		50-60	3
		60-70	2
		70-80	3
		80-3.5 yr.	10

¹All specimens studied following sex differentiation on sixth day were females²Day of hatching.

found to be a good fixative for embryos of early stages since it satisfactorily preserved cytoplasmic yolk inclusions in the primordial germ cells. The material was sectioned at 4 to 6 μ and stained in hematoxylin and eosin, iron hematoxylin or Mallory's triple (McFarlane, '44) stain. Specimens fixed in the acetic-osmic-bichromate mixture were stained employing Bensley's anilin-acid fuchsin-Wright's blood stain method (Swift, '15).

An attempt was made to distinguish the germ cells of early quail embryos by fixing them in chilled Gendre fluid and staining for glycogen by the periodic acid-Schiff (PAS) technic and in cold acetone for staining with alkaline phosphatase employing Gomori's ('46) and Burstone's ('58) modifications.

OBSERVATIONS

Development of the undifferentiated gonad. The formation of the gonads may conveniently be considered as beginning with the arrival of the primordial germ cells (PGCs) in the peritoneal epithelium midway between the cranial aspect of the mesonephric ridge and the developing dor-

sal mesentery. In the Japanese quail² this happens at about 48 to 60 hours incubation. Prior to this stage, the germ cells can be seen in the endoderm of the blastoderm space between ectoderm and mesoderm, blood islets (fig. 1), and the splanchnopleur, revealing the extragonadal origin of these cells.

The PGCs of the quail resemble those described by Swift ('14) in the chick, in size (14 to 16 μ), shape (spherical to ovoid), prominent nuclei (7 to 10 μ) and above all in a cytoplasm filled with fat globules (fig. 1). When stained for glycogen with the PAS reagent, these cells did not show any significant reaction. It is interesting to note this connection that Meyer ('61), Dorn and Clawson ('62) and Clawson and Dorn ('63) observed that glycogen can be used as a diagnostic characteristic of the early germ cells in the chick. Attempts to stain these cells with alkaline phosphatase stain also failed in this species although it has been found to be highly successful in the case of mouse embryos (Chiquoine, '57; Mintz, '59) and others.

By three to three and one half days of incubation, the genital ridges were visible

elongated, narrow, light-colored bodies the medial-ventral side of the mesohric ridges extending from behind the hialic end of the Wolffian body to about mm caudally. They are composed of a minimal epithelium of two to three layers, an underlying tissue of loosely arranged mesenchymal cells (fig. 2). A lateral asymmetry as concerns the number of germ cells and the size of the gonads is already evident at this time. Among ten embryos examined, seven showed a somewhat larger left (30 to 60 μ in thickness) than right (25 to 55 μ) gonad and the germ cells were distributed in approximately a 5:2 ratio between left and right. In the remaining embryos both gonads were approximately the same size, however, distribution of the germ cells showed a 4:3 ratio in favor of the left gonad. By the fourth day of incubation bud-like projections from the germinal epithelium were noticeable, indicating the beginning proliferation of the first or primary set of sex cords. This proliferation is active by four and one half days and is practically terminated by five and one half days (fig. 3). The mesenchyme cells appear to distribute themselves between the cords, to form the connective tissue stroma rather than contributing to the formation of the cords themselves. The cords consist mainly of epithelial cells with a few germ cells embedded in them. When proliferation is complete, a layer of connective tissue stroma appears under the epithelium representing the primary tunica albuginea.

In general, the PGCs up to this time (5 to 6 days) have retained their original size and shape. A few of them, however, are somewhat smaller and this is apparently the result of mitotic division. One noticeable change at this time is the disappearance of the cytoplasmic fat globules. The size of the germ cells, however, remains the most significant identifying characteristic during this period.

Sex differentiation and development of gonads to time of hatching. The period of development from sex differentiation to the time of hatching may be arbitrarily divided, for convenience of description, into two stages: (1) from six to nine days of incubation when most of the cortical cords

are formed and (2) from ten days to hatching when differentiation of the germ cells and involution of the right gonad in females appear to be the most important events.

From six to nine days of incubation. Proliferation of the primary or medullary cords is terminated by five and one half to six days, at which time a definite determination of sex can be made. In addition to the fact that the left gonad in females is larger than the right, the germinal epithelium of the left is also much thicker (3 to 5 cells or 25 to 30 μ). In the right gonad on the other hand, the epithelium has diminished to little more than a single layer of cells (fig. 4). In male embryos, as the first proliferation comes to an end, both right and left gonads acquire an epithelium similar to that of the right in females, i.e., a single layer of cuboidal cells.

Sex differentiation is further evident when the cortical cords, or cords of second proliferation begin to appear as bud-like projections from the epithelium of the left gonad of females starting on the sixth day of incubation. This proliferation becomes very pronounced during the succeeding days, especially between seven and nine days. Although a sporadic division of germ cells was noticed in earlier stages, it is during the height of cortical proliferation that the active phase of mitotic division of these cells was seen. The resulting daughter cells are smaller and show no trace of cytoplasmic fat depositions. Unlike the medullary cords, the cortical cords consist mainly of germ cells and a few somatic cells derived from the germinal epithelium.

In none of the 25 embryos examined between six and nine days of incubation did we find any trace of a cortex or proliferation of cortical cords in the rudimentary right gonad. As mentioned earlier, the epithelium of this gonad is already a thin, single layered, structure by six days of incubation.

The medulla of both left and right gonads in females continued to increase in size during the period of cortical proliferation. At seven days of incubation the medulla of the left had reached a thickness of 170 to 190 and the right 130 to 150 μ .

This increase is mainly due to the mitotic activity of the cells of the medullary cords. By seven and one half to eight days, the medullary cords of both gonads in female embryos began to show certain atrophic changes. The first indication of this was visible when some of the cords, especially those towards the hilar area, acquired a lumen (fig. 5). These cords gradually became distended with the lining cells becoming cuboidal and later somewhat more flattened. Some of the cords became loosely arranged and broke up into small isolated groups of cells. Some of these cells underwent cytological changes becoming vesicular and vacuolated, resembling the "fat laden" cells described in the chick embryo by Brode ('28), while others underwent necrosis and gradually disappeared.

From ten days of incubation to hatching. The left ovary. By the tenth day, cortical proliferation may cease in the medial ventral areas of the ovary where the cortical cords remain detached and separated from the epithelium by a discontinuous connective tissue stroma which represents the developing secondary or ovarian tunica albuginea. The cessation of proliferation of cortical cords gradually spreads in all directions from the medial ventral region of the ovary, so that at the time of hatching, proliferation of these cords may be seen only in the dorsal lips or folds of the cortex close to the mesovarium.

By the eleventh day, some of the oogonia at the inner aspect of the cortex revealed the early meiotic changes. Their nuclei enlarged and began to show deeply staining chromosomes similar to those seen in typical leptotene stages of meiosis. Furthermore, the chromosomes became polarized, that is to say they were not randomly distributed but lay clumped to one side with a clear space at the opposite pole of the nucleus, thus resembling the synizesis arrangement (fig. 6). This transformation continued and spread over the entire cortex as incubation advanced and hatching time approached. Meanwhile, by 13 to 14 days, the older oocytes, located at the inner aspect of the cortex, underwent further meiotic prophase changes in anticipation of the growth phase. All of the oocytes appeared to enter this growth phase but only a fraction of them continued to grow

and acquire a follicular envelope. The older ones underwent involution and beginning at 14 days of incubation.

During the period from 10 to 16 days, the medulla of the left ovary also revealed some growth. This growth was largely confined to the outer sub-cortical medulla and in consequence this became very compact and sharply distinguished from the inner vacuolated medullary zone. The "fat laden" cells are prevalent in the medulla at this stage (fig. 6). While the oogonia of the cortex were undergoing meiotic changes, some of the germ cells located in the medulla showed similar changes resulting in the synizesis arrangement of their chromosomes. However, these changes in the latter did not proceed much further, instead, they underwent necrosis and gradually disappeared from the medulla.

The rudimentary right gonad. The rudimentary right gonad of the female ceased to grow between eight and ten days of incubation. In fact it began to show signs of involution by the eighth day, and at the time of hatching it measured approximately 1.5 to 2 mm in length and 0.5 mm in width while the left ovary had an average length of 4 mm and a width of 1.5 mm. This disparity in size between the right and left female gonads was more evident in their thickness, the right rudimentary gonad ranging from 45 to 60 μ as compared to 220 to 300 μ for the left ovary (fig. 8). The germinal epithelium at this stage is so thin that it is barely distinguishable from the visceral peritoneum. In none of the 12 embryos examined, between ten days at the time of hatching, did we observe cortical cords or a cortex in the right rudimentary gonad, nor were any germ cells seen in the germinal epithelium.

The atrophic changes seen in the medulla of the right gonad, beginning eight to nine days of incubation, continued at an accelerated rate during the rest of the incubation period. The lacunae of the lacinated medullary cords gradually became larger and in consequence the lining epithelium became thinner (fig. 7). Conversion of medullary cells into "fat laden" cells continued but as the embryos grew older, this transformation decreased.

The number of germ cells in the medulla

the right rudimentary gonad also increased as development advanced. At the time of hatching, a cross section of this gonad might reveal one or two and occasionally none at all. None of the germ cells observed showed meiotic changes such as were seen in the left ovary.

Development of gonads in the post-hatch period. The left ovary. A detailed discussion on the growth and development of the left ovary during the post-hatch period is not intended, hence only certain relevant changes will be noted.

The mitotic division of germ cells seems to have ceased in all areas of the cortex by the first day after hatching. Even as early as the first day of hatching, the growing oocyte may be surrounded by a follicular covering (fig. 10). This was particularly so in embryos at required 17 or more days to hatch. As stated earlier, not all oocytes acquire a follicular envelope; only a small percentage do so while those that did not, disappeared. The formation of ovarian follicles, as well as the development of oocytes, was first seen along the medial ventral area of the ovary and then spread to other areas. By the eighth day after hatching, follicles could be seen in all areas of the ovarian cortex. The older follicles attained full growth and ruptured between 45 and 75 days.

Soon after hatching, an increase in number was noticed in the epithelial cells of the cortex of the left ovary some of which differentiated into "interstitial" cells. These cells were especially abundant in the inner layer of growing follicles.

A medulla is recognizable in the left ovary of the adult. The medullary cells of the outer compact zone intermingle with the interstitial elements of the cortex and thus lose their identity in the post-hatch period. The reticular zone of the medulla in the adult ovary is confined to the hilus and consists mostly of connective tissue infiltrated with blood vessels. Loose epithelial cells were seen in the early post-hatch stages but in mature ovaries, they have either disappeared or have become modified in such a way that they are no longer distinguishable from other connective tissue cells. The "fat laden" cells of the medulla gradually disappear in the early post-hatch period, so that in ovaries from

birds beyond ten days of age these cells are seldom seen.

Germ cells were as a rule, not seen in the medulla of the left ovary after hatching. However, in one four day old bird a few were found in some of the sections. Scattered cells with fairly large nuclei may be seen in the medulla of adult ovaries, however, their identity as germ cells is doubtful.

The rudimentary right gonad. The rudimentary right gonad of the female continued to regress for some days after hatching and attained its smallest size sometime between seven and ten days. At this time it is visible as an elongated, narrow, flattened bit of tissue lying on the ventral surface of the post caval vein and/or the medial surface of the right mesonephric remnant. A wide individual variation was observed in the size of these gonads which generally ranged from 1 to 2 mm in length and 0.2 to 0.6 in width.

In none of the 53 right gonads examined histologically, from hatching to sexual maturity, was there any evidence of a cortex. The epithelium covering the gonad was invariably thin, flattened and similar to the peritoneal lining of the coelom (figs. 9, 11, 12).

The medulla of the right gonad showed some variations as the birds approached sexual maturity. Usually, it was composed of loose masses of epithelial cells derived from the original medullary cords, a few "fat laden" cells, connective tissue stroma and some blood cells (fig. 11). In a few cases small solid cords of epithelial cells were seen. Distended luminated cords and masses of lymphocytes were also observed in the stroma. Fibrous connective tissue was increasingly prevalent in the older gonads. In a few the bulk of the gonad was composed of fibroblast-like cells with very few epithelial cells in evidence. In such cases, it seems that the epithelial cells have either largely disappeared or have transformed into fibrous connective tissue-like cells. The number of "fat laden" cells also showed considerable individual variation while in some cases none of these cells could be found.

Germ cells were seen in the right gonad as late as three to four days posthatch after which they could no longer be found

This increase is mainly due to the mitotic activity of the cells of the medullary cords. By seven and one half to eight days, the medullary cords of both gonads in female embryos began to show certain atrophic changes. The first indication of this was visible when some of the cords, especially those towards the hilar area, acquired a lumen (fig. 5). These cords gradually became distended with the lining cells becoming cuboidal and later somewhat more flattened. Some of the cords became loosely arranged and broke up into small isolated groups of cells. Some of these cells underwent cytological changes becoming vesicular and vacuolated, resembling the "fat laden" cells described in the chick embryo by Brode ('28), while others underwent necrosis and gradually disappeared.

From ten days of incubation to hatching. The left ovary. By the tenth day, cortical proliferation may cease in the medial ventral areas of the ovary where the cortical cords remain detached and separated from the epithelium by a discontinuous connective tissue stroma which represents the developing secondary or ovarian tunica albuginea. The cessation of proliferation of cortical cords gradually spreads in all directions from the medial ventral region of the ovary, so that at the time of hatching, proliferation of these cords may be seen only in the dorsal lips or folds of the cortex close to the mesovarium.

By the eleventh day, some of the oogonia at the inner aspect of the cortex revealed the early meiotic changes. Their nuclei enlarged and began to show deeply staining chromosomes similar to those seen in typical leptotene stages of meiosis. Furthermore, the chromosomes became polarized, that is to say they were not randomly distributed but lay clumped to one side with a clear space at the opposite pole of the nucleus, thus resembling the synizesis arrangement (fig. 6). This transformation continued and spread over the entire cortex as incubation advanced and hatching time approached. Meanwhile, by 13 to 14 days, the older oocytes, located at the inner aspect of the cortex, underwent further meiotic prophase changes in anticipation of the growth phase. All of the oocytes appeared to enter this growth phase but only a fraction of them continued to grow

and acquire a follicular envelope. The underwent involution and beginning at 14 days of incubation.

During the period from 10 to 16 days, medulla of the left ovary also received some growth. This growth was confined to the outer sub-cortical area of the medulla and in consequence the became very compact and sharply distinguished from the inner vacuolated lar zone. The "fat laden" cells are prevalent in the medulla at this stage (fig. 6). While the oogonia of the cortex were undergoing meiotic changes, some of the germ cells located in the medulla showed similar changes resulting in the synizesis arrangement of their chromosomes. However, these changes in the latter did not proceed much further, instead, they underwent necrosis and gradually disappeared from the medulla.

The rudimentary right gonad. The rudimentary right gonad of the female ceased to grow between eight and ten days of incubation. In fact it began to show signs of involution by the eighth day, and at the time of hatching it measured approximately 1.5 to 2 mm in length and 0.5 mm in width while the left ovary had an average length of 4 mm and a width of 1.5 mm. This disparity in size between the right and left female gonads was more evident in their thickness, the right rudimentary gonad ranging from 45 to 60 μ as compared to 220 to 300 for the left ovary (fig. 8). The germinal epithelium at this stage is so thin that it is barely distinguishable from the visceral peritoneum. In none of the embryos examined, between ten days and the time of hatching, did we observe cortical cords or a cortex in the right rudimentary gonad, nor were any germ cells seen in the germinal epithelium.

The atrophic changes seen in the medulla of the right gonad, beginning at eight to nine days of incubation, continued at an accelerated rate during the rest of the incubation period. The lacunae of the lacinated medullary cords gradually became larger and in consequence the lining epithelium became thinner (fig. 7). The conversion of medullary cells into "fat laden" cells continued but as the embryos grew older, this transformation decreased.

The number of germ cells in the medulla

and cortical cords as well as in other events of later development.

In the chick, an extragonadal origin of PGCs became apparent from our studies in the quail, for these cells were found in the entoderm of the blastoderm, in the space between the ectoderm and mesoderm, in the blood stream, and in the mesonephros prior to their arrival in the gonadal area at two to two and one half days of incubation. Firket ('14), although agreeing with the concept of an extragonadal origin of the germ cells in the chick, does not believe that the definitive oocytes arise from these cells. Instead, he believes that these cells undergo degeneration beginning at 15 days of incubation and that they are subsequently replaced by new cells arising from the germinal epithelium. Such a view was previously reported by Dantschakoff ('08) and more recently by Benberg and Garwacki ('38). Swift ('15) and Goldsmith ('28) on the other hand, maintain that it is the PGCs that later give rise to the definitive oocytes. In the quail we were able to follow the course of the PGCs from the time of their arrival in the gonad, through mitotic divisions, and later, through the transformation of oogonia into oocytes, some of which became enveloped as follicles. However, we observed that in the quail many of the PGCs undergo degeneration and disappear, beginning at days of incubation, but it is the survivors that develop into the definitive oocytes. Firket ('13, '14), Swift ('15), Blocker ('33), Stanley and Witsch ('40), Clawson and Domm ('63) and others, have observed that in chick embryos the PGCs collect preferentially in the left gonad, sometimes two to five times greater numbers than in the right, as early as 96 hours of incubation. Prior to two and one half to three days the thickness of the germinal epithelium and the number of incorporated germ cells were more or less equal on left and right sides. A similar phenomenon was observed in our quail embryos as early as three days of incubation. The germinal epithelium of the left gonad was thicker than that of the right and the germ cells showed a 5:2 ratio in favor of the left. However, this disparity was not so pronounced in any of the younger embryos examined. Some of these showed a near uniformity in the size of left

and right gonads and in these the ratio was approximately 4:3. As is now generally known, in the female domestic fowl and the quail, as well as most other birds, only the left ovary becomes functional while the right ceases to develop at an early age and persists throughout life as a rudimentary gonad. In the male on the other hand, both left and right gonads become functional. In general, we may therefore assume that those embryos which show a pronounced asymmetry of the gonads are genetically determined females. However, a more extensive study on the distribution of the germ cells in the quail is necessary before a fixed ratio can be established.

Contrary to the prevailing view that in the domestic fowl, the medullary cords proliferate from the germinal epithelium, (Hoffman, 1892, D'Hollander, '04, Firket, '14, Swift, '15, '16, Benoit, '24, '51, Goldsmith, '28, Brode, '28, Essenberg and Garwacki, '38, Willier, '39, and others), Witschi ('35, '60) reports that in birds these cords are derived from the mesenchymal blastema of the indifferent gonad. Blocker ('33) in his studies on the English sparrow *Passer domesticus* earlier came to the same conclusion.

Bud-like projections were seen to arise from the germinal epithelium of quail embryos of four to four and one half days of incubation which by further proliferation appear to give rise to the medullary cords. Our study did not permit us to determine whether any cells of the mesenchymal blastema contributed to the formation of the medullary cords.

From the studies of Domm ('27), Brode ('28) and Willier ('39) it is known that the medullary tissue does not completely disappear in the female chick although Firket ('20) believed that it does. Brode and Willier both reported that it persists in the left ovary as well as in the rudimentary right gonad after transforming into one of the following structures: distended tubules which may temporarily contain germ cells, clusters of cords of clear or "fat laden" cells and isolated medullary cord cells. In the quail we found a similar transformation of the medulla of the left and right gonads. The difference between the domestic fowl and the quail seems to lie chiefly in the degree of atrophy that occurs and

although occasional large nuclei lacking distinct cell walls were seen in the medulla. The identity of the latter as germ cells was questionable.

The rudimentary right gonad in older birds. The right gonad sites of ten older females ranging in age from 230 days to three and one half years were studied histologically. A rudimentary gonad was found in all of these cases (fig. 12). The epithelial cells were fewer in number but there was more fibrous connective tissue when compared with the younger stages. The so-called "fat laden" cells were rarely observed in any of these gonads but masses of lymphocytes were frequently seen.

The development of Mullerian and Wolffian ducts. Mullerian ducts. The tubal ridges, that later contribute to the formation of the Mullerian ducts were usually visible during the third day of incubation as thickened lines of peritoneum along the dorso-lateral side of the mesonephros, lying immediately lateral to the mesonephric duct. By three and one half days, the cranial end of each ridge began to invaginate and to form a groove which soon transformed into a tube, the Mullerian duct. The tube was open at the cranial end but closed caudally. The part thus formed was relatively short. The major portion of the duct was formed by a posterior elongation which reached the cloaca at about six to six and one half days incubation.

In female embryos, development of the Mullerian ducts was uniform on either side up to eight days at which time both ducts showed a length of 6 to 6.5 mm. At this time the right Mullerian duct ceased to grow and showed signs of atrophy. This began at the cranial end and by the fourteenth day of incubation the tube had disappeared except for a short cloacal stump measuring about 2.5 to 3 mm in length. In adult females this rudimentary cloacal remnant was found attached to the right side of the cloaca as reported in the brown Leghorn fowl (Domm, '27). It was found to be somewhat larger in laying than in non-laying females presumably because of its responsiveness to estrogenic hormones.

The left oviduct on the other hand continued to grow throughout the entire em-

bryonic as well as early postembryonic period. In the period between 35 to 45 days, a tremendous increase in size and coiling took place in preparation for ovulation and laying. A noticeable increase in vascularization was also observed at this period. At the time of ovulation the oviduct was large, approximately 15 to 30 cm. in length, highly convoluted, and took up most of the space in the body cavity between the ovary and the cloaca.

It is of interest to note in this connection that in males regression of the Mullerian ducts occurred simultaneously in both left and right ducts and that it began three and one half days of incubation. Unlike the female, atrophy of these ducts in the male begins at the caudal end and progresses cranially, rather rapidly, since by the 11th day they have practically disappeared except for a small thread-like remnant which had usually disappeared by the fourteenth day.

Wolffian ducts. The mesonephric duct persists in the adult female as a minute straight, thread-like ridge, lying in close association with and parallel to, the ureter on the ventral surface of the metanephros. Anteriorly, it is connected to the mesonephric remnant, consisting of a few convoluted tubules, the epoophoron, and posteriorly to the cloaca.

DISCUSSION

In comparing the development of the gonads of the quail, and those of the chick which is well known to students of avian embryology, it is clear that, despite the difference in incubation periods viz., 16 to 17 days for the quail and 21 for the chick, the degree of development of the gonads at the time of hatching is about the same. Consequently, embryonic development requiring 21 days for the chick is completed in a shorter period in the quail. Hence, there is evidently a speeding up of development in the case of the quail. For example, in the chick, Swift ('14, '15) and others have found that the PGCs appear in the presumptive germinal epithelium by three and one half days of incubation whereas in the quail we found that this occurred as early as two to two and one half days. Such an acceleration was observed in the proliferation of the medul-

- um, C., and J. A. Stanford 1959 Coturnix quail America. 48th Convention International Association of Game, Fish and Conservation Commissioners, 1-119.
- tschakoff, V. 1908 Entwicklung des Blutes bei n Vogeln. Anat. Hefte., 37: 471-589.
- um, L. V. 1927 New experiments on ovariectomy d the problem of sex inversion in the fowl. J. Exp. ol., 48: 31-173.
- um, L. V., and R. C. Clawson 1962 The glycogen ntent of primordial germ cells in normal and corti- l treated chick embryos. Excerpta Medica. Intern. ngr. Sera. No., 51: 415.
- enberg, J. M., and J. K. Garwacki 1938 On the tigin and development of the definitive germ cells in e domestic fowl. Western J. Surg. Obstet. Gynecol., 5: 145-152.
- et, J. 1913 Recherches sur les gonocytes prima- es (Urgeschlechtszellen) pendant la periode indifférence sexuelle et le développement de ovarie chez le poulet. Anat. Anz., 44: 166-175.
- 1914 Recherches sur l'organogenèse des landes sexuelles chez les oiseaux. Arch. Biol., Paris, 9 201-351.
- 1920 Recherches sur l'organogenèse des landes sexuelles chez les oiseaux. II. Arch. Biol., Paris, 30: 393-516.
- lay, C. F. 1925 Studies on the sex differentiation n fowls. Brit. J. Exp. Biol., 2: 439-468.
- ldsmith, J. B. 1928 The histology of germ cells in he domestic fowl. J. Morph., 46: 275-315.
- lioni, C. 1946 The study of enzymes in tissue sec- tions. Am. J. Clin. Path., 16: 347-352.
- ffmann, C. K. 1892 Étude sur le developpement de l'appareil urogenital des oiseaux. Verhand. der K. Akad. van Wetenschappen—Amsterdam, 1: 1-54.
- llander, F. d' 1904 Recherches sur l'oogenese et sur la structure et la Signification du noyau vitellin de Balbiani chez les oiseaux. Arch. d'anat. Micr., 7: 117-180.
- nnankeri, J. V., and L. V. Domm 1963 Prelim- inary observations on the effects of sinistral ovari- ectomy in the Japanese quail (Coturnix coturnix japonica). Anat. Rec., 145 329-330.
- 1964 The development of ovary in the Japa- nese quail (Coturnix coturnix japonica). Anat. Rec., 148 293
- Lewis, L. B. 1946 A study of some effects of sex hormones upon the embryonic reproductive system of the white Pekin duck. Physiol. Zool., 19: 282-329.
- McFarlane, D. 1944 An easily controlled regressive trichromatic staining method. Stain Tech., 19: (1) 29-37.
- Meyer, D. B. 1961 The intra-embryonic migration of primordial germ cells in staged chick embryos. Anat. Rec., 139: 314.
- Mintz, B. 1959 Continuity of the female germ cell line from embryo to adult. Arch. d'Anat. Micr. et de Morph. Exp., 48: 155-172.
- Padgett, C. M., and W. D. Ivey 1959 Coturnix quail as a laboratory research animal. Science, 129: 267-268
- 1960 The normal embryology of the coturnix quail. Anat. Rec., 137: 1-11.
- Phillips, J. C. 1928 Wild birds introduced or trans- planted in North America. U.S.D.A. Tech. Bull., 61: 1-63.
- Stanley, A. J., and E. Witschi 1940 Germ cell migra- tion in relation to asymmetry in the sex glands of hawks. Anat. Rec., 76: 329-342.
- Swift, C. H. 1914 Origin and early history of the primordial germ cells in the chick. Am. J. Anat., 15: 483-518.
- 1915 Origin of the definitive sex-cells in the female chick and their relation to the primordial germ cells. Am. J. Anat., 18: 441-470.
- 1916 Origin of the sex-cords and definitive spermatogonia in the male chick. Am. J. Anat., 20: 375-410.
- Willer, B. H. 1939 The embryonic development of sex. Sex and Internal Secretions, 2nd Ed. Eds., Allen, Danforth and Doisy, Williams and Wilkins Co., Balti- more. 64-114.
- Witschi, E. 1935 Origin of asymmetry in the repro- ductive system of birds. Am. J. Anat., 56: 119-141.
- 1960 Sex and secondary sexual characters. Biology and Comparative Physiology of Birds. Ed., A. J. Marshall, Academic Press, New York and London. 2: 115-168.

consequently in the amount of medullary tissue that persists, especially in the right gonad. In the chicken, cords of clear or unmodified medullary cells and a considerable number of "fat laden" cells are quite common in the rudimentary right gonad of adults. In the quail on the other hand, medullary cells, aggregated in a cord-like fashion, were observed only in exceptional cases; they usually occurred as scattered isolated cells. The "fat laden" cells were relatively rare and sometimes even completely absent. Our observations indicate that atrophy of the right gonad is more severe in the quail than in the chick which would seem to be supported by the earlier disappearance of the germ cells from the rudimentary right gonad. In the chick, Brode ('28) observed germ cells in the medulla of both the left ovary and the right rudimentary gonad up to three to four weeks after hatching while in our studies on the quail these cells were either absent or could no longer be recognized beyond four days after hatching.

One of the important and interesting observations on the rudimentary right gonad of the quail was the absence of cortical tissue. According to Brode ('28) in the domestic fowl, 39% of the embryonic right gonads and 20% of the adult revealed either a cortex or cortical cords. The presence of cortical tissue has also been reported in the developing right gonad of the English sparrow (Blocker, '33) and the Pekin duck (Lewis, '46). The absence of this tissue in the right gonad of the quail is of particular importance in studies on the hypertrophied rudimentary right gonad following sinistral ovariectomy. Finlay ('25) and Domm ('27) postulated that the rudimentary right gonad of the brown Leghorn fowl may develop into an ovotestis or an ovary only when cortical elements are present in the rudimentary right gonad at the time of ovariectomy, and Domm (loc. cit.) maintained that the presence of a normal sized right ovary in poulards was contingent on the amount of cortical tissue present in the right gonad at the time the left ovary was removed. Our observations on the hypertrophied rudimentary right gonad of the quail are in agreement with this view, namely, that cortex will not develop, *de novo*, since in a total of 50

ovariectomies (Kannankeril and Domm '63, '64) not a single case showed ovarian tissue in this gonad. If the hypothesis of Finlay and Domm (loc. cit.) is valid this result would be expected since cortical elements were found in any of quail embryos studied. The reason for the apparent complete absence of cortex in rudimentary right gonads of the quail in contrast to the chick and some other forms is not known. We may tentatively conclude that in the quail, the genetic and/or hormonal inhibitory control of cortical development in the right gonad is complete whereas in those forms where it is incomplete, occurs this control is either incomplete or lacking.

ACKNOWLEDGEMENTS

The authors are greatly indebted to Mrs. Lucia Smelte for her able technical assistance during the course of this investigation and to Dr. James E. Woods, Research Associate in Anatomy, for helpful suggestions regarding problems in incubation and rearing of the birds. The authors also acknowledge their indebtedness to Dr. Les A. Emmert, Assistant Professor of Anatomy, for a critical reading of the manuscript and for advice and counsel on some of the histochemical procedures and to John A. Maurer for assistance in the preparation of the microphotographs.

LITERATURE CITED

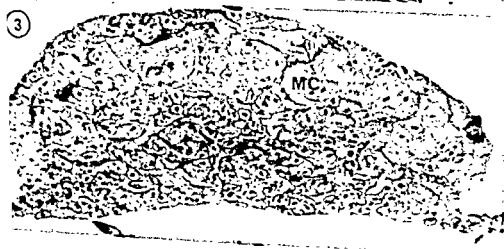
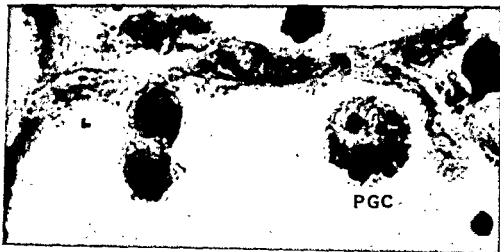
- Benoit, J. 1924 Sur la signification de la glande rudimentaire droite chez la poule. *C. R. Acad. Sci.*, 178: 341-344.
- 1951 Différenciation sexuelle chez les oiseaux au cours du développement normal et de l'ovariotomie. *Sexualité expérimentale par ovariectomie. Que sur la Différenciation Sexuelle chez les oiseaux.* Centre National de la Recherche Scientifique. Paris. 213-232.
- Blocker, H. W. 1933 Embryonic history of the cells in *Passer domesticus*. *Acta Zool. Stockhol.* 111-162.
- Brode, M. D. 1928 The significance of the asymmetry of the ovaries of the fowl. *J. Morph. Physiol.* 46: 1-10.
- Burstone, H. S. 1958 Histochemical comparison of Naphthol AS-phosphates for the demonstration of phosphatases. *J. Nat. Canc. Inst.* 20: 601-613.
- Chiquotne, A. D. 1954 The identification, origin and migration of the primordial germ cells in the mouse embryo. *Anat. Rec.* 118: 135-146.
- Clawson, R. C., and L. V. Domm 1963 The glycogen content of primordial germ cells in chick embryos. *Proc. Soc. Exp. Biol. Med.* 112: 533-537.

- am, C., and J. A. Stanford 1959 Coturnix quail America. 48th Convention International Association of Game, Fish and Conservation Commissioners, 1-119.
- Aschakoff, V. 1908 Entwicklung des Blutes bei Vogel. Anat. Hefte., 37: 471-589.
- am, L. V. 1927 New experiments on ovariectomy and the problem of sex inversion in the fowl. J. Exp. Biol., 48: 31-173.
- am, L. V., and R. C. Clawson 1962 The glycogen content of primordial germ cells in normal and cortisone treated chick embryos. Excerpta Medica. Intern. Congr. Sera. No., 51: 415.
- erg, J. M., and J. K. Garwacki 1938 On the origin and development of the definitive germ cells in the domestic fowl. Western J. Surg. Obstet. Gynecol., 3: 145-152.
- et, J. 1913 Recherches sur les gonocytes primaires (Urgeschlechtszellen) pendant la période d'indifférence sexuelle et le développement de l'ovaire chez le poulet. Anat. Anz., 44: 166-175.
- 1914 Recherches sur l'organogenèse des glandes sexuelles chez les oiseaux. Arch. Biol., Paris, 9: 201-351.
- 1920 Recherches sur l'organogenèse des glandes sexuelles chez les oiseaux. II. Arch. Biol., Paris, 30: 393-516.
- ay, G. F. 1925 Studies on the sex differentiation in fowls. Brit. J. Exp. Biol., 2: 439-468.
- Adsmith, J. B. 1928 The histology of germ cells in the domestic fowl. J. Morph., 46: 275-315.
- moni, C. 1946 The study of enzymes in tissue sections. Am. J. Clin. Path., 16: 347-352.
- offmann, C. K. 1892 Etude sur le développement de l'appareil urogénital des oiseaux. Verhan. der K. Akad. van Wetenschappen - Amsterdam, 1. 1-54.
- llander, F. d' 1904 Recherches sur l'oogenèse et sur la structure et la Signification du noyau vitellin de Balbiani chez les oiseaux. Arch. d'anat. Micr., 7: 117-180.
- nnankeril, J. V., and L. V. Domm 1963 Preliminary observations on the effects of surgical ovariectomy in the Japanese quail (Coturnix coturnix japonica) Anat. Rec., 145: 329-330.
- 1964 The development of ovary in the Japanese quail (Coturnix coturnix japonica). Anat. Rec., 48: 293
- Lewis, L. B. 1946 A study of some effects of sex hormones upon the embryonic reproductive system of the white Pekin duck. Physiol. Zool., 19: 282-329.
- McFarlane, D. 1944 An easily controlled regressive trichromatic staining method. Stain Tech., 19: (1) 29-37.
- Meyer, D. B. 1961 The intra-embryonic migration of primordial germ cells in staged chick embryos. Anat. Rec., 139: 314.
- Mintz, B. 1959 Continuity of the female germ cell line from embryo to adult. Arch. d'Anat. Micr. et de Morph. Exp., 48: 155-172.
- Padgett, C. M., and W. D. Ivey 1959 Coturnix quail as a laboratory research animal. Science, 129: 267-268.
- 1960 The normal embryology of the coturnix quail. Anat. Rec., 137: 1-11.
- Phillips, J. C. 1928 Wild birds introduced or transplanted in North America. U.S.D.A. Tech. Bull., 61: 1-63.
- Stanley, A. J., and E. Witschi 1940 Germ cell migration in relation to asymmetry in the sex glands of hawks. Anat. Rec., 76: 329-342.
- Swift, C. H. 1914 Origin and early history of the primordial germ cells in the chick. Am. J. Anat., 15: 483-516.
- 1915 Origin of the definitive sex-cells in the female chick and their relation to the primordial germ cells. Am. J. Anat., 18: 441-470.
- 1916 Origin of the sex-cords and definitive spermatogonia in the male chick. Am. J. Anat., 20: 375-410.
- Willier, B. H. 1939 The embryonic development of sex. Sex and Internal Secretions, 2nd Ed. Eds., Allen, Danforth and Doisy, Williams and Wilkins Co., Baltimore. 64-114.
- Witschi, E. 1935 Origin of asymmetry in the reproductive system of birds. Am. J. Anat., 56: 119-141.
- 1960 Sex and secondary sexual characters. Biology and Comparative Physiology of Birds, Ed., A. J. Marshall, Academic Press, New York and London. 2: 115-168.

PLATE 1

EXPLANATION OF FIGURES

- 1 Photomicrograph of a primordial germ cell (PGC) located in a blood islet of an embryo of two and one half days incubation. Note the large size of the nucleus and the lipid granules in the cytoplasm. $\times 1500$.
- 2 Photomicrograph of the left (L) and right (R) gonads of a three and one half day embryo. Note the difference in distribution of germ cells between left and right gonads. $\times 600$.
- Cross section of the left gonad of a four and one half day embryo showing the ingrowth from the germinal epithelium of the primary or medullary sex cords (MC). $\times 600$.



EXPLANATION OF FIGURES

- 4 Cross section through the peripheral portion of the left and right gonads of a six day female embryo. Note the thin, single layered, germinal epithelium (GE) of the right gonad and the thick multilayered epithelium of the left gonad. The latter also shows small bud-like projections indicating the beginning of proliferation of the secondary or cortical cords (CC). MC, medullary cords. $\times 530$.
- 5 Cross section of the rudimentary right gonad of an eight day female embryo. Note the absence of any cortex or cortical cords, also the loosely arranged medullary cords and the lacunae (L) in certain of the cords. $\times 260$.
- 6 Cross section of the left ovary of an 11 day female embryo showing a portion of the cortex and the underlying medullary tissue. Note the oocytes in synizesis (O) at the inner aspect of the cortex and islets of "fat laden" cells (FLC) in the medulla. $\times 650$.
- 7 Cross section of the rudimentary right gonad of an 11 day female embryo. Note the lone germ cell (GC) in the degenerating medullary tissue and the "fat laden" cells (FLC). $\times 475$.

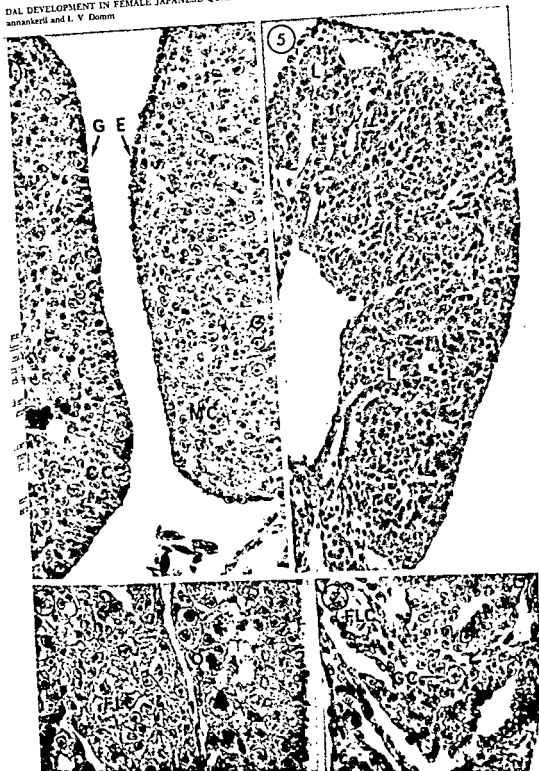
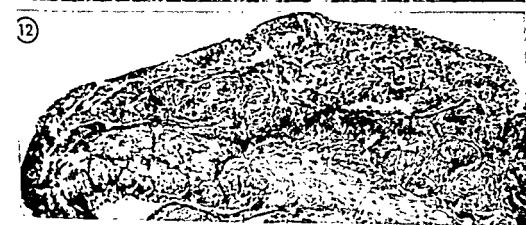
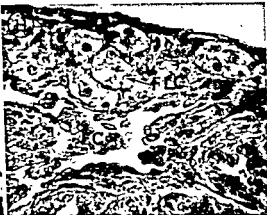
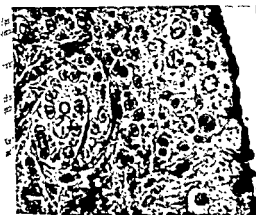
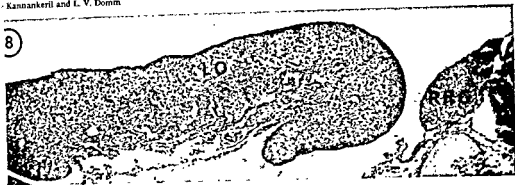
DAL DEVELOPMENT IN FEMALE JAPANESE QUAIL
annankeri and I. V. Domm

PLATE 2

EXPLANATION OF FIGURES

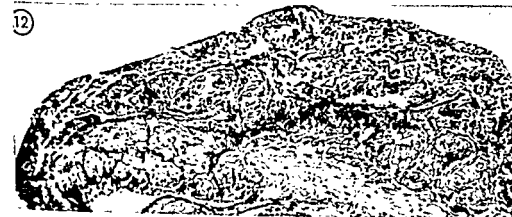
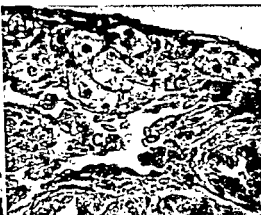
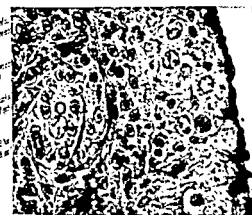
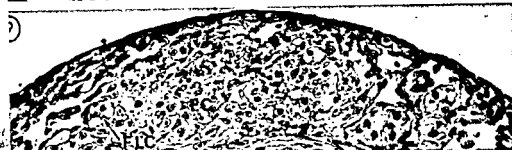
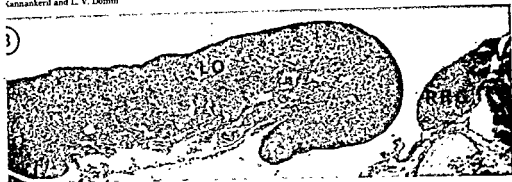
- 4 Cross section through the peripheral portion of the left and right gonads of a six day female embryo. Note the thin, single layered, germinal epithelium (GE) of the right gonad and the thick multilayered epithelium of the left gonad. The latter also shows small bud-like projections indicating the beginning of proliferation of the secondary or cortical cords (CC). MC, medullary cords. $\times 530$.
- 5 Cross section of the rudimentary right gonad of an eight day female embryo. Note the absence of any cortex or cortical cords, also the loosely arranged medullary cords and the lacunae (L) in certain of the cords. $\times 260$.
- 6 Cross section of the left ovary of an 11 day female embryo showing a portion of the cortex and the underlying medullary tissue. Note the oocytes in synizesis (O) at the inner aspect of the cortex and islets of "fat laden" cells (FLC) in the medulla. $\times 650$.
- 7 Cross section of the rudimentary right gonad of an 11 day female embryo. Note the lone germ cell (GC) in the degenerating medullary tissue and the "fat laden" cells (FLC). $\times 475$.

ADAMAL DEVELOPMENT IN FEMALE JAPANESE QUAIL
Kannankeril and L. V. Domm



EXPLANATION OF FIGURES

- 8 Cross section of the rudimentary right gonad and the left ovary of a 14 day embryo. Note the wide disparity in size between the two gonads, LO, left ovary; RRG, rudimentary right gonad. $\times 135$.
- 9 Cross section of the rudimentary right gonad of a newly hatched quail (17 days of incubation). Note the "fat laden" cells (FLC) and other loose epithelial cells (EC). $\times 450$.
- 10 A part of the cortex of the left ovary of the newly hatched quail shown in figure 9. Note the oocyte (O) being enveloped by follicle cells (FC). $\times 600$.
- 11 Cross section of the rudimentary right gonad of seven day post-hatch quail. Note the groups of "fat laden" cells (FLC) and loosely arranged epithelial cells (EC). $\times 500$.
- 12 Cross section of the rudimentary right gonad of a two year old quail. Note the increase in fibrous connective tissue cells. Compare figures 5, 9, and 11. $\times 200$.

ADAL DEVELOPMENT IN FEMALE JAPANESE QUAIL
Cannankeril and L. V. Domm

Observations on Epidermal Differentiation in the Fetal Rat¹

MARY A. BONNEVILLE²

Dermatologic Genetics Laboratory, New England Center Hospital, Boston, Massachusetts

ABSTRACT Study of fetal rat epidermis has revealed the presence of a single layer of non-keratinizing cells, the periderm, that covers the free surface of the skin during embryonic life. The periderm resembles structurally the epithelium lining the amniotic cavity, and the two are believed to be similar in function and embryonic origin.

Observations of keratinization have shown that keratohyalin granules formed initially during fetal life may differ in structure from those formed during later fetal life and in the adult. Those formed first contain lipidlike globules embedded in a dense granular matrix. Those formed next contain dense patches of finely granular material embedded in a less dense matrix. Granules formed late in fetal life have a homogeneous structure and resemble those of adult skin.

As in adult epidermis, tonofibrils, abundant in epidermal cells prior to cornification, probably contribute to formation of the keratohyalin granules. Also, as in adult tissue, ribosomes lie close to the surfaces of developing keratohyalin granules and seem to be involved in their formation.

Electron microscopic examination of human fetal skin (Bonneville, '64; athnach and Wyllie, '65; Hashimoto et al., '66) has revealed that the free surface of the epidermis is covered by a layer of non-cornified cells, beneath which lie the basal cells of the thin stratum corneum. This layer has been called the periderm, and it is believed to share its origin and function with the epithelial lining of the amniotic cavity (Bonneville, '64). In order to confirm that the presence of a periderm is a general feature in development of mammalian epidermis, investigation of fetal rat skin at various gestational ages is undertaken. Fine structural details of its development and evidence for its persistence during the fetal life of the albino rat are presented in this study.

Preliminary observations of the fetal rat skin revealed that following primary fixation with glutaraldehyde (Sabatini et al., '63) and postfixation with osmium tetroxide, the keratohyalin granules in the stratum corneum or so cell layers that undergo cornification exhibit marked structural differences from granules previously observed in the epidermis of embryo mice (Seneff, '57), of newborn rats (Matoltsy, '62) and of mature mammalian skin, as reviewed by Brody ('64), Odland ('64) and Odland and Clark ('64). In some instances

they display morphological variability similar to that described by Farbman ('66a) in rat tongue. This study therefore contains a detailed description of the unusual keratohyalin granules found in fetal rat skin in an attempt to evaluate the significance of these images and to add to the general understanding of the cornification process.

METHODS AND MATERIALS

Pregnant female albino rats were obtained from the Charles River Breeding Laboratories, Wilmington, Massachusetts. Samples of skin were taken from the scapular region of fetuses at various ages of gestation ranging from 10-19 days. In this study, the animals described are referred to both by crown-rump (C-R) length and by their approximate gestational age.

The morphological observations of skin development recounted in this paper were made on skin fixed in 6.25% glutaraldehyde (Sabatini et al., '63) in Sorensen's buffer (pH 7.4) for two hours. After thor-

¹This investigation was supported in part by four grants from the United States Public Health Service, Research Grant 5-R01-GM 10299 and Training Grant 5T-01-AM 05220 to Tufts University School of Medicine (Dr. Walter F. Lever, Principal Investigator), Research Grant GM 1591 to New England Medical Center Hospitals (Dr. George F. Widgram, Principal Investigator) and Research Grant CA-00592 to Brown University (Dr. Hermann B. Chase, Principal Investigator).

²Present address: The Biological Laboratories, Harvard University, 16 Divinity Avenue, Cambridge, Massachusetts 02138.

ough rinsing in buffer, the tissues were postfixed in 1% OsO₄ in Sorensen's buffer (pH 7.4) for two hours. All specimens were dehydrated in ethanol and embedded in Epon (Luft, '61). Sections for both light and electron microscopy were made on a Porter-Blum MT-1 ultramicrotome. For light microscopy, one to two μ thick sections were mounted on glass slides and stained with toluidine blue. Those for the electron microscope were cut with a diamond knife and stained with aqueous uranyl acetate followed by lead citrate (Reynolds, '63). Observations were made on RCA electron microscopes, Models 3F and 3G, and on the Siemens Elmiskop I.

OBSERVATIONS

The periderm

In the youngest fetus examined (crown-rump length, C-R, 15 mm; ca ten days gestation) the skin from the scapular area consists generally of only two cell layers (fig. 1). The layer of flattened cells bordering the free surface of the epithelium is continuous with the lining of the amniotic cavity. During the whole of fetal life this outermost epidermal layer, referred to here as periderm, never undergoes cornification. Its fate during differentiation of the epidermis may be followed in light and electron micrographs.

Light microscopy. Before any fully cornified cells have formed (fig. 2), the young epidermis (C-R, 20 mm; ca 12 days gestation) has differentiated into three layers that correspond to layers found in mature tissue. The basal layer, the stratum germinativum, consists of a single row of low columnar cells. These underlie approximately two layers of rounded cells, the stratum spinosum. They, in turn, are covered by two layers of flattened cells, the stratum granulosum, that contain small dark-staining keratohyalin granules. The most superficial cell layer, the periderm, is made up of cells with rounded nuclei and cytoplasm devoid of granules.

As development proceeds (C-R, 28 mm; ca 15-16 days), the number of cell layers in the granulosum increases (fig. 3). In certain regions of the most superficial granular layer large individual keratohyalin granules may be identified, while

in other areas the intergranular space is filled with dark-staining material. At this stage the periderm layer is thin, but most of its flattened cells are occasionally bulging into the amniotic cavity. Still later during gestation (C-R, 35 mm; ca 18 days), when cornification of a second layer has begun (fig. 4), the periderm is difficult to detect in light micrographs and is best examined with the electron microscope.

Electron microscopy. The periderm has been found in all specimens of fetal skin examined so far. Usually the periderm appears as a thin layer with short protrusions on its free surface (fig. 5). In certain instances, however, the free surface is expanded by villuslike structures that may be branched (fig. 7). It is in this condition that the periderm most resembles the amniotic epithelium (fig. 8) in which it is continuous. When the periderm rests on cornified cells, it is usually thinner than at earlier stages (fig. 9).

During most of fetal life the structure of the periderm is that of healthy functioning tissue. Its cytoplasm contains many fine fibrils, some microtubules, free ribosomes and mitochondria (figs. 5, 7, 9). The nuclei appear viable and do not undergo degenerative changes comparable to the striking nuclear alterations that occur in cells undergoing cornification (Farbman, '66a). During the last 5 days of fetal life its cytoplasm appears well organized (fig. 12) and may undergo some degenerative changes.

Early in development the periderm is attached to the underlying granular layer by desmosomes alone (fig. 5), but from about the twelfth day of gestation extracellular lamellar material becomes abundant in the intercellular space (figs. 7, 9). This material is believed to be derived from membrane-coating granules (MCG's) or keratinosomes¹ (see following section). Late in development (one or two days before birth) the periderm, though still present (fig 12), is less firmly attached because the intercellular material and desmosomes linking it to the cornified

¹Both terms currently in use for these granules are characteristic of differentiating epidermis are admittedly unsatisfactory, since they are not descriptive of structure or function. These terms are retained, however, because they are familiar to a number of workers and because I hesitate to suggest another name before their function is known.

beneath it have disappeared (at least the material sampled in this study), probably in preparation for shedding of the epiderm at birth.

Keratohyalin granules

The most superficial layer of the stratum corneum. Keratohyalin granules appear first in the layer immediately beneath the epiderm (fig. 5) at about the eleventh of gestation. The granules comprise at least two kinds of material: dense homogeneous globular elements that resemble liposomes and a matrix of fine dense particles in which the globules are embedded. Lipoprotein membranes separating the components of the granule from each other or from the surrounding cytoplasm have not been detected.

These granules do exhibit, however, certain relationships with other cytoplasmic structures. Tonofibrils frequently approach individual tonofilaments are apparently embedded in the periphery of the granules, especially when the latter are small (fig. 6). The fibrils are not particularly well developed or abundant in the surrounding cytoplasm, and many profiles of the larger, more mature granules do not show this relationship. Ribosomes, on the other hand, are present in large numbers throughout the cytoplasm, and often they appear to blend into the matrix of the granules (fig. 6). It seems likely that the liposomes are a normal component of the keratohyalin granules as other workers have suggested (Rogers, '64; Rhodin and others, '62).

When keratohyalin granules first appear, the surrounding cytoplasm possesses, in addition to the tonofibrils and ribosomes already mentioned, many small bodies known as membrane-coating granules or ratiinosomes (fig. 5). Small Golgi regions and mitochondria are also present. The cells often enclose a large granule (fig. 5), the significance of which is unknown. As the cells become flattened (about the 14th day) the enlarged keratohyalin granules occupy relatively more of the cytoplasmic volume (fig. 7). Recognizable structures in the surrounding cytoplasm consist largely of ribosomes. The contents of the membrane coating granules or keratinosomes are believed to contribute to the inter-

cellular lamellar material, as has been postulated in a number of fine structural studies of epidermis (Farbman, '64; Frithiof and Wersäll, '65; Matoltsy and Parakkal, '65; Matoltsy, '66; Bonneville et al., '68).

About the sixteenth day of gestation, the profile of the large heterogeneous granules may still be seen (fig. 9). The intergranular cytoplasm consists of a homogeneous material, the density of which is nearly equal to that of the matrix of the granule. As in normal and psoriatic epidermis the plasma membrane of such cells has become "thickened" (Matoltsy and Parakkal, '65; Farbman, '66b; Bonneville et al., '68) and appears as a dense outline around the cell. Beneath it is a thin layer of fine, dense granular material.

During the last days of fetal life the intergranular areas of these cells appear as a flattened scale. The "thickened" membrane encloses a homogeneous material almost as dense as itself (fig. 12). The original heterogeneous keratohyalin granules may still be seen, however, giving this layer, when observed in light micrographs, a beaded appearance (fig. 4). This layer has also been observed at the surface of the epidermis of the newborn rat. There is, therefore, no shedding of horny layers until after birth.

The second through fourth layers of the stratum corneum. The next deeper layer (the second beneath the epiderm) and the two to three below it become cornified, each lagging behind the one above it. In none of the succeeding layers, however, do the keratohyalin granules appear as in the first layer described above. None contain the lipidlike globules but rather consist of a matrix of fine granular material with irregular patches (figs. 7, 9, 10). Often a nucleoid, apparently of matrix material, is free of the denser granular component (fig. 10). Ribosomes are closely associated with the surface of these keratohyalin granules at all stages of their development, but tonofibrils are closely related to them only during the early ones (fig. 11). At this time the dense patches are apparently confined to the periphery of the granules, and tonofibrils are usually embedded in their surfaces (fig. 11). In spite of the heterogeneous nature of these granules, no

ough rinsing in buffer, the tissues were postfixed in 1% OsO₄ in Sorensen's buffer (pH 7.4) for two hours. All specimens were dehydrated in ethanol and embedded in Epon (Luft, '61). Sections for both light and electron microscopy were made on a Porter-Blum MT-1 ultramicrotome. For light microscopy, one to two μ thick sections were mounted on glass slides and stained with toluidine blue. Those for the electron microscope were cut with a diamond knife and stained with aqueous uranyl acetate followed by lead citrate (Reynolds, '63). Observations were made on RCA electron microscopes, Models 3F and 3G, and on the Siemens Elmiskop I.

OBSERVATIONS

The periderm

In the youngest fetus examined (crown-rump length, C-R, 15 mm; ca ten days gestation) the skin from the scapular area consists generally of only two cell layers (fig. 1). The layer of flattened cells bordering the free surface of the epithelium is continuous with the lining of the amniotic cavity. During the whole of fetal life this outermost epidermal layer, referred to here as periderm, never undergoes cornification. Its fate during differentiation of the epidermis may be followed in light and electron micrographs.

Light microscopy. Before any fully cornified cells have formed (fig. 2), the young epidermis (C-R, 20 mm; ca 12 days gestation) has differentiated into three layers that correspond to layers found in mature tissue. The basal layer, the stratum germinativum, consists of a single row of low columnar cells. These underlie approximately two layers of rounded cells, the stratum spinosum. They, in turn, are covered by two layers of flattened cells, the stratum granulosum, that contain small dark-staining keratohyalin granules. The most superficial cell layer, the periderm, is made up of cells with rounded nuclei and cytoplasm devoid of granules.

As development proceeds (C-R, 28 mm; ca 15-16 days), the number of cell layers in the granulosum increases (fig. 3). In certain regions of the most superficial granular layer large individual keratohyalin granules may be identified, while

in other areas the intergranular filled with dark-staining material. At this stage the periderm layer is thin, but some of its flattened cells are occasionally bulging into the amniotic cavity. Still during gestation (C-R, 35 mm; ca 18 days), when cornification of a second layer has begun (fig. 4), the periderm is difficult to detect in light micrographs. It is best examined with the electron microscope.

Electron microscopy. The periderm has been found in all specimens of fetal skin examined so far. Usually the periderm appears as a thin layer with short protrusions on its free surface (fig. 5). In certain instances, however, the free surface is expanded by villuslike structures that may be branched (fig. 7). It is in this condition that the periderm most resembles the amniotic epithelium (fig. 8), in which it is continuous. When the periderm rests on cornified cells, it is usually flatter than at earlier stages (fig. 9).

During most of fetal life the structure of the periderm is that of a healthy functioning tissue. Its cytoplasm contains many fine fibrils, some in tubules, free ribosomes and mitochondria (figs. 5, 7, 9). The nuclei appear viable and do not undergo degenerative changes comparable to the striking nuclear alterations that occur in cells undergoing cornification (Farbman, '66a). During the last days of fetal life its cytoplasm appears well organized (fig. 12) and may undergo some degenerative changes.

Early in development the periderm is attached to the underlying granular layer by desmosomes alone (fig. 5), but about the twelfth day of gestation lamellar material becomes abundant in the intercellular space (figs. 7, 9). This material is believed to be derived from membrane-coating granules (MCG) or keratinosomes² (see following section). Late in development (one or two days before birth) the periderm, though present (fig 12), is less firmly attached because the intercellular material and desmosomes linking it to the cor-

²Both terms currently in use for these granules characteristic of differentiating epidermis are unsatisfactory, since they are not descriptive of its function. These terms are retained, however, because they are familiar to a number of workers and because they suggest another name before their function is known.

bers that form in the fetal epidermis. densely staining globules embedded in granular matrix may be discerned even in the surrounding cytoplasm is filled with cornified material (fig. 12). They then give the layer a beaded appearance when viewed in light micrographs (fig. 4). This structure is not shed during fetal life and has been seen at all developmental stages examined.

The significance of this difference between the keratohyalin granules initially formed and those that follow is not clear.

Globules within them have the appearance of lipid material, but regardless of their chemical composition, it is apparent that the synthetic processes leading to the formation of the globules are not reduced in cornification of succeeding layers.

The heterogeneity of granules in the second through fourth cell layers undergoing cornification (figs. 9, 10, 11) is a characteristic of developing rat epidermis. When these granules are small, dense patches occur at the periphery of a granule in close association with the ends of tonofibrils that seem to be embedded in the surface of the granule (fig. 11). As the granules enlarge, the number of dense patches increases and over tonofibrils are embedded in the surface (fig. 9, 10). One might imagine the patches as representing tonofibrillar material that has been incorporated into the granule and simultaneously transformed to a dense granular material. It seems likely that the patches would arise both from the fibrils and the matrix material within the granule. The nucleoid-like area (fig. 10) would then represent the small granule that existed before incorporation of the tonofibrils began. This process would account for the disappearance of tonofibrils in cells in which granules are large (fig. 9).

This interpretation would agree with the proposals of Rogers ('64), Brody ('64), Glanville ('64), and Roth and Clark ('64) that tonofibrils become associated with a matrix material derived from keratohyalin granules and are in one way or another involved in the formation of the horny layer found in fully cornified cells. In

the fetal rat skin as in the human epidermis described by Brody ('64) the fibrils would seem to undergo transformation as they are incorporated into the keratohyalin granules, inasmuch as tonofibrillar elements cannot be recognized within the granules. The suggestion made here that the tonofibrils are incorporated into the granules differs from that of Farberman ('66a), who feels that the tonofibrils are not incorporated into the dense outer region of heterogeneous keratohyalin granules observed in rat tongue epithelium. Until specific components of both the fibrils and keratohyalin granules have been identified histochemically and/or after isolation and comparisons made between materials from the two sources, it will be difficult to choose with certainty between the two interpretations.

Dense peripheral patches occur in large keratohyalin granules of the fifth cell layer undergoing cornification (fig. 13). It is not known whether these patches are of similar origin and nature to others described above, but it is tentatively assumed that the keratohyalin granules of the fifth cornified layer may form in a manner generally like those in preceding layers.

Small keratohyalin granules forming late in fetal life are apparently homogeneous (fig. 14). Although tonofibrils are closely associated with their outer surfaces, no patches of material can be detected in the peripheral regions of the granules. This may be due to an increased concentration of matrix material that would prevent detection of any patches present. Alternatively, changes in the mode of formation of the granules and in the composition of the granules could be occurring. The specific factors that might influence these changes are, of course, unknown.

Just as in the present study of fetal rat skin, the close association of ribosomes with keratohyalin granules has been noted generally in fine structural studies of epidermis, and their probable role in granule formation has been proposed (Rogers, '64; Rhodin and Reith, '62). It is not apparent, however, whether ribosomes (or their derivatives) occur within the

trace of a similar heterogeneity can be observed in the flattened plates that make up the second, third and fourth cell layers when fully cornified (fig. 12).

The fifth through seventh layer of the stratum corneum. Once the stratum corneum achieves a thickness of four layers, cornification has already been initiated and continues, of course, in the underlying layers. The keratohyalin granules in these layers differ, however, from those previously described. In the fifth layer that undergoes keratinization extremely dense homogeneous deposits are found at the periphery of the granules (fig. 13), the structure of which is made up primarily of fine, dense granular matrix. The deposits are not uniform in shape and project from the granule in such a way as to give it an irregular polygonal profile. After osmium fixation alone the deposits have not been observed, and the granules appear polygonal. Both tonofibrils and ribosomes are closely associated with the surface of such keratohyalin granules.

When the sixth and seventh cell layers beneath the periderm have begun to cornify and have formed small-to-medium sized keratohyalin granules, no internal heterogeneity can be detected (fig. 14). The round-to-oval profiles of the granules that develop late in fetal life are made up of homogeneous dense material. As in the case of all types of granules studied, ribosomes and tonofilaments seem to blend into the material at the surface of the granule (fig. 14).

DISCUSSION

The periderm

This study has shown that throughout fetal life the epidermis of the rat has on its free surface a single layer of cells that do not undergo keratinization. A similar layer has been observed in human fetal skin (Bonneville, '64; Breathnach and Wyllie, '65; Hashimoto et al., '66). The author designated it as the periderm⁴ in the belief that it corresponded to the most superficial non-keratinizing layer of human fetal epidermis described by light microscopists (Arey, '54). In regard to fine structure the human periderm cells resemble one cell type found in the epithelial lining of

the amniotic cavity (Bourne, '62; Scher, '63; and Thomas, '65). It was postulated that the periderm is similar in origin and may share at least some of the functions of the amniotic epithelium. Late in fetal life, before cornification occurs, the periderm may perhaps effect exchange between the amniotic cavity and fetus. These interpretations may reasonably be extended to the rat periderm which, though less highly developed, has structural properties of an absorptive epithelium and resembles the epithelial lining of the amniotic cavity. In the clear evidence of secretory activity in the amniotic epithelium of the periderm has not been seen as it has in human tissue (Thomas, '65; Breathnach and Wyllie, '65). Secretory cells may be present in small numbers but were not observed in the samples examined in this study.

Two to three days before birth the periderm apparently becomes detached from the underlying epidermis, due to breakdown of desmosomes and other intercellular materials. The mechanisms effecting these changes are unknown.

Keratohyalin granules

It should perhaps be stressed at the outset that the appearance of keratohyalin granules, as described in this paper, resulted from the double fixation with glutaraldehyde followed by osmium. With this procedure was the loss of outer three to four granular layers prevented, for in spite of cautious handling these layers were sloughed off after osmium fixation alone, thus it was impossible to compare the structure of developing granules after different preparative procedures.

The initial formation of keratohyalin granules occurs in the cell layer immediately beneath the periderm, and has been demonstrated in this study. These granules differ not only from those observed in adult epidermis but also from

⁴ The term periderm has also been used to designate a layer in the embryonic chick epidermis (Elton-Jackson, quoted by Fellenz). In the chick the periderm is eight-to-ten cells in thickness and contains droplets of keratin-like material. It therefore does not seem to correspond strictly to the periderm described in this study. At the time I applied this term to fetal epidermis I was unaware of its use in regard to chick tissues.

ners that form in the fetal epidermis. Intensely staining globules embedded in granular matrix may be discerned even as the surrounding cytoplasm is filled with cornified material (fig. 12). They then shed the layer a beaded appearance when viewed in light micrographs (fig. 4). This is not shed during fetal life and has been seen at all developmental stages examined.

The significance of this difference between the keratohyalin granules initially shed and those that follow is not clear. The globules within them have the appearance of lipid material, but regardless of their chemical composition, it is apparent that the synthetic processes leading to the formation of the globules are not produced in cornification of succeeding layers.

The heterogeneity of granules in the third and through fourth cell layers undergoing cornification (figs. 9, 10, 11) is a characteristic of developing rat epidermis. When these granules are small, dense patches occur at the periphery of a granule in close association with the bundles of tonofibrils that seem to be embedded in the surface of the granule (fig. 11).

As the granules enlarge, the number of dense patches increases and fewer tonofibrils are embedded in the surface (fig. 9, 10). One might imagine the patches as representing tonofibrillar material that has been incorporated into the granule and simultaneously transformed to a dense granular material. It seems likely that the patches would arise both from the fibrils and the matrix material within the granule. The nucleoid-like area (fig. 10) would then represent the small granule that existed before incorporation of the tonofibrils began. This process would account for the disappearance of tonofibrils in cells in which granules are large (fig. 9).

This interpretation would agree with the proposals of Rogers ('64), Brody ('64), and Roth and Clark ('64) that tonofibrils become associated with a matrix material derived from keratohyalin granules and are in one way or another involved in the formation of the horny material found in fully cornified cells. In

the fetal rat skin as in the human epidermis described by Brody ('64) the fibrils would seem to undergo transformation as they are incorporated into the keratohyalin granules, inasmuch as tonofibrillar elements cannot be recognized within the granules. The suggestion made here that the tonofibrils are incorporated into the granules differs from that of Farbman ('66a), who feels that the tonofibrils are not incorporated into the dense outer region of heterogeneous keratohyalin granules observed in rat tongue epithelium. Until specific components of both the fibrils and keratohyalin granules have been identified histochemically and/or after isolation and comparisons made between materials from the two sources, it will be difficult to choose with certainty between the two interpretations.

Dense peripheral patches occur in large keratohyalin granules of the fifth cell layer undergoing cornification (fig. 13). It is not known whether these patches are of similar origin and nature to others described above, but it is tentatively assumed that the keratohyalin granules of the fifth cornified layer may form in a manner generally like those in preceding layers.

Small keratohyalin granules forming late in fetal life are apparently homogeneous (fig. 14). Although tonofibrils are closely associated with their outer surfaces, no patches of material can be detected in the peripheral regions of the granules. This may be due to an increased concentration of matrix material that would prevent detection of any patches present. Alternatively, changes in the mode of formation of the granules and in the composition of the granules could be occurring. The specific factors that might influence these changes are, of course, unknown.

Just as in the present study of fetal rat skin, the close association of ribosomes with keratohyalin granules has been noted generally in fine structural studies of epidermis, and their probable role in granule formation has been proposed (Rogers, '64; Rhodin and Reith, '62). It is not apparent, however, whether ribosomes (or their derivatives) occur within the

granules, surrounded by the dense material that is produced, presumably, under their influence. Histochemical studies of epidermis (Leutenberger and Lund, '51; Szodoray and Nagy-Vezekényi, '64) have indicated that the nucleoprotein may be included within the keratohyalin granules as a densely staining homogeneous matrix material is forming. The latter probably corresponds to the granules isolated by Matoltsy ('62) that are resistant to the action of trypsin and to urea in 1 to 3M concentrations. The spatial relationship between the ribosomes and the matrix during granule formation, however, has not been determined in more detail. It seems likely that a large number of ribosomes would form a functional unit that gives rise to a keratohyalin granule. As yet there is no morphological evidence that a focus of synthetic activity has been formed until its product can be detected.

ACKNOWLEDGMENTS

I am indebted to a number of investigators who have a long-standing interest in skin and who each kindly provided in part the laboratory facilities used during this investigation. My sincerest thanks are due to Dr. Walter F. Lever, Tufts University School of Medicine; Dr. Hermann B. Chase and Dr. J. Walter Wilson, Brown University; and Dr. George F. Wilgram, New England Center Hospital. In addition I wish to express my gratitude to Miss Jo Ann Hammons, who assisted in preparation of material for microscopy, and to Miss Janice Glenn for her help in preparing the manuscript and illustrations.

LITERATURE CITED

- Arcy, L. B. 1954 Developmental Anatomy. A Text-book and Laboratory Manual of Embryology. 6th ed. W. B. Saunders Company, Philadelphia.
- Bonneville, M. A. 1964 The periderm of human fetal skin. In: Electron Microscopy 1964, Proceedings of the Third European Regional Conference, Vol. B, Biology. M. Tlilbach, ed. Publishing House of the Czechoslovak Academy of Sciences, Prague, 565-566.
- Bonneville, M. A., M. Weinstock and G. F. Wilgram 1968 An electron microscope study of cell adhesion in psoriatic epidermis. *J. Ultrastruct. Res.* In Press.
- Bourne, G. 1962 The Human Amnion and Chorion. Year Book Medical Publishers, Inc., Chicago.
- Breathnach, A. S., and L. M. Wyllie 1963 The structure of cells forming the surface layer of epidermis in human fetuses at fourteen and six weeks. *J. Invest. Derm.*, 45: 179-189.
- Brody, I. 1964 Different staining methods for electronmicroscopic elucidation of the tonofibril differentiation in normal epidermis. In: Epidermis. W. Montagna and W. C. Lobitz, Jr., eds. Academic Press, New York, 251-273.
- Farbman, A. I. 1964 Electron microscope studies of small cytoplasmic structure in rat oral epithelium. *Cell Biol.*, 21: 491-495.
- Farbman, A. I. 1966a Morphological variability of keratohyalin. *Anat. Rec.*, 154: 275-285.
- Farbman, A. I. 1966b Plasma membrane changes during keratinization. *Anat. Rec.*, 156: 269-274.
- Fell, H. B. 1964 The experimental study of keratinization in organ culture. In: The Epidermis. W. Montagna and W. C. Lobitz, Jr., eds. Academic Press, New York, 61-81.
- Frithiof, L., and J. Wersäll 1965 A highly ordered structure in keratinizing human oral epithelium. *Ultrastruct. Res.*, 12: 371-379.
- Hashimoto, K., B. G. Gross, R. J. Di Bella and W. Lever 1966 The ultrastructure of the skin of human embryos. IV. The Epidermis. *J. Invest. Derm.*, 47: 317-335.
- Leutenberger, C., and H. Z. Lund 1951 The chemical nature of the so-called keratohyaline granules of the stratum granulosum of the skin. *Exp. Cell Res.*, 2: 150-152.
- Luft, J. H. 1961 Improvements in epoxy embedding methods. *J. Biophysic. Biochem. Cytol.*, 9: 409-414.
- Matoltsy, A. G. 1962 Mechanism of keratinization. In: Fundamentals of Keratinization. E. O. Böhler and R. F. Sognnaes, eds. A. A. S. Publication No. 70, Washington, D. C., 1-25.
- Matoltsy, A. G. 1966 Membrane-coating granules of the epidermis. *J. Ultrastruct. Res.*, 15: 510-515.
- Matoltsy, A. G., and P. F. Parakkal 1965 Membrane-coating granules of keratinizing epithelia. *J. Biol.*, 24: 297-307.
- Menefee, M. G. 1957 Some fine structure changes occurring in epidermis of embryo mice during differentiation. *J. Ultrastruct. Res.*, 1: 49-61.
- Odland, G. F. 1964 Tonofilaments and keratohyalin. In: The Epidermis. W. Montagna and W. C. Lobitz, Jr., eds. Academic Press, New York, 237-249.
- Reynolds, E. S. 1963 The use of lead citrate at pH as an electron-opaque stain in electron microscopy. *J. Cell Biol.*, 17: 208-212.
- Rhodin, J. A. G., and E. J. Reith 1962 Ultrastructure of keratin in oral mucosa, skin, esophagus, claw hair. In: Fundamentals of Keratinization. E. O. Böhler and R. F. Sognnaes, eds. A. A. S. Publication No. 70, Washington, D. C., 61-91.
- Rogers, G. E. 1964 Structural and biochemical features of the hair follicle. In: The Epidermis. W. Montagna and W. C. Lobitz, Jr., eds. Academic Press, New York, 179-236.
- Roth, S. I., and W. H. Clark, Jr. 1964 Ultrastructural evidence related to the mechanism of keratin synthesis. In: The Epidermis. W. Montagna and W. C. Lobitz, Jr., eds. Academic Press, New York, 303.
- Sabatier, D., K. Bensch and R. J. Barnett 1964 Cytochemistry and electron microscopy. The

on of cellular ultrastructure and enzymatic activity by aldehyde fixation. *J. Cell Biol.*, 17: 19-58.

Idt, W. 1963 Struktur und Funktion des Amnionepithels von Mensch und Huhn. *Z. Zellforsch.*, 64: 642-660.

Szodoray, L., and C. Nagy-Vezekényi. 1964 Histochemical studies of keratohyalin in human epidermis. *J. Invest. Derm.*, 42: 157-159.

Thomas, C. E. 1965 The ultrastructure of human amnion epithelium. *J. Ultrastruct. Res.*, 13: 65-84.

PLATE 1

EXPLANATION OF FIGURES

- 1 Light micrograph of fetal rat epidermis, crown-rump length (C-R), 15 mm; ten days gestation. Two cell layers are present, resting on fetal connective tissue (ct). The flattened superficial layer (arrows), bordering the amniotic cavity, will form the periderm. The basal layer will give rise to the four multicellular layers of mature skin. $\times 630$.
- 2 Light micrograph of fetal rat epidermis, C-R, 20 mm; 11-12 days gestation. The stratum germinativum (ge), a layer of low columnar cells, lies beneath two layers of rounded cells, the stratum spinosum (sp). The stratum granulosum (gr) is represented by a single layer of cells immediately beneath the periderm (p). The latter is devoid of cytoplasmic granules. $\times 630$.
- 3 Light micrograph of fetal rat epidermis, C-R, 28 mm; 14 days gestation. Evidence of the presence of a periderm (p) may be seen. The stratum corneum consists of a single cell layer. The keratohyalin granules peculiar to this layer give it a beaded appearance (co). In certain areas, cornification is not complete and individual granules may be seen (arrows). Both the stratum granulosum (gr) and the stratum spinosum (sp) are three to four layers thick. $\times 630$.
- 4 Light micrograph of fetal rat epidermis, C-R, 35 mm; 18-19 days gestation. Periderm, though present, is thin and difficult to detect in light micrographs. The beaded appearance of the most superficial layer of the stratum corneum is still apparent (arrows). Large keratohyalin granules are present in five to six layers of the stratum granulosum (gr). $\times 630$.

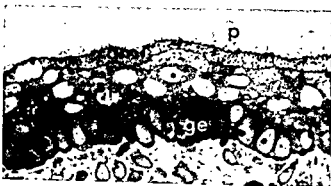
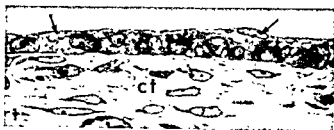


PLATE 1

EXPLANATION OF FIGURES

- 1 Light micrograph of fetal rat epidermis, crown-rump length (C-R), 15 mm; ten days gestation. Two cell layers are present, resting on fetal connective tissue (ct). The flattened superficial layer (arrows), bordering the amniotic cavity, will form the periderm. The basal layer will give rise to the four multicellular layers of mature skin. $\times 630$.
- 2 Light micrograph of fetal rat epidermis, C-R, 20 mm; 11-12 days gestation. The stratum germinativum (ge), a layer of low columnar cells, lies beneath two layers of rounded cells, the stratum spinosum (sp). The stratum granulosum (gr) is represented by a single layer of cells immediately beneath the periderm (p). The latter is devoid of cytoplasmic granules. $\times 630$.
- 3 Light micrograph of fetal rat epidermis, C-R, 28 mm; 14 days gestation. Evidence of the presence of a periderm (p) may be seen. The stratum corneum consists of a single cell layer. The keratohyalin granules peculiar to this layer give it a beaded appearance (co). In certain areas, cornification is not complete and individual granules may be seen (arrows). Both the stratum granulosum (gr) and the stratum spinosum (sp) are three to four layers thick. $\times 630$.
- 4 Light micrograph of fetal rat epidermis, C-R, 35 mm; 18-19 days gestation. Periderm, though present, is thin and difficult to detect in light micrographs. The beaded appearance of the most superficial layer of the stratum corneum is still apparent (arrows). Large keratohyalin granules are present in five to six layers of the stratum granulosum (gr). $\times 630$.

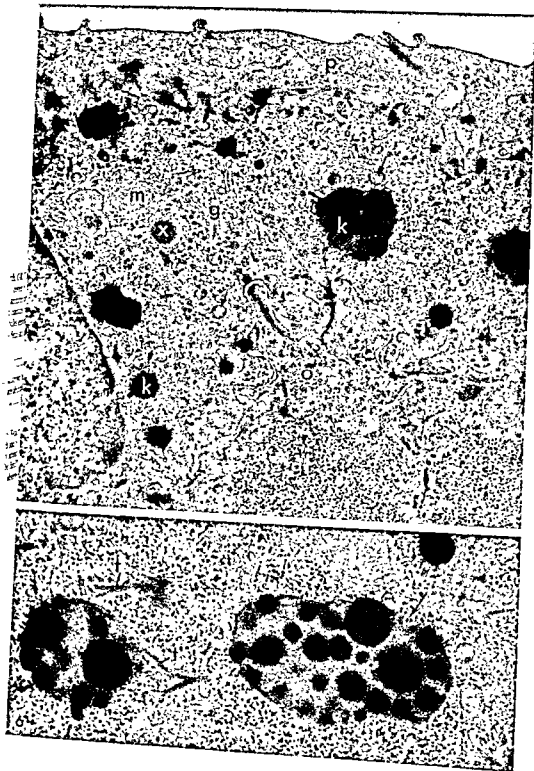


PLATE 2

EXPLANATION OF FIGURES

- 5 Cross section of epidermis from fetal rat (crown-rump length, C-R, 25 mm; 13-14 days gestation). A thin epithelial layer, the periderm (p), covers the free surface of the epidermis and forms part of the lining of the amniotic cavity. It is attached by desmosomes to the underlying layer, which contains small keratohyalin granules (k). The granules comprise lipidlike globules embedded in a dense matrix. Such granules are unique to this layer of the fetal skin and, as far as the author is aware, have not been observed in mature mammalian epidermis. In early stages of cornification, the cytoplasm surrounding the keratohyalin granules contains Golgi membranes (g), ribosomes, and mitochondria (m). The latter often enclose a large granule (x) of unknown significance. Keratinosomes or membrane-coating granules (arrows) are abundant. Glycogen deposits (gl), typical of cells in the stratum spinosum of fetal epidermis, may also be identified. $\times 20,800$.
- 6 Keratohyalin granules in cell layer immediately beneath periderm. Fetal rat, C-R, 25 mm; 13-14 days gestation. Tonofibrils (t) frequently approach and blend into the surface of the keratohyalin granules. Ribosomes also may appear to be embedded in the peripheral regions of the granule (arrows). The lipidlike droplets and the dense granular matrix of the granules may be observed. $\times 39,600$.

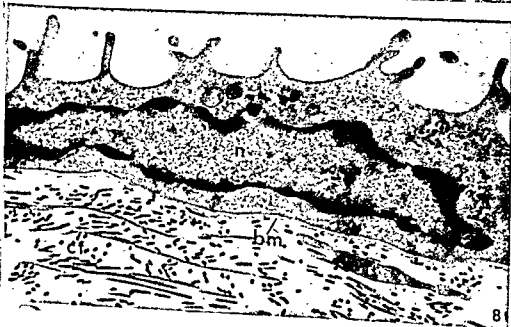
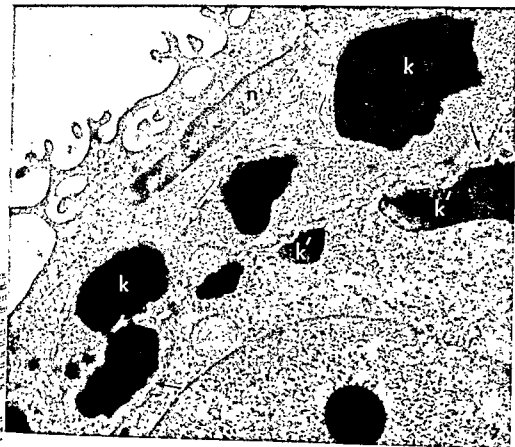


PLATE 3

EXPLANATION OF FIGURES

- 7 Periderm and stratum granulosum of fetal rat epidermis (crown-rump length, 28 mm; 14 days gestation). The periderm cell has an irregular free surface. Such villuslike projections serve to expand the cell surface. A portion of the nucleus (n) of the periderm cell is present. The cell underlying the periderm is flattened so that the large keratohyalin granules (k) form a series of bulges in the cell's profile. Note that the lipidlike globules may be observed within the granules and that the surrounding cytoplasm is rich in ribosomes. Smaller keratohyalin granules (k') occur in the cell lying deep to the first granular layer. Their internal structure is heterogeneous, consisting of a granular matrix, within which denser patches of material are encompassed. Fine lamellar plates, believed to be derived from the keratinosomes, lie in the intercellular spaces (arrows). $\times 17,500$.
- 8 Epithelial cell of amnion of fetal rat (C-R, 35 mm; 18-19 days gestation). Microvilli project into amniotic cavity. No evidences of cornification are seen in the cytoplasm surrounding the flattened nucleus (n). A thin basement membrane (bm) separates the epithelium from the delicate collagen network of the underlying connective tissue (ct). Compare epithelial cell with periderm shown in figure 7. $\times 19,200$.

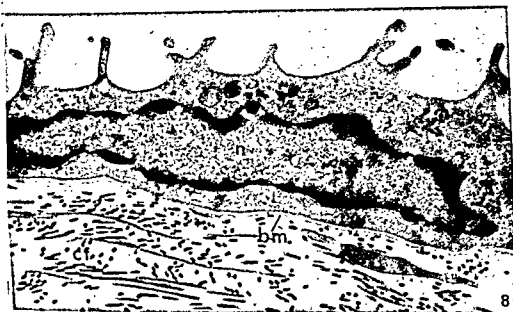
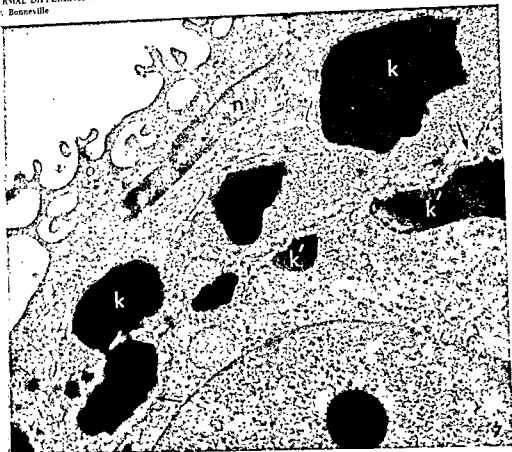


PLATE 3

EXPLANATION OF FIGURES

- 7 Periderm and stratum granulosum of fetal rat epidermis (crown-rump length, 28 mm; 14 days gestation). The periderm cell has an irregular free surface. Such villuslike projections serve to expand the cell surface. A portion of the nucleus (n) of the periderm cell is present. The cell underlying the periderm is flattened so that the large keratohyalin granules (k) form a series of bulges in the cell's profile. Note that the lipidlike globules may be observed within the granules and that the surrounding cytoplasm is rich in ribosomes. Smaller keratohyalin granules (k') occur in the cell lying deep to the first granular layer. Their internal structure is heterogeneous, consisting of a granular matrix, within which denser patches of material are encompassed. Fine lamellar plates, believed to be derived from the keratinosomes, lie in the intercellular spaces (arrows). $\times 17,500$.
- 8 Epithelial cell of amnion of fetal rat (C-R, 35 mm; 18-19 days gestation). Microvilli project into amniotic cavity. No evidences of cornification are seen in the cytoplasm surrounding the flattened nucleus (n). A thin basement membrane (bm) separates the epithelium from the delicate collagen network of the underlying connective tissue (ct). Compare epithelial cell with periderm shown in figure 7. $\times 19,200$.

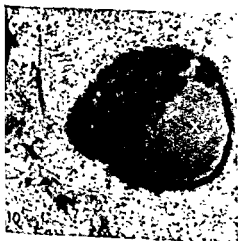
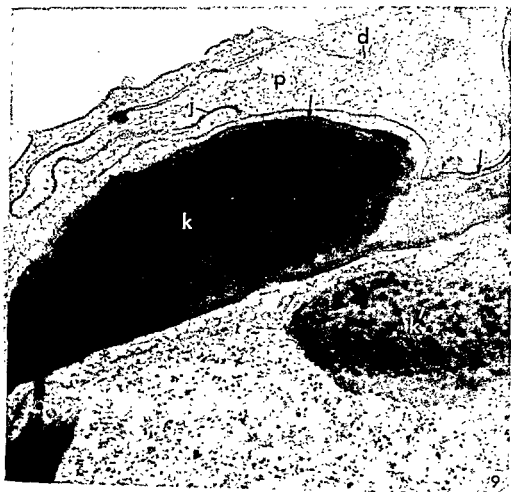


PLATE 4

EXPLANATION OF FIGURES

- 9 Periderm (p) overlies single layer of cornified cells in the epidermis of fetal rat (C-R, 30 mm; 16 days gestation). Plasma membranes of adjacent periderm cells interdigitate. Desmosomes (d) and close junctions of adjacent cell membranes (j) apparently aid in formation of a tightly sealed covering for the differentiating stratum corneum. The large heterogeneous keratohyalin granules (k) that occur in the cornified cell layer at an earlier stage in development (compare figs. 5, 7) may still be seen, but they are surrounded by additional horny material. A thin layer of dense granular material (arrows) separates the granule as well as the intergranular deposits from the "thickened" plasma membrane. Beneath the corneum, cells of the stratum granulosum contain large keratohyalin granules (k'). Note the dense patches of material that characterize the granules. The cytoplasm that surrounds them is usually devoid of tonofilaments. Fine lamellar plates, believed to be derived from keratinosomes, may be seen intercellularly between the two layers of keratinizing cells (*). $\times 34,000$.
- 10 Keratohyalin granule within fetal rat epidermis (C-R, 30 mm; ca 16 days gestation). Granule seen here is forming within the second or third layer of cells beneath the periderm. Dense patches of material are embedded in a less dense matrix. In nucleoid-like area (x) no patches occur. Few tonofibrils are associated with granules at this stage of development, but ribosomes usually adhere closely to the surface of the granule. $\times 42,000$.
- 11 Keratohyalin granule within fetal rat epidermis (C-R, 30 mm). This granule lies in the cell layer immediately beneath that containing the granule seen in figure 10. Note the frequent association between tonofibrils (t) and the surface of the granule. A few dense patches (arrows) of material lie at the periphery of the granule. It is postulated that the patches may arise as fibrillar material is incorporated into the granule. $\times 42,000$.

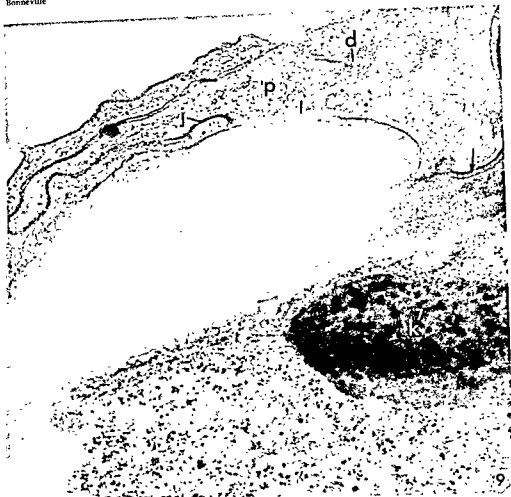
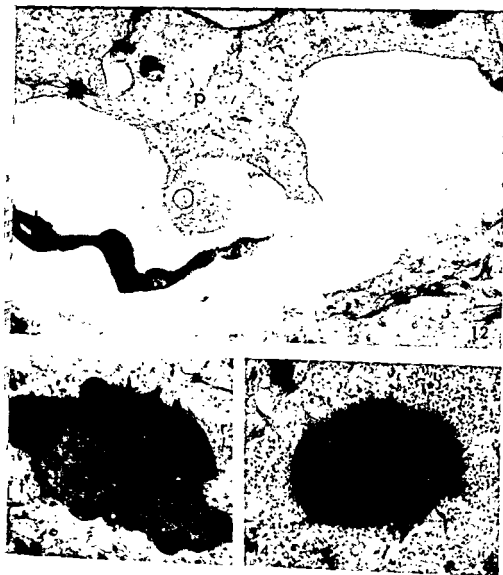


PLATE 5

EXPLANATION OF FIGURES

- 12 Periderm and stratum corneum of fetal rat skin (C-R, 35 mm; 18-19 days gestation). The periderm layer (p) is not firmly attached to the underlying horny cells as it is at earlier stages of development. In the cornified layer immediately below the periderm aggregates of large lipidlike droplets are found in the keratohyalin granules (k) as they are at an earlier stage of development (compare figs. 5, 7). Succeeding layers (co), however, do not form similar granules. Spaces between horny cells are preparation artifacts. $\times 26,400$.
- 13 Keratohyalin granule in fifth cell layer beneath the periderm (C-R, 35 mm). Large irregular dense bodies of homogeneous material are embedded in the periphery of the granule, which consists in the main of a deeply staining granular matrix. Tonofibrils (t) seem to blend into the surface of the granule. Ribosomes (r) also lie near the granule, and it seems feasible that some of them may be embedded in the dense granular matrix. $\times 23,200$.
- 14 Keratohyalin granule forming in the seventh cell layer beneath the periderm (C-R, 35 mm). Note that the tonofibrils and the ribosomes are both closely associated with the surface of the granule. In this granule and those that form later in fetal life and after birth, no internal heterogeneity can be detected. $\times 32,400$.



Electron Microscopic Study of Uterine Arteries During Pregnancy

ERNEST N. ALBERT² AND DANIEL C. PEASE¹

Department of Anatomy, School of Medicine, University of California, Los Angeles, California

ABSTRACT The mesometrial arteries of pregnant guinea pigs are not mere blood conducting channels. Instead they are dynamic in nature. The cells forming the intima and media exhibited significant structural modifications during pregnancy. The endothelial cells became hypertrophied and attenuated. Their cytoplasm showed an increase in the amount of ribosomes, rough endoplasmic reticulum and lysosome-like bodies during pregnancy. Dense bodies that were often closely associated with the Golgi apparatus were seen in pregnant animals. These bodies exhibited a gradation in size within each cell and were thought to be the precursors of the lysosome-like bodies. Similar structures were also seen in smooth muscle cells of the mesometrial arteries of pregnant animals.

The endothelium of these arteries was often discontinuous in full term pregnant animals. In that case, the underlying smooth muscle cells provided the lining surface. Irrespective of which type of cells formed the lumen of these arteries, they became coated with a "fuzzy" layer which specifically stained intensely with phosphotungstic acid, suggesting that this layer might be a mucoprotein. The smooth muscle cell of the arterial media also became hypertrophied during pregnancy. The cytoplasm exhibited a gradual increase in free ribosomes and rough endoplasmic reticulum, mitochondria and microtubules throughout pregnancy. During the latter half of pregnancy many smooth muscle cells developed extensive amounts of smooth endoplasmic reticulum whose vesicles often were filled with an electron opaque secretory material. It is suggested that the development of unusually large quantities of smooth endoplasmic reticulum might be associated with steroid metabolism. Unusually thick basement membranes were formed around the modified smooth muscle cells of full term pregnant animals and the surfaces of these cells often exhibited large numbers of microvilli. The microvilli seemed to disrupt the continuous patterns of the basement membrane.

In electron microscopic studies of the vascular system, the efforts of most investigators have been directed principally towards the large arteries and the capillaries. As a result of this, only a few electron microscopic reports are available on the morphology and function of the smaller "tributing" arteries (Moore and Ruska, 1961; Movat and Fernando, '63; Bunce, '65; Adin, '62, '67). The scarcity of the existing literature on this subject also may be due to the general impression that all uterine arteries have essentially the same morphology and that they are merely blood distributing channels. However the mesometrial arteries of the pregnant guinea pig do not fit into this simple category. It has been shown that the endothelial and smooth muscle cells of these arteries are capable of carrying out a wide variety of functions (Albert, '67a,b; Albert and Pease, '67). Their intimal and medial cells demonstrated cyclic alterations during pregnancy and post-partum involution. The cells of the intima and media were

thought to be involved in the degradation and synthesis of elastic fibers during pregnancy and post-partum involution respectively. Although our histochemical stains supported the view that cells of the intima and media resembled endothelial and smooth muscle cells, we had but limited morphological criteria upon which to base decisions. It was also reported that the endothelial lining of mesometrial arteries became discontinuous during pregnancy, and was reconstructed during post-partum involution. There was, however, a possibility that this might have been due to an artifact of fixation. Hypertrophy and hyperplasia of intimal cells was also apparent, but it was not clear as to how and what cytoplasmic organelles caused these changes in size and number. These questions prompted us to begin a thorough study of the morphological alterations that occur in mesometrial arteries of pregnant

¹ Supported in part by grants of the National Heart Institute.
² Present address: Department of Anatomy, School of Medicine, The George Washington University, 1335 H St. N.W., Washington D.C. 20005

rather of plates or islands of elastic since its pattern has been seen only in two dimensions.

Smooth muscle cells. The three or four cell thick media of the mesometrial artery was formed by a pure population of smooth muscle cells. All muscle cells were enveloped by a continuous thin basement membrane (figs. 1, 4-6). Collagen fibers and occasional fragments of elastic fibers were dispersed throughout the cytoplasm.

The smooth muscle cells (figs. 1, 4, 6) were long and spindle-shaped. They contained prominent nuclei that conformed to the shape of the cell. The main part of the cytoplasm was occupied with longitudinally oriented myofibrils and associated dense bodies, characteristic of smooth muscle, which could be detected amongst the myofibrils (figs. 4-6). There were electron dense granules immediately below the plasma membrane that resembled the dense bodies of the cytoplasm (figs. 4-6). Often continuities between the dense bodies of the cytoplasm and the dense patches under the cell membranes were observed (figs. 4, 5), suggesting that they may be fundamentally the same. Most of the cytoplasmic organelles were located at the nuclear poles between the bundles of myofilaments. In general, the cytoplasmic organelles were abundant. Of the organelles, free ribosomes and mitochondria were most common. Few microtubules and vesicles of Golgi or of smooth or rough surfaced endoplasmic reticulum could be seen.

Group II: Mesometrial arteries from 1-5 week pregnant quinea pigs

Endothelial cells. The first obvious differentiation in the endothelial cells, as a result of pregnancy, was a shape change. In transverse sections the cells apparently flattened greatly, perhaps as a response to the increasing size of the arterial lumen, and the corresponding increase in surface area (fig. 7). The cells were not notably flattened in the early stages of pregnancy, however, by implication their volume had increased substantially (figs. 7, 8). The extent of the attenuations was dependent on the stage of pregnancy.

The surfaces of endothelial cells were covered by a continuous dark staining "fuzzy" layer which followed the membrane contours into open pits and vesicles (fig. 7).

This is in contrast to the non-pregnant animals which demonstrated a patchy layer on the endothelial surfaces.

The cytoplasm of endothelial cells in one to three week pregnant animals gave indications of increased metabolic activity. This was reflected in an increase in the number of free ribosomes, while the other organelles did not show noticeable change (fig. 7). By the fifth week of pregnancy, however, the endothelial cells did demonstrate a significant increase in the rough endoplasmic reticulum and also the Golgi vesicles (fig. 8). Pinocytotic vesicles and plasma membrane infoldings could be distinguished from other smooth surfaced vesicles by the presence of dark staining surfaces (fig. 7). These were thought to be due to the "fuzzy" coating that lined the luminal surface of endothelial cells.

Lysosome-like bodies became increasingly apparent after the first three or four weeks of pregnancy (fig. 8). These bodies were of various sizes. Filamentous structures and occasional microtubules also were seen in some endothelial cells of pregnant animals. Patches of thicker basement membrane can usually be seen under the endothelium at this stage of pregnancy.

Smooth muscle cells. Like the endothelial cells, smooth muscle cells also showed an hypertrophy which was reflected after conception by an increase in the organelles. The muscle cells became progressively enlarged. However, with the progress of gestation the myofibrillar zones did not seem to increase. Rather, it was those areas of cytoplasm occupied by organelles which remarkably expanded. This became dramatically evident by the fifth week of pregnancy as demonstrated by figure 9 in which it can be seen that there was by now much rough and smooth surfaced endoplasmic reticulum, prominent Golgi zones, quantities of free ribosomes, patches of glycogen, and probably more than the original number of mitochondria. Thus, areas occupied by myofibrils came to be conspicuously delineated at the periphery of the cells and separated from the main cytoplasmic mass, located centrally. There was no obvious change in the number and distribution of microtubules. Nuclei did increase in size, and developed prominent and patterned nucleoli.

During early pregnancy, vesicular structures with electron dense contents were

animals using the higher resolution and better methods of tissue preparation of electron microscopy.

MATERIALS AND METHODS

Pregnant guinea pigs were used for the present investigation. The animals were divided into three groups. Group I consisted of adult non-pregnant female guinea pigs and served as the control group. Groups II and III represented the experimental animals at various stages of pregnancy. One to five week pregnant animals were put into Group II, and six to nine week pregnant animals into Group III. These animals were sacrificed at weekly intervals throughout their pregnancy.

All guinea pigs were anesthetized by an intraperitoneal injection of sodium pentobarbital. Their thoracic cavities were opened and the descending part of the aorta cannulated with plastic tubing. The animals were then perfused for five minutes with 5% glutaraldehyde in 0.2 M Collidine buffer (Bennett and Luft, '58). After perfusion, the abdominal cavities were opened and arterial segments of mesometrial arteries closest to the myometrium were dissected out and further fixed in buffered glutaraldehyde for one hour. Following aldehyde fixation, the tissues were washed in two ten minutes changes of collidine buffer, and post-fixed in 1% buffered osmium tetroxide for an additional hour. After osmication, the tissues were washed again in the buffer and dehydrated in ascending series of alcohols. The specimens were then embedded in Vestopal W. After sectioning they were doubly stained with uranyl acetate and lead citrate (Venable and Coggeshall, '65). Some of the sections were also stained with 5% aqueous phosphotungstic acid (Pease, '64).

OBSERVATIONS

General observations

In the adult nulliparous animal, all mesometrial arteries appeared alike to the naked eye. But in the pregnant animal, some of the arteries were conspicuously larger in diameter and exhibited decidedly greater tortuosity. The arteries that directly supplied the placenta were the largest and most coiled. These will be referred to as "placental" arteries, and the

others as "peripheral." The placental arteries consistently exhibited pronounced alterations in their morphology during pregnancy, while the peripheral arteries demonstrated minimal and inconsistent changes, depending upon the distance the peripheral artery from the placenta. The part of all placental vessels closest to the uterine horn exhibited marked changes. Thus, for the sake of consistency all our tissues from pregnant animals were selected from the placental arteries before they entered the myometrium.

The observations which follow on three groups of animals (non-pregnant, early and late-pregnant) are described under individual headings.

Group I: Mesometrial arteries of non-pregnant animals

The endothelial cells. The endothelial cells usually were closely packed, and cuboidal. They were separated from the muscular media by their basement membrane, the internal elastic lamina, and a few scattered collagenous fibers (figs 1-4). The endothelial cell surfaces were usually smooth with some undulations and occasional cytoplasmic processes extending into the lumen. There were hints of specialized, but incomplete surface lining the vascular lumen. This amorphous layer became quite prominent on the luminal surface of endothelial cells in mesometrial arteries at full term as described later.

The cytoplasm of the endothelial cells contained some mitochondria, a few strands of rough endoplasmic reticulum and free ribosomes. The ribosomes were either scattered individually or occurred in groups as polysomes. The Golgi zone in these cells was usually small and vestigial. Many in-pocketings of the plasma membrane along with deeper vesicles, generally of a pinocytotic type, were observed on all surfaces—luminal, medial and intercellular (fig. 2). Some cells contained fibrillar structures scattered throughout the cytoplasm (fig. 3). Lysosome-like structures were few or absent. The endothelial cells rested upon a thin basement membrane.

The internal elastic membrane was regarded as probably a complete fenestrated sheet (fig. 2). However it cannot be ruled out that it at times may have been

1 rather of plates or islands of elastic
2 since its pattern has been seen only
3 o dimensions.

ooth muscle cells. The three or four
thick media of the mesometrial arte-
vas formed by a pure population of
il smooth muscle cells. All muscle
were enveloped by a continuous thin
nent membrane (figs. 1, 4-6). Collage-
fibers and occasional fragments of
a were dispersed throughout the

smooth muscle cells (figs. 1, 4, 6)
long and spindle-shaped. They con-
ed prominent nuclei that conformed to
shape of the cell. The main part of the
plasm was occupied with longitudi-
y oriented myofibrils and associated
se bodies," characteristic of smooth
cle, which could be detected amongst
n (figs. 4-6). There were electron dense
ues immediately below the plasma-
na that resembled the dense bodies of
cytoplasm (figs. 4-6). Often continu-
between the dense bodies of the cyto-
m and the dense patches under the cell
branes were observed (figs. 4, 5), sug-
ing that they may be fundamentally
same. Most of the cytoplasmic organ-
were located at the nuclear poles
een the bundles of myofilaments. In
ral, the cytoplasmic organelles were
abundant. Of the organelles, free ribo-
and mitochondria were most com-
in. Few microtubules and vesicles of
lgi, or of smooth or rough surfaced endo-
smic reticulum could be seen.

Group II: Mesometrial arteries from
1-5 week pregnant quinea pigs

endothelial cells. The first obvious
dification in the endothelial cells, as a
ult of pregnancy, was a shape change.
transverse sections the cells apparently
dened greatly, perhaps as a response to
reasing size of the arterial lumen, and
corresponding increase in surface area
t. 7). The cells were not notably flattened
the early stages of pregnancy, however,
by implication their volume had
reased substantially (figs. 7, 8). The
ent of the attenuations was dependent
on the stage of pregnancy.
urfaces of endothelial cells were cov-
d by a continuous dark staining "fuzzy"
er which followed the membrane con-
rs into open pits and vesicles (fig. 7)

This is in contrast to the non-pregnant ani-
mals which demonstrated a patchy layer
on the endothelial surfaces.

The cytoplasm of endothelial cells in one
to three week pregnant animals gave indi-
cations of increased metabolic activity.
This was reflected in an increase in the
number of free ribosomes, while the other
organelles did not show noticeable change
(fig. 7). By the fifth week of pregnancy,
however, the endothelial cells did demon-
strate a significant increase in the rough
endoplasmic reticulum and also the Golgi
vesicles (fig. 8). Pinocytotic vesicles and
plasma membrane infoldings could be
distinguished from other smooth surfaced
vesicles by the presence of dark staining
surfaces (fig. 7). These were thought to be
due to the "fuzzy" coating that lined the
luminal surface of endothelial cells.

Lysosome-like bodies became increas-
ingly apparent after the first three or four
weeks of pregnancy (fig. 8). These bodies
were of various sizes. Filamentous struc-
tures and occasional microtubules also
were seen in some endothelial cells of preg-
nant animals. Patches of thicker basement
membrane can usually be seen under the
endothelium at this stage of pregnancy.

Smooth muscle cells. Like the endo-
thelial cells, smooth muscle cells also
showed an hypertrophy which was
reflected after conception by an increase in
the organelles. The muscle cells became
progressively enlarged. However, with the
progress of gestation the myofibrillar zones
did not seem to increase. Rather, it was
those areas of cytoplasm occupied by organ-
elles which remarkably expanded. This
became dramatically evident by the fifth
week of pregnancy as demonstrated by
figure 9 in which it can be seen that there
was by now much rough and smooth sur-
faced endoplasmic reticulum, prominent
Golgi zones, quantities of free ribosomes,
patches of glycogen, and probably more
than the original number of mitochondria.
Thus, areas occupied by myofibrils came to
be conspicuously delineated at the periph-
ery of the cells and separated from the
main cytoplasmic mass, located centrally.
There was no obvious change in the num-
ber and distribution of microtubules.
Nuclei did increase in size, and developed
prominent and patterned nucleoli.

During early pregnancy, vesicular struc-
tures with electron dense contents were

detected, often closely associated with the Golgi complex. Some of these vesicles had a homogeneous matrix while others had translucent centers (figs. 9, 18). In general the smaller ones which were closest to the Golgi zones, had translucent matrices, while the larger ones were homogeneous. This became more apparent in later stages of pregnancy.

The dense patches that were seen in smooth muscle of arteries from non-pregnant animals, located immediately below the plasma membrane were also observed in muscle cells of pregnant animals. They appeared to be larger in size and number and seemed to alternate with cell surface protrusions associated with pinocytotic vesicles. This alternating pattern was more prevalent in smooth muscle of mesometrial arteries from pregnant than non-pregnant animals. The basement membranes surrounding the smooth muscle cells of arteries from pregnant animals become conspicuously thicker than those seen around muscle cells in arteries of non-pregnant guinea pigs (compare figs. 6 and 9).

Group III: Mesometrial arteries from 6-9 week pregnant guinea pigs

The endothelial cells. The pattern of the endothelium and its cells presented a peculiar problem in 6-9 week pregnant animals. In the non-pregnant animals it was generally observed that endothelial cells overlapped each other, but this was not commonly the case in near term guinea pigs. Instead, the endothelial cells in this stage of pregnancy often did not even form a continuous lining around the vascular lumina leaving denuded areas of underlying smooth muscle cells. This could partly be attributed to the increase in the size of the lumen of these vessels during pregnancy. At times cells became so attenuated that their cytoplasm seemed to be at the point of breaking or pinching off (fig. 10), and in the event that this would happen the underlying cells would be without an endothelial covering. Under these circumstances, cells of the media would come in direct contact with the blood as shown in figure 11, and apparently serve the same functions as the original endothelial cells.

The luminal surface of mesometrial arteries of full term pregnant animals also

was coated with a fuzzy, dark staining layer irrespective of whether the endothelium or smooth muscle formed the lining. This layer is overlying the endothelium in figure 10 and at the surface of denuded smooth muscle in figures 11 and 17. Plasma membranes of smooth muscle cells underlying an intact endothelium were not covered by such a layer (fig. 10). The "fuzzy" layer covering the luminal surfaces of the arteries (whether they were endothelium or smooth muscle), showed a specific affinity to PTA, while none of the other cytoplasmic membranes exhibited such reactions (fig. 12).

Lest it be thought that the denuded muscle cells were artificially created, it should be emphasized that there were profound changes to be observed in these animals in the subendothelial zone. Irrespective of whether the entire endothelium was intact or not, in most animals, all traces of the internal elastic membrane had disappeared by the ninth week of pregnancy. However in some subendothelial areas where the elastica was absent, and the endothelium was intact, the basement membrane and other fibrous components were normally preserved. In other subendothelial zones, conspicuous cavities could be seen underlying an attenuated endothelium (fig. 10). In this latter case the basement membrane and fibrous elements were absent, and microvillous processes which had appeared on the surface of muscle cells invaded these cavities (fig. 10).

The cytoplasm of endothelial cells from 6-9 week pregnant animals showed continued signs of high metabolism (fig. 1). The cells had become greatly hypertrophied. Golgi zones were quite prominent, rough endoplasmic reticulum, mitochondria, and free ribosomes were abundant and evenly distributed throughout the cytoplasm. Many rounded vascular structures were in close association with the Golgi zones, and at times appeared to be budding off from the Golgi vesicles (figs. 12-14). These rounded structures were partially completely filled with a dense homogeneous matrix. They seemed to be identical with those already described in smooth muscle cells of arteries from pregnant animals in group II (compare figs. 9 and 11 with 12-14). These dense bodies seemed to increase gradually in size and resembled lysosomal structures (fig. 12).

smooth muscle cells. During the early stages of pregnancy, all the muscle became hypertrophied and exhibited form changes in their organelles. But, at later stages of gestation, these cells began to demonstrate individual variation.

While some of the hypertrophied cells could readily be identified as smooth muscle, others had changed to such an extent that they hardly could be recognized. Occasionally, the entire media consisted of modified cells. This observation was made on thick sections. Part of such an area is shown in figure 17. The contrast between highly modified smooth muscle cells and those that did not alter significantly is shown in figure 16 in which the cell demonstrated great modification while the cell in the lower right corner remained minimally altered. Even the most modified cells could be recognized as derived from smooth muscle for they variably retained fibrillar zones in some parts of their cytoplasm (figs. 15, 16, 17 and 19, arrows). Typically fibrillar material appeared to have been displaced peripherally by a great hyperplasia of the rest of the cytoplasm, so that fibrillar zones became conspicuous as bands immediately underlying the surface, and often penetrating as complete septa (fig. 15). That the fibrillar zones represent modifications of the contractile system is indicated by the regular presence of the "dense bodies" characteristic of smooth muscle (figs. 15 and 19). The most prominent feature of modified smooth muscle cells of pregnancy was the appearance of an extensive amount of smooth endoplasmic reticulum. In some cells most of the smooth endoplasmic reticular vesicles were filled with an electron dense material (figs. 15, 19), while those of others were empty (fig. 16). It appeared that the rough endoplasmic reticulum first became prominent during early pregnancy. The agranular reticulum appeared in substantial quantities later in pregnancy, and continued to increase with the progress of gestation. We were unable to decide whether the increase in the smooth endoplasmic reticulum was at the expense of the rough or whether it was an independent formation. Large numbers of mitochondria (figs. 10, 15) and microtubules (fig. 21) also were seen distributed throughout their cytoplasm.

The modified smooth muscle cells elaborated an unusually large amount of a dense material which formed the basement membrane. The thickness of this layer varied considerably from cell to cell, and from animal to animal, and indeed was often discontinuous. Thus dimensions became meaningless (compare figs. 19-22). Nevertheless the thinnest basement membrane was significantly thicker than the ordinary layers seen in non-pregnant animals. Figures 21 and 22 demonstrate continuous basement membranes. Figure 19 illustrates patches of basement membrane separated by microvilli, while figure 20 shows a thick basal lamina, formed of several interrupted layers. This layered appearance gave the impression that such lamina may have formed intermittently. In the absence of basement membranes or when incomplete membranes were present, unusual quantities of microvilli ordinarily seemed to be present (fig. 19). These microvilli were often extraordinarily long and numerous (fig. 19). They gave the impression that they were responsible for the discontinuity of the basement membrane.

DISCUSSION

The morphological changes observed during pregnancy in mesometrial arteries, and their implied physiological alterations, have demonstrated clearly the dynamic nature of these vessels during pregnancy.

Our observations showed that the intima and media of non-pregnant mesometrial arteries were formed exclusively by endothelial and smooth muscle cells. This is in full agreement with the conclusions of Pease and Molinari ('60) on the pial vessels of cat and monkey, and Pease and Paule ('60) on the rat aorta.

During pregnancy both smooth muscle and endothelial cells showed striking alterations in their shapes and numbers and the arrangement of their cytoplasmic components. By term the smooth muscle cells had changed so much that they bore very little resemblance to their original morphology, and were hardly recognizable any longer as such.

It was evident from the present study that smooth muscle developed a substantial capacity for synthetic activity as pregnancy progressed. Muscle cells of

detected, often closely associated with the Golgi complex. Some of these vesicles had a homogeneous matrix while others had translucent centers (figs. 9, 18). In general the smaller ones which were closest to the Golgi zones, had translucent matrices, while the larger ones were homogeneous. This became more apparent in later stages of pregnancy.

The dense patches that were seen in smooth muscle of arteries from non-pregnant animals, located immediately below the plasma membrane were also observed in muscle cells of pregnant animals. They appeared to be larger in size and number and seemed to alternate with cell surface protrusions associated with pinocytotic vesicles. This alternating pattern was more prevalent in smooth muscle of mesometrial arteries from pregnant than non-pregnant animals. The basement membranes surrounding the smooth muscle cells of arteries from pregnant animals become conspicuously thicker than those seen around muscle cells in arteries of non-pregnant guinea pigs (compare figs. 6 and 9).

Group III: Mesometrial arteries from 6-9 week pregnant guinea pigs

The endothelial cells. The pattern of the endothelium and its cells presented a peculiar problem in 6-9 week pregnant animals. In the non-pregnant animals it was generally observed that endothelial cells overlapped each other, but this was not commonly the case in near term guinea pigs. Instead, the endothelial cells in this stage of pregnancy often did not even form a continuous lining around the vascular lumina leaving denuded areas of underlying smooth muscle cells. This could partly be attributed to the increase in the size of the lumen of these vessels during pregnancy. At times cells became so attenuated that their cytoplasm seemed to be at the point of breaking or pinching off (fig. 10), and in the event that this would happen the underlying cells would be without an endothelial covering. Under these circumstances, cells of the media would come in direct contact with the blood as shown in figure 11, and apparently serve the same functions as the original endothelial cells.

The luminal surface of mesometrial arteries of full term pregnant animals also

was coated with a fuzzy, dark layer irrespective of whether endothelium or smooth muscle cells were present.

This layer is overlying the endothelium in figure 10 and at the surface of denuded smooth muscle in figures 11 and 17. The membranes of smooth muscle cells underlying an intact endothelium were not covered by such a layer (fig. 10). The "fuzzy" layer covering the luminal surfaces of the arteries (whether they were endothelial or smooth muscle), showed a specific reaction to PTA, while none of the other cytoplasmic membranes exhibited such reactions (fig. 12).

Lest it be thought that the denuded cells were artificially created, it should be emphasized that there were profound changes to be observed in these animals in the subendothelial zone. Irrespective of whether the entire endothelium was intact or not, in most animals, all traces of internal elastic membrane had disappeared by the ninth week of pregnancy. However in some subendothelial zones where the elastica was absent, and the endothelium was intact, the basement membrane and other fibrous components were normally preserved. In certain subendothelial zones, conspicuous cavities could be seen underlying an attenuated endothelium (fig. 10). In this latter case, basement membrane and fibrous elements were absent, and microvillous processes which had appeared on the surface of endothelial cells invaded these cavities (fig. 10).

The cytoplasm of endothelial cells in 6-9 week pregnant animals showed continued signs of high metabolism (fig. 12). The cells had become greatly hypertrophied. Golgi zones were quite prominent, rough endoplasmic reticulum, mitochondria, and free ribosomes were abundant and evenly distributed throughout the cytoplasm. Many rounded vasicular structures were in close association with the Golgi zones, and at times appeared to be budding off from the Golgi vesicles (figs. 12). These rounded structures were partially or completely filled with a dense homogeneous matrix. They seemed to be identical with those already described in smooth muscle cells of arteries from pregnant animals in group II (compare figs. 9 and 12-14). These dense bodies seem to increase gradually in size and resemble lysosomal structures (fig. 12).

the smooth muscle cells. During the later stages of pregnancy, all the muscle became hypertrophied and exhibited normal changes in their organelles. But, in the later stages of gestation, these cells began to demonstrate individual variations. While some of the hypertrophied cells could readily be identified as smooth muscle, others had changed to such an extent that they hardly could be recognized. Occasionally, the entire media consisted of modified cells. This observation was made on thick sections. Part of such a media is shown in figure 17. The contrast between highly modified smooth muscle cells and those that did not alter significantly is shown in figure 16 in which the central cell demonstrated great modification, while the cell in the lower right corner was minimally altered. Even the most modified cells could be recognized as derived from smooth muscle for they variably retained fibrillar zones in some parts of their cytoplasm (figs. 15, 16, 17 and 19, arrows). Typically fibrillar material appeared to have been displaced peripherally by a great hyperplasia of the rest of the cytoplasm, so that fibrillar zones became conspicuous as bands immediately underlying the surface, and often penetrating as incomplete septa (fig. 15). That the fibrillar zones represent modifications of the contractile system is indicated by the regular presence of the "dense bodies" characteristic of smooth muscle (figs. 15 and 19). The most prominent feature of modified smooth muscle cells of pregnancy was the appearance of an extensive amount of smooth endoplasmic reticulum. In some cells most of the smooth endoplasmic reticular vesicles were filled with an electron dense material (figs. 15, 19), while those of others were empty (fig. 16). It appeared that the rough endoplasmic reticulum first became prominent during early pregnancy. The agranular reticulum appeared in substantial quantities later in pregnancy, and continued to increase with the progress of gestation. We were unable to decide whether the increase in the smooth endoplasmic reticulum was at the expense of the rough or whether it was an independent formation. Large numbers of mitochondria (figs. 10, 15) and microtubules (fig. 21) also were seen distributed throughout their cytoplasm.

The modified smooth muscle cells elaborated an unusually large amount of a dense material which formed the basement membrane. The thickness of this layer varied considerably from cell to cell, and from animal to animal, and indeed was often discontinuous. Thus dimensions became meaningless (compare figs. 19-22). Nevertheless the thinnest basement membrane was significantly thicker than the ordinary layers seen in non-pregnant animals. Figures 21 and 22 demonstrate continuous basement membranes. Figure 19 illustrates patches of basement membrane separated by microvilli, while figure 20 shows a thick basal lamina, formed of several interrupted layers. This layered appearance gave the impression that such lamina may have formed intermittently. In the absence of basement membranes or when incomplete membranes were present, unusual quantities of microvilli ordinarily seemed to be present (fig. 19). These microvilli were often extraordinarily long and numerous (fig. 19). They gave the impression that they were responsible for the discontinuity of the basement membrane.

DISCUSSION

The morphological changes observed during pregnancy in mesometrial arteries, and their implied physiological alterations, have demonstrated clearly the dynamic nature of these vessels during pregnancy.

Our observations showed that the intima and media of non-pregnant mesometrial arteries were formed exclusively by endothelial and smooth muscle cells. This is in full agreement with the conclusions of Pease and Molinari ('60) on the pial vessels of cat and monkey, and Pease and Paule ('60) on the rat aorta.

During pregnancy both smooth muscle and endothelial cells showed striking alterations in their shapes and numbers and the arrangement of their cytoplasmic components. By term the smooth muscle cells had changed so much that they bore very little resemblance to their original morphology, and were hardly recognizable any longer as such.

It was evident from the present study that smooth muscle developed a substantial capacity for synthetic activity as pregnancy progressed. Muscle cells of

mesometrial arteries from non-pregnant animals contained very little rough endoplasmic reticulum, ribosomes or Golgi vesicles. But during pregnancy there was an extensive development of all these organelles. Additionally, the smooth surfaced endoplasmic reticulum expanded in a truly remarkable manner, discussed below.

Although in general smooth muscle cells have not been noted for appreciable synthetic activity, certain recent reports have shown this to be the case in special situations. Thus, uterine smooth muscle has been shown to develop an extensive synthetic apparatus during pregnancy (Laguens and Lagrutta, '64) and under estrogen stimulation (Ross and Klebanoff, '67; Laguens, '64). Gorski and Nelson ('65) also showed an increase in ribosomes in uterine muscle in estrogen stimulated rats. These authors suggested that uterine smooth muscle was probably participating in the secretion of collagen as well as non-collagenous proteins. Parker and Odland ('66) have implicated smooth muscle as manufacturing collagen in atherosclerotic plaques. Pease et al. ('60) have emphasized that the presence of only smooth muscle and endothelial cells in the intima and media of pial and aortic vessels demonstrated that these cells must have been responsible for the synthesis of elastica and collagen, as well as the basement membranes found in those arteries.

One of the most unexpected observations in the smooth muscle of mesometrial arteries of full term pregnant guinea pigs was the development of an extensive agranular reticulum, and the presence of electron dense material in its vesicles. This, coupled with the presence of large numbers of microvilli on cell surfaces, gave the smooth muscle the appearance of secretory cells.

Our electron microscopic studies have not given any specific clues as to the nature of the electron opaque material found in the smooth endoplasmic vesicles. However, the occurrence of large amounts of smooth endoplasmic reticulum often has been associated with steroid secreting cells; interstitial cells of testes (Christensen, '65; Fawcett and Burgos, '60); ovarian cells (Muta, '58); adrenal cortex (Enders and Lyons, '64; Sheridan and Belt,

'64; Sabatini et al., '62) and others. Jones and Fawcett ('65) have... generous doses of progesterone cause significant increase in the agranular reticulum of liver cells. Finally, the identification of specific enzymes necessary for the biosynthesis of androgens has been located biochemically in the components of the agranular reticulum of testicular cells by Lynn and Brown ('65). Based upon these reports, the idea that smooth muscle under certain conditions may be linked to steroid metabolism seems reasonable.

The observations demonstrated that myofibrils were pushed towards the periphery of the cytoplasm during pregnancy. While the cell was increasing its mass, apparently there was no corresponding increase in the number of the myofibrils. These morphological features indicate that it was not the contractile system that was being specialized by pregnancy, but rather other mechanisms.

Another observation of significant interest was the presence of a patchy endothelium on the mesometrial arteries of term pregnant animals. In the absence of complete endothelial covering, the smooth muscle cells apparently served as the luminal surface. Normally one would expect partially denuded blood vessels to react as in the case of an injury to endothelium. But there was no evidence of such a reaction in the present circumstances.

We observed the presence of a thick, dark staining layer on the endothelial surface of pregnant animals. This same layer was seen to cover the denuded smooth muscle cells in the absence of an endothelium. In such a layer was not present on the surfaces of smooth muscle cells where the endothelium was intact. Therefore it is possible that this "fuzzy" layer acted as a protective coat, preventing thrombus formation (or other complications) just effectively when it covered denuded smooth muscle as when it overlay endothelium.

The original demonstration of a specialized surface coat lining vascular lumens was by Chambers and Zweifach ('60). They thought this to be an adsorbed protein constituent of blood plasma. Observing enhanced staining of this layer with ruthenium red,

in red, Luft, ('65) suggested that it might contain mucopolysaccharides. In the present study it was shown that the internal surfaces of mesometrial arteries in pregnant animals stained specifically with phosphotungstic acid, while none of the other cytomembranes were stained. Phosphotungstic acid has been shown empirically by Pease ('66) also to be a fairly specific stain for polysaccharides.

It may be well to point out that the incomplete endothelium seen in full term pregnant animals was not due to improper techniques of fixation, dehydration or embedding. The reality of this observation is further substantiated by the fact that the fuzzy layer on denuded smooth muscle must have formed while these cells were in contact with the normal blood flow. Breaks in the endothelial lining had been due to the techniques of tissue preparation, for this layer would not have been present on the smooth muscle surfaces. Other reasons for the actual existence of exposed muscle cells have already been incorporated in the "Observations."

During pregnancy some of the smooth muscle cells elaborated unusually thick basement membranes and/or irregular masses of similar material. The thickness and pattern of these varied from cell to cell and animal to animal. This observation is in no means unique as increases in thickness of basement membranes have been reported as a result of aging and species differences (Donahue and Pappas, '61; Bloom et al., '59; Stehbens and Silver, '65) as well as in relation to the site of the vessel (Pease, '60). Pathological thickenings of basement membranes also have been described often (Zacks et al., '62; Lannigan et al., '64). However, in the present observations it should be emphasized that the endothelial basement membrane thickened only when the underlying smooth muscle showed morphological alterations. Furthermore, the most pronounced thickening of the basement membranes was seen only around extensively modified smooth muscle cells. To the best of our knowledge, this sort of excessive formation associated with smooth muscle cells has not been described before.

Aside from the modifications that take place in individual cells during pregnancy,

the basic arterial skeleton undergoes profound alterations. The internal elastic membrane was always absent in vessels in late pregnancy. Very few collagenous fibers were seen in the intima and media of these vessels by the end of pregnancy. Instead, unusually thick basement membranes and microvilli occupied the intercellular spaces.

LITERATURE CITED

- Albert, E. 1967a. The effect of pregnancy on the elastic membranes of mesometrial arteries in the guinea pig. *Am. J. Anat.*, 120: 611.
- 1967b. An electron microscopic study of uterine arteries during pregnancy. (*Abst.*) *Anat. Rec.*, 157: 204.
- Albert, E., and B. Bhussary 1967. The effects of multiple pregnancies and age on the elastic tissue of uterine arteries in the guinea pig. *Am. J. Anat.*, 121: 259.
- Bennett, S., and J. Luft 1959. S-Collidine as a basis for buffering fixatives. *J. Biophys. Biochem. Cytol.*, 6: 113.
- Bloom, P., J. Hartman and R. Vernier 1959. An electron microscopic evaluation of the width of normal glomerular basement membrane in man at various ages. *Anat. Rec.*, 133: 257.
- Bunce, D. 1965. Structural differences between distended and collapsed arteries. *Angiology*, 16: 53.
- Caesar, R., G. Edwards and H. Ruska 1957. Architecture and nerve supply of mammalian smooth muscle tissue. *J. Biophys. Biochem. Cytol.*, 3: 867.
- Chambers, R., and B. Zweifach 1947. Intercellular cement and capillary permeability. *Physiol. Rev.*, 27: 436.
- Christensen, A. 1965. The fine structure of testicular interstitial cells in guinea pigs. *J. Cell Biol.*, 26: 911.
- Donahue, S., and A. Pappas 1961. The fine structure of capillaries in cerebral cortex of the rat at various stages of development. *Am. J. Anat.*, 108: 331.
- Enders, A., and W. Lyons 1964. Observations on the fine structure of lutein cells. II. The effect of hypophysectomy and mammatrophic hormone in the rat. *J. Cell Biol.*, 22: 127.
- Fawcett, D., and M. Burgos 1960. Studies on the fine structure of the mammalian testis. II. The human interstitial tissue. *Am. J. Anat.*, 107: 245.
- Gorski, J., and N. Nelson 1965. Ribonucleic acid synthesis in the rat uterus and its early response to estrogen. *Arch. Biochem. Biophys.*, 110: 284.
- Jones, A., and D. Fawcett 1966. Hypertrophy of the agranular endoplasmic reticulum in hamster liver induced by phenobarbital. With a review on the functions of this organelle in liver. *J. Histochem. Cytochem.*, 14: 215.
- Laguens, R. 1964. Effects of estrogen upon the fine structure of uterine smooth muscle cell of the rat. *J. Ultrastr. Res.*, 10: 578.
- Laguens, R., and J. Lagrutta 1964. Fine structure of human uterine muscle in pregnancy. *Am. J. Obstet. Gynecol.*, 89: 1040.
- Lannigan, R., J. Blainey and D. Brewer 1964. Electron microscopy of the diffuse glomerular lesion in diabetes mellitus with special reference to early changes. *J. Pathol. Bacteriol.*, 88: 255.

mesometrial arteries from non-pregnant animals contained very little rough endoplasmic reticulum, ribosomes or Golgi vesicles. But during pregnancy there was an extensive development of all these organelles. Additionally, the smooth surfaced endoplasmic reticulum expanded in a truly remarkable manner, discussed below.

Although in general smooth muscle cells have not been noted for appreciable synthetic activity, certain recent reports have shown this to be the case in special situations. Thus, uterine smooth muscle has been shown to develop an extensive synthetic apparatus during pregnancy (Laguens and Lagrutta, '64) and under estrogen stimulation (Ross and Klebanoff, '67; Laguens, '64). Gorski and Nelson ('65) also showed an increase in ribosomes in uterine muscle in estrogen stimulated rats. These authors suggested that uterine smooth muscle was probably participating in the secretion of collagen as well as non-collagenous proteins. Parker and Odland ('66) have implicated smooth muscle as manufacturing collagen in atherosclerotic plaques. Pease et al. ('60) have emphasized that the presence of only smooth muscle and endothelial cells in the intima and media of pial and aortic vessels demonstrated that these cells must have been responsible for the synthesis of elastica and collagen, as well as the basement membranes found in those arteries.

One of the most unexpected observations in the smooth muscle of mesometrial arteries of full term pregnant guinea pigs was the development of an extensive agranular reticulum, and the presence of electron dense material in its vesicles. This, coupled with the presence of large numbers of microvilli on cell surfaces, gave the smooth muscle the appearance of secretory cells.

Our electron microscopic studies have not given any specific clues as to the nature of the electron opaque material found in the smooth endoplasmic vesicles. However, the occurrence of large amounts of smooth endoplasmic reticulum often has been associated with steroid secreting cells; interstitial cells of testes (Christensen, '65; Fawcett and Burgos, '60); ovarian cells (Muta, '58); adrenal cortex (Enders and Lyons, '64; Sheridan and Belt,

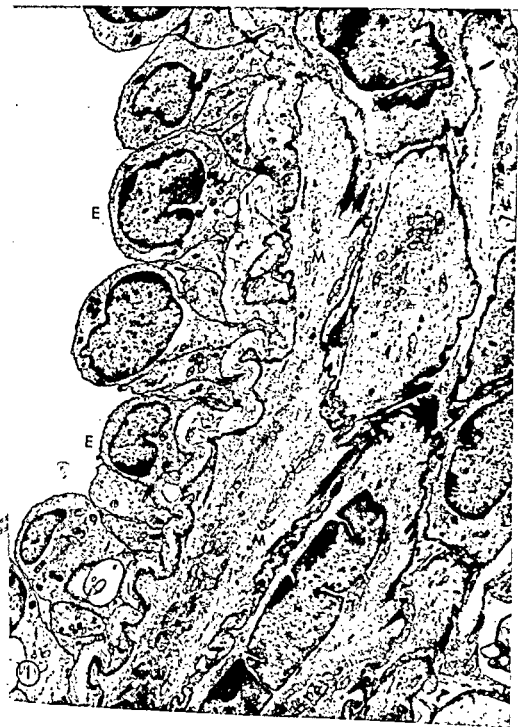
'64; Sabatini et al., '62) and others. Jones and Fawcett ('65) have reported generous doses of progesterone cause significant increase in the agranular reticulum of liver cells. Finally, the activation of specific enzymes necessary for the biosynthesis of androgens has been located biochemically in the membrane components of the agranular reticulum of testicular cells by Lynn and Brown ('64). Based upon these reports, the idea of smooth muscle under certain conditions may be linked to steroid metabolism seems reasonable.

The observations demonstrated that myofibrils were pushed towards the periphery of the cytoplasm during pregnancy. While the cell was increasing its mass apparently there was no corresponding increase in the number of the myofibrils. These morphological features indicate that it was not the contractile system that was being specialized by pregnancy, but rather other mechanisms.

Another observation of significant interest was the presence of a patchy endothelium on the mesometrial arteries of full term pregnant animals. In the absence of complete endothelial covering, the smooth muscle cells apparently served as the luminal surface. Normally one would expect partially denuded blood vessels to react as in the case of an injury to endothelium. But there was no evidence of such reaction in the present circumstances.

We observed the presence of a thick, dark staining layer on the endothelial surface of pregnant animals. This same layer was seen to cover the denuded smooth muscle cells in the absence of an endothelium. Such a layer was not present on the surfaces of smooth muscle cells where the endothelium was intact. Therefore it is possible that this "fuzzy" layer acted as a protective coat, preventing thrombus formation (or other complications) just as effectively when it covered denuded smooth muscle as when it overlay endothelium.

The original demonstration of a specialized surface coat lining vascular lumens was by Chambers and Zweifach, ('44). They thought this to be an adsorbed protein constituent of blood plasma. Observing enhanced staining of this layer with ruthenium



- Luft, J. 1965 Fine structure of capillaries: the endocapillary layer. (Abst.) *Anat. Rec.*, 151: 380.
- Lynn, W., and R. Brown 1958 The conversion of progesterone to androgens by testes. *J. Biol. Chem.*, 22: 1015.
- Moore, D., and M. Ruska 1957 The fine structure of capillaries and small arteries. *J. Biophys. Biochem. Cytol.*, 3: 457.
- Movat, M., and N. Fernando 1963 The fine structure of terminal vascular bed. I. Small arteries with an internal elastic lamina. *Exp. Molec. Pathol.*, 2: 549.
- Muta, T. 1958 The fine structure of the interstitial cell in the mouse ovary studied with electron microscope. *Kurume Med. J.*, 5: 167.
- Pease, D. C. 1960 The basement membrane: substratum of histological order and complexity. In: *Trans. 4th Internat. Conf. Elect. Micro.*, vol. II, Berlin 1958. W. Bargmann et al. ed. Springer-Verlag, Berlin, 139.
- 1964 *Histological Techniques for Electron Microscopy*. Academic Press, New York, London, 237.
- 1966 Polysaccharides associated with the exterior surface of epithelial cells: Kidney, intestine, brain. *J. Ultrast. Res.*, 15: 555.
- Pease, D., and W. Paule 1960 Electron microscopy of elastic arteries: The thoracic aorta of the rat. *J. Ultrast. Res.*, 3: 469.
- Pease, D., and S. Molinari 1960 Electron microscopy of muscular arteries: Pial vessels of the cat and monkey. *J. Ultrast. Res.*, 3: 447.
- Parker, F., and G. Odland 1966 A light micro., histochemical, and electron microscopic study of experimental atherosclerosis in rabbit carotid artery and a comparison with rabbit aorta sclerosis. *Am. J. Pathol.*, 48: 451.
- Rhodin, J. 1962 Fine structure of vascular wall in mammals with special reference to smooth muscle component. *Physiol. Rev.*, 42: 48.
- 1967 The ultrastructure of mammary arterioles and precapillary sphincters. *J. Ultrast. Res.*, 18: 181.
- Ross, R., and S. Klebanoff 1967 Fine structural changes in uterine smooth muscle and fibroblasts in response to estrogen. *J. Cell Biol.*, 32: 155.
- Sabatini, D., E. DeRobertis and H. F. Mar 1962 Submicroscopic study of the effect of estradiol on the adrenocortex of the rat. *Endocrinology*, 70: 390.
- Sheridan, M., and W. Belt 1964 Fine structure of guinea pig adrenal cortex. *Anat. Rec.*, 149: 71.
- Stehbens, W., and M. Silver 1965 Unusual development of basement membrane about small blood vessels. *J. Cell Biol.*, 26: 669.
- Venable, J., and R. Coggeshall 1965 A simple lead citrate stain for use in electron microscopy. *J. Cell Biol.*, 25: 407.
- Zacks, S., J. Pegues and F. Elliot 1962 Intercapillary muscle capillaries in patients with diabetes mellitus. A light and electron microscope study. *Metabolism*, 11: 381.

PLATE I

EXPLANATION OF FIGURE

- 1 Cross section of the mesometrial artery from a non-pregnant guinea pig. Endothelial cells (E), internal elastic membrane (I), and smooth muscle cells (M). $\times 5,500$.

TRON MICROSCOPY OF UTERINE ARTERIES
N. Albert and Daniel C. Pease

PLATE 2

EXPLANATION OF FIGURES

- 2 Higher power micrograph of an endothelial cell from the mesometrial artery of a non-pregnant animal. Notice the amount and distribution of the organelles. There are hints of a dark staining surface layer (S). Pinocytotic vesicles are present on all surfaces of the cell in the center. Fenestrated internal elastic membrane (I). $\times 19,300$.
- 3 Another higher power micrograph of a similar cell as in figure 2. Notice the presence of fibrillar structures in the cytoplasm. $\times 41,300$.

TRON MICROSCOPY OF UTERINE ARTERIES
N. Albert and Daniel C. Pease

PLATE 3

EXPLANATION OF FIGURES

- 4 Smooth muscle cell from mesometrial artery of a non-pregnant animal. The cytoplasm is filled with myofibrils. Dense bodies (D) are seen associated with the myofibrils. Some of them are attached to the dark plaques below the plasmalemma (arrows). $\times 42,000$.
- 5 Shows the basement membrane associated with smooth muscle of non-pregnant animals. Notice the continuity between the dense body and the dark plaques below the plasma membrane (arrow). $\times 43,100$.
- 6 Also shows the thin continuous basement membrane (arrow), myofibrils and dense bodies. $\times 43,100$.



PLATE 3

EXPLANATION OF FIGURES

- 4 Smooth muscle cell from mesometrial artery of a non-pregnant animal. The cytoplasm is filled with myofibrils. Dense bodies (D) are seen associated with the myofibrils. Some of them are attached to the dark plaques below the plasmalemma (arrows). $\times 42,000$.
- 5 Shows the basement membrane associated with smooth muscle of non-pregnant animals. Notice the continuity between the dense body and the dark plaques below the plasma membrane (arrow). $\times 43,100$.
- 6 Also shows the thin continuous basement membrane (arrow), myofibrils and dense bodies. $\times 43,100$.

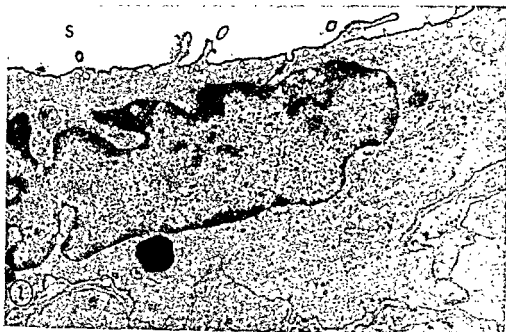


PLATE 4

EXPLANATION OF FIGURES

- 7 Endothelial cell from a three week pregnant guinea pig. Notice the presence of a "fuzzy" dark staining surface layer (S). This can also be seen covering the pits and vesicles associated with the plasma membrane (arrow). Free ribosomes are present either individually or in groups as polysomes. $\times 21,000$.
- 8 Endothelial cell from a five week pregnant animal. Notice the increase in the cytoplasmic organelles over those seen in figure 2, large and small lysosome-like bodies and patches of thick basement membrane (arrow). $\times 13,500$.

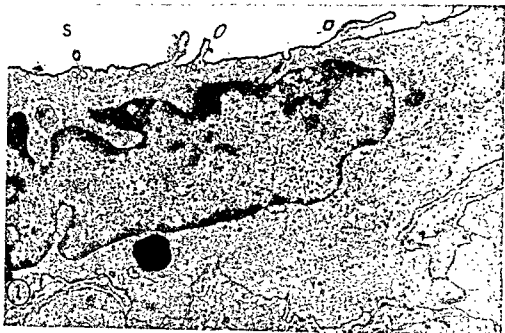


PLATE 5

EXPLANATION OF FIGURE

- 9 Smooth muscle cell from a five week pregnant guinea pig. Bulk of the cytoplasm is filled with large quantities of organelles, while the myofibrils (M) are pushed toward the periphery. Notice the presence of vesicular structures around the Golgi zone (arrows). These are shown at higher magnification in figure 18. During pregnancy thicker basement membranes also are associated with muscle cells. $\times 32,700$.

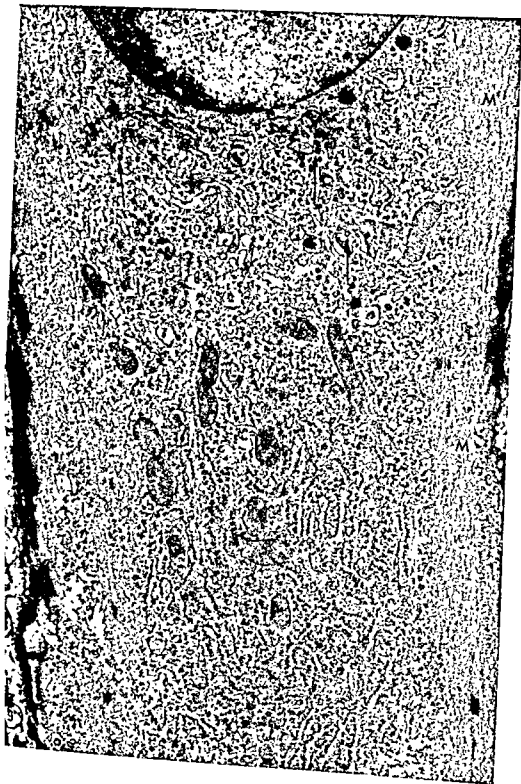


PLATE 5

EXPLANATION OF FIGURE

- 9 Smooth muscle cell from a five week pregnant guinea pig. Bulk of the cytoplasm is filled with large quantities of organelles, while the myofibrils (M) are pushed toward the periphery. Notice the presence of vesicular structures around the Golgi zone (arrows). These are shown at higher magnification in figure 18. During pregnancy thicker basement membranes also are associated with muscle cells. $\times 32,700$.

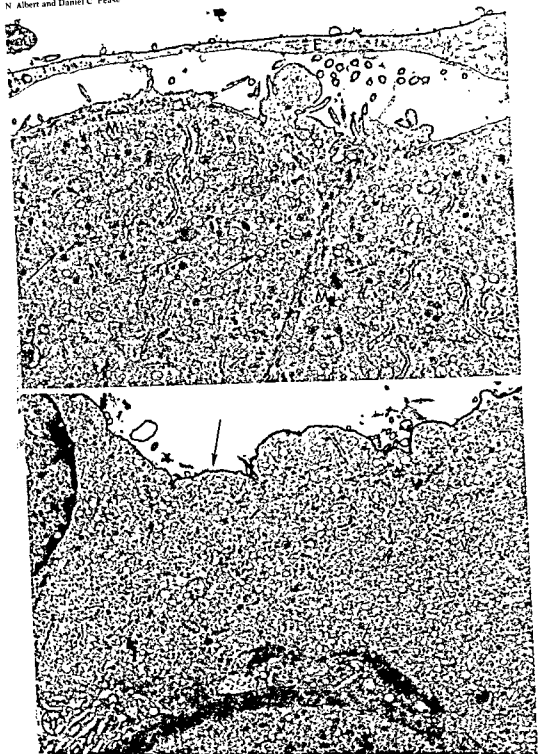
ELECTRON MICROSCOPY OF UTERINE ARTERIES
N. Albert and Daniel C. Pease

PLATE 6

EXPLANATION OF FIGURES

- 10 Taken from an eight week pregnant guinea pig. The endothelial cell (E) is lining the vascular lumen by a thin attenuated process. The surface layer is coated by the "fuzzy" dark staining layer, but the underlying muscle cell surfaces do not have this layer. Smooth muscle cell processes and microvilli are seen invading the subendothelial zone. The endothelial basement membrane and the internal elastic membrane are absent. The cytoplasm of muscle cells is packed with rough and smooth endoplasmic reticulum. Some of the agranular vesicles contain electron dense material while others are empty (arrows). A thin band of myofibrils (M) is seen around the periphery and also projecting into the cytoplasm. $\times 19,300$.
- 11 Same stage of pregnancy as figure 10. The endothelium is absent. Smooth muscle surface is coated with the "fuzzy" layer (arrow). $\times 18,000$.



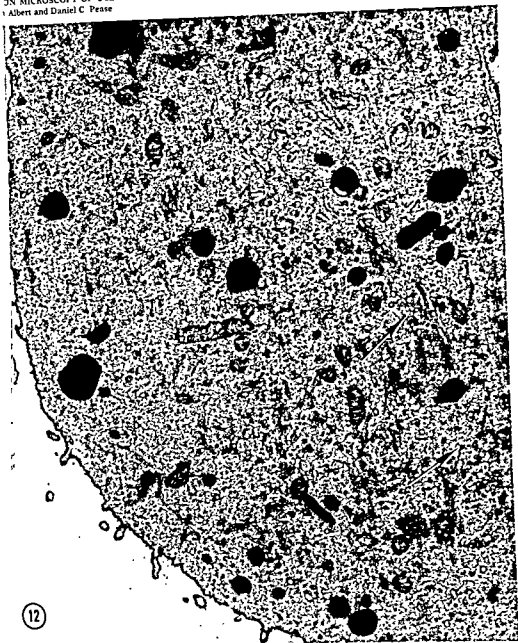
PLATE 7

EXPLANATION OF FIGURES

- 12 Endothelial cell from a nine week pregnant animal. Surface of the cell is coated with the dark "fuzzy" layer. The cytoplasm is filled with organelles. The Golgi is quite prominent. Notice the presence of vesicular structures closely associated with the Golgi zones (arrow). Some of them have a homogeneously dense matrix. Many of these vesicles are budding off from the membranous stacks of Golgi. This is more clearly shown in figures 13 and 14. Smaller homogeneous dense bodies appear to be increasing in size and are thought to be forming the lysosome-like bodies (L). $\times 12,250$.
- 13 Higher magnification of the Golgi in figure 12. Some vesicular structures in close association with the Golgi (arrow). $\times 25,200$.
- 14 Another Golgi zone at higher magnification. Notice the vesicle that appears to be pinching off from the main membranous cistern (arrow). On the opposite side some dense material is seen inside the Golgi vesicle. $\times 48,700$.

ON MICROSCOPY OF UTERINE ARTERIES

Albert and Daniel C. Pease



12



PLATE 8

EXPLANATION OF FIGURES

- 15 Modified smooth muscle cell from a nine week pregnant animal. Notice that the cytoplasm contains rough and smooth endoplasmic reticulum. Some of the agranular reticulum vesicles are filled with an electron dense material (arrow). The myofibrils are in the periphery. Dense bodies (D) associated with the myofibrils can be easily identified. $\times 43,100$.
- 16 Same stage as in figure 15. The cell in the center can hardly be recognized as a smooth muscle cell. Almost all of the agranular reticulum vesicles are empty. The cell in the lower right corner has hardly altered during pregnancy. $\times 43,100$.



PLATE 8

EXPLANATION OF FIGURES

- 15 Modified smooth muscle cell from a nine week pregnant animal. Notice that the cytoplasm contains rough and smooth endoplasmic reticulum. Some of the agranular reticulum vesicles are filled with an electron dense material (arrow). The myofibrils are in the periphery. Dense bodies (D) associated with the myofibrils can be easily identified. $\times 43,100$.
- 16 Same stage as in figure 15. The cell in the center can hardly be recognized as a smooth muscle cell. Almost all of the agranular reticulum vesicles are empty. The cell in the lower right corner has hardly altered during pregnancy. $\times 43,100$.

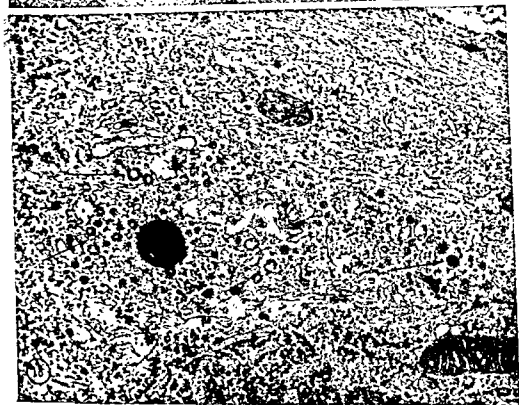
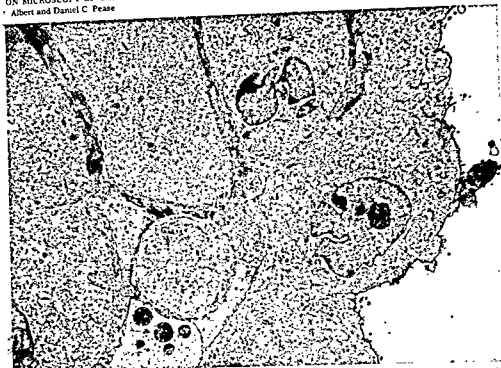


PLATE 9

EXPLANATION OF FIGURES

- 17 Part of the media of a mesometrial artery taken from a nine week pregnant animal. The endothelium is absent. The entire media is formed of modified smooth muscle cells. $\times 4,500$.
- 18 Part of smooth muscle cell from five week pregnant animal. Notice the rounded structures with homogeneous matrices. Some of them have translucent centers (arrows). These are thought to be identical to those described in figures 9 and 12-14. $\times 45,000$.

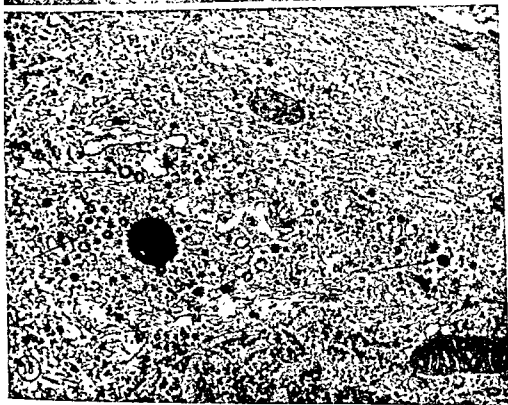


PLATE 10

EXPLANATION OF FIGURES

- 19 Represents one of the several patterns of basement membranes observed in late (6-9 weeks) pregnancy. Note the patches of thick basement membrane (arrows) alternating with well developed microvilli. Dense bodies (D). $\times 53,200$.
- 20 This also represents one of the late stages of pregnancy. Notice the different pattern of the basement membrane. $\times 22,800$.

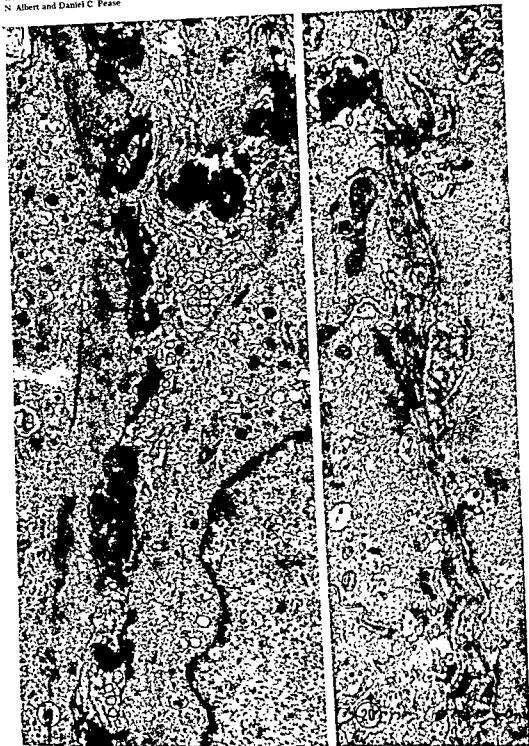
RON MICROSCOPY OF UTERINE ARTERIES
N. Albert and Daniel C. Pease

PLATE 10

EXPLANATION OF FIGURES

- 19 Represents one of the several patterns of basement membranes observed in late (6-9 weeks) pregnancy. Note the patches of thick basement membrane (arrows) alternating with well developed microvilli. Dense bodies (D). $\times 53,200$.
- 20 This also represents one of the late stages of pregnancy. Notice the different pattern of the basement membrane. $\times 22,800$.

PLATE 10

EXPLANATION OF FIGURES

- 19 Represents one of the several patterns of basement membranes observed in late (6-9 weeks) pregnancy. Note the patches of thick basement membrane (arrows) alternating with well developed microvilli. Dense bodies (D). $\times 53,200$.
- 20 This also represents one of the late stages of pregnancy. Notice the different pattern of the basement membrane. $\times 22,800$.

TRON MICROSCOPY OF UTERINE ARTERIES

t N. Albert and Daniel C. Pease



PLATE 11

EXPLANATION OF FIGURES

- 21-22 Show a continuous and homogeneous basement membrane. Although the magnifications are not the same, the basement membrane in figure 21 is proportionally thicker than that in figure 22. Also note the presence of microtubules (arrows) in figure 21. Figure 21, $\times 49,000$; figure 22, $\times 21,500$.
- 23 Denuded smooth muscle surface as seen after staining with phosphotungstic acid. Only the surface layer is stained. None of the other membranous components show any affinity for this stain. $\times 71,500$.

IRON MICROSCOPY OF UTERINE ARTERIES
N. Albert and Daniel C. Pease

PLATE 11

EXPLANATION OF FIGURES

- 21-22 Show a continuous and homogeneous basement membrane. Although the magnifications are not the same, the basement membrane in figure 21 is proportionally thicker than that in figure 22. Also note the presence of microtubules (arrows) in figure 21. Figure 21, $\times 49,000$; figure 22, $\times 21,500$.
- 23 Denuded smooth muscle surface as seen after staining with phosphotungstic acid. Only the surface layer is stained. None of the other membranous components show any affinity for this stain. $\times 71,500$.

Renal Morphology of the English Sole (*Parophrys vetulus*)

RUTH ELLEN BULGER AND BENJAMIN F. TRUMP

Department of Pathology, University of Washington Medical School, Seattle,
Washington and Department of Pathology, Duke University Medical Center,
Durham, North Carolina

ABSTRACT The nephron of the English sole, *Parophrys vetulus*, is composed of the following regions: a renal corpuscle with few capillary loops and an extensive mesangial area with mesangial cell processes insinuated between endothelium and podocyte basement membrane; a ciliated neck segment with mucous-containing cells; the first major brush border segment with a broad vacuolated apical zone most closely resembling the mammalian proximal convoluted tubule, a second major brush border segment with the tallest most eosinophilic cells; a gradual transition to a third major brush border segment with lower, more basophilic cells; no distal convolution and a collecting tubule which empties into a collecting duct system. Granulated cells in the arteriolar media appeared to be modified smooth muscle cells.

Unique features of fish kidneys have provided the basis for theories concerning renal physiology and make these organs valuable in correlative studies of structure and function (see reviews of Marshall, '34; Smith, '51; Forster, '61).

Isolated flounder kidney tubules are ideal for physiologic studies of transport processes *in vitro* because of the ease with which they may be isolated and maintained for several hours in oxygenated balanced salt solutions (Forster, '48; Forster and Taggart, '50; Taggart and Forster, '51; Forster and Hong, '58; Hong and Forster, '59). Active transport may be assessed by the rate and degree of intraluminal dye accumulation.

We have used flounder tubules in a multicentered investigation of cell injury (Trump and Bulger, '65, '67). To establish normal controls, a detailed study was made of the structure of the kidney of a local species of flounder, the English sole, *Parophrys vetulus*, and forms the basis of this report.

MATERIALS AND METHODS

Approximately 50 representatives of a local species of flounder, the English sole, *Parophrys vetulus*, were used for this study. The majority of fish were obtained from Puget Sound and were fixed immediately or maintained in recirculating salt water aquaria for short periods before use; a few fish were caught by hook and line and fixed immediately.

The fish were stunned by a blow on the head and the body cavity was quickly opened. Kidneys were fixed by perfusion via the renal portal system or by immersion of pieces in fixative solutions. In addition, small pieces were rapidly frozen in isopentane and subsequently freeze-dried and fixed in formaldehyde vapor. The fixative solutions used included the following: 1. 4% phosphate-buffered formaldehyde (Gridley, '60); 2. 6.25% glutaraldehyde buffered in 0.1 M cacodylate with and without post-fixation with 2% osmium tetroxide buffered with *s*-collidine (Sabatini et al., '63); 3. Helly's solution (Gridley, '60); 4. 2% osmium tetroxide buffered with *s*-collidine (Bennett and Luft, '59); 5. Millonig's solution (Millonig, '62); 6. 10% acrolein buffered in phosphate (Luft, '59); 7. 0.6% or 3% potassium permanganate in water or buffered in cacodylate or veronal acetate (Luft, '56); or 8. a combined fixative containing 6.25% glutaraldehyde and 2% osmium tetroxide buffered in *s*-collidine (Trump and Bulger, '66). Tissues fixed in the first three solutions were dehydrated in ethanol and embedded in a mixture of paraffin and Piccolyte while tissues fixed with methods 2, 4-8 were dehydrated in ethanol and embedded in Epon epoxy resin (Luft, '61).

Paraffin sections were occasionally examined unstained or were stained with hematoxylin and eosin (H&E), the periodic-acid-Schiff technique (PAS), or Gomori's trichrome (Gridley, '60). Serial sections were made and nephrons were



hat the "membrane" was located on the pedicel. The basement membrane was reflected along the podocytic and did not completely encircle the lary. Coated caveoli were frequently on the plasmalemma adjacent to the ment membrane and desmosomes seen between adjacent processes. A of narrow, short filaments (or fuzz) ated into Bowman's space from the r surface of the plasmalemma of the cyte. The mitochondria were elond or irregular in shape with a pale six and a few short cristae. A moderate ber of cisternae of rough-surfaced oplasmic reticulum were present, espe y in the cell body region. Abundant oth-surfaced vesicles and free RNP cles were identified. The Golgi appa frequently was extensive, consisting of iple cisternae and vesicles on both aces. Multivesicular bodies were racterized by a few internal vesicles e a condensation of material in one on on the cytoplasmic side of the limit membrane. Cytosomes (as defined by sson and Trump, '64) with a pale or lerate matrical density contained a ety of materials including amorphous sties, filaments, membranes or occa al dense rhomboidal crystals. Bundles filaments traversed the cell bodies and e especially concentrated in the larger processes. The nuclei showed fre nt indentations and had homogeneous yomatin after fixation with osmium eide.

2. Bowman's space. Bowman's space obtained a flocculent material. There s, however, a much higher concentra of flocculent material in the capillary mens.

3. Endothelium. Although the endo elium lining the afferent arteriole was ck and filled with vesicles, the endothe n of the capillary loops was of the thin ety containing both vesicles and pores. e capillaries were surrounded by a flocc ent material which was indistinguisha from the mesangial matrix. In some ons this material formed a thin layer der the endothelium but in general no ntinuous layer of condensed material s found. In some regions endothelial ocesses extended from the basal surface e the endothelial cells, penetrating the

mesangial matrix to lie adjacent to the basement membrane of the podocyte. In a few regions, the endothelium lay adjacent to the podocytic basement membrane without an intervening layer of mesangium. The endothelium often was closely associated with mesangial processes and desmosomes were seen between the two cell types. The endothelial pores appeared open and were not bridged by a distinct diaphragm.

E. Mesangial region. The mesangial region was extensive being composed of many mesangial cells and an abundant mesangial matrix. The mesangial cells were found not only in the axial region of the capillary loops, as seen in normal mammalian glomeruli, but frequently had long processes insinuated between the podocytic basement membrane and the capillary endothelium, thus encircling the capillary loops. Rounded mesangial processes also extended into depressions in the endothelial cytoplasm and occasionally into the capillary lumens. The mesangial cells were characterized by extremely irregular nuclei and a cytoplasm filled with fine filaments. The extensive mesangial matrix which surrounded the cells consisted mainly of a fine flocculent material of low density permeated by fine filaments. The filaments often ran singly but large aggregates were seen. Areas showing a moderate density also could be identified. The mesangial matrix blended into the basement membrane.

II. Neck (figs. 1, 6)

Near the urinary pole of the renal corpuscle, the cells of the parietal layer became more cuboidal and finally columnar and formed a funnel-like structure marking the beginning of the neck segment. The neck segment varied in length but was usually short. The cells of the neck segment were narrow and columnar with basal nuclei which were elongate or irregular in shape. The cytoplasm was scanty and basophilic containing apical PAS-positive granules and cilia. The diameter of this segment was small with respect to the rest of the nephron. Electron micrographs demonstrated cells of irregular shape showing some lateral interlocking. In addition to the junctional complexes, tight junction regions were seen between adja-

followed to determine the sequence of the morphologic regions. Epon sections were stained with toluidine blue (Trump et al., '61).

Acid phosphatase was demonstrated on frozen sections of formaldehyde-fixed tissue using the technique of Barka and Anderson ('63).

OBSERVATIONS

The kidney of the English sole, *Parophrys vetulus*, lay in a retroperitoneal position on the dorsal and caudal surfaces of the body cavity. Along the dorsal aspect of the body cavity, the kidney was bounded by the backbone and the ribs, and along the caudal aspect, it abutted upon the fused transverse processes of the first caudal vertebra. The kidney formed a single midline structure except in the most anterior region (the head kidney) where the kidney tissue split at approximately the level of the heart and two small projections continued anteriorly.

The kidney was composed of nephrons embedded in hematopoietic tissue. The nephrons consisted of a renal corpuscle, a neck, three major segments with brush borders and a collecting tubule which connected with the system of collecting ducts. This division of the nephron was based on the study of numerous light and electron microscopic preparations as well as reconstructions from serial sections by light microscopy. Some minor variations in the last regions of the nephron, such as dual collecting ducts, could occasionally be found. Scattered throughout the hematopoietic tissue were islands of cells which contained abundant pigment deposits. Few nephrons were found in the head kidney. Located in the hematopoietic tissue of this region, interrenal and suprarenal tissues were identified. Along the dorsal surface of the kidney, the spherular corpuscles of Stannius could be found. Vessels were seen throughout the kidney substance. Nerves and associated ganglion cells coursed along the larger arteries. Also, in long stretches of the media of arterioles, rounded cells filled with PAS-positive granules were seen. These granules contained high acid phosphatase activity.

1. Renal corpuscle (figs. 1, 5)

The renal corpuscle consisted of the following structures: a parietal layer of Bow-

man's capsule generally composed of squamous cells; a visceral layer consisting of irregular shaped branching cells; Bowman's space between these two capillary layers; a system of capillary loops; and an abundant mesangial area.

A. Parietal layer. The parietal layer was lined by squamous cells containing flattened nuclei slightly irregular in shape. Occasional cilia were seen emerging from depressions in the cytoplasm. The mitochondria were large and elongated, contained a pale matrix and few cristae which often appeared as circular profiles and therefore at least some appeared to be tubular. The endoplasmic reticulum consisted of a moderate number of rough surfaced cisternae and occasional circular profiles, and small irregular cisternae smooth-surfaced elements. A moderate number of free ribonucleoprotein (RNP) particles were present in the cytoplasm. The Golgi apparatus, seen adjacent to the nucleus, was inconspicuous being composed of only a few short cisternae and vesicles. Single membrane-bound bodies consisted of multivesicular bodies and a second type characterized by a more dense matrix of intermediate density. The cytoplasmic matrix was filled with a large number of filaments. Filaments of several dimensions were seen forming a thick layer around the entire cell adjacent to the plasmalemma while a network of larger filaments permeated the remaining cytoplasm. The parietal cells rested on a relatively thin basement membrane. Near the urinary pole the cells increased in height and frequently cells of differing morphology were seen lying between the parietal and visceral layers. These cells were interpreted as wandering cells.

B. Visceral layer. The visceral layer was lined by cells (podocytes) of an extremely complex shape similar to that demonstrated by Zimmermann ('55) in mammalian visceral epithelial cells. The cell consisted of a rounded cell body with several large processes extending peripherally. The large processes gave off smaller processes (pedicels) which interdigitated with other small processes forming a layer adjacent to the basement membrane. The pedicels were connected by a filtration "membrane" similar to that seen in mammalian renal corpuscles but differ-

that the "membrane" was located on the pedicel. The basement membrane was reflected along the podocytic and did not completely encircle the artery. Coated caveoli were frequently seen in the plasmalemma adjacent to the basement membrane and desmosomes were seen between adjacent processes. A network of narrow, short filaments (or fuzz) extended into Bowman's space from the apical surface of the plasmalemma of the podocyte. The mitochondria were elongated or irregular in shape with a pale matrix and a few short cristae. A moderate number of cisternae of rough-surfaced endoplasmic reticulum were present, especially in the cell body region. Abundant smooth-surfaced vesicles and free RNP granules were identified. The Golgi apparatus frequently was extensive, consisting of multiple cisternae and vesicles on both surfaces. Multivesicular bodies were characterized by a few internal vesicles and a condensation of material in one region on the cytoplasmic side of the limiting membrane. Cytosomes (as defined by Esson and Trump, '64) with a pale or moderate matrical density contained a variety of materials including amorphous densities, filaments, membranes or occasionally dense rhomboidal crystals. Bundles of filaments traversed the cell bodies and were especially concentrated in the larger processes. The nuclei showed frequent indentations and had homogeneous chromatin after fixation with osmium tetroxide.

Bowman's space. Bowman's space contained a flocculent material. There was, however, a much higher concentration of flocculent material in the capillary lumens.

Endothelium. Although the endothelium lining the afferent arteriole was thick and filled with vesicles, the endothelium of the capillary loops was of the thin variety containing both vesicles and pores. The capillaries were surrounded by a flocculent material which was indistinguishable from the mesangial matrix. In some regions this material formed a thin layer under the endothelium but in general no continuous layer of condensed material was found. In some regions endothelial processes extended from the basal surface of the endothelial cells, penetrating the

mesangial matrix to lie adjacent to the basement membrane of the podocyte. In a few regions, the endothelium lay adjacent to the podocytic basement membrane without an intervening layer of mesangium. The endothelium often was closely associated with mesangial processes and desmosomes were seen between the two cell types. The endothelial pores appeared open and were not bridged by a distinct diaphragm.

E. Mesangial region. The mesangial region was extensive being composed of many mesangial cells and an abundant mesangial matrix. The mesangial cells were found not only in the axial region of the capillary loops, as seen in normal mammalian glomeruli, but frequently had long processes insinuated between the podocytic basement membrane and the capillary endothelium, thus encircling the capillary loops. Rounded mesangial processes also extended into depressions in the endothelial cytoplasm and occasionally into the capillary lumens. The mesangial cells were characterized by extremely irregular nuclei and a cytoplasm filled with fine filaments. The extensive mesangial matrix which surrounded the cells consisted mainly of a fine flocculent material of low density permeated by fine filaments. The filaments often ran singly but large aggregates were seen. Areas showing a moderate density also could be identified. The mesangial matrix blended into the basement membrane.

II. Neck (figs. 1, 6)

Near the urinary pole of the renal corpuscle, the cells of the parietal layer became more cuboidal and finally columnar and formed a funnel-like structure marking the beginning of the neck segment. The neck segment varied in length but was usually short. The cells of the neck segment were narrow and columnar with basal nuclei which were elongate or irregular in shape. The cytoplasm was scanty and basophilic containing apical PAS-positive granules and cilia. The diameter of this segment was small with respect to the rest of the nephron. Electron micrographs demonstrated cells of irregular shape showing some lateral interlocking. In addition to the junctional complexes, tight junction regions were seen between adja-

cent lateral plasmalemmas in a more basal position.

Cilia emerged in groups of approximately twelve from some apical cell profiles. The cilia were of the usual structure. The basal bodies were connected with an extensive system of striated rootlets. A few apical microvilli extended into the lumen. The majority of the cells contained apical mucous granules (which contained a flocculent material of low concentration). The membranes of the granules often were incomplete. The mitochondria were few in number, irregular in shape and large in size. The rough-surfaced endoplasmic reticulum was well-developed consisting mainly of branching cisternae; free ribosomes were abundant. In fortuitous sections, the Golgi apparatus was extensive consisting not only of vesicles and cisternae, but also of pale vacuoles. The nuclei were irregular having deep cytoplasmic indentations. Wandering cells were occasionally seen in the neck region. The basement membrane varied in thickness but frequently was irregular in contour. Smooth muscle cells sometimes surrounded the tubule, but a complete muscular coat was lacking.

III. First major segment with a brush border (figs. 1, 2, 7)

A. Light microscopy. The first major segment was composed of tall columnar cells with occasional long cilia projecting into the lumen. The cells possessed a tall PAS-positive brush border. There was a large apical zone which contained vacuoles but lacked mitochondria. A diffuse PAS-positivity was seen in this zone as well. The nucleus lay in the mid to basal region of the cell and appeared circular although irregularities in shape were frequent. The nuclei sometimes appeared rounder, lighter and slightly larger than those of the second major segment. The cytoplasm below the apical zone was eosinophilic although a slight basophilic cast could be seen. After applying Gomori's trichrome procedure with chromotrope 2R staining, this zone was seen to be filled with large elongate or circular mitochondria; PAS-positive granules were seen in the cytoplasm as well. Small acid phosphatase-positive granules were found throughout the cytoplasm. Occasional cells with intensely stained nuclei were seen between the tubular cells which were interpreted as wandering cells of blood origin. Similar cells were seen throughout the rest of the nephron. The PAS-positive basement membrane was thick, and a smooth muscle layer lay external to it.

B. Electron microscopy. The cells comprising the first major segment were tall and columnar. The apical surface was covered by long, tightly packed microvilli. After osmium tetroxide fixation, the plasmalemmas covering adjacent microvilli often appeared as a row of vesicles; this appearance was not noted after fixation with glutaraldehyde or permanganate and was interpreted as artifactual membrane rearrangement. Bundles of filaments from the interior of the microvilli swept down into the cell. Similar filaments from the apical cytoplasm were concentrated at the lateral plasmalemma in the region of the intermediate junction. Tight junctions were seen along the lateral plasmalemma in a more basal position. In addition to the junctional complexes, a single basal body, associated centriole and striated rootlet fibers were seen in the apical cytoplasm.

A broad zone of apical cytoplasm underlying the microvillus border contained circular, tubular and vacuolar profiles identical with those seen in the mammalian proximal tubule.

An extensive system of smooth-surfaced membranes occupied the basal cytoplasm, most of which represented plasma membranes when the tissue was well fixed. After potassium permanganate fixation procedures, two types of membranes were observed in the basal cytoplasm (fig. 12). A few were similar in thickness and configuration to the membranes of the endoplasmic reticulum while the majority were similar to and confluent with the basal plasmalemmas. After fixation with osmium tetroxide, only a few of the membranes connected with the basal plasmalemma. Instead they formed large cisternae oriented perpendicular to the basement membrane or occasionally formed circular whorls. Near the basal plasmalemma, cisternae appeared to convert into tubules.

10). After primary fixation with glutaraldehyde-containing fixatives, the membranes were more frequently seen in continuity with the basal plasmalemma (fig. 11). The mitochondria were large and elongated, containing an abundant number of cristae, a moderately dense matrix substance and some matrical granules. Mitochondria were in apposition to the smooth-faced membranes of the basal cytoplasm. The rough-surfaced component of the endoplasmic reticulum was fairly abundant throughout the cytoplasm and frequently oriented along the lateral cell membranes. The smooth-surfaced component consisted of vesicles or irregularly shaped cisternae. The Golgi apparatus was adjacent to the nucleus.

The class of single membrane-bounded bodies were small in size, of round, elongated or irregular structures with a matrix density similar to that of the mitochondria. Their close spatial relationship to the membranes of both smooth- and rough-surfaced endoplasmic reticulum, their connections with the smooth-surfaced membranes and their presence in this cell type, make it likely that these represent microbodies.

Cytosomes were especially abundant and demonstrated marked variation in fine structure. The type most frequently seen contained a pale to moderately dense flocculent material. A second population of cytosomes seen in this region contained coarse and fine filamentous material. This latter type of cytosome is found only in this segment. In the flounder, *Paralichthys hostigma*, acid phosphatase activity has been demonstrated in bodies of similar morphology (Trump, Green, and Hickman, unpublished observations).

The basement membrane showed considerable variation in thickness and homogeneity. It was generally several times thicker than that seen covering rat kidney tubules. Although it commonly appeared as a single thick layer, a few tubules had a basement membrane coating showing a definite reticulated network. A thin layer of collagen fibrils surrounded the basement membrane, and beyond this a layer of smooth muscle cells formed a peripheral investment. These cells were filled with

fine filaments and dense plaque-like structures.

IV. Second and third major segments with a brush border (figs. 2, 3, 8, 9)

A. Light microscopy. The second major segment was composed of columnar cells that were frequently even taller than those comprising the first major segment. The cytoplasm was intensely acidophilic. A prominent brush border demonstrating a slight PAS-positivity covered the luminal surface and occasional cilia projected into the lumen. Although the small apical region contained no mitochondria or vacuoles, the remaining cytoplasm was filled with large elongate mitochondria (fig. 8). The mitochondria were longer and more numerous than those seen in the first major segment which accounted for the extreme acidophilia and chromotrope 2R staining. The mitochondria were generally oriented perpendicular to the basement membrane of the tubule and frequently extended the entire height of the cell. A few cells in the early part of this segment contained extremely large mitochondria, especially near the base. Oval nuclei usually occupied a midposition in the cells although sometimes they lay slightly basally. PAS-positive droplets were seen in the cytoplasm as well and were especially concentrated in the apical region. Acid phosphatase-positive granules were concentrated in the apex. A thick PAS-positive basement membrane, which showed some variation in thickness, and which was embraced by a layer of smooth muscle cells, surrounded the tubule. At the transition zone between the first and second major segments some intermingling of cell types could be seen.

The second and third major segments had many morphological features in common. In fact there appeared to be a gradual transition between them. Typical cells of the third major segment, however, were lower being cuboidal to low columnar and the brush border was much less conspicuous. This segment had a diameter which was smaller than that of the first or second major segments. An extremely small apical zone was present which lacked mitochondria and vacuoles; however, mitochondria filled the remaining cytoplasm.

cent lateral plasmalemmas in a more basal position.

Cilia emerged in groups of approximately twelve from some apical cell profiles. The cilia were of the usual structure. The basal bodies were connected with an extensive system of striated rootlets. A few apical microvilli extended into the lumen. The majority of the cells contained apical mucous granules (which contained a flocculent material of low concentration). The membranes of the granules often were incomplete. The mitochondria were few in number, irregular in shape and large in size. The rough-surfaced endoplasmic reticulum was well-developed consisting mainly of branching cisternae; free ribosomes were abundant. In fortuitous sections, the Golgi apparatus was extensive consisting not only of vesicles and cisternae, but also of pale vacuoles. The nuclei were irregular having deep cytoplasmic indentations. Wandering cells were occasionally seen in the neck region. The basement membrane varied in thickness but frequently was irregular in contour. Smooth muscle cells sometimes surrounded the tubule, but a complete muscular coat was lacking.

III. First major segment with a brush border (figs. 1, 2, 7)

A. Light microscopy. The first major segment was composed of tall columnar cells with occasional long cilia projecting into the lumen. The cells possessed a tall PAS-positive brush border. There was a large apical zone which contained vacuoles but lacked mitochondria. A diffuse PAS-positivity was seen in this zone as well. The nucleus lay in the mid to basal region of the cell and appeared circular although irregularities in shape were frequent. The nuclei sometimes appeared rounder, lighter and slightly larger than those of the second major segment. The cytoplasm below the apical zone was eosinophilic although a slight basophilic cast could be seen. After applying Gomori's trichrome procedure with chromotrope 2R staining, this zone was seen to be filled with large elongate or circular mitochondria; PAS-positive granules were seen in the cytoplasm as well. Small acid phosphatase-positive granules were found throughout the cytoplasm. Occasional cells intensely stained nuclei were between the tubular cells which interpreted as wandering cells of blood. Similar cells were seen throughout the rest of the nephron. The PAS-positive basement membrane was thick, and a smooth muscle layer lay external to it.

B. Electron microscopy. The cells comprising the first major segment were tall and columnar. The apical surface was covered by long, tightly packed microvilli. After osmium tetroxide fixation, plasmalemmas covering adjacent microvilli often appeared as a row of vesicles; this appearance was not noted after fixation with glutaraldehyde or permanganate and was interpreted as artifactual membrane rearrangement. Bundles of filaments from the interior of the microvilli swept down into the cell. Similar filaments from the apical cytoplasm concentrated at the lateral plasmalemma in the region of the intermediate junction. Tight junctions were seen along the lateral plasmalemma in a more basal position in addition to the junctional complexes of the single basal body, associated centrioles. Striated rootlet fibers were seen in the basal cytoplasm.

A broad zone of apical cytoplasm underlying the microvillus border contained circular, tubular and vacuolar profiles identical with those seen in the mammalian proximal tubule.

An extensive system of smooth-surfaced membranes occupied the basal cytoplasm, most of which represented plasma membranes when the tissue was well fixed. After potassium permanganate fixation procedures, two types of membranes were observed in the basal cytoplasm (fig. 12). A few were similar in thickness and orientation to the membranes of the endoplasmic reticulum while the majority were similar to and confluent with the lateral plasmalemmas. After fixation with osmium tetroxide, only a few of the membranes connected with the basal plasmalemma. Instead they formed large cisternae oriented perpendicular to the basement membrane or occasionally formed circular whorls. Near the basal plasmalemma, cisternae appeared to convert into tubules.

collecting tubule. The cytoplasm was phillie and the mitochondria were geny inconspicuous. The cell apices jently contained PAS-positive gran- and occasional acid phosphatase- droplets. The oval nuclei were gate along the axis of the tubule. A -positive basement membrane and a oth muscle coat surrounded the tubule.

Electron microscopy. The lumen of collecting tubule was widely dilated contained profiles of cilia. Occasional rovilli were seen on the apical surface. majority of the mucous granules seen he apex of the cell lay apical to a layer ilaments associated with the desmo- es which formed a thick layer across cell apex although occasional mucous plets were seen basal to it. A single al body was occasionally found in the cal cytoplasm.

lumerous small elongate mitochondrial files containing abundant cristae were n throughout the remaining cytoplasm. listernae of rough-surfaced endoplas- c reticulum were extremely abundant oughout the cytoplasm and many of the ternae had dilated lumens. The smooth- faced endoplasmic reticulum was tensive as well. The Golgi apparatus was tremely large. Elements of the rough- faced endoplasmic reticulum were quently seen adjacent to the external ce of the Golgi apparatus. Several Golgi sternae were seen lying in a closely paral- l fashion and the internal face of the olgi consisted of numerous vesicles and me enlarged vacuoles containing a flocc- ilent material of low density.

VI. Collecting duct system (fig. 14)

A Light microscopy. The collecting ubule emptied into a collecting duct ystem in which the ducts converged to rm larger channels finally emptying into mesonephric duct. The epithelial cells lining the collecting duct system started as ow columnar, but increased in height in he larger channels. They possessed a well- efined brush border. The lumen was pa- ent, large and contained long cilia from he unciliated epithelial cells; the termi- al bars were distinct. Immediately below he luminal border was a layer of numer-

ous small darkly PAS-positive granules. The apical zone beneath this layer con- tained scattered PAS-positive granules. Larger PAS-positive granules were found just above the nucleus. The nuclei were elongate perpendicular to the axis of the tubule and slight irregularities in shape were noted. Cells presumed to be wander- ing cells were extremely abundant in this region and often stained intensely with the PAS technique. Besides a thick basement membrane, the ducts were surrounded by many layers of smooth muscle, connective tissue elements and capillaries.

B. Electron microscopy. The cells lin- ing the larger collecting ducts of the kidney were similar in morphology to those lining the collecting tubules previously described although they were taller. A layer of micro- villi was seen on the luminal border; the apical cytoplasm contained large numbers of mucous granules; and the remaining cytoplasm was filled with small mitochon- dria containing numerous cristae and a pale matrix. Many of the mitochondrial profiles were elongate and, in the basal cytoplasm, lay adjacent to the smooth-sur- faced membrane. A network of elements of the rough-surfaced endoplasmic reticulum lay between the numerous mitochondria. The Golgi apparatus, lying at the level of the nucleus, consisted of cisternae, a large number of small vesicles and large vacuoles of intermediate density. The nucleus tended to lay below the midlevel of the cell. The epithelium comprising the larger collecting ducts was surrounded by several layers of smooth muscle cells and connective tissue elements. Wandering cells were frequently seen between the lat- eral cell borders in this region in a manner similar to that seen in collecting tubules.

VII. Wandering cells

A variety of cells were seen lying between the lateral cell borders of the kid- ney tubular cells. The cell most frequently seen contained numerous ribosomes, a few vesicles, an irregular nucleus, an occa- sional mitochondria, a small amount of rough-surfaced endoplasmic reticulum. Cells containing cylindrical bodies of com- plex structure were frequently identified. Other cell profiles contained numerous vesicles of varying density, small mito-

The mitochondria were smaller in size and number than those seen in the second major segment and smaller but more numerous than those in the first major segment. A marked basophilic component was also noted in the entire cytoplasm of this latter segment after H&E staining. The apex contained PAS- and acid phosphatase-positive granules. The oval nuclei lay in a basal position. The basement membrane was thick and stained with the PAS technique. A layer of smooth muscle cells was seen surrounding the tubule.

B. Electron microscopy. The apical surface of each region was covered by tall microvilli which were not as tightly packed as those found in the first major segment. The appearance of the apical cytoplasm in the second and third major segments was similar in morphology although the region was much broader in the second major segment. This apical zone contained numerous smooth-surfaced vesicles and/or irregular-shaped units which varied in size and density. Following glutaraldehyde fixation, the apical vesicles were not as prominent. Irregular-shaped units were more frequently seen and the apical zone contained numerous filaments, microtubules and a background matrix of considerable density. A single basal body was occasionally seen in this apical region. Occasional large invaginations and large apical vacuoles were seen in the apical cytoplasm of these two regions which appeared to correspond to the large apical dye-containing structures seen in isolated tubules (Trump and Bulger, '67).

An extensive system of smooth-surfaced membranes was seen in the basal cytoplasm similar to those described for the first major segment. These membranes sometimes formed whorls surrounding various organelles. Tight junction regions were seen along adjacent lateral cell membranes in both segments beneath the level of the junctional complex.

Large numbers of elongated mitochondria filled the cytoplasm of these two segments. The mitochondrial matrix was dense and contained a few short cristae. Matrical granules were also identified. A few cells of the second major segment had extremely large mitochondria in the cell base.

Scattered units of the rough-surfaced endoplasmic reticulum were seen throughout the cytoplasm but were especially concentrated in the apical region. The cisternae were frequently parallel with lateral cell borders. The rough-surfaced endoplasmic reticulum was especially prominent in the third major segment which most likely accounts for the pronounced basophilia of this segment. An extensive network of irregular-shaped elements of the smooth-surfaced endoplasmic reticulum were seen throughout the cytoplasm.

The Golgi apparatus was most frequently seen lateral to the nucleus and consisted of several parallel cisternae and an associated group of vesicles. Dilated lumens were seen in the cisternae most lateral to the nucleus.

Cytosomes, cytosegresomes, multivesicular bodies and microbodies were seen in both of these two segments. Cytosegresomes were present with both pale matrix and dark matrix and contained a variety of materials including myelin figures and filaments. Cytosegresomes, containing recognizable organelles, were present. A few of the cytosegresomes were surrounded by a sac formed from two membranes which contained dense material.

Another class of single membrane-bounded bodies were seen in these segments. They were frequently associated with the endoplasmic reticulum and contained a central core area and therefore were presumed to be microbodies. In the cells of the second major segment, the microbodies appeared to be small and frequently seen around the nucleus. In the third major segment, the microbodies were considerably larger in size and widely distributed throughout the cytoplasm.

V. The collecting tubule (figs. 4, 13)

A. Light microscopy. The collecting tubule was composed of low cuboidal cells and its diameter was generally smaller than that of the third major segment. The luminal border of the cell was rectilinear with the long axis of the cell parallel to the axis of the tubule (fig. 3). The length of the segment was variable and could be extremely long. In some instances more than one major segment emptied into

collecting tubule. The cytoplasm was hilic and the mitochondria were generally inconspicuous. The cell apices contained PAS-positive granules and occasional acid phosphatase-positive droplets. The oval nuclei were placed along the axis of the tubule. A positive basement membrane and a smooth muscle coat surrounded the tubule. *Electron microscopy.* The lumen of collecting tubule was widely dilated and contained profiles of cilia. Occasional microvilli were seen on the apical surface. The majority of the mucous granules seen at the apex of the cell lay apical to a layer of filaments associated with the desmosomes which formed a thick layer across the cell apex although occasional mucous droplets were seen basal to it. A single dilated body was occasionally found in the apical cytoplasm.

Numerous small elongate mitochondrial profiles containing abundant cristae were distributed throughout the remaining cytoplasm. Cisternae of rough-surfaced endoplasmic reticulum were extremely abundant throughout the cytoplasm and many of the cisternae had dilated lumens. The smooth-surfaced endoplasmic reticulum was extensive as well. The Golgi apparatus was extremely large. Elements of the rough-surfaced endoplasmic reticulum were frequently seen adjacent to the external face of the Golgi apparatus. Several Golgi cisternae were seen lying in a closely parallel fashion and the internal face of the Golgi consisted of numerous vesicles and some enlarged vacuoles containing a flocculent material of low density.

VI. Collecting duct system (fig. 14)

A. Light microscopy. The collecting duct emptied into a collecting duct system in which the ducts converged to form larger channels finally emptying into the mesonephric duct. The epithelial cells lining the collecting duct system started as low columnar, but increased in height in the larger channels. They possessed a well-defined brush border. The lumen was patent, large and contained long cilia from the uniciliated epithelial cells; the terminal bars were distinct. Immediately below the luminal border was a layer of numer-

ous small darkly PAS-positive granules. The apical zone beneath this layer contained scattered PAS-positive granules. Larger PAS-positive granules were found just above the nucleus. The nuclei were elongate perpendicular to the axis of the tubule and slight irregularities in shape were noted. Cells presumed to be wandering cells were extremely abundant in this region and often stained intensely with the PAS technique. Besides a thick basement membrane, the ducts were surrounded by many layers of smooth muscle, connective tissue elements and capillaries.

B. Electron microscopy. The cells lining the larger collecting ducts of the kidney were similar in morphology to those lining the collecting tubules previously described although they were taller. A layer of microvilli was seen on the luminal border; the apical cytoplasm contained large numbers of mucous granules; and the remaining cytoplasm was filled with small mitochondria containing numerous cristae and a pale matrix. Many of the mitochondrial profiles were elongate and, in the basal cytoplasm, lay adjacent to the smooth-surfaced membrane. A network of elements of the rough-surfaced endoplasmic reticulum lay between the numerous mitochondria. The Golgi apparatus, lying at the level of the nucleus, consisted of cisternae, a large number of small vesicles and large vacuoles of intermediate density. The nucleus tended to lay below the midlevel of the cell. The epithelium comprising the larger collecting ducts was surrounded by several layers of smooth muscle cells and connective tissue elements. Wandering cells were frequently seen between the lateral cell borders in this region in a manner similar to that seen in collecting tubules.

VII. Wandering cells

A variety of cells were seen lying between the lateral cell borders of the kidney tubular cells. The cell most frequently seen contained numerous ribosomes, a few vesicles, an irregular nucleus, an occasional mitochondrion, a small amount of rough-surfaced endoplasmic reticulum. Cells containing cylindrical bodies of complex structure were frequently identified. Other cell profiles contained numerous vesicles of varying density, small mito-

chondria, abundant mitochondria and intracytoplasmic filaments and other cell profiles were seen filled with expanded cisternae of the endoplasmic reticulum. Cells were identified which contained dense granules presumed to be some type of granulocyte of blood origin.

DISCUSSION

Teleost nephrons have been reported to show an extensive diversity in morphology (Huot, '02; Audige, '10; Verne, '22; Edwards, '28, '29-30, '33, '35; Marshall and Grafflin, '28; Marshall, '29, '34; Grafflin, '29, '31, '33, '37a,b,c; Nash, '31; Defrise, '32; Guyton, '35; Smith, '51; Forster, '53, '61; Black, '57; Newstead and Ford, '60; Bulger, '65), and teleosts live in widely varied environments with profoundly differing needs with respect to salt and water balance. These observations stimulated comparative studies of kidney physiology and anatomy which have advanced the understanding of renal physiology (Marshall, '34). For example, the existence of aglomerular kidneys gave credibility to the proposed mechanism of tubular secretion (see review of Marshall, '34).

Many light microscopy studies were done between 1920 and 1937 of a wide variety of fish kidneys including Edwards' extensive investigations ('28, '29-30, '33, '35). Edwards ('35) listed several types of renal morphology in fish. Marine teleosts were divided into the following groups: 1. Unisegmental aglomerular tubules lacking a distal convolution; a. Entirely aglomerular as exemplified by *Sygnathidae*; b. Partly aglomerular as exemplified by *Muraenidae* (*Muraena helena*) and *Lophiidae* (*Lophius piscatorius* and *Lophius bodegassa*); c. Glomerular with slightly patent or nonpatent necks as exemplified by *Gadidae* (*Merluccius vulgaris*); 2. Plurisegmental glomerular tubules lacking a distal convolution; a. Glomerular but lacking an intermediate segment as exemplified by *Trachinidae* (*Trachinus vipera*), *Scorpaenidae* (*Scorpaena*) *scrofa* and *Myoxocephalus octodactylus* and others; b. Glomerular with an intermediate segment resembling some of the tubules of *Muraenidae* (*Muraena helena*). This classification does not include the collecting tubule system.

Forster ('61) was under the impression that the nephron of the common flounder was uniform enough to be considered consisting solely of tubules resembling mammalian proximal tubules. Our results indicate, however, that the kidney of the flounder, *Parophrys vetulus*, is similar in morphology to that of other glomerular marine fish in Edwards' ('35) class 2a, a plurisegmental glomerular tubule, lacking distal convolutions and lacking an intermediate segment. Only the cells of the first major segment resembled the mammalian proximal tubule. Although an intermediate segment and a distal convolution are lacking in this fish, it seems to us that applying the term "proximal convolution" for the entire nephron will lead to confusion; it should be noted that most of the nephron (segments 2 and 3) is quite different both structurally and functionally from any part of the mammalian tubule.

Glomerular development is not extensive in marine teleosts (Nash, '31) and, in general, marine teleosts have low glomerular filtration rates (Grafflin, '37a; Forster, '53). In fact, certain marine species are aglomerular (Huot, '02). It is not surprising that the English sole renal corpuscle, when compared with the well-studied mammalian species, are characterized by several morphologic features which seem to reflect the low glomerular filtration rate. These features include: a paucity of capillary loops; a relatively thick-walled capillary with only a few pores; an extensive system of mesangial cells with processes which often encircle the capillary; and an abundant mesangial matrix. In this regard, Hickman (personal communication) has shown that some individuals of the flounder species, *Paralichthys lethostigma*, may be functionally aglomerular, possessing glomeruli of similar morphology to those described here.

Two morphologic features of the flounder renal glomerulus indicate a close relationship between the podocyte and the glomerular basement membrane. First, the basement membrane lies adjacent to the pedicel border and does not completely surround the capillary. Instead, the basement membrane follows the podocytes at inflection points leaving a broad zone of capillary to abut only on the mesangium. Second, as the mesangial cells send their

esses around the capillary loops, they triably lie between the podocytic basement membrane and the capillary. A similar morphologic relationship is seen in certain renal diseases such as chronic glomerulonephritis (Faith and Trump, '66). Except for the feature already noted, the structure of the glomerulus resembles that seen in mammalian species. Two exceptions were noted: desmosomes are frequently seen between parts of the podocytes, and filtration slit "membranes" are located high on the pedicels therefore at some distance from the basement membrane.

The cells of the neck region are characterized by cilia and mucous granules. Several cilia can be seen emerging from a single cellular profile. Groups of cilia can be seen in the lumen, generally numbering approximately 12. It, therefore, seems likely that multiple cilia arise from single cells in groups of approximately 12. The beating of the cilia may serve to propel urine along the nephron. Marshall ('34) noted that ciliated neck segments are found only in species with relatively low blood pressure. Mucous granules are seen in the majority of the remaining cellular profiles. The number of granules shows much variation from region to region. Cells containing mucous granules also have a well-developed rough-surfaced endoplasmic reticulum. Occasionally a single granulum can be seen arising from a mucous containing cell.

Cells of the first major segment are characterized by an extensive brush border and a broad apical zone containing numerous tubular and vesicular profiles and large vacuoles similar to those found in the proximal tubules of a variety of mammalian species (Rhodin, '62, '63; Ericsson, '64, '65), fresh water teleosts (Gritzka, '63; Bulger, unpublished observations), and odocoetes (Himmelhoch and Karnovsky, '61). These structures have been associated with the uptake of filtered proteins (Straus, '57, '62, '64; Miller, '60; Miller and Glade, '64; Ericsson, '64, '65) or other macromolecules (Trump, '61). Unpublished observations in our laboratory have indicated that these apical tubules participate in the endocytosis of ferritin or other colloidal particles injected into the tubular lumen. This is in marked contrast to the

handling of similar particles in other regions of the nephron. Also this region has extremely large cytosomes which show acid phosphatase activity and thus contains all of the structures usually associated with highly endocytic cells. Cytoresosomes, most of which probably represent foci of autophagy, were only occasionally seen in this or other regions of the normal nephron. This is in marked contrast to tubules incubated *in vitro* where numerous foci of autophagy occurred (Trump and Bulger, '67).

Aglomerular marine toadfish have no filtered protein and also are the only vertebrate studied which lack the apical zone of tubules and vacuoles (Bulger, '65; Trump and Bulger, '67). It seems conceivable, therefore, that the apical structures that have been associated with endocytosis in mammals are present only in teleosts which possess glomerular filtration; in aglomerular fish the luminal surface of cells lining the tubule is not exposed to particles of colloidal size since these cannot enter through the peritubular capillaries and basement membranes. It therefore seems no accident that this segment specialized for endocytosis is not present in aglomerular fish so far studied (Bulger, '65). There would seem to be at least two ways in which this might be controlled. The first is that these structures may actually be induced by the presence of material such as protein in the tubular lumen. The other possibility might be that these segments degenerate during embryogenesis along with the glomeruli because of some common factor such as blood supply. This last hypothesis seems to be favored by the fact that aglomerular fish also lack a neck region which would seem to be rather useful in these fish.

Cells of the second and third major segment also have a specialized brush border though less so than in the first but lack the apical tubules and vacuoles. The apical zone contains some smooth-surfaced membranes whose configuration depends on the fixative employed. This zone is similar to that found in the aglomerular toadfish (Bulger, '65) and probably functions in a similar manner.

All three major segments have certain features in common. One prominent similarity is the presence of an extensive

chondria, abundant mitochondria and intracytoplasmic filaments and other cell profiles were seen filled with expanded cisternae of the endoplasmic reticulum. Cells were identified which contained dense granules presumed to be some type of granulocyte of blood origin.

DISCUSSION

Teleost nephrons have been reported to show an extensive diversity in morphology (Huot, '02; Audige, '10; Verne, '22; Edwards, '28, '29-'30, '33, '35; Marshall and Grafflin, '28; Marshall, '29, '34; Grafflin, '29, '31, '33, '37a,b,c; Nash, '31; Defrise, '32; Guyton, '35; Smith, '51; Forster, '53, '61; Black, '57; Newstead and Ford, '60; Bulger, '65), and teleosts live in widely varied environments with profoundly differing needs with respect to salt and water balance. These observations stimulated comparative studies of kidney physiology and anatomy which have advanced the understanding of renal physiology (Marshall, '34). For example, the existence of aglomerular kidneys gave credibility to the proposed mechanism of tubular secretion (see review of Marshall, '34).

Many light microscopy studies were done between 1920 and 1937 of a wide variety of fish kidneys including Edwards' extensive investigations ('28, '29-'30, '33, '35). Edwards ('35) listed several types of renal morphology in fish. Marine teleosts were divided into the following groups: 1. Unisegmental aglomerular tubules lacking a distal convolution; a. Entirely aglomerular as exemplified by *Sygnathidae*; b. Partly aglomerular as exemplified by *Muraenidae* (*Muraena helena*) and *Lophiidae* (*Lophius piscatorius* and *Lophius bodegassa*); c. Glomerular with slightly patent or nonpatent necks as exemplified by *Gadidae* (*Merluccius vulgaris*); 2. Plurisegmental glomerular tubules lacking a distal convolution; a. Glomerular but lacking an intermediate segment as exemplified by *Trachinidae* (*Trachinus vipera*), *Scorpaenidae* (*Scorpaena*) *scrofa* and *Myoxocephalus octodidimspinus* and others; b. Glomerular with an intermediate segment resembling some of the tubules of *Muraenidae* (*Muraena helena*). This classification does not include the collecting tubule system.

Forster ('61) was under the impression that the nephron of the common flounder was uniform enough to be considered consisting solely of tubules resembling mammalian proximal tubules. Our re-examination, however, of the kidney of flounder, *Parophrys vetulus*, is similar in morphology to that of other glomerular marine fish in Edwards' ('35) class 2a, a plurisegmental glomerular tubule, lacking distal convolutions and lacking an intermediate segment. Only the first major segment resembled the mammalian proximal tubule. Although an intermediate segment and a distal convolution are lacking in this fish, it seems to us that applying the term "proximal convolution" for the entire nephron will lead to confusion; it should be noted that most of a nephron (segments 2 and 3) is quite different both structurally and functionally from any part of the mammalian tubule.

Glomerular development is not extensive in marine teleosts (Nash, '31) and, in general, marine teleosts have low glomerular filtration rates (Grafflin, '37a; Forster, '53). In fact, certain marine species are aglomerular (Huot, '02). It is not surprising that the English sole renal corpuscle when compared with the well-studied mammalian species, are characterized by several morphologic features which to reflect the low glomerular filtration rate. These features include: a paucity of capillary loops; a relatively thick-walled capillary with only a few pores; an extensive system of mesangial cells with processes which often encircle the capillary; and an abundant mesangial matrix. In this regard Hickman (personal communication) has shown that some individuals of the eel species, *Paralichthys lethostomus*, may be functionally aglomerular, possessing glomeruli of similar morphology to those described here.

Two morphologic features of the flounder renal glomerulus indicate a close relationship between the podocyte and the glomerular basement membrane. First, the basement membrane lies adjacent to the pedicel border and does not completely round the capillary. Instead, the basement membrane follows the podocytes at inflection points leaving a broad zone of capillary to abut only on the mesangium. Second, as the mesangial cells send the

ses around the capillary loops, they ably lie between the podocytic basement membrane and the capillary. A similar morphologic relationship is seen in certain diseases such as chronic glomerulonephritis (Faith and Trump, '66). Except for the feature already noted, the structure of the glomerulus resembles seen in mammalian species. Two exceptions were noted: desmosomes frequently seen between parts of the cytes, and filtration slit "membranes" located high on the pedicels therefore at some distance from the basement brane.

Cells of the neck region are characterized by cilia and mucous granules. Sev-cilia can be seen emerging from a cellular profile. Groups of cilia can be seen in the lumen, generally numbering approximately 12. It, therefore, is likely that multiple cilia arise from cells in groups of approximately 12. Beating of the cilia may serve to propel urine along the nephron. Marshall ('34) noted that ciliated neck segments are found only in species with relatively low pressure. Mucous granules are seen in the majority of the remaining cellular files. The number of granules shows variation from region to region. Cells containing mucous granules also have a well-developed rough-surfaced endoplasmic reticulum. Occasionally a single lumen can be seen arising from a mucous containing cell.

Cells of the first major segment are characterized by an extensive brush border and a broad apical zone containing numerous tubular and vesicular profiles and large vacuoles similar to those found in the proximal tubules of a variety of mammalian species (Rhodin, '62, '63; Ericsson, '65), fresh water teleosts (Gritzka, '63; Bulger, unpublished observations), and oocytes (Himmelhoch and Karnovsky, '61). These structures have been associated with the uptake of filtered proteins (Straus, '57, '62, '64; Miller, '60; Miller and Wade, '64; Ericsson, '64, '65) or other macromolecules (Trump, '61). Unpublished observations in our laboratory have indicated that these apical tubules participate in the endocytosis of ferritin or other colloidal particles injected into the tubular lumen. This is in marked contrast to the

handling of similar particles in other regions of the nephron. Also this region has extremely large cytosomes which show acid phosphatase activity and thus contains all of the structures usually associated with highly endocytic cells. Cytoresomes, most of which probably represent foci of autophagy, were only occasionally seen in this or other regions of the normal nephron. This is in marked contrast to tubules incubated *in vitro* where numerous foci of autophagy occurred (Trump and Bulger, '67).

Aglomerular marine toadfish have no filtered protein and also are the only vertebrate studied which lack the apical zone of tubules and vacuoles (Bulger, '65; Trump and Bulger, '67). It seems conceivable, therefore, that the apical structures that have been associated with endocytosis in mammals are present only in teleosts which possess glomerular filtration; in aglomerular fish the luminal surface of cells lining the tubule is not exposed to particles of colloidal size since these cannot enter through the peritubular capillaries and basement membranes. It therefore seems no accident that this segment specialized for endocytosis is not present in aglomerular fish so far studied (Bulger, '65). There would seem to be at least two ways in which this might be controlled. The first is that these structures may actually be induced by the presence of material such as protein in the tubular lumen. The other possibility might be that these segments degenerate during embryogenesis along with the glomeruli because of some common factor such as blood supply. This last hypothesis seems to be favored by the fact that aglomerular fish also lack a neck region which would seem to be rather useful in these fish.

Cells of the second and third major segment also have a specialized brush border though less so than in the first but lack the apical tubules and vacuoles. The apical zone contains some smooth-surfaced membranes whose configuration depends on the fixative employed. This zone is similar to that found in the aglomerular toadfish (Bulger, '65) and probably functions in a similar manner.

All three major segments have certain features in common. One prominent similarity is the presence of an extensive

system of smooth-surfaced membranes in the basal cytoplasm, which most likely appears to be plasma membranes. Differences were seen in the configuration of these smooth-surfaced membranes after primary fixation with osmium tetroxide, glutaraldehyde or potassium permanganate. Such a system was therefore described as constituting part of the smooth-surfaced endoplasmic reticulum in *Fundulus heteroclitus* (Gritzka, '63). However, following glutaraldehyde fixation, connections of these membranes with the basal plasmalemma were frequently seen by us. Two types of membranes were distinguished following permanganate fixation, the most abundant of which invariably connected with the basal plasmalemma forming long narrow interdigitating processes in the basal cytoplasm. Although it is presently impossible to distinguish which one represents the *in vivo* state, it seems more likely that membrane breakdown is occurring following osmium tetroxide fixation. A similar system of elaborate basal plasma membranes was noted in the basal cytoplasm of the aglomerular teleost, *Opsanus tau* (Bulger, '65).

The plasma membranes lie adjacent to the numerous mitochondria found in the cytoplasm of all three major segments. A similar association of mitochondria and membranes is frequently found in other ion transporting tissues (see Bulger, '65 for review). This association correlates well with the physiologic role of these cells in active transport. It has been shown that all of the three major segments are capable of transporting chlorphenol red (Trump and Bulger, '67).

The presence of a class of single membrane limited bodies, containing a moderate matrix density and an occasional central crystalline core area, and lying adjacent to units of endoplasmic reticulum, was noted. These bodies probably correspond with the microbodies found in the liver and kidney of other vertebrate species.

Large flask-shaped structures were sometimes found in the apical cytoplasm of all three major segments which occasionally were seen to be confluent with the lumen. Similar structures formed with great rapidity and in large numbers when colloidal particles were injected retrograde

into the nephron (Bulger & Trump, unpublished observations).

The urine of marine teleosts, in general and of the southern flounder, *Paralichthys lethostigma*, which has recently been studied by Hickman (personal communication), is composed primarily of magnesium sulfate with smaller amounts of sodium, potassium, calcium, and other anions. Magnesium, which represents the major constituent, is derived from sea water, is probably excreted almost entirely by tubular secretion, even when filtration rates of urine are at maximal levels. *Paralichthys lethostigma* not more than 3% of the magnesium or sulfate excreted is filtered (Hickman, personal communication). The sodium concentration is somewhat variable; however, it appears that virtually all sodium and most of the chloride are reabsorbed actively against the concentration gradient. Even when filtration stops, as it appears to do in some individuals, sodium and chloride, that leak into the lumen, must still be reabsorbed (Hickman, personal communication). The presence of sodium and chloride secretion by a leak-type of mechanism is suggested by the presence of these ions in relatively large amounts in aglomerular species during laboratory diuresis at which time reabsorptive mechanism is evidently blocked (Forster and Berglund, '56).

There are no data presently available concerning these various secretory and reabsorptive mechanisms in the English sole nephron. Our ultrastructure studies together with previously reported studies on aglomerular nephrons (Bulger, '65) can lead to tentative interpretations. Since the aglomerular fish has a region resembling the second and third brush border segments and since calcium and magnesium reabsorptive mechanisms are present in teleost species, it would seem that divalent ion secretory systems might be found in these regions. Such an interpretation is supported by the finding of microcrystalline deposits within the endoplasmic reticulum of the second and third brush border regions of *Paralichthys lethostigma*. Similar microcrystalline deposits can be seen in thin sections of urine sediment by electron microscopy and x-ray diffraction of such urine sediments reveal the presence of calcium monohydrate

hate ($\text{CaHPO}_4 \cdot 2\text{H}_2\text{O}$) (Trump and Jan, unpublished observations). The of sodium reabsorption is more difficult to assign. In comparison with other excreting tissues, it would seem that all the brush border segments, and to a degree the collecting ducts, have the of mitochondrial-plasmalemma association that seem to be important in this.

region morphologically similar to the tubule of the mammal (Rhodin, '62, or the goldfish (Bulger, unpublished observations) was found in this nephron. There was no juxtaglomerular apparatus although large granulated cells were running for considerable distances in media of arterioles which appeared to present juxtaglomerular cells. The related cells appeared to be modified epithelial muscle cells. In this regard, Connell and Kaley ('64) demonstrated the presence of renin in the kidneys of the eel, *Paralichthys*.

The cells of the collecting tubules and excretory collecting ducts were characterized by apical mucous granules. The abundant small mitochondria and moderate amounts of smooth-surfaced membranes found in these cells indicate that these cells play an active role in the functioning of the tubule instead of being merely a passive system of conduits.

Smooth muscle cells were seen surrounding the entire flounder renal tubule. Evansley and Scott ('63) noted systolic muscular action in the renal tubules of the eel. We have also observed this in eel renal tubules. Such muscular action might play a role in the propulsion of the filtrate down the nephron. The beating of ciliated cells in the neck region and the long cilia from cells of the remaining tubular regions is likely to play a role in fluid movement as well. Marshall ('34) has noted that ciliated neck and intermediate segments disappear coincidentally with the acquisition of a relatively high blood pressure as seen in birds and mammals.

ACKNOWLEDGMENTS

The authors wish to express their thanks to Dr. Tom English of the University of Washington and Dr. Allan C. DeLacy for assistance with collection and maintenance of fish, and to Judy Strum, Dawn

Bockus, Liz Caldwell, Rene Collman, Ingrid Klock, and Franque Remington for their excellent technical assistance.

This investigation was supported by grants AM-07919 and AM-10922 from the U.S.P.H.S.

LITERATURE CITED

- Audige, J. 1910 Contribution à l'étude des reins des poissons téléostéens. Arch. Zool. Exp. et Gen., T., 4: 275-624.
- Barka, T., and P. J. Anderson 1963 Histochemistry: Theory, Practice and Bibliography. Hoeber Medical Division, Harper and Row, Publishers, Inc., New York.
- Bennett, H. S., and J. H. Luft 1959 α -Collidine as a basis for buffering fixatives. J. Biophys. Biochem. Cytol., 6: 113-114.
- Black, V. S. 1957 Excretion and Osmoregulation. In: Physiology of Fishes, Vol. I. Margaret E. Brown, ed. 163-205.
- Bulger, R. E. 1965 The fine structure of the glomerular nephron of the toadfish, *Opsanus tau*. Am. J. Anat., 117: 171-192.
- Connell, C. M., and G. Kaley 1964 Evidence for the presence of "renin" in kidneys of marine fish and amphibia. Biol. Bull., 127: 366-367.
- Defrise, A. 1932 Cytophysiological studies of the nephrocytes of unisegmental glomerular and glomerular nephrons. Anat. Rec., 54: 185-195.
- Edwards, J. C. 1928 Studies on glomerular and glomerular kidneys. I. Anatomical. Am. J. Anat., 42: 75-107.
- 1929-1930 Studies on glomerular and glomerular kidneys. III. Cytological. Anat. Rec., 44: 15-27.
- 1933 Functional sites and morphological differentiation in the renal tubules. Anat. Rec., 55: 343-367.
- 1935 The epithelium of the renal tubule in bony fish. Anat. Rec., 63: 263-279.
- Ericsson, J. L. E. 1964 Absorption and decomposition of homologous hemoglobin in renal proximal tubular cells. An experimental light and electron microscopic study. Acta Path. Microbiol. Scand., 168 (Supplement): 1-121.
- 1965 Transport and digestion of hemoglobin in the proximal tubule. II. Electron microscopy. Lab. Invest., 14: 16-39.
- Ericsson, J. L. E., and B. F. Trump 1964 Electron microscopic studies of the epithelium of the proximal tubule of the rat kidney. I. The intracellular localization of acid phosphatase. Lab. Invest., 13: 1427-1456.
- Faith, G. C., and B. F. Trump 1966 The glomerular capillary wall in human kidney disease: Acute glomerulonephritis, system lupus erythematosus and preeclampsia-eclampsia. Lab. Invest., 15: 1682-1719.
- Forster, R. P. 1948 Use of thin kidney slices and isolated renal tubules for direct study of cellular transport kinetics. Science, 108: 65-67.
- 1953 A comparative study of renal function in marine teleosts. J. Cell. and Comp. Physiol., 42: 487-509.
- 1961 Kidney Cells. In: The Cell. Vol. 5 Jean Brachet & Alfred Mirsky, eds. 89-161.
- Forster, R. P., and Berglund, F. 1956 Osmotic diuresis and its effect on total electrolyte distribution in

system of smooth-surfaced membranes in the basal cytoplasm, which most likely appears to be plasma membranes. Differences were seen in the configuration of these smooth-surfaced membranes after primary fixation with osmium tetroxide, glutaraldehyde or potassium permanganate. Such a system was therefore described as constituting part of the smooth-surfaced endoplasmic reticulum in *Fundulus heteroclitus* (Gritzka, '63). However, following glutaraldehyde fixation, connections of these membranes with the basal plasmalemma were frequently seen by us. Two types of membranes were distinguished following permanganate fixation, the most abundant of which invariably connected with the basal plasmalemma forming long narrow interdigitating processes in the basal cytoplasm. Although it is presently impossible to distinguish which one represents the *in vivo* state, it seems more likely that membrane breakdown is occurring following osmium tetroxide fixation. A similar system of elaborate basal plasma membranes was noted in the basal cytoplasm of the aglomerular teleost, *Opsanus tau* (Bulger, '65).

The plasma membranes lie adjacent to the numerous mitochondria found in the cytoplasm of all three major segments. A similar association of mitochondria and membranes is frequently found in other ion transporting tissues (see Bulger, '65 for review). This association correlates well with the physiologic role of these cells in active transport. It has been shown that all of the three major segments are capable of transporting chlorphenol red (Trump and Bulger, '67).

The presence of a class of single membrane limited bodies, containing a moderate matrix density and an occasional central crystalline core area, and lying adjacent to units of endoplasmic reticulum, was noted. These bodies probably correspond with the microbodies found in the liver and kidney of other vertebrate species.

Large flask-shaped structures were sometimes found in the apical cytoplasm of all three major segments which occasionally were seen to be confluent with the lumen. Similar structures formed with great rapidity and in large numbers when colloidal particles were injected retrograde

into the nephron (Bulger & Trump, unpublished observations).

The urine of marine teleosts, in general of the southern flounder, *Paralichthys lethostigma*, which has recently been studied by Hickman (personal communication), is composed primarily of magnesium sulfate with smaller amounts of sodium, potassium, calcium, and other anions. Magnesium, which represents the major constituent, is derived from sea water and is probably excreted almost entirely by tubular secretion, even when filtrate rates of urine are at maximal levels. *Paralichthys lethostigma* not more than 3% of the magnesium or sulfate excreted is filtered (Hickman, personal communication). The sodium concentration is somewhat variable; however, it appears that virtually all sodium and most of the chloride are reabsorbed actively against the concentration gradient. Even when filtration stops, as it appears to do in some individuals, sodium and chloride, that leak into the lumen, must still be reabsorbed (Hickman, personal communication). The presence of sodium and chloride secretion by a leak-type of mechanism is suggested by the presence of these ions in relatively large amounts in aglomerular species during laboratory diuresis at which time the reabsorptive mechanism is evidently blocked (Forster and Berglund, '56).

There are no data presently available concerning these various secretory and reabsorptive mechanisms in the English sole nephron. Our ultrastructure studies together with previously reported studies on aglomerular nephrons (Bulger, '65) can lead to tentative interpretations. Since the aglomerular fish has a region resembling the second and third brush border segments and since calcium and magnesium secretory mechanisms are present in these species, it would seem that divalent cation secretory systems might be found in these regions. Such an interpretation is supported by the finding of microcrystalline deposits within the endoplasmic reticulum of the second and third brush border regions of *Paralichthys lethostigma*. Similar microcrystalline deposits can be seen in thin sections of urine sediment by electron microscopy and x-ray diffraction of such urine sediments reveal the presence of calcium monohydrate.

- p. B. F., and C. P. Hickman Unpublished observations.
- p. B. F., E. A. Smuckler and E. P. Benditt 1961 Method for staining epoxy sections for light microscopy. *J. Ultrastruct. Res.*, 5: 343-348.
- Verne, J. 1922 Contribution à l'étude des reins agglomérulaires. L'appareil renal des poissons *Lophobranchies*. *Arch. de Anat. Microscop.*, T., 18: 357-407.
- Zimmermann, K. W. 1915 Über das epithel des glomerularen Endkammerblattes der Saugerniere. *Anat. Anz.*, 48: 335-341.

- plasma and urine of the aglomerular teleost, *Lophius americanus*. J. Gen. Physiol., 39: 349-59.
- Forster, R. P., and S. K. Hong 1958 *In vitro* transport of dyes by isolated renal tubules of the flounder as disclosed by direct visualization. Intracellular accumulation and transcellular movement. J. Cell. and Comp. Physiol., 51: 257-272.
- Forster, R. P., and J. V. Taggart 1950 Use of isolated renal tubules for the examination of metabolic processes associated with active cellular transport. J. Cell. and Comp. Physiol., 35: 251-270.
- Grafflin, A. L. 1929 The pseudoglomeruli of the kidney of *Lophius piscatorius*. Am. J. Anat., 44: 441-54.
- 1931 The structure of the renal tubule of the toadfish. Bull. Johns Hopkins Hosp., 48: 269-271.
- 1933 Glomerular degeneration in the kidney of the daddy sculpin (*Myoxocephalus scorpius*). Anat. Rec., 57: 59-79.
- 1937a Observations upon the aglomerular nature of certain teleostean kidneys. J. Morph., 61: 165-173.
- 1937b The structure of the nephron in fishes. Anat. Rec., 68: 287-303.
- 1937c The structure of the nephron in the sculpin, *Myoxocephalus octodecimspinosus*. Anat. Rec., 68: 145-163.
- Gridley, M. F. 1960 Manual of Histologic and Special Staining Techniques, 2nd edition. The Blakiston Division, McGraw-Hill Book Co., Inc., New York.
- Gritzka, T. L. 1963 The ultrastructure of the proximal convoluted tubule of the euryhaline teleost, *Fundulus heteroclitus*. Anat. Rec., 145: 235-236.
- Guyton, J. S. 1935 The structure of the nephron in the South American lungfish, *Lepidosiren paradoxa*. Anat. Rec., 63: 213-229.
- Hickman, C. P. Personal communication.
- Himmelhoch, F. R., and M. J. Karnovsky 1961 Oxidative and hydrolytic enzymes in the nephron of *necturus maculosus*. J. Biophys. Biochem. Cytol., 9: 893-908.
- Hong, S. K., and R. P. Forster 1959 Further observations on the separate steps involved in the active transport of chlorphenol red by isolated renal tubules of the flounder *in vitro*. J. Cell. and Comp. Physiol., 53: 237-242.
- Huot, A. 1902 Recherches sur les poissons Lophobranchies. Ann. d. Sci. (Zool. et Paleont.), T. 14: 197-288.
- Luft, J. H. 1956 Permanganate—A new fixative for electron microscopy. J. Biophys. Biochem. Cytol., 2: 799-801.
- 1959 The use of acrolein as a fixative for light and electron microscopy. Anat. Rec., 133: 305.
- 1961 Improvements in epoxy resin embedding methods. J. Biophys. Biochem. Cytol., 9: 409-414.
- Marshall, E. K., Jr. 1929 The aglomerular kidney of the toadfish (*Opsanus tau*). Bull. Johns Hopkins Hosp., 45: 95-101.
- 1934 The comparative physiology of the kidney in relation to theories of renal secretion. Physiol. Rev., 14: 133-159.
- Marshall, E. K., Jr., and A. L. Grafflin 1928 The structure and function of the kidney of *Lophius piscatorius*. Bull. Johns Hopkins Hosp., 43: 205-236.
- Miller, F. 1960 Hemoglobin absorption by the cells of the proximal convoluted tubule in mouse kidney. J. Biophys. Biochem. Cytol., 8: 689-718.
- Miller, F., and G. E. Palade 1964 Lysosomal renal protein absorption droplets. J. Cell Biol. 519-552.
- Millonig, G. 1962 Further observations on a phosphate buffer for osmium solutions in fixation. Proc. of the Fifth International Congress for Electron Microscopy. S. S. Breese, Jr., ed. Vol. 2, New Academic Press, p. 8.
- Nash, J. 1931 The number and size of glomeruli of the kidneys of fishes, with observations on the physiology of the renal tubules of fishes. Am. J. 47: 425-445.
- Newstead, J. D., and P. Ford 1960 Studies on development of the kidney of the Pacific pinkfish (*Oncomorhynchus gorbuscha* Walbaum) III. Development of the mesonephros with particular reference to the mesonephric tubule. Can. J. Zool. 38.
- Rhodin, J. A. G. 1962 Electron Microscopy of Kidney. In: Renal Disease (D. A. K. Black et al. 117-156, Blackwell Scientific Publications, Philadelphia, Pennsylvania).
- 1963 Structure of the Kidney. In: Diseases of the Kidney (M. B. Strauss and L. G. Welt, eds. 1-29, Little, Brown and Company, Boston, Massachusetts).
- Sabatini, P. D., K. Bensch and R. J. Barmett 1961 Cytochemistry and electron microscopy. The preservation of cellular ultrastructure and enzymatic activity by aldehyde fixation. J. Cell Biol., 17: 1-15.
- Smith, H. W. 1951 The Kidney: Structure and Function in Health and Disease, Oxford University Press, New York.
- Straus, W. 1957 Changes in "droplet" fractions of rat kidney cells after intraperitoneal injection of white. J. Biophys. Biochem. Cytol., 3: 933-94.
- 1962 Colorimetric investigation of the effect of an intravenously injected protein (horseradish peroxidase) by rat kidney and effects of copper by egg white. J. Cell Biol., 12: 231-246.
- 1964 Cytochemical observations on the relationship between lysosomes and phagosomes in kidney and liver by combined staining for acid phosphatase and intravenously injected horseradish peroxidase. J. Cell Biol., 20: 497-507.
- Taggart, J. V., and R. P. Forster 1950 Renal transport. Effect of 2, 4-dinitrophenol and related compounds on phenol red transport in the renal tubules of the flounder. Am. J. Physiol., 161: 167-170.
- Townsend, P. M., and M. A. Scott 1963 Secretory muscular action of the kidney tubules of flounder. Fish Res. Bd. Canada, 20: 243-244.
- Trump, B. F. 1961 An electron microscope study of the uptake, transport and storage of cell material by the cells of the vertebrate nephron. Ultrastruct. Res., 5: 291-310.
- Trump, B. F., and R. E. Bulger 1965 Effect of nitrile on ultrastructure of isolated nephrons. Fed. Proc., 24: 616.
- 1966 New ultrastructural characteristics of cells fixed in a glutaraldehyde-osmium tetroxide mixture. Lab. Invest., 15: 368-379.
- 1967 Studies of cellular injury in flounder tubules. I. Correlation between morphological and function of control tubules and observations on autophagocytosis and mechanical cell damage. Invest., 16: 453-482.
- Trump, B. F., K. Green, and C. P. Hickman 1968 Observations.



Abbreviations

I, First major segment	I, Intercellular space
II, Second major segment	LD, Lipid droplets
III, Third major segment	M, Mitochondria
BB, Brush border	Mb, Microbodies
BM, Basement membrane	MC, Mesangial cells
C, Cytosomes	MG, Mucous granules
Cap, Capillaries	MM, Mesangial matrix
Cl, Cilia	Mv, Microvilli
CT, Collecting tubule	N, Neck region
ERG, Endoplasmic reticulum, granular	P, Podocyte
F, Filaments	SM, Smooth muscles
Go, Golgi apparatus	Ve, Vesicles

PLATE 1

EXPLANATION OF FIGURES

Figures 1-4 were taken of kidney embedded in a mixture of paraffin and Piccolyte. The tissue for picture 4 was stained with the PAS technique and counterstained with hematoxylin. The others were taken from tissues stained according to the Gomori trichrome technique.

- 1 Portions of a renal corpuscle showing abundant mesangium and peripheral small capillaries (Cap). Neck segment (N), first major segment (I) and second major segment (II) are seen embedded in the abundant hematopoietic tissue. $\times 475$.
- 2 Two transition regions from the first (I) to the second (II) major segments. Cells of the second major segment are characterized by large, densely staining mitochondria. Certain cells have extremely large mitochondria (arrows). Note intermingling of cell types in junctional regions, especially marked in transition on left. $\times 520$.
- 3 A transition zone between a third major segment (III) and a collecting tubule (CT). Note the shape of the luminal border of the collecting tubule cells (arrow). $\times 630$.
- 4 A collecting duct with tall columnar cells containing apical PAS-positive mucous granules (arrow), smaller PAS-positive granules (double arrow), and a thick basement membrane. Numerous densely-staining nuclei of wandering cells can be identified in the tubule wall. The tubule is surrounded by a thick layer containing collagen and smooth muscle cells. $\times 510$.

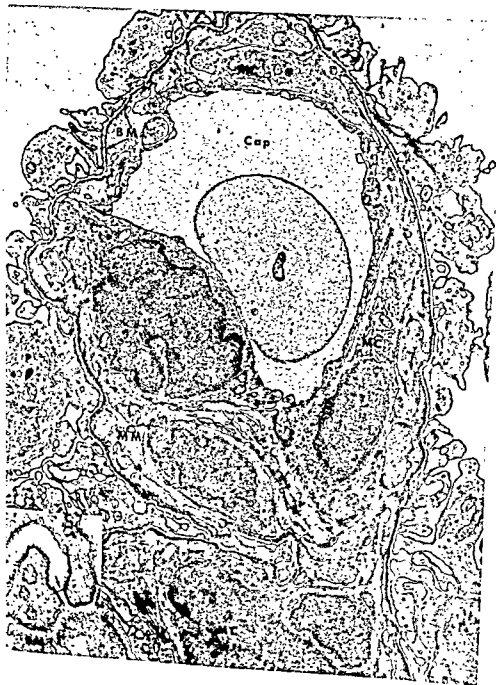


PLATE 2

EXPLANATION OF FIGURE

- 5 Electron micrograph showing a portion of a renal corpuscle. The podocytes (P) have small processes, called "pedicels," which rest on the basement membrane (BM) and surround the capillaries (Cap). The mesangial cells (MC) are numerous and have cell processes which extend peripherally and frequently almost encircle the capillary. The mesangial matrix (MM), which surrounds the mesangial cells, is abundant. The insert is a higher magnification picture showing the relationship between the pedicels and the basement membrane (BM). The filtration slit "membrane" (arrows) lies high on the pedicel. Fixed by vascular perfusion in osmium tetroxide buffered with *s*-collidine. $\times 11,700$. Insert $\times 47,400$.



PLATE 3

EXPLANATION OF FIGURE

- 6 Electron micrograph of the neck segment showing cellular profiles containing numerous mucous granules (MG) and a cellular profile containing the basal bodies of several cilia (Ci). Cilia are also seen in the lumen of the tubule. Fixed by immersion in osmium tetroxide buffered with *s*-collidine. $\times 13,900$.



PLATE 4

EXPLANATION OF FIGURE

- 7 Electron micrograph of the first major segment with a brush border. The first segment is characterized by an apical layer of microvilli (BB), abundant cytosomes (C), microbodies (Mb) and mitochondria (M). The apical cytoplasm contains vacuoles, vesicles and dense tubules similar in appearance to those seen in rat proximal convoluted tubule cells. Cilia (Ci) are seen in the tubular lumen. The tubule is surrounded by a thick basement membrane (BM) and a layer of smooth muscle cells (SM). Fixed by vascular perfusion with osmium tetroxide buffered with *s*-collidine. $\times 7,400$.

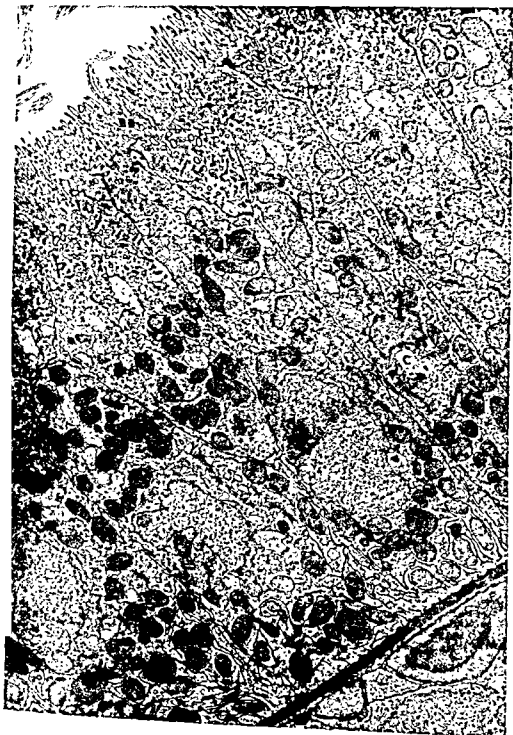


PLATE 4

EXPLANATION OF FIGURE

- 7 Electron micrograph of the first major segment with a brush border. The first segment is characterized by an apical layer of microvilli (BB), abundant cytosomes (C), microbodies (Mb) and mitochondria (M). The apical cytoplasm contains vacuoles, vesicles and dense tubules similar in appearance to those seen in rat proximal convoluted tubule cells. Cilia (Cl) are seen in the tubular lumen. The tubule is surrounded by a thick basement membrane (BM) and a layer of smooth muscle cells (SM). Fixed by vascular perfusion with osmium tetroxide buffered with *s*-collidine. $\times 7,400$.

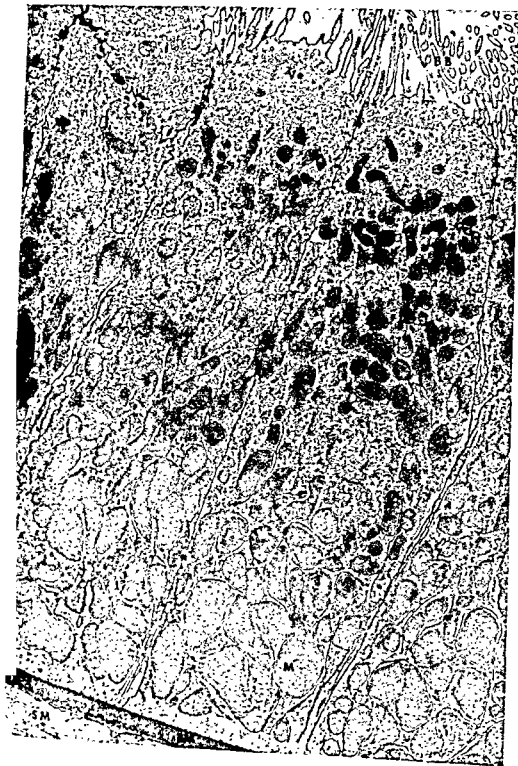


PLATE 5

EXPLANATION OF FIGURE

- 8 An electron micrograph of the second major segment with a brush border. The profiles of the second major segment are characterized by long microvilli (BB), an apical layer of cytoplasm filled with vesicles (Ve), and abundant mitochondria (M) filling the rest of the cytoplasm. The first few cells of this region sometimes have some extremely large mitochondria (M) in the basal cytoplasm. A thick basement membrane (BM) and a layer of smooth muscle cells (SM) surround the tubule. Fixed by perfusion with osmium tetroxide buffered with *s*-collidine. $\times 5,900$.

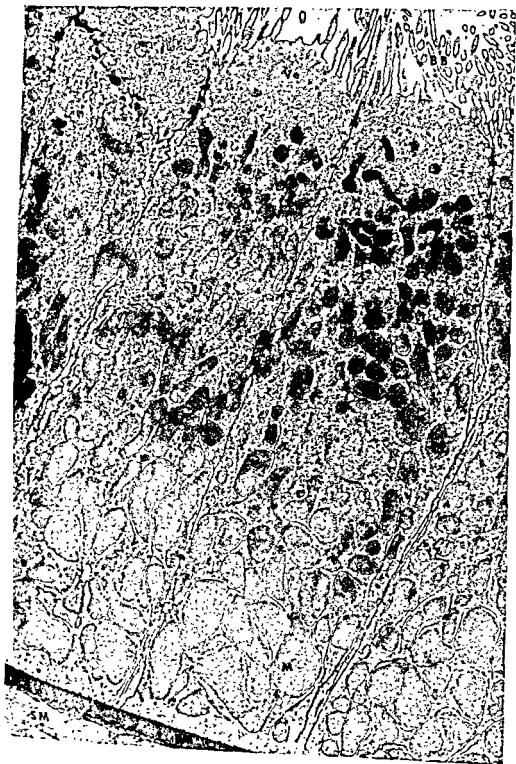


PLATE 6

EXPLANATION OF FIGURE

- 9 Electron micrograph of the third major segment with a brush border. The cells of the third major segment are similar in appearance to those of the second segment although they are lower in height, contain more rough-surfaced endoplasmic reticulum (ERG) and have a smaller apical zone of vesicles (Ve). Note slight expansion of lateral intercellular space (I). The tubule is surrounded by a thick basement membrane (BM) and a layer of smooth muscle cells (SM). Fixed by immersion in osmium tetroxide buffered with *s*-collidine. $\times 9,200$.



PLATE 6

EXPLANATION OF FIGURE

- 9 Electron micrograph of the third major segment with a brush border. The cell of the third major segment are similar in appearance to those of the second segment although they are lower in height, contain more rough-surface endoplasmic reticulum (ERG) and have a smaller apical zone of vesicles (Ve). Note slight expansion of lateral intercellular space (I). The tubule is surrounded by a thick basement membrane (BM) and a layer of smooth muscle cells (SM). Fixed by immersion in osmium tetroxide buffered with s-collidine. $\times 9,200$.



PLATE 7

EXPLANATION OF FIGURES

- 10 Electron micrograph showing the basal cytoplasm of a tubular cell fixed in osmium tetroxide. The smooth-surfaced membrane (arrows) seen in the basal cytoplasm do not often connect with the basal plasmalemma. Fixed by vascular perfusion. $\times 28,400$.
- 11 Electron micrograph showing the basal cytoplasm of the tubular cell after fixation in a mixture of osmium tetroxide and glutaraldehyde. The smooth-surfaced membranes in the basal cytoplasm more frequently connect with the basal plasmalemma (arrows). Fixed by immersion. $\times 27,700$.
- 12 Electron micrograph showing the basal cytoplasm of a tubular cell after fixation in potassium permanganate. The basal plasmalemma is continuous with the smooth-surfaced membranes of the basal cytoplasm. However, occasional membranes are seen (arrows) which do not connect with the basal plasmalemma and appear to be endoplasmic reticulum. Fixed by immersion. $\times 69,700$.

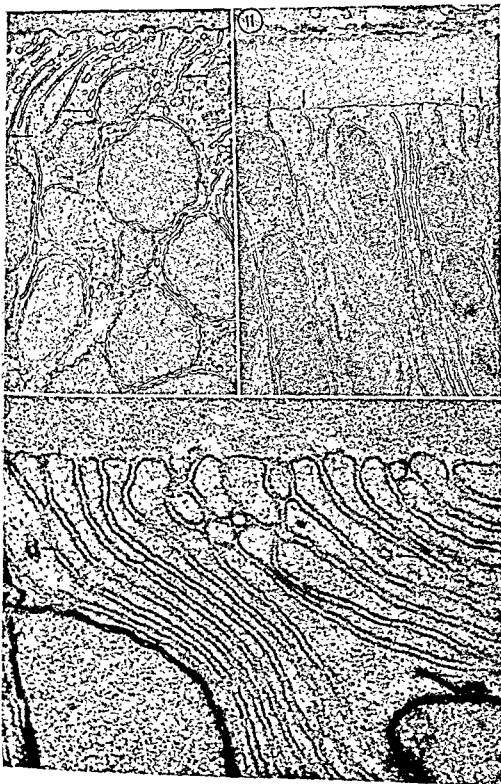


PLATE 8

EXPLANATION OF FIGURE

- 13 Electron micrograph of a collecting tubule. The collecting tubules are characterized by apical mucous granules (MG) with a layer of fine filaments (F) lying basal to most of the granules. The mitochondria are smaller than those found in the other regions of the tubule although they are abundant. A well developed Golgi apparatus (Go) and occasional lipid droplets (LD) are seen. Fixed by immersion in osmium tetroxide buffered in *s*-collidine. $\times 13,000$.

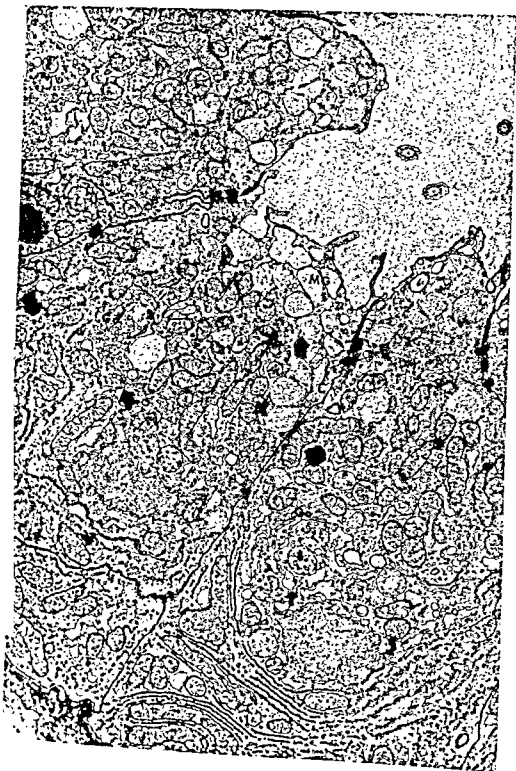


PLATE 8

EXPLANATION OF FIGURE

- 13 Electron micrograph of a collecting tubule. The collecting tubules are characterized by apical mucous granules (MG) with a layer of fine filaments (F) lying basal to most of the granules. The mitochondria are smaller than those found in the other regions of the tubule although they are abundant. A well-developed Golgi apparatus (Go) and occasional lipid droplets (LD) are seen. Fixed by immersion in osmium tetroxide buffered in *s*-collidine. $\times 13,000$.



PLATE 9

EXPLANATION OF FIGURE

- 14 Electron micrograph of a large collecting duct. A large collecting duct is characterized by a layer of apical microvilli (Mv), a layer of mucous granules (MG), a large Golgi apparatus (Go), abundant but small mitochondria (M) and a thick coat of smooth muscle cells (SM) surrounding the tubule. Fixed by immersion in osmium tetroxide buffered with *s*-collidine. $\times 4,100$.



Uptake of Ferritin by Ileal Absorptive Cells in Suckling Rats. An Electron Microscope Study¹

DANIEL O. GRANEY²

Departments of Anatomy, University of California, San Francisco, California and Harvard Medical School, Boston, Massachusetts

ABSTRACT An electron microscopic study of the small intestine of rats from birth to 15 days of age has demonstrated a gradient of both structure and function along the length of the small intestine. During this period of development, only the ileum was found to absorb intact exogenous ferritin or colostral proteins. In newborn rats ferritin particles or milk proteins are incorporated by ileal absorptive cells into tubular invaginations of the apical plasmalemma which connect with vacuoles or cisternae in the apical cytoplasm. The ferritin particles are then transported by another vacuolar system to the supranuclear region where several such vacuoles coalesce to form a single supranuclear vacuole. After the first feeding the supranuclear vacuole is established in the ileal cells so that additional ingested proteins, whether ferritin or from milk, are transported from the cisternae directly to the supranuclear vacuole. There was no evidence in the present study to indicate that ferritin is transmitted from the ileal cell to the circulation. The subject of protein transport by the intestinal epithelium is reviewed briefly.

The mucosa of the ileum in neonatal guinea pigs, rodents, and carnivores differs markedly from the adult ileum in its morphology (Clark, '59; Kraehenbuhl, 1960; and Blanc, '66), cytochemical (Corl and Padykula, '65), and physiological characteristics (Brambell, '58, '66). Ileal absorptive cells from neonatal animals of these groups can incorporate ingested protein and transfer certain immune globulins from the absorptive cell into the circulation. This is an important mechanism for passive immunization of the newborn. Maternal antibodies secreted into the colostrum and milk can be absorbed and utilized by the suckling animal until active antibody synthesis is established. The incorporation and transport of protein by the ileum of suckling rats ceases about three weeks after birth when there is a transition to the typical adult type (Halliday, 1955a,b; Clark, '59). In some animals from the above species, particularly the rat and dog, there is also a prenatal transfer of antibody via the yolk sac and intestine. This is not an important pathway quantitatively in these animals, but in the rabbit and monkey prenatal transfer of proteins via the yolk sac and placenta, respectively, is the principal means of passive immunization.

In those species which absorb intact proteins during the suckling period, the fine structure of the intestinal absorptive cells in the ileum is distinguished from adult absorptive cells by the presence of many small apical cytoplasmic vesicles and a large supranuclear vacuole (Möllen-dorff, '24; Smith, '25; Comline, Roberts and Titchen, '51b; Comline, Pomeroy and Titchen, '53; Hill and Hardy, '56; Clark, '59; Payne and Marsh, '62; Anderson, '63; Grane, '64; Cornell and Padykula, '65; Kraehenbuhl et al., '66). Clark ('59) studied the uptake of proteins during the early postnatal period in rats and mice by examining the passage of gamma globulins and electron-dense particles across the intestinal mucosa. Three hours after feeding bovine gamma globulins he was able to localize them with a fluorescein-labeled antibody in the supranuclear inclusions of absorptive cells in the midportion of the small intestine and in associated lacteals and mesenteric lymph nodes. Electron microscopic studies with colloidal tracers revealed the uptake of gold and saccharated iron oxide particles into apical cytoplasmic

¹ This work was supported by grants CM 406-06 and HE 04512 from the USPHS, National Institutes of Health, and Predoctoral Fellowship No. GM-21,246.

² Present address: Department of Biological Structure, University of Washington School of Medicine, Seattle, Washington 98105.

Preparation of tissues

animals were anesthetized by an injection of nembutal (0.04 gm body weight) and a laparotomy performed to expose the intestinal tract. Small samples of the proximal jejunum and terminal ileum were excised, cut in small blocks and immediately placed in fixative.

The fixatives used were 3% glutaraldehyde in 0.1 M sodium cacodylate or phosphate buffer (Millonig, '62) and 1% osmium tetroxide in phosphate buffer (Millonig, '62) for one to two hours prior to dehydration. The tissues were either rapidly dehydrated in graded alcohols or, in some cases, were dehydrated in acetone and then fixed in the block with 0.5-1% potassium permanganate according to the method of Parsons ('61). After dehydration the tissues were embedded in Epon Araldite (Luft, '61). Thick sections (1-2 μ) were cut on an ultramicrotome and stained either by light microscopy after staining with toluidine blue or by electron microscopy. Thin sections were mounted on copper grids with a substrate consisting of either formvar or celloidin and a carbon film and were doubly stained with uranyl acetate (Watson, '58) and alkaline lead citrate (Ryenolds, '63; Venable and Coggeshall, '65).

OBSERVATIONS

Regional variations in the gross morphology of the small intestine

The duodenum and jejunum in the normal suckling animal can be distinguished from the ileum by their creamy white color in contrast to the brownish-yellow or amber color of the ileum (Möllerndorff, '24). The distinctive regional coloration of the small intestine corresponds with regional differences in absorptive function of the small intestine that are observed after feeding suckling animals ferritin or colloidal tracers, e.g., carbon or trypan blue.

After young rats are gavaged with a solution of ferritin, there is no change in the creamy color of the jejunum when examined at intervals of 0.5, 1, 2, 4, 6 or 24 hours. When the intestine is opened, the presence of the tracer is revealed by a

reddish-brown color in the lumen of the jejunum 30 minutes after feeding, but all of the tracer can be washed away from the mucosal surface by gentle rinsing in saline. In contrast, one hour after feeding ferritin the normal amber color of the upper ileum changes to an intense reddish brown. By two hours after gavage, the ferritin solution completely traverses the small intestine, and the entire ileal mucosa is a reddish-brown color. This is in striking contrast to the pale jejunal mucosa. If other tracers are used, such as trypan blue, hemoglobin or carbon, the amber color of the ileum becomes masked by the color of the tracer. None of the tracers used could be washed from the ileal mucosa with saline rinses, and the pigmentation was still present 24 hours after feeding (the longest time point studied).

These simple macroscopic observations suggest that the jejunum is not important in the uptake of ferritin or particulate tracers. However, light and electron microscopic studies of this area were undertaken in order to verify these conclusions and to compare the cytological features of jejunal and ileal mucosa at various times and under both conditions of fasting and suckling.

Light microscopy

Jejunum. The cytological detail of columnar absorptive cells in the jejunal mucosa of newborn rats (prior to suckling) and fasting young rats is very similar to that of the adult. The apical cytoplasm in all of these cells has a coarse granularity which is probably due to the presence of mitochondria (figs. 1, 3, 5). Particulate inclusions are not prominent. However, in tissues fixed within 30 minutes after young rats are allowed to suckle, the jejunal absorptive cells contain variable amounts of lipid which is distributed in droplets throughout the apical cytoplasm and in the Golgi apparatus (fig. 3). Four hours after suckling, most of the jejunal cells have been cleared of obvious fat droplets (fig. 5).

The initial uptake of lipid by the intestinal mucosa occurs in cells located on the apices of the intestinal villi and later by cells situated along the sides and base of the villi as described previously in the

tubules, membrane-limited vesicles and the supranuclear vacuole. These findings were interpreted as evidence for pinocytotic activity in these cells. It was noted that the colloidal particles appeared to be retained by the lining cells, while some of the gamma globulins were discharged into the lamina propria. It has been shown by others (Comline, Roberts and Titchen, '51a; Hill and Hardy, '56; May and Whaler, '58; Pierce and Johnson, '60) that proteins are usually transported from the lamina propria by lymphatic rather than blood capillaries. More recently, it has been shown that proteins of 70,000 M.W. or less are absorbed via portal blood (Balfour and Comline, '59; Pierce, Risdall and Shaw, '64).

In the current study, ferritin, a naturally occurring electron-dense protein, was introduced into the gastrointestinal tract of suckling rats in order to study further the absorption of intact protein at this stage of development. In particular, it was of interest to determine whether this tracer protein would be transferred from the intestinal lining cells to the lamina propria and thus establish the successive steps in the pathway of protein absorption.

MATERIALS AND METHODS

Animals and experimental grouping

Long-Evans and Charles River rats from newborn to 15 days of age were divided into the following groups:

Controls. (1) Newborn rats separated from the mother prior to suckling, (2) newborn rats separated from the mother 0.5, 1 and 2 hours after suckling, and (3) young rats, 4-15 days of age, separated from the mother 0.5, 1, 2, 3, 4, 6 and 8 hours after suckling. Some of these animals were maintained in a fasting state (no solid or liquid food) for periods up to 24 hours.

Lipid studies. Two 15-day-old rats were separated from the mother and given 1 ml of Mazola corn oil via a gastric tube. The animals were subsequently killed after intervals of one and two hours respectively.

Ferritin studies. Ferritin was administered to newborn rats prior to suckling and to suckling rats up to 15 days of age. A small polyethylene tube (P.E. 10-50) was

passed into the esophagus of an anesthetized animal and 0.1 or 0.2 ml of a lyophilized ferritin solution was injected from a tuberculin syringe attached to the tube.

Preparation of gross specimens

Five 5-day-old suckling rats were used for a special macroscopic study of the small intestine. One animal was a normal suckling control and the remaining four each received one of the following solutions by gastric tube: (1) 0.2 ml of a 1% ferritin solution, (2) 0.5 ml of a 1% blue solution, (3) 0.2 ml of a 10% hemoglobin solution, and (4) 0.3 ml of an India ink solution. The animals were killed 2 hours after gavage and the entire small intestine from gastroduodenal junction to caecum was excised and placed in normal saline. A pair of fine scissors was used to open the intestine and expose the mucosa. The specimen was then rinsed in several changes of physiological salt solution and fixed *in toto* in 10% calcium-formol.

Dialysis procedure for ferritin solutions

The ferritin solution used in this study was obtained from either of two commercial sources (Nutritional Biochemical Corporation, Cleveland, Ohio; Pentex Corporation, Kankakee, Illinois). Both commercial preparations of ferritin, approximately 10 gm% in concentration, were similarly crystallized from extracts of horse spleen with cadmium sulfate. It was, therefore, necessary to dialyze the ferritin solution against a chelating agent, ethylene-di-nitrilo-tetracetic acid (EDTA), to remove toxic cadmium contamination (for details see Farquhar and Palade, '64). The ferritin solution was then rendered isotonic by a subsequent dialysis against Gey's balanced salt solution for 72 hours with three changes (Wissig, '64).

The final dialyzed solution of ferritin was passed through a Millipore (0.45 μ) and refrigerated in a sterile amber-stoppered serum bottle. Under these conditions the ferritin solution may be stored for at least 6 months without significant deterioration. Small quantities may be removed as needed with a syringe and needle.

Preparation of tissues

animals were anesthetized by an eritoneal injection of nembutal (0.04 n body weight) and a laparotomy performed to expose the intestinal Small samples of the proximal jeju- and terminal ileum were excised, cut mall blocks and immediately placed ative.

fixatives used were 3% glutaralde- in 0.1 M sodium cacodylate or phos- buffer (Millonig, '62) and 1% osmi- troxide in phosphate buffer (Millonig, or one to two hours prior to dehydra- The tissues were either rapidly de- ated in graded alcohols or, in some , were dehydrated in acetone and ed in the block with 0.5-1% po- m permanganate according to the od of Parsons ('61). After dehydra- the tissues were embedded in Epon alditite (Luft, '61). Thick sections (1- were cut on an ultramicrotome and ined either by light microscopy after ing with toluidine blue or by electron oscopy. Thin sections were mounted opper grids with a substrate consisting ther formvar or celloidin and a carbon and were doubly stained with uranyl ate (Watson, '58) and alkaline lead ts (Ryenolds, '63; Venable and Cogges- l, '65).

OBSERVATIONS

Regional variations in the gross morphology of the small intestine

The duodenum and jejunum in the nor- al suckling animal can be distinguished m the ileum by their creamy white color contrast to the brownish-yellow or am- r color of the ileum (Möllendorff, '24). ne distinctive regional coloration of the all intestine corresponds with regional ifferences in absorptive function of the all intestine that are observed after eeding suckling animals ferritin or col- idal tracers, e.g., carbon or trypan blue.

After young rats are gavaged with a so- ation of ferritin, there is no change in the reamy color of the jejunum when exam- ned at intervals of 0.5, 1, 2, 4, 6 or 24 ours. When the intestine is opened, the esence of the tracer is revealed by a

reddish-brown color in the lumen of the jejunum 30 minutes after feeding, but all of the tracer can be washed away from the mucosal surface by gentle rinsing in saline. In contrast, one hour after feeding ferritin the normal amber color of the up- per ileum changes to an intense reddish brown. By two hours after gavage, the ferritin solution completely traverses the small intestine, and the entire ileal mucosa is a reddish-brown color. This is in striking contrast to the pale jejunal mucosa. If other tracers are used, such as trypan blue, hemoglobin or carbon, the amber color of the ileum becomes masked by the color of the tracer. None of the tracers used could be washed from the ileal mucosa with saline rinses, and the pigmentation was still present 24 hours after feeding (the longest time point studied).

These simple macroscopic observations suggest that the jejunum is not important in the uptake of ferritin or particulate tracers. However, light and electron micro- scopic studies of this area were undertaken in order to verify these conclusions and to compare the cytological features of jejunal and ileal mucosa at various times and under both conditions of fasting and suckling.

Light microscopy

Jejunum. The cytological detail of col- umnar absorptive cells in the jejunal mu- cosa of newborn rats (prior to suckling) and fasting young rats is very similar to that of the adult. The apical cytoplasm in all of these cells has a coarse granularity which is probably due to the presence of mitochondria (figs. 1, 3, 5). Particulate in- clusions are not prominent. However, in tissues fixed within 30 minutes after young rats are allowed to suckle, the jejunal ab- sorptive cells contain variable amounts of lipid which is distributed in droplets throughout the apical cytoplasm and in the Golgi apparatus (fig. 3). Four hours after suckling, most of the jejunal cells have been cleared of obvious fat droplets (fig. 5).

The initial uptake of lipid by the intes- tinal mucosa occurs in cells located on the apices of the intestinal villi and later by cells situated along the sides and base of the villi as described previously in the

adult rat (Hewitt, '54; Palay and Karlin, '59b; Ladman, Padykula and Strauss, '63).

The uptake of milk lipid by the jejunal mucosa in ferritin-fed animals appeared to be the same as in normal control animals. There was no evidence of ferritin uptake by the jejunal absorptive cells, e.g., dense vacuoles; and jejunal tissue from either ferritin-fed or control animals could not be distinguished by light microscopic study.

Ileum. The appearance of ileal absorptive cells in the newborn rat prior to suckling (fig. 2) is similar to the jejunal absorptive cells in the same animal. In some young, the ileal absorptive cells contain a few small vesicles in the apical cytoplasm, deep to the area of the terminal web. Their number was variable, but in no case were there as many vesicles in the newborn as in the suckled or ferritin-fed animals.

After the young have suckled, the appearance of the ileal absorptive cells changes conspicuously, acquiring a unique character which distinguishes them from other absorptive cells in the proximal part of the intestine. A large vacuolar structure appears in the supranuclear area, displacing the nucleus toward the base of the cell (figs. 4, 9). In the suckling pig, a large cytoplasmic vacuole is formed at the base of the absorptive cell and the nucleus assumes an apical position (Payne and Marsh, '62; Mattisson and Karlsson, '66; Sibalin and Björkman, '66; Vodovar and Fléchon, '66). The contents of the vacuoles vary. They may contain either homogeneous dense material, clumps of dense material aggregated about the periphery of the vacuole; or their contents may appear as a meshwork of finely vacuolated, flocculent material. The size of the vacuole varies depending upon whether it is located in an absorptive cell on the apex or base of a villus. The largest vacuoles were usually located in cells on the apex of the villus, with a gradation in size to the smallest located in absorptive cells on the base of the villus. Cells in the crypts of Lieberkühn do not contain supranuclear vacuoles. The apparent local absorption gradient located in an apico-basal direction along the height of the villi is reminiscent of that observed during absorption of fat in the jejunum of suckling young and that reported for the adult jejunum during fat

absorption (Hewitt, '54; Palay and Karlin, '59b). The vacuole persists in the supranuclear region even when the animal is fasted for periods of up to 24 hours (fig. 7).

Fine structure

The fine structure of intestinal epithelial cells of suckling rats has been described previously (Clark, '59; Kraebühl et al., '66; Dunn, '67). However, some structural features have not been considered heretofore and, in particular, the cytological differences between the proximal half of the small intestine (duodenum to jejunum) and the distal half (ileum) have not been emphasized. These differences which are not apparent in the adult, represent a longitudinal differentiation of ultrastructure in the small intestine of the suckling rat and presumably underlie the specialized absorptive function of the proximal and distal small intestine.

Jejunum. The fine structure of jejunal absorptive cells from either newborn rats (prior to suckling) or suckling rats (which are subsequently fasted) is indistinguishable and is comparable to the fine structure of jejunal absorptive cells in fasted adult rats (Palay and Karlin, '59a; Cardé, Badenhhausen and Porter, '67).

When jejunal absorptive cells of young rats were examined 30 minutes to 2 hours after suckling, osmiophilic droplets, presumably lipid, were observed distending the endoplasmic reticulum of the apical cytoplasm. At later periods, the Golgi vesicles and intercellular spaces become distended with lipid droplets, appearing finally in the lamina propria. The matrix of these lipid droplets often appears extracted and sometimes only a thin shell of dense material remains. This was more consistent finding after glutaraldehyde fixation than with osmium fixation. In an attempt to produce better visualization of the pathway of lipid through the jejunal cell, Mazola corn oil was given by gastric tube to two suckling rats and the jejunums subsequently fixed in osmium (fig. 8). The pathway of the lipid through the jejunal cells appears to be the same whether the animal is fed milk or corn oil. In either case, it is not sufficiently different from the studies of adult jejunum

and Karlin, '59b; Cardell et al., '67) to warrant discussion here.

In the jejunal cells of suckling rats absorb lipid in quantity, the present investigation has not demonstrated the capacity of these cells to absorb protein. Ferritin was not observed in the jejunal cells, at any time interval, after it was administered to either fasting or suckling rats, even though its presence in the jejunal lumen could be verified by the color of the contents at the time of autopsy.

There were no obvious differences between jejunal and ileal lining cells of newborn rats (prior to suckling) when studied by light microscopy, but an electron microscopic examination reveals a fundamental difference in their ultrastructure. The plasmalemma in the intermicrovillus spaces of ileal absorptive cells forms invaginations extending for some distance into the apical cytoplasm (figs. 10, 11). These invaginations often branch and anastomose with others from neighboring intermicrovillus spaces as they penetrate the cytoplasm. The resulting labyrinth of interconnected tubules is confined to a band or zone across the apical part of the cell, intermingled with mitochondria and elements of the endoplasmic reticulum (figs. 10, 11). Ultimately, the tubules terminate in a vacuolar structure or perhaps a better term is cistern, since there are vacuoles of similar size which apparently do not have tubular connections (figs. 10, 11, 14). Within the lumen of these tubules and cisternae there is a fine, flocculent material, but prior to suckling the quantity of this material is not significant. After suckling, however, the dominant feature of these cells is the abundance of this flocculent material throughout the tubular labyrinth and within the cisternae. This substance is similar to that described by Clark ('59) and is a proteinaceous material, presumably derived from the milk and succus entericus. In addition, large vacuoles without obvious tubular connections contain this material also and appear to coalesce, forming the single, large vacuole in the supranuclear region described earlier in this paper. An amorphous material identical to that in the supranuclear vacuole was noted also in the intercellular space (fig. 9). The supranuclear vacuole persists in

ileal absorptive cells, at least in those on the upper three-fourths of the villus, even when the animal is fasted for 18-24 hours (fig. 6). With the normal feeding cycle of the young, this means that supranuclear vacuoles are present in the ileum from the first meal until about three weeks after birth when the ileal cells are gradually replaced by cells typical of the mucosa of the adult. After fasting the cells on the basal part of the villus resemble the ileal cells from newborn animals, i.e., they contain a tubular apparatus with its associated cisternae but lack supranuclear vacuoles. The flocculent material within the tubular apparatus is sparse. Presumably, these are differentiating cells which have migrated up the villus during the fasting period.

After ferritin gavage, individual ferritin molecules were identified in the intestinal lumen, intermicrovillus spaces, and within the invaginations of the apical plasmalemma of ileal lining cells (figs. 11-14). Within 1.5 hours after administration of ferritin the tubular apparatus contains the ferritin tracer, as do the associated vacuoles or cisternae (figs. 13, 14). Vacuoles without associated tubules are predominant in the supranuclear area and contain ferritin in high concentration also. It is not clear whether the smooth-surfaced vacuoles bud off from the cisternae or represent cisternae which have lost their tubular connections. In any event, these vacuoles migrate to the supranuclear area where they coalesce, forming a single large vacuole (fig. 14). The progressive increase in size of this vacuole, as successive ferritin-filled vacuoles migrate from the apical area and fuse with it, ultimately results in formation of the definitive supranuclear vacuole. The nucleus is gradually displaced basally to accommodate the expanding vacuole.

On occasion, ferritin particles are seen in crystalline patterns within the smooth-surfaced vacuoles adjacent to the supranuclear vacuole as well as in the supranuclear vacuole itself. More often, the content of the tubular apparatus, apical vacuoles, and supranuclear vacuoles is heterogeneous, consisting of both ferritin particles and a fine, flocculent material

similar to that observed in suckling controls.

The successive steps in the formation of the supranuclear vacuole described above pertain to the newborn rat and the changes which occur after the first meal, whether it consists of milk or ferritin. In older suckling animals, the supranuclear vacuole is already established, so that when additional protein is ingested and taken into the apical tubules and cisternae, the smooth-surfaced vacuoles shuttle the protein directly to the existing supranuclear vacuole. In this study, the supranuclear vacuole appears to represent the terminus of the absorptive pathway for ferritin in the intestinal epithelial cell. It was not observed in association with the Golgi apparatus and there was no evidence to indicate that ferritin was transported from the lining cells to the intercellular space or lamina propria. This is in disagreement with the report of Kraehenbuhl, Gloor and Blanc ('67). A few particles were observed free in the cytoplasm, but these might represent endogenous ferritin or ferritin artifactually released from the tubules and vacuoles. The use of glutaraldehyde fixation proved crucial in this regard. Multiple attempts with osmium tetroxide as a primary fixative in combination with a spectrum of buffer systems, consistently resulted in the diffuse distribution of ferritin molecules throughout the cytoplasm of jejunal absorptive cells, the intercellular space, and the lamina propria. Ferritin was retained within membrane-limited systems only when glutaraldehyde was used as the primary fixative.

DISCUSSION

Morphological and functional gradients in the small intestine

The existence of an apico-basal gradient in the structure and function of an adult intestinal villus has been recognized for some time (review by Padykula, '62). The results of the present study have emphasized a longitudinal or proximo-distal gradient in the ultrastructural characteristics of the intestinal lining cells of suckling rats which is related to regional differences in their specific absorptive functions.

The proximal part of the small intestine actively absorbs lipid, but it does not absorb intact protein. This interpretation is supported by the observation that neither ferritin nor aggregates of amorphous precipitated material originating from the milk were identified in lining cells of the duodenum or jejunum of the young rat. Moreover, there is no tubular apparatus; the apical cytoplasm of jejunal lining cells is comparable to that found in the ileum, and therefore, the jejunum appears to lack the morphological apparatus necessary for absorption of intact proteins.

In two papers reporting ferritin absorption by the jejunum of adult rats (Card et al., '67; Casley-Smith, '67) the experiments were done using ligated intestinal segments and a much higher concentration of ferritin than the one employed in the study. The quantity of ferritin taken up under these conditions was very small compared with that absorbed by the ileum of suckling rats; therefore, the ability of the jejunum to absorb significant amounts of intact protein under normal conditions remains to be demonstrated. The ileum of the suckling rat absorbs protein primarily but it can absorb lipid also. Cornell and Padykula ('65) have shown that the ileum of the suckling rat can absorb an emulsified lipid when it is injected into the intestinal lumen. From the observations in the present study and those of Cornell and Padykula ('65), the apical tubular apparatus and supranuclear vacuole do not play an obvious role in the absorption of lipid, at least particulate lipid. In view of the current concepts of lipid absorption (Cardell et al., '67); Strauss and Ito, '65) it is conceivable that free fatty acids and other soluble lipids enter the tubular labyrinth where they diffuse into the apical cytoplasm and subsequently become esterified in the endoplasmic reticulum. Under normal physiological conditions, however, it appears that only small quantities of lipid reach the distal part of the small intestine because of the efficiency with which lipid is absorbed in the proximal part. In addition to the differences in structure and function described above, there are variations in the enzymatic activities between the proximal and distal small intestine which is further evidence of a linea

functional gradient; both β -glucuronidase (Heringova, Jirsova and Koldovsky, '65) and β -galactosidase (Koldovsky and Chytil, '65) activities are higher in the ileum than in the jejunum of suckling animals. Acid phosphatase activity is greater in the ileum and has been demonstrated by histochemical means to be in association with the perinuclear vacuole and adjacent small vacuoles (Cornell and Padykula, '65; Sherry, '66).

Alkaline phosphatase activity, however, is greater in the duodenum than in either the jejunum or ileum (Moog, '51, '62; Koldovsky, Faltova, Hahn and Vacek, '61). It is interesting to note that whereas alkaline phosphatase activity increases after day 15, β -glucuronidase and β -galactosidase activities decrease. All of the changes in the activities of the enzymes mentioned above can be delayed by adrenalectomy or induced precociously by administration of cortisone (Moog, '62; Koldovsky and Chytil, '65; Heringova et al., '65). It should be emphasized that in addition to regional qualitative differences in the morphological, enzymatic, and functional features which distinguish the jejunum and ileum, there are also quantitative changes occurring within each of these regions during the course of the suckling period. In the rat, this period is 21 days, but in other animals it may be considerably less. These points have not always been appreciated by some investigators, resulting in erroneous generalizations about intestinal histophysiology.

Mechanism of protein uptake by intestinal epithelial cells

Schechtman ('56) has emphasized that there are two distinct steps in the movement of proteins across a cellular layer. The first step, in the case of the intestinal epithelial cell, is the uptake of the protein at the surface of the cell and the second is the discharge of protein from the lateral and/or basal surface of the cell. The tacit assumption is that proteins cannot enter the lamina propria by passing directly through the intercellular spaces. There is no evidence at present for the intercellular passage of protein through the intestinal epithelium. There is, however, both physiological and immunological data (Brambell,

'58, '67; Clark, '59) which show that proteins are incorporated nonselectively into intestinal lining cells of certain suckling animals. A variety of proteins and colloidal particles can be incorporated into the cell, e.g., albumin, gamma globulin, saccharated iron oxide (Clark, '59), ferritin (Graney, '64, '65; Kraehenbuhl et al., '67) and peroxidase (Straus, '65), but only specific proteins are discharged from the cells. The mechanism of this discharge will be discussed in the following section.

The rat is born with an antibody titer approximately one-sixteenth that of the maternal serum, but by the second or third day after birth it is equal to or exceeds that in the maternal serum (Halliday, '55b). During the postnatal period, the rat continues to absorb intact antibodies until day 20, although the quantity absorbed begins to decrease after day 15 (Culbertson, '39; Halliday, '57; Clark, '59).

The rate of transfer can be quite rapid; measurable quantities of antibody appear in the circulation of the young rat within 30 minutes after feeding immune serum. By three hours the circulating titer has attained a maximum concentration (Halliday, '55a).

Clark ('59) first suggested that protein was incorporated into the intestinal epithelial cells of suckling rats and mice by the process of pinocytosis. This concept has been reiterated for the suckling puppy (Rubin, '66), piglet (Mattisson and Karlsson, '66; Sibalín and Björkman, '66; Vodovar and Flechon, '66) and rat (Kraehenbuhl et al., '67). The morphological observations of the present study do not seem to be completely consistent with this concept. Ferritin particles enter the apices of the lining cell through a tubular labyrinth and not by incorporation into vacuoles resulting from folding of the surface membrane as in the original concept of pinocytosis (Lewis, '31). Similarly, there was no pinocytotic uptake of ferritin in *quania* (Palade, '53) by vesicles of either the smooth-surfaced or coated variety, although this phenomenon has been observed in several other systems (Wissig, '58; Fawcett, '65).

An alternative viewpoint is that the apical tubules and their cisternal terminals are a relatively stable system within the

apical cytoplasm and that the lumen of this system is confluent with the intestinal lumen, i.e., extracellular. This would provide an access for nonspecific diffusion of protein, or other substances for that matter, from the intestinal lumen through the apical tubules and into the cisternae or vacuolar terminals of the tubules. The precise means by which protein moves from the cisternae to the supranuclear vacuole remains elusive. From Clark's studies ('59) and the results obtained with ferritin there is little doubt that the nonselective incorporation of protein proceeds past the point of the cisternae and as far as the supranuclear vacuole. Whether this occurs by a pinching off of small vesicles from the cisternae or from a separate vacuolar system is unknown. There is histochemical evidence which supports to some extent the concept of two separate membrane systems. Cornell and Padykula ('65) have shown that the apical cisternae (apical droplet in their terminology) are rich in esterase, whereas the supranuclear vacuole and adjacent small vacuoles contain both acid phosphatase and esterase activities. Since the supranuclear vacuole is formed in newborn young by the successive coalescence of vacuoles in the supranuclear region, some form of a vesicular transport system must be operating.

Selective discharge of protein from intestinal lining cells

An electron microscopic examination of the ileum from at least ten rats removed at intervals varying from 30 minutes to 24 hours after feeding ferritin has not demonstrated the passage of ferritin beyond the point of the supranuclear vacuole. This disagrees with the results of Kraehenbuhl et al. ('67) who described the movement of ferritin to the basal area of the supranuclear vacuole where some of the particles were incorporated into Golgi vesicles while others appeared to migrate freely through the cytoplasm and lateral cell membrane into the intercellular space. They noted ferritin in blood and lymphatic capillaries within the lamina propria also. The free movement of ferritin through the cytoplasm and lateral cell membrane is open to question on the grounds of inadequate fixation. Their results, however,

seemed to be substantiated by immunological data. Using a double-diffusion technique with an Ouchterlony plate they obtained a precipitin line between ferritin antibody and sera from young rats that had received ferritin solution 60-90 minutes previously by intraduodenal injection. In early pilot experiments of the present study, ferritin was administered to young rats by injecting the solution directly through the anterior abdominal wall into the stomach, which, in the suckling rat, was full of milk and readily visualized. However, when the abdomen was opened to remove a sample of intestinal tissue it was obvious that a seepage of ferritin had occurred through the needle hole into the peritoneal cavity, even though the injection was made with a 30-gauge needle. To avoid such leakage the gavage method was subsequently employed. It seems possible that a similar leakage could occur from the duodenum particularly during the pumping action of peristaltic movements. Therefore, the intestinal uptake of ferritin reported by Kraehenbuhl et al. ('67) may actually represent absorption of ferritin from the peritoneal cavity via diaphragmatic lymphatics.

Transmission of proteins from intestinal lining cells to the circulation of young rats is a highly selective process. Apparently these cells can distinguish between various classes of serum proteins (Bangham and Terry, '57) as well as homologous and heterologous proteins. When immune sera are prepared from a single antigen in different species and fed separately to suckling rats, the highest titer of circulating antibody is attained with homologous serum, while a lower titer is noted with heterologous sera from more distally related species (Halliday, '57). This and other related evidence suggested that the structure or configuration of a protein is important in the process of selective transmission. It has been demonstrated that fragments of pepsin refined (Brambell, Hemmings and Oakley, '59) or papain digested antibodies (Brambell, Hemmings, Oakley and Porter, '60) are transmitted to the circulation at quite different rates. Fragments I and II, produced by papain digestion (Porter, '58, '59) contain the antibody reactive sites but are not trans-

ated to the circulation whereas Fragment III, the antigenic part of the antibody transmitted readily (Brambell et al., '60). Brambell, Halliday and Morris ('58) have postulated that the mechanism of selection may be related to receptor sites which act as a receptor-substrate system recognizing a specific part of the protein. Pierce and Smith ('67a) have noted that interpretation of some of the studies by Brambell et al. is complicated by the fact that their serum assays detected only complete serum agglutinins and did not account for incomplete antibodies. This is particularly significant in light of recent findings by Morris ('65) demonstrating incomplete agglutinins in the sera of young rats after feeding heterologous immune sera. Similar data were obtained by Pierce and Smith ('67a) using newborn pigs. In view of these facts, some reassessment of the mechanism of selective transmission of proteins seems necessary; previous experiments should be repeated using more refined immunological techniques.

Molecular weights and size of proteins have been discounted in the past as a determinant of the transmissibility of proteins (Brambell, '58, '66; Hemmings and Jones, '62). However, its significance may be more important than previously realized. For example, a very small protein such as bovine insulin, 36,000 M.W. in dimeric form, is transmitted to the circulation of suckling mice (Kelly, '60) and rats (Mosinger, Placer and Koldovsky, '59) in sufficient quantities to induce hypoglycemia. But very large proteins, IgM immunoglobulins, 10⁶ M.W. and ferritin, 150,000 M.W. are not transmitted (Morris, '65; Graney, '64).

Besides some of the sophisticated immunological and *in vitro* techniques now available, recent advances have been made in tagging antibodies with electron opaque markers. This method should allow one to follow the pathway of discharged proteins at the ultrastructural level. The evidence at present, though purely circumstantial, indicates that proteins are discharged at the lateral cell membrane, pass through the intercellular space and enter the lamina propria. A similar pathway has been described for the yolk sac (Padykula, Deren and Wilson, '66). Amorphous pre-

cipitated material, identical to the contents of the supranuclear vacuole and blood capillaries of the lamina propria, is often observed in the intercellular spaces of the ileum during suckling, but it is not observed in the jejunum. This material is not observed in the intercellular spaces of the jejunal or ileal epithelium of the adult rat. There is, however, a similar precipitated material in the intercellular spaces of intestinal epithelium in humans who have certain protein losing enteropathies, e.g., intestinal lymphangiectasia (Dobbins, '66).

Digestion and fate of ferritin and colostral protein

There are at least two enzymatic environments which ingested proteins must survive before reaching the circulation, the first is in the lumen of the gastrointestinal tract and the second is in the ileal lining cell itself. Proteolytic activity in the small intestine of newborn rats is high, and does not differ significantly from the activity in adult intestine (Noack, Koldovsky, Friedrich, Heringova, Jirsova and Schenk, '66). Survival of proteins in the intestinal lumen is apparently related to a low activity of digestive enzymes in the stomach. Mosinger et al. ('59) have shown that the proteolytic activity of the gastric contents is low in newborn rats, but increases significantly after day 21. These changes correspond with the morphological development of the parietal and chief cells in the gastric glands (Manville and Lloyd, '32; Kammeraad, '42; Hill, '56).

Acid phosphatase and other hydrolytic enzymes have been localized histochemically in the supranuclear vacuole of ileal lining cells (Cornell and Padykula, '65; Straus, '65; Shervy, '66) which would indicate an active lysosomal activity in these cells. It should be mentioned from a comparative standpoint, an apical tubular apparatus with an esterase positive vacuolar system and a second vacuolar system with both esterase and acid phosphatase activities is found in other cell types besides the ileal lining cell, e.g., cells of the proximal convoluted tubule of the kidney (Straus, '64) and yolk sac endoderm (Padykula, '58; Sorokin and Padykula, '64; Lambson, '66). It is not known whether all proteins

must pass through the supranuclear vacuole prior to discharge, or if transmitted proteins bypass the vacuole. It is known that only about 10% of ingested proteins are actually transmitted across the epithelium (Morris, '65; Bamford, '66; Pierce and Smith, '67a,b); the remaining presumably are degraded by the lining cells.

It has been suggested (Brambell et al., '58; Leissring and Anderson, '61; Anderson, '65; Morris, '64; Brambell, '66) that the protein distributed about the periphery of supranuclear vacuoles, may be adsorbed or bound to the limiting membrane of the vacuole. It was further speculated that the binding of the protein may in some way protect it from the proteolytic activity in the vacuole. In the present study there was no evidence to indicate specific binding of ferritin to either the surface membrane or the limiting membranes of the tubular system or supranuclear vacuole. Using the tetrad structure of the micellar core of ferritin as a criterion of its integrity, there was no evidence of ferritin degradation 18 hours after feeding. This is not a good parameter, however, since all ferritin molecules are not necessarily oriented favorably to visualize the micelles. In addition, Mاتيoli and Baker ('63) have described a ferritinic form of hemosiderin as an intermediate in the degradation of ferritin to nonferritinic hemosiderin. The half-life of intestinal lining cells in the suckling animals is about 20% longer than in the adult (Koldovsky, Sunshine and Kretchmer, '66) so that considerable intracellular digestion of protein may occur before the cells are sloughed into the intestinal lumen.

ACKNOWLEDGMENTS

The author gratefully acknowledges the valuable assistance of Steven L. Wissig and Don W. Fawcett for their criticism of the manuscript.

LITERATURE CITED

- Anderson, J. W. 1963 Ultrastructural correlates of protein transport. *J. Cell Biol.*, 19: 4A-5A.
- 1965 Ultrastructural correlates of intestinal protein absorption. In: *Macromolecular Aspects of Protein Absorption and Excretion in the Mammalian Intestine*. Rept. of 50th Ross Conf. on Pediatric Res. D. C. Heiner, ed. Ross Laboratories, Columbus, 46-50.
- Balfour, W. E., and R. S. Comline 1959 The specificity of the intestinal absorption of immunoglobulin molecules by the new-born calf. *J. Physiol.*, 148: 77-78.
- Bamford, D. R. 1966 Studies *in vitro* of the passage of serum proteins across the intestinal wall of young rats. *Proc. Roy. Soc. (London)*, Ser. B, 166: 30-45.
- Bangham, D. R., and R. J. Terry 1957 The absorption of 131 I labelled homologous and heterologous serum proteins fed orally to rats. *Biochem. J.*, 66: 579-583.
- Brambell, F. W. R. 1958 The passive immunity of the young mammal. *Biol. Rev. Camb. Phil. Soc.*, 33: 488-531.
- 1966 The transmission of immunity from mother to young and the catabolism of immunoglobulins. *Lancet*, no. 7473, Serial 19 November, 1087-1093.
- Brambell, F. W. R., R. Halliday and I. G. McEwen 1958 Interference by human and bovine serum and serum protein fractions with the sorption of antibodies by suckling rats and mice. *Proc. Roy. Soc. (London)*, Ser. B, 151: 1-11.
- Brambell, F. W. R., W. A. Hemmings and C. Oakley 1959 The relative transmission of natural and pepsin-refined homologous and heterologous antigens from the uterine cavity to the foetal circulation in the rabbit. *Proc. Roy. Soc. (London)*, Ser. B, 150: 312-317.
- Brambell, F. W. R., W. A. Hemmings, C. L. Oakley and R. R. Porter 1960 The relative transmission of the fractions of papain hydrolyzed homologous γ -globulin from the uterine cavity to the foetal circulation in the rabbit. *Proc. Roy. Soc. (London)*, Ser. B, 151: 478-482.
- Cardell, Robert R., Jr., Susan Badenhansen and Keith R. Porter 1967 Intestinal triphosphate absorption in the rat. An electron microscopic study. *J. Cell Biol.*, 34: 123-155.
- Casley-Smith, J. R. 1967 The passage of ferritin into jejunal epithelial cells. *Experientia*, 23: 370-371.
- Clark, Sam L., Jr. 1959 The ingestion of proteins and colloidal materials by columnar absorptive cells of the small intestine in suckling rats and mice. *J. Biophysic. Biochem. Cytol.*, 5: 41-49.
- Comline, R. S., H. E. Roberts and D. A. Titch 1951a Route of absorption of colostrum globulin in the newborn animal. *Nature*, 167: 562-563.
- 1951b Histological changes in the epithelium of the small intestine during protein absorption in the newborn animal. *Nature*, 168: 84-85.
- Comline, R. S., R. W. Pomeroy and D. A. Titch 1953 Histological changes in the intestine during colostrum absorption. *J. Physiol.*, 101: 6P.
- Cornell, Richard, and H. A. Padykula 1963 Cytochemical study of intestinal absorption in the postnatal rat. *Anat. Rec.*, 151: 339.
- Culbertson, J. T. 1939 The immunization of rats of different age groups against *Trypanosoma lewisi* by the administration of special antiserum *per os*. *J. Parasitol.*, 25: 181-192.

- ns, W. O., III 1966 Electron microscopic study of the intestinal mucosa in intestinal phagocytosis. *Gastroenterology*, 51: 1004-17.
- ., J. S. 1967 The fine structure of the absorptive epithelial cells of the developing small intestine of the rat. *J. Anat.*, 101: 57-68.
- har, Marilyn, and George E. Palade 1961 Mercurial permeability: II. Ferritin transfer across the glomerular capillary wall in newborn rats. *J. Expil. Med.*, 114: 699-716.
- xtt, Donald W. 1965 Surface specialization of absorbing cells. *J. Histochem. Cytochem.*, 13: 75-81.
- ey, D. O. 1964 The uptake of ferritin by endocytosis in intestinal lining cells of suckling rats. *Anat. Rec.*, 148: 286.
- 1965 Uptake of ferritin by intestinal lining cells of suckling rats. In: *Macromolecular Aspects of Protein Absorption and Excretion in the Mammalian Intestine*. Rept. of 50th Conf. on Pediatric Res. D. C. Heiner, ed. Ross Laboratories, Columbus, 18-27.
- iday, R. 1955a The absorption of antibodies from immune sera by the gut of the young rat. *Proc. Roy. Soc. (London) Ser. B*, 43: 408-413.
- 1955b Prenatal and postnatal transmission of passive immunity to young rats. *Proc. Roy. Soc. (London) Ser. B*, 144: 427-430.
- 1957 The absorption of antibody from immune sera and from mixtures of sera by the gut of the young rat. *Proc. Roy. Soc. (London) Ser. B*, 148: 92-103.
- ummings, W. A., and R. E. Jones 1962 The occurrence of macroglobulin antibodies in maternal and foetal sera of rabbits as determined by gradient centrifugation. *Proc. Roy. Soc. (London) Ser. B*, 157: 27-32.
- ringova, A., V. Jirsova and O. Koldovsky 1965 Postnatal development of β -glucuronidase in the jejunum and ileum of rats. *Can. J. Biochem. Physiol.*, 43: 173-178.
- twitt, W. 1954 A histochemical study of fat absorption in the small intestine of the rat. *Quart. J. Microscop. Sci.*, 95: 153-157.
- ll, K. J. 1956 Gastric development and antibody transference in the lamb, with some observations on the rat and guinea-pig. *Quart. J. Expil. Physiol.*, 41: 421-432.
- ll, K. J., and W. S. Hardy 1956 Histological and histochemical observations on the intestinal cells of lambs and kids absorbing colostrum. *Nature*, 178: 1353-1354.
- umeraad, A. 1942 The development of the gastro-intestinal tract of the rat. I. Histogenesis of the epithelium of the stomach, small intestine and pancreas. *J. Morph.*, 70: 323-351.
- elly, W. A. 1960 Passage of insulin through the wall of the gastro-intestinal tract of the infant rat. *Nature*, 184: 1245-1246.
- oldovsky, O., E. Faltova, P. Hahn and Z. Vacek 1961 The functional development of the gastro-intestinal tract in rats. In: *The Development of Homeostasis*. E. F. Adolph, ed. Publishing House of the Czechoslovak Academy of Sciences, Prague, 133-163.
- Koldovsky, O., and F. Chytil 1965 Postnatal development of β -galactosidase activity in the small intestine of the rat. Effect of adrenalectomy and diet. *Biochem. J.*, 94: 266-270.
- Koldovsky, O., P. Sunshine and N. Kretschmer 1966 Cellular migration of intestinal epithelia in suckling and weaned rats. *Nature*, 212: 1389-1390.
- Kraehenbuhl, J.-P., E. Gloor and B. Blanc 1966 Morphologie comparée de la muqueuse intestinale de deux espèces animales aux possibilités d'absorption protéique neonatale différentes. *Z. Zellforsch. Mikroskop. Anat.*, 70: 209-219.
- 1967 Réorption intestinale de la ferritine chez deux espèces animales aux possibilités d'absorption protéique néonatale différentes. *Z. Zellforsch. Mikroskop. Anat.*, 76: 170-186.
- Ladman, Aaron J., H. A. Padykula and E. W. Strauss 1963 A morphological study of fat transport in the human jejunum. *Am. J. Anat.*, 112: 389-420.
- Lambson, Roger O. 1966 An electron microscopic visualization of transport across rat visceral yolk sac. *Am. J. Anat.*, 118: 31-37.
- Leissring, J. C., and J. W. Anderson 1961 The transfer of serum proteins from mother to young in the guinea pig. III. Postnatal studies. *Am. J. Anat.*, 109: 175-179.
- Lewis, W. H. 1931 Pinocytosis. *Bull. Johns Hopkins Hosp.*, 49: 17-23.
- Luft, John H. 1961 Improvements in epoxy embedding methods. *J. Biophysic. Biochem. Cytol.*, 9: 409-414.
- Manville, I. A., and R. W. Lloyd 1932 The hydrogen ion concentration of the gastric juice of fetal and newborn white rats. *Am. J. Physiol.*, 100: 394-401.
- Matioli, Gastone T., and Richard F. Baker 1963 Denaturation of ferritin and its relationship with hemosiderin. *J. Ultrastruct. Res.*, 8: 477-490.
- Mattsson, A. G. M., and B. W. Karlsson 1966 Electron microscopic and immunochemical studies on the small intestine of newborn piglets. *Arkiv Zool.*, 18: 575-587.
- May, A. J., and B. C. Whaler 1958 The absorption of *Colistridium botulinum* Type A toxin from the alimentary canal. *Brit. J. Expil. Pathol.*, 39: 307-316.
- Millonig, G. 1962 Further observations on a phosphate buffer for osmium solutions in fixation. In: *Electron Microscopy*. Sydney S. Breese, Jr., ed. Vol. II, Academic Press, New York and London, P-8.
- Möllendorff, Von Wilhelm 1924 Ueber die anteilnahme des darmepithels an der verarbeitung enteral und parenteral zugeführter saurer Farbstoffe. *Munch. Med. Wochenschrift*, 71: 569-572.
- Moog, F. 1951 The functional differentiation of the small intestine. II. The differentiation of phosphatase in the duodenum of the mouse. *Expil. Zool.*, 118: 187-208.
- 1962 Developmental adaptations of alkaline phosphatases in the small intestine. *Federation Proc.*, 21: 51-56.

- Morris, I. G. 1964 The transmission of antibodies and normal gamma globulins across the young mouse gut. *Proc. Roy. Soc. (London)* Ser. B, 160: 276-292.
- 1965 The transmission of anti-*Brucella abortus* agglutinins across the gut in young rats. *Proc. Roy. Soc. (London)* Ser. B, 163: 402-416.
- Mosinger, B., Z. Placer and O. Koldovsky 1959 Passage of insulin through the wall of the gastro-intestinal tract of the infant rat. *Nature*, 184: 1245-1246.
- Noack, R., O. Koldovsky, M. Friedrich, A. Heringova, V. Jirsova and G. Schenk 1966 Proteolytic and peptidase activities of the jejunum and ileum of the rat during postnatal development. *Biochem. J.*, 100: 775-778.
- Padykula, H. A. 1958 A histochemical and quantitative study of enzymes of the rat's placenta. *J. Anat.*, 92: 118-129.
- Padykula, Helen A. 1962 Recent functional interpretations of intestinal morphology. *Federation Proc.*, 21: 873-879.
- Padykula, Helen A., J. J. Deren and T. H. Wilson 1966 Development of structure and function in the mammalian yolk sac. I. Development, morphology and vitamin B12 uptake of the rat yolk sac. *Dev. Biol.*, 13: 311-348.
- Palade, George 1953 Fine structure of blood capillaries. *J. Appl. Phys.*, 24: 1424.
- Palay, S. L., and L. J. Karni 1959a An electron microscopic study of the intestinal villus. I. The fasting animal. *J. Biophysic. Biochem. Cytol.*, 5: 363-371.
- 1959b An electron microscopic study of the intestinal villus. II. The pathway of fat absorption. *J. Biophysic. Biochem. Cytol.*, 5: 373-383.
- Parsons, D. F. 1961 A simple method for obtaining increase contrast in Araldite sections by using postfixation staining of tissues with potassium permanganate. *J. Biophysic. Biochem. Cytol.*, 11: 492-497.
- Payne, L. C., and C. Marsh 1962 Absorption of gamma globulin by the small intestine. *Federation Proc.*, 21: 909-912.
- Pierce, A. E., and P. Johnson 1960 Ultra-centrifuge and electrophoretic studies on the proteinuria of the newborn calf. *J. Hyg.*, 58: 247-260.
- Pierce, A. E., P. C. Risdall and B. Shaw 1964 Absorption of orally administered insulin by the newly born calf. *J. Physiol.*, 171: 203-215.
- Pierce, A. E., and M. W. Smith 1967a The intestinal absorption of pig and bovine immune lactoglobulin and human serum albumin by the new-born pig. *J. Physiol.*, 190: 1-18.
- 1967b The *in vitro* transfer of bovine immune lactoglobulin across the intestine of new-born pigs. *J. Physiol.*, 190: 19-34.
- Porter, R. R. 1958 Separation and isolation of fractions of rabbit gamma-globulin containing the antibody and antigenic combining site. *Nature*, 181: 670-671.
- 1959 The hydrolysis of rabbit gamma globulin and antibodies with crystalline trypsin. *Biochem. J.*, 73: 119-126.
- Reynolds, E. S. 1963 The use of lead citrate at high pH as an electron-opaque stain in electron microscopy. *J. Cell Biol.*, 17: 208-212.
- Rubin, C. E. 1966 Electron microscopic study of triglyceride absorption in man. *Gastroenterology*, 50: 65-77.
- Schechtman, A. M. 1956 Uptake and transport of macromolecules by cells with special reference to growth and development. In: *National Review of Cytology*. G. Bourne and F. Danielli, eds. Vol. 5, Academic Press, New York, 303-322.
- Shervey, Paul 1966 Observations on the development and histochemistry of the intestinal inclusion bodies of the suckling rat. *Anat. Rec.*, 154: 422.
- Sibalin, M., and N. Björkman 1966 On the structure and absorptive function of the jejunal villi during the early suckling period. *Exptl. Cell Res.*, 44: 165-174.
- Smith, T. 1925 Hydropic stages in the intestinal epithelium of new-born calves. *J. Exp. Med.*, 41: 81-88.
- Sorokin, S. P., and H. A. Padykula 1964 Differentiation of the rat's yolk sac in organ culture. *Am. J. Anat.*, 114: 457-479.
- Strauss, E., and S. Ito 1965 Autoradiography and biochemical study of linolenic acid-¹⁴C absorption by hamster intestine from micelles *in vitro*. *J. Cell Biol.*, 27: 101A.
- Straus, Werner 1964 Cytochemical observations on the relationship between lysosomes and phagosomes in kidney and liver by combined staining for acid phosphatase and by venously injected horseradish peroxidase. *Cell Biol.*, 20: 497-507.
- 1965 Cytologic observations on protein uptake and transport in kidney and liver. *Macromolecular Aspects of Protein Absorption and Excretion in the Mammalian Intestine*. Rept. of 50th Ross Conf. on Pediatric Res. D. Heiner, ed. Ross Laboratories, Columbus, 45.
- Venable, John H., and Richard Coggeshall 1964 A simplified lead citrate stain for use in electron microscopy. *J. Cell Biol.*, 25: 407-408.
- Vodovar, N., and J.-E. Flechon 1966 La cellule épithéliale absorbante de l'intestin grege d'ultrastructure. *Ann. Biol. Animale Biochim. Biophys.*, 6: 13-32.
- Watson, M. L. 1958 Staining of tissue sections for electron microscopy with heavy metals. *Biochem. Biophys. Cytol.*, 4: 475-478.
- Wissig, Steven L. 1958 An electron microscopic study of the permeability of capillaries in the rat. *Anat. Rec.*, 130: 467-468.
- Wissig, S. L. 1964 Personal communication.

Note added in proof: Since this manuscript was submitted for publication, two significant review articles related to this topic have appeared in *The Handbook of Physiology*, Section 6: Alimentary Canal, Volume III. Intestinal Absorption, page 1099 and I. G. Morris, page 1491.

PLATE 1

EXPLANATION OF FIGURES

The following six figures are photomicrographs of the small intestine from three different animals: newborn rat prior to suckling, nine-day-old suckling rat and a ten-day-old rat fasted for 18 hours prior to sacrifice. Each pair of photographs represent Epon sections of jejunal and ileal tissue taken from the same animal and stained with toluidine blue. Magnification in figures 1-6 is the same, $\times 1744$.

- 1 Jejunum of newborn rat prior to suckling. There are no obvious inclusions visible in the cytoplasm.
- 2 Ileum of newborn rat prior to suckling. Morphological pattern of the ileum not significantly different from jejunum (fig. 1).
- 3 Jejunum of nine-day-old suckling rat. Lipid droplets are observed in Golgi apparatus, intercellular spaces and lamina propria.
- 4 Ileum of nine-day-old suckling rat. Numerous clear vacuoles are noted in the apical cytoplasm. Supranuclear area occupied by large vacuole containing amorphous dense material.
- 5 Jejunum of ten-day-old suckling rat fasted for 18 hours prior to sacrifice. At this stage, cytoplasm is completely clear of lipid material. Typical fasting state.
- 6 Ileum of ten-day-old suckling rat fasted for 18 hours prior to sacrifice. Apical vacuoles and a supranuclear vacuole are still observed in the cytoplasm of the lining cells.

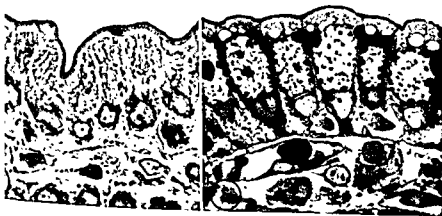
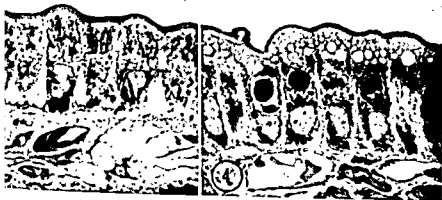
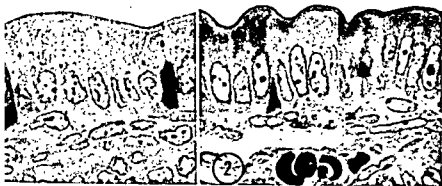


PLATE 2

EXPLANATION OF FIGURES

- 7 Jejunum of 15-day-old suckling rat fasted for 18 hours prior to sacrifice. Electron micrograph showing mitochondria, membranes of the smooth- and rough-surfaced endoplasmic reticulum. Note absence of any extensive plasmalemmal invaginations. $\times 29,000$.
- 8 Jejunum of 15-day-old suckling rat, two hours after receiving 1 ml of corn oil. Osmiophilic droplets, presumably lipid, are observed in both smooth- and rough-surfaced endoplasmic reticulum. $\times 25,000$.

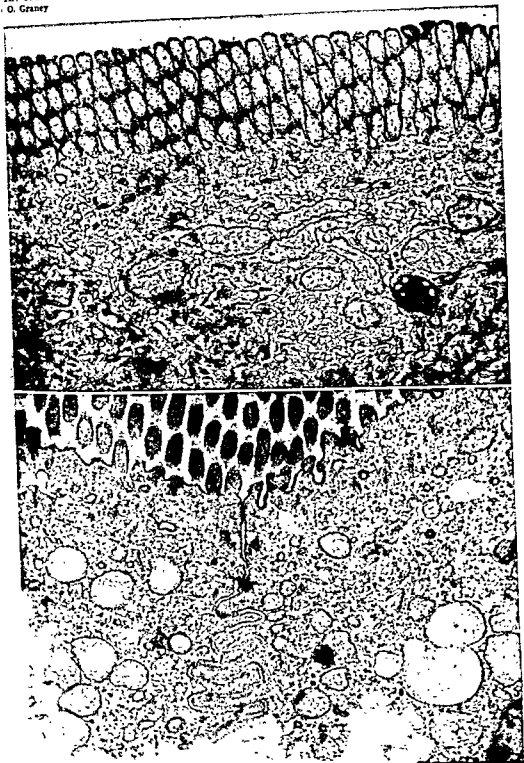
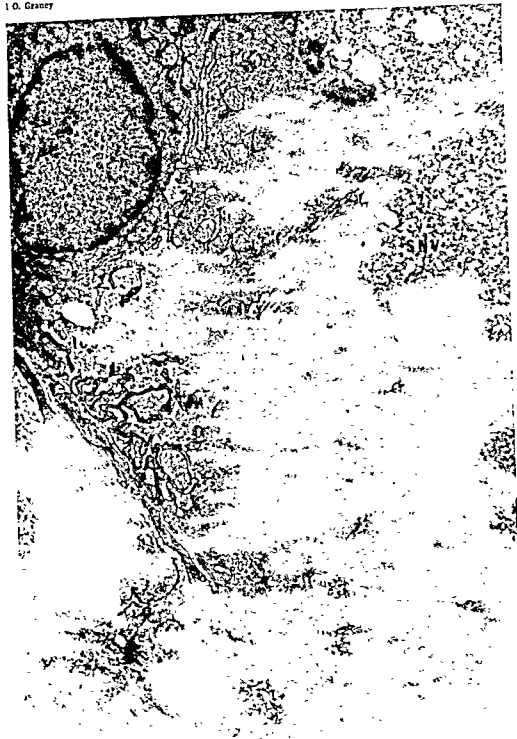
TIN UPTAKE BY ILEAL LINING CELLS
O. Graney

PLATE 2

EXPLANATION OF FIGURES

- 7 Jejunum of 15-day-old suckling rat fasted for 18 hours prior to sacrifice. Electron micrograph showing mitochondria, membranes of the smooth- and rough-surfaced endoplasmic reticulum. Note absence of any extensive plasmalemmal invaginations. $\times 29,000$.
- 8 Jejunum of 15-day-old suckling rat, two hours after receiving 1 ml of corn oil. Osmiophilic droplets, presumably lipid, are observed in both smooth- and rough-surfaced endoplasmic reticulum. $\times 25,000$.

ITIN UPTAKE BY ILEAL LINING CELLS
I. O. Grady

Uptake of Ferritin by Ileal Absorptive Cells in Suckling Rats. An Electron Microscope Study¹

DANIEL O. GRANEY²

Departments of Anatomy, University of California, San Francisco, California and Harvard Medical School, Boston, Massachusetts

ABSTRACT An electron microscopic study of the small intestine of rats from birth to 15 days of age has demonstrated a gradient of both structure and function along the length of the small intestine. During this period of development, only the ileum was found to absorb intact exogenous ferritin or colostral proteins. In newborn rats ferritin particles or milk proteins are incorporated by ileal absorptive cells into tubular invaginations of the apical plasmalemma which connect with vacuoles or cisternae in the apical cytoplasm. The ferritin particles are then transported by another vacuolar system to the supranuclear region where several such vacuoles coalesce to form a single supranuclear vacuole. After the first feeding the supranuclear vacuole is established in the ileal cells so that additional ingested proteins, whether ferritin or from milk, are transported from the cisternae directly to the supranuclear vacuole. There was no evidence in the present study to indicate that ferritin is transmitted from the ileal cell to the circulation. The subject of protein transport by the intestinal epithelium is reviewed briefly.

The mucosa of the ileum in neonatal ungulates, rodents, and carnivores differs markedly from the adult ileum in its morphological (Clark, '59; Kraehenbuhl, Moor and Blanc, '66), cytochemical (Correll and Padykula, '65), and physiological characteristics (Brambell, '58, '66). Ileal absorptive cells from neonatal animals of these groups can incorporate ingested protein and transfer certain immune globulin from the absorptive cell into the circulation. This is an important mechanism of passive immunization of the newborn. Maternal antibodies secreted into the colostrum and milk can be absorbed and utilized by the suckling animal until active antibody synthesis is established. The intake and transport of protein by the ileum of suckling rats ceases about three days after birth when there is a transition to the typical adult type (Halliday, Clark, '59). In some animals from other species, particularly the rat and rabbit, there is also a prenatal transfer of proteins via the yolk sac and intestine. This is not an important pathway quantitatively in these animals, but in the rabbit and monkey prenatal transfer of proteins via the yolk sac and placenta, respectively, is the principal means of passive immunization.

In those species which absorb intact proteins during the suckling period, the fine structure of the intestinal absorptive cells in the ileum is distinguished from adult absorptive cells by the presence of many small apical cytoplasmic vesicles and a large supranuclear vacuole (Möllen-dorff, '24; Smith, '25; Comline, Roberts and Titchen, '51b; Comline, Pomeroy and Titchen, '53; Hill and Hardy, '56; Clark, '59; Payne and Marsh, '62; Anderson, '63; Graney, '64; Cornell and Padykula, '65; Kraehenbuhl et al., '66). Clark ('59) studied the uptake of proteins during the early postnatal period in rats and mice by examining the passage of gamma globulins and electron-dense particles across the intestinal mucosa. Three hours after feeding bovine gamma globulins he was able to localize them with a fluorescein-labeled antibody in the supranuclear inclusions of absorptive cells in the midportion of the small intestine and in associated lacteals and mesenteric lymph nodes. Electron microscopic studies with colloidal tracers revealed the uptake of gold and saccharated iron oxide particles into apical cytoplasmic

¹ This work was supported by grants GM 406-06 and HE 04512 from the USPHS, National Institutes of Health, and Predoctoral Fellowship No. GM-21,346.

² Present address: Department of Biological Structure, University of Washington School of Medicine, Seattle, Washington 98105.

Preparation of tissues

The animals were anesthetized by an injection of nembutal (0.04 gm body weight) and a laparotomy performed to expose the intestinal tract. Small samples of the proximal jejunum and terminal ileum were excised, cut into small blocks and immediately placed in fixative.

The fixatives used were 3% glutaraldehyde in 0.1 M sodium cacodylate or phosphate buffer (Millonig, '62) and 1% osmium tetroxide in phosphate buffer (Millonig, '62) for one to two hours prior to dehydration. The tissues were either rapidly dehydrated in graded alcohols or, in some cases, were dehydrated in acetone and placed in the block with 0.5-1% potassium permanganate according to the method of Parsons ('61). After dehydration the tissues were embedded in Epon 812 or Araldite (Luft, '61). Thick sections (1-2 μ) were cut on an ultramicrotome and stained either by light microscopy after staining with toluidine blue or by electron microscopy. Thin sections were mounted on copper grids with a substrate consisting of either formvar or celloidin and a carbon film and were doubly stained with uranyl acetate (Watson, '58) and alkaline lead citrate (Ryenolds, '63; Venable and Coggeshall, '65).

OBSERVATIONS

Regional variations in the gross morphology of the small intestine

The duodenum and jejunum in the non-suckling animal can be distinguished from the ileum by their creamy white color contrast to the brownish-yellow or amber color of the ileum (Möllendorff, '24). The distinctive regional coloration of the intestine corresponds with regional differences in absorptive function of the intestine that are observed after feeding suckling animals ferritin or tracers, e.g., carbon or trypan blue. After young rats are gavaged with a solution of ferritin, there is no change in the color of the jejunum when examined at intervals of 0.5, 1, 2, 4, 6 or 24 hours. When the intestine is opened, the presence of the tracer is revealed by a

reddish-brown color in the lumen of the jejunum 30 minutes after feeding, but all of the tracer can be washed away from the mucosal surface by gentle rinsing in saline. In contrast, one hour after feeding ferritin the normal amber color of the upper ileum changes to an intense reddish brown. By two hours after gavage, the ferritin solution completely traverses the small intestine, and the entire ileal mucosa is a reddish-brown color. This is in striking contrast to the pale jejunal mucosa. If other tracers are used, such as trypan blue, hemoglobin or carbon, the amber color of the ileum becomes masked by the color of the tracer. None of the tracers used could be washed from the ileal mucosa with saline rinses, and the pigmentation was still present 24 hours after feeding (the longest time point studied).

These simple macroscopic observations suggest that the jejunum is not important in the uptake of ferritin or particulate tracers. However, light and electron microscopic studies of this area were undertaken in order to verify these conclusions and to compare the cytological features of jejunal and ileal mucosa at various times and under both conditions of fasting and suckling.

Light microscopy

Jejunum. The cytological detail of columnar absorptive cells in the jejunal mucosa of newborn rats (prior to suckling) and fasting young rats is very similar to that of the adult. The apical cytoplasm in all of these cells has a coarse granularity which is probably due to the presence of mitochondria (figs. 1, 3, 5). Particulate inclusions are not prominent. However, in tissues fixed within 30 minutes after young rats are allowed to suckle, the jejunal absorptive cells contain variable amounts of lipid which is distributed in droplets throughout the apical cytoplasm and in the Golgi apparatus (fig. 3). Four hours after suckling, most of the jejunal cells have been cleared of obvious fat droplets (fig. 5).

The initial uptake of lipid by the intestinal mucosa occurs in cells located on the apices of the intestinal villi and later by cells situated along the sides and base of the villi as described previously in the

tubules, membrane-limited vesicles and the supranuclear vacuole. These findings were interpreted as evidence for pinocytotic activity in these cells. It was noted that the colloidal particles appeared to be retained by the lining cells, while some of the gamma globulins were discharged into the lamina propria. It has been shown by others (Comline, Roberts and Titchen, '51a; Hill and Hardy, '56; May and Whaler, '58; Pierce and Johnson, '60) that proteins are usually transported from the lamina propria by lymphatic rather than blood capillaries. More recently, it has been shown that proteins of 70,000 M.W. or less are absorbed via portal blood (Balfour and Comline, '59; Pierce, Risdall and Shaw, '64).

In the current study, ferritin, a naturally occurring electron-dense protein, was introduced into the gastrointestinal tract of suckling rats in order to study further the absorption of intact protein at this stage of development. In particular, it was of interest to determine whether this tracer protein would be transferred from the intestinal lining cells to the lamina propria and thus establish the successive steps in the pathway of protein absorption.

MATERIALS AND METHODS

Animals and experimental grouping

Long-Evans and Charles River rats from newborn to 15 days of age were divided into the following groups:

Controls. (1) Newborn rats separated from the mother prior to suckling, (2) newborn rats separated from the mother 0.5, 1 and 2 hours after suckling, and (3) young rats, 4-15 days of age, separated from the mother 0.5, 1, 2, 3, 4, 6 and 8 hours after suckling. Some of these animals were maintained in a fasting state (no solid or liquid food) for periods up to 24 hours.

Lipid studies. Two 15-day-old rats were separated from the mother and given 1 ml of Mazola corn oil via a gastric tube. The animals were subsequently killed after intervals of one and two hours respectively.

Ferritin studies. Ferritin was administered to newborn rats prior to suckling and to suckling rats up to 15 days of age. A small polyethylene tube (P.E. 10-50) was

passed into the esophagus of an unanesthetized animal and 0.1 or 0.2 ml of a dialyzed ferritin solution was injected from a tuberculin syringe attached to the tubing.

Preparation of gross specimens

Five 5-day-old suckling rats were used for a special macroscopic study of the small intestine. One animal was a non-suckling control and the remaining four each received one of the following solutions by gastric tube: (1) 0.2 ml of a 1% ferritin solution, (2) 0.5 ml of a 1% blue solution, (3) 0.2 ml of a 10% hemoglobin solution, and (4) 0.3 ml of an 1% ink solution. The animals were killed 24 hours after gavage and the entire intestine from gastroduodenal junction to caecum was excised and placed in saline. A pair of fine scissors was used to open the intestine and expose the mucosa. The specimen was then rinsed in several changes of physiological salt solution and fixed *in toto* in 10% calcium-formol.

Dialysis procedure for ferritin solution

The ferritin solution used in this study was obtained from either of two commercial sources (Nutritional Biochemical Corporation, Cleveland, Ohio; Pentex Incorporated, Kankakee, Illinois). Both commercial preparations of ferritin, approximately 10 gm% in concentration, were similarly crystallized from extracts of horse spleen with cadmium sulfate. It was, therefore, necessary to dialyze the ferritin solution against a chelating agent, ethylene-di-nitrilo-tetracetic acid (EDTA), to remove toxic cadmium contaminants (for details see Farquhar and Palade, '61). The ferritin solution was then rendered isotonic by a subsequent dialysis against Gey's balanced salt solution for 72 hours with three changes (Wissig, '64).

The final dialyzed solution of ferritin was passed through a Millipore filter (0.45 μ) and refrigerated in a sterile rubber-stoppered serum bottle. Under these conditions the ferritin solution may be stored for at least 6 months without any significant deterioration. Small quantities may be removed as needed with a sterile syringe and needle.

Karlin, '59b; Cardell et al., '67) to want discussion here.

Although the jejunal cells of suckling absorb lipid in quantity, the present investigation has not demonstrated the capacity of these cells to absorb protein. Ferritin was not observed in the jejunal cells, any time interval, after it was administered to either fasting or suckling rats, though its presence in the jejunal lumen could be verified by the color of the contents at the time of autopsy.

Ileum. There were no obvious differences between jejunal and ileal lining cells in newborn rats (prior to suckling) when studied by light microscopy, but an electron microscopic examination reveals a fundamental difference in their ultrastructure. The plasmalemma in the intermicrovillus spaces of ileal absorptive cells forms invaginations extending for some distance to the apical cytoplasm (figs. 10, 11). These invaginations often branch and anastomose with others from neighboring intermicrovillus spaces as they penetrate the cytoplasm. The resulting labyrinth of interconnected tubules is confined to a band or zone across the apical part of the cell, intermingled with mitochondria and elements of the endoplasmic reticulum (figs. 10, 11). Ultimately, the tubules terminate in a vacuolar structure or perhaps a better term is cistern, since there are vacuoles of similar size which apparently do not have tubular connections (figs. 10, 11, 14). Within the lumen of these tubules and cisternae there is a fine, flocculent material, but prior to suckling the quantity of this material is not significant. After suckling, however, the dominant feature of these cells is the abundance of this flocculent material throughout the tubular labyrinth and within the cisternae. This substance is similar to that described by Clark ('59) and is a proteinaceous material, presumably derived from the milk and succus entericus. In addition, large vacuoles without obvious tubular connections contain this material also and appear to coalesce, forming the single, large vacuole in the supranuclear region described earlier in this paper. An amorphous material identical to that in the supranuclear vacuole was noted also in the intercellular space (fig. 13). The supranuclear vacuole persists in

ileal absorptive cells, at least in those on the upper three-fourths of the villus, even when the animal is fasted for 18-24 hours (fig. 6). With the normal feeding cycle of the young, this means that supranuclear vacuoles are present in the ileum from the first meal until about three weeks after birth when the ileal cells are gradually replaced by cells typical of the mucosa of the adult. After fasting the cells on the basal part of the villus resemble the ileal cells from newborn animals, i.e., they contain a tubular apparatus with its associated cisternae but lack supranuclear vacuoles. The flocculent material within the tubular apparatus is sparse. Presumably, these are differentiating cells which have migrated up the villus during the fasting period.

After ferritin gavage, individual ferritin molecules were identified in the intestinal lumen, intermicrovillus spaces, and within the invaginations of the apical plasmalemma of ileal lining cells (figs. 11-14). Within 1.5 hours after administration of ferritin the tubular apparatus contains the ferritin tracer, as do the associated vacuoles or cisternae (figs. 13, 14). Vacuoles without associated tubules are predominant in the supranuclear area and contain ferritin in high concentration also. It is not clear whether the smooth-surfaced vacuoles bud off from the cisternae or represent cisternae which have lost their tubular connections. In any event, these vacuoles migrate to the supranuclear area where they coalesce, forming a single large vacuole (fig. 14). The progressive increase in size of this vacuole, as successive ferritin-filled vacuoles migrate from the apical area and fuse with it, ultimately results in formation of the definitive supranuclear vacuole. The nucleus is gradually displaced basally to accommodate the expanding vacuole.

On occasion, ferritin particles are seen in crystalline patterns within the smooth-surfaced vacuoles adjacent to the supranuclear vacuole as well as in the supranuclear vacuole itself. More often, the content of the tubular apparatus, apical vacuoles, and supranuclear vacuoles is heterogeneous, consisting of both ferritin particles and a fine, flocculent material

adult rat (Hewitt, '54; Palay and Karlin, '59b; Ladman, Padykula and Strauss, '63).

The uptake of milk lipid by the jejunal mucosa in ferritin-fed animals appeared to be the same as in normal control animals. There was no evidence of ferritin uptake by the jejunal absorptive cells, e.g., dense vacuoles; and jejunal tissue from either ferritin-fed or control animals could not be distinguished by light microscopic study.

Ileum. The appearance of ileal absorptive cells in the newborn rat prior to suckling (fig. 2) is similar to the jejunal absorptive cells in the same animal. In some young, the ileal absorptive cells contain a few small vesicles in the apical cytoplasm, deep to the area of the terminal web. Their number was variable, but in no case were there as many vesicles in the newborn as in the suckled or ferritin-fed animals.

After the young have suckled, the appearance of the ileal absorptive cells changes conspicuously, acquiring a unique character which distinguishes them from other absorptive cells in the proximal part of the intestine. A large vacuolar structure appears in the supranuclear area, displacing the nucleus toward the base of the cell (figs. 4, 9). In the suckling pig, a large cytoplasmic vacuole is formed at the base of the absorptive cell and the nucleus assumes an apical position (Payne and Marsh, '62; Mattisson and Karlsson, '66; Sibalin and Björkman, '66; Vodovar and Fléchon, '66). The contents of the vacuoles vary. They may contain either homogeneous dense material, clumps of dense material aggregated about the periphery of the vacuole; or their contents may appear as a meshwork of finely vacuolated, flocculent material. The size of the vacuole varies depending upon whether it is located in an absorptive cell on the apex or base of a villus. The largest vacuoles were usually located in cells on the apex of the villus, with a gradation in size to the smallest located in absorptive cells on the base of the villus. Cells in the crypts of Lieberkühn do not contain supranuclear vacuoles. The apparent local absorption gradient located in an apico-basal direction along the height of the villi is reminiscent of that observed during absorption of fat in the jejunum of suckling young and that reported for the adult jejunum during fat

absorption (Hewitt, '54; Palay and Karlin, '59b). The vacuole persists in the supranuclear region even when the animal is fasted for periods of up to 24 hours (fig. 6).

Fine structure

The fine structure of intestinal epithelial cells of suckling rats has been described previously (Clark, '59; Kraehenbuhl et al., '66; Dunn, '67). However, some structural features have not been considered heretofore and, in particular, the cytological differences between the proximal half of the small intestine (duodenum and jejunum) and the distal half (ileum) have not been emphasized. These differences, which are not apparent in the adult, represent a longitudinal differentiation of ultrastructure in the small intestine of the suckling rat and presumably underlie the specialized absorptive function of the proximal and distal small intestine.

Jejunum. The fine structure of jejunal absorptive cells from either newborn rats (prior to suckling) or suckling rats (which are subsequently fasted) is indistinguishable and is comparable to the fine structure of jejunal absorptive cells in fasted adult rats (Palay and Karlin, '59a; Cardell, Badenhhausen and Porter, '67).

When jejunal absorptive cells of young rats were examined 30 minutes to 24 hours after suckling, osmophilic droplets, presumably lipid, were observed distending the endoplasmic reticulum of the apical cytoplasm. At later periods, the Golgi vesicles and intercellular spaces became distended with lipid droplets, appearing finally in the lamina propria. The matrix of these lipid droplets often appears contracted and sometimes only a thin shell of dense material remains. This was more consistent finding after glutaraldehyde fixation than with osmium fixation. In an attempt to produce better visualization of the pathway of lipid through the jejunal cell, Mazola corn oil was given to the gastric tube to two suckling rats and their jejunums subsequently fixed in osmium (fig. 8). The pathway of the lipid through the jejunal cells appears to be the same whether the animal is fed milk or corn oil. In either case, it is not sufficiently different from the studies of adult jejunum (Palay

1 Karlin, '59b; Cardell et al., '67) to rant discussion here.

41 the jejunal cells of suckling a absorb lipid in quantity, the present igation has not demonstrated the ca- these cells to absorb protein. Fer- was not observed in the jejunal cells, any time interval, after it was admin- to either fasting or suckling rats, m though its presence in the jejunal nen could be verified by the color of the , at the time of autopsy.

Ileum. There were no obvious differ- ces between jejunal and ileal lining cells newborn rats (prior to suckling) when idied by light microscopy, but an elec- m microscopic examination reveals a difference in their ultrastruc-

The plasmalemma in the intermicro- spaces of ileal absorptive cells forms extending for some distance the apical cytoplasm (figs. 10, 11). ese invaginations often branch and an- tomose with others from neighboring termicrovillus spaces as they penetrate e cytoplasm. The resulting labyrinth of urtherconnected tubules is confined to a and or zone across the apical part of the ill, intermingled with mitochondria and of the endoplasmic reticulum 10, 11). Ultimately, the tubules ter- in a vacuolar structure or perhaps better term is cistern, since there are acuoles of similar size which apparently do not have tubular connections (figs. 10, 1, 14). Within the lumen of these tubules cisternae there is a fine, flocculent ial, but prior to suckling the quantity of this material is not significant. After however, the dominant feature of cells is the abundance of this floccu- ial throughout the tubular laby- nth and within the cisternae. This sub- is similar to that described by Clark '59) and is a proteinaceous material, pre- umably derived from the milk and succus

In addition, large vacuoles with- obvious tubular connections contain material also and appear to coalesce, orming the single, large vacuole in the clear region described earlier in paper. An amorphous material identi- to that in the supranuclear vacuole was also in the intercellular space (fig.). The supranuclear vacuole persists in

ileal absorptive cells, at least in those on the upper three-fourths of the villus, even when the animal is fasted for 18-24 hours (fig. 6). With the normal feeding cycle of the young, this means that supranuclear vacuoles are present in the ileum from the first meal until about three weeks after birth when the ileal cells are gradually re- placed by cells typical of the mucosa of the adult. After fasting the cells on the basal part of the villus resemble the ileal cells from newborn animals, i.e., they con- tain a tubular apparatus with its associ- ated cisternae but lack supranuclear vac- uoles. The flocculent material within the tubular apparatus is sparse. Presumably, these are differentiating cells which have migrated up the villus during the fasting period.

After ferritin gavage, individual ferritin molecules were identified in the intestinal lumen, intermicrovillus spaces, and within the invaginations of the apical plasma- lemma of ileal lining cells (figs. 11-14). Within 1.5 hours after administration of ferritin the tubular apparatus contains the ferritin tracer, as do the associated vacu- oles or cisternae (figs. 13, 14). Vacuoles without associated tubules are predomi- nant in the supranuclear area and contain ferritin in high concentration also. It is not clear whether the smooth-surfaced vacu- oles bud off from the cisternae or represent cisternae which have lost their tubular connections. In any event, these vacuoles migrate to the supranuclear area where they coalesce, forming a single large vacu- ole (fig. 14). The progressive increase in size of this vacuole, as successive ferritin- filled vacuoles migrate from the apical area and fuse with it, ultimately results in for- mation of the definitive supranuclear vacu- ole. The nucleus is gradually displaced basally to accommodate the expanding vacu- ole.

On occasion, ferritin particles are seen in crystalline patterns within the smooth- surfaced vacuoles adjacent to the supra- nuclear vacuole as well as in the supra- nuclear vacuole itself. More often, the content of the tubular apparatus, apical vacuoles, and supranuclear vacuoles is heterogeneous, consisting of both ferritin particles and a fine, flocculent material

similar to that observed in suckling controls.

The successive steps in the formation of the supranuclear vacuole described above pertain to the newborn rat and the changes which occur after the first meal, whether it consists of milk or ferritin. In older suckling animals, the supranuclear vacuole is already established, so that when additional protein is ingested and taken into the apical tubules and cisternae, the smooth-surfaced vacuoles shuttle the protein directly to the existing supranuclear vacuole. In this study, the supranuclear vacuole appears to represent the terminus of the absorptive pathway for ferritin in the intestinal epithelial cell. It was not observed in association with the Golgi apparatus and there was no evidence to indicate that ferritin was transported from the lining cells to the intercellular space or lamina propria. This is in disagreement with the report of Kraehenbuhl, Gloor and Blanc ('67). A few particles were observed free in the cytoplasm, but these might represent endogenous ferritin or ferritin artifactiously released from the tubules and vacuoles. The use of glutaraldehyde fixation proved crucial in this regard. Multiple attempts with osmium tetroxide as a primary fixative in combination with a spectrum of buffer systems, consistently resulted in the diffuse distribution of ferritin molecules throughout the cytoplasm of jejunal absorptive cells, the intercellular space, and the lamina propria. Ferritin was retained within membrane-limited systems only when glutaraldehyde was used as the primary fixative.

DISCUSSION

Morphological and functional gradients in the small intestine

The existence of an apico-basal gradient in the structure and function of an adult intestinal villus has been recognized for some time (review by Padykula, '62). The results of the present study have emphasized a longitudinal or proximo-distal gradient in the ultrastructural characteristics of the intestinal lining cells of suckling rats which is related to regional differences in their specific absorptive functions.

The proximal part of the small intestine actively absorbs lipid, but it does not absorb intact protein. This interpretation is supported by the observation that neither ferritin nor aggregates of amorphous precipitated material originating from the milk were identified in lining cells of the duodenum or jejunum of the young rat. Moreover, there is no tubular apparatus in the apical cytoplasm of jejunal lining cells comparable to that found in the ileum; therefore, the jejunum appears to lack the morphological apparatus necessary for absorption of intact proteins.

In two papers reporting ferritin absorption by the jejunum of adult rats (Cardell et al., '67; Casley-Smith, '67) the experiments were done using ligated intestinal segments and a much higher concentration of ferritin than the one employed in the study. The quantity of ferritin taken up under these conditions was very small compared with that absorbed by the ileum of suckling rats; therefore, the ability of the jejunum to absorb significant amounts of intact protein under normal conditions remains to be demonstrated. The ileum of the suckling rat absorbs protein primarily but it can absorb lipid also. Cornell and Padykula ('65) have shown that the ileum of the suckling rat can absorb an emulsified lipid when it is injected into the intestinal lumen. From the observations in the present study and those of Cornell and Padykula ('65), the apical tubular apparatus and supranuclear vacuole do not play an obvious role in the absorption of lipid, at least particulate lipid. In view of the current concepts of lipid absorption (Cardell et al., '67; Strauss and Ito, '65) it is conceivable that free fatty acids and other soluble lipids enter the tubular lumen where they diffuse into the apical cytoplasm and subsequently become esterified in the endoplasmic reticulum. Under normal physiological conditions, however, it appears that only small quantities of lipid reach the distal part of the small intestine because of the efficiency with which lipid is absorbed in the proximal part. In addition to the differences in structure and function described above, there are variations in the enzymatic activities between the proximal and distal small intestine which is further evidence of a line-

functional gradient; both β -glucuronidase (Heringova, Jirsova and Koldovsky, '65) and β -galactosidase (Koldovsky and Chytil, '65) activities are higher in the ileum than in the jejunum of suckling animals. Acid phosphatase activity is greater in the ileum. It has been demonstrated by histochemistry means to be in association with the paranuclear vacuole and adjacent small vacuoles (Cornell and Padykula, '65; Sherry, '66).

Alkaline phosphatase activity, however, is greater in the duodenum than in either the jejunum or ileum (Moog, '51, '62; Koldovsky, Faltova, Hahn and Vacek, '61). It is interesting to note that whereas alkaline phosphatase activity increases after day 10, β -glucuronidase and β -galactosidase activities decrease. All of the changes in the activities of the enzymes mentioned above can be delayed by adrenalectomy or induced precociously by administration of exogenous cortisone (Moog, '62; Koldovsky and Chytil, '65; Heringova et al., '65). It should be emphasized that in addition to regional qualitative differences in the morphological, enzymatic, and functional features which distinguish the jejunum and ileum, there are also quantitative changes occurring within each of these regions during the course of the suckling period. In the rat, this period is 21 days, but in other animals it may be considerably less. These points have not always been appreciated by some investigators, resulting in erroneous generalizations about intestinal histophysiology.

Mechanism of protein uptake by intestinal epithelial cells

Schechtman ('56) has emphasized that there are two distinct steps in the movement of proteins across a cellular layer. The first step, in the case of the intestinal epithelial cell, is the uptake of the protein at the surface of the cell and the second is the discharge of protein from the lateral and/or basal surface of the cell. The tacit assumption is that proteins cannot enter the lamina propria by passing directly through the intercellular spaces. There is no evidence at present for the intercellular passage of protein through the intestinal epithelium. There is, however, both physiological and immunological data (Brambell,

'58, '67; Clark, '59) which show that proteins are incorporated nonselectively into intestinal lining cells of certain suckling animals. A variety of proteins and colloidal particles can be incorporated into the cell, e.g., albumin, gamma globulin, saccharated iron oxide (Clark, '59), ferritin (Graney, '64, '65; Kraehenbuhl et al., '67) and peroxidase (Straus, '65), but only specific proteins are discharged from the cells. The mechanism of this discharge will be discussed in the following section.

The rat is born with an antibody titer approximately one-sixteenth that of the maternal serum, but by the second or third day after birth it is equal to or exceeds that in the maternal serum (Halliday, '55b). During the postnatal period, the rat continues to absorb intact antibodies until day 20, although the quantity absorbed begins to decrease after day 15 (Culbertson, '39; Halliday, '57; Clark, '59).

The rate of transfer can be quite rapid; measurable quantities of antibody appear in the circulation of the young rat within 30 minutes after feeding immune serum. By three hours the circulating titer has attained a maximum concentration (Halliday, '55a).

Clark ('59) first suggested that protein was incorporated into the intestinal epithelial cells of suckling rats and mice by the process of pinocytosis. This concept has been reiterated for the suckling puppy (Rubin, '66), piglet (Mattisson and Karlsson, '66; Sibalin and Björkman, '66; Vodovar and Flechon, '66) and rat (Kraehenbuhl et al., '67). The morphological observations of the present study do not seem to be completely consistent with this concept. Ferritin particles enter the apices of the lining cell through a tubular labyrinth and not by incorporation into vacuoles resulting from folding of the surface membrane as in the original concept of pinocytosis (Lewis, '31). Similarly, there was no pinocytotic uptake of ferritin in *quania* (Palade, '53) by vesicles of either the smooth-surfaced or coated variety, although this phenomenon has been observed in several other systems (Wissig, '58; Fawcett, '65).

An alternative viewpoint is that the apical tubules and their cisternal terminals are a relatively stable system within the

apical cytoplasm and that the lumen of this system is confluent with the intestinal lumen, i.e., extracellular. This would provide an access for nonspecific diffusion of protein, or other substances for that matter, from the intestinal lumen through the apical tubules and into the cisternae or vacuolar terminals of the tubules. The precise means by which protein moves from the cisternae to the supranuclear vacuole remains elusive. From Clark's studies ('59) and the results obtained with ferritin there is little doubt that the nonselective incorporation of protein proceeds past the point of the cisternae and as far as the supranuclear vacuole. Whether this occurs by a pinching off of small vesicles from the cisternae or from a separate vacuolar system is unknown. There is histochemical evidence which supports to some extent the concept of two separate membrane systems. Cornell and Padykula ('65) have shown that the apical cisternae (apical droplet in their terminology) are rich in esterase, whereas the supranuclear vacuole and adjacent small vacuoles contain both acid phosphatase and esterase activities. Since the supranuclear vacuole is formed in newborn young by the successive coalescence of vacuoles in the supranuclear region, some form of a vesicular transport system must be operating.

Selective discharge of protein from intestinal lining cells

An electron microscopic examination of the ileum from at least ten rats removed at intervals varying from 30 minutes to 24 hours after feeding ferritin has not demonstrated the passage of ferritin beyond the point of the supranuclear vacuole. This disagrees with the results of Kraehenbuhl et al. ('67) who described the movement of ferritin to the basal area of the supranuclear vacuole where some of the particles were incorporated into Golgi vesicles while others appeared to migrate freely through the cytoplasm and lateral cell membrane into the intercellular space. They noted ferritin in blood and lymphatic capillaries within the lamina propria also. The free movement of ferritin through the cytoplasm and lateral cell membrane is open to question on the grounds of inadequate fixation. Their results, however,

seemed to be substantiated by immunological data. Using a double-diffusion technique with an Ouchterlony plate they tained a precipitin line between ferritin antibody and sera from young rats which had received ferritin solution 60-90 minutes previously by intraduodenal injection. In early pilot experiments of the present study, ferritin was administered to young rats by injecting the solution directly through the anterior abdominal wall into the stomach, which, in the rat, was full of milk and readily visualized. However, when the abdomen was opened to remove a sample of intestinal tissue it was obvious that a seepage of ferritin had occurred through the needle hole into the peritoneal cavity, even though the injection was made with a 30-gauge needle. To avoid such leakage the gavage method was subsequently employed. It is possible that a similar leakage could occur from the duodenum particularly during the pumping action of peristaltic movements. Therefore, the intestinal uptake of ferritin reported by Kraehenbuhl et al. ('67) may actually represent absorption of ferritin from the peritoneal cavity via diaphragmatic lymphatics.

Transmission of proteins from intestinal lining cells to the circulation of young rats is a highly selective process. Apparently these cells can distinguish between various classes of serum proteins (Bangham and Terry, '57) as well as homologous and heterologous proteins. When immune sera are prepared from a single antigen in different species and fed separately to suckling rats, the highest titer of circulating antibody is attained with homologous serum, while a lower titer is noted with heterologous sera from more distally related species (Halliday, '57). This and other related evidence suggested that the structure or configuration of a protein is important in the process of selective transmission. It has been demonstrated that fragments of pepsin refined (Brambell, Hemmings and Oakley, '59) or papain digested antibodies (Brambell, Hemmings, Oakley and Porter, '60) are transmitted to the circulation at quite different rates. Fragments I and II, produced by papain digestion (Porter, '58, '59) contain the antibody reactive sites but are not trans-

ed to the circulation whereas Fragment III, the antigenic part of the antibody, is transmitted readily (Brambell et al., '60). Brambell, Halliday and Morris ('58) have concluded that the mechanism of selection is related to receptor sites which act as a receptor-substrate system recognizing a specific part of the protein. Pierce and Smith ('67a) have noted that interpretation of some of the studies by Brambell et al. is complicated by the fact that their *in vitro* assays detected only complete serum agglutinins and did not account for incomplete antibodies. This is particularly significant in light of recent findings by Morris ('65) demonstrating incomplete agglutinins in the sera of young rats after feeding heterologous immune sera. Similar results were obtained by Pierce and Smith ('67a) using newborn pigs. In view of these facts, some reassessment of the mechanism of selective transmission of proteins seems necessary; previous experiments should be repeated using more refined immunological techniques.

Molecular weights and size of proteins have been discounted in the past as a determinant of the transmissibility of proteins (Brambell, '58, '66; Hemmings and Mes, '62). However, its significance may be more important than previously realized. For example, a very small protein such as bovine insulin, 36,000 M.W. in monomeric form, is transmitted to the circulation of suckling mice (Kelly, '60) and its (Mosinger, Placer and Koldovsky, '59) in sufficient quantities to induce hypoglycemia. But very large proteins, IgM immunoglobulins, 10⁶ M.W. and ferritin, 50,000 M.W. are not transmitted (Morris, '65; Graney, '64).

Besides some of the sophisticated immunological and *in vitro* techniques now available, recent advances have been made in tagging antibodies with electron opaque markers. This method should allow one to follow the pathway of discharged proteins at the ultrastructural level. The evidence at present, though purely circumstantial, indicates that proteins are discharged at the lateral cell membrane, pass through the intercellular space and enter the lamina propria. A similar pathway has been described for the yolk sac (Padykula, Jørgensen and Wilson, '66). Amorphous pre-

cipitated material, identical to the contents of the supranuclear vacuole and blood capillaries of the lamina propria, is often observed in the intercellular spaces of the ileum during suckling, but it is not observed in the jejunum. This material is not observed in the intercellular spaces of the jejunal or ileal epithelium of the adult rat. There is, however, a similar precipitated material in the intercellular spaces of intestinal epithelium in humans who have certain protein losing enteropathies, e.g., intestinal lymphangiectasia (Dobbins, '66).

Digestion and fate of ferritin and colostral protein

There are at least two enzymatic environments which ingested proteins must survive before reaching the circulation, the first is in the lumen of the gastrointestinal tract and the second is in the ileal lining cell itself. Proteolytic activity in the small intestine of newborn rats is high, and does not differ significantly from the activity in adult intestine (Noack, Koldovsky, Friedrich, Heringova, Jirsova and Schenk, '66). Survival of proteins in the intestinal lumen is apparently related to a low activity of digestive enzymes in the stomach. Mosinger et al. ('59) have shown that the proteolytic activity of the gastric contents is low in newborn rats, but increases significantly after day 21. These changes correspond with the morphological development of the parietal and chief cells in the gastric glands (Manville and Lloyd, '32; Kammeraad, '42; Hill, '56).

Acid phosphatase and other hydrolytic enzymes have been localized histochemically in the supranuclear vacuole of ileal lining cells (Cornell and Padykula, '65; Straus, '65; Shervey, '66) which would indicate an active lysosomal activity in these cells. It should be mentioned from a comparative standpoint, an apical tubular apparatus with an esterase positive vacuolar system and a second vacuolar system with both esterase and acid phosphatase activities is found in other cell types besides the ileal lining cell, e.g., cells of the proximal convoluted tubule of the kidney (Straus, '64) and yolk sac endoderm (Padykula, '58; Sorokin and Padykula, '64; Lambson, '66). It is not known whether all proteins

must pass through the supranuclear vacuole prior to discharge, or if transmitted proteins bypass the vacuole. It is known that only about 10% of ingested proteins are actually transmitted across the epithelium (Morris, '65; Bamford, '66; Pierce and Smith, '67a,b); the remaining presumably are degraded by the lining cells.

It has been suggested (Brambell et al., '58; Leissring and Anderson, '61; Anderson, '65; Morris, '64; Brambell, '66) that the protein distributed about the periphery of supranuclear vacuoles, may be adsorbed or bound to the limiting membrane of the vacuole. It was further speculated that the binding of the protein may in some way protect it from the proteolytic activity in the vacuole. In the present study there was no evidence to indicate specific binding of ferritin to either the surface membrane or the limiting membranes of the tubular system or supranuclear vacuole. Using the tetrad structure of the micellar core of ferritin as a criterion of its integrity, there was no evidence of ferritin degradation 18 hours after feeding. This is not a good parameter, however, since all ferritin molecules are not necessarily oriented favorably to visualize the micelles. In addition, Matioli and Baker ('63) have described a ferritin form of hemosiderin as an intermediate in the degradation of ferritin to nonferritin hemosiderin. The half-life of intestinal lining cells in the suckling animals is about 20% longer than in the adult (Koldovsky, Sunshine and Kretchmer, '66) so that considerable intracellular digestion of protein may occur before the cells are sloughed into the intestinal lumen.

ACKNOWLEDGMENTS

The author gratefully acknowledges the valuable assistance of Steven L. Wissig and Don W. Fawcett for their criticism of the manuscript.

LITERATURE CITED

- Anderson, J. W. 1963 Ultrastructural correlates of protein transport. *J. Cell Biol.*, 19: 4A-5A.
- 1965 Ultrastructure correlates of intestinal protein absorption. In: *Macromolecular Aspects of Protein Absorption and Excretion in the Mammalian Intestine*. Rept. of 50th Ross Conf. on Pediatric Res. D. C. Heiner, ed. Ross Laboratories, Columbus, 46-50.
- Balfour, W. E., and R. S. Comline 1959 The specificity of the intestinal absorption of γ -globulin by the new-born calf. *J. Physiol.*, 148: 77-78.
- Bamford, D. R. 1966 Studies in vitro of the passage of serum proteins across the intestinal wall of young rats. *Proc. Roy. Soc. (Lond.) Ser. B*, 166: 30-45.
- Bangham, D. R., and R. J. Terry 1957 The absorption of 125 I-labelled homologous and heterologous serum proteins fed orally to rats. *Biochem. J.*, 66: 579-583.
- Brambell, F. W. R. 1958 The passive immunity of the young mammal. *Biol. Rev. Camb. Phil. Soc.*, 33: 489-531.
- 1966 The transmission of immunity from mother to young and the catabolism of immunoglobulins. *Lancet*, no. 7473, Saturday 19 November, 1087-1093.
- Brambell, F. W. R., R. Halliday and I. G. Macdonald 1958 Interference by human and bovine serum and serum protein fractions with the adsorption of antibodies by suckling rats and mice. *Proc. Roy. Soc. (London)*, Ser. B, 146: 1-11.
- Brambell, F. W. R., W. A. Hemmings and C. L. Oakley 1959 The relative transmission of natural and pepsin-refined homologous and heterologous γ -globulin from the uterine cavity to the foetal circulation in the rabbit. *Proc. Roy. Soc. (London)*, Ser. B, 150: 312-317.
- Brambell, F. W. R., W. A. Hemmings, C. L. Oakley and R. R. Porter 1960 The relative transmission of the fractions of papain hydrolyzed homologous γ -globulin from the uterine cavity to the foetal circulation in the rabbit. *Proc. Roy. Soc. (London)*, Ser. B, 151: 478-482.
- Cardell, Robert R., Jr., Susan Badenhausen and Keith R. Porter 1967 Intestinal triglyceride absorption in the rat. An electron microscopic study. *J. Cell Biol.*, 34: 123-155.
- Casley-Smith, J. R. 1967 The passage of ferritin into jejunal epithelial cells. *Experientia*, 23: 370-371.
- Clark, Sam L., Jr. 1959 The ingestion of proteins and colloidal materials by columnar absorptive cells of the small intestine in suckling rats and mice. *J. Biophysic. Biochem. Cytol.*, 5: 41-49.
- Comline, R. S., H. E. Roberts and D. A. Titcher 1951a Route of absorption of colostrum globulin in the newborn animal. *Nature*, 167: 521-562.
- 1951b Histological changes in the epithelium of the small intestine during protein absorption in the newborn animal. *Nature*, 168: 84-85.
- Comline, R. S., R. W. Pomeroy and D. A. Titcher 1953 Histological changes in the intestine during colostrum absorption. *J. Physiol.*, 102: 6P.
- Cornell, Richard, and H. A. Padykula 1965 A cytochemical study of intestinal absorption in the postnatal rat. *Anat. Rec.*, 151: 339.
- Culbertson, J. T. 1939 The immunization of rats of different age groups against *Trypanosoma lewisi* by the administration of specific antiserum per os. *J. Parasitol.*, 25: 181-182.

- Ans, W. O., III 1966 Electron microscopic study of the intestinal mucosa in intestinal disease. *Gastroenterology*, 51: 1004-1017.
- Bar, J. S. 1967 The fine structure of the absorptive epithelial cells of the developing small intestine of the rat. *J. Anat.*, 101: 57-68.
- Bar, Marilyn, and George E. Palade 1961 Permeability: II. Ferritin transfer across the glomerular capillary wall in neonatal rats. *J. Exptl. Med.*, 114: 699-716.
- Brett, Donald W. 1965 Surface specialization of absorbing cells. *J. Histochem. Cytochem.*, 13: 75-91.
- Bray, D. O. 1964 The uptake of ferritin by necrosis in intestinal lining cells of suckling rats. *Anat. Rec.*, 148: 286.
- 1965 Uptake of ferritin by intestinal lining cells of suckling rats. In: *Macromolecular Aspects of Protein Absorption and Excretion in the Mammalian Intestine*. Rept. of 50th Conf. on Pediatric Res. D. C. Heiner, ed. Ross Laboratories, Columbus, 18-27.
- Bray, R. 1955a The absorption of antibodies from immune sera by the gut of the young rat. *Proc. Roy. Soc. (London) Ser. B*, 408-413.
- 1955b Prenatal and postnatal transmission of passive immunity to young rats. *Proc. Roy. Soc. (London) Ser. B*, 144: 427-430.
- 1957 The absorption of antibody from sera and from mixtures of sera by the gut of the young rat. *Proc. Roy. Soc. (London) Ser. B*, 148: 92-103.
- Bray, W. A., and R. E. Jones 1962 The effect of macroglobulin antibodies in fetal and foetal sera of rabbits as determined by gradient centrifugation. *Proc. Roy. Soc. (London) Ser. B*, 157: 27-32.
- Bray, W. A., V. Jirsova and O. Koldovsky 1965 Postnatal development of β -glucuronidase in the jejunum and ileum of rats. *Can. J. Biochem. Physiol.*, 43: 173-178.
- Bray, W. 1954 A histochemical study of fat absorption in the small intestine of the rat. *Quart. J. Microscop. Sci.*, 95: 153-157.
- Bray, K. J. 1956 Gastric development and antibody transference in the lamb, with some observations on the rat and guinea-pig. *Quart. J. Physiol.*, 41: 421-432.
- Bray, K. J., and W. S. Hardy 1956 Histochemical observations on the intestinal cells of lambs and kids absorbing colostrum. *Nature*, 178: 1353-1354.
- Bray, W. A. 1942 The development of the gastro-intestinal tract of the rat. I. Histogenesis of the epithelium of the stomach, small intestine and pancreas. *J. Morph.*, 70: 323-351.
- Bray, W. A. 1960 Passage of insulin through the wall of the gastro-intestinal tract of the infant rat. *Nature*, 184: 1245-1246.
- Bray, W. A., O. E. Faltova, P. Hahn and Z. Vacek 1961 The functional development of the gastro-intestinal tract in rats. In: *The Development of Homeostasis*. E. F. Adolph, ed. Publishing House of the Czechoslovak Academy of Sciences, Prague, 155-163.
- Koldovsky, O., and F. Chytil 1965 Postnatal development of β -galactosidase activity in the small intestine of the rat. Effect of adrenalectomy and diet. *Biochem. J.*, 94: 266-270.
- Koldovsky, O., P. Sunshine and N. Kretschmer 1966 Cellular migration of intestinal epithelia in suckling and weaned rats. *Nature*, 212: 1389-1390.
- Kraehenbuhl, J.-P., E. Gloor and B. Blanc 1966 Morphologie comparée de la muqueuse intestinale de deux espèces animales aux possibilités d'absorption protéique neonatale différentes. *Z. Zellforsch. Mikroskop. Anat.*, 70: 209-219.
- 1967 Résorption intestinale de la ferritine chez deux espèces animales aux possibilités d'absorption protéique néonatale différentes. *Z. Zellforsch. Mikroskop. Anat.*, 76: 170-186.
- Ladman, Aaron J., H. A. Padykula and E. W. Strauss 1963 A morphological study of fat transport in the human jejunum. *Am. J. Anat.*, 112: 389-420.
- Lambson, Roger O. 1966 An electron microscopic visualization of transport across rat visceral yolk sac. *Am. J. Anat.*, 118: 31-32.
- Leissring, J. C., and J. W. Anderson 1961 The transfer of serum proteins from mother to young in the guinea pig. III. Postnatal studies. *Am. J. Anat.*, 109: 175-179.
- Lewis, W. H. 1931 Pinocytosis. *Bull. Johns Hopkins Hosp.*, 49: 17-23.
- Luft, John H. 1961 Improvements in epoxy embedding methods. *J. Biophysic. Biochem. Cytol.*, 9: 409-414.
- Manville, I. A., and R. W. Lloyd 1932 The hydrogen ion concentration of the gastric juice of fetal and newborn white rats. *Am. J. Physiol.*, 100: 394-401.
- Mattioli, Gastone T., and Richard F. Baker 1963 Denaturation of ferritin and its relationship with hemosiderin. *J. Ultrastruct. Res.*, 8: 477-490.
- Mattison, A. G. M., and B. W. Karlsson 1966 Electron microscopic and immunochemical studies on the small intestine of newborn piglets. *Arkiv Zool.*, 18: 575-587.
- May, A. J., and B. C. Whaler 1958 The absorption of *Colistridium botulinum* Type A toxin from the alimentary canal. *Brit. J. Exptl. Pathol.*, 39: 307-316.
- Millonig, G. 1962 Further observations on a phosphate buffer for osmium solutions in fixation. In: *Electron Microscopy*. Sydney S. Breese, Jr., ed. Vol. II, Academic Press, New York and London, P-8.
- Möllendorff, Von Wilhelm 1924 Ueber die anteilnahme des darmepithels an der verarbeitung enteral und parenteral zugeführter saurer Farbstoffe. *Munch. Med. Wochenschrift*, 71: 569-572.
- Moog, F. 1951 The functional differentiation of the small intestine. II. The differentiation of phosphatase in the duodenum of the mouse. *Exptl. Zool.*, 118: 187-208.
- 1962 Developmental adaptations of alkaline phosphatases in the small intestine. *Federation Proc.*, 21: 51-56.

- Morris, I. G. 1964 The transmission of antibodies and normal gamma globulins across the young mouse gut. *Proc. Roy. Soc. (London)* Ser. B, 160: 276-292.
- 1965 The transmission of anti-*Brucella abortus* agglutinins across the gut in young rats. *Proc. Roy. Soc. (London)* Ser. B, 163: 402-416.
- Mosinger, B., Z. Placer and O. Koldovsky 1959 Passage of insulin through the wall of the gastro-intestinal tract of the infant rat. *Nature*, 184: 1245-1246.
- Noack, R., O. Koldovsky, M. Friedrich, A. Heringova, V. Jirsova and G. Schenk 1966 Proteolytic and peptidase activities of the jejunum and ileum of the rat during postnatal development. *Biochem. J.*, 100: 775-778.
- Padykula, H. A. 1958 A histochemical and quantitative study of enzymes of the rat's placenta. *J. Anat.*, 92: 118-129.
- Padykula, Helen A. 1962 Recent functional interpretations of intestinal morphology. *Federation Proc.*, 21: 873-879.
- Padykula, Helen A., J. J. Deren and T. H. Wilson 1966 Development of structure and function in the mammalian yolk sac. I. Development, morphology and vitamin B12 uptake of the rat yolk sac. *Devel. Biol.*, 13: 311-348.
- Palade, George 1953 Fine structure of blood capillaries. *J. Appl. Phys.*, 24: 1424.
- Palay, S. L., and L. J. Karlin 1959a An electron microscopic study of the intestinal villus. I. The fasting animal. *J. Biophysic. Biochem. Cytol.*, 5: 363-371.
- 1959b An electron microscopic study of the intestinal villus. II. The pathway of fat absorption. *J. Biophysic. Biochem. Cytol.*, 5: 373-383.
- Parsons, D. F. 1961 A simple method for obtaining increase contrast in Araldite sections by using postfixation staining of tissues with potassium permanganate. *J. Biophysic. Biochem. Cytol.*, 11: 492-497.
- Payne, L. C., and C. Marsh 1962 Absorption of gamma globulin by the small intestine. *Federation Proc.*, 21: 909-912.
- Pierce, A. E., and P. Johnson 1960 Ultra-centrifuge and electrophoretic studies on the proteinuria of the newborn calf. *J. Hyg.*, 58: 247-260.
- Pierce, A. E., P. C. Risdall and B. Shaw 1964 Absorption of orally administered insulin by the newly born calf. *J. Physiol.*, 171: 203-215.
- Pierce, A. E., and M. W. Smith 1967a The intestinal absorption of pig and bovine immune lactoglobulin and human serum albumin by the new-born pig. *J. Physiol.*, 190: 1-18.
- 1967b The *in vitro* transfer of bovine immune lactoglobulin across the intestine of new-born pigs. *J. Physiol.*, 190: 19-34.
- Porter, R. R. 1958 Separation and isolation of fractions of rabbit gamma-globulin containing the antibody and antigenic combining sites. *Nature*, 181: 670-671.
- 1959 The hydrolysis of rabbit gamma globulin and antibodies with crystalline pepsin. *Biochem. J.*, 73: 119-126.
- Reynolds, E. S. 1963 The use of lead citrate at high pH as an electron-opaque stain in electron microscopy. *J. Cell Biol.*, 17: 208-212.
- Rubin, C. E. 1966 Electron microscopic study of triglyceride absorption in man. *Gastroenterology*, 50: 65-77.
- Schechtman, A. M. 1956 Uptake and transport of macromolecules by cells with special reference to growth and development. In: *International Review of Cytology*, G. Bourne and F. Danielli, eds. Vol. 5, Academic Press, New York, 303-322.
- Shervey, Paul 1966 Observations on the development and histochemistry of the intestinal inclusion bodies of the suckling rat. *Anat. Rec.*, 154: 422.
- Sibalin, M., and N. Björkman 1966 On the structure and absorptive function of the jejunal villi during the early suckling period. *Exptl. Cell Res.*, 44: 165-174.
- Smith, T. 1925 Hydronic stages in the intestinal epithelium of new-born calves. *J. Exp. Med.*, 41: 81-88.
- Sorokin, S. P., and H. A. Padykula 1964 Differentiation of the rat's yolk sac in organ culture. *Am. J. Anat.*, 114: 457-479.
- Strauss, E., and S. Ito 1965 Autoradiographic and biochemical study of linolenic acid C^{14} absorption by hamster intestine from mixed micelles *in vitro*. *J. Cell Biol.*, 27: 101A.
- Straus, Werner 1964 Cytochemical observations on the relationship between lysosomes and phagosomes in kidney and liver by combined staining for acid phosphatase and intravenously injected horseradish peroxidase. *J. Cell Biol.*, 20: 497-507.
- 1965 Cytologic observations on protein uptake and transport in kidney and liver. In: *Macromolecular Aspects of Protein Absorption and Excretion in the Mammalian Intestine*. Rept. of 50th Ross Conf. on Pediatric Res. D. C. Heiner, ed. Ross Laboratories, Columbus, 46-55.
- Venable, John H., and Richard Coggeshall 1965 A simplified lead citrate stain for use in electron microscopy. *J. Cell Biol.*, 25: 407-408.
- Vodovar, N., and J.-E. Flechon 1966 La cellule épithéliale absorbante de l'intestin grêle du porc. Ultrastructure. *Ann. Biol. Animale Biochim. Biophys.*, 6: 13-32.
- Watson, M. L. 1958 Staining of tissue sections for electron microscopy with heavy metals. *J. Biophysic. Biochem. Cytol.*, 4: 475-478.
- Wissig, Steven L. 1958 An electron microscopic study of the permeability of capillaries in man. *Anat. Rec.*, 130: 467-468.
- Wissig, S. L. 1964 Personal communication.

Note added in proof: Since this manuscript was submitted for publication, two significant review articles related to this topic have appeared in *The Handbook of Physiology*, Section 6: Alimentary Canal, Volume III. Intestinal Absorption, American Physiological Society, Washington, D. C., 1968. See J. J. Deren, page 1099 and I. G. Morris, page 1491.

PLATE 1

EXPLANATION OF FIGURES

The following six figures are photomicrographs of the small intestine from three different animals: newborn rat prior to suckling, nine-day-old suckling rat and a ten-day-old rat fasted for 18 hours prior to sacrifice. Each pair of photographs represent Epon sections of jejunal and ileal tissue taken from the same animal and stained with toluidine blue. Magnification in figures 1-6 is the same, $\times 1744$.

- 1 Jejunum of newborn rat prior to suckling. There are no obvious inclusions visible in the cytoplasm.
- 2 Ileum of newborn rat prior to suckling. Morphological pattern of the ileum not significantly different from jejunum (fig. 1).
- 3 Jejunum of nine-day-old suckling rat. Lipid droplets are observed in Golgi apparatus, intercellular spaces and lamina propria.
- 4 Ileum of nine-day-old suckling rat. Numerous clear vacuoles are noted in the apical cytoplasm. Supranuclear area occupied by large vacuole containing amorphous dense material.
- 5 Jejunum of ten-day-old suckling rat fasted for 18 hours prior to sacrifice. At this stage, cytoplasm is completely clear of lipid material. Typical fasting state.
- 6 Ileum of ten-day-old suckling rat fasted for 18 hours prior to sacrifice. Apical vacuoles and a supranuclear vacuole are still observed in the cytoplasm of the lining cells.

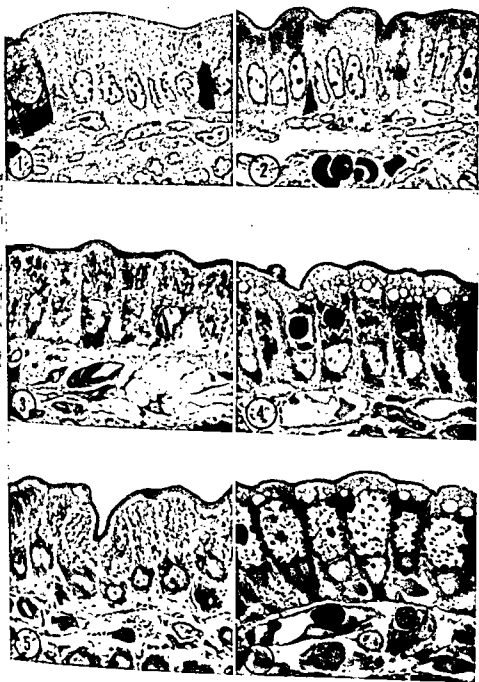


PLATE 2

EXPLANATION OF FIGURES

- 7 Jejunum of 15-day-old suckling rat fasted for 18 hours prior to sacrifice. Electron micrograph showing mitochondria, membranes of the smooth- and rough-surfaced endoplasmic reticulum. Note absence of any extensive plasmalemmal invaginations. $\times 29,000$.
- 8 Jejunum of 15-day-old suckling rat, two hours after receiving 1 ml of corn oil. Osmiophilic droplets, presumably lipid, are observed in both smooth- and rough-surfaced endoplasmic reticulum. $\times 25,000$.

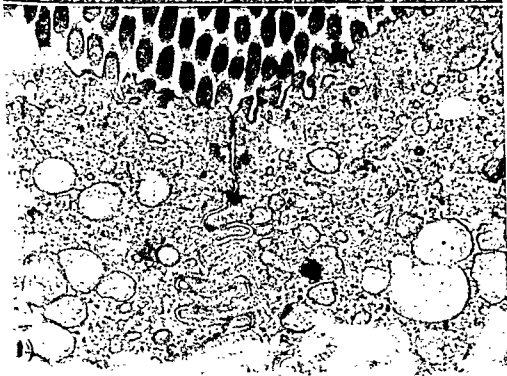
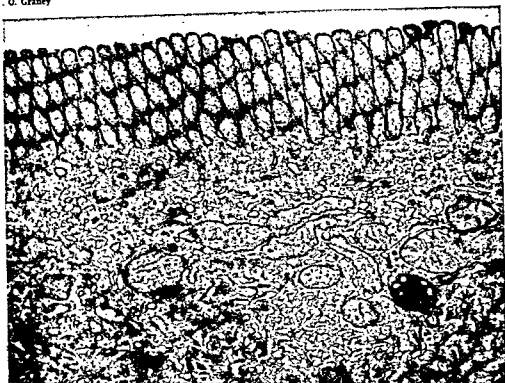


PLATE 3

EXPLANATION OF FIGURE

- 9 Ileum of 15-day-old suckling rat. Compare amorphous precipitated material in supranuclear vacuole (SNV) with similar material in the intercellular space (ICS), lamina propria (LP) and the blood capillary marked by the red blood cell (RBC). $\times 13,600$.

TIN UPTAKE BY ILEAL LINING CELLS

I O. Graney

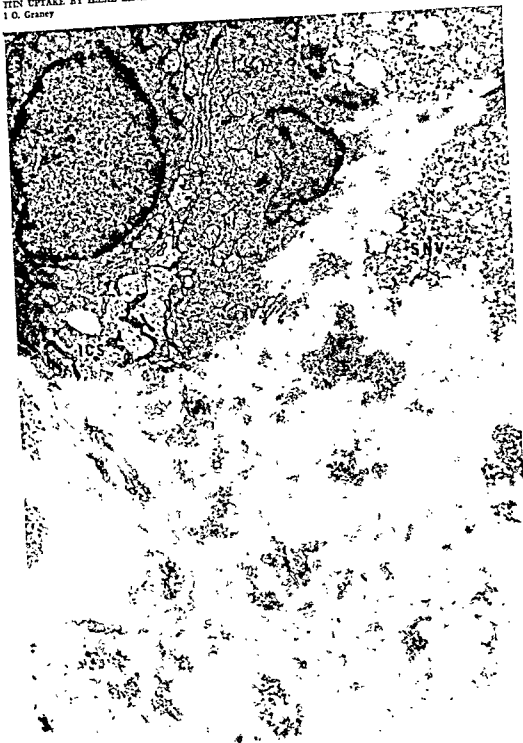


PLATE 4

EXPLANATION OF FIGURES

- 10 Ileum of 15-day-old suckling rat fasted 18 hours prior to sacrifice. Several cisternae (C) with tubular (arrows) connections are seen in the apical cytoplasm. The cisternae and some of the vacuoles (V), particularly those situated deeper in the apical cytoplasm, contain an amorphous precipitated material. $\times 14,700$.
- 11 Ileum of ten-day-old suckling rat two hours after receiving 0.15 ml of ferritin. Low magnification electron micrograph illustrating the distribution of ferritin in the apical tubular system, apical vacuoles (arrows) and supranuclear vacuole (SNV). $\times 12,320$.

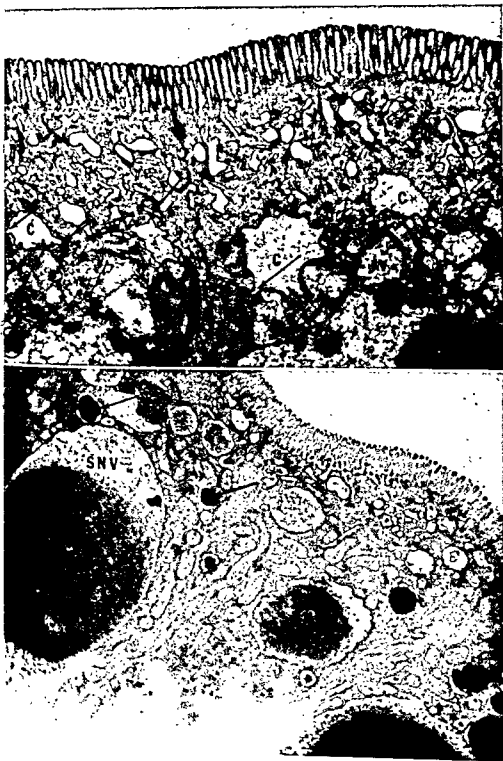


PLATE 5

EXPLANATION OF FIGURE

- 12 Ileum of ten-day-old rat two hours after ferritin gavage. Ferritin particles (arrows) are seen in the lumen of plasmalemmal invaginations and in tubules situated deeper in the apical cytoplasm. $\times 102,000$. *Inset* illustrates detail of the tearad (arrow) of ferric hydroxide micelles in the center of the ferritin molecule. $\times 216,000$.

IRON UPTAKE BY ILEAL LINING CELLS
I. O. Graney



PLATE 6

EXPLANATION OF FIGURE

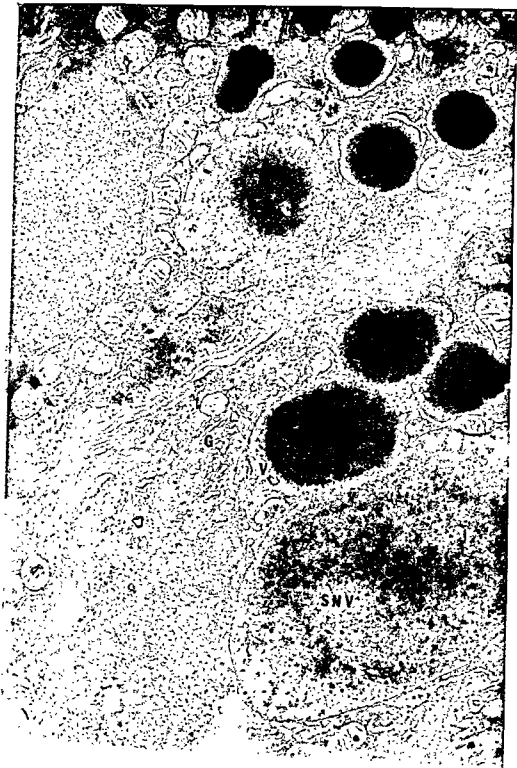
- 13 Ileum of 15-day-old rat 1.5 hours after ferritin gavage. Three tubules (T) are shown connecting with a large vacuole or cistern (C), containing ferritin. The intestinal lumen is toward the top of the figure. $\times 135,000$.



PLATE 7

EXPLANATION OF FIGURE

- 14 Ileum of ten-day-old rat two hours after ferritin gavage. Medium sized vacuoles containing concentrated ferritin appear to be coalescing in the supranuclear region of the lining cell shown in the upper half of the figure. The cell in the lower half of the figure already contains a rather large supranuclear vacuole (SNV). Another vacuole (V) is seen fusing the supranuclear vacuole. The Golgi apparatus (G) does not contain ferritin. $\times 21,420$.



Morphological Features of Brown Adipose Cell Maturation *in vivo* and *in vitro*^{1,2}

ROBERT F. DYER*

Department of Anatomy and Cell Biology, School of Medicine,
University of Pittsburgh, Pittsburgh, Pennsylvania

ABSTRACT The maturation of brown adipose cells, derived at various time intervals from interscapular brown fat pads of neonatal rats, has been investigated electron microscopically. The major changes in *in vivo* brown adipose cells are related to lipid accumulation. In older animals, fat droplets are separated by a membrane complex, and membranous fragments are seen within large lipid inclusions. The ultrastructural characteristics of monolayer cultures of brown fat cells, isolated from neonatal brown fat pads by tryptic dissociation, and maintained for one to six days on a reconstituted collagen matrix, have also been investigated. Adipose cells *in vitro* are morphologically similar to control brown fat cells, and lipid accumulation closely parallels that seen *in vivo*. *In vitro* lipid droplet coalescence, impossible to visualize *in vivo*, has been documented by time-lapse cinematography, and membrane complexes similar to those observed *in vivo* are seen. Major changes in cultivated fat cells, compared to *in vivo* cells, involve extensive glycogen deposition and breakdown of cytoplasmic ribosomal rosettes. Older cultures contain adipose cells exhibiting characteristics of white fat cells. Effects of tissue culture environment upon the brown fat cells, and the possible conversion of the brown fat cell into a white fat cell are discussed.

Since the original description of brown adipose tissue (Gesner, 1551), the relationship of the brown fat cell to the white cell has been a controversial subject. The investigators are of the opinion that brown adipose tissue is an immature form of white fat (Auerbach, '02; Sheldon, '24; non, '62), while others maintain that brown and white fat are separate tissue entities (Rasmussen, '23; Napolitano, '63). Ultrastructural studies have demonstrated at the morphological characteristics of immature forms of brown and white fat cells are distinctly different (Napolitano, '5). If brown fat cells do mature into white fat cells, then brown adipose cells would be required to undergo significant morphological and biochemical changes.

One morphological characteristic of the brown (multilocular) fat cell is the presence of numerous lipid droplets within its cytoplasm, in contrast to the single lipid droplet contained in the mature white (unilocular) fat cell. If conversion of a multilocular fat cell into a unilocular fat cell occurs, such a process would most likely involve the coalescence of preexisting lipid droplets within the multilocular cell. There are reports in the literature

that brown fat lipid droplets do coalesce, both *in vivo* (Sheldon, '24) and in organ culture systems (Sidman, '56a), but critical documentation of this phenomenon has been lacking.

It is impossible to observe the dynamic process of coalescence *in vivo* or in organ culture. However, monolayer tissue cultures provide an approach for the controlled observation of living cells, and adipose cells exhibiting the light microscopic characteristics of brown fat cells can be maintained in monolayer culture systems (Masters, '65). The cultivated adipose cells, if exposed to insulin, accumulate lipid with time *in vitro*. Time-lapse cinematographic studies of such a lipogenic system might be expected to provide documentation of lipid droplet coalescence, and investigations of this nature are reported.

¹ Submitted in partial fulfillment of the requirements for the degree of Doctor of Philosophy in the Department of Anatomy and Cell Biology, in the Graduate School of the School of Medicine, University of Pittsburgh, Pittsburgh, Pennsylvania, 1968.

² Supported by training grant ST1HD-40, Department of Health, Education and Welfare.

* Present address: Department of Anatomy, Louisiana State University Medical Center, New Orleans, Louisiana 70112.

These tissues were also fixed in a cold solution of 1% osmium tetroxide in phosphate buffer pH 7.2 (Palade, '52), and dehydrated in alcohols. The embedding medium was Vestopal W (Kellenberger, Swab and Ryter, '56) or Maraglas (Spur, Kattine and Freeman, '63).

In addition to examining the *in vivo* developmental sequence, electron microscopic observations were conducted on cultivated adipose cells maintained on reconstituted collagen. Cultures were fixed *in situ* in 1% osmium tetroxide in phosphate buffer (pH 7.2) for one-two hours. Following alcohol dehydration, a razor blade was used to strip the gel matrix from the cover slip, and the matrix together with the attached cells were processed as an ordinary piece of tissue. These were embedded flat in Vestopal W. After polymerization, the light microscope was used to select cells for electron microscopy. Selected areas were cut out with a jeweler's saw and mounted in a blank Vestopal capsule with Tray Resin.*

All tissues were sectioned on a Huxley microtome and double stained with lead citrate (Reynolds, '63) and uranyl acetate (Watson, '58). All observations were made with a Philips EM 200 electron microscope.

Time-lapse cinematography. Time-lapse cinematography was used to study the rate of lipid droplets within the cultivated adipose cells. Trypsinized cell suspensions were prepared as previously described, and the cells were introduced into a Sykes-type perfusion chamber (Sykes and Moore, '60). After 48 hours incubation, the culture medium was changed and the perfusion chamber was inverted and secured to a glass slide with paraffin. In one series of experiments the growth medium was replaced with Krebs-Ringer phosphate buffer (pH 7.2) (Cohen, '49) after the initial 9 hour incubation. The slide and attached chamber was placed on the stage of an AO Spencer phase-contrast microscope which was housed in a constant temperature incubator (37°C). The progress of these cultures was monitored by time-lapse cinematography with exposures at the rate of one frame per minute.

RESULTS

Control electron microscopy. The following observations are concerned with the ultrastructural features and morphological alterations of rat brown adipose tissues during the first nine days after birth.

The brown fat cell of the neonatal rat contains a spherical or elliptical nucleus which is centrally or slightly eccentrically located (fig. 1, N). The nuclear chromatin is clumped, and localized at the periphery of the nucleus. The nucleoli are conspicuous within the nucleoplasm, and exhibit a distinct *pars fibrosa* and *pars granulosa* (fig. 2, NU).

Newborn brown fat cells contain relatively little lipid, and nuclear displacement occurs with an increase in the size of cytoplasmic lipid inclusions. In figure 7 (4 days post partum), the nucleus at N1 is still centrally located, but the nucleus at N2 is being impinged upon by lipid droplets, resulting in displacement toward the periphery of the cell. The majority of brown fat cell nuclei in older animals have been similarly displaced (fig. 9, N).

There are large numbers of mitochondria in brown fat cells of the newborn animal. These mitochondria are pleomorphic, and cristae orientation is quite variable. Three types of cristae orientation, characteristic of brown fat mitochondria, can be seen in figure 4, where M1 depicts cristae which are perpendicular to the long axis of the mitochondrion, and M2 contains cristae which are almost parallel to the long axis. The mitochondrion labeled M3 contains cristae which are both parallel and perpendicular to the long axis. These specializations in mitochondrial morphology provide a distinct criterion for establishing that cultivated adipose cells are representative of brown fat cells.

Ribosomes are found in great abundance in brown fat cells. The majority of these ribosomes exist as aggregates which are not membrane associated (figs. 2, 3, R), but membrane-bound ribosomes are occasionally found (fig. 2, MBR). Most brown fat cells contain little agranular reticulum, but exceptions to this have been observed. The fat cell in figure 3 contains large amounts of smooth reticulum (SR), which

*L. D. Caulk Co., Milford, Delaware.

Although the ultrastructure of newborn, rat brown fat tissue has been described (Napolitano and Fawcett, '58), electron microscopic studies dealing with temporally-related morphological changes have not been reported. It should also be important to demonstrate that the *in vitro* adipose cell morphology and maturational sequences are similar to that seen *in vivo*. Therefore, ultrastructural characterization of brown adipose cells from newborn rats at various stages of development, and similar studies on the cultivated adipose cells, will be presented. Electron microscopic studies of maturing brown adipose cells might also provide information relating to lipid-droplet coalescence and cell transformation.

MATERIALS AND METHODS

Tissue culture procedures. Brown fat cell monolayer cultures were established as described by Masters ('65). Interscapular brown fat pads from newborn Wistar rats were aseptically removed, diced, and dissociated by agitation in a calcium-magnesium free isotonic solution of 0.25% trypsin (1:300) at pH 7.2 (Moscona, '52). Suspended cells were collected by centrifugation at 1000 rpm for five minutes, and were resuspended in culture medium composed of Eagle's medium (Eagle, '55) containing 2X amino acids, Hanks balanced salt solution (Hanks and Wallace, '49), and 10% bovine fetal serum. Insulin is a requirement for the accumulation of lipid in cultivated brown fat cells (Masters, '65), and was added at a concentration of 10 gamma/ml (0.2 units/ml) of medium. Penicillin was added also at a concentration of 100 units/ml.

Cell viability was determined by exposing the cell sample to trypan blue, which stains non-viable cells (Pappenheimer, '17), and cell counts were made in a hemocytometer. Leighton tubes containing flying-cover slips were inoculated with 5×10^5 cells/ml, and monolayer cultures as described by Earle, Schilling and Shelton ('50) were established. The cultures were incubated at 37°C.

Cultivated cells which were to be examined with the electron microscope were maintained on a reconstituted collagen matrix. Attachment of the fat cells to the

collagen matrix provides for retention of cell to cell and cell to matrix relationships and allows circumvention of some of the technical problems associated with the handling of fat-laden cells during electron microscopic preparative techniques.

The reconstituted collagen was prepared by a modification of the technique described by Ehrmann and Gey ('56). Tendon from two rat tails were placed in a 0.1% solution of acetic acid (pH 3.5) and allowed to stand overnight in the cold. This procedure solubilizes the collagen in the tendon material. The resulting viscous solution was then filtered through large-pore gauze material to remove remnants of the tendon. Solid sodium acetate was added to the clarified collagen solution in sufficient quantity to raise the pH to 5 (ionic strength 0.125). Under these conditions the collagen precipitates out of solution in fibrillar form. The fibrils were collected by centrifugation, and all but a small amount of supernatant poured off. A drop or two of acetic acid was added to the fibril pellet, which lowered the pH and solubilized the collagen. The resulting concentrated collagen solution was then layered on cover slips which were placed in a loosely covered container and exposed to ammonium hydroxide vapors. The vapors raised the pH of the collagen solution and a transparent collagen gel was formed. Gel sterilization was effected by placing the cover slips in 70% alcohol which also partially dehydrates the gel, resulting in a firmer matrix. Equilibration of the gel was carried out by placing the collagen-coated cover slips in several changes of Eagle's medium. The end product forms a non-toxic, biological matrix which is suitable for the support of cells *in vitro* and strong enough to withstand handling and preparative procedures for electron microscopy (Dyer and Ruby, '63).

Electron microscopy. In order to establish brown fat cell maturational sequences interscapular brown fat pads were removed from rats at days one, two, four, six and nine post partum. Tissues were fixed overnight in cold 4% glutaraldehyde (Sabatini, Bensch and Barnett, '63) buffered in McEwen's buffer (McEwen, '56), post-osmicated for one-two hours and dehydrated in a graded series of alcohols. Some

The fat-containing cell in figure 17 is closely apposed to a fibroblastic cell (B), which is in contact with the surface of the reconstituted collagen matrix (C). The differences in mitochondrial size and complexity between the two cells are striking. The fibroblast nucleus (N) is flattened, and the cytoplasmic morphology is distinct from the fat-containing cell. Small fat droplets are seen occasionally in fibroblastic cells, but fat droplets comparable in size to those seen in cultivated adipose cells have not been observed. The fibroblasts do not contain glycogen, nor do they exhibit pinocytotic activity.

A third cell type, not seen until four days *in vitro*, is depicted in figure 18. This cell contains a large, centrally located fat inclusion, and the nucleus (N), displaced peripherally, is flattened against the cell surface. The cytoplasm contains many small vesicles and structures of a paracrystalline nature. The mitochondria are small, and their internal structure is uncomplicated. These cells do not contain accumulations of glycogen, in contrast to brown fat cells in culture. This third cell type is similar to a white adipose cell, but should be pointed out that it may represent a differentiated white fat cell originally present in the brown fat tissue at the time of trypsinization.

Adipose cells after one day *in vitro* are representative of brown fat cells one day post partum. Cultivated fat-cell nuclei (fig. 12, N), nucleoli (fig. 13, NU), and mitochondria (fig. 13, M) are structurally similar to those observed in control brown fat cells. However, ribosomal rosettes, abundant in *in vitro* cells, are not nearly as evident in cultivated adipose cells. The cultivated fat cells do contain numerous free ribosomes. Glycogen, rarely seen in control brown fat cells, is a common feature of adipose cells *in vitro* (fig. 12, G). Large quantities of glycogen accumulate with time in culture (fig. 15, G).

There are major changes in the cultivated adipose cells associated with lipid accumulation. Lipid inclusions in 24 hour cultivated cells (figs. 12 and 13, LD) are similar in size and number to those observed in control cells one day post partum.

There is an increase in lipid droplet size after two days *in vitro*. The fat inclusion labeled LD in figure 14 is 14 μ in diameter, which is three times the size of the largest droplets in one day cultivated cells, and is similar in size to lipid droplets observed in *in vivo* brown fat cells four days post partum. The nuclei of two day cultivated fat cells are peripherally located (fig. 14, N).

The multilocular fat cells after four days *in vitro* show a slight increase in the number of large lipid inclusions (fig. 16). In figure 16, there is a peripheral rim of lesser density within the larger fat droplets LD1, LD2 and LD3, which is 0.3–0.4 μ in width. LD1 and LD2 contain also, profiles of lesser density which correspond in size to the smaller cytoplasmic lipid inclusions.

Cultivated fat cells six days *in vitro* contain numerous large lipid droplets, many of which are in contact with one another. In figure 19, LD1 is impinging upon an adjacent fat droplet at A, and is being impinged upon by a second droplet at B. High magnification of the interface at A reveals that the droplets are separated by a membrane complex (fig. 20), which is comparable to the membrane complexes observed between and within lipid droplets of control brown fat cells (figs. 10, 11, arrows).

There are many fat-containing cells after six days *in vitro* which are morphologically quite different from multilocular fat cells in one, two and four day cultures (fig. 21). Such cells contain large lipid inclusions (LD) which measure up to 20 μ in diameter, and occasionally, small lipid droplets are closely associated with these inclusions (arrow). The nuclei (N1 and N2) of these fat-laden cells are oval or triangular in shape, and are located near the cell periphery. Glycogen bodies (G) are usually present, and parallel arrays of endoplasmic reticulum (ER) are more apparent than in earlier cultivated fat cells. These cell types are similar in some respects to both the recognizable brown fat cell *in vitro*, and the unilocular fat cell seen in the four day culture system.

Time-lapse cinematography. The preceding electron microscopic evidence strongly suggests that lipid droplet coales-

is randomly dispersed throughout the cytoplasm.

Glycogen has not been observed in brown fat cells of very young animals, but glycogen is frequently seen in the cytoplasm of capillary endothelial cells two days after birth (fig. 6, G). These particles are 250–350 Å in diameter, and exhibit the morphological characteristics and staining reactions of cellular beta glycogen as described by Revel ('64). Small quantities of similar glycogen particles were initially seen in brown fat cells six days post partum.

There is an extensive vascular system permeating brown fat tissue, and brown fat cells are routinely found adjacent to one or more capillaries (fig. 1, C). Vesicles associated with pinocytotic activity are frequently seen at the surface of the brown fat cell and the capillary endothelial cell (fig. 2, P). Pinocytosis is not restricted to the brown fat cell plasma membrane opposite capillary endothelial cells. Pinocytotic vesicles may be seen in many instances lining the surface membranes of two opposed brown fat cells (fig. 3). In figure 3, the formation of pinocytotic vesicles can be seen at P, and at P1 secondary vesicles are seen forming from the initial invagination of the plasma membrane. Similar vesicular structures, termed microvesicular rosettes by Williamson ('64), have been described at the cell surface of white adipose cells acutely depleted of lipid.

The most noticeable cytological changes in brown fat cells are related to lipid accumulation. Brown adipose cells one day after birth contain lipid droplets which vary in diameter from 0.2–4 μ . Although the larger droplets are found in many cells (fig. 1, LD), some cells contain only small amounts of lipid in the form of incipient droplets (figs. 2, 4, LD).

Brown fat cells two days post partum exhibit an increased lipid content, mainly due to an increase in the number of small lipid inclusions (fig. 5, LD). Many of these small droplets are on the order of 1 μ in diameter, which corresponds to the size of chylomicrons. Large numbers of chylomicrons are seen in capillary lumina of the two day old rat (fig. 5, CH), in contrast to the unfed, newborn animal. Fat parti-

cles the size of chylomicrons have not been seen in the extracellular spaces between capillaries and fat cells, confirming previous observations (Napolitano, '63).

There is an increase in lipid droplet size four days post partum, resulting in increased cell size, and a corresponding decrease in the dimensions of the extracellular spaces. The lipid droplet labeled A in figure 7 is 15 μ in diameter, which is three times the size of the largest droplets seen in the newborn. Smaller lipid droplets are round and in some cases are apposed to these larger fat inclusions (fig. 7). It is possible to visualize membrane complexes surrounding two closely apposed lipid droplets (fig. 8). Each membrane complex measures 70 Å, and presents the morphological characteristics of a unit membrane. It is not known whether these membrane complexes represent true unit membrane or simply a lipo-protein interface.

Brown fat cells six days post partum contain large lipid inclusions similar in size to those observed after four days post partum (fig. 9, LD), but there does appear to be a significant decrease in the number of smaller lipid droplets.

Brown fat cells nine days post partum contain many adjacent lipid droplets (fig. 10, LD1 and LD2) separated only by an intervening membrane complex. The membrane complex in figure 10 (arrow) is displaced into one of the lipid droplets. Figure 11 (arrow) demonstrates the presence of a membrane fragment, morphologically similar to that described in figure 1 within a lipid inclusion. The fragment measures 150–200 Å in width, and is composed of two outer dense lines and a central zone which is bisected by a third dense line. A lamellar array of membrane (LMS) is found also at the periphery of the lipid droplet in figure 11.

Tissue culture electron microscopy. Three cell types have been observed in the culture system. Figure 17 depicts two of these cell types. The cell containing lipid inclusions (LD), and the large pleomorphic mitochondria (M), exhibits the general morphology of control brown fat cells. Cytoplasmic vesicles (V), and vesicles of pinocytotic origin (P) are observed frequently within these cells.

The fat-containing cell in figure 17 is closely apposed to a fibroblastic cell (F), which is in contact with the surface of the reconstituted collagen matrix (C). The differences in mitochondrial content and complexity between the two cells are striking. The fibroblast nucleus (N) is flattened, and the cytoplasmic morphology is distinct from the fat-containing cell. Small fat droplets are seen occasionally in fibroblastic cells, but fat droplets comparable in size to those seen in cultivated adipose cells have not been observed. The fibroblasts do not contain glycogen, nor do they exhibit pinocytotic activity.

A third cell type, not seen until four days *in vitro*, is depicted in figure 18. This cell contains a large, centrally located fat inclusion, and the nucleus (N), displaced peripherally, is flattened against the cell surface. The cytoplasm contains many small vesicles and structures of a particulate nature. The mitochondria are small, and their internal structure is uncomplicated. These cells do not contain accumulations of glycogen, in contrast to brown fat cells in culture. This third cell type is similar to a white adipose cell, but should be pointed out that it may represent a differentiated white fat cell originally present in the brown fat tissue at the time of trypsinization.

Adipose cells after one day *in vitro* are representative of brown fat cells one day post partum. Cultivated fat-cell nuclei (fig. 12, N), nucleoli (fig. 13, NU), and mitochondria (fig. 13, M) are structurally similar to those observed in control brown fat cells. However, ribosomal rosettes, abundant in *in vivo* cells, are not nearly so evident in cultivated adipose cells. The cultivated fat cells do contain numerous free ribosomes. Glycogen, rarely seen in control brown fat cells, is a common feature of adipose cells *in vitro* (fig. 12, G). Large quantities of glycogen accumulate with time in culture (fig. 15, G).

There are major changes in the cultivated adipose cells associated with lipid accumulation. Lipid inclusions in 24 hour cultivated cells (figs. 12 and 13, LD) are similar in size and number to those observed in control cells one day post partum.

There is an increase in lipid droplet size after two days *in vitro*. The fat inclusion labeled LD in figure 14 is 14 μ in diameter, which is three times the size of the largest droplets in one day cultivated cells, and is similar in size to lipid droplets observed in *in vivo* brown fat cells four days post partum. The nuclei of two day cultivated fat cells are peripherally located (fig. 14, N).

The multilocular fat cells after four days *in vitro* show a slight increase in the number of large lipid inclusions (fig. 16). In figure 16, there is a peripheral rim of lesser density within the larger fat droplets LD1, LD2 and LD3, which is 0.3–0.4 μ in width. LD1 and LD2 contain also, profiles of lesser density which correspond in size to the smaller cytoplasmic lipid inclusions.

Cultivated fat cells six days *in vitro* contain numerous large lipid droplets, many of which are in contact with one another. In figure 19, LD1 is impinging upon an adjacent fat droplet at A, and is being impinged upon by a second droplet at B. High magnification of the interface at A reveals that the droplets are separated by a membrane complex (fig. 20), which is comparable to the membrane complexes observed between and within lipid droplets of control brown fat cells (figs. 10, 11, arrows).

There are many fat-containing cells after six days *in vitro* which are morphologically quite different from multilocular fat cells in one, two and four day cultures (fig. 21). Such cells contain large lipid inclusions (LD) which measure up to 20 μ in diameter, and occasionally, small lipid droplets are closely associated with these inclusions (arrow). The nuclei (N1 and N2) of these fat-laden cells are oval or triangular in shape, and are located near the cell periphery. Glycogen bodies (G) are usually present, and parallel arrays of endoplasmic reticulum (ER) are more apparent than in earlier cultivated fat cells. These cell types are similar in some respects to both the recognizable brown fat cell *in vitro*, and the unilocular fat cell seen in the four day culture system.

Time-lapse cinematography. The preceding electron microscopic evidence strongly suggests that lipid droplet coales-

is randomly dispersed throughout the cytoplasm.

Glycogen has not been observed in brown fat cells of very young animals, but glycogen is frequently seen in the cytoplasm of capillary endothelial cells two days after birth (fig. 6, G). These particles are 250–350 Å in diameter, and exhibit the morphological characteristics and staining reactions of cellular beta glycogen as described by Revel ('64). Small quantities of similar glycogen particles were initially seen in brown fat cells six days post partum.

There is an extensive vascular system permeating brown fat tissue, and brown fat cells are routinely found adjacent to one or more capillaries (fig. 1, C). Vesicles associated with pinocytotic activity are frequently seen at the surface of the brown fat cell and the capillary endothelial cell (fig. 2, P). Pinocytosis is not restricted to the brown fat cell plasma membrane opposite capillary endothelial cells. Pinocytotic vesicles may be seen in many instances lining the surface membranes of two opposed brown fat cells (fig. 3). In figure 3, the formation of pinocytotic vesicles can be seen at P, and at P1 secondary vesicles are seen forming from the initial invagination of the plasma membrane. Similar vesicular structures, termed microvesicular rosettes by Williamson ('64), have been described at the cell surface of white adipose cells acutely depleted of lipid.

The most noticeable cytological changes in brown fat cells are related to lipid accumulation. Brown adipose cells one day after birth contain lipid droplets which vary in diameter from 0.2–4 μ . Although the larger droplets are found in many cells (fig. 1, LD), some cells contain only small amounts of lipid in the form of incipient droplets (figs. 2, 4, LD).

Brown fat cells two days post partum exhibit an increased lipid content, mainly due to an increase in the number of small lipid inclusions (fig. 5, LD). Many of these small droplets are on the order of 1 μ in diameter, which corresponds to the size of chylomicrons. Large numbers of chylomicrons are seen in capillary lumina of the two day old rat (fig. 5, CH), in contrast to the unfed, newborn animal. Fat parti-

cles the size of chylomicrons have not been seen in the extracellular spaces between capillaries and fat cells, confirming previous observations (Napolitano, '63).

There is an increase in lipid droplets four days post partum, resulting in increased cell size, and a corresponding increase in the dimensions of the extracellular spaces. The lipid droplet labeled A in figure 7 is 15 μ in diameter, which is ten times the size of the largest droplets seen in the newborn. Smaller lipid droplets are round and in some cases are apposed to these larger fat inclusions (fig. 7). It is possible to visualize membrane complexes surrounding two closely apposed lipid droplets (fig. 8). Each membrane complex measures 70 Å, and presents the morphological characteristics of a unit membrane. It is not known whether these membrane complexes represent true unit membranes or simply a lipo-protein interface.

Brown fat cells six days post partum contain large lipid inclusions similar in size to those observed after four days post partum (fig. 9, LD), but there does appear to be a significant decrease in the number of smaller lipid droplets.

Brown fat cells nine days post partum contain many adjacent lipid droplets (10, LD1 and LD2) separated only by intervening membrane complex. The membrane complex in figure 10 (arrow) is placed into one of the lipid droplets. Figure 11 (arrow) demonstrates the presence of a membrane fragment, morphologically similar to that described in figure 8, within a lipid inclusion. The fragment measures 150–200 Å in width, and is composed of two outer dense lines and a central zone which is bisected by a third dense line. A lamellar array of membrane (LMS) is found also at the periphery of the lipid droplet in figure 11.

Tissue culture electron microscope. Three cell types have been observed in the culture system. Figure 17 depicts two of these cell types. The cell containing lipid inclusions (LD), and the large morphic mitochondria (M), exhibits the general morphology of control brown fat cells. Cytoplasmic vesicles (V), and vesicles of pinocytotic origin (P) are observed frequently within these cells.

degeneration, but this is the least tenable interpretation if one considers that lipid accumulation is an index of cell viability.

The presence of large accumulations of lipid in the cultivated cell can also be considered with regard to *in vitro* conditions. *In vivo* control mechanisms which maintain the delicate balance of insulin exposure and glucose availability are lost. Insulin is a requirement for lipid in the cultivated brown fat cell, and it is known that this hormone can alter the rate of glucose incorporation in cultivated cells (Sidman, '56b; Vann, Renberg and Lewin, '63). On this basis, it would be reasonable to expect that the constant exposure of the fat cell to insulin and glucose, combined with the reduced extracellular fluid volume ratio *in vitro*, would result in an unusually high glucose incorporation into the cell.

Pinocytosis, which is a common feature of the cultivated fat cell, reflects changes in membrane properties consequent to insulin exposure. Pinocytosis is probably the major factor which determines the incorporation rate of glucose into the cultivated brown adipose cell. A similar role for pinocytosis has been postulated for insulin-stimulated white adipose cells (Barnett and Ball, '60). Since neither glycogen accumulation nor excessive pinocytotic activity is evident in the fibroblastic cells in the culture system, it is possible that insulin exhibits a selectivity toward the cultivated brown fat cell, and/or that the cell is extremely sensitive to the hormone.

Turning now to a consideration of the cytoplasmic lipid component of the brown fat cell, it is apparent that there are time-related alterations in lipid content of *in vitro* and experimental cells. The cells of these systems exhibit an increase in lipid content with the passage of time. The lipid inclusions in the cultivated cells become larger than those droplets in the *in vivo* cells, and associated with this increase in size is a corresponding decrease in the number of fat inclusions. *In vivo* control mechanisms and lipid utilization may alter the size of lipid droplets in the *in vivo* brown fat cells.

The smallest visible lipid droplets in the fat cell are approximately 0.2 μ in

diameter. These lipid inclusions are apparently synthesized within the cytoplasm of the brown fat cell, and are not incorporated as pre-formed extracellular lipid bodies. Although the capillary lumina *in vivo* contain chylomicrons, no such structures have ever been seen in the capillary cytoplasm or in the extracellular space between the capillary endothelial cell and the brown fat cell. Lipid accumulation also occurs *in vitro* in the absence of visible lipid structures in the culture medium, and is dependent upon the presence of insulin which facilitates the influx of glucose into the cell. Previous reports in the literature also indicate that lipid inclusions are formed within the fat cell and are not incorporated as preexisting structures (Napolitano, '65).

Membrane-bound lipid droplets have been demonstrated in this study, both *in vivo* and *in vitro*, in brown fat cells. The definitive membrane has been seen surrounding only the larger fat inclusions, supporting a similar claim by Simon ('65). Filamentous structures, surrounding lipid droplets in developing white adipose cells (Wood, '67), have not been observed in this investigation.

If the smaller droplets are not membrane-bound, this would indicate that the presence of a membrane is not necessary for the initial synthesis of lipid and suggests that membrane formation occurs after a critical droplet size is reached. It is possible also that the smaller fat inclusions are membrane-bound, and that the plane of section is not favorable for the visualization of such a membrane.

Recent metabolic evidence suggests that lipid in adipose cells is contained within compartments (Wertheimer, '65); a large compartment serving as a relatively inert storage site in which lipid turnover is very slow, and a second smaller compartment consisting of lipid in a very rapid state of turnover. The presence or absence of a membrane surrounding the lipid droplets might be related to such compartmentalization. The presence of a membrane around larger droplets might act as a physical barrier to lipolysis, thereby preserving a portion of the cytoplasmic lipid component. These large membrane-bound inclusions could represent the lipid com-

cence occurs in the cultivated fat cells after a period of time in culture. Time-lapse cinematography was utilized in an attempt to visualize the process of coalescence, and the results of these studies follow.

Figures 22-27 are sequential frames of a time-lapse film which demonstrates coalescence of fat inclusions in 48 hour cultivated cells placed in Krebs-Ringer phosphate buffer. Figure 22 shows two cells (a and b), which contain numerous lipid droplets. Cell a contains at least ten lipid droplets, and six are present in cell b. Cell b is triangular in shape and measures $17\ \mu$ along one side. The lipid inclusions in cell b are $5.5\ \mu$ in diameter, and the droplets in cell a measure $4\ \mu$.

After approximately 30 minutes in phosphate buffer, coalescence is seen to occur almost simultaneously in both cells. In frame D (fig. 23, arrow), the coalescence of two lipid droplets in cell b can be seen, and further coalescence in cell b is observed in figure 24, frames G and I (arrows).

In figure 25, further coalescence is seen in cell b (frame J, arrow), and cell a in figure 25 is seen also to undergo coalescence of lipid droplets (frames J and L, arrows).

The remaining frames follow the pattern of coalescence and the final frames depict two cells, each of which contain a large, single lipid inclusion (fig. 27). The fat droplet in cell a (fig. 27, frame P) now measures $8.2\ \mu$ and the inclusion in cell b (fig. 27, frame P) is $11\ \mu$ in diameter. These droplets are double in diameter as compared with the individual droplets seen in figure 22. However, the total volume of lipid in each cell is comparable before and after coalescence.

Coalescence has also been observed with time-lapse cinematography in cells maintained on standard tissue culture medium. However, these cells have not been observed to undergo total coalescence to a unilocular stage. In addition, cells in the process of dying have been recorded with time-lapse cinematography. The lipid droplets contained in these cells were seen to fragment into smaller droplets, rather than fusing to form larger fat droplets.

DISCUSSION

The morphological data accumulated in this investigation have provided additional insight into the cytodifferentiation of the brown fat cell. The general ultrastructural features of brown adipose tissue that have been reported previously (Lever, T. Napolitano and Fawcett, '58; and Napolitano, '65). However, studies designed to follow *in vivo* morphological alterations as a function of time, or ultrastructural characterization of cultivated brown fat cells, and the temporally-related changes which these cells undergo, have not been attempted prior to this investigation. The present study demonstrates that cultivated adipose cells, derived from brown fat tissues, are representative of brown fat cells and that the *in vitro* maturational sequences are similar to those observed *in vivo*. The cultivated fat cells are not absolutely comparable to control cells, because they have been trypsinized and exposed to an artificial physical and chemical environment. However, these factors appear not to have significantly disturbed the fat cell maturation, as evidenced by the accumulation of lipid with time.

An ultrastructural comparison of the *in vivo* and *in vitro* brown adipose cells indicated two major differences. First, control cells contain large numbers of ribosomal rosettes, whereas cultivated cells contain fewer ribosomal aggregates; the ribosomes existing as individual particles. Secondly, the majority of *in vivo* cells do not contain appreciable amounts of glycogen. In contrast, the cultivated cells contain copious quantities of glycogen.

The above differences can be considered a result of culture conditions. The apparent diminution of ribosomal rosettes in cultivated fat cells might reflect a decrease in the production of enzymes which are not employed *in vitro*. The tissue culture environment would place more emphasis on lipogenesis, with little or no need for lipolysis. This physiological shift could result in a decreased production of lipolytic enzymes, resulting in disruption of ribosomal aggregates. It could be argued that the ribosomal changes are a result

degeneration, but this is the least ten-
interpretation if one considers that
accumulation is an index of cell via-

he presence of large accumulations of
ogen in the cultivated cell can also be
sidered with regard to *in vitro* condi-
s. *In vivo* control mechanisms which
tain the delicate balance of insulin
posure and glucose availability are lost
itro. Insulin is a requirement for lipid
umulation in the cultivated brown fat
e, and it is known that this hormone can
ease the rate of glucose incorporation
cultivated cells (Sidman, '56b; Vann,
renberg and Lewin, '63). On this basis,
ould be reasonable to expect that the
stant exposure of the fat cell to insulin
d glucose, combined with the reduced
extracellular fluid volume ratio in
ro, would result in an unusually high
ucose incorporation into the cell.

Pinocytosis, which is a common feature
the cultivated fat cell, reflects changes
membrane properties consequent to in-
lin exposure. Pinocytosis is probably the
ajor factor which determines the incor-
poration rate of glucose into the cultivated
own adipose cell. A similar role for pino-
tosis has been postulated for insulin-
stimulated white adipose cells (Barnett
ad Ball, '60). Since neither glycogen ac-
cumulation or excessive pinocytotic activ-
ity is evident in the fibroblastic cells in
the culture system, it is possible that in-
ulin exhibits a selectivity toward the cul-
ivated brown fat cell, and/or that the cell
extremely sensitive to the hormone.

Turning now to a consideration of the
cytoplasmic lipid component of the brown
at cell, it is apparent that there are time-
elated alterations in lipid content of *in*
two and experimental cells. The cells of
both systems exhibit an increase in lipid
content with the passage of time. The lipid
nclusions in the cultivated cells become
arger than those droplets in the *in vivo*
cells, and associated with this increase in
droplet size is a corresponding decrease in
the number of fat inclusions. *In vivo* con-
trol mechanisms and lipid utilization may
restrict the size of lipid droplets in the *in*
vitro brown fat cells.

The smallest visible lipid droplets in the
brown fat cell are approximately 0.2μ in

diameter. These lipid inclusions are ap-
parently synthesized within the cytoplasm
of the brown fat cell, and are not incor-
porated as pre-formed extracellular lipid
bodies. Although the capillary lumina *in*
vitro contain chylomicrons, no such struc-
tures have ever been seen in the capillary
cytoplasm or in the extracellular space be-
tween the capillary endothelial cell and
the brown fat cell. Lipid accumulation also
occurs *in vitro* in the absence of visible
lipid structures in the culture medium, and
is dependent upon the presence of insulin
which facilitates the influx of glucose into
the cell. Previous reports in the literature
also indicate that lipid inclusions are
formed within the fat cell and are not in-
corporated as preexisting structures (Na-
politano, '65).

Membrane-bound lipid droplets have
been demonstrated in this study, both *in*
vivo and *in vitro*, in brown fat cells. The
definitive membrane has been seen sur-
rounding only the larger fat inclusions,
supporting a similar claim by Simon ('65).
Filamentous structures, surrounding lipid
droplets in developing white adipose cells
(Wood, '67), have not been observed in
this investigation.

If the smaller droplets are not mem-
brane-bound, this would indicate that the
presence of a membrane is not necessary
for the initial synthesis of lipid and sug-
gests that membrane formation occurs
after a critical droplet size is reached. It
is possible also that the smaller fat in-
clusions are membrane-bound, and that the
plane of section is not favorable for the
visualization of such a membrane.

Recent metabolic evidence suggests that
lipid in adipose cells is contained within
compartments (Wertheimer, '65); a large
compartment serving as a relatively inert
storage site in which lipid turnover is very
slow, and a second smaller compartment
consisting of lipid in a very rapid state of
turnover. The presence or absence of a
membrane surrounding the lipid droplets
might be related to such compartmental-
ization. The presence of a membrane
around larger droplets might act as a phys-
ical barrier to lipolysis, thereby preserv-
ing a portion of the cytoplasmic lipid
component. These large membrane-bound
inclusions could represent the lipid com-

partment which turns over very slowly. The absence of a membrane around the smaller droplets would facilitate the addition of lipid to an existing droplet, and the lipid material would be also subject to rapid breakdown by cytoplasmic lipase. These non-membrane bound lipid inclusions could represent the lipid compartment which turns over very rapidly.

Coalescence of lipid droplets has been observed in the cultivated multilocular fat cell. The phenomenon of coalescence is not necessarily associated with degeneration of cultivated fat cells, for when cell death is observed *in vitro* in the time-lapse system, lipid breakdown rather than coalescence is seen to accompany the death of the cell. It is also unlikely that the time-lapse film has captured coalescence in a fibroblast, for fibroblasts in culture are spindle-shaped and contain only small amounts of lipid material, whereas the multilocular fat cells are epitheloid in shape, and lipid droplets the size of which are seen to coalesce are found only in those cultivated fat cells with the ultrastructural characteristics of the *in vivo* brown fat cell. For the above reasons, it is concluded that coalescence is a phenomenon that occurs in viable brown fat cells *in vitro*. Since it is impossible to visualize the process of coalescence *in vivo*, one cannot assume that those events which occur *in vitro* also occur *in vivo*. The increase in lipid droplet size with time *in vivo* need not be a result of coalescence, for lipid droplet size could increase by addition of newly formed lipid to existing fat inclusions.

There are certain morphological characteristics of apposed lipid droplets in cultivated and control fat cells which could be associated with the process of coalescence. The membrane complexes observed between fat droplets *in vitro* may represent the initial stages of droplet coalescence, and similar membrane complexes are seen separating fat droplets in control brown fat cells. Discontinuities of this membrane structure, observed in control cells, have not been seen between lipid droplets *in vitro*, but since coalescence of two droplets can occur in a one minute time span, as shown by the time-lapse results, it would be extremely difficult to capture membrane

fragmentation at the ultrastructural level in a system that contains relatively few cells compared to the control system.

Fragmented portions of membranes also appear free within lipid droplets. If time-lapse fragmentation of intervening membrane between two lipid droplets were to occur as a result of coalescence, one would expect to see such fragments within newly formed lipid droplets. The localization of membranous inclusions in lipid droplets supports the postulation that coalescence does occur *in vivo*.

The problem of conversion of brown cells into white fat cells can also be discussed on the basis of the results of this study. If transformation of a multilocular fat cell into a unilocular fat cell were to occur, then one necessary, morphological change would be the coalescence of the numerous lipid droplets of the multilocular cell into a single lipid inclusion. The time-lapse results demonstrate such a morphological change. Conversion would result also in total nuclear displacement to the cytoplasm, with subsequent flattening of the nucleus as the lipid inclusion enlarged, and there would be changes in the cytoplasmic organelles, especially with regard to mitochondrial morphology and number. Some cultivated cells are morphologically different from recognizable brown fat cells and exhibit some structural features of the white adipose cell, and cell types which strongly resemble white cells also have been seen *in vitro*. However, the present investigation does not provide sufficient evidence to the effect that these cells are brown fat cells in the process of transformation *in vitro*.

It is possible that some control mechanisms which are functional *in vitro* are lost *in vitro*, resulting in conversion of cultivated brown fat cell into a cell which exhibits some of the morphological characteristics of a white fat cell. That such a control mechanism does exist *in vivo* is supported by the fact that brown adipocytes are maintained as a specific entity throughout the life-span of the animal, and that in a non-hibernating animal such as the rat, the tissue sites occupied by brown fat cells in the newborn contain large amounts of white adipocytes and very few brown adipose cells.

on this basis that some investigators find that brown fat can be transformed into white adipose tissue. The results of *in vitro* study neither confirm nor deny such a postulation, but they are consistent with the notion that such conversions are possible.

In conclusion, the brown fat cell exhibits striking morphological changes during its differentiation. The most apparent, temporally-related, morphological alterations which these cells undergo involve the size and physical character of the lipid pool. Morphological data from both *in vivo* and *in vitro* systems strongly suggest that lipid synthesis is initially associated with the maturation of small droplets which subsequently increase in size, become surrounded by a membrane, and finally fuse with one another by the process of coalescence. The problem of conversion of the brown fat cell into a white fat cell remains an open question, but that such a conversion can occur is suggested by the *in vitro* evidence.

Since the cultivated cell is no longer exposed to *in vivo* control mechanisms, the potentialities of the cell become more apparent in the tissue culture system, provided that the artificial environment does not interfere with the emergence of such potentialities. That the fat cells *in vitro* are representative of control brown fat cells cannot be disputed. Some reservations must be maintained, however, concerning the extent to which *in vivo* and *in vitro* data may be compared. This investigation is provided an experimental system and laid a basic foundation for further correlative studies which might lead to the elucidation of the physiological, biochemical, and morphological properties and capabilities of the brown fat cell.

LITERATURE CITED

- Urbach, M. 1902 Das braune Fettgewebe bei schweizerischen und deutschen Nagern und Insectivoren. Arch. mikr. Anat., 60: 291-338.
- Arnett, R. J., and E. G. Ball 1960 Metabolic and ultrastructural changes induced in adipose tissue by insulin. J. Biophys. Biochem. Cytol., 8: 83-101.
- Olsen, P. P. 1949 Suspending media for animal tissues. In: Manometric Techniques and Tissue Metabolism. W. W. Umbreit, R. H. Harris and J. F. Stauffer, eds. Burgess Publishing Co., Minneapolis, Minn., 118-119.
- Dyer, R., and J. Ruby 1963 Electron microscope observations of the attachments of cultured cells to a reconstituted collagen matrix. Abst. Anat. Rec., 145: 224.
- Eagle, H. 1953 Nutrition needs of mammalian cells in tissue culture. Science, 122: 501-504.
- Earle, W. R., E. L. Schilling and E. Shelton 1950 Production of malignancy *in vitro*. X. Continued description of cells at the glass interface of the cultures. J. Nat. Cancer Inst., 10: 1067-1104.
- Ehrmann, R. L., and G. O. Gey 1956 The growth of cells on a transparent gel of reconstituted rat-tail collagen. J. Nat. Cancer Inst., 16: 1375-1404.
- Gesner, C. 1551 Medici Tigurini Historiae Animalium. Liber II. Tiguri apud C. Froschoverum, 840-843.
- Hanks, J. H., and R. E. Wallace 1949 Relation of oxygen and temperature in the preservation of tissues by refrigeration. Proc. Soc. Exp. Biol. Med., 71: 196-200.
- Kellenberger, E., W. Schwab and A. Ryter 1956 L'utilisation d'un copolymère du groupe des polyesters comme matériel d'inclusion en ultramicrotomie. Experientia, 12: 421-422.
- Lever, J. D. 1957 The fine structure of brown adipose tissue in the rat with observations on the cytological changes following starvation and adrenalectomy. Anat. Rec., 128: 361-377.
- Masters, E. 1965 Monolayer cultures of brown fat cells. Proc. Soc. Exp. Biol. Med., 119: 44-46.
- McEwen, L. M. 1956 The effect on the isolated rabbit heart of vagal stimulation and its modification by cocaine, hexamethonium and ouabain. J. Physiol., 131: 678-689.
- Moscona, A. 1952 Cell suspensions from organ rudiments of chick embryos. Exp. Cell Res., 3: 535-539.
- Napolitano, L. 1963 The differentiation of white adipose cells. J. Cell Biol., 18: 663-679.
- 1965 Handbook of Physiology. Section 5: Adipose Tissue. A. E. Renold and G. F. Cahill, Jr., Eds., American Physiological Society, Washington, D. C., Chap. 12: 109-123.
- Napolitano, L., and D. W. Fawcett 1958 The fine structure of brown adipose tissue in the newborn mouse and rat. J. Biophys. Biochem. Cytol., 4: 685-692.
- Palade, G. E. 1952 A study of fixation for electron microscopy. J. Exp. Med., 95: 285-298.
- Pappenheimer, A. M. 1917 Experimental studies upon lymphocytes. I. The reactions of lymphocytes under various experimental conditions. J. Exp. Med., 25: 633-650.
- Rasmussen, A. T. 1923 The so-called hibernating gland. J. Morph., 38: 147-206.
- Revel, J. P. 1964 Electron microscopy of glycogen. J. Histo. Cytochem., 12: 104-114.
- Reynolds, E. S. 1963 The use of lead citrate at high pH as an electron-opaque stain in electron microscopy. J. Cell Biol., 17: 208-212.
- Sabatini, D. D., K. Bensch and R. J. Barnett 1963 Cytochemistry and Electron microscopy: The preservation of cellular ultrastructure and enzymatic activity by aldehyde fixation. J. Cell Biol., 17: 19-58.

- Sheldon, E. F. 1924 The so-called hibernating gland in mammals: A form of adipose tissue. *Anat. Rec.*, 28: 331-347.
- Sidman, R. L. 1956a Histogenesis of brown adipose tissue *in vivo* and in organ culture. *Anat. Rec.*, 124: 581-602.
- 1956b The direct effect of insulin on organ cultures of brown fat. *Anat. Rec.*, 124: 723-739.
- Simon, G. 1962 Genèse et structure du tissu adipeux chez l'homme, *Acta Anat.*, 48: 232-241.
- 1965 Handbook of Physiology. Section 5: Adipose Tissue. A. E. Renold and G. F. Cahill, Jr., Eds., American Physiological Society, Washington, D. C., Chap. 11: 101-107.
- Spurlock, B. O., V. C. Kattine and J. A. Freeman 1963 Technical modifications in Maraglas embedding. *J. Cell Biol.*, 17: 203-207.
- Sykes, J. A., and E. B. Moore 1960 A simple tissue culture chamber. *Texas Rep. Biol. Med.*, 18: 288-297.
- Vann, L. S., S. T. Nerenberg and C. J. Lee 1963 Glucose uptake by HeLa cells as enhanced by insulin. *Exp. Cell Res.*, 32: 355-357.
- Watson, M. L. 1958 Staining of tissue sections for electron microscopy with heavy metals. *J. Biophys. Biochem. Cytol.*, 4: 475-478.
- Wertheimer, H. E. 1965 Handbook of Physiology. Section 5: Adipose Tissue. A. E. Renold and G. F. Cahill, Jr., Eds., American Physiological Society, Washington, D. C., Chap. 2: 5-11.
- Williamson, J. R. 1964 Adipose tissue: Morphological changes associated with lipid mobilization. *J. Cell Biol.*, 20: 57-74.
- Wood, E. M. 1967 An ordered complex of elements surrounding the lipid droplets in developing adipose cells. *Anat. Rec.*, 157: 437-446.

Abbreviations

C, Capillary	MBR, Membrane-bound ribosomes
CH, Chylomicron	N, Nucleus
ER, Endoplasmic reticulum	NP, Nuclear pore
FIB, Fibroblast	NU, Nucleolus
G, Glycogen	P, Pinocytotic vesicle
LD, Lipid droplet	R, Ribosome
LMS, Lamellar-membrane system	RBC, Red blood cell
M, Mitochondrion	RC, Reconstituted collagen
	SR, Agranular reticulum
	V, Cytoplasmic vesicle

PLATE 1

EXPLANATION OF FIGURES

- 1 Day one post partum. A general survey electron micrograph demonstrating the tissue organization of the newborn, rat interscapular brown fat pad. Each adipose cell is adjacent to at least one capillary (C), some of which contain a red blood cell (RBC). There are large extracellular spaces in this tissue, relative to tissues in older animals. (LD, lipid droplet; N, nucleus). $\times 3400$.
- 2 Day one post partum. A portion of a brown fat cell and an adjacent capillary. The adipose cell contains small lipid droplets (LD), numerous mitochondria (M), ribosomal rosettes (R), and small amounts of membrane-bound ribosomes (MBR). Pinocytotic vesicles (P) are located along the surface of the fat cell and the capillary endothelial cell. (NU, nucleolus). $\times 8250$.

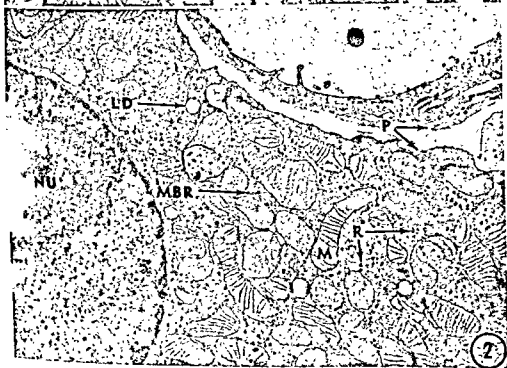
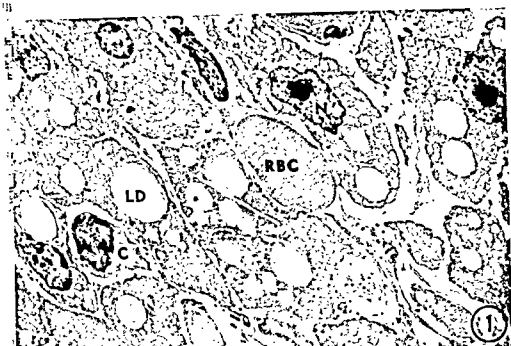


PLATE 2

EXPLANATION OF FIGURES

- 3 Day one post partum. Adjacent adipose cells exhibiting numerous ribosomal rosettes (R), and elements of smooth reticulum (SR). Pinocytotic vesicle formation is observed at P, and P1 indicates a microvesicular rosette. $\times 9600$.
- 4 Day one post partum. Portions of brown fat cells containing large numbers of mitochondria. M1, M2 and M3 depict the patterns of cristae orientation characteristics of brown fat cell mitochondria. (LD, droplet). $\times 5600$.



PLATE 2

EXPLANATION OF FIGURES

- 3 Day one post partum. Adjacent adipose cells exhibiting numerous ribosomal rosettes (R), and elements of smooth reticulum (SR). Pinocytotic vesicle formation is observed at P, and P1 indicates a microvesicular rosette. $\times 9600$.
- 4 Day one post partum. Portions of brown fat cells containing large numbers of mitochondria. M1, M2 and M3 depict the patterns of cristae orientation characteristics of brown fat cell mitochondria. (LD, droplet). $\times 5600$.

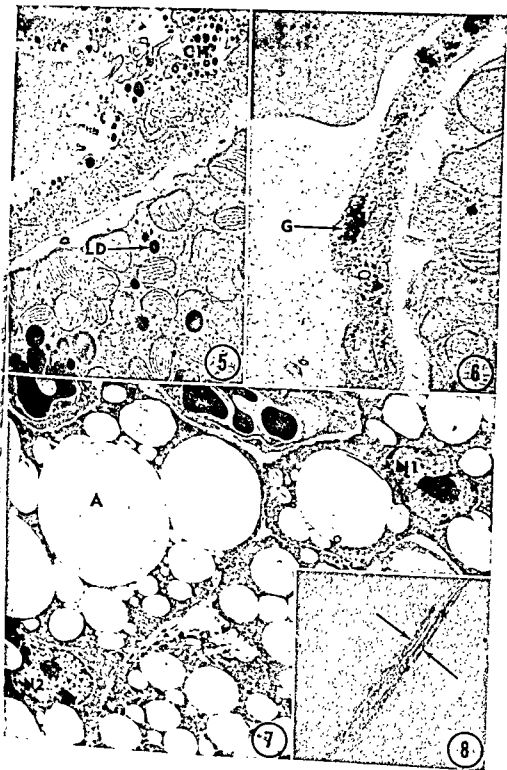


PLATE 3

EXPLANATION OF FIGURES

- 5 Day two post partum. Portions of a brown fat cell and an adjacent capillary. The capillary lumen contains large numbers of chylomicrons (CH). Numerous lipid droplets (LD) are present in the brown adipose cell. $\times 18,720$.
- 6 Day two post partum. Portions of a capillary and a brown fat cell. Cytoplasmic glycogen (G) is present in the capillary endothelial cell. $\times 25,000$.
- 7 Day four post partum. A survey electron micrograph demonstrating large numbers of lipid inclusions in the brown fat cells four days after birth. The weak osmophilia of the lipid is due to preparative procedures. Note the close association of surrounding lipid droplets to the droplet labeled A. There is a general increase in cell size due to lipid accumulation, and a corresponding decrease in extracellular space. (N, nucleus). $\times 2975$.
- 8 Day four post partum. Two large lipid droplets separated from each other by tri-partite membrane complexes (arrows). $\times 146,250$.

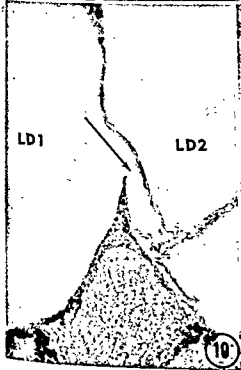
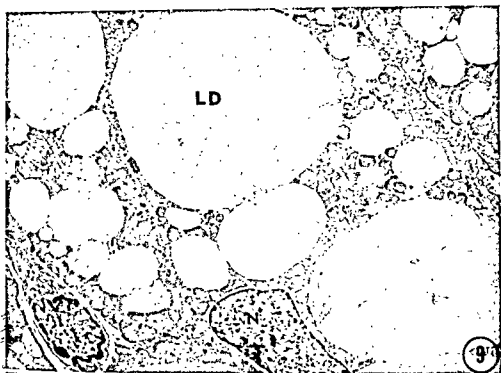


PLATE 4

EXPLANATION OF FIGURES

- 9 Day six post partum. A survey electron micrograph demonstrating large lipid inclusions (LD) in the adipose cells. The extracellular spaces between these fat-laden cells are very small. (N, nucleus). $\times 5000$.
- 10 Day nine post partum. A membrane complex between two lipid droplets (LD1 and LD2). Note the lateral displacement of the membrane complex at the arrow. $\times 95,800$.
- 11 Day nine post partum. A membranous fragment (arrow) within a lipid droplet (LD). A lamellar-membrane system (LMS) is seen at the periphery of the lipid droplet. $\times 100,625$.

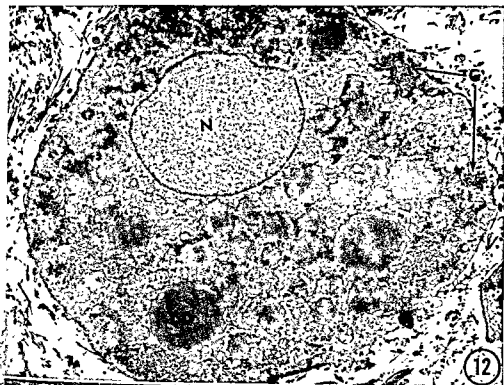


PLATE 5

EXPLANATION OF FIGURES

- 12 Day one *in vitro*. A cultivated adipose cell exhibiting the general morphological characteristics of *in vitro* brown fat cells, except for large glycogen accumulations (G). Note the numerous small lipid inclusions (LD), and the spherical, eccentric nucleus (N). $\times 7660$.
- 13 Day one *in vitro*. A cultivated brown fat cell containing a prominent nucleolus (NU), and exhibiting pores in the nuclear envelope (NP). The mitochondria (M) are characteristic of control brown fat cells. (LD, lipid droplet). $\times 18,000$.

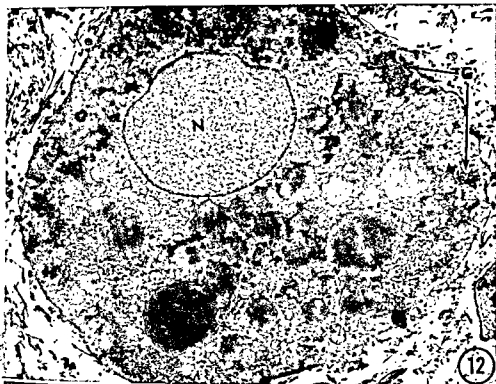


PLATE 6

EXPLANATION OF FIGURES

- 14 Day two *in vitro*. Portions of a cultivated adipose cell exhibiting the morphological characteristics of *in vivo* brown fat cells four days post partum. (LD, lipid droplet; N, nucleus). $\times 5200$.
- 15 Day two *in vitro*. Two cultivated brown fat cells which contain large accumulations of glycogen (G). $\times 16,380$.
- 16 Day four *in vitro*. An adipose cell containing numerous lipid droplets, some of which exhibit a peripheral rim of lesser density (LD1, LD2 and LD3). Note the apposition of small fat inclusions to LD1 and LD2. LD1 and LD2 contain profiles of lesser density which correspond in size to the smaller lipid droplets. $\times 6200$.

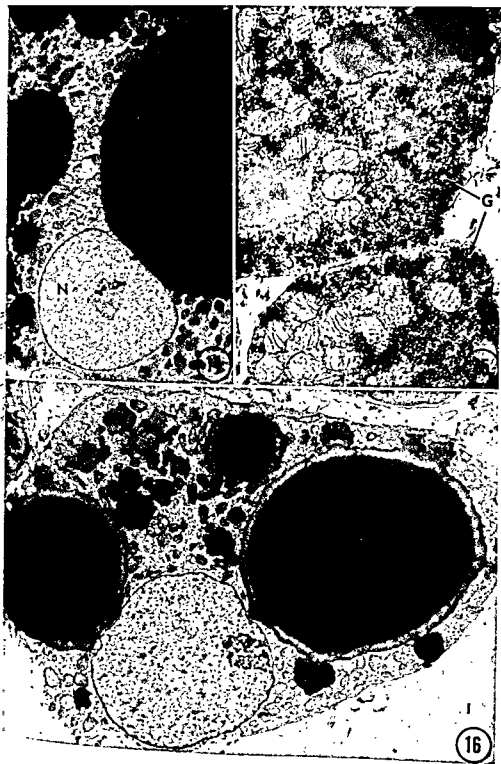


PLATE 7

EXPLANATION OF FIGURES

- 17 Day four *in vitro*. This micrograph depicts the two cell types found in the culture system. The fat cell contains lipid droplets (LD), cytoplasmic vesicles (V), numerous, large, complex mitochondria (M), and the cell surface is lined with pinocytotic vesicles (P). The fibroblastic cell (FIB) is strikingly different from the cultivated fat cells. Notice in particular the differences in mitochondrial morphology. The fibroblastic cell (FIB) is attached to the surface of the reconstituted collagen matrix (RC). (N, nucleus). $\times 12,250$.
- 18 Day four *in vitro*. A cell containing a single, large lipid droplet and a peripherally displaced and flattened nucleus (N). This cell exhibits the general morphological characteristics of a white fat cell. $\times 7950$.



PLATE 8

EXPLANATION OF FIGURES

- 19 Day six *in vitro*. A portion of a cultivated multilocular adipose cell. Note the apposition of adjacent lipid droplets at A and B to the lipid inclusion labeled LD1. $\times 11,690$.
- 20 Day six *in vitro*. A high magnification of the interlocking interface at A in figure 19, revealing the membrane complex at this region (arrow). $\times 100,625$.
- 21 Day six *in vitro*. A number of adipose cells containing large lipid droplets, (LD), glycogen bodies (G), and displaced nuclei (N1, N2). Small lipid inclusions are frequently seen at the periphery of the larger droplets (arrow). (ER, endoplasmic reticulum). $\times 3600$.

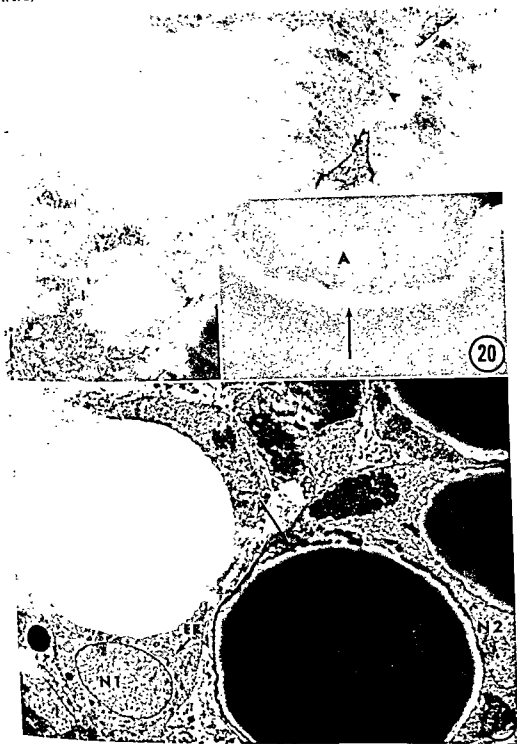


PLATE 8

EXPLANATION OF FIGURES

- 19 Day six *in vitro*. A portion of a cultivated multilocular adipose cell. Note the apposition of adjacent lipid droplets at A and B to the lipid inclusion labeled LD1. $\times 11,690$.
- 20 Day six *in vitro*. A high magnification of the interlocking interface at A in figure 19, revealing the membrane complex at this region (arrow). $\times 100,625$.
- 21 Day six *in vitro*. A number of adipose cells containing large lipid droplets, (LD), glycogen bodies (G), and displaced nuclei (N1, N2). Small lipid inclusions are frequently seen at the periphery of the larger droplets (arrow). (ER, endoplasmic reticulum). $\times 3600$.

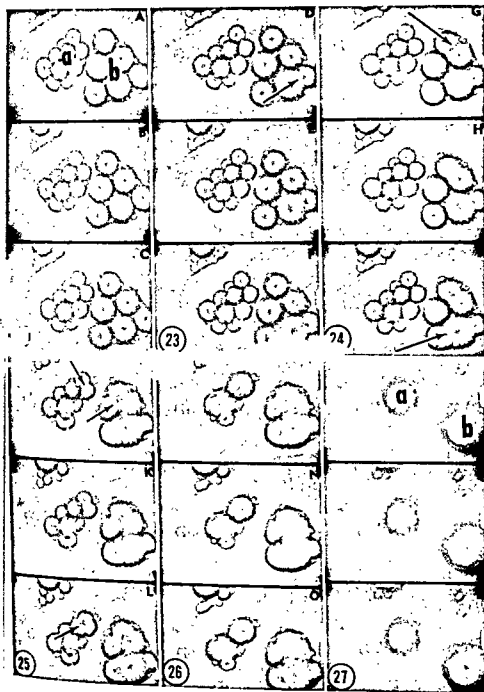


PLATE 9

EXPLANATION OF FIGURES

- 22-27 Day two *in vitro*. Sequential frames of a time-lapse film. Two fat-containing cells are seen (fig. 22, frame A, a and b). Lipid-droplet coalescence is observed at the arrows in figure 23 (frame D), figure 24 (frame G and I), and figure 25 (frame J and L). Figure 27 depicts two unilocular fat cells (frame P, a and b), formed by the coalescence of lipid droplets. $\times 1375$.

e Ultrastructure of the Crevicular ithelium of Cat Gingiva¹

J. B. GAVIN²

Department of Anatomy, Northwestern University Medical and
Dental Schools, Chicago, Illinois

ABSTRACT The ultrastructure of the crevicular epithelium of clinically healthy cat gingiva was similar to that of other non-keratinizing oral epithelia. However, it differed in that the intercellular spaces were wide and extended as a continuous network from the basal lamina to the epithelial surface. Basal cells contained numerous mitochondria, Golgi apparatus, free ribosomes and a fine feltwork of evenly distributed tonofilaments. Hemidesmosomes were present in relation to the basal lamina. Cells in the intermediate layers showed a decrease in the number of organelles and an increase in concentration of tonofilaments. Superficial cells were further flattened and the remaining organelles commonly showed degenerative changes. Epithelial cells showed prominent microvilli extending into the intercellular spaces. Some of these formed desmosomes with similar processes of adjacent cells. Occasional randomly distributed tight junctions were also observed. Inactive basal melanocytes, more superficial Langerhans cells and leucocytes were seen between epithelial cells. The great majority of leucocytes were neutrophils and many of these ruptured as they approached the epithelial surface scattering their specific granules into the intercellular spaces. These findings are discussed in relation to the peculiar permeability of the gingival crevicular region of the oral mucosa to tissue fluid and leucocytes.

Electron microscopy has been used to investigate the structure of gingival epithelium in both animals (Albright, '60; Arn, '65) and in man (Kurahashi and Kuma, '62; Listgarten, '64; Stern, '65; Asterhouse, '65; Haim, '66; Schroeder and Ellade, '66) but these studies have dealt most exclusively with the keratinizing epithelium which forms the outer or masticatory surface of gingiva. Stern ('62) and Listgarten ('66) studied the fine structure of the attached epithelial cuff of gingiva and elucidated the nature of the gingivo-epithelial junction. Thilander ('63) studied the action of enzymes on the stratum spinosum of the crevicular epithelium and Weinstein et al. ('67) examined it following the intravenous administration of saccharated iron oxide. However, the fine structure of this epithelial lining of the gingival crevice has not been comprehensively described.

Using intravenous tracers Brill and Krasse ('58) and Brill and Bjorn ('59) demonstrated that a protein-containing fluid can pass through the clinically healthy crevicular epithelium at not through other regions of oral and nasal mucosa. Recently Weinstein et al.

('67) described differences in composition between this gingival fluid and serum which suggest that permeability of the crevicular epithelium is a selective one. Sharry and Krasse ('60) and Loe ('61) demonstrated that the gingival crevice is also the site of entry into the mouth of salivary leucocytes.

The present investigation was undertaken to describe fully the fine structure of crevicular epithelium, and to provide a basis for understanding the permeability of this region of the oral mucosa.

MATERIAL AND METHOD

Strips (the marginal 2-3 mm, fig. 1) of clinically healthy gingiva were excised from the labial and buccal surfaces of canine and premolar teeth of ten mongrel cats. They were immediately sliced transversely at 0.5-1 mm intervals in a drop of fixative, and fixation was continued for one hour, either in ice-cold, phosphate-buffered (pH 7.3) 1% osmium tetroxide solution containing 5.4% glucose (Milonig, '62), or in veronal-acetate buffered

¹ This investigation was supported by a United States Public Health Service International Postdoctoral Research Fellowship (F-05-TW-863-01).

² Present address: Department of Anatomy, University of Saskatchewan, Saskatoon, Canada.

grouped and oriented into prominent bundles, as in keratinizing gingival epithelium (fig. 5).

Small circular vesicles, often arranged in lines in close relation to the cell membrane, were common in the cytoplasm of basal cells. Indentations and invaginations of the basal cell plasma membranes suggested pinocytotic activity (figs. 1, 2). Occasional dense rounded bodies with a finely granular, or sometimes multilamellar, matrix were present within the cytoplasm of crevicular epithelial cells (figs. 3, 3) and larger lipid droplets were also common (fig. 10).

The desmosomes of crevicular epithelium consisted of opposing zones of cell membrane specialization, subjacent cytoplasmic electron density and tonofilament concentration, as seen in the hemidesmosomes, separated by an intercellular interval of some 200 Å (fig. 9). The intercellular lamellae which form part of the desmosomal complex in keratinizing gingival epithelium were often not as apparent as in similarly treated crevicular epithelium. Tight junctions, characterized by a fusion of the outer leaflets of adjacent cell membranes and the absence of adjacent cytoplasmic modification, were occasionally seen amongst groups of desmosomes. They appeared to be randomly distributed and were not characteristically found in the superficial strata (fig. 9).

Passing from the basal to intermediate cell layers there was a progressive flattening of the epithelial cells, nuclear outlines tended to become more irregular, and there was a diminution in the number of mitochondria. Conversely, the number of tonofilaments tended to increase (figs. 4, 8) but unlike keratinizing gingival epithelium there was no tendency for them to form prominent bundles (fig. 5). In the superficial cells cytoplasmic lipid droplets were more common (fig. 10) but cytoplasmic organelles were fewer and tended to be poorly defined and degenerate. Intracellular lysosome-like bodies at this level often had bizarre forms and membranous whorls resembling myelin figures were also observed.

At all levels the intercellular spaces were wide (figs. 3, 6, 8, 10, 11, 13) with localized dilatations up to several microns in

width. A finely granular material (figs. 6, 11), generally similar in appearance to the ground substance of connective tissue, filled the intercellular spaces which formed an interconnecting network extending from the basal lamina dense to the external environment. In the intermediate (fig. 8) and superficial (fig. 13) layers, the intercellular spaces frequently contained cellular debris and membrane-bound dense bodies which exhibited a variety of shapes (fig. 13). Some resembled the intracellular lysosome-like bodies already described. Microvilli of various lengths projected from epithelial cells into the intercellular spaces and often contacted similar processes from adjacent cells (fig. 8).

Basal melanocytes were recognised by their characteristically indented nucleus and a cytoplasm rich in mitochondria but devoid of tonofilaments and cytoplasmic granules (fig. 7). These cells were found close to the epithelial basal lamina but were usually separated from it by fine processes of the adjacent Malpighian cells. They did not form desmosomes with the epithelial cells (fig. 7). Melanocyte processes were seen in the intercellular spaces at all levels. Langerhans cells with similarly indented nuclei and cytoplasm rich in mitochondria were present in the intermediate and superficial layers.

Leucocytes were also present within the intercellular spaces of crevicular epithelium. Although lymphocytes and larger cells of the monocyte series were observed, neutrophils were the most common type. The latter were readily recognised by their nuclear polymorphism and rich cytoplasmic content of densely staining "specific granules" (fig. 11). The cell membranes of neutrophils in the more superficial parts of the epithelium frequently showed discontinuities not evident in the plasma membranes of adjacent epithelial cells (fig. 11). Rupture of these migrating neutrophils (figs. 11, 12) as they approached the salivary environment seemed the most likely explanation for the presence of lysosome-like bodies within the intercellular spaces of the crevicular epithelium.

DISCUSSION

Although the fine structure of the crevicular epithelium was found to be gen-

(pH 7.3) 2% osmium tetroxide containing 4.5% sucrose (Caulfield, '57). After dehydration in graded ethanol and infiltration with propylene oxide, the triangular gingival slices were embedded flat in discs of Araldite (Luft, '61) or in an Araldite and Epon mixture (Yamamoto, '66).

The polymerized discs were then viewed with a dissecting microscope to distinguish the strongly osmiophilic keratinizing epithelium, the lightly stained crevicular epithelium and the virtually unstained connective tissue, each of which formed one margin of the slice of gingiva. As an additional check on the localisation of the block face, 1 μ sections were cut and stained with 0.5% alkaline methylene blue for light microscopy. Sections (700–1200 Å in thickness) were stained with uranyl acetate (Watson, '58) and lead citrate (Reynolds, '63) and examined with a Hitachi HU-11A electron microscope.

OBSERVATIONS

Under the light microscope the crevicular epithelium varied from 3–4 cells in thickness over connective tissue papillae to several times this thickness between them (figs. 1, 2). Wide-bore capillaries were numerous just deep to the basement membrane separating the collagenous connective tissue from the basal epithelial cells (fig. 2). The germinative cells stained deeply with methylene blue and were frequently observed in mitosis (fig. 2). In the intermediate layers, cells showed a transition from the cuboidal or low columnar basal cells to the more flattened superficial cells, a change accompanied by a loss of basophilia and nucleolar prominence (fig. 2). Although sometimes smooth, the surface of the crevicular epithelium was often ragged (fig. 2).

With the electron microscope the junction of the epithelium and connective tissue was seen to be irregular due to projections and invaginations of the basal epithelial cells (fig. 4). The junctional zone or "basement membrane" consisted of two lamellae. A relatively clear layer, the lamina lucida, some 250–400 Å thick separated the plasma membranes of the basal cells from an electron dense layer, the lamina densa, which was of similar thickness (figs. 4, 5, 6). Fine fibrils about 100 Å

in diameter with faint but irregular transverse striations radiated from the lamina densa between the larger (250–600 Å) light staining and characteristically oriented collagen fibres most of which were parallel to the basal lamina. These fine fibrils were more numerous beneath keratinizing gingival epithelium (fig. 5) than deep to the crevicular epithelium (fig. 4). The lamina densa was continuous across the spaces between basal cells but there was little distinction between the lamina lucida and the intercellular material (fig. 6).

Hemidesmosomes were present at the junction of the crevicular epithelium and connective tissue (fig. 4) but were not as numerous as those beneath keratinizing gingival epithelium. At the half desmosome, the epithelial cell membrane showed an increased separation of its component leaflets and an intensification in staining of the inner one. The subjacent cytoplasm exhibited a diffuse electron density which shaded off into the concentration of tonofilaments usually present. On the connective tissue side of the modified plasma membrane an additional dense lamina 60 Å thick, and separated from the cell membrane by 100 Å, was present in the lamina lucida. There was a tendency for the lamina densa in these regions to show an increased density.

The basal epithelial cells had centrally placed ovoid nuclei bounded by a nuclear membrane containing nuclear pores. Mitochondria were numerous in these cells, particularly in the basal parts of the cytoplasm and in the vicinity of the Golgi apparatus (fig. 3). One or two electron dense granules were frequently present within these mitochondria in relation to the inner mitochondrial membrane. The series of parallel lamellae and vesicles which comprised the Golgi apparatus tended to be arranged parallel to the nuclear membrane and quite close to it (fig. 3). Rough surfaced endoplasmic reticulum was not present in any significant amounts but free ribosomes, often grouped to form polyribosomes, were abundant and distributed throughout the cytoplasm amongst the even feltwork of short fine tonofilaments. The tonofilaments of crevicular epithelium (fig. 3) were not as numerous, nor were

LITERATURE CITED

- staff, and to Associate Professor W. D. Miller of the Department of Anatomy of the University for their help, guidance and constructive criticism during this investigation.
- Light, J. T. 1960 Electron microscopic study of keratinization as observed in gingiva and cheek mucosa. *Ann. N. Y. Acad. Sci.*, 85: 351-1.
- Miller, D. L. 1960 The hormonal induction of vaginal leukocytic exudate in the germ-free mouse. *Am. J. Path.*, 37: 769-773.
- Miller, N. 1959 Influence of capillary permeability on flow of tissue fluid into human gingival pockets. *Acta Odont. Scand.*, 17: 23-33.
- Miller, N., and H. Björn 1959 Passage of tissue fluid into human gingival pockets. *Acta Odont. Scand.*, 17: 11-22.
- Miller, N., and B. Krasse 1958 The passage of tissue fluid into the clinically healthy gingival pocket. *Acta Odont. Scand.*, 16: 233-246.
- Miller-Grant, K., and R. M. Browne 1966 The gingival fluid of the labial aspect of the upper incisors in the rabbit. *Arch. Oral Biol.*, 11: 55-471.
- Miller, J. B. 1957 Effects of varying the vehicle for OsO_4 in tissue fixation. *J. Biophys. Biochem. Cytol.*, 3: 827-829.
- Miller, J. M., and J. M. Tormey 1966 Role of long extracellular channels in fluid transport across epithelia. *Nature*, 210: 817-820.
- Miller, J. 1963 Diffusion of histamine into the gingival crevice and through the crevicular epithelium. *Acta Odont. Scand.*, 21: 271-276.
- Miller, M. G., and G. E. Palade 1964 Functional organization of amphibian skin. *Proc. Nat. Acad. Sci.*, 51: 569-577.
- Miller, J. 1965 Cell junctions in amphibian skin. *J. Cell Biol.*, 26: 263-291.
- Miller, J. B., and A. A. Collins 1961 The occurrence of bacteria within the clinically healthy gingival crevice. *J. Periodont.*, 32: 198-202.
- Miller, G. 1966 Les Parodontopathies. Rapports et Communications du XVIII^e Congrès de l'Association pour les Recherches sur les Parodontopathies (Arpa Internationale) Berlin, 22-26. Mai 1966. Georg & Cie S.A., Genève, 1-7.
- Miller, J. F. 1966 Distribution and fine structure of globule leucocytes in respiratory and digestive tracts of the laboratory rat. *Anat. Rec.*, 156: 439-454.
- Miller, Y., and S. Takuma 1962 Electron microscopy of human gingival epithelium. *Bull. Tokyo Dent. Coll.*, 3: 29-43.
- Miller, M. A. 1964 The ultrastructure of human gingival epithelium. *Am. J. Anat.*, 114: 43-69.
- Miller, J. 1966 Electron microscopic study of the gingivo-dental junction of man. *Am. J. Anat.*, 119: 147-178.
- Löe, H. 1961 Physiological aspects of the gingival pocket. *Acta Odont. Scand.*, 19: 387-396.
- Luft, J. H. 1961 Improvements in epoxy resin embedding methods. *J. Biophys. Biochem. Cytol.*, 9: 409-414.
- Millonig, G. 1962 Electron Microscopy, Fifth Internat. Congr. Electron Microscopy, Academic Press, New York, 2: 8.
- Orban, B. J. 1957 Oral Histology and Embryology. 4th ed. C. V. Mosby Co., St. Louis, 256.
- Reynolds, E. S. 1963 The use of lead citrate at high pH as an electron-opaque stain in electron microscopy. *J. Cell Biol.*, 17: 208-212.
- Rizzo, A. A., and C. T. Mitchell 1966 Chronic allergic inflammation induced by repeated deposition of antigen in rabbit gingival pockets. *Periodontics*, 4: 4-10.
- Rovin, S., E. R. Costich and H. A. Gordon 1966 The influence of bacteria and irritation in the initiation of periodontal disease in germ-free and conventional rats. *J. Periodont. Res.*, 1: 193-203.
- Schroeder, H. E., and J. Theilade 1966 Electron microscopy of normal human gingival epithelium. *J. Periodont. Res.*, 1: 95-119.
- Sharry, J. J., and B. Krasse 1960 Observations on the origin of salivary leukocytes. *Acta Odont. Scand.*, 18: 347-358.
- Stern, I. B. 1962 The fine structure of the ameloblast-enamel junction in rat incisors; epithelial attachment and cuticular membrane. In: Electron Microscopy, Fifth Internat. Congr. Electron Microscopy, Academic Press, New York, 2: QQ-6.
- Miller, J. 1965 Electron microscopic observations of oral epithelium. I. Basal cells and basement membrane. *Periodontics*, 3: 224-238.
- Thilander, H. 1963 The effect of leukocytic enzyme activity on the structure of the gingival pocket epithelium in man. *Acta Odont. Scand.*, 21: 431-451.
- Miller, J. 1964 Permeability of gingival pocket epithelium. *Internat. Dent. J.*, 14: 416-421.
- Waterhouse, J. P. 1965 The gingival part of the human periodontium. *Dent. Pract.*, 15: 409-415.
- Weinstein, E., I. D. Mandel, A. Salkind, H. I. Oshrain and G. D. Pappas 1967 Studies of gingival fluid. *Periodontics*, 5: 161-166.
- Watson, M. L. 1958 Staining of tissue sections for electron microscopy with heavy metals. *J. Biophys. Biochem. Cytol.*, 4: 475-478.
- Yamamoto, I. 1966 Ultrastructural changes in mesenteric lymph nodes of mice infected with *Salmonella enteritidis*. *J. Infect. Dis.*, 116: 8-20.
- Zelickson, A. S., and J. F. Hartmann 1962 An electron microscopic study of normal human non-keratinizing oral mucosa. *J. Invest. Derm.*, 38: 99-107.
- Miller, J. 1963 Electron microscopy of skin and mucous membrane. Charles C Thomas, Springfield, Illinois, 64-78.

erally similar to that of non-keratinizing oral epithelia (Zelickson and Hartmann, '62, '63) it differed in two significant respects, namely, the continuity of its intercellular spaces with the oral cavity and the presence within it of large numbers of leucocytes.

Prominent intercellular spaces, like those of crevicular epithelium, are also seen in amphibian epidermis but in the latter, belts of membrane fusion (zonulae occludentes) bind the superficial cells into a continuous sheet (Farquhar and Palade, '64, '65). Diamond and Tormey ('66) have reviewed the role of long extracellular channels in the transport of fluid across epithelia. However, in the epithelia they discuss (intestine, gall bladder, kidney) the intercellular spaces are closed externally by tight junctions as in amphibian epidermis. Such tight junctions as were observed between the cells of the crevicular epithelium appeared to be insufficient in number to form such a barrier, and the few present were not limited to the superficial layer of cells. The possibility that the presence of such wide intercellular spaces was a fixation artefact was eliminated by comparing the crevicular epithelium with the keratinizing epithelium in the same slice of gingiva. In the latter epithelium, as in non-keratinizing oral epithelium (Zelickson and Hartmann, '62, '63), the superficial intercellular spaces were virtually obliterated.

Although a study using saccharated iron oxide as an electron-dense tracer (Weinstein et al., '67) did not produce conclusive evidence of intercellular passage, it seems probable that the width and continuity of the intercellular spaces is the morphological basis for the outward movement of tissue fluid (Brill and Krasse, '58; Brill and Bjorn, '59) through the crevicular epithelium, but not through other regions of healthy oral mucosa. The recovery of intravenous sodium fluorescein has been used to demonstrate the flow of this gingival fluid in the dog (Brill and Krasse, '58), man (Brill and Bjorn, '59), and rabbit (Brown-Grant and Browne, '66) and we have found that it also enters the gingival crevice in the cat (unpublished results). The differences in ratios of components between this fluid and serum (Weinstein

et al., '67) indicate that it is not a simple transudate. Two morphological features of the crevicular epithelium could be related to this selectivity. They are the epithelial basal lamina which appeared to form the only continuous "barrier" between the connective tissue and the oral cavity, and the prominent microvilli which suggest cellular modification of the content of the intercellular spaces.

Similarly, the wide intercellular spaces could be the route for inward passage of materials through this epithelium. Eysenbach-Gamborg ('63) has demonstrated that histamine placed in the gingival crevice produces changes in the underlying vasculature while Rizzo and Mitchell ('66) have produced both a local and a systemic antibody response to the repeated application of albumin to the crevicular region.

In view of this inward permeability, the presence of leucocytes in the gingival tissues could be interpreted as an inflammatory response to the bacterial flora of the gingival crevice (Gavin and Collins, '61). However, Orban ('57) believes that the presence of such cells does not, in itself, constitute a pathological condition. This latter view is supported by the presence of leucocytes in the gingiva of germ-free mice (Rovin, Costich and Gordon, '66) and in other mucous membranes of the genital (Beaver, '60), respiratory and digestive tracts (Kent, '66) which are not commonly inflamed. Until it is determined whether gingival leucocytes represent an actual, or only a potential, defense mechanism, the histological control of the selection of healthy gingiva will remain unreliable. Many of the neutrophils observed in the crevicular epithelium appeared to be deintegrating and discharging their granules into the intercellular spaces. Indeed, the prominence of these spaces in the material examined might be related to this leucocytic degranulation, for both leucocytic enzymes and hyaluronidase increase their width (Thilander, '63). The latter enzyme may be a product of the crevicular bacterial flora (Thilander, '64).

ACKNOWLEDGMENTS

The author is indebted to Professor J. C. Hampton, Chairman of the Department of Anatomy at Northwestern University and

LITERATURE CITED

- aff, and to Associate Professor W. D. [unclear] of the Department of Anatomy of [unclear] University for their help, guidance and constructive criticism during this investigation.
- Light, J. T. 1960 Electron microscopic study of keratinization as observed in gingiva and oral mucosa. *Ann. N. Y. Acad. Sci.*, 85: 351-366.
- McCr, D. L. 1960 The hormonal induction of gingival leukocytic exudate in the germ-free mouse. *Am. J. Path.*, 37: 769-773.
- N. 1959 Influence of capillary permeability on flow of tissue fluid into human gingival pockets. *Acta Odont. Scand.*, 17: 23-33.
- N., and H. Björn 1959 Passage of tissue fluid into human gingival pockets. *Acta Odont. Scand.*, 17: 11-22.
- N., and B. Krasse 1958 The passage of tissue fluid into the clinically healthy gingival pocket. *Acta Odont. Scand.*, 16: 233-246.
- McGrath, K., and R. M. Browne 1966 The gingival fluid of the labial aspect of the upper incisors in the rabbit. *Arch. Oral Biol.*, 11: 435-471.
- Field, J. B. 1957 Effects of varying the vehicle for OsO₄ in tissue fixation. *J. Biophys. Biochem. Cytol.*, 3: 827-829.
- Moond, J. M., and J. M. Tormey 1966 Role of long extracellular channels in fluid transport across epithelia. *Nature*, 210: 817-820.
- Berg, J. 1963 Diffusion of histamine into the gingival crevice and through the crevicular epithelium. *Acta Odont. Scand.*, 21: 271-276.
- Gohar, M. G., and G. E. Palade 1964 Functional organization of amphibian skin. *Proc. Nat. Acad. Sci.*, 51: 569-577.
- 1965 Cell junctions in amphibian skin. *Cell Biol.*, 26: 263-291.
- Lin, J. B., and A. A. Collins 1961 The occurrence of bacteria within the clinically healthy gingival crevice. *J. Periodont.*, 32: 198-202.
- Am, G. 1966 Les Parodontopathies. Rapports et Communications du XVIII^e Congrès de l'Association pour les Recherches sur les Parodontopathies (Arpa Internationale) Berlin, 22-26. Mai 1966. Georg & Cie S.A., Genève, 1-7.
- nt, J. F. 1966 Distribution and fine structure of globule leucocytes in respiratory and digestive tracts of the laboratory rat. *Anat. Rec.*, 156: 439-454.
- Urahashi, Y., and S. Takuma 1962 Electron microscopy of human gingival epithelium. *Bull. Tokyo Dent. Coll.*, 3: 29-43.
- Stegarten, M. A. 1964 The ultrastructure of human gingival epithelium. *Am. J. Anat.*, 114: 43-69.
- 1966 Electron microscopic study of the gingivo-dental junction of man. *Am. J. Anat.*, 119: 147-178.
- Løe, H. 1961 Physiological aspects of the gingival pocket. *Acta Odont. Scand.*, 19: 387-396.
- Luft, J. H. 1961 Improvements in epoxy resin embedding methods. *J. Biophys. Biochem. Cytol.*, 9: 409-414.
- Millonig, G. 1962 Electron Microscopy, Fifth Internat. Congr. Electron Microscopy, Academic Press, New York, 2: 8.
- Orban, B. J. 1957 Oral Histology and Embryology. 4th ed. C. V. Mosby Co., St. Louis, 256.
- Reynolds, E. S. 1963 The use of lead citrate at high pH as an electron-opaque stain in electron microscopy. *J. Cell Biol.*, 17: 208-212.
- Rizzo, A. A., and C. T. Mitchell 1966 Chronic allergic inflammation induced by repeated deposition of antigen in rabbit gingival pockets. *Periodontics*, 4: 4-10.
- Rovin, S., E. R. Costich and H. A. Gordon 1966 The influence of bacteria and irritation in the initiation of periodontal disease in germ-free and conventional rats. *J. Periodont. Res.*, 1: 193-203.
- Schroeder, H. E., and J. Theilade 1966 Electron microscopy of normal human gingival epithelium. *J. Periodont. Res.*, 1: 95-119.
- Sharry, J. J., and B. Krasse 1960 Observations on the origin of salivary leukocytes. *Acta Odont. Scand.*, 18: 347-358.
- Stern, I. B. 1962 The fine structure of the ameloblast-enamel junction in rat incisors; epithelial attachment and cuticular membrane. In: *Electron Microscopy, Fifth Internat. Congr. Electron Microscopy*, Academic Press, New York, 2: QQ-6.
- 1965 Electron microscopic observations of oral epithelium. I. Basal cells and basement membrane. *Periodontics*, 3: 224-238.
- Thilander, H. 1963 The effect of leukocytic enzyme activity on the structure of the gingival pocket epithelium in man. *Acta Odont. Scand.*, 21: 431-451.
- 1964 Permeability of gingival pocket epithelium. *Internat. Dent. J.*, 14: 416-421.
- Waterhouse, J. P. 1965 The gingival part of the human periodontium. *Dent. Pract.*, 15: 409-415.
- Weinstein, E., I. D. Mandel, A. Salkind, H. I. Oshrain and G. D. Pappas 1967 Studies of gingival fluid. *Periodontics*, 5: 161-166.
- Watson, M. L. 1958 Staining of tissue sections for electron microscopy with heavy metals. *J. Biophys. Biochem. Cytol.*, 4: 475-478.
- Yamamoto, I. 1966 Ultrastructural changes in mesenteric lymph nodes of mice infected with *Salmonella enteritidis*. *J. Infect. Dis.*, 116: 8-20.
- Zelickson, A. S., and J. F. Hartmann 1962 An electron microscopic study of normal human non-keratinizing oral mucosa. *J. Invest. Derm.*, 38: 99-107.
- 1963 Electron microscopy of skin and mucous membrane. Charles C Thomas, Springfield, Illinois, 64-78.

PLATE 1

EXPLANATION OF FIGURES

- 1 Light micrograph of cat gingiva showing keratinized masticatory epithelium (ME), the crevicular epithelium (CE) related to the gingival crevice, and the attached epithelial cuff (AEC) related to the space (E) occupied by the enamel prior to decalcification. These epithelia cover a collagenous tissue (CT) which is well supplied with capillaries (c). The horizontal line indicates the level of the scalpel cut used to obtain specimens of crevicular epithelium. Paraffin section, Masson's trichrome stain. $\times 40$.
- 2 Light micrograph of crevicular epithelium showing the basophilic basal epithelial cells one of which is in mitosis (mf), the more flattened intermediate cells (i) which have prominent nucleoli, and the lightly staining, somewhat ragged superficial cells (s). Several capillaries (c) are present just deep to the epithelium. Araldite section, methylene blue stain. $\times 400$.
- 3 Electron micrograph of parts of four basal cells of crevicular epithelium. Such cells have an ovoid nucleus (N), numerous mitochondria containing small dense granules (M), Golgi vesicles (G), pinocytotic vesicles (P), lysosome-like granules (L), and a fine feltwork of tonofilaments (T). These cells are separated from one another except at the desmosomes (D) by the intercellular spaces (S) into which microvilli (MV) project. $\times 12,500$.

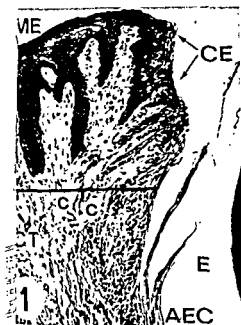


PLATE 2

EXPLANATION OF FIGURES

- 4 Electron micrograph of the convoluted junction between crevicular epithelium (E) and the underlying connective tissue (C). The junction consists of a lamina lucida (ll) and a lamina densa (ld) from which fine fibrils (ff) radiate between the lightly staining collagen fibres beneath. The basal epithelial cell membrane shows invaginations reminiscent of pinocytosis (p) and an increase in electron density at hemidesmosomes (hd). $\times 25,000$.
- 5 Electron micrograph of the junction between keratinizing gingival epithelium and the underlying collagenous tissue. The aggregation of tonofilaments (TF) into bundles is shown within the epithelial cells which form hemidesmosomes (hd). Fine fibrils (small arrows) radiate from the lamina densa (ld) between underlying collagen fibres (large arrows). $\times 45,000$.
- 6 Electron micrograph of the junction of crevicular epithelium (E) and the underlying connective tissue (C). The dilated intercellular space (S) is separated from the connective tissue ground substance by the lamina densa (arrows). $\times 20,000$.
- 7 Electron micrograph of a basal melanocyte in crevicular epithelium. This cell has a prominently indented nucleus (N) and a cytoplasm rich in mitochondria (m) but devoid of tonofilaments. Processes of adjacent epithelial cells (E) separate the melanocyte from the basal lamina and underlying connective tissue (C). $\times 13,500$.

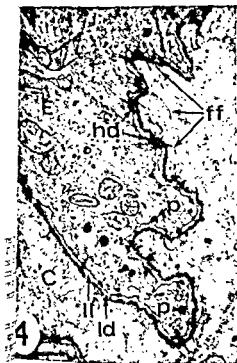


PLATE 3

EXPLANATION OF FIGURES

- 8 Electron micrograph of portions of several intermediate cells of crevicular epithelium. These show desmosomes (D) perinuclear mitochondria (m) and microvilli (mv) which project into the wide intercellular space (S) containing a free dense body (arrow). $\times 10,000$.
- 9 Electron micrograph of the contact relationship of two intermediate level cells of crevicular epithelium (E). Portions of three desmosomes (D) and two regions of tight junction (arrows) interrupt the continuity of the intercellular space (S). $\times 50,000$.
- 10 Electron micrograph of portions of three flattened superficial cells of crevicular epithelium. They contain a lipid droplet (Li) and a lysosome-like body (L). The intercellular spaces (S) also contain free dense bodies (arrows). $\times 15,000$.

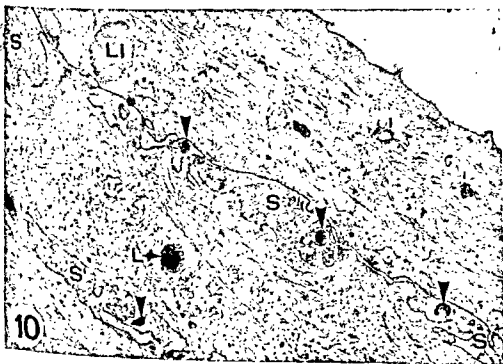


PLATE 4

EXPLANATION OF FIGURES

- 11 Electron micrograph of several intermediate level cells (E) of crevicular epithelium. The dilated intercellular space (S) contains a neutrophil leukocyte identified by its polymorphic nucleus (N) and by its cytoplasmic granules. Arrows indicate breaks in the cell membrane of the neutrophil but adjacent epithelial cell membranes are intact. $\times 6,000$.
- 12 Electron micrograph of part of a superficial cell of crevicular epithelium (E) and related intercellular space (S). This space contains a process from a neutrophilic leukocyte which has ruptured and is discharging its cytoplasmic granules into the intercellular space. $\times 25,000$.
- 13 Electron micrograph of an intercellular space between superficial cells (E) of the crevicular epithelium. It contains cellular debris (CD) and numerous dense bodies (arrows) which are ovoid (1), indented (2), elongated (3), round (4) or irregular (5) in form (cf. fig. 12). $\times 22,000$.

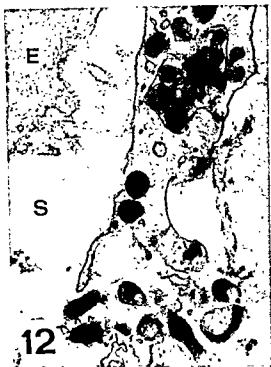


PLATE 4

EXPLANATION OF FIGURES

- 11 Electron micrograph of several intermediate level cells (E) of crevicular epithelium. The dilated intercellular space (S) contains neutrophil leukocyte identified by its polymorphic nucleus (N) and by its cytoplasmic granules. Arrows indicate breaks in the cell membrane of the neutrophil but adjacent epithelial cell membranes are intact. $\times 6,000$.
- 12 Electron micrograph of part of a superficial cell of crevicular epithelium (E) and related intercellular space (S). This space contains process from a neutrophilic leukocyte which has ruptured and is discharging its cytoplasmic granules into the intercellular space $\times 25,000$.
- 13 Electron micrograph of an intercellular space between superficial cell (E) of the crevicular epithelium. It contains cellular debris (CD) and numerous dense bodies (arrows) which are ovoid (1), indented (2), elongated (3), round (4) or irregular (5) in form (cf. fig. 12) $\times 22,000$.

The Fine Structure of the Adrenal Cortex of the 13-lined Ground Squirrel¹

WILLIAM G. SELIGER² AND WAYNE F. SMITH

Department of Anatomy, Colorado State University, Fort Collins, Colorado

ABSTRACT The adrenal cortex of the 13-lined ground squirrel was examined by means of phase contrast and electron microscopy. At the most, two cell types were observed. One of these two types was observed in three morphologically different stages of activity. They had some common characteristics, although they were very different in general appearance. The findings substantiate Symington's ('60, '61) statements that the zona reticularis contains the active cells and the zona fasciculata contains the inactive cells of the deep adrenal cortex. The cell types do not stay within the bounds of the three classical zones, and it is suggested these be used for general topography only. A number of modifications and derivations of mitochondria are described, one of which lends strength to Lever's ('55) suggestion that mitochondria might be converted into lipoidal masses.

Sheridan and Belt ('64) state, "Fine morphology of an organ is usually similar in most instances from one species to another. This generality, however, does not apply in the case of the mammalian adrenal cortex since there has been considerable variability among the species that have been observed."

Due to the recorded differences and because the periductular steroid cells resemble and functionally replace the adrenal cortex of the adrenalectomized 13-lined ground squirrel (Seligier, Blair and Lossman, '66), an investigation of the ultrastructural morphology of the adrenal cortex of this animal was considered a vital first step in our study of the origin, differentiation and controlling factors of these cells.

MATERIALS AND METHODS

Fourteen male and fourteen female 13-lined ground squirrels (*Citellus tridecemlineatus*, Mitchell) were used in this investigation. All had been trapped as juvenile animals and had been in captivity approximately a year.

A great deal of care was exercised to attempt to keep the environmental conditions and the mechanics of sacrifice and tissue-handling constant. Half of the animals in each group were decapitated while asleep. The other half were carefully lifted from their cages with a gloved hand, carried rapidly to the laboratory and killed

immediately by a sudden cervical blow. The adrenal glands were removed and immediately sliced serially while immersed under the fixative.

Fixation was accomplished with 6.25% glutaraldehyde, buffered to pH 7.7 with Sorensen's phosphate buffer, chilled to 4°C. After being rinsed in buffer, the tissue was stained with cold 1% osmium tetroxide in the same buffer. A graded series of ethyl alcohol was used for dehydration. Propylene oxide was the clearing agent. Epon 812 (Luft, '61) was used as the embedding material. The tissue was stained by uranyl acetate followed by lead acetate.

OBSERVATIONS

Phase contrast microscopic observations

Despite apparent control of environment and processing methods, phase contrast study of 2 μ sections reveals a wide variation in the adrenal cortices of the animals studied.

The outermost cells contain large, round or oval, smooth-walled vacuoles. These cells occupy the zona glomerulosa and, to a variable degree, the outer portion of the zona fasciculata. Their location varies in different specimens and, to some extent,

¹ Supported by National Science Foundation grant GB-4439 and in part by American Cancer Society project 1. N. 83B, National Institutes of Health Research Career Award 1-K3-DE-18-557-01 and Colorado State University Faculty Improvement grant 179.

² Present address: Medical College of Georgia, School of Dentistry, Augusta, Georgia 30902.

mentioned in the electron microscopic observations.

Electron microscopic observations

The round-vacuole cells are polygonal with vesicular, generally round nuclei. Cells located near the capsule are somewhat elongated and have flattened nuclei. The nuclei possess a narrow, rather clear nuclear cistern and obvious nuclear pores, evenly dispersed granular material in the center, and peripherally concentrated chromatin which projects toward the center at several regions, one of which often has a nucleolus on its summit. The extranuclear compartments contain large numbers of round, membrane-bound vacuoles, the majority of which are usually situated on one side of the cell (usually containing a blood vessel), causing the nucleus to be eccentric. A flattened, elongated, agranular sac or series of sacs are usually closely pressed against the outer surface of these vacuoles.

The matrix of the cytoplasmic compartment, including the intervals between vacuoles, is moderately dense and contains sparsely scattered small vesicles of agranular endoplasmic reticulum interspersed with groups of ribosomes and mitochondria. The mitochondria are usually round or oval. They have a dense, faintly granular matrix and contain primarily tubulo-saccular cristae. Most mitochondria contain some vesicular and lamellar-form cristae. The perinuclear Golgi complex is often observed, but occasionally one is located near the plasma-membrane.

Osmiophilic, membrane-enclosed rods are found in the perinuclear zone of the round-vacuole cells of some of the animals (fig. 4). Many of the rods show clear areas within their confines (fig. 6). Often more than one rod is found in a membranous sac. Large, irregular membrane-enclosed forms of similar texture and density also have been observed. Some specimens also show similar rods which are not membrane-enclosed, but merely surrounded by the cytoplasmic matrix. Some of these cells contain osmiophilic, membrane-enclosed forms which vary from round to club or cup shaped. These structures have not been analysed but have the ultrastructural appearance of lysosomes.

In the deeper regions of the round-vacuole cell layer, there is a gradual change. First the mitochondria become modified by a loss of the dense matrix and a loss or reduction of the cristae. Often the cristae are seen in longitudinally organized bundles of tubular membranes. These modified mitochondria commonly show internally located membrane-enclosed areas, either clear, full of osmiophilic material, or as multilayered, partially collapsed sacs. These latter occasionally appear to be in the process of being extruded from the mitochondria (fig. 8), and other examples located near the mitochondrial wall appear to have their outer membrane fused with the inner membrane of the mitochondrial wall. Similar multilayered, collapsed figures are occasionally seen in the cytoplasmic compartments of these cells.

The first irregular vacuoles observed deep to the round vacuoles are round with a scalloped outline (fig. 5). These cells also contain small vacuoles which appear to be enlarged examples of the vesicular endoplasmic reticulum of these cells, and it appears as if the scalloped outline of the irregular vacuoles is caused by the remnants of the small vacuoles which are coalescing into the large vacuoles. The deeper lying irregular vacuoles have the outlines of partially collapsed sacs (fig. 7). Often one of the latter will have a pseudopod-like process which extends into an adjacent vacuole or mitochondrion, and occasionally a mitochondrion will have a similar process which extends inside of an irregular vacuole.

Lysosome-like structures appear in higher numbers in these cells than in the previous form. The cytoplasm is filled with vesicular, agranular endoplasmic reticulum which is interspersed with groups of ribosomes.

Many of these cells show dilated nuclear cisterns which have a varicose appearance and accentuate the nuclear pores. The dilated nuclear cisterns are commonly associated with the presence of the small vacuoles described above.

The electron photomicrographs of the transitional halo cells show a sparsity or, most often, an absence of vacuoles. They show the presence of vesicular endoplasmic reticulum and, occasionally, tubules of

in various areas of the same specimen (fig. 1). Occasionally cells of this type extend deep into the zona fasciculata, and some sections show a transition zone followed by another layer of these round-vacuole cells. Occasionally an isolated cell of this type is found anywhere in the other parts of the adrenal cortex. These cells are arranged in compact, block-like groups, two or three cells wide, with blood vessels and connective tissue stroma separating adjoining groups. The large, round vacuoles are of various sizes but essentially of one size within any one cell. Most of the vacuoles appear clear and refractile. A small number of cells, often near the capsule, show vacuoles which are filled with osmiophilic material or vacuoles which have peripheral zones of osmiophilic material and clear centers. The various types are usually uniform for an individual cell. To determine if different degrees of osmium penetration caused this difference, usual fixation and osmification procedures were employed on some tissues. These blocks were thoroughly rinsed and re-osmified with extensive agitation. Most of the vacuoles appear clear. These findings, plus some of our observations on cells showing clear vacuoles and also showing intensely osmified structures within the confines of the same cells, lead to the conclusion that the various forms of these vacuoles indicate the degree of saturation of their enclosed lipoidal material.

The second cell form, the irregular-vacuole cell, often appears to blend gradually with the round-vacuole cell. In some deeper areas, the round-vacuole cells contain both irregular, non-refractile vacuoles and smooth, round, refractile vacuoles (fig. 1). In areas like this it is impossible to draw a line of demarcation between the two cell forms. In other areas the two cell forms appear as contiguous cells and a distinct line of demarcation can be drawn. Between these two cell forms, cells are found occasionally which show no cytoplasmic detail with phase contrast microscopy. This cell is designated as a transitional halo cell and is associated morphologically with the halo cell (fourth cell form).

The cytoplasmic compartments of the irregular-vacuole cells are filled with non-refractile, irregular, "clear" spaces. This

gives a foamy appearance to the cells (fig. 2). Examination with the phase contrast microscope at high magnification discloses that many of these "clear" spaces actually do contain light gray material. The electron photomicrographs show that these spaces containing the light gray material are actually modified mitochondria.

The irregular-vacuole cells are found deep to the round-vacuole cells, and their extent varies. They vary inversely with the fourth form, the halo cell, which occupies the remainder of the deep adrenal cortex to the cortico-medullary junction, except for one or two layers of transitional halo cells (third form) sandwiched between the irregular-vacuole cells and the halo cells. Three of the decapitated animals' adrenal cortices show these irregular-vacuole cells present, almost exclusively, deep to the round-vacuole cell layer and extending to the medulla. The remaining decapitated animals and a number of hand-held control animals have irregular-vacuole cells deep to the round-vacuole cells, occupying from half to three-quarters of the remaining deep adrenal cortex. The balance of hand-held control animals show layers of irregular-vacuole cells that vary from a narrow irregular layer to approximately a third of the cortex deep to the round-vacuole cells.

The halo cells are designated "halo" cells because the nuclei are closely encircled by a varying degree of gray, halo-like masses. The gray masses vary: Some appear to be homogeneous, some to be composed of small gray particles, and others have irregular or flattened clear spaces scattered throughout them (fig. 3). The electron photomicrographs show the gray masses to be concentrated accumulations of mitochondria. Except for size, these halo cells are the same, whether they are found in the zona reticularis or the zona fasciculata. The irregular-vacuole cells and the halo cells occupy the majority of the cortex deep to the round-vacuole cells and are inversely proportional to each other in the volume they occupy.

Small black structures become common in the deeper cells of the round-vacuole cell area and occur with a greater frequency in the deeper cells of the adrenal cortex. They are the lysosome-like bodies

sample of both in the round-vacuole region of the gland. We agree with ('55) that these are not degenerative but rather are probably in a different of activity. The "dark" cells appear a greater concentration of mitochondria, dense cytoplasmic matrix and compact and irregular nuclei.

The cell membranes of contiguous cells from regular separated pairs of plasma membranes to slight dilations of the intercellular spaces, some of which contain a process or microvillus from one of the cells. Occasionally, there is a large intercellular space with an extreme folding of the membranes or a great number of microvilli. This last arrangement is commonly found in the deeper portions of the gland at the point where the parenchymal cells meet at the base of a sinusoid. The parenchymal cell membranes facing the sinusoidal endothelium show many caveolae, and in the outer portions of the gland, the caveolae are generally larger and usually connected to the surface by a tube. It is common to find a junctional complex made up of a narrow intercellular space surrounded by a mass of terminal bar substance (fig. 13). The endothelial lining of the sinusoids in the adrenal cortex appears to have an increasing number of diaphragm-covered fenestrae in the deeper parts of the gland. In the zona reticularis, the fenestrae are often so close together that the sectioned endothelium appears beaded.

Zonation

A phase contrast study of 2 μ sections of the adrenal cortex shows great variability in the cells' locations and boundaries plus the apparently gradual blending of the cell forms. Since special care had been taken to attempt to control the conditions of the care and sacrifice of these animals, this was very unexpected. In an attempt to understand this, sections were cut from blocks of Epon-embedded tissues from a pilot study concerned with stimulation and inhibition of the adrenal cortex. Two animals had been killed — one hour and 24 hours — after administration of 4 units/kg of ACTH gel (stimulated animals). Two animals (for each drug) had been killed — one and 24 hours — after receiving 10

mg/kg cortisone acetate; 10 mg/kg hydroxycortisone acetate; and 5 mg/kg desoxycortisone acetate (inhibited animals).

All one-hour animals showed a rather normal pattern of cells, typical of the hand-held control animals. This consisted of an outer layer of round-vacuole cells followed by a variable layer of irregular-vacuole cells, not exceeding half of the remainder of the adrenal cortex. The remainder of the area down to the junction with the medullary cells was filled with halo cells. The tissues from the 24-hour animals which were inhibited showed predominantly irregular-vacuole cells deep to the round-vacuole cell layer, and the stimulated glands showed halo cells, almost exclusively, deep to the round-vacuole cell layer.

This information is the result of only a pilot study, but it indicates that the wide variation that occurred in the adrenal cortices of the control glands of these animals was due to a variation in the degree of stress they felt under seemingly identical environments. These findings substantiate Symington's ('60, '61) statements that the zona reticularis contains the active cells and the zona fasciculata the inactive cells of the deep adrenal cortex.

DISCUSSION

Our findings in the 13-lined ground squirrel's adrenal cortex indicate that the three classical zones should be used only for general orientation and localization. Since there is considerable variation in the location of the cells, the glands should be subdivided according to cell forms and the volumes they occupy. This great variability of the cells' locations and boundaries, plus the gradual blending of cell forms, suggests that no more than two cell types, in various stages of production and activity, are involved. The variation in the ratio and position of the cell forms appears to be a result of hidden stresses.

It is naive to believe that animals kept under outwardly identical environmental conditions would be under the same degree of stress. The general health of these animals could vary a great deal without being obvious. Variation in the degree of adjustment to captivity, the cage size, different eating and drinking habits, the odors of

endoplasmic reticulum organized into bundles which present a honeycomb-like appearance on cross section (fig. 11). There are no ribosomes or obvious matrix present between these tubules. Most of the mitochondria are elongated and thin except at the ends, and are arranged into cupped masses which DeRobertis and Sabatini ('58) refer to as "chondriospheres" (fig. 10). A smooth-walled membranous sac is pressed intimately between the adjacent mitochondria of these masses (fig. 10). This arrangement causes the contiguous mitochondrial surfaces to appear thickened or more intensely stained. The internal membranes of these mitochondria are vesicular and occasionally tubular, but the intense contrast between matrix and internal membranes which is seen in other mitochondria is absent.

Although the general appearance of these cells is very different from the halo cells, the mitochondria-membranous sac relationships are the same. Intermediate forms containing chondriospheres as well as the aligned mitochondria which are characteristic of halo cells have been observed (fig. 11).

The halo cells occupy a variable amount of the deeper portion of the zona fasciculata and the entire zona reticularis. The cells of the zona reticularis are smaller and lose the column-like arrangement, but they are morphologically the same in both zones. The nuclei are generally round, with peripherally concentrated chromatin and often contain a central nucleolus which may be in a ring form or in the form of a folded columnonema. The nuclear cisterns vary from the narrow, regular type to the varicose type which is associated with the dilation of certain intermitochondrial sacs to be described.

The mitochondria occur in packed masses which closely encircle the nuclei to a variable extent. They vary in shape from round or elongated to branching, in the same cells. Their internal membranes are tubulo-saccular, vesicular and lamellar-form in one mitochondrion. Occasionally, a number of very elongated mitochondria occur in parallel groups orientated radially from the nucleus with parallel lamellar-form cristae running the entire length of the mitochondria (fig. 16). Elongated sacs

of granular endoplasmic reticulum occur between adjacent mitochondria (fig. 13). They are often flattened to the extent that the lumina are very narrow. Halo cells which have varicose nuclear cisterns and a preponderance of modified mitochondria usually show dilated intermitochondrial sacs (figs. 14, 15). No direct connection has been observed between the nuclear cistern and these intermitochondrial sacs. Occasionally, cells from the junction between the outermost halo cells and the transitional halo cells show mitochondria arranged in this same manner but possessing agranular intermitochondrial sacs (fig. 11).

The cytoplasmic compartments of the halo cells are packed with vesicles of smooth endoplasmic reticulum which are interspersed with small clumps of ribosomes.

Generalities

Centrioles are commonly found in cells of all forms and regions (fig. 13). A cilium was observed in one round-vacuole cell. Wheatly ('67) recorded similar observations in the rat adrenal cortex.

The lysosome-like structures are present in cells of all forms. They are least common in the round-vacuole cells. In the deeper regions, similar dark structures are seen which contain empty round vacuoles several of which are often larger than the osmophilic portions of the structures (fig. 15).

A multivacuole structure has been observed in cells of all forms. This large structure is full of empty-appearing vacuoles which usually maintain a slightly stained, constant-width interspace which gives the appearance of a network of tubules (fig. 17). Select sections show a double-membrane outer wall, and sufficient examples of transition between these structures and mitochondria have been observed to state that they are derived from these organelles (fig. 18). Some of these structures have thick walls, which are made up of concentric layers of osmophilic lamellae giving them a myelin-like appearance.

"Light" and "dark" cells have been observed among all cell forms and in all zones of the adrenal cortex. Figure 4 contains

sample of both in the round-vacuole region of the gland. We agree with ('55) that these are not degenerative but rather are probably in a different of activity. The "dark" cells appear to contain a greater concentration of mitochondria, dense cytoplasmic matrix and compact and irregular nuclei.

The cell membranes of contiguous cells are from regular separated pairs of plasma membranes to slight dilations of the intercellular spaces, some of which contain a process or microvillus from one of the cells. Occasionally, there is a large intercellular space with an extreme folding of the membranes or a great number of microvilli. This last arrangement is commonly found in the deeper portions of the gland at the point where the parenchymal cells meet at the base of a sinusoid. The parenchymal cell membranes facing the sinusoidal endothelium show many caveolae, and in the deeper portions of the gland, the caveolae are generally larger and usually connected to the surface by a tube. It is common to find a junctional complex made up of a narrow intercellular space surrounded by a mass of terminal bar substance (fig. 13). The endothelial lining of the sinusoids in the adrenal cortex appears to have an increasing number of diaphragm-covered fenestrae in the deeper parts of the gland. In the zona reticularis, the fenestrae are often so close together that the sectioned endothelium appears beaded.

Zonation

Phase contrast study of 2 μ sections of the adrenal cortex shows great variability in the cells' locations and boundaries plus an apparently gradual blending of the cell forms. Since special care had been taken to attempt to control the conditions of the care and sacrifice of these animals, this was very unexpected. In an attempt to understand this, sections were cut from blocks of Epon-embedded tissues from a pilot study concerned with stimulation and inhibition of the adrenal cortex. Two animals had been killed — one hour and 24 hours — after administration of 4 units/kg of ACTH gel (stimulated animals). Two animals (for each drug) had been killed — one and 24 hours — after receiving 10

mg/kg cortisone acetate; 10 mg/kg hydrocortisone acetate; and 5 mg/kg desoxycortisone acetate (inhibited animals).

All one-hour animals showed a rather normal pattern of cells, typical of the hand-held control animals. This consisted of an outer layer of round-vacuole cells followed by a variable layer of irregular-vacuole cells, not exceeding half of the remainder of the adrenal cortex. The remainder of the area down to the junction with the medullary cells was filled with halo cells. The tissues from the 24-hour animals which were inhibited showed predominantly irregular-vacuole cells deep to the round-vacuole cell layer, and the stimulated glands showed halo cells, almost exclusively, deep to the round-vacuole cell layer.

This information is the result of only a pilot study, but it indicates that the wide variation that occurred in the adrenal cortices of the control glands of these animals was due to a variation in the degree of stress they felt under seemingly identical environments. These findings substantiate Symington's ('60, '61) statements that the zona reticularis contains the active cells and the zona fasciculata the inactive cells of the deep adrenal cortex.

DISCUSSION

Our findings in the 13-lined ground squirrel's adrenal cortex indicate that the three classical zones should be used only for general orientation and localization. Since there is considerable variation in the location of the cells, the glands should be subdivided according to cell forms and the volumes they occupy. This great variability of the cells' locations and boundaries, plus the gradual blending of cell forms, suggests that no more than two cell types, in various stages of production and activity, are involved. The variation in the ratio and position of the cell forms appears to be a result of hidden stresses.

It is naive to believe that animals kept under outwardly identical environmental conditions would be under the same degree of stress. The general health of these animals could vary a great deal without being obvious. Variation in the degree of adjustment to captivity, the cage size, different eating and drinking habits, the odors of

other animals, noises, and lighting could affect the animals differently. Jones ('63) felt the 13-lined ground squirrels he used were subjected to different degrees of stress due to the positions of their cages in the battery.

Although some viruses — especially insect viruses — are rod-shaped, and incomplete ones could have clear areas within them, the described rods and the similar large irregular masses are probably similar to the rods of crystalloid material shown in the interstitial cells of the testes (Fawcett, '66). To date, demonstration of a crystalloid matrix in these rods and masses has not been possible.

The mitochondria seem to have no definite shape in the various parts of the adrenal cortex, but most of them appear round or oval on section. They seem to be more commonly elongated in the deeper-lying halo cells.

The mitochondria containing the membrane-bound osmiophilic structures indicate that some product is formed and is being stored in the mitochondria. Another internal configuration, myelin figures, appear to be formed within the mitochondria by apposition of ever increasing numbers of membranes. The myelin-like figures have been observed apparently penetrating the walls of the mitochondria. It is not certain they are being extruded, but since it appears they are built up within the mitochondria, this assumption seems logical. These forms may collapse after voiding their contents to the exterior of the mitochondria. The single, clear, round, membrane-bound vacuoles seen within the mitochondria may be the beginning of these myelin-like figures.

The large, multivacuole structures described appear to be the result of modification and enlargement of mitochondria. What appear to be more advanced stages show thick osmiophilic laminated walls. Some of the above observations appear to reinforce Lever's ('55) statement that mitochondria may form the lipoidal material of these cells. When one of these structures is present in a cell, it is common to see others within the confines of that cell.

There is an almost constant relationship between the degree of varicosity of the nuclear cistern and the degree of dilation of some of the endoplasmic reticulum membranes. The rough membranes that occur between the organized mitochondria in the internal cells are often very dilated. Since the nuclear cistern is considered to be continuous, to some degree, with the endoplasmic reticulum, this is not an unexpected finding. This same relationship also seems to exist in the irregular cells, with some of the smaller vacuoles or membranous sacs. It is our belief that these smaller vacuoles are actually dilated examples of the vesicles of the endoplasmic reticulum which fill these cells.

ACKNOWLEDGMENT

We would like to acknowledge Doctor P. Epling, of our department, for his advice, and for allowing us to use various pieces of equipment from his electron microscope laboratory.

LITERATURE CITED

- De Robertis, E., and D. Sabatini 1958 1
chondrial changes in the adreno-cortex of
mal hamsters. *J. Biophysics and Bio-*
Cytol., 4: 667-673.
- Fawcett, D. 1966 *An Atlas of Fine Struc-*
The Cell. W. B. Saunders Company, Phil-
phia and London.
- Jones, I. C. 1963 Ovary of the thirteen-
ground squirrel after adrenalectomy.
Endocrinol., 26: 265.
- Lever, J. D. 1955 Electron microscopic
variations on the adrenal cortex. *Am. J. Anat.*
409-430.
- Luft, J. H. 1961 Improvements in epoxy
embedding methods. *J. Biophys. Bio-*
Cytol., 9: 409-414.
- Seligman, W. G., A. J. Blair and H. W. Mos-
1966 Differentiation of adrenal cortex-till
sue at the hilum of the gonads in respon-
adrenalectomy. *Am. J. Anat.*, 118: 615-621.
- Sheridan, M. N., and W. D. Belt 1964
structure of the guinea pig adrenal
Anat. Rec., 149: 73-98.
- Symington, T. 1960 *Biochemical* 2.
(18): 40. Cambridge University Press.
- Symington, T. 1961 The morphology and
ing of the human adrenal cortex. *Proce-*
of conference on the human adrenal
Livingstone, Edinburgh.
- Wheatley, D. N. 1967 Cilia and centri-
the rat adrenal cortex. *J. of Anat.*, 101: 22

PLATE 1

EXPLANATION OF FIGURES

In all three photomicrographs the small, dark structures in the cytoplasmic compartments are the lysosome-like structures of the electron photomicrographs.

- 1 Area of the junction of round-vacuole cells (R) with irregular-vacuole cells (I). Mixed form (M) containing mostly round vacuoles. Hand-held control female animal, phase contrast photomicrograph. $\times 1,600$.
- 2 Area full of irregular-vacuole cells from the zona fasciculata. Hand-held control female animal, phase contrast photomicrograph. $\times 1,600$.
- 3 Cells with "halos" of mitochondria (H) around the nuclei. A cell with dilated intermitochondrial sacs (D). The nuclei of the latter are usually darker and have more irregular outlines. Hand-held control female animal, phase contrast photomicrograph. $\times 1,600$.

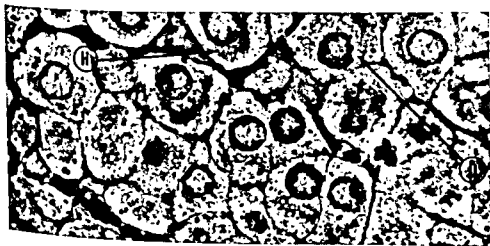
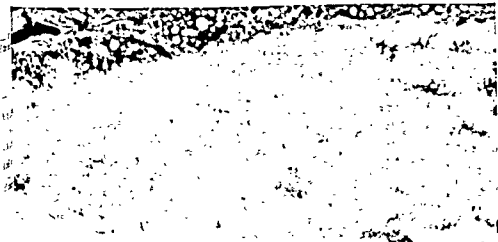
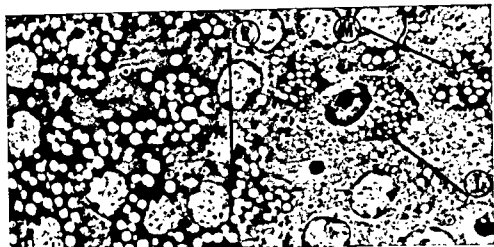


PLATE 2

EXPLANATION OF FIGURES

- 4 Round-vacuole cells from the zona glomerulosa. Portions are seen of two "light" cells, left, and two "dark" cells, right. Membrane-bound rods (R) are seen in the "light" cells. Modified mitochondria (MM) and a Golgi complex (G) are seen in the "dark" cells. Hand-held control female. $\times 6,400$.
- 5 Portions of cells from deep in the round-vacuole cell layer. Cell to the right shows scalloped irregular vacuole (S) with surrounding small vacuoles. The mitochondrion below the scalloped vacuole has a process (P). The cell to the left shows a typical round vacuole (R) for comparison. Hand-held control female. $\times 16,000$.
- 6 A group of membrane-enclosed rods and two of the larger irregular structures of similar texture. The nucleus of this round-vacuole cell is just evident in the upper right corner (from the zona glomerulosa). Hand-held control female. $\times 28,000$.

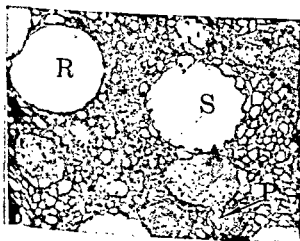
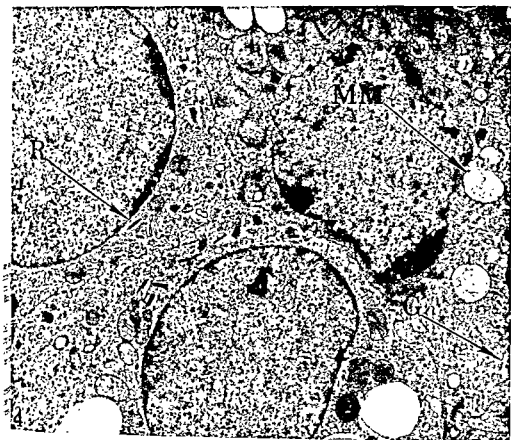


PLATE 2

EXPLANATION OF FIGURES

- 4 Round-vacuole cells from the zona glomerulosa. Portions are seen of two "light" cells, left, and two "dark" cells, right. Membrane-bound rods (R) are seen in the "light" cells. Modified mitochondria (MM) and a Golgi complex (G) are seen in the "dark" cells. Hand-held control female. $\times 6,400$.
- 5 Portions of cells from deep in the round-vacuole cell layer. Cell to the right shows scalloped irregular vacuole (S) with surrounding small vacuoles. The mitochondrion below the scalloped vacuole has a process (P). The cell to the left shows a typical round vacuole (R) for comparison. Hand-held control female. $\times 16,000$.
- 6 A group of membrane-enclosed rods and two of the larger irregular structures of similar texture. The nucleus of this round-vacuole cell is just evident in the upper right corner (from the zona glomerulosa). Hand-held control female. $\times 28,000$.

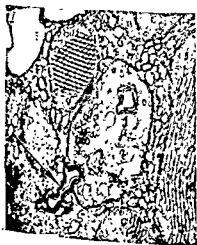
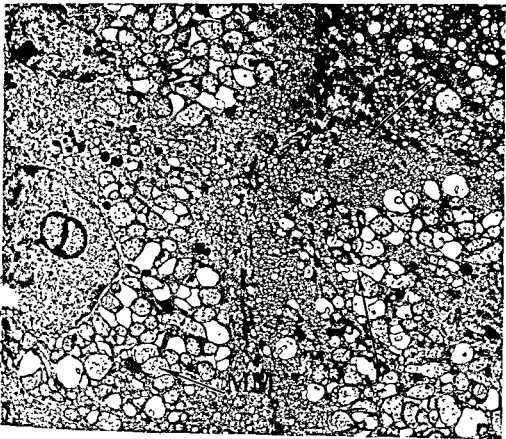


PLATE 3

EXPLANATION OF FIGURES

- 7 Portions of four irregular-vacuole cells. Modified mitochondria (MM) and irregular vacuoles, many of which have pseudopod-like processes (P), are very plentiful. The small vacuoles (sV) which appear to be dilated, vesicular endoplasmic reticulum also are very plentiful. Hand-held control female. $\times 9,000$.
- 8 Mitochondria from an irregular-vacuole cell, one of which shows tangentially sectioned, organized tubular cristae. The other shows myelin figure-like structures, one of which appears to be in the process of being extruded (arrow) (from the zona fasciculata). Hand-held control male animal. $\times 25,000$.
- 9 A portion of an irregular-vacuole cell showing the extensive contact often present between the modified mitochondria (arrows) and the clear-appearing irregular vacuoles (from the zona fasciculata). Hand-held control female. $\times 22,000$.

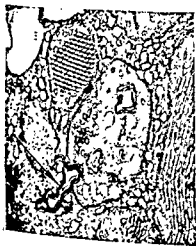
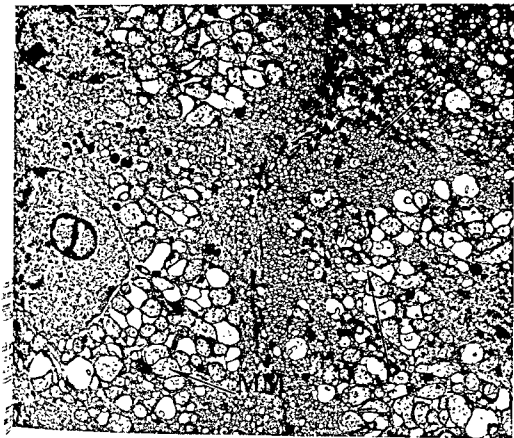


PLATE 4

EXPLANATION OF FIGURES

- 10 Portion of a transitional halo cell. Mitochondria are elongated and cupped into chondriospheres. Arrows indicate the ends of the collapsed agranular sacs located between contiguous mitochondria (from the outer zona fasciculata). Hand-held control female. $\times 23,000$.
- 11 Transitional halo cell from a slightly deeper portion of the gland than the cell shown in figure 10. It shows an intermediate form containing both chondriospheres (right) and aligned mitochondria similar to those seen in halo cells (left). The arrows indicate the ends of the intermitochondrial sacs. Surrounding these mitochondria is organized tubular agranular endoplasmic reticulum viewed on cross section (from the outer zona fasciculata). Hand-held control female. $\times 13,000$.
- 12 Portion of a halo cell showing the organization of mitochondria and granular intermitochondrial sacs (from the zona reticularis). Hand-held control female. $\times 10,000$.
- 13 Portions of two halo cells showing a centriole (C) and cell junction complexes (J). Hand-held control female. $\times 9,000$.

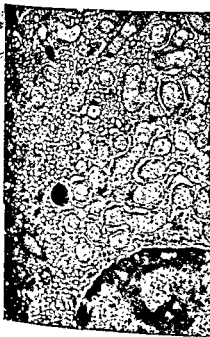
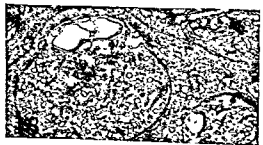
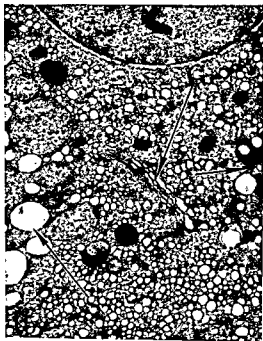


PLATE 5

EXPLANATION OF FIGURES

- 14 Portions of two halo cells. Cell A shows marked dilation of the nuclear cistern, the intermitochondrial sacs and a large number of the small vacuoles believed to be enlarged vesicles of smooth endoplasmic reticulum, and modified mitochondria. Cell B shows a narrow, regular nuclear cistern, undilated intermitochondrial sacs, unmodified mitochondria and a more regular cytoplasmic matrix (from the zona reticularis). Hand-held control female. $\times 5,600$.
- 15 A cell similar to that shown in figure 14 showing dilated, granular intermitochondrial sacs cut on cross section (S), a Golgi complex (G), and several of the osmophilic bodies containing large clear vacuoles (arrow). Hand-held control female. $\times 15,000$.
- 16 Portion of a halo cell showing various forms of mitochondria seen in these cells. Hand-held control female. $\times 15,000$.
- 17 Multivacuole structure (arrow). Hand-held control female. $\times 6,000$.
- 18 These two mitochondria are the best examples observed of the transition between the multivacuole structures and mitochondria. The dark granular material is precipitate. Hand-held control male. $\times 18,000$.



Innervation of the Bone Marrow Laboratory Animals^{1,2}

WENCESLAO CALVO

*Abteilung für Klinische Physiologie der Universität Ulm,
Parkstr. 11, 79 Ulm, Germany*

ABSTRACT The nerve pattern of the bone marrow of the monkey, rabbit, rat and mouse was studied in serial sections specially stained to demonstrate myelinated and nonmyelinated nerve fibers. Features that are common to the different species studied were found in the bone marrow of the femur of the rat in a simple arrangement.

A scheme is proposed based on thirteen photomicrographs demonstrating the nerve pattern of the bone marrow and the relation of the nerve fibers with the arterial tree, the sinusoids and the blood forming cells. This scheme shows that the necessary anatomical conditions exist permitting a direct influence of the nervous system on the function of the bone marrow. These conditions are the presence of myelinated nerve fibers traversing the parenchyma of the marrow, and the existence of nonmyelinated fibers ending in sphincterlike structures at the origin of the arterioles.

Single myelinated nerve fibers and small bundles of both myelinated and nonmyelinated fibers lie in close contact with the endothelial wall of the sinuses during long trajects. Only the very thin endothelium of the sinuses separates the newly formed blood and the nerve fibers. An interaction between both elements is possible along these areas of contact.

The function of an organ cannot be fully understood without considering also the nervous system, yet the study of the innervation of the bone marrow has long been neglected. Its study is of interest in normal morphology and physiology, and may prove to be of importance in pathology.

The purpose of this paper is to present observations concerning the presence, the structure and the distribution of the nerve fibers in bone marrow of normal adult animals commonly used in the laboratory, as well as the relations between the nerve fibers and the cells of the parenchyma, the arterial vessels and the sinusoids. It is hoped that the description of the normal architecture of the bone marrow, with the nerve pattern included, may throw some light on the understanding of the mechanisms that regulate the proliferation and release of the blood cells, and also on the maintenance of homeostasis and on the adaptation of the function of the bone marrow to different stimulations. The photomicrographs of normal nerve fibers demonstrated here with well standardised histological methods may serve later for comparison with pathological material.

MATERIAL AND METHODS

The bone marrow of the long bones of the normal adult mouse, rat, rabbit and monkey was studied. For the demonstration of the nonmyelinated fibers, the marrow was impregnated en bloc by the silver nitrate method of Cajal after fixation and decalcification of the bone with the fluid of Castro ('25). The femur, tibia and humerus of the small animals (mice and rats), with their bone marrow inside, was embedded in paraffin and cut entirely in serial sections, 10 μ thick. This method permits the study of the bone marrow in relation to the bone. The marrow of the large animals (rabbit and monkey) was extracted from the bone as cylinders of approximately 15 mm in length and impregnated with the silver nitrate. Cylinders of marrow from the area of the nutrient foramen, the diaphysis and the distal epiphysis were studied separately. From these regions, serial sections were cut and at intervals a number of slides were counter-

¹ Research supported by the Association Contract "Hematology" between the European Atomic Energy Community (Euratom) and the Gesellschaft für Strahlenforschung mbH.

² This publication is contribution 298 of the Euratom Biology Division.

stained with the Masson's trichrome or with Hematoxylin-Eosin. The sections counterstained with these methods provided evidence of the selectivity of the silver impregnation for nerve fibers and gave information concerning the relations between the nerve fibers and the other structures of the bone marrow. Blocks of tissue from the same region were fixed in formalin and stained with the Luxol fast blue-Periodic-acid-Schiff-Hematoxylin technique as described by Margolis and Pickett ('56) for the demonstration of the myelinated fibers and the blood vessels. The reticulum fibers were stained in sections of this formalin fixed material with the method of Wilder and compared with the nerve fibers for additional control of selectivity of the silver impregnation of the nerve fibers by the Cajal — Castro method. In some cases, the nerve and the nutrient artery with a fragment of tissue at the level of the nutrient foramen were fixed and stained with osmic acid for demonstrating myelinated fibers and fat. A total of 330 long bones were prepared of which 27,000 sections were cut and studied.

RESULTS

General findings

The long bones of the animals have a small foramen in a constant position, the so-called nutrient foramen. The nutrient artery and a nerve pass through foramen, providing the blood supply and the nerve supply for the marrow. This is well defined from its origin in the spinal nerve that corresponds to the territory in which the foramen is located, until its termination in the periosteum and the bone marrow. Following the nomenclature given by Gros (1846) we call diaphysary nerves those nerve trunks extending between the corresponding spinal nerve and the foramen. The diaphysary nerve gives branches that spread over the periosteum and also branches that penetrate into the bone cavity. The latter are the medullary branches of the diaphysary nerve and constitute the subject of our study. The medullary branches immediately upon entering the marrow cavity, divide repeatedly and give off numerous nerve bundles that follow a distribution roughly parallel to the

branches of the nutrient artery spreading throughout the marrow, both distally and proximally to the nutrient foramen. Each nerve bundle contains a number of nerve fibers surrounded by a thin membrane of connective tissue, the perineurium. These bundles have both myelinated and nonmyelinated fibers. The nonmyelinated fibers are thinner than those covered with myelin. With the reduced silver nitrate of Cajal — Castro, these fibers are selectively impregnated by the silver salt and appear as black wirelike structures sharply demarcated on a yellowish background. The structure which becomes impregnated corresponds to the neurofibrillary component of the nerve fiber. The neurilemma remains almost unstained but it can be distinguished as a pale sheath around the neurofibrils. The oval nuclei, sparsely distributed along the nerve fibers, are of the Schwann cells that form the neurilemmal sheath. The different cells and connective tissue fibers of the marrow are faintly stained but the various structural types of blood vessels are recognizable. The distinction between arteries and capillaries is very easy owing to the clear demarcation of the muscular wall of the vessels in which every smooth muscle cell is stained brown with the osmic acid method used and appears clearly separated from the others.

The myelinated fibers are thicker and less numerous than the nonmyelinated. They can be found isolated among the cells of the bone marrow or in the nerve bundles intermixed with nonmyelinated fibers. The osmic acid stains the myelin black leaving the nonmyelinated fibers unstained. The relation between myelinated fibers, cells and blood vessels can be beautifully demonstrated by the Luxol fast blue-Periodic acid-Schiff-Hematoxylin method. The myelinated fibers are stained in sky blue color, the blood vessels in bright red and the nuclei of the cells in blue-violet.

In most of the long bones studied, nerves enter the bone cavity at one point only, but in the humerus of the rat there are two separated entries. The main entry is through the nutrient foramen located in the proximal part of the bone. A smaller entry is located near the trochlea.

Innervation of very small areas of marrow was observed in the long s, by the entry of single nerve fibers sgh some of the largest Haversian ls.

summary then, except for the minor e contributions mentioned above, most e bone marrow is innervated by nerve ches entering with the nutrient artery ugh the nutrient foramen. The nerve ches divide repeatedly and are related a) the arterial component of marrow ulation (b) the sinusoidal part of the row circulation and (c) the paren- ma.

a) *Innervation of the arterial tree.* : outstanding features of the innerva- i of the bone marrow is the close associ- on of the nerve pattern with the arterial tem. All arteries of the marrow are ompanied by nerve bundles (fig. 1) t form a wide-meshed network with inches often winding around the arter-. The main branches of the nutrient ry are surrounded by a number of ve bundles each of them containing merous nerve fibers (fig. 2). The thin- branches of the artery are accompanied only one or two bundles, each having y two or three nerve fibers (fig. 3). The rterioles and the capillaries often are ac- companied by only one naked fiber at- ched to the vessel wall. The thicker ve bundles are individually ensheathed s a thin membrane of connective tissue rd may lie either in close contact with : arterial wall, or run parallel to the ves- el, leaving a few cells of the parenchyma :ween nerve and artery. Thin nonmye- ated fibers leave the nerve bundles, ach the wall of the arteries and spread along the smooth muscle fibers dividing epeatedly into branches that end in con- :act with the muscle fibers. Particularly ch is the innervation of the circular layer e smooth muscle fibers located around e opening of the initial part of some of e branches of the nutrient artery (fig. 1). The presence of well innervated annu- : muscle fibers is a characteristic of the :inctors working under immediate nerv- : control.

The capillaries are in contact with very in nonmyelinated fibers only in certain :arts of their course. The fibers may follow

the capillary in intimate contact with its endothelial wall for some distance, then leave the vessel and join another capillary that results from the division of a neigh- bouring vessel (fig. 5). It appears as if a number of these very thin nerve fibers never reach another vessel but divide fur- ther and eventually end among the cells of the parenchyma.

(b) *Innervation of the sinusoidal tree.* The sinusoids appear to be poorly innerv- ated in comparison with the arterial ves- sels. In some sections of the diaphysary marrow it is possible to see isolated myelin fibers alongside the wall of the central sinus (fig. 6). They can be followed for a long way, straight and undivided, chang- ing their course only to curve a little around the walls of the mouths of the sinus recti, which in this area enter the central sinus perpendicularly. In the epiph- ysary marrow, the central sinus rami- fies towards the trabecular bone of the epiphysis following the long axis of the bone. Some of the myelinated fibers de- scribed along the central sinus in the diaph- ysary marrow continue along the wall of the sinusoids as they ramify towards the epiphysis. The fibers become very thin and disappear among the cells of the paren- chyma or end in contact with the endothe- lium of the sinusoids. Other fibers, either isolated or in loose bundles, run parallel to the central sinus approximately at mid- dle distance from the sinus to the endo- steum, establishing contact with numer- ous sinusoids (fig. 7). The small bundles of nerve fibers become loose because they are not ensheathed by the perineurium as in the main nerve trunks. When the bun- dles meet the wall of a sinusoid, their fi- bers spread and follow the rounding of the sinusoidal wall, rejoining again on the other side as the bundle proceeds towards the epiphysis. In this form all the fibers of each bundle make contact with the endothelium of numerous sinusoids.

Myelinated and nonmyelinated fibers that lie in contact with the wall of the sinusoids are separated from the blood only by the thin sinusoidal wall. The fibers end by dividing into extremely thin naked fi- bers that taper away in contact with the endothelium of the sinuses.

(c) *Innervation of the parenchyma.* From repeated division of the nerve entering the bone cavity, sharply demarcated nerve bundles detach and proceed proximally and distally across the parenchyma of the bone marrow following the length of the bones independently of the arterial branches. An exchange of fibers occurs between some of the nerve bundles in the form a chiasmata (fig. 8). The nerve bundles divide into thinner branches in their course towards either epiphyses. They are composed of a number of nerve fibers (two to seven) both myelinated and nonmyelinated. Other branches consist of a few nonmyelinated elements.

The nerve bundles give off single myelinated fibers (fig. 9) that travel a long way undivided across the parenchyma before they end by ramifying freely among the blood forming cells (fig. 10).

No one cell type or group of cells of the parenchyma appear to have special attraction for the nerve fibers. The same single nerve fiber touches successively but indiscriminately every cell that lies in its path. Nonmyelinated fibers follow a more tortuous course. After a long path among the cells of the parenchyma they end in the wall of an arteriole, on a capillary (fig. 11), or wander for some distance among the blood forming cells as very thin naked fibers (i.e., nerve fibers without Schwann cells).

The usual linear course of the fibers is occasionally modified by parenchymal cells lying in their path (fig. 12).

Fat globules appearing in the way of the nerve fibers also cause them to take a curved path (fig. 13).

A few nonmyelinated fibers turn from the axial direction towards the surface of the marrow cylinder ending among the elements of the endosteum or penetrating occasionally into a Haversian canal. The Haversian canals can therefore be innervated by either fibers entering the bone cavity from the periosteum or by fibers originating within the parenchyma as branches of the medullary nerve bundles.

The nerve fibers are asymmetrically distributed in the bone marrow. They are abundant in the vicinity of the nutrient foramen (upper third of the femur), but sparsely distributed in the distal epiphyses. The nerve fibers are mostly to be found

midway between the endosteum and the central sinus of the marrow cylinder.

DISCUSSION

The above separate description of the innervation of the sinusoids and innervation of the parenchyma is artificial, and was intended for descriptive simplicity since sinusoids and blood forming cells form a labyrinth of vessels and islands of cells intimately related to each other.

The long bones of the laboratory animals have a bone marrow with similar architectural characteristics. In the marrow of the femur of the rat exist the basic anatomical details in almost diagrammatic simplicity. Therefore this marrow was chosen for the detailed description.

The findings presented leave no doubt that the bone marrow is innervated by myelinated and nonmyelinated nerve fibers. These fibers form a characteristic pattern that in part parallels the vascular architecture and in part appears related to the cellular parenchyma. The vascular architecture has been studied extensively by Fliedner et al. ('56) who proposed a schema that describes the marrow as an organ with a well defined relation between vessels and parenchyma. The present study complements their description by adding the nerve pattern to the study of the bone marrow as a well innervated organ. It now appears possible to propose the following scheme (fig. 14) for the relation between nerves, vessels, and marrow cells. The wide central sinus collects the blood carried by the sinusoids. The arteries divide giving branches on either side of the central sinus and end in capillaries that pervade the marrow throughout. The arteries and arterioles are shown as tubular with lines across that represent smooth muscle fibers, while in the capillaries the fibers are absent. In the upper part of the figure a fragment of the diaphyseal bone appears perforated by innervated Haversian canals.

The nerve pattern comprehends the main findings and is composed and based on the 13 photomicrographs described on the previous pages. The number of the photomicrographs corresponds with the same number on the scheme. The relation between the nerve fibers and the nutritive

ssels are shown in numbers one to five. mulation of these nerve fibers will in-
ence the blood flow by changing the
meter of the lumen of the arteries that
pends on the degree of contraction of
the innervated smooth muscle fibers of the
terial wall. The nerve bundles that ap-
ar to have a course independent of the
trient blood vessels are described as re-
ted to the parenchymal cells and the
usoids. The numbers 6 to 13 illustrate
e peculiarities of these relations. In
umber 7 a group of myelinated fibers
versing the parenchyma spread and
nd around the wall of the sinusoids that
pear across their path. Changes in diam-
er of the sinusoids are likely to stimulate
e nerve fibers. Myelinated nerve fibers are
so bent by the cells, as demonstrated in
umber 12. An increase in cellularity can
rve the nerve fibers in many areas caus-
g an elongation of the fibers that is also
likely to originate nerve impulses. Only a
ery thin, fenestrated endothelium sepa-
ates the newly formed blood from the
erve fibers that lie in contact with the
wall of the sinuses. This circumstance
permits an interaction between nerve fi-
ers and blood. The composition of the
newly formed blood may affect the conduc-
ivity of the nerve fibers, while the stim-
ulation of the nerve fibers may induce the
elease of substances that influence the
permeability of the vessels' wall.

The presence of myelinated fibers in the
bone marrow was mentioned by Variot und
Remy (1880) and by Castro ('29) and
were interpreted as afferent fibers respon-
sible for the transmission of nerve impulses
to the brain where they could be evaluated
as pain. The existence of these afferent
fibers is well proved by the repeated clin-
ical observation of patients that feel pain
during the performance of a bone mar-
row aspiration.

The nonmyelinated fibers were first
found in the marrow by Variot and Remy
(1880). Ottolenghi ('02) described the in-
timate relations that these fibers establish
with the arteries, and Castro ('29) dem-
onstrated anatomically the autonomic na-
ture of the nerves of the bone marrow of

the occipital bones by following the nerve
fibers in serial sections to their origin in
the superior cervical ganglion.

An indirect influence of the nervous
system on the blood cell count by way of
nerve fibers carried by the splanchnic and
vagi nerves ending in the abdominal vis-
cera, was schematically presented by Ko-
miya ('56). Our scheme demonstrates that
the myelinated and nonmyelinated nerve
fibers carried by the spinal nerves estab-
lish intimate anatomical relations with the
bone marrow structures permitting a di-
rect influence of the nervous system on the
bone marrow function. This direct influ-
ence does not exclude but rather comple-
ments the other regulatory mechanisms
that are known to influence the physiology
of the bone marrow.

ACKNOWLEDGMENTS

The author expresses his gratitude to
Professor Dr. T. M. Fliedner, Dr. E. B.
Harriss, Dr. W. Bauer and Dr. F. J. Pre-
torius for helpful criticism, and gratefully
acknowledges the excellent technical as-
sistance of Mrs. M. Neumann and Miss
Ch. Pannach.

LITERATURE CITED

- Castro, F. de 1925 Technique pour la colora-
tion du système nerveux quand il est pourvu
de ses étuis osseux. Trav. Lab. Rech. Biol.
Univ. Madrid., 23: 427-446.
- 1929 Quelques observations sur l'interven-
tion du système nerveux autonome dans
l'ossification, innervation du tissu osseux et
de la moelle osseuse. Trav. Lab. Rech. Biol.
Univ. Madrid., 26: 215-244.
- Fliedner, T. M., S. Sandkühler and R. Stodtmeis-
ter 1956 Untersuchungen über die Gefäss-
architektur des Knochenmarkes der Ratte.
Z. Zellforsch., 45: 328-338.
- Gros, M. 1846 Note sur les nerfs des os C. R.
Acad. Sci. (Paris) 23: 1106-1108.
- Komiya, E. 1956 Die zentralnervöse Regula-
tion des Blutbildes. G. Thieme, Stuttgart.
- Margolis, G., and J. P. Pickett 1956 Lab. In-
vest., 5: 459-473. Ref. in Manual of Histologic
and Special Staining Technics. McGraw-Hill,
New York, 1960.
- Ottolenghi, D. 1902 Sur les nerfs de la moelle
des os. Arch. Ital. Biol., 37: 73-80.
- Variot, P., and Ch. Remy 1880 Sur les nerfs
de la moelle des os. J. Anat. Physiol., 6: 273-
284.

PLATE I

EXPLANATION OF FIGURES

Bone marrow, femur, rat. Reduced silver nitrate of Cajal-Castro

- 1 One of the main branches of the nutrient artery divides. The smooth muscle fibers are clearly demonstrated. Two of the nerve bundles (arrow) accompanying the blood vessels are visible in this section. Each nerve bundle is composed of numerous nerve fibers. $\times 500$.
- 2 Cross section of one of the main branches of the nutrient artery in the vicinity of the nutrient foramen. The blood vessel appears surrounded by five nerve bundles, each containing a different number of nerve fibers. $\times 500$.
- 3 An arteriole accompanied by three nerve fibers. The nerve fibers contact the layer of smooth muscle fibers of the arterial wall. $\times 800$.



PLATE 2

EXPLANATION OF FIGURES

Bone marrow, femur, rat. Reduced silver nitrate of Cajal-Castro

- 4 A thin branch of the nutrient artery gives off an arteriole on the right hand side of the figure. One of the nerve fibers accompanying the artery (arrow) ends in a bulbous sphincterlike structure at the beginning of the arteriole. $\times 500$.
- 5 In the center of the figure a capillary divides (arrow). One isolated nerve fiber bends at the level of the division and follows one of the branches of the vessel in intimate contact with its endothelial wall. The fiber appears interrupted in the photograph but it can be followed in the serial sections as it crosses from the left (top) to the right of the vessel wall (bottom of the figure). $\times 800$.
- 6 A thick nerve fiber (arrow) is visible in the wall of the central sinus. Only the endothelial wall of the sinus separates the fiber from the newly formed blood carried by the vessel. The nerve fiber disappears in the center of the figure bent by the sinus ending perpendicularly to the central sinus, but in the serial sections the fiber can be followed a long distance attached to the wall of the sinus. $\times 800$.



PLATE 3

EXPLANATION OF FIGURES

Bone marrow, Femur, Rat.

- 7 In the lower half of the figure, an arteriole is followed by a nerve bundle. Another bundle of nerve fibers appears out of focus in the upper left of the figure and becomes clearly visible (arrow) at the right, where the nerve fibers spread and curve around one of the sinusoids appearing in the path of these fibers. Reduced silver nitrate. $\times 800$.
- 8 The lower half of the figure shows an exchange of fibers between two nerve bundles, producing a chiasma. In the upper half, another nerve bundle appears at the right. Reduced silver nitrate. $\times 800$.
- 9 A myelinated nerve fiber traverses the parenchyma in intimate contact with the various cell types of the marrow. The arrow shows a node of Ranvier. Osmic acid. $\times 2,500$.

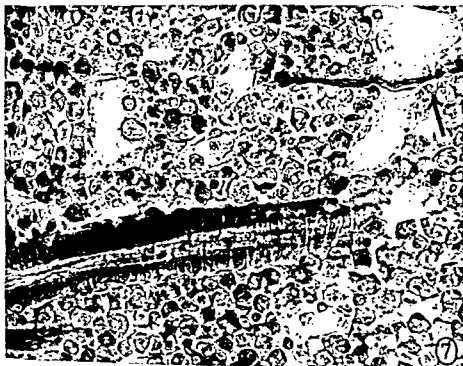
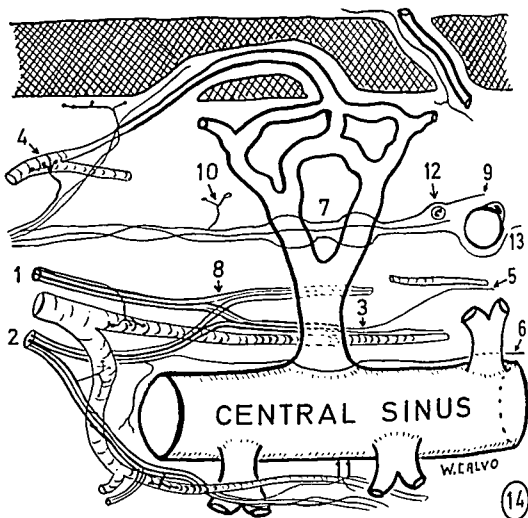


PLATE 4

EXPLANATION OF FIGURES

- 10 A nerve fiber (arrow) ramifies in the center of the figure, ending among the cells of the parenchyma. Bone marrow. Femur. Rat. Reduced silver nitrate. $\times 2,000$.
- 11 Nonmyelinated fiber (arrow) reaches the wall of a capillary, divides and disappears among the cells in the vicinity. Bone marrow. Femur. Rat. $\times 800$.
- 12 Myelinated fiber arching around a cell at the right hand side of the figure. The myelin appears as an unstained sheath around the fiber. The nucleus of a Schwann cell is shown at the left (arrow). Bone marrow. Femur. Rat. $\times 2,000$.
- 13 Two nerve fibers following the curvature of a fat globule in the center of the figure. Bone marrow. Femur. Rabbit. $\times 800$.





EXPLANATION OF FIGURE

- 14 Schematic representation of nerve pattern of bone marrow. The relation of the nerve fibers with the arterial tree, the sinusoids and the parenchyma of the organ are based on the 13 photomicrographs described in the text. The numbers of the photographs correspond with the same numbers in the scheme. The innervation of the nutrient vessels are shown in numbers one to five. The innervation of the sinuses and the parenchymal cells in numbers 6 to 13. Harversian canals innervated by fibers originated from nerve bundles within the bone marrow and in the periosteum are represented in the upper part of the figure.

Ultrastructural Changes in the Sperm Head during Fertilization in the Rabbit

J. M. BEDFORD¹

The Worcester Foundation for Experimental Biology,
Shrewsbury, Massachusetts

ABSTRACT Spermatozoa have been observed with the electron microscope at various stages of their approach to and penetration of the rabbit ovum. No significant change in fine structure is observed in uterine sperm, or in many of the sperm at the periphery of the granulosa investment around the ovum. By contrast, a majority of sperm lying between the granulosa cells or on the surface of the zona pellucida display various stages of the "acrosome reaction"; this involves fusion and vesicle formation between the plasma membrane and the outer membrane of the acrosome. Loss of these vesicular elements, and content of the acrosome cap, takes place before sperm begin to penetrate the substance of the zona. The constricted posterior "equatorial" segment of the acrosome cap does not take part in the acrosome reaction and remains with its content intact during penetration of the zona; neither does the content of the apical sub-acrosomal region (perforatorium) or post-acrosomal region appear to change in traversing the zona. The hypothetical zona lysis is thus presumed to be closely associated with the persistent inner membrane of the acrosome, which now becomes the limiting membrane around the anterior part of the sperm nucleus.

No "penetration filament" has been observed, but sperm within the zona pellucida of ageing eggs are often preceded by a straight or curved fissure in the substance of the zona. The possible nature of capacitation and its relation to the acrosome reaction and to the process of penetration, are discussed briefly.

The ultra-structural features of mammalian spermatozoa have by now been fairly well documented (Fawcett, '58, '65; Iwatt and Ito, '65; Blom and Birch-Anderson, '65; Nicander and Bane, '62, '66; Locke and Almquist, '64; Hadek, '63b; Bedford, '64, '67b; Kojima, '66). Although species differences are seen in the form and proportions of certain organelles, the sperm head is always constructed according to the following basic arrangement. The dense nucleus is covered rostrally by the acrosome cap, a membrane limited sac filled with a fairly homogeneous material which is presumed to possess hyaluronidase activity, though this has not as yet been demonstrated unequivocally. Between the inner membrane of the acrosome and the frontal border of the nucleus, except in man (Bedford, '67b), is found the "perforatorium" or "apical body," which is, in fact, a subacrosomal space of variable size occupied in most species by electron dense material. This material may possibly extend posteriorly as a thin layer over the whole subacrosomal surface of the nu-

cleus, to become confluent with material enveloping the post-acrosomal region (Bedford, '67b). The sperm head is covered by a plasma membrane which is always closely applied to the post-acrosomal region, but appears rather more loosely apposed to the surface of the acrosome.

Although we have a fair understanding of the structural arrangement of the mammalian sperm head, our present conception of the events which occur in sperm during their approach to and penetration of the egg is scanty at best; little is known, moreover, of the precise function or fate of the sperm organelles during fertilization. The substance of the acrosome cap has been shown to be absent in rodent and rabbit sperm penetrating the zona pellucida (Austin and Bishop, '58b; Moricard, '61; Austin, '63; Hadek, '63a; Piko and Tyler, '64), and this has sometimes left an impression that structural changes in the acrosome cap occur during capacita-

¹ Present address: Department of Anatomy and the International Institute for the Study of Human Reproduction, Columbia University, College of Physicians and Surgeons, New York, N. Y. 10032.

tion. Rabbit uterine sperm, however, do not show obvious structural modifications which can be equated with the physiological change of capacitation when examined with the light, or the electron microscope (Adams and Chang, '62; Bedford, '63a, '64; Austin, '63), though evidence from *in vitro* fertilization experiments shows these sperm to be functionally capacitated. Furthermore, the fact that some component of seminal plasma can reversibly inhibit the capacitated state (Chang, '57; Bedford and Chang, '62), seems to militate against the idea that profound structural changes occur in sperm as a feature of capacitation *per se*.

It has not proved possible to visualize clearly the acrosome cap of living rabbit spermatozoa, but, in phase contrast microscope observation of guinea pig and rodent sperm moving within the cumulus oophorus, the acrosome cap often appears elevated or separated from the sperm head before it reaches the surface of the zona pellucida (Austin and Bishop, '58b; Ohnuki, '59; Yanagimachi, '66). In the present investigation, the question of the significance and fate of the rabbit acrosome during the approach to and penetration of the ovum has been studied with the electron microscope. The results show that with the exception of the narrow posterior segment, the substance and outer membrane of the acrosome are lost before commencement of penetration into the zona pellucida. Breakdown of the acrosome in the vicinity of the egg apparently occurs as a result of multiple fusion between the plasma membrane and outer membrane of the acrosome cap; this latter process has been discussed recently by Barros, Bedford, Franklin and Austin ('67).

MATERIALS AND METHODS

Relatively few spermatozoa are present in the ampulla of the oviduct following natural mating. For this reason, in the present study $2.0-2.5 \times 10^5$ rabbit sperm obtained from the cauda epididymidis were inseminated in 0.025 ml of Ringer solution into each oviduct of oestrous rabbits, two hours before administration of an ovulation injection of 50 i.u. human chorionic gonadotrophin. The timing of

these events was arranged to allow ample opportunity for the sperm to become fully capacitated in the Fallopian tube, before arrival of the ova (Adams and '62). Ova were flushed from the Fallopian tubes with 4% glutaraldehyde in phosphate or collidine buffer. In the course of observations, the ova were recovered about 12.5 hours after the ovulation injection — at this time the bulk of the cumulus oophorus had dispersed, but most ova were completely covered by cells of the corona radiata together with variable numbers of cumulus cells. The eggs with the greatest mass of surrounding granulosa cells were later chosen for sectioning. In the second series, eggs were recovered 17–18 hours after an ovulation injection; the majority of these were completely naked of corona cells, and showed a central area in the ooplasm, typical of pronuclear stage.

Ova were allowed to fix in phosphate collidine buffered 4% glutaraldehyde for two hours, and after immersion for several hours in either phosphate or collidine buffer alone, were transferred to 1% osmic acid for one hour. Soon after exposure to osmic acid, the ova become brown and are more easily seen. The eggs were dehydrated in ascending concentrations of alcohol up to 100% alcohol, during one hour, followed by immersion in propylene oxide for two hours. Great care was taken not to disturb the eggs during dehydration, as the surrounding granulosa cells tend to become detached rather easily at this stage. After dehydration, the eggs were placed in capsules containing Epon, and were embedded for several days at 60°C; it was necessary to push the eggs to the bottom of the capsule with a fine wire, as they usually would not sink by way of gravity through the viscous resin. Sections were cut with an automatic microtome (Porter-Bloss Sorvall) using a diamond knife. They were stained with uranyl acetate and lead citrate, and were examined in a Philips 200 electron microscope.

OBSERVATIONS

Many spermatozoa were observed at various stages of their approach to, and penetration of the zona pellucida. Rath-

expectedly, sperm were seen occasionally also within corona cells around several ova. The examples shown in figures 4 and 5 both have lost the content and outer membrane of the acrosome, but other instances were observed where intact sperm heads had come to lie within the corona cell.

The pattern of change in morphology of the sperm head, in relation to its spatial position, was never clear-cut, but the following general impression and sequence of events nevertheless made itself evident. Most spermatozoa situated at the periphery of the granulosa cell coat showed no change in the continuity of the plasma membrane, or in the form and consistency of the acrosome cap; thus their structure did not differ essentially from that of the majority of mature epididymal or ejaculated rabbit sperm (Hadek, '63b; Bedford, '64). However, a minority of free sperm at the periphery did exhibit various degrees of acrosomal change. In some of these, the plasma and outer membranes had content of the acrosome had disappeared (see fig. 3); in others, the plasma membrane had apparently fused at various points with the outer acrosome membrane, to form a chain of vesicles arrayed around the rostral half of the nucleus (see figs. 1, 2).

In contrast to sperm present at the periphery of the cells about the egg, a majority of the sperm seen within the granulosa mass, wedged in the interstices of the cells, showed a variety of stages of the process of acrosomal breakdown (acrosome reaction). Some of these sperm had reached the point of vesiculation (figs. 1, 2) with concomitant release of the contents of the acrosome. In others the process was complete, leaving only the sharply outlined inner membrane of the acrosome as a shroud for the anterior half of the nucleus (fig. 3). Unchanged sperm heads were present on occasion between the corona cells, and on one egg covered only sparsely by such cells, two intact sperm were adherent to the surface of the zona pellucida (figs. 7, 8). However, most sperm among the corona cell processes near to the surface of the zona in young fertilizable eggs (fig. 1), showed some degree of acrosomal change.

As reported by Barros et al. ('67), sperm displaying vesiculation of the plasma and outer acrosomal membranes are often to be found adhering to the zona surface (fig. 2). By contrast, sperm entering (fig. 6) or within the zona (figs. 9, 10, 11) do not retain any acrosomal material, with the exception of that present in the stable posterior (equatorial) segment (fig. 12), which remains intact during sperm passage as far as the peri-vitelline space (fig. 16). Observation of more than 100 sperm at different stages of penetration of the zona, in several ova, indicates that all remnants of the outer acrosome/plasma membrane vesicular complex are lost before penetration begins (fig. 6). Thus it is the rostral part of the inner membrane of the acrosome which must first interact with the substance of the zona pellucida during the initial phase of penetration, and it is this relatively stable membrane which, after the "acrosome reaction," becomes the limiting cell membrane over the anterior surface of the sperm head. At this stage the plasma membrane still remains intact over the posterior part of the head and over the tail (fig. 14), and thus breakdown of the original plasma membrane is confined to that region which covers the acrosome. Following the acrosome reaction, continuity of the cell surface is ensured by fusion of the equatorial segment with the remaining plasma membrane; this arrangement is shown in a sperm traversing the zona pellucida in figure 12, and can be seen in a diagrammatic representation of the acrosome reaction in text-figure 1.

The absence of any change in density or quality of the zona beneath the point of contact with the plasma membrane of the intact sperm head (figs. 7, 8), contrasts with the obvious digestion which precedes the bared inner acrosome membrane of sperm beginning to penetrate the zona. The examples shown in figures 6 and 13, might suggest that the sperm traverses the zona only through a narrow fissure; in many freshly ovulated eggs, however, the sperm begins to enter within a wide cone of superficial digestion which narrows to become a slit in the deeper regions of the zona.

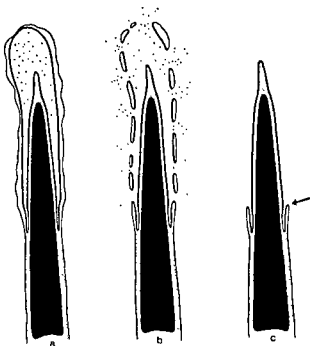


Fig. 1 Diagrammatic representation of the acrosome reaction in rabbit spermatozoa. (a) Intact sperm head as seen in samples of ejaculate, epididymal and capacitated uterine spermatozoa. (b) The outer membrane of the acrosome cap fuses at several points, progressively, with the overlying plasma membrane, to form a series of vesicles around the rostral part of the sperm head — the acrosomal content escapes through the ports which appear between the vesiculated membranes. (c) The vesicles are shed, leaving the sharply defined inner acrosome membrane as the limiting border of the anterior sperm head; continuity of the sperm surface is ensured by fusion at the anterior border of the persistent "equatorial" segment between the acrosome and plasma membranes which remain (arrowed).

An interesting difference in the reaction of the zona pellucida to sperm entry, was observed in young and ageing eggs, respectively. Very rarely was there any space beyond the leading edge of sperm heads traversing the zona in eggs recovered one to two and one-half hours after ovulation. Sperm heads within the zona of eggs recovered six to eight hours after ovulation, on the other hand, frequently were preceded by a narrow channel of variable length (fig. 15) which followed a straight or sometimes a curved course through the zona.

Once the sperm has undergone the acrosome reaction and has lost the outer vesiculated elements, no further structural changes occur in traversing the zona pel-

lucida. Perivitelline sperm appear no different, structurally, from those about to penetrate (cf. figs. 3, 16), and no indication was obtained that the material which occupies the sub-acrosomal space (peritritorium) or the post-acrosomal in any way dissipated during passage through the zona.

It has not been possible thus far to clarify the mode of entry of the sperm into the vitellus. In figure 20, however, it can be seen that the filamentous elements of the tail entering the vitellus, devoid of the plasma membrane so obviously present during penetration of the zona (fig. 14). A similar picture is presented also by the tail which still is adjacent to the fully formed male pronucleus (fig. 22). A cross-section of a sperm head (fig. 17), fixed approximately 30–60 minutes after penetration, at the beginning of the swelling process is often described with the phase-contrast microscope. The surrounding envelope which has swollen away from the nucleus may be nuclear membrane, but this is not certain. The beginnings of rarefaction in the nucleus, faintly discernible in figure 17, are shown clearly at higher magnification in another section of this same sperm head (fig. 18). Sections in figures 18 and 19, also show strands or fibrils of material beginning to detach themselves from the relatively dense fabric of the nucleus. One is impressed with the dynamic nature of the process whereby such a chromatin is transformed in four hours into a definitive male pronucleus (fig. 21).

DISCUSSION

The form and rostral position of the acrosome cap of mammalian sperm suggest an important role for this organelle in fertilization, but its function has remained uncertain. It is known that the acrosome cap is no longer present in sperm which have penetrated the egg (Austin and Bishop, '58b; Hadek, '63; Austin, '63; Piko and Tyler, '64), but the extent of its involvement at the time of passage through the zona pellucida has been unclear. Present observations suggest that the majority of the content of the acrosome is lost before penetration.

zona pellucida begins. Sperm at the t stage of entry, in which the leading t of the sperm head intrudes into the stance of the zona, do not retain any nant of the outer membrane and con- of the acrosome, except that remain- in the equatorial region. The persistent ter acrosomal membrane of penetrating rm is sharply outlined, and displays no ternal "fuzz," indicative of residues of rosomal content associated with its sur- e. The material in the persistent pos- for equatorial region of the acrosome, d the substance occupying the sub-acro- mal and post-acrosomal spaces, did not pear changed or diminished during pas- ge of sperm through the zona pellucida the peri-vitelline space. If one assumes at penetration of the zona is facilitated sperm lysins, it is reasonable to argue present evidence that this postulated ic activity is closely associated with the ble inner membrane of the acrosome p. The nature of the zona lysin is uncer- in. It is unlikely to be hyaluronidase, for, hile impure preparations of bovine or ine testicular hyaluronidase (300-500 u/mg — Sigma) will dissolve the rabbit ma, similar or higher concentrations of ctrophoretically pure testicular hyaluro- idase (ca. 3000 tru/mg — Mann Bio- chemicals) will not do so (unpublished). is more reasonable to speculate that me type of proteolytic activity is in- olved at this stage, since the zona pelli- da is susceptible to trypsin (Smithberg, '63; Chang and Hunt, '57) to pronase (Mintz, '62), and, significantly perhaps, to e proteolytic lipoglycoprotein complex olated from ram sperm by Srivastava, adams and Hartree ('65). Recently, an nzyme(s) with proteolytic activity towards emoglobin, having a pH optimum of 6.8- 7.0, has been detected in acrosomal pre- parations (Hartree and Allison — personal communication). The significance of the table, persistent, posterior remnant of the acrosome, which corresponds to the "equa- torial" region seen in the light microscope, is equally unclear. Its existence is probably ubiquitous, as it has been found in cen- tral sagittal sections of sperm from sev- eral mammalian species, (Nicander and Bane, '66), including man (Bedford, '67b)

and rodents (unpublished). Since the con- tent and form of this segment do not ap- pear to change in passing through the zona, its function, if any, may relate to events occurring during entry into the vitellus.

It is difficult at present to ascribe any function to the substance of the protrud- ing apical sub-acrosomal space or "perfor- atorium," during penetration of the zona (see Dan, '67; Colwin and Colwin, '67); more information is needed in mammals about the mode of fusion of the fertilizing sperm with the vitelline membrane, before a firm idea of the significance of this ap- ical region can be gained. There are marked species differences in the form and size of the apical space, which varies from the prominent hook in rodent sperm (Cler- mont, Einberg, Leblond and Wagner, '55; Austin and Bishop, '58a), to the negligible protuberance in sperm from the cat and horse (Nicander and Bane, '66); the per- foratorium as a special structure or rostral concentration of sub-acrosomal ma- terial is entirely absent in ejaculated human spermatozoa (Bedford, '67b). Evidence has been obtained that the cytoplasmic material of the "perforatorium" may ex- tend posteriorly as a thin layer over the sub-acrosomal surface of the nucleus to join that present in the post-acrosomal space (Hadek, '63b; Bedford, '67b). These facts raise a question as to whether the localized apical concentration of this sub- acrosomal material, as such, has special functional significance. The material which overlies the post-acrosomal and other regions of the nuclear surface may be equally important in possible roles in- volving activation of the vitelline surface or of ooplasmic organelles.

As yet, there has been no clear demon- stration of the nature of capacitation. Sperm recovered from the rabbit uterus 12 hours after mating are presumed to be functionally capacitated, since some will definitely fertilize *in vitro* (Dauzier and Thibault, '56, '59; Chang, '59). There is, however, a distinct difference in the fine structure of a majority of uterine sperm (Bedford, '64), tubal sperm outside the granulosa mass, or ejaculate sperm adher- ing to the rabbit ovum (Hadek, '63b), which appear intact, and most sperm

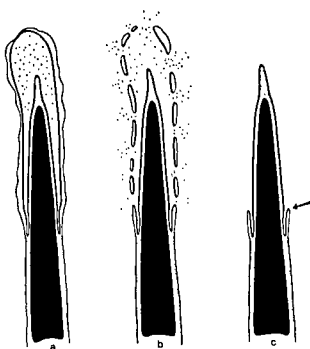


Fig. 1 Diagrammatic representation of the acrosome reaction in rabbit spermatozoa. (a) Intact sperm head as seen in samples of ejaculate, epididymal and capacitated uterine spermatozoa. (b) The outer membrane of the acrosome cap fuses at several points, progressively, with the overlying plasma membrane, to form a series of vesicles around the rostral part of the sperm head—the acrosomal content escapes through the ports which appear between the vesiculated membranes. (c) The vesicles are shed, leaving the sharply defined inner acrosome membrane as the limiting border of the anterior sperm head; continuity of the sperm surface is ensured by fusion at the anterior border of the persistent "equatorial" segment between the acrosome and plasma membranes which remain (arrowed).

An interesting difference in the reaction of the zona pellucida to sperm entry, was observed in young and ageing eggs, respectively. Very rarely was there any space beyond the leading edge of sperm heads traversing the zona in eggs recovered one to two and one-half hours after ovulation. Sperm heads within the zona of eggs recovered six to eight hours after ovulation, on the other hand, frequently were preceded by a narrow channel of variable length (fig. 15) which followed a straight or sometimes a curved course through the zona.

Once the sperm has undergone the acrosome reaction and has lost the outer vesiculated elements, no further structural changes occur in traversing the zona pel-

lucida. Perivitelline sperm appear no different, structurally, from those about to penetrate (cf. figs. 3, 16), and no indication was obtained that the material which occupies the sub-acrosomal space (perioratorium) or the post-acrosomal region, in any way dissipated during passage through the zona.

It has not been possible thus far to clarify the mode of entry of the fertilizing sperm into the vitellus. In figure 20, however, it can be seen that the "remnants of the tail entering the vitellus, devoid of the plasma membrane so obviously present during penetration of the zona (fig. 14). A similar picture is presented also by the tail which still lies adjacent to the fully formed male pronucleus (fig. 22). A cross-section of a fertilizing sperm head (fig. 17), fixed approximately 30–60 minutes after penetration, the beginning of the swelling process often described with the phase "microscope. The surrounding environment which has swollen away from the nucleus may be nuclear membrane; this is not certain. The beginnings of rarefaction in the nucleus, faintly discernible in figure 17, are shown at higher magnification in another of this same sperm head (fig. 18). Sections in figures 18 and 19, also reveal strands or fibrils of material beginning to detach themselves from the relatively dense fabric of the nucleus. One is impressed with the dynamic nature of the process whereby such a chromatin is transformed in four hours into a definitive male pronucleus (fig. 21).

DISCUSSION

The form and rostral position of the acrosome cap of mammalian sperm suggest an important role for this organ in fertilization, but its function has remained uncertain. It is known that the acrosome cap is no longer present in sperm which have penetrated the mammalian egg (Austin and Bishop, '58b; Hadek, '63; Austin, '63; Piko and Tyler, '64), but the extent of its involvement at the point of passage through the zona pellucida has been unclear. Present observations reveal that the majority of the content of the acrosome is lost before penetration

zona pellucida begins. Sperm at the stage of entry, in which the leading part of the sperm head intrudes into the substance of the zona, do not retain any remnant of the outer membrane and content of the acrosome, except that remaining in the equatorial region. The persistent periacrosomal membrane of penetrating sperm is sharply outlined, and displays no external "fuzz," indicative of residues of acrosomal content associated with its surface. The material in the persistent posterior equatorial region of the acrosome, and the substance occupying the sub-acrosomal and post-acrosomal spaces, did not appear changed or diminished during passage of sperm through the zona pellucida or the perivitelline space. If one assumes that penetration of the zona is facilitated by sperm lysins, it is reasonable to argue from present evidence that this postulated proteolytic activity is closely associated with the inner membrane of the acrosome. The nature of the zona lysis is uncertain. It is unlikely to be hyaluronidase, for, while impure preparations of bovine or rabbit testicular hyaluronidase (300–500 μ /mg — Sigma) will dissolve the rabbit zona, similar or higher concentrations of electrophoretically pure testicular hyaluronidase (ca. 3000 μ /mg — Mann Biochemicals) will not do so (unpublished). It is more reasonable to speculate that some type of proteolytic activity is involved at this stage, since the zona pellucida is susceptible to trypsin (Smithberg, '53; Chang and Hunt, '57) to pronase (Mintz, '62), and, significantly perhaps, to the proteolytic lipoglycoprotein complex isolated from ram sperm by Srivastava, Adams and Hartree ('65). Recently, an enzyme with proteolytic activity towards haemoglobin, having a pH optimum of 6.8–7.0, has been detected in acrosomal preparations (Hartree and Allison — personal communication). The significance of the stable, persistent, posterior remnant of the acrosome, which corresponds to the "equatorial" region seen in the light microscope, is equally unclear. Its existence is probably ubiquitous, as it has been found in central sagittal sections of sperm from several mammalian species, (Nicander and Bane, '66), including man (Bedford, '67b)

and rodents (unpublished). Since the content and form of this segment do not appear to change in passing through the zona, its function, if any, may relate to events occurring during entry into the vitellus.

It is difficult at present to ascribe any function to the substance of the protruding apical sub-acrosomal space or "perforatorium," during penetration of the zona (see Dan, '67; Colwin and Colwin, '67); more information is needed in mammals about the mode of fusion of the fertilizing sperm with the vitelline membrane, before a firm idea of the significance of this apical region can be gained. There are marked species differences in the form and size of the apical space, which varies from the prominent hook in rodent sperm (Clermont, Einberg, Leblond and Wagner, '55; Austin and Bishop, '58a), to the negligible protuberance in sperm from the cat and horse (Nicander and Bane, '66); the perforatorium as a special structure or rostral concentration of sub-acrosomal material is entirely absent in ejaculated human spermatozoa (Bedford, '67b). Evidence has been obtained that the cytoplasmic material of the "perforatorium" may extend posteriorly as a thin layer over the sub-acrosomal surface of the nucleus to join that present in the post-acrosomal space (Hadek, '63b; Bedford, '67b). These facts raise a question as to whether the localized apical concentration of this sub-acrosomal material, as such, has special functional significance. The material which overlies the post-acrosomal and other regions of the nuclear surface may be equally important in possible roles involving activation of the vitelline surface or of ooplasmic organelles.

As yet, there has been no clear demonstration of the nature of capacitation. Sperm recovered from the rabbit uterus 12 hours after mating are presumed to be functionally capacitated, since some will definitely fertilize *in vitro* (Dauzier and Thibault, '56, '59; Chang, '59). There is, however, a distinct difference in the fine structure of a majority of uterine sperm (Bedford, '64), tubal sperm outside the granulosa mass, or ejaculate sperm adhering to the rabbit ovum (Hadek, '63b), which appear intact, and most sperm

among the granulosa cells in the vicinity of the fresh egg in which the outer elements of the acrosome have disappeared (fig. 3) or are undergoing vesiculation (figs. 1, 2). This raises the possibility that substances in the vicinity of the mammal egg stimulate or initiate the acrosome reaction (text-fig. 1), and that viable rabbit sperm are able to react in this manner only after the prior conditioning which constitutes capacitation. Such sperm-stimulating substance(s), obviously comparable to the "fertilisin" of sea urchin eggs (Lillie, '19), could emanate from the surrounding granulosa cells and/or the ovum. The cells of the corona radiata around ovulated eggs often display a well-preserved and extensive ribosome-studded endoplasmic reticulum as well as a widespread system of Golgi lamellae. Clearly, these cells may still discharge some secretory function after ovulation. It should be noted, however, that some fresh rabbit ova remain fertilizable, though less so, after loss of the cells of the corona radiata (Chang and Bedford, '62; Bedford and Chang, '62); thus their presence is not essential for fertilization.

The exact significance of capacitation at fertilization is not wholly clear, but it is evident that sperm penetration through the zona pellucida is able to occur only after capacitation has been accomplished. Apparently, this functional change in the sperm also ensures establishment of initial contact between the gametes early in the fertile life of the egg, probably by facilitating sperm passage across the granulosa cell "barrier" (Austin, '60; Bedford, '67a). The mode of the acrosome reaction, discussed by Barros et al. ('67), and in the present paper (text-fig. 1), make it seem likely that capacitation involves changes of a destabilizing nature in the plasma membrane of the sperm. This membrane, though morphologically unchanged following capacitation, would then be able to react appropriately to the hypothetical stimulatory substances arising from the granulosa cell/egg mass, by local breakdown and fusion with the underlying outer membrane of the acrosome. This vesiculation reaction would in turn allow coordinated release in the vicinity of the egg, of the acrosomal content,

which, by virtue of its presumed hyaluronidase activity must act to dissipate the matrix between the granulosa cells (Barros et al., '67). In the second place, loss of the outer acrosomal elements involved in the vesiculation reaction serves to reveal the inner membrane of the acrosome; this latter phenomenon appears an essential pre-requisite for penetration of the zona substance (cf. figs. 6, 9, 10, 11). In the above scheme of events the decapacitator factor in seminal plasma (Chang, '57; Bedford and Chang, '62a) might be presumed to inhibit the fertilizing ability of capacitated sperm by acting to block membrane receptors or to "stabilize" the plasma membrane in some other way, so as to prevent the onset of the vesiculation reaction. These last speculative suggestions are now open to experimental investigation.

In the present study, a few intact sperm were situated between the granulosa cells but it must be remembered that abnormally large numbers of sperm were deposited at the site of fertilization. The intact sperm shown in figures 4 and 5 were adherent over relatively denuded parts of the zona. Since the sperm were taken from the cauda epididymidis it is possible that these may still have been relatively immature, but this finding, nevertheless, raises the question as to whether all viable spermatozoa in the ejaculate are capable of undergoing capacitation.

The plasma membrane of mammalian sperm, though physically continuous, appears to be regionally differentiated in character, as judged by differences in the antigenic nature of the surface over the head and tail, respectively (Henle, Henle and Chambers, '38; Smith, '49) by the auto-agglutination behavior in various media (Kato, '36; Bedford, '65), and by the typical tail-anode orientation of mature mammalian sperm in an electric field (Nevo, Michaeli and Schindler, '61; Barrham, '61; Bedford, '63). It is interesting, therefore, that in capacitated sperm approaching the ovum, the plasma membrane breaks down only locally, where it overlies the acrosome. The cell surface about the posterior part of the head and the tail (fig. 14) is apparently untouched by the factors which promote the coordinate

face breakdown seen during the acrosome reaction. In a collation of available evidence concerning the nature of the acrosome reaction, Colwin and Colwin ('67) bring to the basic morphological similarity of event in widely separated groups including the Enteropneusta, Echinodermata, Mollusca, and speculatively, in Mammalia. Present evidence shows their speculation with regard to mammals to be correct; thus the inner acrosome membrane of the mammalian sperm can be considered as the homologue of the membrane which delineates the acrosomal filament or tubule, extruded during the acrosome reaction in Arbacia or Saccoglossus. There is, however, no extension of this membrane as a concomitant of the acrosome reaction in rabbit sperm. Phase contrast microscope studies of fertilized ova from the rabbit, pig and sheep, have shown that appears to be a filament extending from the rostral border of sperm within the zona pellucida (Dickmann, '64; Dickmann and Dziuk, '64; Dziuk and Dickmann, '65). In the phase contrast microscope this element may precede the sperm as a light zone (fig. 15 — inset) or as a dark filamentous projection, depending upon the exact level of focus (personal observation). No filament has been observed in the electron microscope in rabbit sperm at various stages of penetration through the zona, (figs. 6, 9, 10, 11, 15) and since the apical border always remained intact in these sperm, it is difficult to visualize how such a filament might arise. In contrast to the concept of filament, it seems more probable that the image of an anterior projection in the phase microscope is produced by the narrow fissure (fig. 15), which appears commonly before sperm within the zona of rabbit eggs recovered at the end of their fertile life. Since this type of channel was rarely seen to precede sperm in the zona of young fertile eggs, it is possible that its appearance is associated with some change in the physical properties of the zona, as a concomitant of the ageing process. The mode of formation of the fissure extending in front of the sperm head, is an open question. It is difficult to imagine

how a process of predigestion could produce such a directional effect in the seemingly homogeneous material of the zona. Although it is conceivable that such a gap might be left after retrograde movement of the sperm within the zona, this suggestion is weakened by the fact that in some cases the fissure is curved to a much greater degree than is the rigid straight sperm nucleus. The remaining possibility that comes to mind is that this fissure develops as a physical split, or rupture of the zona substance brought about by forward movement of the sperm at a time when the ageing zona is becoming less resilient. In this case one would assume that sperm in this situation have reached the limit of their penetration and are probably destined to remain within the zona.

The finding of sperm within several corona cells was unexpected, and to the author's knowledge this has not been observed heretofore. It should be remembered, however, that relatively a large number of sperm were placed at the site of fertilization, and one cannot be certain that movement of some sperm into corona cells occurs after natural mating. Although both examples in plate 3 show sperm which have already undergone the acrosome reaction, several structurally intact sperm have been observed within corona cells. This implies that the entry process was probably phagocytic rather than the result of active penetration by the sperm. The reason for the withdrawal and incarceration of some sperm by the cells which surround the ovum, is not readily apparent, though this might conceivably serve to shield the female gamete from "defective" spermatozoa.

ACKNOWLEDGMENTS

The author wishes to express his gratitude to Dr. L. F. Cavazos, Department of Anatomy, Tufts University Medical School, for his kindness in making available the electron microscope facilities of his department, and to Miss Shirley Gray for her technical assistance. Text-figure 1 was drawn by R. J. Demarest.

This study has been supported by grants HD-03472 and GM 14370 awarded to Dr. M. C. Chang.

LITERATURE CITED

- Adams, C. E., and M. C. Chang 1962 Capacitation of rabbit spermatozoa in the Fallopian tube and in the uterus. *J. Exp. Zool.*, 151: 159-166.
- Austin, C. R. 1960 Capacitation and release of hyaluronidase. *J. Reprod. and Fertil.*, 1: 310-311.
- 1961 *The Mammalian Egg*. Blackwell, Oxford.
- 1963 Acrosome loss from the rabbit spermatozoon in relation to entry into the egg. *J. Reprod. and Fertil.*, 6: 313-314.
- Austin, C. R., and M. W. H. Bishop 1958a Some features of the acrosome and perforatorium in mammalian spermatozoa. *Proc. R. Soc. B.*, 148: 234-240.
- 1958b Role of the rodent acrosome and perforatorium in fertilization. *Proc. R. Soc. B.*, 148: 241-248.
- Bangham, A. D. 1961 Electrophoretic characteristics of ram and rabbit spermatozoa. *Proc. R. Soc. B.*, 155: 292-305.
- Barros, C., J. M. Bedford, L. E. Franklin and C. R. Austin 1967 Membrane vesiculation as a feature of the mammalian acrosome reaction. *J. Cell Biol.*, 34: C1-C5.
- Bedford, J. M. 1963a Morphological reaction of spermatozoa in the female reproductive tract of the rabbit. *J. Reprod. and Fertil.*, 6: 245-255.
- 1963b Changes in the electrophoretic properties of rabbit spermatozoa during passage through the epididymis. *Nature*, 200: 1178-1180.
- 1964 Fine structure of the sperm head in ejaculate and uterine spermatozoa of the rabbit. *J. Reprod. and Fertil.*, 7: 221-228.
- 1965 Non-specific tail-tail agglutination of mammalian spermatozoa. *Exp. Cell Res.*, 38: 654-659.
- 1967a The importance of capacitation for establishing contact between eggs and sperm in the rabbit. *J. Reprod. and Fertil.*, 13: 365-367.
- 1967b Observations on the fine structure of spermatozoa of the Bush Baby (*Galago senegalensis*), The African Green Monkey (*Cercopithecus aethiops*) and Man. *Am. J. Anat.*, 121: 443-460.
- Bedford, J. M., and M. C. Chang 1962a Removal of decapacitation factor from seminal plasma by high speed centrifugation. *Am. J. Physiol.*, 202: 179-181.
- 1962b Fertilization of rabbit ova, *in vitro*. *Nature*, 193: 898-899.
- Blom, E., and A. Birch-Anderson 1965 The ultrastructure of the Bull Sperm. II. The Sperm Head. *Nord Vet.*, 17: 193-212.
- Chang, M. C. 1957 A detrimental effect of seminal plasma on the fertilizing capacity of sperm. *Nature*, 179: 258-259.
- 1959 Fertilization of rabbit ova *in vitro*. *Nature*, 184: 466-467.
- Chang, M. C., and D. M. Hunt 1957 Effects of proteolytic enzymes on the zona pellucida of fertilized and unfertilized mammalian eggs. *Exp. Cell Res.*, 11: 497-499.
- Chang, M. C., and J. M. Bedford 1962 Fertilizability of rabbit ova after removal of the corona radiata. *Fertil. and Steril.*, 13: 421-423.
- Clermont, Y., E. Einberg, C. P. Leblond and S. Wagner 1955 The perforatorium—an extension of the nuclear membrane of the spermatozoon. *Anat. Rec.*, 121: 1-12.
- Colwin, L. H., and A. L. Colwin 1967 Membrane fusion in relation to sperm-egg association. Chapter 7. In: *Fertilization*. Vol. 1. C. B. Metz and A. Monroy, eds. Academic Press.
- Dan, J. C. 1967 Acrosome reaction and lysis. Chapter 6. In: *Fertilization*. Vol. 1. C. B. Metz and A. Monroy, eds. Academic Press.
- Dauzier, L., and C. Thibault 1956 Recherches expérimentales sur la maturation des gamètes mâles chez les mammifères par l'étude de la fécondation *in vitro* de l'oeuf de Lapine. *Proc. III. Int. Congr. Anim. Reproduc.* Cambridge, Section I, Pp. 58-62.
- 1959 Données nouvelles sur la fécondation *in vitro* de l'oeuf de la Lapine et de Brébis. *C. R. Acad. Sci.*, 248: 2655-2656.
- Dickmann, Z. 1964 The passage of spermatozoa through and into the zona pellucida of the rabbit egg. *J. Exp. Biol.*, 41: 177-182.
- Dickmann, Z., and P. J. Dziuk 1964 Sperm penetration of the zona pellucida of the rabbit egg. *J. Exp. Biol.*, 41: 603-608.
- Dziuk, P. J., and Z. Dickmann 1965 Sperm penetration through the zona pellucida of the sheep egg. *J. Exp. Zool.*, 158: 237-239.
- Fawcett, D. W. 1958 The structure of the mammalian spermatozoon. *Int. Rev. Cytol.*, 195-235.
- 1965 The anatomy of the mammalian spermatozoon with particular reference to the guinea pig. *Z. Zellforsch.*, 67: 279-296.
- Fawcett, D. W., and S. Ito 1965 The fine structure of bat spermatozoa. *Am. J. Anat.*, 116: 567-610.
- Hadek, R. 1963a Submicroscopic changes in the penetrating spermatozoon of the rabbit. *Ultrastruct. Res.*, 8: 161-169.
- 1963b Study on the fine structure of the rabbit sperm head. *J. Ultrastruct. Res.*, 110-122.
- Henle, W., G. Henle and L. S. Chambers 1965 Studies on the antigenic structure of some mammalian spermatozoa. *J. Exp. Med.*, 121: 335-352.
- Kato, K. 1936 Experimental studies on the agglutination of mammalian spermatozoa with special reference to its bearing upon fertilization. *Mem. Fac. Sci. & Agr., Taihoku Univ.*, 19: 1-73.
- Kojima, Y. 1966 Electron microscopic study of the bull spermatozoon. *Jap. J. Vet. Res.*, 14: Nos. 1 and 2.
- Lillie, F. 1919 *Problems of Fertilization*. University of Chicago Press.
- Mintz, B. 1962 Experimental study of the developing mammalian egg: removal of the zona pellucida. *Science*, 138: 594-595.

- icard, R. 1960 Observations de microscopie électronique sur des modifications acrosomiques lors de la pénétration spermatique dans l'oeuf des mammifères. C. R. Soc. Biol., Paris, 154: 187-2189.
- o, A. C., I. Michaeli and H. Schindler 1961 Electrophoretic properties of bull and of rabbit spermatozoa. Exp. Cell Res., 23: 69-83.
- ander, L., and A. Bane 1962 Fine structure of boar spermatozoa. Z. Zellforsch., 57: 390-405.
- 1966 Fine structure of the sperm head in some mammals, with particular reference to the acrosome and sub-acrosomal substance. Z. Zellforsch., 72: 496-515.
- uki, Y. 1959 Some morphological observations of mouse spermatozoa in relation to insemination. Zool. Mag., Tokyo, 68: 275. Biol. Abst. 1960 35: 46462.
- o, L., and A. Tyler 1964 Fine structural studies of sperm penetration in the rat. Proc. V. Int. Congr. Anim. Reprod., Trento, Vol. II. 372-377.
- Saacke, R. G., and J. O. Almquist 1964 Ultrastructure of bovine spermatozoa. I. The head of normal ejaculated sperm. Am. J. Anat., 115: 143-162.
- Smith, A. U. 1949 Some antigenic properties of mammalian spermatozoa. Proc. R. Soc. B., 136: 46-66.
- Smithberg, M. 1953 The effect of different proteolytic enzymes on the zona pellucida of mouse ova. Anat. Res., 117: 554.
- Srivastava, C. E., C. E. Adams and E. F. Hartree 1965 Enzymic action of acrosomal preparations on the rabbit ovum *in vitro*. J. Reprod. and Fertil., 10: 61-67.
- Yanagimachi, R. 1966 Time and process of sperm penetration into the hamster ova, *in vivo* and *in vitro*. J. Reprod. and Fertil., 11: 359-370.

LITERATURE CITED

- Adams, C. E., and M. C. Chang 1962 Capacitation of rabbit spermatozoa in the Fallopian tube and in the uterus. *J. Exp. Zool.*, 151: 159-166.
- Austin, C. R. 1960 Capacitation and release of hyaluronidase. *J. Reprod. and Fertil.*, 1: 310-311.
- 1961 *The Mammalian Egg*. Blackwell, Oxford.
- 1963 Acrosome loss from the rabbit spermatozoon in relation to entry into the egg. *J. Reprod. and Fertil.*, 6: 313-314.
- Austin, C. R., and M. W. H. Bishop 1958a Some features of the acrosome and perforatorium in mammalian spermatozoa. *Proc. R. Soc. B.*, 148: 234-240.
- 1958b Role of the rodent acrosome and perforatorium in fertilization. *Proc. R. Soc. B.*, 148: 241-248.
- Bangham, A. D. 1961 Electrophoretic characteristics of ram and rabbit spermatozoa. *Proc. R. Soc. B.*, 155: 292-305.
- Barros, C., J. M. Bedford, L. E. Franklin and C. R. Austin 1967 Membrane vesiculation as a feature of the mammalian acrosome reaction. *J. Cell Biol.*, 34: C1-C5.
- Bedford, J. M. 1963a Morphological reaction of spermatozoa in the female reproductive tract of the rabbit. *J. Reprod. and Fertil.*, 6: 245-255.
- 1963b Changes in the electrophoretic properties of rabbit spermatozoa during passage through the epididymis. *Nature*, 200: 1178-1180.
- 1964 Fine structure of the sperm head in ejaculate and uterine spermatozoa of the rabbit. *J. Reprod. and Fertil.*, 7: 221-228.
- 1965 Non-specific tail-tail agglutination of mammalian spermatozoa. *Exp. Cell Res.*, 38: 654-659.
- 1967a The importance of capacitation for establishing contact between eggs and sperm in the rabbit. *J. Reprod. and Fertil.*, 13: 365-367.
- 1967b Observations on the fine structure of spermatozoa of the Bush Baby (*Galago senegalensis*), The African Green Monkey (*Cercopithecus aethiops*) and Man. *Am. J. Anat.*, 121: 443-460.
- Bedford, J. M., and M. C. Chang 1962a Removal of decapacitation factor from seminal plasma by high speed centrifugation. *Am. J. Physiol.*, 202: 179-181.
- 1962b Fertilization of rabbit ova, *in vitro*. *Nature*, 193: 898-899.
- Blom, E., and A. Birch-Anderson 1965 The ultrastructure of the Bull Sperm. II. The Sperm Head. *Nord Vet.*, 17: 193-212.
- Chang, M. C. 1957 A detrimental effect of seminal plasma on the fertilizing capacity of sperm. *Nature*, 179: 258-259.
- 1959 Fertilization of rabbit ova *in vitro*. *Nature*, 184: 466-467.
- Chang, M. C., and D. M. Hunt 1957 Effects of proteolytic enzymes on the zona pellucida of fertilized and unfertilized mammalian eggs. *Exp. Cell Res.*, 11: 497-499.
- Chang, M. C., and J. M. Bedford 1962 Fertilizability of rabbit ova after removal of the corona radiata. *Fertil and Steril.*, 13: 421-425.
- Clermont, Y., E. Einberg, C. P. Leblond and S. Wagner 1955 The perforatorium — as a tension of the nuclear membrane of the spermatozoon. *Anat. Rec.*, 121: 1-12.
- Colwin, L. H., and A. L. Colwin 1967 Membrane fusion in relation to sperm-egg association. Chapter 7. In: *Fertilization*. Vol. 1. C. B. Metz and A. Monroy, eds. Academic Press.
- Dan, J. C. 1967 Acrosome reaction and lysosomes. Chapter 6. In: *Fertilization*. Vol. 1. C. B. Metz and A. Monroy, eds. Academic Press.
- Dauzier, L., and C. Thibault 1956 Recherches expérimentales sur la maturation des gamètes mâles chez les mammifères par l'étude de la fécondation *in vitro* de l'oeuf de Lapine. *Proc. III. Int. Congr. Anim. Reproduc.* Cambridge Section I. Pp. 58-62.
- 1959 Données nouvelles sur la fécondation *in vitro* de l'oeuf de la Lapine et de la Brébis. *C. R. Acad. Sci.*, 248: 2655-2656.
- Dickmann, Z. 1964 The passage of spermatozoa through and into the zona pellucida of the rabbit egg. *J. Exp. Biol.*, 41: 177-182.
- Dickmann, Z., and P. J. Dziuk 1964 Sperm penetration of the zona pellucida of the rat egg. *J. Exp. Biol.*, 41: 603-608.
- Dziuk, P. J., and Z. Dickmann 1965 Sperm penetration through the zona pellucida of the sheep egg. *J. Exp. Zool.*, 158: 237-239.
- Fawcett, D. W. 1958 The structure of the mammalian spermatozoon. *Int. Rev. Cytol.*, 7: 195-235.
- 1965 The anatomy of the mammalian spermatozoon with particular reference to the guinea pig. *Z. Zellforsch.*, 67: 279-296.
- Fawcett, D. W., and S. Ito 1965 The fine structure of bat spermatozoa. *Am. J. Anat.*, 116: 567-610.
- Hadek, R. 1963a Submicroscopic changes in the penetrating spermatozoon of the rabbit. *J. Ultrastruct. Res.*, 8: 161-169.
- 1963b Study on the fine structure of the rabbit sperm head. *J. Ultrastruct. Res.*, 9: 110-122.
- Henle, W., G. Henle and L. S. Chambers 1955 Studies on the antigenic structure of some mammalian spermatozoa. *J. Exp. Med.*, 63: 335-352.
- Kato, K. 1936 Experimental studies on the agglutination of mammalian spermatozoa with special reference to its bearing upon fertilization. *Mem. Fac. Sci. & Agr., Taihoku Imp. Univ.*, 19: 1-73.
- Kojima, Y. 1966 Electron microscopic study of the bull spermatozoon. *Jap. J. Vet. Res.*, 14: Nos. 1 and 2.
- Lillie, F. 1919 *Problems of Fertilization*. Univ. of Chicago Press.
- Mintz, B. 1962 Experimental study of the developing mammalian egg: removal of the zona pellucida. *Science*, 138: 594-595.



PLATE 1

EXPLANATION OF FIGURES

- 1 A rabbit sperm is approaching the zona pellucida (Z) between corona cells (C) and corona cell processes (P). The acrosome cap has been transformed into a series of vesicles which still cover the rostral region of the sperm head. $\times 13,000$. Inset: higher magnification to show the arrangement of the vesiculated acrosome. $\times 27,000$.
- 2 Transverse section of a rabbit sperm head on the surface of the zona pellucida of a fertilized ovum, recovered approximately two and one-half hours after ovulation. The outer investment of the acrosome has undergone vesiculation (av), with loss of the acrosomal content. No change is evident in the zona substance (Z) in contact with the vesiculating acrosomal elements. $\times 23,600$.

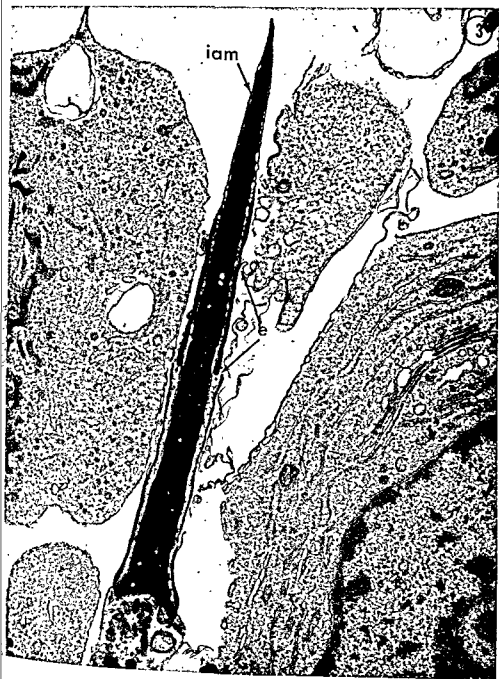


PLATE 2

EXPLANATION OF FIGURES

- 3 Rabbit sperm between corona cells (C) approaching the surface of the zona pellucida, which lies out of view beyond the upper border of the plate. In this case the vesiculated acrosomal investment has been discharged before contact with the zona pellucida, exposing the inner membrane (i.a.m.) of the acrosome cap. Note the intact posterior remnant of the cap (c) which persists during penetration of the zona. $\times 40,000$.



PLATE 3

EXPLANATION OF FIGURES

- 4-5 Both figures show rabbit sperm nuclei lying within corona cells. Examples have been observed of intact sperm similarly placed within corona cells. Note the distribution of Golgi lamellae and ribosome-studded endoplasmic reticulum within the cells. $\times 15,800$.

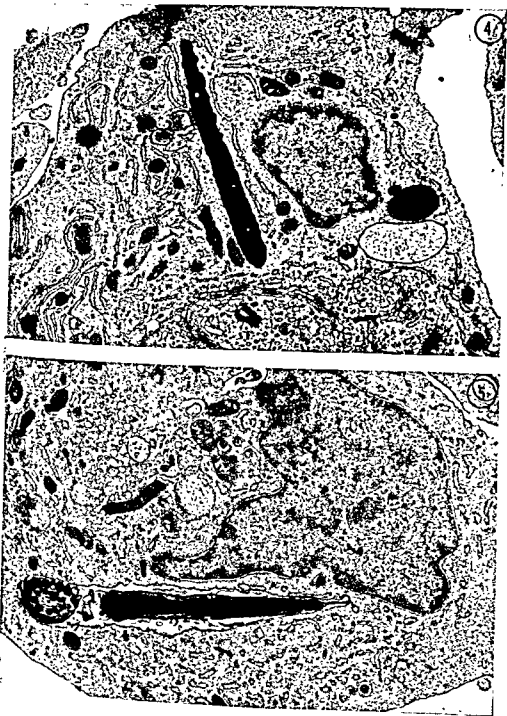


PLATE 4

EXPLANATION OF FIGURE

- 6 Rabbit sperm head beginning to penetrate the zona pellucida. No acrosomal vesicles remain about the rostral surface of the head; thus, the zona interacts solely with the inner membrane of the acrosome cap during the initial stages of penetration. This ovum has already been activated by another sperm as evidenced by the absence of cortical granules in the vitellus. $\times 17,000$.



PLATE 5

EXPLANATION OF FIGURES

- 7 An intact sperm head is adhering to a relatively denuded part of the zona surface (Z), though a corona cell (C) is seen immediately above the sperm head. The zona pellucida appears in no way affected by contact with the sperm plasma membrane (arrowed).
× 38,000.
- 8 Sperm head with intact acrosome cap, and most of the covering plasma membrane (arrowed), adhering to a denuded region of the zona pellucida (Z) of a fertilized ovum recovered about two and one-half hours after ovulation. Although the sperm head has indented the surface, no change is apparent in the substance of the zona.
× 38,000.

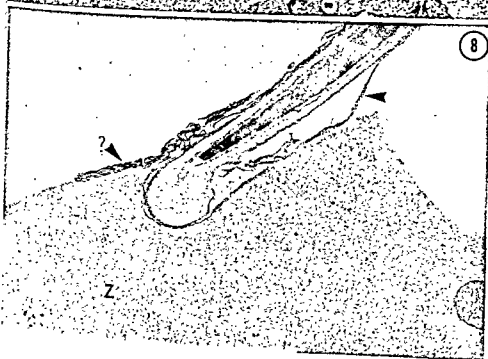
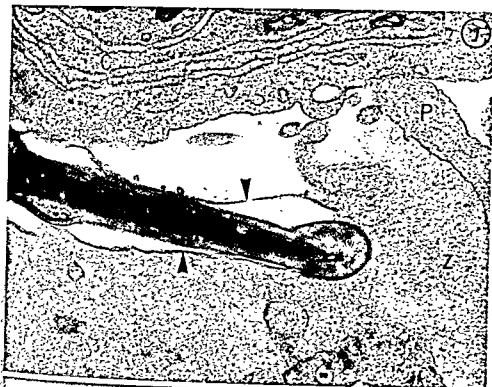


PLATE 6

EXPLANATION OF FIGURES

- 9-11 Examples of sperm lodged wholly within the zona pellucida of freshly ovulated ova. No vesiculated acrosomal elements remain about the sperm head. All figures $\times 22,000$.

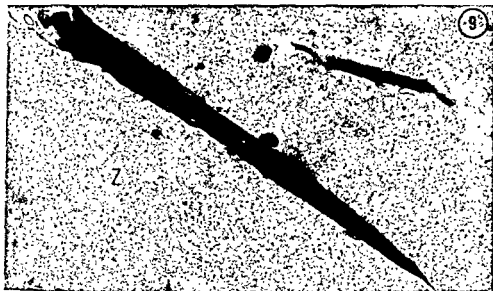


PLATE 6

EXPLANATION OF FIGURES

- 9-11 Examples of sperm lodged wholly within the zona pellucida of freshly ovulated ova. No vesiculated acrosomal elements remain about the sperm head. All figures $\times 22,000$.

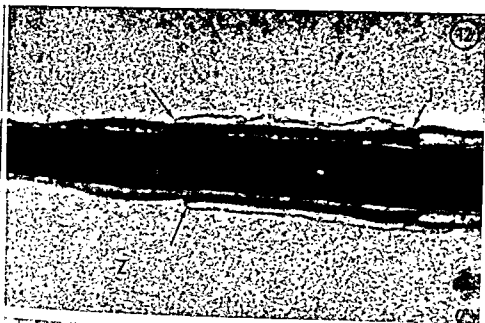


PLATE 7

EXPLANATION OF FIGURES

- 12 Central portion of a sperm head lying within the zona of a freshly ovulated ovum. Arrows denote the point of fusion between the outer membrane of the acrosome cap and the overlying plasma membrane which extends caudally to cover the posterior head and tail surface; J. indicates the posterior limit of the acrosome cap. $\times 70,000$.
- 13 Section of a fertilized ovum recovered approximately six hours after ovulation. This shows the typical form of the penetration curve (p.c.) formed by sperm in traversing the zona pellucida (Z). A sperm head is seen in the peri-vitelline space at the right of the picture, and a remnant of a corona cell process (p) is still present within the substance of the zona. $\times 11,800$.

ZS

14

15



Z

16

V

PLATE 8

EXPLANATION OF FIGURES

- 14 Section of sperm tail below the zona surface (ZS). At this stage the plasma membrane remains intact over the posterior head and the tail region of the sperm. $\times 56,000$.
- 15 Sperm head lodged within the zona pellucida of a fertilized ovum recovered approximately seven hours after ovulation. The fissure which precedes the head, is seen commonly in eggs taken at this stage, and is thought to be responsible for the appearance of a projection (see inset) which sometimes extends from the rostral border of such sperm viewed with the phase microscope. $\times 25,500$.
- 16 Sperm head lying in the peri-vitelline space of a fertilized egg. Note that the space of the perforatorium is occupied by electron-dense material. The posterior equatorial segment of the acrosome also remains intact in peri-vitelline sperm. $\times 25,500$.

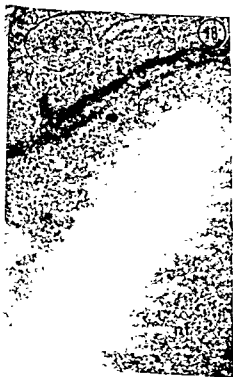
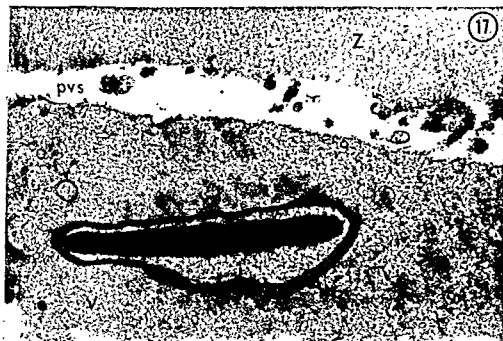


PLATE 9

EXPLANATION OF FIGURES

- 17 Section of the fertilizing sperm head in an ovum recovered about two hours after ovulation. The swelling envelope around the dense nucleus may be nuclear membrane. $\times 23,500$.
- 18-19 Higher magnification of sections of a fertilizing sperm head. Note the appearance of areas of rarefaction within the dense nucleus (arrow), and fibrils (NF), emanating from the surface of the dense nuclear chromatin. Figure 18, $\times 64,000$; figure 19, $\times 69,000$.

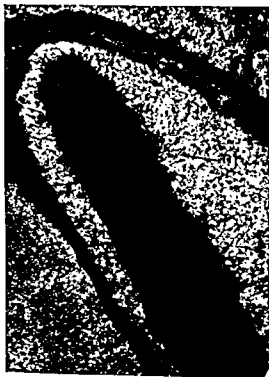
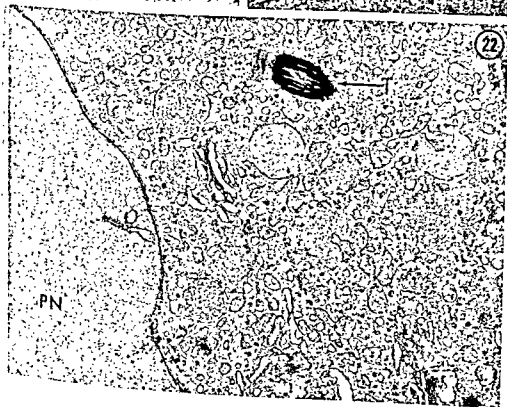


PLATE 10

EXPLANATION OF FIGURES

- 20 Tail of the fertilizing sperm (T) entering the vitellus. Note the absence of a limiting membrane around the tail filaments within the ooplasm (cf. fig. 14). It is uncertain whether the membranes within the peri-vitelline space derive from the vitelline surface, from the limiting membrane of the sperm, or from both. $\times 51,000$.
- 21 Appearance of the male pronucleus in an egg recovered about six hours after ovulation. Note the homogeneous nucleoplasm, and the prominent nucleoli, which are not membrane bound. At this stage the pronuclei become surrounded by many newly formed Golgi vesicles and lamellae. $\times 8,000$.
- 22 Higher power of part of a male pronucleus (PN); the sperm tail (T) often lies in close apposition to the pronucleus at this stage. $\times 25,000$.



Autoradiographic Investigation of Calvarial Growth in the Rat¹

VINCENT DE ANGELIS*

Department of Orthodontics, Harvard University School of
Dental Medicine, Boston, Massachusetts

ABSTRACT Results of autoradiographic investigations utilizing tritiated proline reveal an intricate mechanism of rat calvarial growth and reshaping from age two days through 75 days. Generalized intramembranous bone growth dominates the growth process from two through eight days; however, this simple bony enlargement is terminated early. At eight days a differential apposition-resorption process begins dorsally in the calvarium and progresses rostrally within a ten day period. This process includes differential apposition on the ectocranial and endocranial periosteal surfaces accompanied by a differential apposition-resorption pattern on the endosteal surfaces. The wave-like process begins in the occipital bone and progresses ventrally to the frontal bone resulting in a flattening of the bony components. At 35 days bone accretion is again generalized on most calvarial surface. However, at 40 days another change in the growth process evolves on the occipital and frontal bones. These bones are now seemingly displaced in a superior direction as bone apposition continues on their superior surfaces, namely, the ectocranial periosteal and endocranial endosteal surfaces and resorption progresses on the two inferior surfaces. The magnitude and duration of the process described in this paper is sufficient to account for calvarial flattening in the absence of bony spatial reorientation due to bending at sutures. The findings described here when compared to proposed *in vitro* studies can help put the importance of the so-called "functional matrix" related to bone growth into its proper perspective.

The specific sites of bone apposition and resorption in the growing rat calvarium are not been clearly defined. The role played by the areas of apposition and resorption in the general growth and reshaping of the calvarium is subject to controversy (Baer, '54; Brash, '34; Brodie, '11; Craven, '56; Giblin and Alley, '42, '44; Massler and Schour, '51; Moss, '54; Young, '62).

Moreover, assessment of the influence of environmental factors such as soft tissue function upon bone growth remains a difficult task. Genetic control over the primordia of bones is generally accepted. However, the point at which environment assumes primary importance, if there be such a point, remains unknown. Function, according to its latest proponent, Moss (Moss and Baer, '56), is of prime importance in bone growth. Consequently, enlargement of the brain, periosteal sliding and other soft tissue systems are considered by him to be determinants of growth of the neurocranium. This hypothesis may well be true; however, definite concepts cannot be postulated without knowledge of

the precise mechanism of bony changes and without experimental evidence that a specific pattern of bone growth would be altered in the absence of soft tissue or functional requirements.

The autoradiography technique (Leblond et al., '50) with tritiated proline was utilized in the experiments described in this paper in order to assess small increments of growth on decalcified sections, a task beyond the resolution afforded by previous Alizarin Red S studies (Cameron, '30; Jarabak, '51; Moore, '49; Schour, '36, '41; Massler and Schour, '51; Baer, '54). The experiments were designed to observe the growth process from birth to seventy-five days in the male albino rat calvarium. In order to prepare for the major study, two preliminary investigations were performed.

The first preliminary experiment was designed to determine the precise pattern and the magnitude of differential apposi-

¹ This project was supported in part by Research grant D-1592 from the National Institute of Dental Research and Training grant 5 T01 DE 00113.

* A post-doctoral Fellow at Forsyth Dental Center and Harvard University School of Dental Medicine and supported by the National Institute of Dental Research at the time this work was done.

TABLE 3

Growth of male albino rat calvarium. Experimental design. Major investigation

Number of animals at each age	Age in days at first injection. ¹ These animals were injected a second time after two days and sacrificed six hours later	Age in days at first injection. ¹ These animals were injected a second time after four days and sacrificed six hours later	Age in days at first injection. ¹ These animals were injected a second time after six days and sacrificed six hours later
2	2, 4, 6, 8, 10, 12, 14, 16, 18, 20, 22, 24, 26, 28, 30, 32, 34, 36, 38, 40, 42, 44	46, 50, 54	58, 64, 70

¹ One microcurie of tritiated proline per gram of body weight.

four days of age and sacrificed six hours later. Two four-day-olds were injected with comparable amounts of proline and again injected at six days of age; then sacrificed six hours later. This injection scheme was continued through animals of 46 days of age. Two 46-day-old animals were injected and again injected at 50 days, then sacrificed six hours later. This four-day injection interval was now used for animals up to 58 days and a six-day period up to 75 days (table 3).

After sacrifice with ether, the tibia and calvarium were removed and fixed in 5% formal-saline, decalcified with formic-acid-sodium-citrate, embedded in paraffin and cut sagittally at 6 μ . The sections were dipped in Kodak NTB 2 emulsion and exposed for 11 to 14 day intervals. They were then processed and post-stained with hematoxylin and eosin.

RESULTS

Sutures. From two through 20 days of age the sutural connective tissue at the parietal-frontal, anterior lambdoidal and posterior lambdoidal sutures diminished in width as generalized intramembranous growth of adjacent bones continued through 18 days (Gans and Sarnat, '51; Pritchard, Scott and Girgis, '56).

At 20 days the sutural growth became more appositional in nature as sheets of osteoblasts lined the bone edge on either side of the suture. The three sutures mentioned remained active through the 75-day experimental period in contrast to the earlier closure if these sutures proposed by Mässler and Schour, '51 (figs. 2, 3).

Endocranial and endocranial surfaces (fig. 1). Apposition on all surfaces of the

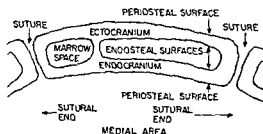


Fig. 1 Diagrammatic representation of calvarial bone with surfaces to be discussed labeled.

frontal, parietal, interparietal and occipital bones through eight days was observed, with no differential pattern exhibited during this period (figs. 4, 5).

At eight days, however, a differential pattern of apposition became evident. The ectocranial periosteal surface of the interparietal bone exhibited marked and rapid growth at the suture ends with little or no change at the medial area of this surface (figs. 6, 7). The endosteal side of this surface, however, was an active site of apposition. The endocranial periosteal surface exhibited more growth at the medial and less at the suture borders. The endosteal side of this surface was an active resorption site. At no time was resorption observed on the endocranial periosteal surface. While the differential pattern continued on the interparietal bone, the generalized apposition on the parietal and frontal bone continued (fig. 8).

At 12 days the parietal bone began the differential growth pattern described for the interparietal bone while the frontal bone still exhibited a generalized apposition and remodelling.

TABLE 1
Preliminary experiment 1
Experimental design

Number of animals injected ¹ in each group	Age of animal when given first injection	Age of animal when given second injection and sacrificed six hours later	Age of animal when given second injection and sacrificed seven days later
2	21	28	
2	28	35	
2	35	42	
2	42	49	
2	21		28
2	28		35

¹One microcurie of tritiated proline per gram of bodyweight.

tion and resorption in the neurocranium as well as the duration of growth at the neurocranial sutures.

The second preliminary experiment was designed to determine an injection regimen leading to the major study of calvarial growth from birth through 75 days. Its purpose was to assess the optimal interval between injections of ³H-proline in representative age groups during the experimental period so that two injections would be far enough apart for good definition and at the same time avoid the loss of the first injection due to remodelling.

METHODS AND MATERIALS

Preliminary experiments

Preliminary experiment 1. Twelve Holtzman male albino rats ranging in age from 21 through 49 days were studied. Two 21-day-old animals were injected with one microcurie of ³H-proline per gram of body weight. These two animals were again injected at 28 days and sacrificed six hours later. This same scheme was followed over the next two seven-day periods. Animals with two injections seven days apart were sacrificed after 14 days and also studied (table 1).

After sacrifice with ether, the tibia and calvarium were removed, fixed in 5% formal-saline, decalcified with formic acid sodium citrate, embedded in paraffin and cut sagittally at 6 μ . These sections were dipped in Kodak NTB 2 emulsion and exposed for five through 14-day intervals.

They were then processed and post-stained with hematoxylin and eosin.

Preliminary experiment 2. Sixteen male albino rats of the Holtzman strain were studied. Four animals were injected with 1 μ Ci of ³H-proline per gram of body weight at 2, 21, 35 and 55 days of age. Two of each group were injected a second time two days later and sacrificed after six hours. The other two in each group were injected once more after four days and sacrificed six hours later (table 2).

The tibia and calvarium were removed from each and treated as in preliminary experiment 1.

RESULTS

The results of the preliminary experiments revealed that a two-day interval between injections was most suitable in animals up to 46 days, four-day intervals from 46 through 58 days, and six-day intervals from 58 through 75 days. The magnitude of the major remodeling process, based on findings of preliminary experiment 1, will be discussed later. The major experiment was then designed, utilizing knowledge from these two pilot studies, to observe the growth process from birth through 75 days.

METHODS AND MATERIALS

Major investigation

Fifty-six Holtzman male albino rats ranging in age from two to 75 days were studied. Following the findings of preliminary experiment 2, two 2-day-old animals were injected intraperitoneally with 1 μ Ci of tritiated-proline per gram of body weight. These animals were injected again

TABLE 2
Preliminary experiment 2
Experimental design

Number of animals injected ¹ in each group	Age in days when first injected. These animals were injected a second time two days later then sacrificed after six hours	Age in days when first injected. These animals were injected a second time four days later then sacrificed after six hours
2	2, 21, 35, 55	2, 21, 35, 55

¹One microcurie of tritiated proline per gram of bodyweight.

larly a reaction to environmental stimuli, such as soft tissue function. Only by organ culture means can the validity of such a concept be tested. While it is true that work by Fell and Robinson ('29) has shown a strong genetic effect in growth of long bones, the changes we have described above in the cranial bones are so much more intricate and time dependent, that these bones lend themselves ideally to further investigations of this kind.

ACKNOWLEDGMENTS

The author is indebted to Drs. James T. King, Coenraad F. A. Moorrees and Miles Crenshaw for their guidance in this study and to Mr. John D. Heeley for his technical assistance.

LITERATURE CITED

- Fell, M. J. 1954 Patterns of growth of the skull as revealed by vital staining. *Human Biol.*, 26: 80-126.
- Gans, J. C. 1934 Some problems in growth and developmental mechanics of bone. *Edinburgh Med. J.*, n.s. 4th, 41: 305-387.
- Robinson, A. G. 1941 On the growth pattern of the human head from the third month of life to the eighth year of life. *Am. J. Anat.*, 68: 209-262.
- Wamer, G. R. 1930 The staining of calcium. *J. Path. and Bact.*, 33: 929-915.
- Wamer, A. H. 1936 Growth in width of the head of the macaca rhesus monkey as revealed by vital staining. *Am. J. Ortho.*, 42: 341-362.
- Wolow, D. H. 1963 Principles of bone remodeling. Courtesy of Charles C Thomas, Springfield, Illinois.
- Fell, H. B., and R. Robinson 1929 The growth, development and phosphatase activity of embryonic avian femora and limb buds cultivated in vitro. *Bioch. J.*, 23: 767-784.
- Gans, B. J., and B. G. Sarnat 1951 Sutural facial growth of the macaque monkey. *Am. J. Ortho.*, 37: 827-841.
- Giblin, N., and A. Alley 1942 A method of determining bone growth in the skull. *Anat. Rec.*, 83: 381-387.
- 1944 Studies in skull growth: coronal suture fixation. *Anat. Rec.*, 88: 143-153.
- Jarabak, J. R. 1951 Alizarin as an indicator of bone growth. Abstract. *J. Dent. Res.*, 30: 512.
- Leblond, C. P., et al. 1950 Radioautographic visualization of bone formation in the rat. *Am. J. Anat.*, 86: 289-342.
- Massler, M., and I. Schour 1951 Growth pattern of the cranial vault in the albino rat as measured by vital staining with alizarin red. *Anat. Rec.*, 110: 83-101.
- Moore, A. W. 1949 Head growth of the Macaque monkey as revealed by vital staining, embedding, and undecalcified sectioning. *Am. J. Ortho.*, 35: 654-671.
- Moss, M. L. 1954 Growth of the calvaria in the rat. *Am. J. Anat.*, 94: 333-362.
- Moss, M. L., and M. J. Baer 1956 Differential growth of the rat skull. *Growth.*, 20: 107-120.
- Pritchard, J. J., J. H. Scott and F. G. Girgis 1956 The structure and development of cranial and facial sutures. *J. Anat.*, 90: 73-86.
- Schour, I. 1936 Measurement of bone growth by alizarin injections. *Proc. Soc. Exper. Biol. and Med.*, 34: 140-141.
- 1941 Vital staining of growing bones and teeth with alizarin red S. *J. Dent. Res.*, 20: 411-418.
- Young, R. W. 1962 Autoradiography studies on postnatal growth of the skull in young rats injected with tritiated glycine. *Anat. Rec.*, 143: 1-13.

At 14 days the same pattern of change occurred in the frontal bone. As differential apposition continued on the periosteal surfaces the marrow spaces exhibited the same interesting pattern of change. The ectocranial endosteal surface was lined with osteoblasts laying down bone while the endocranial endosteal surface was actively resorbing bone as evidence by many Howship's lacunae filled with osteoclasts, and no apposition occurred at this surface. This intricate pattern continued on the occipital, interparietal, parietal and frontal bones until 35 days.

At 35 days, the differential pattern of apposition and resorption was lost and a more generalized system of growth was exhibited on all periosteal surfaces (fig. 9).

At approximately 40 days, the frontal and occipital bones showed a different pattern than that previously described. Apposition now was evident on the entire ectocranial periosteal surface and the entire endocranial endosteal surface while resorption occurred on the ectocranial endosteal surface and endocranial periosteal surfaces (fig. 10).

DISCUSSION

Growth of the neurocranium up to eight days was shown to be a result of generalized intramembranous bone growth which occurred within a fibrous connective tissue capsule and progresses from each bone center radially until the presumptive sutures are compressed into the adult form (Pritchard, Scott and Girgis, '56).

However, after eight days a differential pattern of apposition and resorption began within this capsule. This pattern started dorsally in the calvarium and progressed rostrally within a few days. The changes described led to a flattening of the occipital, interparietal, parietal and frontal bones. These bones flattened individually until 35 days when they apparently reached their final configuration and thereafter grew in a more generalized, uniform manner.

At approximately 40 days another change in pattern was noticed at the occipital and frontal bones. These bones were now displaced in a superior direction similar to the process in long bones called "drift" by Enlow ('63) (fig. 11).

In view of this finding, Enlow's concept of alteration of environment in long bones may apply to membranous bones as well. Enlow states that during lengthening of long bone by epiphyseal growth, changes along the shaft are induced by the altered environment as muscle attachments change and periosteal sliding occurs.

In light of my investigations, the flat bone counterpart of the epiphysis may be the suture and the outer and inner tables of the calvarial bones can be compared to the shaft of long bone. Thereby, the sutures, acting as pacemakers like the epiphyses, may induce concurrently adaptive growth changes along the length of membranous bones between them as function and environment are altered.

The magnitude and importance of the differential pattern of apposition and resorption described was made clear by preliminary experiment 1. In this experiment it was established that a ³H-proline injection given 14 days prior to sacrifice was now located at the resorptive endocranial endosteal surface of the parietal bones. This surface therefore replaced itself in a 14-day period from 21 days through 35 days (fig. 12). An apposition-resorption pattern of this magnitude can easily lead to a change of shape of this bone, and the concurrent process in the other components of the calvarium could certainly result in the flattening of the calvarium with growth. This flattening process was also described by Baer ('54) but it was explained by the spatial reorientation of each bone by a bending at the sutures. The conclusions obtained from my own investigations indicate that very little reorientation is needed.

The results of the foregoing experiments indicate the specific sites of alteration of growth in the calvarial bones at different stages of development. The next question is to consider the various influences which control these alterations in growth, environmental or genetic. While there is no doubt that both these factors play a role, it is our intention to undertake organ culture experiments to ascertain if similar changes are brought about in the absence, as far as possible, of usual environmental conditions. Moss's theory, for example, is that bone growth and remodeling is pri-

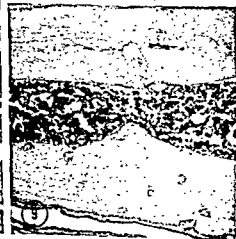
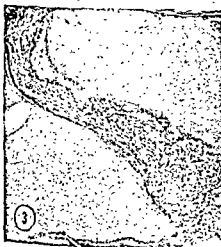
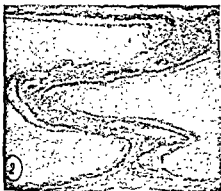


PLATE 1

EXPLANATION OF FIGURES

- 2 Parietal-frontal suture. Animal injected at 70 days and 75 days, then sacrificed six hours later. Note continued growth of both bones at the suture. ($\times 110$, H & E).
- 3 Anterior lambdoidal suture. Animal injected at same intervals as in figure 2. Growth takes place at this suture also. ($\times 110$, H & E).
- 4 Parietal Bone — generalized intramembranous growth at age six days in control animals. Osteoblasts evident on all surfaces. Ectocranial surface (a). Endocranial surface (b). All other photomicrographs will have same orientation. ($\times 110$, H & E).
- 5 Same age as figure 4. Autoradiograph shows generalized labeling of bone surfaces ($\times 110$, H & E).
- 6 Interparietal bone — medial area. Animal injected at eight days and ten days, then sacrificed six hours later. Note apposition on ectocranial endosteal surface and endocranial periosteal surface. The ectocranial periosteal surface appears quiescent while the endocranial endosteal surface is rapidly resorbing as shown in figure 12. ($\times 110$, H & E).
- 7 Lateral portion of same bone as in figure 6. The periosteal ectocranial surface at this site (arrow) is actively depositing bone in contrast to the medial area distant from the suture. ($\times 200$, H & E).
- 8 Parietal bone — medial area, same age period as in figures 6 and 7. Bone apposition on both periosteal surfaces with no apposition at endosteal side. No differential pattern is evident here. ($\times 110$, H & E).
- 9 Frontal bone — medial area. Animal injected at age 34 days and 36 days, then sacrificed six hours later. General periosteal apposition has returned. ($\times 110$, H & E).

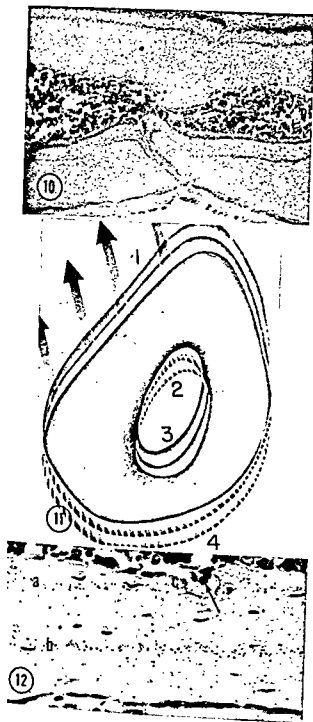
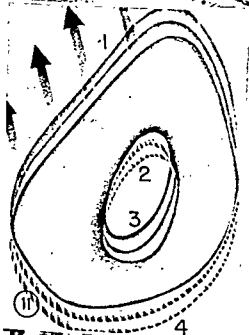
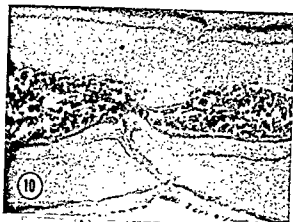


PLATE 2

EXPLANATION OF FIGURES

- 10 Frontal bone — medial area. Animal injected at ages 42 days and 44 days, then sacrificed six hours later.
- 11 Cross section of long bone from Enlow. Drift phenomenon similar to that process described in calvarial bone of figure 10.
- 12 Parietal bone — medial area. Animal injected at 21 days and 28 days, then sacrificed at 35 days. 21 day injection (a), 28 day injection (b), endocranial endosteal resorbing surface (c). Osteoclast at label given 14 days prior to sacrifice (arrow). This bone surface has replaced itself in a 14 day period. ($\times 440$, H & E).





1e Fine Structure of Uterine Smooth Muscle of the 1t Uterus at Various Time Intervals Following :Single Injection of Estrogen ¹

WALTER J. BO, D. LOUISE ODOR AND MARTHA ROTHROCK
*Department of Anatomy, Bowman Gray School of Medicine,
Wake Forest University, Winston-Salem, North Carolina*

ABSTRACT The fine structure of smooth muscle cells of the rat uterus was studied at 6, 12, 24, 48, 72 and 96 hours after a single subcutaneous injection of estradiol dipropionate (10 μ g). The control rats were ovariectomized, but did not receive hormone treatment. Changes in the ultrastructure of the muscle cells occurred soon after estrogen stimulation. An increase in the number of ribosomes on the outer nuclear membrane and evagination of the membrane into the surrounding cytoplasm was noted at six hours. The amount and dilatation of the granular endoplasmic reticulum (GER) increased gradually from 6 to 96 hours. At 24 and 48 hours the mitochondria appeared to increase in number and at later time intervals they increased in size. The Golgi complex was more prominent at 72 and 96 hours than at the earlier time intervals. An increase in free ribosomes was observed at 6 and 12 hours, but a marked accumulation of them occurred at 24 hours and continued to 96 hours. The glycogen granules were very pronounced at 24 and 48 hours with a reduction at 72 and 96 hours. Many pinocytotic vesicles and dense bodies were present in the controls and at 6 and 12 hours. A decrease in number occurred in both at the later time intervals. Organelles accumulated at the nuclear poles beginning at 24 hours and extending to 96 hours. The observations made provide additional information on the fine structure of uterine smooth muscle cells following estrogen stimulation and support previous biochemical studies on glycogen concentration and RNA synthesis in the rat uterus.

Estrogen increases the glycogen concentration of the rat uterus (Boettiger, '46). The polysaccharide is localized primarily in smooth muscle cells (Bo and Atkinson, '62) and appears shortly after initiation of hormone treatment (Walaas, '52; Bitman, '54; Mench and Wrenn, '65; Bo, Maraspin and Smith, '67). Similarly, glycogen synthetase activity increases in the myometrium of the rat uterus soon after estrogen stimulation (Bo and Smith, '64; Bo, Maraspin and Smith, '67). Shortly after estrogen treatment there is also an increase in the amount of phospholipids, RNA synthesis and protein synthesis in the rat uterus (Aizawa and Mueller, '61; Mueller, Ijzerman and Jervell, '58; Noteboom and Gorski, '63).

The literature contains a few reports which attempt to correlate the fine structure of uterine smooth muscle cells with the chemical changes that occur following estrogen stimulation. Laguens ('64) reported an increase in the number and size of the nucleoli at 6, 12, 24 hours after a single injection of estrogen (10 μ g). At 48

and 72 hours the large nucleoli lay peripherally and in the cytoplasm some ribosomes, rough endoplasmic reticulum (RER) and slightly enlarged mitochondria were present. Ross and Klebanoff ('67) observed that muscle cells in the diestrous rat uterus were elongated, spindle-shaped, contained ellipsoid nuclei and cytoplasmic organelles present were located adjacent to the nucleus. In the cytoplasm the RER had only a few scattered ribosomes on its membranes, Golgi complexes were well developed, scattered free ribosomes appeared and numerous vesicles occurred at the surfaces of the cells. At estrus, Ross and Klebanoff ('67) noticed a marked increase in the amount of RER and Golgi complexes; the surface of the smooth muscle cells had numerous outpocketings and infoldings. Following estrogen stimulation for three consecutive days the fine structure of uterine smooth muscle was similar to the estrous condition (Ross and Klebanoff, '67).

¹ This investigation was supported by USPHS grants AM-08029-04 and HD-00606. The authors are grateful to Dr. Norman Sulkin for making the electron microscope available.

In order to better understand the progressive ultrastructural changes that occur in the smooth muscle cells of the rat uterus following estrogen stimulation, this investigation was designed to study the cells at different time intervals following a single subcutaneous injection of the hormone. The study will attempt to correlate, where possible, the changes with some of the chemical alterations known to occur.

MATERIAL AND METHODS

Twenty-four adult virgin female rats (weighing 200 ± 10 gm) of the Wistar strain (Charles River) were used. All the animals were bilaterally ovariectomized and maintained four to a cage with free access to food. Ten days following ovariectomy four control animals were killed; the remaining rats received a single subcutaneous injection of $10 \mu\text{g}$ estradiol dipropionate* in 0.1 ml cottonseed oil. The animals (3 or 4 at each time interval) were killed with ether vapor at 6, 12, 24, 48, 72 and 96 hours after administering the hormone. The uterus was quickly removed, placed in a cold solution of 2% osmium tetroxide buffered with veronal acetate (pH 7.4) and cut in small pieces. The tissue was fixed for one hour, dehydrated through a graded series of alcohols and embedded in an epoxy resin, Epon 812. The sections were cut with a Porter-Blum ultramicrotome and stained for 30 minutes with lead citrate (Reynolds, '63).

RESULTS

Ovariectomized animals. In many areas a relatively large amount of intracellular connective tissue was present and the smooth muscle cells were small and spindle-shaped. Only a few elongated and centrally located nuclei appeared in the smooth muscle cells. In a few areas the outer nuclear membrane formed small evaginations into the cytoplasm and only a few ribosomes were attached to the membranes. The myofilaments were parallel to the long axis of the cell, but absent in areas containing organelles. The plasma membrane was fairly free of evaginations throughout its extent.

The few mitochondria present lay primarily close to the periphery of the cell although some of them were present at the

nuclear poles. The shape of mitochondria varied, being either elongated, round, or short rod-like structures with well developed lamellar cristae. Only a very small amount of granular endoplasmic reticulum (GER) was noted along the sides of the nucleus and at the nuclear poles. Well defined Golgi complexes appeared lateral to the nucleus. Small vesicles made up the complex with only a few cisternal elements. Numerous pinocytotic vesicles were attached to or near the plasma membrane. Several multivesicular bodies lay beside the nucleus. A few ribosomes were scattered around the nucleus and along the plasma membrane. The rare glycogen granules appeared close to the plasma membrane or at the nuclear poles. Dense bodies present had a variable morphology. Some of them contained linear, closely packed structures, while others had small rounded dense structures of various sizes surrounded by a light background matrix (figs. 1, 2).

Six hours following estrogen treatment. Several changes in the structure of uterine smooth muscle cells manifested themselves at this time interval. The nucleoli appeared to be closer to the nuclear envelope than in the control rats. More ribosomes were located on the outer nuclear membrane than in the controls; numerous evaginations of the membrane projected into the cytoplasm. These evaginations became especially prominent at the nuclear poles. In addition to being present along the plasma membrane mitochondria and GER occurred at the nuclear poles. Mitochondria varied in shape as in the control group of animals. The amount of GER increased and some of it was dilated, forming branching cisternae. The Golgi complex, located at the side of the nucleus and at the nuclear poles, contained more vesicular than cisternal elements. More free ribosomes and glycogen granules located at the sides of the nucleus and at the nuclear poles existed than in the ovariectomized rats. The dense bodies varied in morphology; the most common form had an enclosing membrane with a small space between the membrane and the contents. The light matrix contained granules of variable size. A few of the

* The estradiol dipropionate was supplied through the courtesy of Ciba Pharmaceutical Products, Summit, New Jersey.

nse bodies had clear vacuoles resembling those in lipofuscin pigment.

Twelve hours after estrogen treatment. With a few exceptions the fine structure of the smooth muscle cells was similar to that at six hours. The cells appeared larger, the plasma membrane protruded in some places into the connective tissue and fewer evaginations of the outer nuclear membrane were present. Glycogen granules, ribosomes and GER increased slightly in amount from that observed at six hours.

Twenty-four hours after estrogen treatment. The muscle cells were more elongated than observed previously due to the distension of the cytoplasm from the nuclear poles. Adjacent muscle cells interdigitated frequently at this time interval. Two nucleoli occurred in a few cells. Evaginations of the outer nuclear membrane were not as pronounced as at 12 and 6 hours. At this time interval the greatest change consisted of the accumulation of organelles at the nuclear poles. The GER increased, its cisternae enlarged, the mitochondria appeared to have increased in number, but the Golgi complex remained approximately the same size as previously. A marked increase in the number of free ribosomes and glycogen granules located both at the nuclear poles and along the cytoplasmic extensions was evident. There were fewer pinocytotic vesicles than noted earlier (fig. 3).

Forty-eight hours after estrogen stimulation. The cells had increased in size and there was more interdigitation of adjacent muscle cells occurred than at the preceding time interval. There were indentations of the nuclear envelope, but these may have resulted from contraction of the muscle cells. The outer nuclear membrane had only a few ribosomes with only a few areas showing evaginations of the membrane into the surrounding cytoplasm. Some of the nucleoli lay closer to the nuclear envelope than in the previous groups. The amount of GER greatly increased and appeared primarily at the nuclear poles and in the cytoplasmic extensions of the cells. In some areas the GER consisted of large tubular-like structures. The Golgi complex lay beside and at the poles of the nucleus; its size did not appear to vary from the preceding time intervals. Although mitochondria

were located primarily at the nuclear poles some occurred next to the nucleus and in the cytoplasmic extensions. Their number appeared to have increased at this time interval.

A marked increase in glycogen concentration occurred at this time interval. Its component particles were located close to the plasma membrane, at the nuclear poles and in the cytoplasmic extensions. Also free ribosomes, located primarily at the nuclear poles and in the cytoplasmic extensions, increased greatly. Very few pinocytotic vesicles were seen along the plasma membrane (figs. 4-6).

Seventy-two hours after estrogen stimulation. At this time interval GER, mitochondria and Golgi complexes became concentrated at the nuclear poles and in the cytoplasmic extensions of the muscle cells. There were fewer glycogen granules than at 48 hours, and they appeared primarily along the plasma membrane (fig. 7).

Ninety-six hours after estrogen stimulation. The structure of the muscle cells was similar to that seen at 72 hours. However, the GER appeared to have increased in amount and often in many areas it was dilated. In some of the cytoplasmic extensions mitochondria, GER, ribosomes and scattered glycogen granules occupied the entire part of the cell (fig. 8).

DISCUSSION

The results demonstrate that the fine structure of the smooth muscle cells of the rat uterus undergo changes soon after estrogen stimulation. At six hours, ribosomes were abundant on the outer nuclear membrane which was evaginated into the surrounding cytoplasm. Although some ribosomes appeared on the outer nuclear membrane and some evagination occurred at later time intervals they were not as pronounced as at six hours. A gradual increase in amount and dilatation of the GER occurred from 6-96 hours. Mitochondria appeared to increase in amount at 24 and 48 hours and at the later time intervals they enlarged. The Golgi complex was seen throughout the periods studied, but seemed to be more prominent at 72 and 96 hours at the nuclear poles. An increase in free ribosomes appeared at 6 and 12 hours, but a marked accumulation of them occurred

at 24 hours and continued to 96 hours. The glycogen granules were very pronounced at 24 and 48 hours followed by a reduction at 72 and 96 hours. Many pinocytotic vesicles and dense bodies were present in the controls and at 6 and 12 hours. A decrease in number of vesicles and bodies occurred at the later time intervals.

The findings of the present study at time intervals (48-96 hours) are similar to the observations made by Ross and Klebanoff ('67) in the uteri of rats during estrus and in ovariectomized rats following estrogen treatment for three days. The glycogen concentration was not discussed by the above investigators. The present data differ from those of Laguens ('64) who did not detect any cytoplasmic changes until 48 hours after a single injection of estrogen (10 μ g); free ribosomes were increased in number, some rough ER appeared and the mitochondria were enlarged. No comment was made on the glycogen concentration at the different time intervals. The observations obtained in the present study on the glycogen concentration at different time intervals following estrogen stimulation are similar to the results of biochemical studies reported previously (Bo, Maraspin and Smith, '67).

Noteboom and Gorski ('63) in a biochemical study did not detect any significant increase in protein synthesis in the nuclear, mitochondrial and ribosomal fractions of uterine cells at two hours after estrogen treatment; four hours after hormone stimulation a marked increase was noted in all the above fractions. It has been suggested by Ui and Mueller ('63) that estrogen stimulates the synthesis of certain proteins in the uterus which are necessary for the synthesis of new RNA and that the new RNA supplies the protein synthesizing machinery the essential information necessary for effecting the early anabolic effects of the hormone. The cellular RNA is primarily ribosomal. Moore and Hamilton ('64) reported that ribosomes were more abundant in the cytoplasm of the cells of the entire uterus following estrogen stimulation than in those deprived of the hormone; 4 to 24 hours after estrogen treatment newly formed ribosomes appeared in the cytoplasm. The increase in

the amount of free ribosomes and GER following estrogen stimulation which was noted in this investigation supports the biochemical results obtained by Moore and Hamilton ('64).

Hamilton ('63) suggested that estrogen stimulates intranuclear reactions resulting in the production or regulation of messenger RNA which precedes the acceleration of protein synthesis. If the synthesis of new RNA is blocked by actinomycin D, the early acceleration of phospholipid and protein synthesis due to estrogen do not occur (Ui and Mueller, '63). Whether the accumulation of glycogen in uterine smooth muscle following estrogen stimulation is dependent on newly synthesized RNA has not been established, but the present ultrastructural study provides suggestive evidence of a linkage of the two phenomena.

The dense bodies were more evident in the smooth muscle cells of the controls and at 6 and 12 hours than at the later time intervals following estrogen stimulation. Whether the dense bodies were lipofuscin pigments or lysosomes was not established. The significance of dense bodies in smooth muscle cells has not been determined. Pigment granules have been observed to accumulate in smooth muscle cells of vitamin E deficient intact rats (Mason and Emmel, '45). Kaunitz, Slanetz and Atkinson ('49) reported that in ovariectomized rats pigmentation did not develop to the degree characteristic of vitamin E deficiency, but following prolonged estrogen treatment during the course of avitaminosis pigmentation developed which was similar to that seen in intact vitamin E deficient rats. They may accumulate in the cell when the normal metabolic activity of the cell is altered. This has been shown to occur in skeletal muscle (Odor, Patel and Pearce, '67).

An increase in the number of mitochondria was noted at 24 hours and 48 hours after estrogen treatment and at 72 and 96 hours the organelle appeared to increase in size. The changes seemed to occur at the time of greatest metabolic activity of the smooth muscle cells. Rouiller ('60) reported that in skeletal and heart muscles there is a relationship between tissue activity and the number of mitochondria

in active striated muscle (red) the mitochondria are numerous and in white striated muscles there are fewer mitochondria. Whether or not the enlargement of mitochondria observed at 72-96 hours was due to change in metabolic activity was not determined. Swelling of mitochondria occurs in various physiological and pathological states (Rouiller, '60).

LITERATURE CITED

- Lawson, Y., and G. C. Mueller 1961 The effect in vivo and in vitro of estrogens on lipid synthesis in the rat uterus. *J. Biol. Chem.*, 236: 381-386.
- Lawson, J., H. C. Cecil, M. L. Mench and T. R. Wrenn 1965 Kinetics of in vivo glycogen synthesis in the oestrogen-stimulated rat uterus. *Endocrinology*, 76: 63-69.
- Lawson, W. J., and W. B. Atkinson 1952 Histological studies on glycogen deposition in the uterus of the rat. I. In intact cyclic animals and in castrates treated with ovarian hormones. *Anat. Rec.*, 113: 91-100.
- Lawson, W. J., L. Maraspin and M. S. Smith 1967 Glycogen synthetase activity in the rat uterus. *J. Endocrinology*, 38: 33-37.
- Lawson, W. J., and M. Smith 1964 Further histochemical observations on uridine diphosphate glucose glycogen transferase activity of the uterus. *J. Histochem. Cytochem.*, 12: 393-394.
- Loettiger, E. G. 1946 Changes in the glycogen and water content of the rat uterus. *J. Cell. and Comp. Physiol.*, 27: 9-14.
- Hamilton, T. H. 1963 Isotopic studies on estrogen-induced accelerations on ribonucleic acid and protein synthesis. *Proc. Nat. Acad. Sci. U.S.A.*, 49: 373-379.
- Kaunitz, H., C. A. Slanetz and W. B. Atkinson 1949 Estrogen response and pigmentation of the uterus in vitamin E-deficient rat. *Proc. Soc. Exp. Biol. Med.*, 70: 302-304.
- Laguens, R. 1964 The effect of estrogen upon the fine structure of the uterine smooth muscle cell of the rat. *J. Ultrastructure Res.*, 10: 578-584.
- Mason, K. E., and A. F. Emmel 1945 Vitamin E and muscle pigment in the rat. *Anat. Rec.*, 92: 33-50.
- Moore, R. J., and T. H. Hamilton 1964 Estrogen-induced formation of uterine ribosomes. *Proc. Nat. Acad. Sci. U.S.A.*, 52: 439-446.
- Mueller, G. C., A. M. Herranen and K. F. Jervell 1958 Studies on the mechanism of action of estrogens. *Recent Progr. in Hormone Research*, 14: 95-139.
- Noteboom, W. D., and J. Gorski 1963 An early effect of estrogen on protein synthesis. *Proc. Nat. Acad. Sci. U.S.A.*, 50: 250-255.
- Odor, D. L., A. N. Patel and L. A. Pearce 1967 Familial hypokalemic periodic paralysis with permanent myopathy. A clinical and ultrastructural study. *J. Neuropath. and Exp. Neurology*, 26: 98-114.
- Reynolds, E. S. 1963 The use of lead citrate at high pH as an electron-opaque stain in electron microscopy. *J. Cell Biol.*, 17: 208-212.
- Ross, R., and S. J. Klebanoff 1967 Fine structural changes in uterine smooth muscle and fibroblasts in response to estrogen. *J. Cell Biol.*, 32: 155-167.
- Rouiller, C. H. 1960 Physiological and pathological changes in mitochondrial morphology. *International Rev. Cytol.*, 9: 227-292.
- Uj, H., and G. C. Mueller 1963 The role of RNA synthesis in early estrogen action. *Proc. Nat. Acad. Sci. U.S.A.*, 50: 256-260.
- Walaas, O. 1952 Effect of oestrogens on the glycogen content of the rat uterus. *Acta endocr., Copenh.*, 10: 175-192.

PLATE 1

EXPLANATION OF FIGURE

- 1 Electron micrograph of several uterine smooth muscle cells from an ovariectomized rat. The smooth muscle cells are small and the intercellular material (IC) is fairly abundant. Along the plasma membrane (PM) are pinocytotic vesicles (PV). In the cytoplasm can be seen several dense bodies (DB) of variable structure. Also present in the cells are a few mitochondria (M), a small amount of granular endoplasmic reticulum (GER) a few scattered free ribosomes (R) and the Golgi complex (GC). $\times 20,720$.



PLATE 2

EXPLANATION OF FIGURE

- 2 Longitudinally cut smooth muscle cells from an ovariectomized rat showing ultrastructural similarities to those seen in figure 1. More mitochondria (M), pinocytotic vesicles (PV) and fewer dense bodies (DB) are visible. $\times 20,720$.

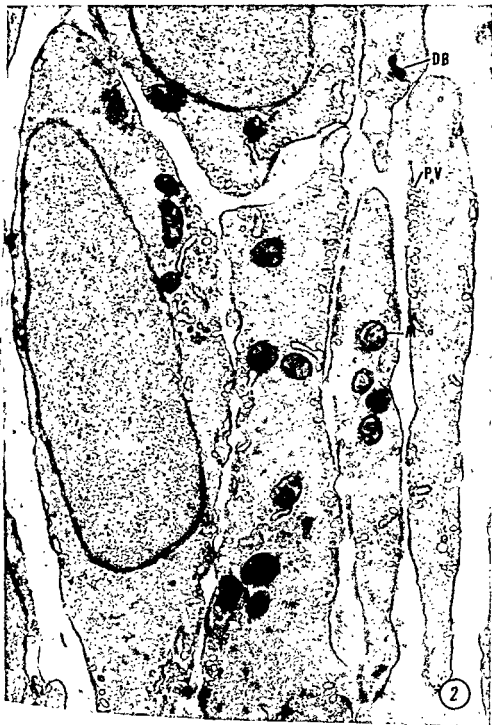


PLATE 3

EXPLANATION OF FIGURES

- 3 An electron micrograph demonstrating the beginning of accumulation of granular endoplasmic reticulum (GER), mitochondria (M), Golgi complex (GC) and free ribosomes (R) at the nuclear pole. A dense body (DB) lies in close relation to the nucleus (N). The rat was autopsied 24 hours after estrogen stimulation. $\times 30,900$.
- 4 This electron micrograph demonstrates a portion of a smooth muscle cell of the uterus from an ovariectomized animal autopsied 48 hours after a single injection of estrogen. There is some interdigitation (ID) of adjacent cells. There is a great accumulation of glycogen (G), free ribosomes (R) and granular endoplasmic reticulum (GER) at the nuclear pole. A few mitochondria (M) and multivesicular bodies (MVB) are located in this area. Ribosomes (R) are present in the outer nuclear membrane (ONM). $\times 20,720$.

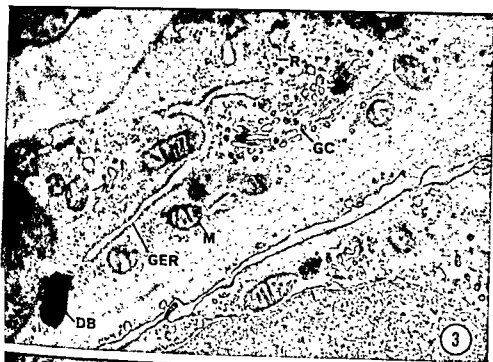


PLATE 4

EXPLANATION OF FIGURES

- 5 Cytoplasmic extensions of two smooth muscle cells are seen in this electron micrograph. Interdigitation (ID) of adjacent cells is evident. Note the marked accumulation of glycogen (G) granules close to the plasma membrane (PM). There are some free ribosomes (R) and scattered mitochondria (M) in the cells. The animal was autopsied 48 hours after estrogen treatment. $\times 20,720$.
- 6 An electron micrograph demonstrating an accumulation of ribosomes (R) and granular endoplasmic reticulum (GER) at the nuclear pole of a smooth muscle cell. Also in this area are a few glycogen (G) granules, a dense body (DB), a few mitochondria (M) and a multivesicular body (MVB). In an adjacent cell (top right) glycogen (G) granules are present. The animal was autopsied 48 hours after estrogen stimulation. $\times 20,720$.

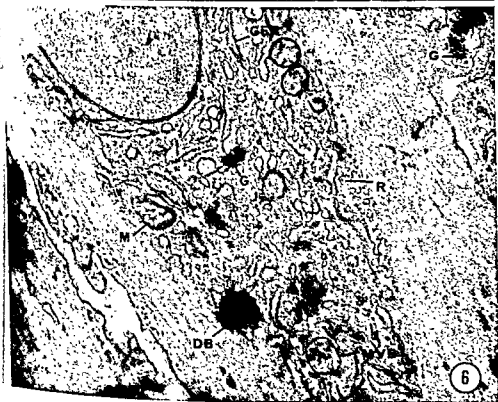
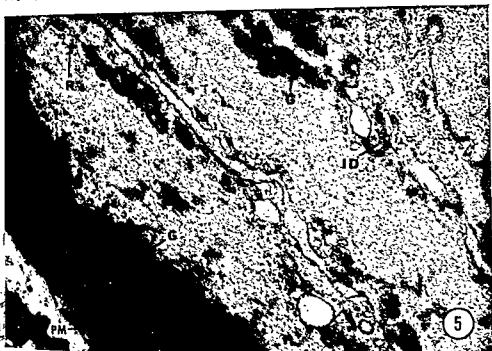
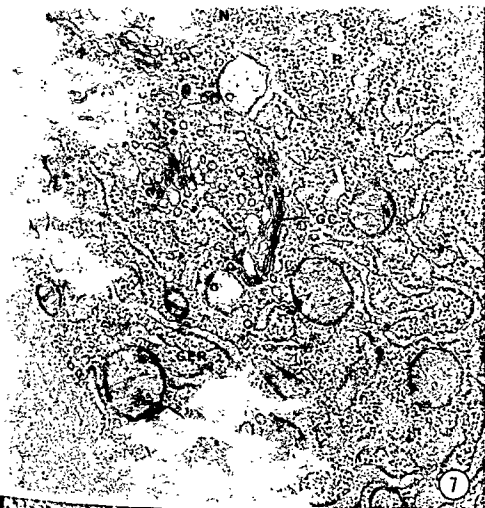


PLATE 5

EXPLANATION OF FIGURES

- 7 This electron micrograph shows an accumulation of structures at the nuclear pole of the smooth muscle cell. Note the presence of the granular endoplasmic reticulum (GER), mitochondria (M), Golgi complex (GC) and free ribosomes (R). A portion of the nucleus (N) can be seen. The rat was autopsied 72 hours after estrogen treatment. $\times 30,900$.
- 8 A cytoplasmic extension of a smooth muscle cell from an animal autopsied 96 hours after estrogen stimulation. Mitochondria (M), granular endoplasmic reticulum (GER), free ribosomes (R), scattered glycogen (G) particles and Golgi complex (GC) occupy almost the entire area. $\times 30,900$.



Phylogenesis of the Placenta and Fetal Membranes of the Tree Shrews (Family Tupaiidae)¹

WINTER PATRICK LUCKETT²

Department of Anatomy, University of Wisconsin Medical School, Madison, Wisconsin

ABSTRACT The paucity of information on the early developmental stages and the necessity for re-evaluation of the phylogenetic implications of the tupaiid fetal membranes have stimulated the present study.

Neonatal tupaiids possess prominent bilateral endometrial pads that run the length of each uterine horn. These gland-free pads are the sites of implantation and placenta-tion in adults. Implantation is bilateral and superficial. Multinucleated giant cells differentiate from the cytotrophoblast of the attachment sites; they facilitate the marginal expansion of the placental disc by detaching the paraplacental epithelium from its basement membrane.

Prominent bilateral chorio-vitelline placentae develop and remain functional through early limb bud stages. Decidual cells fuse to form "decidual knots" during this period.

The bilateral chorio-allantoic placentae are labyrinthine endotheliochorial. The trophoblast of the labyrinth is entirely syntrophoblastic, similar to the condition in the armadillo placenta. Epithelioid mesenchymal cells in the labyrinth are strikingly similar to those of the shrew placenta. The large allantoic vesicle and free vascular yolk sac persist. Amniogenesis occurs by folding.

Uterine glands remain secretory throughout pregnancy; iron is probably supplied to the fetus in this manner.

The tree shrews of Southeast Asia possess many characteristics that suggest affinities with the mammalian orders Insectivora and Primates, but the absence of unquestioned fossil tupaiids obscures their precise phylogenetic relationships. Many authors classify the family Tupaiidae within the suborder Prosimii of the Primates (Fiedler, '56; Clark, '62; Buettner-Janusch, '66). Recent re-examinations of the skeleton and dentition (van Valen, '65; McKenna, '66) and the nervous system (Campbell, '66), as well as immunological comparisons of serum proteins (Goodman, '67), suggest that the Tupaiidae are not as closely related to the prosimian Primates as previously believed.

The lack of unquestioned fossil remains necessitates the search for comparative anatomical and biochemical characteristics that may be useful in determining the phylogenetic affinities of tree shrews. Mossman's ('37, '53) extensive comparative analysis suggests that the developmental characteristics of the placenta and fetal membranes have remained conservative features during the evolution of mammals, presumably because of their relative isolation

from the selective effects of the external environment. This conservative nature of the fetal membranes suggests that they have considerable significance in characterizing the higher taxa, particularly at the ordinal and subordinal levels.

Hubrecht (1894b, 1895, 1899, '08) examined over 450 *Tupaia javanica* in all stages of pregnancy. The single fetus in each uterine horn is connected to two bilateral placental discs. Hubrecht observed further that implantation, formation of the yolk sac placentae, and their subsequent replacement by the chorio-allantoic placentae all occur on the lateral walls of each horn. These specialized sites are evident in the virgin uterine horn as gland-free endometrial "cushions." Hubrecht reported that the invasive chorio-allantoic villi surround the maternal capillaries, and that the capillary endothelium then degenerates, resulting in the circulation of maternal blood within trophoblastic lacunae.

¹This work was supported by predoctoral fellowship 5-F1-GM-10,136 from the National Institutes of Health, and NIH grant HD 00277-11.

²Present address: Department of Anatomy, Columbia University College of Physicians and Surgeons, 630 W. 168th St., N. Y., N. Y. 10032.

On the basis of Hubrecht's description, de Lange ('33) included the placentation of *Tupaia* within the labyrinthine hemochorial type of Grosser ('09).

Mossman ('39) stated that the placenta of the tree shrew is endotheliochorial, but he presented no evidence supporting this view. Actually, his conclusions were based upon his unpublished observations of several specimens of *Tupaia javanica* that J. P. Hill had obtained from the Hubrecht Laboratory (Mossman, '67a).

Van der Horst ('49) disagreed with Hubrecht concerning the fate of the maternal capillary endothelium in the placental labyrinth. He traced the endothelial continuity between the maternal arterioles entering the placenta and the capillaries in the labyrinth. He stated that maternal capillary endothelium persists in late stages of pregnancy and classified the *Tupaia* placenta as endotheliochorial.

Meister and Davis ('56, '58) examined placental material from *Tupaia minor* and *Tupaia tana* (= *Lyonogale tana* Conisbee '53), consisting of one early and two late stages of chorio-allantoic placentation. They described the earlier stage as labyrinthine endotheliochorial, but they believed that the maternal endothelium is lost in the labyrinth of the near term specimens, and thus classified them as labyrinthine hemochorial. Meister and Davis concluded that the fetal membranes of *Tupaia* are significantly different from those of the Insectivora, but they found a similarity between the fetal membranes of *Tupaia* and those of the more generalized members of the families Cebidae and Cercopithecidae of the Primates. This evidence of the placenta and fetal membranes has been used to support the contention that the tupalids are closely related to the Primates (Clark, '62; Buettner-Janusch, '66).

Recent studies of the placentation of *Tupaia* and *Anathana* support van der Horst's ('49) conclusion that the endotheliochorial relationship persists in late stages of pregnancy (Hill, '65; Verma, '65). Furthermore, Hill contended that there is no justification for classifying the tupalids with the Primates on the basis of their placentation.

The lack of agreement about certain details of placentation, the paucity of infor-

mation available on the earlier developmental stages of the fetal membranes, and the necessity for re-evaluation of the phylogenetic implications of the morphogenesis of their fetal membranes have stimulated the present study.

MATERIALS AND METHODS

The 52 specimens examined during this study belong to 4 of the 6 genera of tupalids recognized by Lyon ('13). Reproductive tracts were obtained from 10 *Tupaia javanica*, 6 *T. longipes*, 6 *T. minor*, 5 *T. glis*, 4 *T. palawanensis*, 1 *T. picta*, 1 *T. chinensis*, 1 *T. montana*, 1 *T. gracilis*, 1 *Lyonogale tana*, 6 *Urogale everetti*, and 1 *Dendrogale murinus*. The material was collected in Malaysia, Thailand and the Philippine Islands through the cooperation of a number of individuals. The majority of the specimens were obtained from Professor Clinton H. Conaway, Department of Zoology, University of Missouri and Doctor Kenneth L. Duke, Department of Anatomy Duke University Medical Center. Professor B. I. Balinsky, Department of Zoology, University of the Witwatersrand, South Africa kindly loaned the collection of slides prepared by the late C. J. van der Horst (see van der Horst, '49). Single preserved reproductive tracts were obtained from each of the following: Barbara Harrison, the Sarawak Museum, Malaysia (see Harrison, '63; Doctor Joseph C. Moore, Chicago Natural History Museum; Professor Clinton N. Woolsey, Department of Neurophysiology, University of Wisconsin Medical School; and Doctor P. D. Nieuwkoop, Hubrecht Laboratory, Utrecht, the Netherlands.

The reproductive tracts were fixed in 10% formalin, Bouin's fixative or AFA (alcohol, formalin and acetic acid), and subsequently stored in 70% alcohol. Paraffin sections were cut at 6-10 μ ; serial sections were mounted and stained from the early stages of pregnancy, whereas only every tenth section was examined from some of the later stages. The ovaries were also sectioned in order to provide additional information about the reproductive history of these animals. Sections were stained with Groat's tetrachrome (unpublished), Harris' hematoxylin and eosin, Masson's trichrome, Movat's pentachrome,

an silver, PAS (Periodic Acid-Schiff), Gomori's basic fuchsin, Turnbull's blue, or Nicholson's iron stain.

Measurements of the greatest diameters and length of the early developmental stages were recorded from serial section slides with the aid of an ocular micrometer. Cross measurements were made of the crown-rump length of preserved embryos whenever possible.

OBSERVATIONS

To understand the uterine changes that occur during pregnancy, it will be useful to consider briefly the uterine histology of the immature and non-pregnant adult tree shrew. The elongate uterine horns unite in a short common corpus; the general external appearance of the uterus has been described previously (Wood Jones, '17; Meister and Davis, '56; Clark, '62).

Non-pregnant uterus

At 12 days postnatum the endometrium of each horn exhibits two characteristic regions: (1) the mesometrial and antimesometrial surfaces bear short, straight tubular glands in the superficial third of the endometrium, and (2) gland-free endometrial pads or cushions occupy the lateral antimesometrial walls and bulge prominently into the uterine lumen. These pads are actually bilateral ridges which extend the entire length of the horn. In cross section the pads are fungiform. (fig. 5).

The subepithelial zone of the endometrial pads consists of densely packed cellular stroma, whereas the stroma of the base of the pads and of the mesometrial and antimesometrial regions is more loosely arranged. The columnar epithelial lining of the pads measures about 13 μ in height. Prominent endometrial pads are also seen in the uterine horns of the neonate, but there is no sign of uterine gland formation at this stage.

Uterine glands extend to the base of the endometrium by 50 days of age. The endometrial pads remain gland-free, although coiled gland tubules occur in the stroma immediately beneath them. Serial sections show that these basal glands curve around the pads to open into the uterine lumen. The pads are similar in appearance to those of earlier stages.

In more mature nulliparous specimens the endometrial pads are less prominent because of the relatively greater thickness of the glandular endometrium (fig. 6). The basal glands are coiled slightly, and the antimesometrial glandular endometrium is about three times as thick as that of the mesometrial region.

During the preovulatory phase of the estrous cycle of mature tupalids the basal halves of the uterine glands are moderately coiled. At this stage the gland-free endometrial pads no longer bulge into the uterine lumen; hyperplasia of the adjacent glandular endometrium has resulted in a relatively uniform thickness of the lateral walls. The arterioles which supply the endometrial pads of parous animals are coiled in the region between the myometrium and the base of the pads, but there is little or no evidence of coiling of the smaller arterioles which directly supply the pads (fig. 7).

Preimplantation stages of pregnancy

In one specimen of *Tupaia glis* the ampulla of each oviduct contains an eight cell stage surrounded by the zona pellucida. These cleavage stages measure $76 \times 84 \mu$ and $82 \times 89 \mu$, exclusive of the zona; in comparison, the average dimensions of ova from six Graafian follicles in *T. glis* are $114 \times 123 \mu$.

The earliest blastocyst found occurs in the isthmus of one oviduct of a specimen of *Urogale everetti*; three late morulae also occur in the same region. The tubal blastocyst measures $107 \times 108 \mu$. A unilaminar blastocyst becomes distributed to the middle region of each uterine horn, even in those cases where double ovulation occurs in one ovary and none in the other. At this stage the inner cell mass is 3-4 cells thick; there is no thinning of the trophoblast (Raubers' layer) covering the inner cell mass.

Two specimens contain expanded free bilaminar blastocysts in the middle of each uterine horn (fig. 8). The cuboidal trophoblastic epithelium is about 10 μ thick and is considerably thinner than in earlier stages. Raubers' layer is complete in the younger of these two blastocysts, but it is reduced in thickness and incomplete in places over the embryonic knot of the older

Abbreviations

A, Amnion	K, Decidual knots
AD, Allantoic duct	L, Labyrinth
AM, Allantoic mesenchyme	M, Macrophage
AP, Attachment plaque	P, Endometrial pad
AV, Allantoic vesicle	PV, Primary villi
B, Basement membrane	S, Syntrophoblast
C, Cytotrophoblast	SC, Smooth chorion
CM, Basal chromatic masses	T, Trophoblast
D, Basal decidua	TG, Trophoblast giant cell
E, Endothelium	U, Uterine epithelium
EC, Endometrial capillaries	UG, Uterine gland
ED, Endoderm	VS, Vascular splanchnopleure
EX, Exocoelom	VV, Vitelline vessels
G, Cytoplasmic granules	Y, Yolk sac cavity

specimen. A squamous endodermal layer forms a continuous internal lining for the blastocyst cavity.

There are no remains of the zona pellucida around any of the expanded free blastocysts. An attenuated zona surrounds the unilaminar uterine blastocysts; but it is uncertain whether loss of the zona results from continued stretching or from its dissolution as a result of acid fixation. The zona still surrounds the expanded unimplanted blastocysts of the badger, ferret, mink and rabbit (Wright, '66; Orsini, '67).

Coiling of the uterine glands increases during passage of the blastocysts from the oviduct to the uterus; they are considerably coiled in uteri containing expanded bilaminar blastocysts. The stroma of the endometrial pads remains densely packed and cellular throughout most of the pre-implantation period, although some stromal edema is evident in the expanded blastocyst stage.

A single *Tupaia longipes* was sacrificed six days following postpartum copulation in captivity. The ovaries contain two generations of corpora lutea: smaller corpora of lactation and larger corpora of pregnancy. A bilaminar blastocyst occurs on the uterine side of the tubo-uterine junction (fig. 9). Rauber's layer is complete and there is no evidence of a zona pellucida; the general appearance of the blastocyst is very similar to that of the expanded bilaminar preimplantation blastocysts of other specimens. This specimen suggests the possibility of lactational delay of implantation in *Tupaia*, similar to the situation described in the mouse and rat (Enzmann, Saphir and Pincus, '32; Krehbiel, '41). Secretory material is abundant in the lumina of the

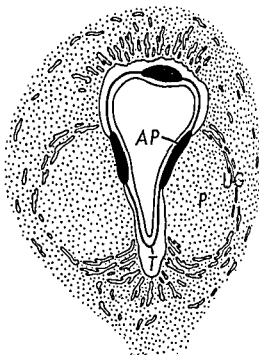


Fig. 1 Diagram of a cross section of the uterus showing implantation of the bilaminar blastocyst. Implantation is bilateral and the embryonic is oriented antimesometrially.

uterine glands at the ovarian end of the horn, and a considerable amount of secretory product surrounds and is adsorbed to the surface of the blastocyst.

Implantation

The initial attachment of the bilaminar blastocyst is accompanied by the intima apposition of the simple cuboidal layer of trophoblast and the epithelium of the lateral endometrial pads. Following this the trophoblast of the attachment site proliferates to form a layer 2-6 cells thick

though the multilayered cytotrophoblast adheres intimately to the uterine epithelium, the apposed plasma membranes appear to remain intact (fig. 10). The two cell types may be distinguished on the basis of their nuclear characteristics. The trophoblastic nuclei are slightly larger and contain one or two large, centrally located nucleoli. Scattered fine chromatin clumps may occur in the nucleus, but its general appearance is open or vesicular. Nuclei of uterine epithelial cells are spherical and contain small nucleoli; the nucleoplasm is relatively homogeneous and basophilic (figs. 10, 11).

A specimen of *Tupaia longipes* in an early stage of implantation bears irregular shallow invaginations or crypts over the entire epithelial lining of the uterine horn. The crypts measure 55–120 μ in depth, and uterine glands open into them except on the gland-free endometrial pads (figs. 11, 12). The attaching trophoblast has partially penetrated into the lumina of the endometrial pad crypts, but there is no apparent rupture of the uterine epithelium.

A slightly later stage of implantation bears prominent bilateral "attachment plaques" approximately 100 μ thick, consisting of the multilayered attaching trophoblast and a nearly complete layer of uterine epithelium. Occasional trophoblastic cells have sent processes between epithelial cells toward the underlying basement membrane, but there is little evidence of epithelial degeneration (fig. 13). Trophoblastic and epithelial nuclei remain distinguishable on the basis of the previously mentioned criteria, and plasma membranes persists between the two cell types.

By the time the attachment plaques are about 130 μ thick, numerous crenated, pyknotic nuclei have appeared in them (fig. 14); these probably represent degenerating uterine epithelial cells. The trophoblastic and epithelial elements of the plaques are radially arranged; this probably reflects the interdigitation of trophoblast and the irregular epithelial crypts seen in an earlier phase of attachment. Some relatively normal appearing epithelial cells occur in the bases of the plaques, but it is impossible to identify some of the other plaque cells with certainty.

The early attaching blastocyst occupies an enlargement of an antimesometrial third of the uterine lumen, and then narrows between its bilateral attachments to the endometrial pads (fig. 1). The embryonic knot of the late preimplantation stage has become an enlarged flattened disc. Nuclei of the pseudostratified epithelium of the disc are arranged in two irregular layers. There is no evidence of a primitive streak in any of these early attaching blastocysts. A thin, homogeneous, acidophilic lamina separates the trophoblast and endoderm in the mesometrial half of the blastocyst; it is analogous to the Reichert's membrane characteristic of rodents, shrews and some bats, but is not nearly as thick.

The endometrial pad stroma is edematous during the initial period of blastocyst attachment. A thin subepithelial zone of stroma is more compact, possibly due to pressure from the expanded blastocyst. In cross sections of the uterus the maternal capillaries form a characteristic radiating pattern throughout the endometrial pad (fig. 15). The stroma of the superficial fifth of the pads is more compact in later attachment stages, apparently due to a slight hypertrophy of the stromal cells rather than to hyperplasia (fig. 13).

Implantation in the tree shrews is therefore bilateral and superficial, and the embryonic shield is oriented antimesometrially. There is no decidual reaction at the initial stage of attachment (fig. 1).

Primitive streak stage

The thickened attachment plaques show little or no evidence of remnants of uterine epithelium. They now consist of two distinct zones (fig. 16). (1) An inner cytotrophoblastic zone 2–5 cells thick is separated from the endoderm by Reichert's membrane. There are scattered mitotic figures in this zone, and the cells are similar to those of earlier implantation stages. (2) An outer zone of hypertrophied trophoblastic cells abuts upon the maternal stroma. At least some of these radially elongated trophoblastic "giant" cells are multinucleate, but plasma membranes separate adjacent multinucleated masses. Mitotic figures were never seen in them. The intensely basophilic cytoplasm of the

giant cells contrasts sharply with the pale staining cytoplasm of the inner cytotrophoblastic cells, and the diameter of giant cell nuclei is about twice that of the cytotrophoblastic cells.

The basement membrane of the uterine epithelium which previously covered the endometrial pads is still demonstrable in the two specimens of this stage (fig. 17). It appears intact beneath the antimesometrial and mesometrial borders of the attached trophoblast, and is continuous with the basement membrane of the uterine epithelium adjacent to the attachment plaques. The basement membrane is incomplete beneath the mid-region of the plaque, where it is penetrated in places by multinucleated giant cells. At both margins of the attachment site wedge-like processes of trophoblastic giant cells seem to detach the uterine epithelium from its underlying basement membrane (fig. 18).

The endometrial pad stroma is composed predominantly of closely packed, enlarged, epithelioid decidual cells with basophilic cytoplasm (figs. 16, 18). There is a gradation from basally located fibroblast-like cells to the closely packed epithelioid cells adjacent to the attachment plaque. The decidual cells have vesicular nuclei with one or two prominent nucleoli. Those decidual cells immediately adjacent to the trophoblast are further modified; their cytoplasm is more basophilic and their nuclei contain increased amounts of clumped chromatin which tend to be located next to the nuclear membrane (fig. 19). Plasma membranes are increasingly difficult to detect around individual hypertrophied stromal cells, and the decidual cells bordering the trophoblast appear to be multinucleated masses. Mitoses are frequent in the compacted decidual cells, but are less numerous in the thin basal zone of unmodified and more edematous stroma.

There is no evidence of blood island formation in either specimen of this stage. Reichert's membrane is continuous with a slightly thinner basement membrane of identical staining affinities which underlies the antimesometrial trophoblast and the embryonic ectoderm. The fact that the extraembryonic mesoderm separates both trophoblast and Reichert's membrane from the endoderm suggests that this membrane

in the tupaiid blastocyst consists largely of the basement membrane of the trophoblast, similar to the condition in the Soricidae (Brambell and Perry, '45; Wimsatt and Wislocki, '47).

Development of chorio-vitelline placentation

Avascular trilaminar omphalopleure covers the antimesometrial surface of the endometrial pads in a specimen of *Lycogale* containing a 6-somite embryo, where the remainder of the surface of the pads is covered by bilaminar omphalopleure. The giant cell layer characteristic of the primitive streak stage is now considerably reduced; only scattered giant cells occur between the multilayered cytotrophoblast and the decidual cells. A few giant cells have penetrated into the decidual zone, but the cytotrophoblast shows no evidence of such penetration.

The decidual cells are densely packed and show numerous mitotic figures. Some of the decidual cells adjacent to the trophoblast form syncytial "decidual knots" consisting of a peripheral ring of nuclei around a central cytoplasmic core (fig. 21). The decidual knot nuclei contain abundant peripheral chromatin clumps. The knots are more numerous adjacent to the attached trophoblast, but they are also found in the deeper regions of the pad.

The incipient placental discs show three prominent zones by the time vascular mesoderm has extended into their antimesometrial margins (figs. 20, 21, 22). (1) The inner trophoblastic zone at the fetal surface of the disc consists of a thin layer of cytotrophoblast which commonly surrounds maternal capillaries. Densely nucleated, its regular processes extend from the cytotrophoblast into the decidua as primary villi; they appear to be syncytial in nature, but this is difficult to ascertain. Frequently one or several giant cells appear to be embedded in the core of the primary villus, but they are almost completely obscured by the surrounding smaller nuclei. Many primary villi completely or partly surround decidual knots (fig. 21).

(2) The decidual zone adjacent to an intermingled with the primary villi is characterized by numerous, more developed decidual knots (fig. 21). In a cross section

a knot the hyperchromatic nuclei are arranged in a semilunar or circular pattern about the periphery, and the center consists of a common acidophilic cytoplasm. The greatest diameter of the serial knots is about 30 μ , and about 9 nuclei are located in the periphery of not in cross section. The irregular spaces in the loosely arranged decidual knot zone may be due to tissue dissolution or to resorption.

(3) The relatively normal basal decidua separated from the flattened uterine decidua that underlie the disc by a thin layer of typical spindle-shaped stromal cells. Mitotic figures are numerous in the basal decidua but are absent in the decidua overlying the chorionic plate. There is a transitional zone between the normal basal decidual cells and decidual cells overlying the chorionic plate (fig. 22). Maternal capillary endothelium remains intact in the decidual knot zone, despite considerable tissue dissolution in this region. These capillaries are often completely surrounded by cytotrophoblast of the fetal surface of the incipient placental disc (fig. 21).

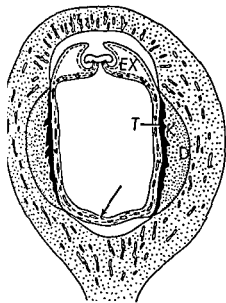


Fig. 2 Diagram of a cross section of the uterus during the period of chorio-vitelline placentalation. The bilaminar omphalopleure (arrow) extends between the mesometrial margins of the developing placental discs. Mesoderm, dashed lines.

In 12-somite embryos mesometrial extension of vascular extraembryonic mesoderm results in the establishment of bilateral chorio-vitelline placental discs (fig. 25). The bilaminar omphalopleure persists temporarily between the mesometrial margins of the placental discs, but the continued mesometrial extension of vascular mesoderm soon results in a vascular trilaminar omphalopleure (fig. 2).

The cytotrophoblast at the fetal surface of the chorio-vitelline placenta varies in thickness from 2-4 cells in the early stages to ten or more cells later. Mitoses are frequent in the cytotrophoblast, especially during the early period of chorio-vitelline placentalation. The maternal capillaries which are surrounded by the cytotrophoblast of the chorionic plate tend to run in a mesometrial-antimesometrial plane (fig. 24). Their endothelium remains intact, and its continuity can be traced with that of the thin-walled, radial arterioles which course through the basal decidua up to the chorionic plate. In many instances maternal capillaries are separated from the fetal vessels of the chorio-vitelline placenta by a layer of cytotrophoblast only 1-2 cells thick.

Densely nucleated, primary trophoblastic villi are well developed in the chorio-vitelline placenta and grade into the cytotrophoblast of the chorionic plate (figs. 23, 24). Mitoses are absent from the multinucleated or syncytial primary villi. Trophoblastic giant cells are rare in the main portion of the chorio-vitelline placental disc. However, paraplacental trophoblastic giant cells are conspicuous throughout chorio-vitelline placentalation; they continue to detach or delaminate the uterine epithelium from its basement membrane in this region, and to invade the paraplacental uterine glands (fig. 26). This paraplacental epithelial delamination appears to play a role in the marginal expansion of the placental discs, since the discs come to occupy the entire lateral walls of the uterine horn.

The zone of decidual knots becomes reduced in thickness in later stages of chorio-vitelline placentalation. The knots may become surrounded by the proliferating cytotrophoblast of the chorionic plate (fig. 27), or they may be partly surrounded by the densely nucleated primary villi (figs. 24,

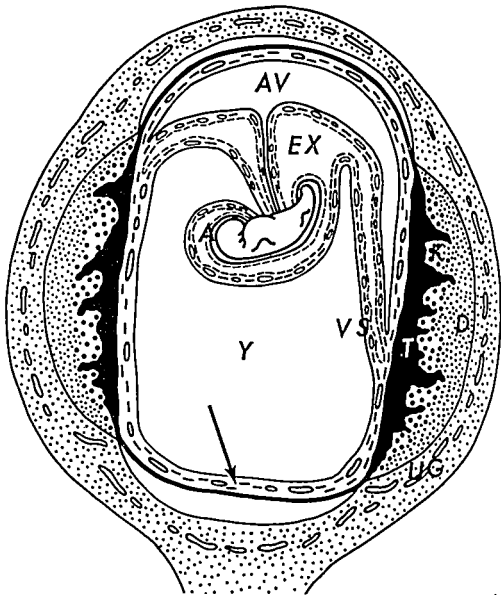


Fig. 3 Diagram of a cross section of the uterus during the transition between chorio-vitelline and chorio-allantoic placentation. The vascular splanchnopleure of the yolk sac still adheres to the mesometrial region of the placental discs, and trilaminar omphalopleure (arrow) persists between the mesometrial borders of the placental discs.

25). Later many decidual knots show increased nuclear pyknosis and a loss of the characteristic peripheral nuclear arrangement (fig. 23). Mitotic figures are abundant in the normal appearing basal decidua, but they are absent in the thinner zone of decidual knots. The basal decidua may form up to half the thickness of the placental disc.

Transition between chorio-vitelline and chorio-allantoic placentation

Two specimens were collected in the early limb bud stage. A very short vitelline

duct connects the yolk sac to the midgut. The patent allantoic duct leaves the ventral body wall and runs antimesometrially to open into the large allantoic vesicle which has spread bilaterally and mesometrially (fig. 3). The vascular allantois has displaced the vascular splanchnopleure of the yolk sac from the surface of the placental discs throughout the antimesometrial half of their extent. The mesometrial portion of each placental disc remains covered by the vascular splanchnopleure of the yolk sac and apparently still functions as a chorio-vitelline placenta (figs. 28, 29)

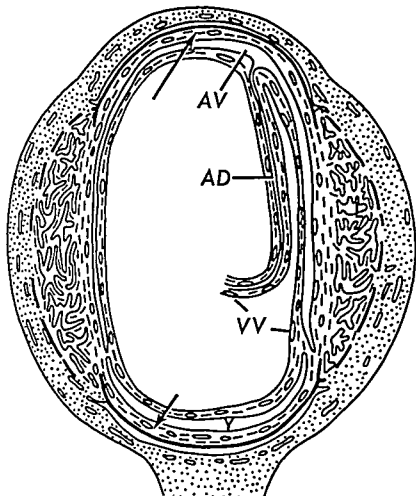


Fig. 4 Diagram of a cross section of the uterus during late pregnancy. The smooth chorion is fused with the outer layer of the allantois and of the yolk sac to form a chorio-allantoic membrane (long arrow) and a chorio-vitelline membrane (short arrow). Vitelline vessels run along the periphery of the umbilical cord and the proximal wall of the allantoic vesicle to vascularize the free yolk sac. No attempt is made to portray the detailed structure of the labyrinth in this diagram.

Short, blunt processes of vascular allantoic mesoderm indent the chorionic plate at the antimesometrial portion of the placental discs, but these vascular buds have not yet penetrated the chorionic plate to form an intimate relationship with the maternal capillaries. The prominent, dense-nucleated primary villi extend throughout 60% of the thickness of the placental disc. Scattered mitoses occur in the chorionic plate and basal decidua, but are lacking in the maternal decidua.

Chorio-allantoic placentation

The placental disc during the progressive establishment of chorio-allantoic placentation consists of four zones which tend to interdigitate with each other: (1) chorionic plate, (2) chorio-allantoic labyrinth, (3) a mixed zone of primary villi and decidual knots, and (4) a reduced zone of basal decidua (fig. 30).

The multilayered cytotrophoblast of the chorionic plate is about 80–180 μ thick during this period, and mitotic figures are

infrequent. Vascular allantoic mesenchymal villi, surrounded by a single layer of trophoblast, penetrate the chorionic plate to form an intimate relationship with maternal capillaries. These villi have carried portions of the chorionic plate with attached primary villi deep into the basal decidua zone (figs. 30, 31) as trophoblastic "cell columns."

The mesenchymal cells of the villus-like processes are hypertrophied and epithelioid in appearance. Their spherical or ovoid nuclei are vesicular and contain prominent nucleoli; their cytoplasm is lightly acidophilic (figs. 33, 35, 37, 38, 39). Transitional cell types occur between these and the spindle-shaped, unmodified mesenchymal cells of the fetal surface of the chorionic plate.

The attenuated layer of trophoblast covering the villus-like processes of the labyrinth is completely syntrophoblastic, and it is continuous with the cytotrophoblast of the chorionic plate and the multinucleated cell columns at the tips of the villus-like processes (fig. 32). Maternal capillary endothelium persists in the developing labyrinth and is considerably hypertrophied in places, especially adjacent to the chorionic plate (fig. 33). The vesicular maternal endothelial nucleus is spherical or ovoid and contains 1-2 prominent basophilic nucleoli. The flattened syntrophoblastic nuclei are filled with densely packed chromatin clumps and are intensely basophilic.

Multinucleated primary villi extend almost to the base of the placental disc, where they interdigitate with decidua knots or the reduced region of unmodified decidua basalis (fig. 31). As development proceeds, the labyrinth comes to occupy more and more of the thickness of the placental disc, while the mixed zone of cell columns and decidua becomes reduced to a thinner region of irregular, densely nucleated masses (fig. 34). These masses probably represent remnants of cell columns; their densely packed nuclei are filled with clumped chromatin, similar to the condition in the cell columns. Occasional decidua knots and small clusters of pyknotic nuclei, which probably represent degenerating decidua knots, also occur.

The major change in the placental during later stages of pregnancy is continued reduction in thickness of basal densely nucleated masses. If multinucleated masses are indeed of cell columns, they would be with the *trophospongium* of other thine placentae, that is, the troph zone that contains only maternal channels. However, the possibility that the basal decidua or decidua may also contribute to the multinucleated masses, and therefore the non-specific "basal chromatic masses" is used to these structures. Some of the basal chromatic masses exhibit two or more cell, and some of these are similar to pyknotic, degenerating decidua knots earlier stages (fig. 35). Villus-like from the labyrinth spread out and flattened against the basal masses. In placentae obtained from term deliveries, the basal chromatic are generally less than 50 μ thick and absent from much of the bases of the placental discs. At parturition the separate from the uterus at the between the chromatic masses and the layer of unmodified stroma that the flattened uterine glands.

Near term placental discs are in cross section, and most of their thickness consists of the labyrinth or zone of intimacy (fig. 36). The villus-like appearance of the labyrinth reflects the fan-like arrangement of the allantoic mesenchymal villi (fig. 37). However, are no true chorio-allantoic villi, as trophoblast which surrounds the capillaries is continuous throughout the labyrinth (fig. 38).

The hypertrophied maternal endothelium persists to term in the labyrinth of the chorio-allantoic placentae. The basement membranes of both the trophoblast and the maternal endothelium are demonstrated by PAS, azan silver and Lory's trichrome staining (figs. 39, 40). The layers that separate the fetal and maternal blood in the chorio-allantoic labyrinth are (1) fetal endothelium, (2) the basement membrane(s) between the fetal endothelium and syntrophoblast, (3) the trophoblast, (4) basement membrane of maternal endothelium, and (5)

endothelium. According to Grosser's ('09) scheme, the chorio-allantoic placenta of the tupaids is therefore endotheliochorial. This endotheliochorial condition is also evident in placentae obtained from normal term deliveries (fig. 41). Hyalinization of the basement membranes of the labyrinth at term renders them visible with routine staining procedures.

Placental circulation in tupaids is similar to that of most species possessing labyrinthine placenta. Maternal arterioles from the myometrium pass through the labyrinth and open into capillaries at the fetal surface of the placental disc. The modified maternal capillaries follow a predominantly radial course to the base of the placental discs, where they drain into uterine veins. Fetal arterioles penetrate deeply into the placental labyrinth before breaking up into capillaries which pursue a rather tortuous course toward the allantoic veins at the fetal surface of the placenta. The countercurrent flow of the tupaids placental circulation follows the general scheme postulated for most, if not all, mammalian placentae (Mossman, '65).

Amniogenesis

The earliest evidence of amniogenesis among the available specimens occurs in a 6-somite embryo of *Lyomys*. The amniotic tail fold covers the caudal tip of the embryo, but there is only a slight suggestion of the amniotic head fold. On the other hand, in a 12-somite *Tupaia javanica* embryo the amniotic head fold extends over the anterior third of the embryo; but there is no suggestion of an amniotic tail fold. In the later stages of chorio-vitelline placenta the amniotic folds extend over the anterior and posterior ends of the embryo, but the amnion remains incomplete over the midregion. The amniotic folds are not completely closed until the allantoic diverticulum fuses with the chorion to initiate chorio-allantoic placenta.

Yolk sac

The antimesometrial wall of the yolk sac is invaginated by the expanded amnion and embryo during the transitional stage between chorio-vitelline and chorio-allantoic placenta. For convenience the antimesometrial concave surface of the yolk

sac may be considered the proximal layer, and the convex mesometrial surface may be considered the distal layer (fig. 3). After its detachment from the surface of the placental disc by the spreading allantois, the yolk sac becomes compressed between the amnion and the mesometrial margins of the placental discs (fig. 4).

In early stages of chorio-allantoic placenta the intestinal loop herniates into the umbilical coelom (fig. 42), but it is no longer connected with the yolk duct. In the mid-mesometrial region of the proximal wall of the yolk sac a short endodermal diverticulum about 0.5 mm long represents the distal remnant of the yolk duct (fig. 43). It is flanked by the two primary branches of the vitelline vein, and its blind end is closely associated with the vitelline artery. There is no herniation of the intestinal loop into the umbilical cord in later stages of chorio-allantoic placenta, and there is no continuity between the endoderm of the midgut and that of the yolk sac. The free yolk sac remains large although compressed throughout the remainder of pregnancy, and it extends the entire anterior-posterior length of the fetus. The single vitelline artery and vein leave the umbilical cord antimesometrially and run laterally and mesometrially between the amnion and allantois toward the yolk sac (fig. 4).

The distal splanchnopleure of the yolk sac vascularizes the overlying mesometrial smooth chorion, forming a chorio-vitelline membrane, and the proximal splanchnopleure of the yolk sac is similarly associated with the amnion to form a vascular amnio-vitelline membrane (fig. 4). During the early stages of chorio-allantoic placenta the distal endoderm of the yolk sac is generally 2-3 times as thick as the proximal layer, particularly toward the mid-mesometrial region (fig. 44). The distal splanchnopleure also possesses a richer vascular supply than does the proximal splanchnopleure. The most pronounced modification of the chorio-vitelline membrane occurs in a specimen of *Tupaia palawanensis*. The mid-mesometrial chorion has invaginated to form a pocket or sac which opens into the uterine lumen (fig. 45). Villus-like processes of the distal endoderm penetrate the folds or plicae

infrequent. Vascular allantoic mesenchymal villi, surrounded by a single layer of trophoblast, penetrate the chorionic plate to form an intimate relationship with maternal capillaries. These villi have carried portions of the chorionic plate with attached primary villi deep into the basal decidua zone (figs. 30, 31) as trophoblastic "cell columns."

The mesenchymal cells of the villus-like processes are hypertrophied and epithelioid in appearance. Their spherical or ovoid nuclei are vesicular and contain prominent nucleoli; their cytoplasm is lightly acidophilic (figs. 33, 35, 37, 38, 39). Transitional cell types occur between these and the spindle-shaped, unmodified mesenchymal cells of the fetal surface of the chorionic plate.

The attenuated layer of trophoblast covering the villus-like processes of the labyrinth is completely syntrophoblastic, and it is continuous with the cytotrophoblast of the chorionic plate and the multinucleated cell columns at the tips of the villus-like processes (fig. 32). Maternal capillary endothelium persists in the developing labyrinth and is considerably hypertrophied in places, especially adjacent to the chorionic plate (fig. 33). The vesicular maternal endothelial nucleus is spherical or ovoid and contains 1-2 prominent basophilic nucleoli. The flattened syntrophoblastic nuclei are filled with densely packed chromatin clumps and are intensely basophilic.

Multinucleated primary villi extend almost to the base of the placental disc, where they interdigitate with decidua knots or the reduced region of unmodified decidua basalis (fig. 31). As development proceeds, the labyrinth comes to occupy more and more of the thickness of the placental disc, while the mixed zone of cell columns and decidua becomes reduced to a thinner region of irregular, densely nucleated masses (fig. 34). These masses probably represent remnants of cell columns; their densely packed nuclei are filled with clumped chromatin, similar to the condition in the cell columns. Occasional decidua knots and small clusters of pyknotic nuclei, which probably represent degenerating decidua knots, also occur.

The major change in the placental discs during later stages of pregnancy is continued reduction in thickness of basal densely nucleated masses. If these multinucleated masses are indeed composed of cell columns, they would be homologous with the *trophospongium* of other labyrinthine placentae, that is, the trophoblastic zone that contains only maternal blood channels. However, the possibility that the basal decidua or decidua knots may also contribute to the multinucleated masses, and therefore the non-specific "basal chromatic masses" is used to refer to these structures. Some of the basal chromatic masses exhibit two or more cell types and some of these are similar to the pyknotic, degenerating decidua knots of earlier stages (fig. 35). Villus-like processes from the labyrinth spread out and become flattened against the basal chromatic masses. In placentae obtained from normal term deliveries, the basal chromatic masses are generally less than 50 μ thick and are absent from much of the bases of the placental discs. At parturition the placentae separate from the uterus at the junction between the chromatic masses and the thin layer of unmodified stroma that overlies the flattened uterine glands.

Near term placental discs are lenticular in cross section, and most of their thickness consists of the labyrinth or zone of vascular intimacy (fig. 36). The villus-like appearance of the labyrinth reflects the predominantly radiate arrangement of the allantoic mesenchymal villi (fig. 37). However, there are no true chorio-allantoic villi, as the trophoblast which surrounds the maternal capillaries is continuous throughout the labyrinth (fig. 38).

The hypertrophied maternal capillary endothelium persists to term in the labyrinth of the chorio-allantoic placentae. The basement membranes of both the syntrophoblast and the maternal endothelium are demonstrated by PAS, azan silver and Mallory's trichrome staining (figs. 39, 40). The layers that separate the fetal and maternal blood in the chorio-allantoic labyrinth are: (1) fetal endothelium, (2) the basement membrane(s) between the fetal endothelium and syntrophoblast, (3) syntrophoblast, (4) basement membrane of the maternal endothelium, and (5) maternal

and Wislocki, '47). The cushions develop as the result of hypertrophy and hyperplasia of endometrial stromal cells, and implantation occurs on the thickened epithelium of these cushions. The soricid endometrial cushions differ from the endometrial pads of the tupaiids in that they contain uterine glands, and their occurrence is cyclic rather than permanent. Similar bilateral stromal enlargements also occur in uteri of American moles with pre-implantation embryos (Prasad, '58). Endometrial modifications also occur in the lateral uterine walls of the insectivorous families Centetidae and Chrysochloridae (Goetz, '37a; Bluntschli, '38; de Lange, '19; Sabie, '60), but the details of their development are incompletely known.

The tupaiid endometrial pads appear to be more homologous to the bilateral mucosal pads of the Soricidae than to the endometrial caruncles of the higher ruminants. Only the highly specialized superfamilies Bovoidea and Cervoidea among the subdivisions of the Artiodactyla possess caruncles. Caruncles are absent in the more generalized suborder Suina (including pigs and the hippopotamus) and in the infraorder Tylopoda (camels and llamas) of the suborder Ruminantia (Mossman, '37; van Lennep, '61). The chevrotains (*Tragulus*) are generally classified as intermediate in position between the Tylopoda and the higher ruminants (Romer, '66), and slightly raised areas of their endometrium opposite the villous regions of the chorionallantois may be interpreted as a primitive form of caruncle development (van Lennep, '61). It appears that the functional similarities of tupaiid endometrial pads and ruminant caruncles are due to convergent evolution.

A dual endometrial arterial supply occurs in the prosimians *Galago senegalensis* (Butler, '62, '64, '67) and *Loris tardigradus* (Ramawarni and Anand Kumar, '65) and in the Old World monkeys, apes and man (Kaiser, '47a). Coiled arterioles supply the more superficial functional zone and shorter, relatively straight arterioles supply the basal glandular endometrium. It has been suggested that the coiled endometrial arterioles of Old World monkeys, apes and man regulate the amount of hemorrhage and tissue loss during men-

struation (Kaiser, '47a,b). There is no definite evidence for menstruation in any of the prosimians. Menstruation is microscopic in amount in the New World monkeys *Cebus*, *Ateles* and *Alouatta*, but coiled arterioles are absent in these genera (Kaiser, '47b).

The distribution of coiled endometrial arterioles in tupaiids differs from that of *Loris*, *Galago* and the higher Primates, since coiled arterioles do not penetrate into the endometrial pads of the tupaiid endometrium. (My personal communication reported by Butler ('67) was based on incomplete observations regarding the occurrence of coiled arterioles in the tupaiid endometrium.) The tupaiid endometrial pads are analogous to the functional layer of the hominoid endometrium, since these regions are involved in implantation, placental and possibly menstruation in both groups. There is some evidence that tree shrews exhibit a slight loss of the epithelium and subepithelial stroma of the endometrial pads following pseudopregnancy (Luckett, '63; Conaway and Sorenson, '66). This may be comparable to the small amount of menstrual loss in the New World monkeys. Pseudopregnant cycles are probably a rare occurrence in wild tree shrews, since postpartum pregnancy appears to be the usual condition and there is no clear evidence for a restricted breeding season. This would account for the nearly complete lack of evidence for menstruation in wild tupaiids.

The only non-primate in which the occurrence of menstruation is well established is the elephant shrew *Elephantulus* (Van der Horst and Gillman, '41). Van der Horst ('54) reported that enormous coiled arterioles in *Elephantulus* are localized in the small mesometrial region where menstruation and implantation normally occur. He also mentioned that uterine coiled arterioles are found in the insectivorous families Centetidae and Erinaceidae, although menstruation has not been reported in either of these families. The phenomenon of menstruation is of little taxonomic value at the present time, because of the lack of experimental or histological evidence for possible microscopic menstruation in Insectivora, prosimian Primates, or other taxa.

formed by the invaginated chorion. The vitelline vessels that supply the distal splanchnopleure and modified chorion are particularly prominent, whereas there is no noticeable specialization of the proximal splanchnopleure of the yolk sac or of its vascular supply.

Allantois

The allantoic duct decreases in diameter during chorio-allantoic placentation, but it remains patent and opens into the large, cup-shaped allantoic cavity which extends over most of the surface of both placental discs and persists until term (fig. 4). The antimesometrial region of the allantois vascularizes the overlying chorion to form a smooth chorio-allantoic membrane, and the proximal wall of the allantois contacts the antimesometrial and lateral regions of the amnion to form an amnio-allantoic membrane. There is no persisting true chorion.

The single specimen of *Dendrogale* is poorly fixed, and hemorrhaging has occurred at the margins of the placental discs. However, some of the paraplacental hemorrhaging may be a normal occurrence, as it is found to a lesser extent in well preserved specimens of the other genera. The bleeding is most noticeable at the antimesometrial margins of the discs, and the trophoblast of the smooth chorio-allantoic membrane appears to phagocytize red blood cells that adhere to its free surface (fig. 46). Nuclei are basally located in the tall columnar trophoblastic cells, and the supranuclear cytoplasm is filled with large vacuoles and fragments of red blood cells. Several pits or invaginations occur in the smooth chorio-allantoic membrane, and these are probably homologous with the chorionic vesicles or areolae seen in many other mammals.

Umbilical cord

The definitive umbilical cord of the tupalids contains the narrow allantoic duct, paired allantoic arteries and a single allantoic vein. The reduced vitelline vessels are located in the periphery of the cord, but there is no remnant of the vitelline duct. The allantoic vessels diverge to supply both placental discs.

Uterus

The uterine glands are secretory throughout pregnancy, but this activity is most intense through the period of chorio-vitelline placentation. From the time of implantation through the period of establishment of the chorio-vitelline placenta, the secretory product accumulates about, and is adsorbed to, the trophoblast of the bilaminar or trilaminar yolk sac. Material of similar consistency and staining affinity accumulates within the lumen of the yolk sac during this period, but this is less evident in later stages of chorio-vitelline placentation.

In parous animals numerous macrophages containing hemosiderin granules occur in the basal interglandular connective tissue. In many places macrophages are intimately associated with the epithelium of the basal glands, and fine granules which resemble hemosiderin in their color and refractivity are seen in the supranuclear cytoplasm of the gland epithelial cells (fig. 47). Turnbull's blue and Hutchison's iron reaction demonstrate the presence of ferrous or ferric ions in the interglandular macrophages and in the supranuclear cytoplasm of the gland epithelial cells (fig. 48).

DISCUSSION

The bilateral endometrial pads or ridges of the tupalid uterus appear to be analogous to the uterine caruncles found in most ruminants. Caruncles are "... specialised non-glandular areas to which the foetal cotyledons become attached, and are essentially local thickenings of the subepithelial dense connective tissue which elsewhere exists as a thin layer immediately beneath the epithelium." (Amoroso, '52). The tupalid endometrial pads and the ruminant caruncles are specialized sites for placental development, and both are gland-free endometrial modifications evident in immature animals. Endometrial pads are prominently developed at the time of birth, and Mossman ('37) reported that caruncles are grossly differentiated in female cow fetuses of 40 cm CR.

Prominent bilateral mucosal folds or endometrial cushions project into the uterine lumen of shrews (family Soricidae) with free uterine blastocysts (Hubrecht 1894a; Brambell and Perry, '45; Wimsatt

vert signs of epithelial degeneration. A slightly later implantation stage shows degenerating epithelial cells which have been separated from their basement membrane by the invading trophoblast.

Enders ('63, '64) suggested that the initial penetration of the endometrium by the armadillo blastocyst is accomplished by the distintegration of a localized region of the uterine epithelium. After the initial penetration there is little additional epithelial loss. The remaining epithelial cells deteriorate only after the invasive trophoblast separates them from their normal vascular relationships. Preliminary observations on the fine structure of implantation in the hamster suggest that after initial attachment of the blastocyst to the endometrium, trophoblastic cells penetrate between epithelial cells and send horizontal processes which detach the epithelial cells from their underlying basement membrane (Luckett, W. P. and M. W. Orsini, unpublished observations). A similar mechanism is postulated for implantation in the tree shrew.

Mitoses are evident in the cytotrophoblast of the attachment plaques, but not in the giant cells. The latter probably arise by fusion of cytotrophoblastic cells, although there is no direct evidence for this. Neither is there any evidence to support Hubrecht's (1899) contention that giant cells are formed by amitotic division of trophoblastic nuclei. The tupaiid giant cells appear to be involved primarily with penetration of the basement membrane of the uterine epithelium and the formation of cores for the subsequent development of the multinucleated primary villi. The disappearance of giant cells from the main body of the placental discs with the establishment of the chorio-vitelline placenta accounts for the reports that giant cells do not occur in the tree shrew placenta (van der Horst, '49; Meister and Davis, '56, '58). These authors lacked the late implantation stages which are characterized by the prominent zone of giant cells.

The basement membrane of the endometrial pad epithelium appears to form a temporary barrier to trophoblastic invasion, since it persists for a longer time than does the overlying epithelium. It is penetrated only after the differentiation of the layer

of multinucleated giant cells. The fine structural studies of implantation in the rabbit (Larsen, '61), rat (Enders and Schlafke, '67) and the hamster (Luckett, W. P. and M. W. Orsini, unpublished observations) also suggest the probability that the basement membrane acts as a temporary barrier to the invasive trophoblast.

Hill ('65) described decidual knot formation in an early stage of chorio-vitelline placentation in *Tupaia minor*. He noted that these masses are formed by the fusion of decidual cells and "... are syncytial formations, maternal in origin and destined eventually to be resorbed and so we may adopt for them the designation maternal symplasma or simply symplasma, a term suggested by Bonnet."

The term symplasma does indicate maternal tissue that loses its cellular boundaries and is destined for destruction, but in almost all cases it connotes uterine epithelium that undergoes this characteristic reaction. Symplasmic reaction of epithelium associated with implantation typically occurs in some of the Old and New World monkeys (Hill, '32). Because the syncytial modifications of the tupaiid endometrium involve decidual cells rather than epithelium, and since the reaction occurs during early chorio-vitelline placentation rather than at implantation, the term "decidual knots" is preferred for these masses.

Hubrecht (1899) used the term "trophospongia" to describe the maternal decidual tissue of *Tupaia*. He made no reference to the decidual knots, although they can be seen in several of his figures. Hubrecht (1889) first used the term trophospongia to describe "... the product of the further continuation of the endothelial proliferation" during the development of the hedgehog placenta. He believed that this proliferated maternal endothelium or trophospongia conducts maternal blood from the endothelial-lined decidual vessels to the trophoblast-lined lacunae at the fetal surface of the placenta. Thus, trophospongia in the hedgehog refers only to modified maternal endothelial cells and not to decidual cells. Unfortunately, the development of the hedgehog placenta has not been re-examined in detail since Hubrecht's publication.

The occurrence of an expanded bilaminar blastocyst in the ovarian end of the uterine horn in an instance of pregnancy during lactation suggests lactational delay of implantation in tree shrews. It is uncertain from most reports of delayed implantation in other species whether blastocysts are distributed throughout the uterine horn during the delay period or whether they accumulate at the ovarian end of the horn. There is some evidence that blastocysts are distributed throughout the uterine horn during the delay period in both the rat (Krehbiel, '41) and the European badger (Canivenc, '66), but information appears to be lacking for other species.

Hopefully, more information will be obtained about possible lactational delay of implantation in tree shrews from a study of these animals in captivity. It will be interesting to determine whether there is actually a delay in attachment, as appears likely in the rat, or whether there is a delay in distribution of the blastocysts to the optimal sites of implantation. The latter phenomenon is suggested in the single delayed specimen of *Tupaia* available.

The irregular epithelial crypts that develop in the surface epithelium of the endometrium, including that of the endometrial pads, are best seen in *Tupaia longipes*. A few crypts are seen just prior to implantation in *T. javanica*, and there is a suggestion of crypt formation in *T. minor* in a later stage of implantation. The crypts seen in *T. longipes* at the time of implantation appear identical to those of nulliparous *T. chinensis* treated with exogenous estrogen plus progesterone (Conaway and Sorenson, '66). Hubrecht (1899) made no mention of epithelial crypts prior to or at the time of implantation in *T. javanica*, but several of his drawings depict the radial arrangement of epithelial and trophoblastic cells seen in the implantation plaque of *T. minor*. This radial arrangement is best interpreted as the result of interdigitation of trophoblastic and epithelial elements at the time of attachment. An analogous condition of crypt formation occurs in the cat during the second week after ovulation, at the time when blastocysts lie free in the uterine lumen (Courrier and Gros, '32; Dawson and Kosters, '44).

Prominent epithelial thickenings are formed in shrews just prior to implantation on both the antimesometrial and lateral walls of the endometrium (Hubrecht, 1894a; Sansom, '37; Brambell and Perry, '45; Wimsatt and Wislocki, '47). The antimesometrial thickenings give rise to epithelial crypts which mark the site of the future development of the chorio-allantoic placenta. Implantation occurs circumferentially on the lateral epithelial thickenings, but there is no crypt development.

The formation of epithelial crypts on the uterine caruncles prior to the formation of trophoblastic villi occurs in the Bovidae (Björkman, '54) and Cervidae (Hamilton, Harrison and Young, '60). The epithelial crypts are the sites of attachment and invasion of trophoblastic villi; crypts do not form in the intercaruncular regions.

Superficial, central implantation or attachment of an expanded blastocyst which fills most or all of the uterine lumen is characteristic of the Tupalidae, the insectivorous groups Soricidae, Talpidae and *Chrysochloris*, the order Carnivora, and all of the taxa with an epitheliochorial or syndesmochorial placenta: Lemuroidea, Lorisioidea, Artiodactyla, Perissodactyla, Pholidota and probably Cetacea (Mossman, '37). In all of these groups the initial attachment is either circumferential or bilateral, but only the Tupalidae, Soricidae, Talpidae and *Chrysochloris* exhibit noticeable endometrial modifications in this region prior to implantation.

There is no evidence to support Hubrecht's (1899) description of the blending together of trophoblast and uterine epithelium at the time of implantation to form a common coalescing plasmodium ("einem gemeinschaftlichen Verschmelzungspasmodium"). Plasma membranes separate trophoblastic and epithelial cells up until the time that epithelial cells begin to degenerate.

The degeneration of epithelial cells in later stages of implantation appears to be initiated by their separation from the basement membrane by the amoeboid activity of the trophoblast rather than by cytolytic activity of the trophoblast. In early implantation stages cytotrophoblastic cells send processes between epithelial cells toward the basement membrane, but there are no

vert signs of epithelial degeneration. A slightly later implantation stage shows degenerating epithelial cells which have been separated from their basement membrane by the invading trophoblast.

Enders ('63, '64) suggested that the initial penetration of the endometrium by the armadillo blastocyst is accomplished by the disintegration of a localized region of the uterine epithelium. After the initial penetration there is little additional epithelial loss. The remaining epithelial cells deteriorate only after the invasive trophoblast separates them from their normal vascular relationships. Preliminary observations on the fine structure of implantation in the hamster suggest that after initial attachment of the blastocyst to the endometrium, trophoblastic cells penetrate between epithelial cells and send horizontal processes which detach the epithelial cells from their underlying basement membrane (Luckett, W. P. and M. W. Orsini, unpublished observations). A similar mechanism is postulated for implantation in the tree shrew.

Mitoses are evident in the cytotrophoblast of the attachment plaques, but not in the giant cells. The latter probably arise by fusion of cytotrophoblastic cells, although there is no direct evidence for this. Neither is there any evidence to support Hubrecht's (1899) contention that giant cells are formed by amitotic division of trophoblastic nuclei. The tupaiid giant cells appear to be involved primarily with penetration of the basement membrane of the uterine epithelium and the formation of cores for the subsequent development of the multinucleated primary villi. The disappearance of giant cells from the main body of the placental discs with the establishment of the chorio-vitelline placenta accounts for the reports that giant cells do not occur in the tree shrew placenta (van der Horst, '49; Meister and Davis, '56, '58). These authors lacked the late implantation stages which are characterized by the prominent zone of giant cells.

The basement membrane of the endometrial pad epithelium appears to form a temporary barrier to trophoblastic invasion, since it persists for a longer time than does the overlying epithelium. It is penetrated only after the differentiation of the layer

of multinucleated giant cells. The fine structural studies of implantation in the rabbit (Larsen, '61), rat (Enders and Schlafke, '67) and the hamster (Luckett, W. P. and M. W. Orsini, unpublished observations) also suggest the probability that the basement membrane acts as a temporary barrier to the invasive trophoblast.

Hill ('65) described decidual knot formation in an early stage of chorio-vitelline placentalation in *Tupaia minor*. He noted that these masses are formed by the fusion of decidual cells and "... are syncytial formations, maternal in origin and destined eventually to be resorbed and so we may adopt for them the designation maternal symplasma or simply symplasma, a term suggested by Bonnet."

The term symplasma does indicate maternal tissue that loses its cellular boundaries and is destined for destruction, but in almost all cases it connotes uterine epithelium that undergoes this characteristic reaction. Symplasmic reaction of epithelium associated with implantation typically occurs in some of the Old and New World monkeys (Hill, '32). Because the syncytial modifications of the tupaiid endometrium involve decidual cells rather than epithelium, and since the reaction occurs during early chorio-vitelline placentalation rather than at implantation, the term "decidual knots" is preferred for these masses.

Hubrecht (1899) used the term "trophospongia" to describe the maternal decidual tissue of *Tupaia*. He made no reference to the decidual knots, although they can be seen in several of his figures. Hubrecht (1889) first used the term trophospongia to describe "... the product of the further continuation of the endothelial proliferation" during the development of the hedgehog placenta. He believed that this proliferated maternal endothelium or trophospongia conducts maternal blood from the endothelial-lined decidual vessels to the trophoblast-lined lacunae at the fetal surface of the placenta. Thus, trophospongia in the hedgehog refers only to modified maternal endothelial cells and not to decidual cells. Unfortunately, the development of the hedgehog placenta has not been re-examined in detail since Hubrecht's publication.

Hubrecht (1899) described the proliferation of intervacular connective tissue to give rise to trophospongiol connective tissue in the tree shrew placenta. His description and figures indicate that trophospongia in this case is maternal decidual tissue. In a later publication ('08) he stated that trophospongia indicates a maternal cell proliferation, but he did not specify whether it is endothelial, stromal or both. The name trophospongia is no longer used to describe maternal tissue, and it is easily confused with the term "trophospongium," which describes a trophoblastic zone that contains maternal blood channels but no fetal capillaries (Orsini, '54).

The loose zone formed by the degenerating decidual knots appears to provide a pathway for the subsequent invasion of primary villi. The reason for the fusion of decidual cells to form knots prior to their degeneration is unknown. Multinucleated primary villi appear to develop around a core of giant cells; they are first evident when avascular mesoderm separates the endoderm and trophoblast of the placental disc. There is no evidence of mitoses in the primary villi, and presumably they differentiate from the cytotrophoblast of the chorionic plate.

Hill ('65) believed that the cytotrophoblast of the chorionic plate becomes transformed into syntrophoblast at the end of the period of chorio-vitelline placentation. However, he reported the occurrence of mitotic figures in this syntrophoblast and admitted that this is an exceptional phenomenon. There are no well-documented cases for mitotic activity occurring in syntrophoblast, and evidence from autoradiography (Richart, '61; Midgley, Pierce, Deneau and Gosling, '63) and electron microscopy (Carter, '64; Pierce, Midgley and Beals, '64; Enders, '65; Boyd and Hamilton, '66) of human and rhesus monkey placentae indicates that syntrophoblast differentiates from cytotrophoblastic cells which are incorporated into the syncytium and subsequently lose their plasmalemmas.

In all stages of chorio-vitelline placentation examined in the present study, the chorionic plate consists of cytotrophoblast which is continuous with the irregular primary villi. Plasma membranes are apparent in structures labeled as "syncytio-

trophoblast" in Plate VII of Hill's ('65) paper. In addition, structures labeled as "symplesma" in his Plates IIIa, Vb, and VI are identical to the multinucleated primary villi described in the present study. One of Hill's figures shows giant cells buried in the cores of two "symplesmic masses" which are really primary villi. The more densely nucleated primary villous processes which have penetrated deeper into the decidual knot zone and can be seen partly surrounding several decidual knots are also labeled as "symplesma" by Hill.

Hubrecht (1899) and van der Horst ('49) have emphasized the difficulties involved in distinguishing between fetal and maternal tissues in the developing chorio-vitelline placenta of *Tupaia*. Nuclear morphology is quite similar in both primary villi and decidual knots, and it is frequently necessary to follow serial sections in order to determine the identity of a particular densely nucleated mass. Hill's ('65) misinterpretation of tissue relationships during chorio-vitelline placentation apparently resulted from the gap in his series of developmental stages. His earliest is an incipient stage of chorio-vitelline placentation, since the bilaminar omphalopleure still covers the major portion of the placental disc. His next stage is transitional between chorio-vitelline and chorio-allantoic placentation. This gap, which covers most of the period of chorio-vitelline placentation, is filled in the present study by nine specimens which consist of all stages of this critical period.

The vascular chorio-vitelline placenta of tupaiids appear to play an important role in fetal-maternal exchange, since they are prominently developed through the early limb bud stage. Maternal capillaries are embedded in the chorionic plate; in many places they are separated from the fetal vitelline capillaries by only 1-2 layers of cytotrophoblast.

Only a single layer of syntrophoblast covers the maternal capillary tubules of the tupaid labyrinth, whereas other mammalian endotheliochorial or hemochorial placentae are generally characterized by having both cytotrophoblastic and syntrophoblastic layers, at least in the early stages. This cytotrophoblast may be reduced or absent near term, and it is believed to give rise to the syntrophoblast. A

noticeable exception to this pattern is the armadillo placenta, which possesses only a single layer of syntrophoblast in the labyrinth, similar to the tupaiid condition (Enders, '60a,b). Cytotrophoblastic cell columns occur at the tips of the early chorio-allantoic villi in the armadillo and apparently act as a source of proliferation for the syntrophoblast of the villi, since the cytotrophoblast does not persist in the chorionic plate.

Chorionic plate cytotrophoblast and the multinucleated cell columns are the most likely sources of syntrophoblast in the tupaiid labyrinth. Mitoses occur in the chorionic plate but not in the cell columns. Both chorionic plate cytotrophoblast and cell columns have disappeared in late stages of pregnancy.

The epithelioid allantoic mesenchymal cells of the tupaiid labyrinth are strikingly similar to those of the shrew placenta (Wimsatt and Wislocki, '47; Mossman and Owers, '63). In both groups these cells differentiate early during the formation of the chorio-allantoic placenta and persist until term. Mossman and Owers ('63) believed that the trophoblast is lost in the labyrinth of the shrew placenta and they classified it as endothelio-endothelial. They suggested that the epithelioid mesenchyme of the shrew placenta is possibly an adaptation to the absence of trophoblast. However, Wimsatt and Wislocki ('47) stated that a thin layer of syntrophoblast persists in the labyrinth, and they classified the shrew placenta as endotheliochorial.

Enders ('60a) reported that the mesenchymal cells of the chorio-allantoic placenta from late pregnant armadillos are rounded, gland-like cells with pronounced cytoplasmic basophilia. The presence of vast amounts of dilated rough endoplasmic reticulum containing moderately electrondense material within their cisternae and of a well developed Golgi complex suggests that these cells are involved in protein secretion (Enders, '60b). Modified mesenchymal cells are not seen in early stages of armadillo placentation.

The epithelioid mesenchymal cells of the shrew and tree shrew placentae do not appear to be closely related to those of the armadillo. They are prominent from the earliest stages, and their cytoplasm does not

exhibit marked basophilia. Histochemical and electron microscopic examinations may provide some evidence of their function.

The persistence of maternal endothelium in the tupaiid labyrinth was previously reported by van der Horst ('49) and Hill ('65). Hubrecht (1899) believed that this endothelium degenerates after it becomes surrounded by syntrophoblast, however, his figures that illustrate this point are not convincing. Maternal capillaries are clearly surrounded by trophoblast in his figure 54; in fact, his stages illustrating "loss" of maternal endothelium are prior to the establishment of the chorio-vitelline placenta. Meister and Davis ('56, '58) believed that the endotheliochorial labyrinth of early stages is converted to the hemochorial type near term, but all of their figures show hypertrophied maternal endothelium adjacent to a thin layer of syntrophoblast. These authors did not attempt to demonstrate the presence of basement membranes by histochemical techniques. Since the three species examined by Hubrecht and Meister and Davis are represented in the present study, the possibility of species differences is ruled out.

The thin incomplete zone of chromatic masses at the base of the placental discs in late stages of pregnancy may represent remnants of both cell columns and decidual knots. The nuclei of both of these cell types become hyperchromatic, and it is impossible to determine whether one or both contribute to the chromatic masses. The basal layer of hyperchromatic and pyknotic nuclei in the placenta of American shrews has been interpreted as syntrophoblast (Wimsatt and Wislocki, '47) or as a symplasmic remnant of uterine gland epithelium (Mossman and Owers, '63). The chromatic masses are strikingly similar in these two families. The possible derivation of these masses from glandular epithelium in soricids and from uterine stroma in tupaiids does not pose a major problem in homology, since both of these tissues are mesodermal derivatives.

Placentae obtained at normal births indicate that separation from the uterus occurs between the zone of basal chromatic masses and the thin zone of unmodified stroma. The present study refutes the con-

tention that the placentae of *Tupaia* degenerate *in situ* after the delivery of the fetus (van Herwerden, '06; Hubrecht, '08). It is possible that the "puerperal" uteri examined by van Herwerden were examples of embryonic resorption. Several uteri with resorbing embryos were seen during the present study, and they show evidence of partial degeneration of the placentae *in situ*.

The appearance of the yolk sac is relatively similar during the early stages of pregnancy in most mammalian orders, but several modifications may occur during later stages of gestation. (1) The yolk sac may become completely vascularized and persist as a relatively large structure, (2) the completely vascularized yolk sac may become extremely reduced or vestigial in later stages, (3) mesoderm and vitelline vessels may never extend to separate the layers of the abembryonic or distal wall of the yolk sac, and the vascular splanchnopleure may then be closely apposed to the persisting bilaminar orphalopleure, resulting in an *incompletely inverted yolk sac*, and (4) a completely inverted yolk sac is formed when the bilaminar omphalopleure is completely lost and the endoderm of the vascular splanchnopleure is directly exposed to the endometrium (Mossman, '37).

A large, free vascular yolk sac occurs in reptiles and birds and probably represents a primitive condition; among eutherian mammals it is retained in the Tupaiidae and the Carnivora. The taxa with a reduced or vestigial vascular yolk sac include the Primates, Artiodactyla, Perissodactyla, Cetacea, Megachiroptera, the family Centetidae of the Insectivora, the family Bradypodidae of the Edentata and several families of Microchiroptera (Mossman, '37; Goetz, '37b; Moghe, '51; Gopalakrishna, '58). Inverted yolk sacs are characteristic of Rodentia, Lagomorpha, most Insectivora and several families of Microchiroptera (Mossman, '37; Wimsatt, '54; Gopalakrishna, '58).

The tupaïid yolk sac is strikingly similar to that of the most primitive family of carnivores, the Viverridae. The free yolk sac of a late stage of pregnancy of *Paradoxurus* occupies a greater cross-sectional area than is usually seen in other carnivores; this appears to be a case of

primitive retention (Moghe, '56; personal observations).

Meister and Davis ('56, '58) reported that the allantoic vesicle of *Tupaia* is large in early pregnancy, becoming small near term; the vesicle does not reach the fetal surface of the placenta at any stage of pregnancy." These authors sectioned the uterus with the fetus *in situ* from an early stage of chorio-allantoic placentation; however, in the three later stages which they studied, only the placental discs appear to have been sectioned. The structure identified as the allantoic vesicle in figure 2 of their 1958 paper bears no resemblance to the allantois seen at any stage of development during the current study. Examination of placental discs alone from later stages provides little information about the nature of the allantoic vesicle, since it is intimately fused with the chorion, amnion and the surface of the placental discs. Examination of serial sections during the present study demonstrates the continuity between urachus, allantoic duct and the large persisting allantoic vesicle.

The retention of a large allantoic vesicle in late stages of pregnancy is characteristic of reptiles, birds and all of the mammalian taxa that possess an epitheliochorial placenta: Artiodactyla, Perissodactyla, Pholidota, Cetacea and Lemuroidea. A large allantoic vesicle is also found in the subungulate orders Proboscidea, Sirenia and Hyracoidea, and in many, but not all, of the taxa that have an endotheliochorial placenta: Carnivora, Tubulidentata, Tupaiidae and Talpinae (Mossman, '37, '57). The only known occurrence of a large allantoic vesicle associated with a hemochorial placenta occurs in several families of Insectivora: Centetidae, Potamogalidae and Chrysochloridae (Goetz, '37b; Strauss, '43; Hill, '38; Hintzsche, '40).

It has been suggested that the presence of a large allantoic vesicle is correlated with the development of a large functional mesonephric kidney (Bremer, '16). Large and apparently functional mesonephroi are found in birds, reptiles, pigs and sheep and all of these forms possess a large allantois. Both mesonephroi and allantoic vesicles are reduced or vestigial in rodents and the human. The best evidence for the correlation between the functional develop-

ment of the mesonephros and the size of the allantois is presented by Davies ('52) for the sheep. Histochemical and morphological evidence suggests that the sheep mesonephros becomes functional on about the 18th day of gestation, and this appears to be correlated with the sudden expansion of the allantoic vesicle and an accumulation of fluid within it. Although the tree shrew possesses a moderately well developed mesonephros, it is uncertain whether its large allantoic vesicle has a functional significance or whether it is another example of primitive retention.

The small depressions of the smooth chorio-allantoic membrane of *Dendrogale* are probably analogous to the variety of paraplacental absorptive areas that occur in all of the groups that possess an epitheliochorial placenta, as well as in the Carnivora, Talpidae and Tubulidentata (Amoroso, '52; Mossman, '57, '67b). Hill ('65) observed several shallow crypts in the trophoblast of the chorio-vitelline membrane in a single specimen of *Tupaia dorsalis*. He suggested that the crypts are possibly vestiges of the chorionic vesicles found in Talpidae, Lemuroidea and the ungulates. The rudimentary development and scarcity of these structures observed in the present study support this suggestion. The phagocytosis of red blood cells in *Dendrogale* by the trophoblast of the vestigial chorionic vesicles and the smooth chorio-allantoic membrane in general supports the hypothesis of Sinha and Mossman ('66) that the placental hematomas characteristic of carnivores are derived from specialized chorionic vesicles or areolae.

Uterine glands are secretory throughout pregnancy in tupiids and in most taxa that possess an epitheliochorial or endotheliochorial placenta; this "histotrophe" appears to play an important role in fetal nutrition (Amoroso, '52).

Macrophages containing hemosiderin, an iron-containing compound related to ferritin, accumulate at the sites of previous placentae in many mammals to form so-called "placental scars" (Nomberg and Conway, '56). The similarity of the supranuclear granules in the cytoplasm of the glandular epithelium to the hemosiderin granules of the macrophages, and the pos-

sitive iron test for both suggest the possibility that hemosiderin is transferred from macrophages to the glandular epithelium in tree shrews. Ferritin does not normally penetrate the cell plasmalemma, but there is good evidence that under both normal and experimental conditions it can enter cells by the process of micropinocytosis (Fawcett, '65). It is quite possible that hemosiderin enters the basal glandular epithelial cells by a similar mechanism.

The occurrence of iron in the apical cytoplasm of the basal uterine glands during pregnancy has been reported in the rat, guinea pig, pig and woman (Wislocki and Dempsey, '45). These authors believed that the presence of iron in the uterine glands is a consequence of pregnancy, since tests for iron are negative in nonpregnant specimens. In contrast, Wislocki and Dempsey were unable to detect iron in the uterine glands of the cat at any time. They attributed this to the presence of placental hematomas in cats and other carnivores as specialized sites of iron uptake from extravasated maternal red blood cells. This hypothesis should be tested on a variety of other mammals, both with and without placental hematomas.

De Lange and Nierstrasz's ('32) report that amniotic folds first appear in the 4-6 somite stage is confirmed by the present study. However, they believed that the amniotic head fold is initially a proamnion, that is, formed by ectoderm and endoderm but lacking mesoderm, similar to the condition in the early avian embryo. They noted the complete closure of the amniotic folds in the 23 somite stage (corresponding to the time when the vascular allantois has reached the wall of the chorion), although the proamnion still covered a considerable portion of the anterior trunk region. There is no evidence for a proamnion in any stage of amniogenesis in the present study. In all specimens the amniotic folds are composed of an ectodermal and mesodermal layer.

De Lange and Nierstrasz ('32) described the formation of an "archamnionic cavity" in the inner cell mass of *Tupaia javanica* prior to implantation, but similar stages were not available for the present study. This cavity in the inner cell mass is formed by a separation of cells; the subsequent

thinning of both Rauber's layer and the roof of the archamniotic cavity results in its opening into the uterine lumen and the flattening of the cup-shaped disc to form the embryonic shield. Archamniotic formation and loss occur prior to implantation, whereas the formation of the true amnion by folding occurs in the 4-6 somite stage. A similar process of archamnion formation and rupture appears to occur also in the musk shrew *Crocidura caerulea* (= *Suncus murinus*) (Sansom, '37), moles (Goetz, '38; Prasad, '58) and in ungulates and carnivores (Goetz, '38). In all of these forms the true amnion is formed by folding.

Although experimental evidence is lacking, the fetal membrane morphogenesis of the tupaiids suggests the possibility of a variety of regions for feto-maternal exchange that frequently overlap temporally. Uterine gland secretion appears to play an important nutritive role from the preimplantation through the early chorio-vitelline placental phases. Secretory activity is reduced during chorio-allantoic placentation, but the increased vascularity and modification of the mid-mesometrial region of the smooth chorio-vitelline membrane suggest that it is involved in the uptake of uterine secretion. Iron appears to be supplied to the fetus in part by uterine gland secretion. The antimesometrial smooth chorio-allantoic membrane is capable of phagocytizing RBC's and is probably involved in absorption of uterine gland secretion. The chorio-vitelline placentae are well developed through the early limb bud stage, and the proximity of fetal and maternal capillaries suggests an efficient exchange mechanism. The degenerating decidual knot zone may provide material for phagocytosis by the trophoblast during the period of chorio-vitelline placentation. The chorio-allantoic placentae replace the chorio-vitelline placentae both topographically and functionally.

The renewed interest in the phylogenetic relationships of the Tupaiidae warrants a detailed re-evaluation of the phylogenetic implications of the tupaiid fetal membranes on a broad comparative basis, and this is the subject of a paper now in preparation. Synopsis of Basic Data on the Fetal Membranes of the Tree Shrews *Tupaia*, *Lyonogale*, *Urogale*, *Dendrogale*, *Anathana*

Implantation:

Orientation (disc): Antimesometrial
Orientation (first attachment): Bilateral
Depth: Superficial

Decidua: Basalis forms "decidual knots," no capsularis

Amniogenesis: "Archamnion" formed by cavitation prior to implantation; true amnion formed by folding

Yolk sac:

Bilaminar omphalopleure: Temporary
Chorio-vitelline placentae: Bilateral; well developed until early limb bud stage

Vascular splanchnopleure: Large, free vascular yolk sac; no inversion of germ layers

Chorio-allantoic Placentae:

Shape: Discoidal
Type: Labyrinthine
Finer morphology: Endotheliochorial
Location: Bilateral

Allantoic vesicle: Large; permanent

Authorities: Hubrecht, 1899; van der Horst, 1949; Hill, 1965; Verma, 1965; Luckett, 1968

ACKNOWLEDGMENTS

I would like to thank Dr. H. W. Mossman and Dr. J. W. Anderson for their critical reading of this manuscript. M. G. Burroughs prepared the diagrams of the fetal membranes.

LITERATURE CITED

- Amoroso, E. C. 1952 Placentation. In: Marshall's Physiology of Reproduction, Vol. II, A. S. Parkes, ed., Longmans, Green and Company, London.
- Björkman, N. 1954 Morphological and histochemical studies on the bovine placenta. *Acta Anat.* 22, Suppl. 22-2: 1-97.
- Bluntschli, H. 1938 Le développement primaire et l'implantation chez un centetiné (*Hemicentetes*). *Compt. Rend. Assoc. Anat.*, 1-8.
- Boyd, J. D., and W. J. Hamilton 1966 Electron microscopic observations on the cytotrophoblastic contribution to the syncytium in the human placenta. *J. Anat.*, 100: 535-548.
- Brambell, F. W. R., and J. S. Perry 1945 The development of the embryonic membranes of the shrews, *Sorex araneus* Linn. and *Sorex minutus* Linn. *Proc. Zool. Soc. Lond.*, 115: 251-278.

- Bremer, J. L. 1916 The interrelations of the mesonephros, kidney and placenta in different classes of animals. *Am. J. Anat.*, 19: 179-210.
- Joettner-Janusch, J. 1966 *Origins of Man*. John Wiley and Sons, New York.
- Suder, H. 1962 A vascular adaptation to early pregnancy in the Senegal bush baby (*Galago senegalensis senegalensis*). *Sudan Med. J.*, 1: 89-97.
- 1964 The reproductive biology of a strepsirrhine (*Galago senegalensis senegalensis*). *Int. Review Gen. Exp. Zool.*, 1: 241-296.
- 1967 The oestrus cycle of the Senegal bush baby (*Galago senegalensis senegalensis*) in the Sudan. *J. Zool.*, 151: 143-162.
- Campbell, C. B. G. 1966 The relationships of the tree shrews: The evidence of the nervous system. *Evol.*, 20: 276-281.
- Canivenc, R. 1966 A study of progestation in the European badger (*Meles meles* L.). In: *Comparative Biology of Reproduction in Mammals*, I. W. Rolands, ed., Academic Press, London and New York.
- Carter, J. E. 1964 Morphological evidence of syncytial formation from the cytotrophoblastic cells. *Obst. Gynec.*, 23: 647-656.
- Clark, W. E. Le Gros 1962 *The Antecedents of Man*. 2nd Edition, Edinburgh University Press, Edinburgh.
- Conaway, C. H., and M. W. Sorenson 1966 Reproduction in tree shrews. In: *Comparative Biology of Reproduction in Mammals*, I. W. Rolands, ed., Academic Press, London and New York.
- Conisbee, L. R. 1953 A list of the names proposed for genera and subgenera of recent mammals. *British Museum (Nat. Hist.)*, London.
- Courrier, R., and G. Gros 1932 Contribution à l'étude du cycle génital chez la chatte. *Comp. Rend. Soc. Biol.*, 110: 51-53.
- Davies, J. 1952 Correlated anatomical and histochemical studies on the mesonephros and placenta of the sheep. *Am. J. Anat.*, 91: 263-300.
- Dawson, A. B., and B. A. Kusters 1944 Preimplantation changes in the uterine mucosa of the cat. *Am. J. Anat.*, 75: 1-37.
- Enders, A. C. 1960a Development and structure of the villous haemochorial placenta of the nine-banded armadillo (*Dasypus novemcinctus*). *J. Anat.*, 94: 34-45.
- 1960b Electron microscopic observations on the villous haemochorial placenta of the nine-banded armadillo (*Dasypus novemcinctus*). *J. Anat.*, 94: 205-215.
- 1963 Fine structural studies of implantation in the armadillo. In: *Delayed Implantation*, A. C. Enders, ed., U. Chicago Press, Chicago.
- 1964 Electron microscopy of an early implantation stage, with a postulated mechanism of implantation. *Dev. Biol.*, 10: 395-410.
- 1965 Formation of syncytium from cytotrophoblast in the human placenta. *Obstet. Gynec.*, 25: 378-386.
- Enders, A. C., and S. Schlafke 1967 A morphological analysis of the early implantation stages in the rat. *Am. J. Anat.*, 120(2): 185-226.
- Enzmann, E. V., N. R. Saphir and G. Pincus 1932 Delayed pregnancy in mice. *Anat. Rec.*, 54: 325-342.
- Fawcett, D. W. 1965 Surface specializations of absorbing cells. *J. Histochem. Cytochem.*, 13: 75-91.
- Fiedler, W. 1956 Übersicht über das System der Primates. In: *Primatologia*, Vol. I, H. Hofer, A. H. Schultz and D. Starck, eds., S. Karger, Basel and New York.
- Gabie, V. 1960 The placentation of *Eremitalpa granti* (Broom). *J. Morph.*, 107: 61-78.
- Goetz, R. H. 1937a Studien zur Placentation der Centetiden. II. Die Implantation und Frühentwicklung von *Hemicentetes semispinosus* (Cuvier). *Z. Anat. Entw.*, 107: 274-318.
- 1937b Studien zur Placentation der Centetiden. III. Die Entwicklung der Fruchthüllen und der Placenta bei *Hemicentetes semispinosus* (Cuvier). *Z. Anat. Entw.*, 108: 161-200.
- 1938 On the early development of the Tenrecoidae (*Hemicentetes semispinosus*). *Bio-Morphosis*, 1: 67-79.
- Goodman, M. 1967 Deciphering primate phylogeny from macromolecular specificities. *Am. J. Phys. Anthropol.*, 26: 255-276.
- Gopalakrishna, A. 1958 Foetal membranes in some Indian microchiroptera. *J. Morph.*, 102: 157-198.
- Grosser, O. 1909 Vergleichende Anatomie und Entwicklungsgeschichte der Eihäute und der Placenta. Wilhelm Braumüller, Vienna and Leipzig.
- Hamilton, W. J., R. J. Harrison and B. A. Young 1960 Aspects of placentation in certain Cervidae. *J. Anat.*, 94: 1-33.
- Harrison, B. 1963 Tree shrew (*Tupaia tana*) — a twin birth and consequences. *Sarawak Mus. J.*, 11: 262-265.
- Herwerden, M. van 1906 Die puerperalen Vorgänge in der Mucosa Uteri von *Tupaia javanica*. *Anat. Hefte*, 32: 155-169.
- Hill, J. P. 1932 The developmental history of the Primates. *Phil. Trans. Roy. Soc. Lond. (B)* 221: 45-178.
- 1938 The microscopic features of the placentation of the water-shrew (*Potamogale velox*). *Bio-Morphosis*, 1: 331-332.
- 1965 On the placentation of *Tupaia*. *J. Zool.*, 146: 278-304.
- Hintsche, E. 1940 Über Beziehungen zwischen Placentarbau, Urniere und Allantois. *Z. Mikr. Anat. Forsch.*, 48: 54-107.
- Horst, C. J. van der 1949 The placentation of *Tupaia javanica*. *Proc. Kon. Ned. Akad. Wet., Amsterdam*, 52: 1205-1213.
- 1954 *Elephantulus* going into anoestrus: Menstruation and abortion. *Phil. Trans. Roy. Soc. Lond. (B)* 238: 27-61.
- Horst, C. J. van der, and J. Gullman 1941 The menstrual cycle in *Elephantulus*. *S. Afr. J. Med. Sci.*, 6: 27-47.
- Hubrecht, A. W. 1889 Studies in mammalian embryology. I. The Placentation of *Erinaceus europaeus*, with remarks on the phylogeny of the placenta. *Quart. J. Micr. Sci.*, 30: 283-404.

1894a Studies in mammalian embryology. III. The placentation of the shrew (*Sorex vulgaris* L.). Quart. J. Micr. Sci., 35: 481-538.

1894b *Spolia nemoris*. Quart. J. Micr. Sci., 36: 77-125.

1895 Die Phylogenese des Amnions und die Bedeutung des Trophoblastes. Verhandl. Kon. Akad. Wetensch., Amsterdam, 2: 1-66.

1899 Ueber die Entwicklung der Placenta von *Tarsius* und *Tupaia*, nebst Bemerkungen ueber deren Bedeutung als haematopoietische Organe. Proc. 4th Internat. Cong. Zool., 343-412.

1908 Early ontogenetic phenomena in mammals and their bearing on our interpretation of the phylogeny of the vertebrates. Quart. J. Micr. Sci., 53: 1-181.

Kaiser, I. H. 1947a Histological appearance of coiled arterioles in the endometrium of rhesus monkey, baboon, chimpanzee and gibbon. Anat. Rec., 99: 199-225.

1947b Absence of coiled arteries in the endometrium of menstruating new world monkeys. Anat. Rec., 99: 353-367.

Krehbiel, R. H. 1941 The effects of lactation on the implantation of ova of a concurrent pregnancy in the rat. Anat. Rec., 81: 43-65.

Lange, D. de, Jr. 1919 Contribution to the knowledge of the placentation of the Cape goldmole (*Chrysochloris*). Bijl. tot Dierk., Amsterdam, 21: 161-173.

1933 Plazentabildung. Handb. Vergleich. Anat., 6: 155-234.

Lange, D. de, Jr., and H. F. Nierstrasz 1932 Tabellarische Übersicht der Entwicklung von *Tupaia javanica* Horsf. Ontogenese der Wirbeltiere in Übersichten, 1: 1-87.

Larsen, J. F. 1961 Electron microscopy of the implantation site in the rabbit. Am. J. Anat., 109: 319-334.

Lennep, E. W. van 1961 The histology of the placenta of the one-humped camel (*Camelus dromedarius* L.) during the first half of pregnancy. Acta Morph. Neerl. Scand., 4: 180-193.

Luckett, W. P. 1963 A histological examination of the female reproductive anatomy of tree shrews. Unpublished M. A. Thesis, University of Missouri.

Lyon, M. W., Jr. 1913 Tree shrews: An account of the mammalian family Tupaiidae. Proc. U. S. Nat. Mus., 45: 1-188.

McKenna, M. C. 1966a Paleontology and the origin of Primates. Folia Primat., 4: 1-25.

1966b Personal Communication.

Meister, W., and D. D. Davis 1956 Placentation of the pigmy treeshrew *Tupaia minor*. Fieldiana: Zool., 35: 73-84.

1958 Placentation of the terrestrial treeshrew (*Tupaia tana*). Anat. Rec., 132: 541-553.

Midgley, A. R., Jr., G. B. Pierce, Jr., G. A. Deneau and J. R. Gosling 1963 Morphogenesis of syncytiotrophoblast in vivo: An autoradiographic demonstration. Science, 141: 349-350.

Moghe, M. A. 1951 Development and placentation of the Indian fruit bat, *Pteropus giganteus* (Brünnich). Proc. Zool. Soc. Lond., 121: 703-721.

1956 Some observations on the foetal membranes of the Indian palmcivet, *Paradoxurus hermaphroditus hermaphroditus* (Schrater). Proc. Nat. Inst. Sci. India, 22: 41-47.

Momberg, H., and C. Conaway 1956 The distribution of placental scars of first and second pregnancies in the rat. J. Embryol. Exp. Morph., 4: 376-384.

Mossman, H. W. 1937 Comparative morphogenesis of the fetal membranes and accessory uterine structures. Contrib. Embryol. Carnegie Inst., 26: 129-246.

1939 The fetal membranes of Insectivora. Anat. Rec., 75: 102.

1953 The genital system and the fetal membranes as criteria for mammalian phylogeny and taxonomy. J. Mamm., 34: 289-298.

1957 The fetal membranes of the aardvark. Mitteilung. Naturforsch. Gesellschaft, Bern, 14: 119-128.

1965 The principal interchange vessels of the chorioallantoic placenta of mammals. In: Organogenesis, R. L. DeHann and H. Ursprung, eds., Holt, Rinehart and Winston, New York.

1967a Personal communication.

1967b In: Fetal Homeostasis, Vol. II, R. M. Wynn, ed., N. Y. Acad. Sci., New York.

Mossman, H. W., and N. Owers 1963 The shrew placenta: Evidence that it is endothelio-endothelial in type. Am. J. Anat., 113: 245-272.

Orsini, M. W. 1954 The trophoblastic giant cells and endovascular cells associated with pregnancy in the hamster, *Cricetus auratus*. Am. J. Anat., 94: 273-331.

1967 Personal communication.

Pierce, G. B., Jr., A. R. Midgley, Jr. and T. F. Beals 1964 An ultrastructural study of differentiation and maturation of trophoblast of the monkey. Lab. Invest., 13: 451-464.

Prasad, M. R. N. 1958 Morphogenesis of the fetal membranes of the American moles *Scalopus aquaticus*, *Scapanus latimanus* and *Parascalops breweri*. Unpublished Ph.D. Thesis, University of Wisconsin.

Ramaswami, L. S., and T. C. Anand Kumar 1965 Some aspects of reproduction of the female slender loris, *Loris tardigradus lydekkerianus* Cabr. Acta Zool., 46: 257-273.

Richart, R. 1961 Studies of placental morphogenesis. I. Radioautographic studies of human placenta utilizing tritiated thymidine. Proc. Soc. Exp. Biol. Med., 106: 829-831.

Romer, A. S. 1966 Vertebrate Paleontology. U. Chicago Press, Chicago.

Sansom, G. S. 1937 The placentation of the Indian musk-shrew (*Crocidura caerulea*). Trans. Zool. Soc. Lond., 23: 267-314.

Sinha, A. A., and H. W. Mossman 1966 Placentation of the sea otter. Am. J. Anat., 119: 521-554.

Strauss, F. 1943 Die Placentation von *Ericulus setosus*. Rev. Suisse Zool., 50: 17-87.

Valen, L. van 1965 Treeshrews, primates, and fossils Evolution, 19: 137-151.

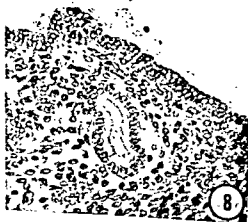
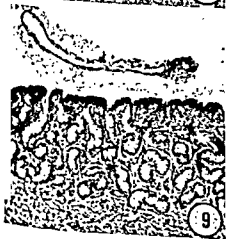
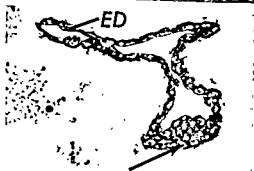
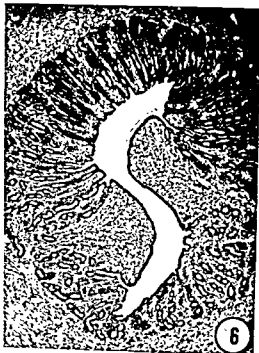
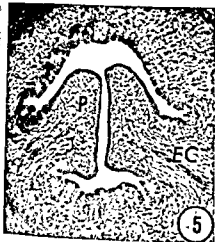
- erma, K. 1965 Notes on the biology and anatomy of the Indian tree-shrew, *Anathana wroughtoni*. *Mamm.*, 29: 289-330.
- Vimsatt, W. A. 1954 The fetal membranes and placentation of the tropical American vampire bat *Desmodus rotundus murinus*. *Acta Anat.*, 21: 285-341.
- Vimsatt, W. A., and G. B. Wislocki 1947 The placentation of the American shrews, *Blarina brevicauda* and *Sorex fumeus*. *Am. J. Anat.*, 80: 361-435.
- Wislocki, G. B., and E. W. Dempsey 1945 Histological reaction of the endometrium in pregnancy. *Am. J. Anat.*, 77: 365-403.
- Wood Jones, F. 1917 The genitalia of *Tupaia*. *J. Anat.*, 51: 118-126.
- Wright, P. 1966 Observations on the reproductive cycle of the American badger (*Taxidea taxus*). In: *Comparative Biology of Reproduction in Mammals*, I. W. Rowlands, ed., Academic Press, London and New York.

The mesometrium is toward the bottom of all figures unless otherwise indicated.

PLATE 1

EXPLANATION OF FIGURES

- 5 Cross section of uterine horn at 12 days postnatum. Note the prominent bilateral endometrial pads and the early glandular development in the mesometrial and antimesometrial regions. *T. longipes* 43. $\times 100$.
- 6 Cross section of uterine horn of immature animal. The increased thickness of the glandular endometrium causes the gland-free pads to appear less prominent. *T. minor* 46. $\times 63$.
- 7 Cross section of uterine horn during tubal blastocyst stage. Gomori's basic fuchsin stain shows the coiled arterioles beneath the pads. The endometrial pad, delimited by arrows, contains no coiled arterioles. *U. everetti* 3. $\times 63$.
- 8 Expanding bilaminar blastocyst unoriented in the uterine lumen. Rauber's layer (arrow) is complete over the embryonic knot. *T. glis* 78. $\times 250$.
- 9 Expanded bilaminar blastocyst near tubo-uterine junction. The delay in distribution of the blastocyst is presumably due to concurrent lactation. The mesometrium is toward the right. *T. longipes* 60. $\times 100$.



The mesometrium is toward the bottom of all figures unless otherwise indicated.

PLATE 1

EXPLANATION OF FIGURES

- 5 Cross section of uterine horn at 12 days postnatum. Note the prominent bilateral endometrial pads and the early glandular development in the mesometrial and antimesometrial regions. *T. longipes* 43. $\times 100$.
- 6 Cross section of uterine horn of immature animal. The increased thickness of the glandular endometrium causes the gland-free pads to appear less prominent. *T. minor* 46. $\times 63$.
- 7 Cross section of uterine horn during tubal blastocyst stage. Gomori's basic fuchsin stain shows the coiled arterioles beneath the pads. The endometrial pad, delimited by arrows, contains no coiled arterioles. *U. everetti* 3. $\times 63$.
- 8 Expanding bilaminar blastocyst unoriented in the uterine lumen. Rauber's layer (arrow) is complete over the embryonic knot. *T. glis* 78. $\times 250$.
- 9 Expanded bilaminar blastocyst near tubo-uterine junction. The delay in distribution of the blastocyst is presumably due to concurrent lactation. The mesometrium is toward the right. *T. longipes* 60. $\times 100$.

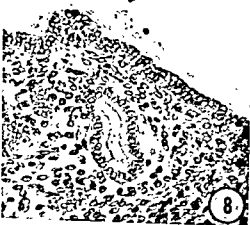
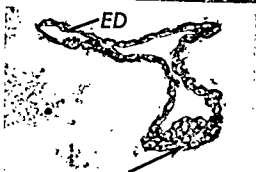
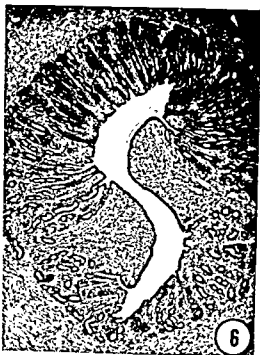


PLATE 2

EXPLANATION OF FIGURES

- 10 Early attachment phase of implantation. The intact uterine epithelium is closely apposed to the trophoblast, and the two cell types may be distinguished by their nuclear morphology. *T. picta* 53. $\times 660$.
- 11 Early stage of implantation. Epithelial crypts occur on the endometrial pad and they are partially invaded by the attached trophoblast. *T. longipes* 82. $\times 400$.
- 12 Uterine horn of early implantation stage, cranial to the attachment site. Epithelial crypts are well developed on both the glandular endometrium and the endometrial pads. The uterine glands are maximally coiled at this period. *T. longipes* 82. $\times 63$.
- 13 Attachment plaque during later stage of implantation. Some trophoblastic cells have insinuated between epithelial cells to reach the underlying basement membrane. Endometrial stromal cells are enlarging to form decidual cells (arrow). *T. minor* 50. $\times 560$.

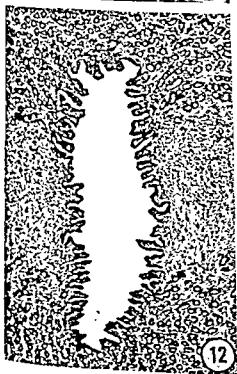


PLATE 3

EXPLANATION OF FIGURES

- 14 Further development of the attachment plaque. The numerous pyknotic nuclei are thought to be remnants of degenerating epithelial cells. Occasional apparently normal epithelial cells are evident. The endodermal lining of the bilaminar yolk sac overlies the attachment plaque. *T. minor* 51. $\times 560$.
- 15 Cross section of endometrial pad during early attachment phase of implantation. Note the radiation of capillaries from the arteriole at the base of the pad. The mesometrium is toward the left. *T. picta* 53. $\times 100$.
- 16 Period of differentiation of the attachment plaque. The trophoblast has differentiated into an inner cytotrophoblastic layer and an outer zone of multinucleated giant cells. The underlying stroma has differentiated into typical decidual tissue. *U. everetti* 4. $\times 250$.
- 17 Differentiated attachment plaque. Silver azan staining demonstrates the continuity of the basement membrane that underlies the uterine epithelium with the basement membrane that separates the trophoblastic giant cells from the decidua. *U. everetti* 4. $\times 250$.

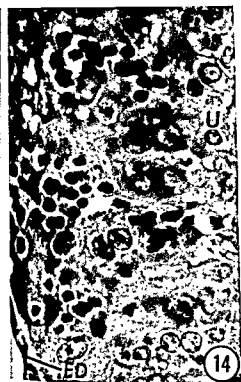


PLATE 4

EXPLANATION OF FIGURES

- 18 Marginal zone of attachment plaque. Trophoblastic giant cells have detached the uterine epithelium from its basement membrane. *U. everetti* 4. $\times 250$.
- 19 Deciduo-trophoblastic junction of late stage of implantation. The decidual cells (arrows) adjacent to the giant cells show increased cytoplasmic basophilia and hyperchromatic nuclei. *U. everetti* 4. $\times 400$.
- 20 Incipient placental disc covered by avascular trilaminar omphalo-pleure. Three characteristic regions are seen in cross section: (1) trophoblastic zone, (2) the zone of degenerating decidual knots, and (3) the basal decidua. *T. palawanensis* 46. $\times 110$.
- 21 Higher magnification near fetal surface of incipient placental disc. Irregular primary villi penetrate into the loose zone of necrotic decidual knots. Note the intact maternal capillaries surrounded by trophoblast. *T. palawanensis*. 46. $\times 250$.

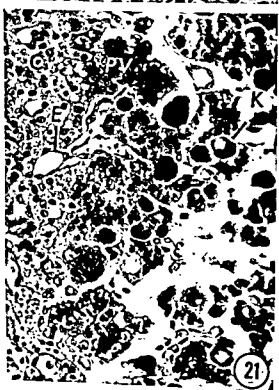
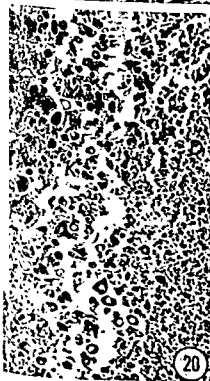
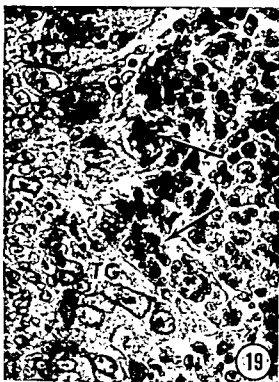


PLATE 5

EXPLANATION OF FIGURES

- 22 Junctional zone of decidua basalis and decidual knots in incipient placental disc. The decidual knots in cross section are characterized by a peripheral ring of nuclei and a central, common cytoplasmic core. Transitional stages occur between the basal decidual cells and the decidual knots. The mesometrium is toward the left. *T. palawanensis* 46. $\times 400$.
- 23 Near fetal surface of chorio-vitelline placenta. Primary villi are continuous with the cytotrophoblast. Some of the decidual knots show signs of degeneration. *T. glis* 76. $\times 250$.
- 24 Higher magnification of a primary villus. Note the intact endothelium of the maternal capillaries surrounded by cytotrophoblast. *T. glis* 76. $\times 400$.
- 25 Vascular chorio-vitelline placental disc. The interdigitated zone of primary villi and the decidual knots occupies about a third of the thickness of the disc. *T. javanica* 2. $\times 38$.

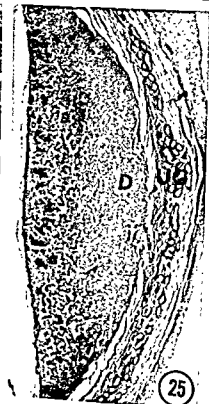
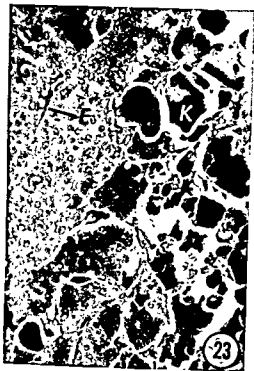
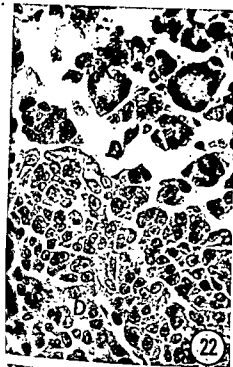


PLATE 6

EXPLANATION OF FIGURES

- 26 Paraplacental region of chorio-vitelline placental disc. Prominent trophoblastic giant cells detach the uterine epithelium in this region. *T. glis* 76. $\times 325$.
- 27 Deciduo-trophoblastic junction of chorio-vitelline placental disc. The densely nucleated primary villi are closely associated with degenerating decidual knots. The mesometrium is toward the left. *T. glis* 76. $\times 275$.
- 28 Initiation of chorio-allantoic placentation. The vascular allantois is detaching the antimesometrial portion of the vascular splanchnopleure of the yolk sac from the surface of the placental disc. *T. javanica* 6. $\times 28$.
- 29 Higher magnification of end of allantoic vesicle shown in fig. 28. Yolk sac splanchnopleure still covers the mesometrial portion of the placental disc. Vascular allantoic mesenchyme is beginning to indent the cytotrophoblast of the surface of the placental disc. *T. javanica* 6. $\times 110$.

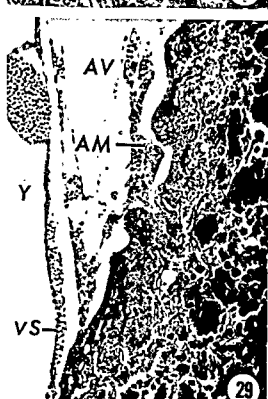
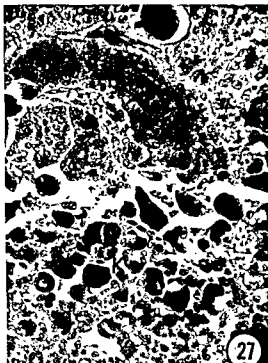


PLATE 7

EXPLANATION OF FIGURES

- 30 Early stage of chorio-allantoic placentation. Four zones are evident at this stage: (1) chorionic plate, (2) labyrinth, (3) the dense zone of primary villi and decidual knots, and (4) the decidua basalis. *T. javanica* 7. $\times 100$.
- 31 Base of the placental disc during early chorio-allantoic placentation. Densely nucleated primary villi interdigitate with the decidua basalis. Scattered decidual knots are evident. *T. javanica* 7. $\times 250$.
- 32 Fetal surface of the placental disc during early chorio-allantoic placentation. Note the continuity between the cytotrophoblast of the chorionic plate and the syntrophoblast of the labyrinth. Shrinkage has separated the syntrophoblast from the allantoic mesenchyme. The mesometrium is toward the left. *T. javanica* 7. $\times 350$.
- 33 Fetal surface of disc during early chorio-allantoic placentation. Note the persistence and hypertrophy of the maternal capillary endothelium adjacent to the chorionic plate cytotrophoblast and to the syntrophoblast of the labyrinth. The mesometrium is toward the left. *T. javanica* 161. $\times 400$.
- 34 Base of the placental disc of a stage later than that of figure 31. The densely multinucleated masses at the base of the disc are probably remnants of the trophoblastic cell columns. Note the accumulation of secretory product in the uterine glands beneath the disc. *T. javanica* 5. $\times 100$.
- 35 Base of placental disc from definitive chorio-allantoic placentation. Basal chromatic masses may represent remnants of cell columns or decidual knots. *T. montana* 62. $\times 300$.

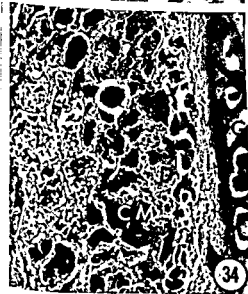
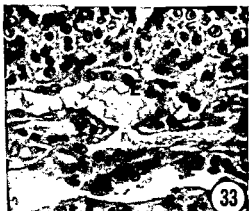
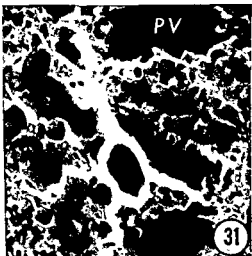
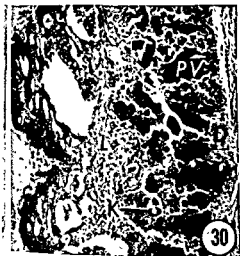


PLATE 8

EXPLANATION OF FIGURES

- 36 Cross section of placental disc from near term pregnancy. Most of the disc is occupied by the labyrinth. Note that the disc separates easily from the underlying stroma immediately beneath the incomplete layer of basal chromatic masses. *T. montana* 62. $\times 25$.
- 37 Labyrinth of near term chorio-allantoic placenta. Note the epithelioid appearance of the allantoic mesenchymal cells. A thin layer of syntrophoblast surrounds the modified endothelium of the maternal capillaries. *T. palawanensis* 68. $\times 250$.
- 38 Labyrinth of near term chorio-allantoic placenta. The interconnection of the trophoblastic lamellae demonstrates the true labyrinthine nature of the tupaiid placenta. *T. montana* 62. $\times 250$.
- 39 Labyrinth of near term chorio-allantoic placenta. A PAS-positive basement membrane separates the syntrophoblast of the labyrinth from the maternal capillary endothelium. *T. gracilis* 26. $\times 672$.

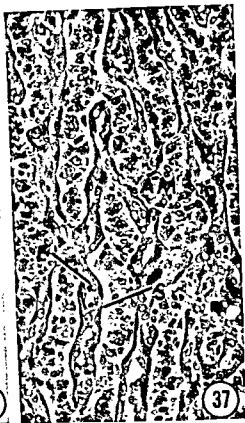
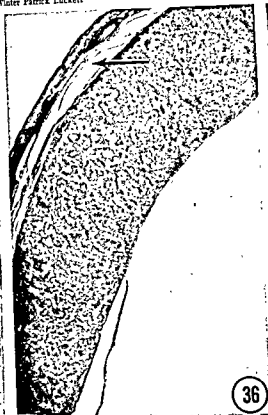
PLACENTATION OF THE TREE SHREWS
Winter Patrick Lockett

PLATE 8

EXPLANATION OF FIGURES

- 36 Cross section of placental disc from near term pregnancy. Most of the disc is occupied by the labyrinth. Note that the disc separates easily from the underlying stroma immediately beneath the incomplete layer of basal chromatic masses. *T. montana* 62. $\times 25$.
- 37 Labyrinth of near term chorio-allantoic placenta. Note the epithelioid appearance of the allantoic mesenchymal cells. A thin layer of syntrophoblast surrounds the modified endothelium of the maternal capillaries. *T. palawanensis* 68. $\times 250$.
- 38 Labyrinth of near term chorio-allantoic placenta. The interconnection of the trophoblastic lamellae demonstrates the true labyrinthine nature of the tupaiid placenta. *T. montana* 62. $\times 250$.
- 39 Labyrinth of near term chorio-allantoic placenta. A PAS-positive basement membrane separates the syntrophoblast of the labyrinth from the maternal capillary endothelium. *T. gracilis* 26. $\times 672$.

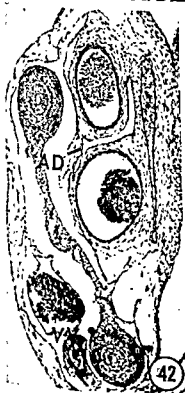
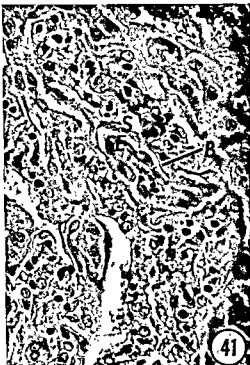
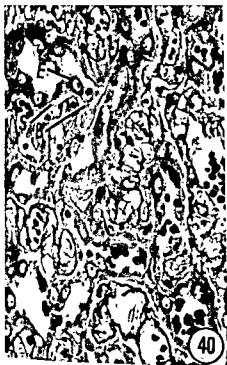


PLATE 9

EXPLANATION OF FIGURES

- 40 Labyrinth of near term chorio-allantoic placenta. Azan silver staining demonstrates a thin, incomplete layer of reticular fibers separating syntrophoblast and maternal endothelium. More prominent reticular fibers separate allantoic mesenchyme and syntrophoblast. *U. everetti* 1. $\times 440$.
- 41 Labyrinth of placenta obtained from normal term birth. The hypertrophied maternal endothelium is separated from the syntrophoblast by a hyalinized basement membrane. *T. chinensis* 45. $\times 400$.
- 42 Umbilical cord during early chorio-allantoic placentation. The allantoic arteries flank the compressed allantoic duct. The intestinal loop and vitelline vessels lie in the umbilical coelom. *T. javanica* 5. $\times 63$.
- 43 Distal remnant of vitelline duct during early chorio-allantoic placentation. The vitelline duct (arrow) is flanked by the primary branches of the vitelline vein. *T. javanica* 7. $\times 76$.

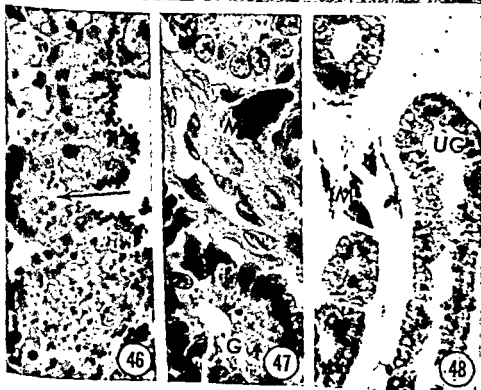


PLATE 10

EXPLANATION OF FIGURES

- 44 Mid-mesometrial region of smooth chorio-vitelline membrane during chorio-allantoic placentation. Note the increased thickness and vascularity of the distal endoderm as compared to the proximal endoderm. The thickened distal wall of the yolk sac is fused with the overlying chorion to form the chorio-vitelline membrane. The mesometrium is toward the right. *U. everetti* 90. $\times 130$.
- 45 Mid-mesometrial modification of the chorio-vitelline membrane. The trophoblast of the invaginated chorion surrounds a pocket that is continuous (arrow) with the uterine lumen. The mesometrium is toward the right. *T. palawanensis* 68. $\times 100$.
- 46 Smooth chorio-allantoic membrane. The trophoblast forms several shallow invaginations (arrow), and it is phagocytizing maternal RBC's that have escaped into the uterine lumen. The mesometrium is toward the left. *D. murinus* 93. $\times 400$.
- 47 Uterine glands during implantation stage. Macrophages containing hemosiderin are scattered in the interglandular connective tissue. The supranuclear cytoplasm of the glandular epithelium contains numerous fine granules that resemble hemosiderin in their color and refractivity. *U. everetti* 4. $\times 1000$.
- 48 Uterine glands during early chorio-allantoic placentation. Turnbull's blue stain demonstrates the presence of iron in the interglandular macrophages and in the cytoplasm of the glandular epithelium. *U. everetti* 90. $\times 400$.

Cortisone-induced Hypertension and Cardiovascular Lesions in Mice¹

THOMAS D. CLARKE,² ALLEN D. ASHBURN and W. LANE WILLIAMS
Department of Anatomy, University of Mississippi School of Medicine,
Jackson, Mississippi

ABSTRACT Daily subcutaneous injections of cortisone acetate (0.5, 1.5 or 2.5 mg) were given to three groups of mice for seven consecutive days. Daily systolic blood pressures of the anesthetized mice were obtained by adapting the method of Friedman and Freed ('49). The maximal arterial pressure increase for the 0.5, 1.5 and 2.5 mg groups was 22%, 31% and 41% respectively. This supports the conclusion that cortisone produces hypertension in mice when administered in large doses. Mural hyalinization, vacuolization and cellular proliferation of coronary arteries were greatest in the 0.5 mg group. The highest incidence of myocardial necrosis, 56%, was in the group receiving 2.5 mg of cortisone daily. The frequency and severity of myocardial and renal cortical necrosis were directly related to the size of the cortisone dose. Adrenal medullary vacuolization and lipid infiltration of the liver were common in all experimental groups.

In mice which received large amounts (25 mg) of cortisone for seven days the arterial walls were normal and there were no periarterial reactions except in arteries adjacent to myocardial abscesses (Ashburn, Williams and Arlander, '62). The coronary arteries were normal and periarteritis was absent when formation of such abscesses was prevented by treatment with penicillin (Ashburn and Williams, '66).

In a study of sequential responses to a single large dose of cortisone medial hyalinization of coronary arteries occurred within 24 hours and exudative and proliferative changes in the arterial walls and perivascular spaces followed hyalinization (Ashburn, Williams and Smith-Vaniz, '68).

The above results indicate that the initial injection of cortisone produces an arterial lesion which is masked when cortisone is continued but is allowed to develop fully if administration of cortisone is terminated after the initial injection.

Other studies show that in rats cortisone may increase blood pressure with (Angelescu, '64) or without demonstrable cardiovascular injury (Crane and Ingle, '64). In this study the actions of a range of cortisone doses upon blood pressure in mice were determined and correlated with

the amount and type of cardiovascular injury.

MATERIALS AND METHODS

Animals. A total of 245 adult nulliparous albino mice of the Taconic Swiss (TS) strain were randomly assigned to seven experimental groups. Animals were three to four months old and weighed 28–32 gm. Water and a nutritionally balanced commercial diet (Purina Laboratory Chow) were available *ad libitum*. The regimen included caudal blood pressure measurements for ten consecutive days at 24 hour intervals. Four experimental groups received daily subcutaneous injections of cortisone acetate (0.5, 1.5 or 2.5 mg) or isotonic saline solution (0.1 ml) immediately following pressure measurements on days three through nine. The final injection of cortisone or saline occurred 24 hours before autopsy. Weights were recorded daily immediately prior to blood pressure measurement.

To correlate the onset, development and incidence of lesions with levels of blood pressure an additional three groups (105 mice) were injected daily with cortisone (0.5, 1.5 or 2.5 mg). Fifteen of these ani-

¹Supported by grants from the National Institute of Health, U.S.P.H.S., HE 04052.

²Predoctoral Trainee in the Anatomical Sciences (ST1 GM 287).

Cortisone-induced Hypertension and Cardiovascular Lesions in Mice¹

THOMAS D. CLARKE,² ALLEN D. ASHBURN AND W. LANE WILLIAMS
Department of Anatomy, University of Mississippi School of Medicine,
Jackson, Mississippi

ABSTRACT Daily subcutaneous injections of cortisone acetate (0.5, 1.5 or 2.5 mg) were given to three groups of mice for seven consecutive days. Daily systolic blood pressures of the anesthetized mice were obtained by adapting the method of Friedman and Freed ('49). The maximal arterial pressure increase for the 0.5, 1.5 and 2.5 mg groups was 22%, 31% and 41% respectively. This supports the conclusion that cortisone produces hypertension in mice when administered in large doses. Mural hyalinization, vacuolization and cellular proliferation of coronary arteries were greatest in the 0.5 mg group. The highest incidence of myocardial necrosis, 56%, was in the group receiving 2.5 mg of cortisone daily. The frequency and severity of myocardial and renal cortical necrosis were directly related to the size of the cortisone dose. Adrenal medullary vacuolization and lipid infiltration of the liver were common in all experimental groups.

In mice which received large amounts (2.5 mg) of cortisone for seven days the arterial walls were normal and there were no periarterial reactions except in arteries adjacent to myocardial abscesses (Ashburn, Williams and Arlander, '62). The coronary arteries were normal and periarthritis was absent when formation of such abscesses was prevented by treatment with penicillin (Ashburn and Williams, '66).

In a study of sequential responses to a single large dose of cortisone medial hyalinization of coronary arteries occurred within 24 hours and exudative and proliferative changes in the arterial walls and perivascular spaces followed hyalinization (Ashburn, Williams and Smith-Vaniz, '68).

The above results indicate that the initial injection of cortisone produces an arterial lesion which is masked when cortisone is continued but is allowed to develop fully if administration of cortisone is terminated after the initial injection.

Other studies show that in rats cortisone may increase blood pressure with (Andershev, '64) or without demonstrable cardiovascular injury (Crane and Ingle, '64). In this study the actions of a range of cortisone doses upon blood pressure in mice were determined and correlated with

the amount and type of cardiovascular injury.

MATERIALS AND METHODS

Animals. A total of 245 adult nulliparous albino mice of the Taconic Swiss (TS) strain were randomly assigned to seven experimental groups. Animals were three to four months old and weighed 28–32 gm. Water and a nutritionally balanced commercial diet (Purina Laboratory Chow) were available *ad libitum*. The regimen included caudal blood pressure measurements for ten consecutive days at 24 hour intervals. Four experimental groups received daily subcutaneous injections of cortisone acetate (0.5, 1.5 or 2.5 mg) or isotonic saline solution (0.1 ml) immediately following pressure measurements on days three through nine. The final injection of cortisone or saline occurred 24 hours before autopsy. Weights were recorded daily immediately prior to blood pressure measurement.

To correlate the onset, development and incidence of lesions with levels of blood pressure an additional three groups (105 mice) were injected daily with cortisone (0.5, 1.5 or 2.5 mg). Fifteen of these ani-

¹ Supported by grants from the National Institute of Health, U.S.P.H.S., HE 04052.

² Predoctoral Trainee in the Anatomical Sciences (ST1 GM 287).

imals were killed daily on days 4 through 10. Blood pressure determinations were monitored only from those mice killed on a given day.

Blood pressure determination. An auscultatory monitor (Carter Electronics) was employed for the caudal determination of systolic blood pressure. The procedure is based upon microphonic detection of low frequency vibrations which first occur when a pneumatic occlusion cuff is deflated to a pressure less than that of the caudal artery. The mice were deeply anesthetized with intraperitoneal sodium pentobarbital, 2.5 mg per mouse. To obviate hypervolemic-induced hypertension, the volume of the injection was 0.05 ml. The anesthetized mice were placed for ten minutes in a wooden $22 \times 22 \times 36$ cm warming box at 37°C to produce caudal vasodilation. Mice were subsequently transferred to a larger container (ambient temperature $36\text{--}37^\circ\text{C}$) containing the occlusion cuff and microphone. The 6 mm circular occlusion cuff containing a latex diaphragm was placed to invest the base of the tail but not abut upon the body of the mouse. The rubber diaphragm liner could occlude the lumen of the cuff at 20 mm Hg and yet sustain inflation pressures over 250 mm Hg. The cuff design followed specifications of human sphygmomanometry. The carbon microphone was placed distal to the cuff but not touching it (about 2 cm from the tail root) in order to eliminate noise caused by respiratory and adventitious body movements. Several minutes were allowed to elapse until the mouse was sufficiently immobile. With the cuff completely deflated pulsations of uniform regularity were detected on an oscilloscope. By an inflation bulb the pressure in the occlusion cuff was increased manually to approximately 50 mm Hg higher than the recorded systolic pressure of the previous day. When pressure in the pneumatic cuff decreased (about 2 mm Hg per second) to the systolic level, a persistent pulsatile contour began abruptly (fig. 1). The respective systolic pressure was read with a Tyco's aneroid manometer. A permanent record was charted by an oscillograph (Grass 50 with a PIK preamplifier). A precise determina-

tion of diastolic pressure was not feasible because of the gradual intensity change of the recorded wave. For each mouse three consecutive pressure determinations were made three to five minutes apart. When they agreed within a range of 10 mm Hg the average of the three was taken as the systolic pressure.

To attest the adequacy of the indirect pressure recording system 12 mice (three from each experimental group) were cannulized in the carotid artery with a 27 gauge needle which was connected with 0.55 mm I.D. polypropylene tubing to a low volume displacement P23De Statham gauge previously calibrated with a one liter mercury manometer. The results were charted so that 1 mm scale deflection equalled 5 mm Hg pressure (fig. 1).

Statistics. Blood pressures and weights of all mice were normalized to day one, regression line showing the correlation between the indirect caudal and the direct carotid arterial pressure was fitted by the method of least squares. Seven mice died during the experiment. These were excluded from the statistical analyses because of their abnormally low blood pressure and precipitous weight loss prior to death.

Histological techniques. These were standard procedures that have been described before (Ashburn, Williams and Arlander, '62). Paraffin-embedded specimens of heart, liver, kidneys, adrenal glands and aorta were sectioned (minimum of 12 sections) at 6μ . Sections stained with hematoxylin and eosin (H & E) and periodic acid-Schiff plus hematoxylin (PASH), with or without prior diastase hydrolysis (PASD). Selected sections were also stained by Masson's trichrome (McManus and Mowry, '60).

RESULTS

Blood pressure

Prior to injection with cortisone or saline the mice had a three day mean systolic blood pressure of 102 mm Hg. When systolic pressures of all mice were normalized to day one, variable gains in blood pressure of the control group were noted in three groups of mice administered cortisone (fig. 2). The first statistically significant

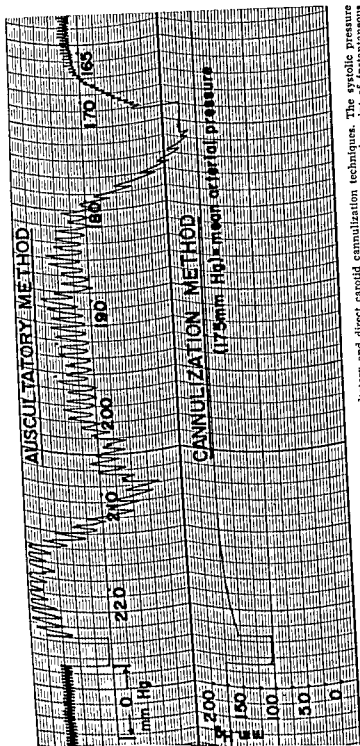


Fig. 1 Comparison of blood pressure values by indirect auscultatory and direct carotid cannulization techniques. The systolic pressure by auscultatory determination is 171 mm Hg. The pressure is equilibrated with the occlusion cuff pressure at the point of instantaneous increase in the frequency and intensity of amplified vibrations. Pulsations preceding the systolic level are due to respiratory and adventitious sounds. Pressure value for the cannulization method represents mean arterial pressure. Paper speed 10 mm/sec.

difference ($p < 0.01$) in blood pressure between the cortisone and saline groups occurred 24 hours after cortisone administration. The most dramatic response was the 41% rise in arterial pressure of mice injected daily with 2.5 mg of cortisone. After the peak on day four the mean systolic blood pressure of the 2.5 mg group decreased significantly below the saline control group ($p < 0.05$) but not below the norm. There was a sustained plateau of blood pressure in the 1.5 mg group; however, the 0.5 mg animals did not differ significantly from those of the controls ($p > 0.05$) for the last three days of the regimen. Blood pressures of the 105 mice killed daily did not differ significantly from the corresponding group receiving the same dose of cortisone.

When the auscultatory technique was validated by direct arterial measurement, a scatter diagram, with the indirect auscultatory pressure as abscissa and the direct

carotid cannulization pressure as ordinate, showed a linear relationship between the two variables. The calculated regression line was $y = 112.2 + 1.14x$. The standard error of estimate (SEE) was 18.2. Correlation of pressures in excess of 190 mm Hg were excluded because of incompatibility.

Changes in body weight. Progressive decreases in mean weight after seven days of cortisone or isotonic saline administration were -16% (2.5 mg), -15% (0.5 mg), -11% (1.5 mg) and -4% (saline control). A statistically significant difference in weight loss between all cortisone and saline control groups ($p < 0.01$) existed at least from day seven the end of the experiment.

Changes in organs

No lesions were observed in the "C" injected control mice. This stock (Taconic

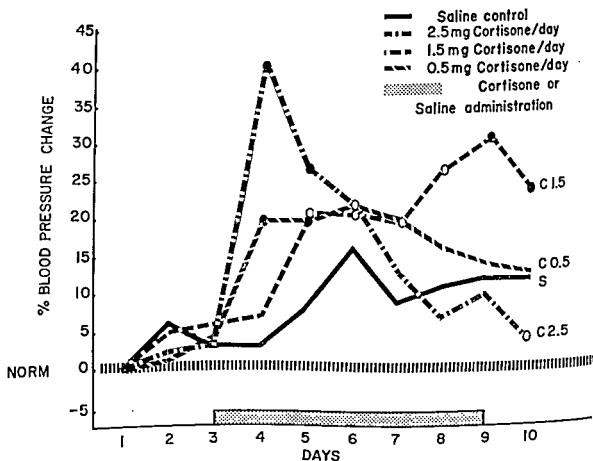


Fig. 2 Percentage shift in mean systolic blood pressure from norm. —●— $p < 0.01$ as compared to saline controls (t-test). —○— $p < 0.05$ as compared to saline controls (t-test).

TABLE 1

Incidence (%) of lesions in mice receiving 0.5, 1.5 or 2.5 mg of cortisone daily for seven days

Types of lesions	0.5	1.5	2.5
	mg/day	mg/day	mg/day
Myocardial necrosis	20	55	56
(a) Right ventricle	20	55	53
(b) Left ventricle	0	25	28
(c) Atrial	0	0	8
Hyalinization of coronary arteries	55	30	2
Adrenal medullary vacuolization	59	31	30

iss) of mice is free of spontaneous dis-
(Ashburn, Williams and Arlander,
).

arts. Foci of myocardial necrosis
observed in all cortisone-injected
(table 1). The right ventricular wall,
ventricular septum and subendocar-
layers of both ventricles were major
of lesions. Atrial necrosis was infre-

Myocardial necrosis was characterized
primary degeneration of the sarcoplasm
condensation and intense pyknosis of
nuclei. The fibers were shrunken and in-
tensely PAS-positive (fig. 3). Use of diase-
 demonstrated that the PAS-positivity
is not due to polysaccharide. Occasion-
ally leukocytes invaded the necrotic areas.
Myocardial necrosis was first observed 24,
and 72 hours respectively after the first
daily injection of 2.5, 1.5 or 0.5 mg of cor-
tisone. The highest incidence was on the
fourth day.

Coronary arteries. In mice receiving
0.5 mg of cortisone arterial lesions were
observed after the second injection. Nu-
merous arteries, inconsistently adjacent to
areas of myocardial necrosis, contained
hyaline, a non-granular, homogeneous sub-
stance which was extremely PAS-positive
and stained red with Masson's trichrome.
Arterial lesions were more frequent in the
right ventricle. In the proximal por-
tions of arteries hyalinization was often
observed (fig. 4), involving only a part of the
arterial wall. Hyalin was primarily within
the intima. The condition resembled "acute
arteritis" (Karsner, '47). In
more advanced lesions and in
distal portions of arteries the entire media
was frequently hyalinized. Arterial walls
often thickened by the hyalin even

though the vessels were dilated. Endothe-
lial cells when present appeared swollen
and nuclei were often pyknotic.

Adventitial and periadventitial fibrosis
of small arteries (fig. 5) occurred within
72 hours after cortisone administration
(0.5 mg). A perivascular response con-
sisting of fibroblasts, macrophages and
mononuclear inflammatory cells was fre-
quent. These proliferative changes involved
the media by the sixth day. The sarcoplasm
of smooth muscle fibers was swollen giv-
ing an impression of medial vacuolization.
The smooth muscle nuclei were pyknotic
and the cellular membranes were more
PAS-positive. These changes appeared to
be sequels to hyalinization.

Beginning on the fourth day in the
groups receiving 2.5 mg of cortisone a
significant number of small coronary ar-
teries showed desquamation of endothelial
cells, fragmentation of the elastica, atrophy
and necrosis of medial smooth muscle
plus initial thrombosis (fig. 6). These ar-
terial lesions lacked a mural or perivascu-
lar inflammatory response. Hyalinization
was infrequent in these severely damaged
arteries. Myocardial veins were normal ex-
cept for dilatation.

Kidneys. Many kidneys had a mottled
appearance. Necrosis of the cortex was
more prevalent than in the medulla. Med-
ullary hemorrhage and tubular ectasia
with degeneration of the epithelial lining
developed in conjunction with widespread
cortical necrosis. A plasma exudate (fig. 7)
occurred within Bowman's space and in
the convoluted tubules in those mice which
sustained for three days or more a blood
pressure in excess of 190 mm Hg. Charac-
teristically in all cortisone-injected mice
glomerular capillaries showed moderate

distention and the mesangium appeared hypercellular. Tuft adhesion or partial to complete glomerular hyalinization was observed in 11% of the 2.5 mg group.

Adrenal glands. Lipid vacuolization of the outer perimeter of the adrenal medulla (fig. 8) was observed in all cortisone groups but was more prevalent in mice receiving the minimal dose (table 1). The cells of the medullary core appeared normal. There was no necrosis.

Livers. The incidence of necrosis was directly related to the cortisone dose, i.e., 32% (2.5 mg), 30% (1.5 mg) and 15% (0.5 mg). Lipid infiltration of the liver was common to at least 45% of all groups. The incidence and severity of liposis increased directly with the size dose of cortisone (84% in 2.5 mg group).

Lungs. Pulmonary congestion, bronchiectasis and diffuse pneumonia were observed in approximately half of the animals but could not be correlated with the dose of cortisone or to changes in other organs.

Other organs. Thymic and splenic involution were frequent. There were no changes in skeletal muscle other than a slightly increased glycogen deposition. Aortas, mesenteric and pancreatic arteries were normal. Splenic vessels, especially the penicillar arterioles, were frequently hyalinized in control and cortisone-injected animals.

DISCUSSION

The reported actions of cortisone on blood pressure are contradictory. Immediate changes of blood pressure in rats, dogs and man are insignificant, but hypertension develops following prolonged administration of large amounts of glucocorticoids (Ingle and Young, '62; Dahl, Heine and Tassinari, '65; Ogawa, Tadokoro, Kiri-hara, Kawakami and Shibata, '65). In rats daily injections of cortisone produced arterial hypertension within two weeks (Sala, Benati, Amira, Ciceri and Cavallero, '51; Bertazzoli, Cavallero and Sala, '52;

Fig. 3 Myocardial necrosis. Dark fibers are necrotic and PAS-positive. (2.5 mg of cortisone for 7 days) PAS plus hematoxylin. $\times 400$.

Fig. 4 Incomplete medial hyalinization of dilated coronary artery. Adjacent myocardial fibers are normal. (0.5 mg of cortisone for 2 days) PAS plus hematoxylin. $\times 500$.



Figures 3-4

Swalton, Loeb, Stoerk, White and Heffernan, '52; Andreichev, '65) or elevated hypertensive pressures to normal (Freed and George, '59; Freed, '61).

Here cortisone produced hypertension in a very rapid manner. The acute rise in blood pressure was approximately reciprocal to dose. Prolonged administration does appear to be a requisite as in rats (Freed and Young, '62; Ogawa, Tadokoro, Kawanishi, Kawakami and Shibata, '65). The mechanism is obscure. Steroid-induced hypertension in other animals usually is related to alterations in electrolytes or increased peripheral resistance, cardiac output or blood viscosity (Cosgriff, Diefenbach, '59; Vogt, '50; Freed, '61; Andreichev, '65; Sambhi, Weil and Udhoji, '65).

The blood pressures of control mice in this study are in close agreement with those reported by other investigators. Discrepant and inconsistent results may be obtained, however, if the occlusion cuff is inflated, ambient temperature, level of anesthesia, caudal pressure gradient, end-tidal pressure and population pressure or age of strain of mice are varied (McMaster, '65; Henry, Meehan, Stephens and Santisteban, '65). The dose of pentobarbital used here is large but it has been used before without complications (Wu and Visscher, '48). Mice under deep anesthesia have less systolic pressure variation than those lightly anesthetized (McMaster, '41). Although the anesthesia may have lowered systolic blood pressures on a given day by at least 10 mm Hg (McMaster, '41; Edwards and Reinecke, '53; Henry, Meehan, Stephens and Santisteban, '65), there was a gradual rise of pressures in control animals. This may be attributed to an aggressive response of the mice to the experimental conditions. The consistently higher pressures by direct carotid cannulation are indicative of the pressure gradient in the length of the mouse tail (Edwards and Reinecke, '53).

In rats focal myocardial necrosis and hypertension followed daily cortisone doses of 5 mg/100 grams of body weight (Andreichev, '64, '65). When the dose was reduced to 2.5 mg, hypertension developed but there was no histological evidence of renal or cardiovascular damage (Knowl-

ton, Loeb, Stoerk, White and Heffernan, '52). Doses of 2.0 mg daily failed to produce hypertension (Friedman, Friedman and Nakashima, '50). In mice DOCA plus salt loading produced chronic hypertension (Rosenblum, Donnenfeld and Aleu, '66). Cardiac hypertrophy and fibrinoid deposits within glomeruli and renal arterioles were found in these animals.

Mural hyalinization of small arteries occurs frequently in animals with hypertension (Goldblatt, Lynch, Hanzal and Somerville, '34; Selye, '46; Wiener, Spiro and Lattes, '65), following immune responses (Karsner, '37), feeding of special diets (Dustin, '62) or following large doses of cortisone (Ashburn, Williams and Smith-Vaniz, '68). Hyalin may be degenerated smooth muscle (Montgomery and Muirhead, '56), plasma proteins (Dustin, '62; Adams, Bayliss and Orton, '67) or basement membrane material (Wiener, Spiro and Lattes, '65).

In this study the smallest dose of cortisone (0.5 mg) produced medial hyalinization of coronary arteries. The hyalinization was followed by a limited perivascular accumulation of fibroblasts and inflammatory cells. The inflammatory response may have been suppressed by the cortisone (Frenkel, '60). The mural and perivascular changes of coronary vessels may be reparative processes similar to those observed during recovery from adrenal enucleation or cortisone administration (Crane and Ingle, '65; Ashburn, Williams and Smith-Vaniz, '68).

LITERATURE CITED

- Adams, C. W. M., O. B. Bayliss and C. C. Orton 1967 Plasma-protein accumulation in arterial degenerations. *J. Atheroscler. Res.*, 7: 473-489.
- Andreichev, A. I. 1964 Myocardial changes in rats subjected to cortisone treatment and certain other conditions. *Fed. Proc. (Transl. Suppl.)*, 23: 1095-1098.
- 1965 Changes in electrocardiogram, myocardial potassium and sodium and in arterial blood pressure of rats on cortisone administration and exposure to certain additional factors. *Fiziol. Zh. SSSR Sechenov.*, 51: 838-843 (in Russian).
- Ashburn, A. D., and W. L. Williams 1966 Hearts and blood vessels of mice receiving cortisone and estrogens. *Anat. Rec.*, 155: 551-562.
- Ashburn, A. D., W. L. Williams and T. R. Arlander 1962 Comparative actions of cortisone, androgens and vitamin B₁₂ on body

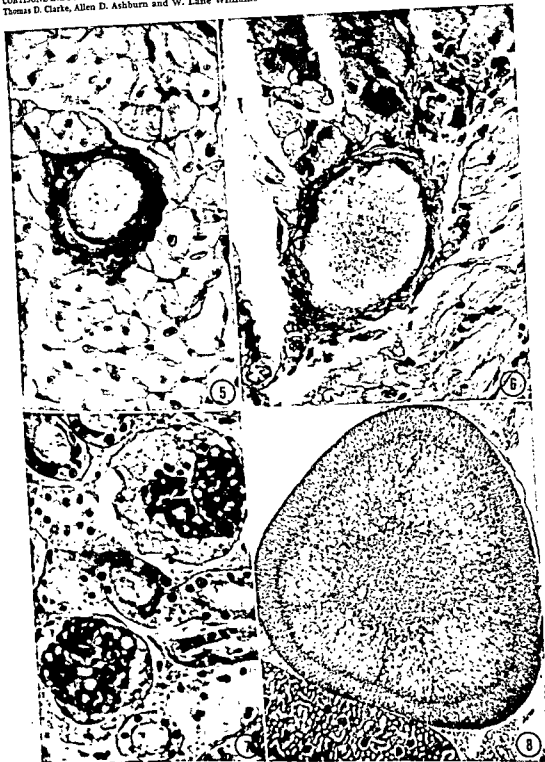
- weight and incidence of disease in mice. *Anat. Rec.*, 144: 1-17.
- Ashburn, A. D., W. L. Williams and G. T. Smith-Vaniz 1968 Arteritis of coronary arteries in mice receiving a single dose of cortisone. *Anat. Rec.*, in press.
- Bertazzoli, C., C. Cavallero and G. Sala 1952 Effect of cortisone on the blood pressure of normal rats. *Nature*, 170: 43.
- Cosgriff, S. W., A. F. Diefenbach and W. Vogt, Jr. 1950 Hypercoagulability of the blood associated with ACTH and cortisone therapy. *Amer. J. Med.*, 9: 752-756.
- Crane, W. A. J., and D. J. Ingle 1964 Effects of stressors on symptoms of corticoid overdosage. *Arch. Path.*, 77: 358-365.
- 1965 Cell proliferation in adrenal-regeneration hypertension. *Arch. Path.*, 79: 169-176.
- Dahl, L. K., M. Heine and L. Tassinari 1965 Effects of chronic excess salt ingestion. Further demonstration that genetic factors influence the development of hypertension: Evidence from experimental hypertension due to cortisone and to adrenal regeneration. *J. Exp. Med.*, 122: 533-545.
- Dustin, P., Jr. 1962 Arteriolar Hyalinosis. In: *International Review of Experimental Pathology*. Vol. 1. G. W. Richter and M. A. Epstein, eds. Academic Press, New York and London, pp. 73-138.
- Edwards, C. C., and R. M. Reinecke 1953 Effect of ischemia of the tail of the mouse on the subsequent local blood pressure. *Amer. J. Physiol.*, 174: 289-292.
- Freed, S. C. 1961 The role of potassium and its relation to sodium in the regulation of blood pressure. *Amer. J. Cardiol.*, 8: 737-740.
- Freed, S. C., and S. St. George 1959 Myocardial sodium and potassium content in relation to blood pressure. *Amer. J. Physiol.*, 197: 214-216.
- Frenkel, J. K. 1960 Evaluation of infection-enhancing activity of modified corticoids. *Proc. Soc. Exp. Biol. Med.*, 103: 552-555.
- Friedman, M., and S. C. Freed 1949 Microphonic manometer for indirect determination of systolic blood pressure in the rat. *Proc. Soc. Exp. Biol. Med.*, 70: 670-672.
- Friedman, S. M., C. L. Friedman and M. Nakashima 1950 Action of cortisone on cardiovascular-renal effects of desoxycorticosterone acetate. *Amer. J. Physiol.*, 163: 319-325.
- Goldblatt, H., J. Lynch, R. F. Hanzal and W. W. Summerville 1934 Studies on experimental hypertension. I. The production of persistent elevation of systolic blood pressure by means of renal ischemia. *J. Exp. Med.*, 59: 347-379.
- Henry, J. P., J. P. Meehan, P. Stephens and G. A. Santisteban 1965 Arterial pressure in CBA mice as related to age. *J. Geront.*, 20: 239-243.
- Ingle, D. J., and S. Young 1962 Effect of cortisone acetate and of certain stressors on blood pressure and on the pathology of heart and kidney in uninephrectomized male rats. *Endocrinology*, 70: 806-814.
- Karsner, H. T. 1937 Primary inflammation of arteries. *Ann. Intern. Med.*, 11: 167-174.
- 1947 Acute inflammations of arteries. *American Lecture Series, American Lectures in Pathology*. No. 6. P. R. Cannon, ed. Charles C. Thomas, Springfield, Illinois, pp. 4-37.
- Knowlton, A. I., E. N. Loeb, H. C. Stoerk, J. P. White and J. F. Heffernan 1952 Induction of arterial hypertension in normal and adrenalectomized rats given cortisone acetate. *J. Exp. Med.*, 96: 187-205.
- McManus, J. F. A., and R. W. Mowry 1951 Staining Methods: Histologic and Histochemical. Paul B. Hoeber, Inc., Medical Book Department of Harper and Brothers, New York pp. 234-236.
- McMaster, P. D. 1941 A method to determine the peripheral arterial blood pressure in the mouse. *J. Exp. Med.*, 74: 29-39.
- Montgomery, P. O'B., and E. E. Muirhead 1959 A differentiation of certain types of fibrinoid and hyalin. *Amer. J. Path.*, 33: 285-291.
- Ogawa, H., S. Tadokoro, R. Kirihara, K. Kawakami and K. Shibata 1965 Studies on hypertensive action of corticosteroids, especially glucocorticoids on rats. *Gunma J. Med. Sci.*, 14: 107-124.
- Rosenblum, W. I., H. Donnerfeld and F. Aln 1966 Effects of increased blood pressure on cerebral vessels in mice. *Arch. Neurol.*, 14: 631-643.
- Sala, G., O. Benati, A. Amira, C. Ciceri and C. Cavallero 1951 Studio sperimentale sugli effetti del cortisone. I. Effetti biochimici su ratto normale. *Sperimentale*, 101: 195-208.
- Sambhi, M. P., M. H. Weil and V. N. Udhoji 1965 Acute pharmacodynamic effects of glucocorticoids. Cardiac output and related hemodynamic changes in normal subjects and patients in shock. *Circulation*, 31: 523-530.
- Selye, H. 1946 General adaptation syndrome and diseases of adaptation. *J. Clin. Endocrinol.*, 6: 117-230.
- Wiener, J., D. Spiro and R. G. Lattes 1965 The cellular pathology of experimental hypertension. II. Arteriolar hyalinosis and fibrinoid change. *Amer. J. Path.*, 47: 457-486.
- Wu, H. C., and M. B. Visscher 1948 Adaptation of the tail plethysmograph to blood pressure measurement in the mouse with some observations on the effects of temperature. *Amer. J. Physiol.*, 153: 330-335.

All photographs are of tissue stained with PAS
plus hematoxylin.

PLATE 1

EXPLANATION OF FIGURES

- 5 Mural and perivascular infiltration of fibroblasts and mononuclear cells. (0.5 mg of cortisone for 3 days) $\times 400$.
- 6 Desquamation of endothelial cells and degeneration of the smooth muscle in the media. Myocardial necrosis is evident above the artery. (2.5 mg of cortisone for 7 days) $\times 400$.
- 7 Plasma exudate within Bowman's space and convoluted tubules. The mouse had a blood pressure in excess of 210 mm Hg for five consecutive days. (2.5 mg of cortisone for 7 days) $\times 400$.
- 8 Adrenal medullary vacuolization. (0.5 mg of cortisone for 7 days) $\times 40$.

CORTISONE-INDUCED HYPERTENSION
Thomas D. Clarke, Allen D. Ashburn and W. Lane Williams

All photographs are of tissue stained with PAS
plus hematoxylin.

PLATE 1

EXPLANATION OF FIGURES

- 5 Mural and perivascular infiltration of fibroblasts and mononuclear cells. (0.5 mg of cortisone for 3 days) $\times 400$.
- 6 Desquamation of endothelial cells and degeneration of the smooth muscle in the media. Myocardial necrosis is evident above the artery. (2.5 mg of cortisone for 7 days) $\times 400$.
- 7 Plasma exudate within Bowman's space and convoluted tubules. The mouse had a blood pressure in excess of 210 mm Hg for five consecutive days. (2.5 mg of cortisone for 7 days) $\times 400$.
- 8 Adrenal medullary vacuolization. (0.5 mg of cortisone for 7 days) $\times 40$.

Studies on the Fine Structure of Ovarian Steroid-secreting Cells in the Rabbit

I. THE NORMAL INTERSTITIAL CELLS¹

J. DAVIES AND CAROLE D. BROADUS

Department of Anatomy, Vanderbilt University Medical School,
Nashville, Tennessee

ABSTRACT In terms of their light microscopic appearance and fine structure the ovarian interstitial cells of the rabbit are typical steroid-secreting cells. They are characterized by an abundance of agranular endoplasmic reticulum, spherical mitochondria with closely packed lamellar cristae, lipid droplets which appear to arise independently of the endoplasmic reticulum, conspicuous Golgi areas, a cytoplasm containing ribosomes and variable numbers of glycogen granules. A feature of the differentiation of the cells from the theca interna of atretic follicles or the stroma is the enlargement of the multiple Golgi areas and the progressive accumulation of agranular endoplasmic reticulum, possibly by "budding" from the Golgi cisternae. "Light" and "dark" cells are observed, the latter being characterized by a more closely packed agranular endoplasmic reticulum which tends to be tubular in type, that of the "light" cell being vesicular. Electron dense material (lipid?) is found in the vesicles and tubules of the agranular endoplasmic reticulum and in the Golgi cisternae; it may indicate a role of these structures in the biosynthesis of steroidal hormone. No fine structural changes specifically associated with pregnancy were observed. Degenerative changes are common and are described. The role of the interstitial cells, especially in relation to the production of 20 alpha-hydroxyprogesterone, is discussed.

The similarities between cells involved in the production of steroidal hormones, long observed by histologists (see Brambell, '62 and Corner, '63 for extensive reviews), have been confirmed in recent years by electron microscopy in a variety of tissues and species, for example the adrenal cortex (Luse, '67; Ross et al., '58; Lever, '59; Zelander, '59; Sabatini and de Robertis, '61), the interstitial cells of the testis (Fawcett and Burgos, '60; Christensen and Fawcett, '61; Carr and Carr, '63; Crabo, '63; Leeson, '63; Christensen, '65; Christensen and Fawcett, '66), the granulosa cells of the Graafian follicle (Wartenberg and Stegner, '60; Björkman, '62; Blanchette, '66), the thecal and interstitial cells of the ovary (Belt and Pearse, '56; Mota, '58), and the corpus luteum (Lever, '56; Enders, '62; Carsten, '65; Blanchette, '66; Flaks and Bresloff, '66; Rennels, '66). These studies and others under experimental conditions after hypophysectomy and treatment with trophic hormones (e.g. those of Sabatini et al., '62; Enders and Lums, '64; Blanchette, '66; Schwarz and Nicker, '67) have resulted in a substantial

body of knowledge on the normal fine structure of these cells and on their subcellular responses to trophic hormones.

The steroid-secreting cells are characterized by an abundance of agranular endoplasmic reticulum, often arranged in concentric whorls around lipid inclusions. The mitochondria vary in form from organ to organ and from one species to another, having conventional lamellar cristae in some, tubular "cristae" in others. The Golgi areas are discrete in some cells; in others they have been described as "diffuse." Foldings and villous modifications of the plasma membranes are common, especially in the luteal cells. Free ribosomes, areas of granular endoplasmic reticulum, granules of glycogen and electron dense "microbodies" of uncertain origin have been described in the cytoplasm. The form of the agranular reticulum is a subject of

¹ This research was supported through funds provided by USPHS grants HD 00132 and HD 00971 and by the Ford Foundation. We also acknowledge financial assistance from the following drug houses: Abbott Laboratories, Ayerst Laboratories, Lilly Research Laboratories, Ortho Research Foundation, Schering Corporation, Sterling-Winthrop Research Institute, Syntex Research, and Wyeth Laboratories.

This confirms the conclusions of others (Guraya and Greenwald, '64). The follicular origin of much of the interstitial tissue is indicated by the frequent occurrence of thickened and hyalinized remnants of the basement membrane of the stratum granulosum ("glassy membranes") embedded in the center of lobular masses of partially or completely differentiated cells. These remnants are especially common in pregnancy. The interstitial tissue of the immature animal is pink and translucent. In adult animals, especially after numerous episodes of pseudopregnancy or pregnancy, it becomes very compact and creamy in appearance.

Interstitial cells at an early stage in their "luteal-like" transformation (fig. 1) are epithelial in appearance. The nucleus is small and compact with indistinct nucleoli. The cytoplasm is granular and markedly acidophilic throughout. In later stages of their differentiation there is hypertrophy involving both nucleus and cytoplasm. Mitoses are rare and even when observed may be related to the stromal elements rather than to the interstitial cells. The nucleus becomes less compact and contains one or more conspicuous nucleoli. The cytoplasm becomes differentiated into a perinuclear acidophilic zone and a peripheral vacuolated zone (fig. 2). The perinuclear zone, which may be shown by a study of sections stained with borax-toluidine blue to contain many of the mitochondria, is a characteristic feature of the normal interstitial cell and its disappearance is an early and significant indication of degeneration. The loss of this acidophilic zone has been found to be a useful criterion for the assessment of functional maintenance of both interstitial and luteal cells in the rabbit, e.g. after hypophysectomy. The peripheral vacuolation is due to the removal of lipid droplets during preparation of the sections. These droplets are lost in the preparation of paraffin-embedded sections but are normally preserved after adequate fixation with osmic acid (figs. 5, 6).

In pseudopregnancy and pregnancy there is a marked hypertrophy of the ovarian interstitial cell (Lane-Clayton, '55) involving both nucleus and cytoplasm (figs. 3, 4), but without any significant in-

crease in number of cells by mitosis (Claesson, '54). There also appears to be a significant accretion of new interstitial tissue by transformation of cells of the theca interna of atretic follicles. The "tempo" of follicular atresia seems to be increased during pregnancy (Halliday, '59) with a new formation of "corpora lutea atretica" or "pesudo corpora lutea" which, after a period of differentiation, become indistinguishable from the main interstitial cell mass. This irregular but progressive accretion of interstitial tissue associated with repeated episodes of pregnancy and pseudopregnancy (fig. 4), probably accounts for the extreme variability in the mass of interstitial tissue in adult rabbits irrespective to their body weight (Davies, '62). In old or senile rabbits the ovaries contain a predominance of interstitial tissue with few residual follicular elements. In a significant percentage (up to 30%) of rabbits obtained from local dealers, from whom no reliable reproductive history of the animal was available, a markedly hypertrophy of the ovarian interstitial tissue was observed over a period of years (Davies, '62). This was accompanied by atrophy of the corpora lutea, which were usually present, massive estrogenic hypertrophy of the uterus, cervix and vagina, hypertrophy of the liver of a type commonly observed after prolonged estrogen administration, severe degeneration of the inner zones of the adrenal cortex, and hypertrophy of the anterior lobe of the pituitary gland. This association of findings in "syndromic pattern" was such that the existence of the other features could be predicted from observation of any one at laparotomy. This "syndrome" appears to represent a spontaneous imbalance of pituitary-adrenal-ovarian function. It is observed so frequently in our experience that it must be considered carefully in all studies of reproductive function in the rabbit.

The vascularity of the ovarian interstitial tissue differs from that of the corpus luteum in the rabbit in that groups of cells rather than individual cells are in immediate contact with blood vessels. The interstitial tissue does not bleed freely on cutting, in contrast to the corpus luteum. Injections with India ink followed by re-

controversy, being described as tubular by some, as combined vesicular and tubular by others. Problems of fixation have greatly complicated the analysis of the probable exact form of the organelles, especially the endoplasmic reticulum and mitochondria. There are many unresolved problems such as the developmental origin of the lipid droplets in relation to the endoplasmic reticulum, and the significance of the droplets and organelles in relation to steroid hormone biosynthesis.

The ovarian interstitial cells studied in this paper are a less well studied population of steroid-secreting cells. They present, however, unique features which make them especially suitable for the experimental analysis of fine structure and function. They are well developed in the rabbit, forming in many adult animals a major proportion of the total ovarian weight even in the presence of corpora lutea, and were described as forming an "interstitial gland" by Limon ('02). Interest in the cells has revived in recent years, chiefly as a result of the studies of Hilliard et al. ('63, '67) who have implicated them in the preovulatory synthesis and release of 20 α -hydroxyprogesterone following mating or gonadotrophic stimulation.

The ovarian interstitial cells as described in this paper have been shown to be typical steroid-secreting cells as far as their fine structure is concerned. They have been studied in non-pregnant ("estrous") and in pseudopregnant and pregnant rabbits. Though hypertrophy of the interstitial cells, involving apparently all cytoplasmic elements, takes place in pseudopregnancy and pregnancy, the changes have been judged to be quantitative and not qualitative in nature, and no specific changes associated with these states of enhanced gonadotrophic function could be determined. The studies reported here are intended as a basis for experimental studies on the interstitial cells of the rabbit after hypophysectomy and treatment with gonadotrophic hormone, to be published later.

MATERIALS AND METHODS

Ovarian interstitial tissue was obtained from New Zealand white rabbits in the following periods and stages of their reproductive life: immature (less than 5

months), mature (non-pregnant or "estrous"), pseudopregnant and pregnant, at term and in the postpartum period. Tissues for light microscopy were fixed in 10% neutral formalin or Bouin's solution. Tissues for electron microscopy were fixed for 40 minutes in buffered osmic acid in which the final concentration of osmic acid was 2%. The fixative was adjusted to a final osmolality of about 350 m.osmols by the addition of 0.3 M phosphate buffer (final concentration of buffer about 0.15 M) at a pH of 7.2-7.4. Osmolality was determined by the method of freezing point depression, using a Fisk osmometer. Increasing the final concentration of osmic acid from 1% to 2% resulted in markedly better and consistent fixation. The use of sucrose for the adjustment of osmolality was found to be disadvantageous, resulting in shrinkage of the cells, and disruption of plasma membranes and those of the organelles. Fixation was also carried out in glutaraldehyde (1.25%) with phosphate buffer at a final osmolality of about 350 m.osmols, followed by osmication in 2% osmic acid-phosphate buffer. Tissues were rapidly dehydrated in ethanol (70%, 80%, 90%, 100%) and in absolute butanol (one hour) followed by clearing in toluene for one hour. They were then embedded in English or American araldite and sectioned on a Porter-Blum MT-2 ultramicrotome. Phase contrast sections were studied for purposes of orientation before final trimming of the face of the block and only those areas showing good preservation of lipid (usually peripheral) were used for thin sectioning. Some were stained with borax-toluidine blue. Thin sections were mounted on 400-mesh uncoated copper grids and stained with uranyl acetate (saturated solution in 50% alcohol) and lead citrate (Reynolds, '63). The sections were examined in a Hitachi HU-11B electron microscope.

OBSERVATIONS

Summary of light microscopic observations

The development of the ovarian interstitial cells is clearly by a "luteal-like" transformation of fibroblastic elements of the theca interna of follicles, both atretic and recently ovulated, and also of the stroma.

ternae and vesicles of the Golgi areas usually contain a small amount of homogeneous material of moderate electron density. The cytoplasm of the interstitial cells at this stage (fig. 9) is densely crowded with small vesicles, presumably of the agranular endoplasmic reticulum. They are predominantly small at first, the largest ones approaching in size that of the dilated vesicles of the Golgi areas. Like the latter they contain electron dense material which completely fills the vesicles in the case of the smallest ones, while in the larger ones it forms a peripheral condensation surrounding an empty central area. The nucleus is surrounded by a continuous outer membrane with multiple areas of contact with the inner nuclear membrane at typical nuclear pores. The cytoplasm is finely granular and contains in addition many free ribosomes arranged singly or in small clusters. There are occasional areas of granular endoplasmic reticulum.

At the stage of differentiation described above and before the deposition of significant amounts of lipid, the interstitial cells show a uniformly granular acidophilic cytoplasm (as in fig. 1). This acidophilia presumably must be attributed to predominantly acidophilic proteins which may include not only those of the mitochondria but also of other elements of the cytoplasm, notably the endoplasmic reticulum. The first indication of the deposition of lipid in the interstitial cell is the appearance of irregular spaces within the peripheral cytoplasm. The spaces frequently appear empty, suggesting that any lipid they may contain at this stage is easily dissolved out during the preparation of the tissues, or that it is of extremely low electron density. It may usually be demonstrated in phase contrast sections as a delicate stippling of droplets not easily distinguished from the mitochondria which are also osmophilic and of comparable size. It has been found impossible to detect a unit membrane circumscribing individual droplets, though there is usually a peripheral condensation of coarsely granular and electron dense material (figs. 9, 12). At this stage in the differentiation of the interstitial cells, therefore, the lipid droplets appear to arise *de novo* within the cytoplasm and independently of the endoplas-

mic reticulum, often in areas rich in free ribosomes. Though some of the early spaces appear empty, other spaces in the same cell or in adjacent cells frequently contain homogeneous electron dense lipid, suggesting marked variation in solubility or osmophilia at this stage.

As the interstitial cells approach the stage of full differentiation (figs. 10, 12) the lipid droplets become more numerous and the cytoplasm becomes crowded with membranes of the Golgi systems and endoplasmic reticulum. The Golgi areas are conspicuous in extent and size and appear in some places in direct continuity with vesicles of the agranular endoplasmic reticulum (fig. 12). The cisterns and vesicles contain electron dense material as described in earlier stages (figs. 10, 12). The mitochondria are uniformly spherical or slightly oval and contain internal membranes of greater complexity. These membranes are arranged in groups of parallel cristae, one group being parallel to another or to the surface of the mitochondrion. Tubular forms of the internal mitochondrial membranes cannot be ruled out, but could be artifactual and result from tangential sections of groups of lamellar cristae. The mitochondrial matrix is finely granular and of considerable electron density. Free ribosomes occur singly or in small clusters but are more scattered, representing either an actual decrease in their numbers compared with earlier stages or a wider distribution throughout the now more extensive cytoplasm. Electron dense granules which are larger and more variable in size than the ribosomes and which are stained selectively with lead salts probably represent glycogen (fig. 12). Electron dense bodies are often observed, particularly in the vicinity of the Golgi areas (fig. 12). Evidence for their possible origin from lipid droplets will be presented later.

Degeneration of interstitial cells occurs frequently even in immature animals. It is characterized by a loss of the formed elements of the cytoplasm (Golgi, mitochondria, endoplasmic reticulum), and by the appearance of "myelin figures" and crystalline structures (cholesterol?). The contents of the crystalline structures, except

construction of the vascular pattern in serial sections indicate that the vascular beds of the interstitial tissue and corpus luteum are independent and no portal system of vessels linking them exists.*

The lipid droplets in the vacuolated areas of the interstitial cell cytoplasm are illustrated following fixation in osmic acid (figs. 5, 6). The droplets are uniform in size (estimated at 1–2 μ) within a single cell but vary considerably from one cell to another. In non-pregnant animals the droplets appear more crowded and relatively numerous. In pregnant animals the droplets appear less densely packed. "Light" and "dark" cells appear in the ovaries of both the non-pregnant and pregnant rabbit (fig. 5). The varying density of the cells, as studied by phase contrast microscopy, is due not only to the degree of crowding of the droplets but also to an increase in the density of the intervening cytoplasm in the "dark" cells.

Degeneration of interstitial cells is common in the ovaries of all mature rabbits whether pregnant or not. It is usually unicellular in type (fig. 7) but is occasionally "lobular" (fig. 8). In each instance the cytological appearance of degenerating cell is the same. The cell is increased in size. There is nuclear pycnosis and a loss of the perinuclear acidophilic zone. Vacuolation of the cytoplasm is complete, and in paraffin-embedded sections the spaces appear larger and the septa between them correspondingly attenuated. Study of frozen sections and sections observed after fixation in osmic acid shows that the large spaces contain lipid droplets which are, however, larger and more varied in size than in the normal cell. They are also less soluble in organic solvents such as acetone than are the droplets of normal cells but are eventually dissolved by prolonged treatment. Late stages in the degeneration of the cells (fig. 7) are associated with swelling, pycnosis, and eventual loss of the nucleus, and apparent disappearance of cytoplasmic material the former site of which is marked by irregular empty spaces.

Electron microscopic observations

The fine structure of the interstitial cells will be described in relation to three princi-

pal stages of their presumed life cycle: (1) immature differentiating cells, (2) mature cells, and (3) degenerating forms.

(1) *Immature differentiating cells.* These are easily studied in young rabbits of less than five months of age. At this time, in our experience, these cells are becoming able to respond to mating with ovulation; there is much variation, however. The interstitial cell mass during this period is pink and rather translucent to the naked eye in contrast to its creamy appearance in the adult animal. Immature interstitial cells, however, may be observed in all stages of their "luteal-like" transformation from fibroblasts of the theca interna of atretic follicles and of the stroma in adult animals (fig. 4), especially during pregnancy.

Interstitial cells in the early stages of differentiation are notable for their relative simplicity of cytoplasmic fine structure. They contain many free ribosomes and occasional elements of the granular endoplasmic reticulum but few of the agranular endoplasmic reticulum. This stage is presumably associated more with protein synthesis and growth. The Golgi areas are discrete but inconspicuous. The plasma membranes are uncomplicated and in simple apposition with each other with occasional areas of contact, forming typical desmosomes. The mitochondria are few and are elongated in form with simple lamellar cristae.

Further differentiation of the interstitial cells is accompanied by increased complexity of cytoplasmic fine structure, in addition to the nuclear changes and cytoplasmic growth observed in the light microscope (fig. 1). The mitochondria are increased in number and, at an early stage, become spherical or oval in form with more complex internal membranes. These membranes are arranged predominantly in lamellar form, rarely in tubular form, and lie in a finely granular matrix. The Golgi areas are now conspicuous and usually multiple. They consist of parallel tubules or cisterns each of which has a dilated vesicular extremity. The cis-

* We are indebted to Miss Jane Davy of St. Thomas's Hospital Medical School, London, England, who carried out these studies during the tenure of a summer fellowship.

16). A thin discontinuous basement membrane envelops the interstitial cells and the cytoplasmic processes and extends around groups of cells but not between individual cells. The basement membrane of the blood vessels in the connective tissue septa is complete.

In interstitial tissue fixed in glutaraldehyde the cytoplasm shows that there is an additional feature not seen after fixation in osmic acid, namely "microtubules" (fig. 17). These microtubules are approximately 270-300 Angstroms in diameter and are rather uniform in caliber. They are easily observed in "light" cells in which there are extensive areas of cytoplasm between the other organelles and inclusions; they are undetectable in "dark" cells.

The mitochondria in both "light" and "dark" cells are similar, and it has not been possible to determine whether they are more numerous in one or another type of cell. They are almost invariably round or slightly oval, rarely elongated, and contain characteristic internal membranes. As previously described, these membranes are arranged in groups of lamellae, one group being at an angle to another or parallel to the surface of the mitochondrion. Tubular "cristae" are rare. The mitochondrial matrix is finely granular and of considerable electron density. It has not been observed to contain large granules at any stage. Ballooning of the outer membranes, vesiculation of the matrix, discontinuities in the outer membranes, and other features described by others in steroid-secreting cells have not been observed.

Free ribosomes become relatively rare in fully differentiated interstitial cells, especially in the so-called "dark" cells. Glycogen granules are also very variable in number. They are generally sparse or absent in apparently well differentiated cells. They are more common in "light" than "dark" cells and, as shown previously (fig. 12), more common in undifferentiated than in differentiated cells. Glycogen is often observed in the endothelial cells of the blood vessels (fig. 18), and this appears to be more common in late pregnancy than at any other time. In late pregnancy the thickening and reduplication of the basement membrane of the interstitial cells, noted in late pregnancy may represent an in-

volitional phenomenon (fig. 18); it has not been observed in non-pregnant animals.

A feature of many interstitial cells at all stages in the mature rabbit is the presence of variable numbers of extremely electron dense bodies. These are often observed in the perinuclear zone associated with the Golgi area (figs. 12, 15). A study of interstitial cells which show other indications of diminishing function or regression (e.g. fig. 19) provides evidence for the origin of these structures from existing lipid droplets. The transformed droplets appear uniformly round, in contrast to the highly irregular homogeneous lipid of fully differentiated cells in young rabbits (c.p. fig. 19 with figs. 13, 14, 16). They also show a peripheral condensation of extremely electron dense material which may encircle the droplet evenly or in the form of a crescent. The absence of an observable limiting membrane around these droplets, and the less intimate relationship between them and the endoplasmic reticulum, confirms the impressions gained from a study of early differentiated cells (see fig. 9) that they exist independently of the endoplasmic reticulum. The transformed droplets also show a gradation in electron density from the periphery to the center (fig. 19). There is frequently a central empty area from which the lipid has apparently been dissolved, suggesting poor penetration of the osmic acid into the droplets during fixation. Other droplets are completely transformed into electron dense bodies similar to those observed previously in the Golgi area (fig. 14); they are considerably reduced in size when compared with the original lipid droplets.

(3) *Degenerating cells.* Degeneration of interstitial cells, as shown by light microscopy (figs. 7, 8) usually involves single isolated cells, but is occasionally lobular in extent. Regression of the interstitial cells is observed in both "light" and "dark" cells. Regression is associated with changes in the mitochondria which show a simplification of the cristae (fig. 19), later gross shrinkage and a marked increase in the electron density of the matrix (fig. 20). The endoplasmic reticulum appears to show marked resistance to degeneration and persists in some form in degenerated cells for an undetermined but probably

for a peripheral condensation of electron dense material, are usually dissolved out.

(2) *Mature interstitial cells.* These are described irrespective of the stage of the reproductive life of the rabbit for the ensuing reasons. The changes in the cells during pregnancy and pseudopregnancy, involving the nuclear and cytoplasmic hypertrophy observable in the light microscope (fig. 4), are seen by electron microscopy to be accompanied by an increase in the number and extent of existing organelles and inclusions (mitochondria, endoplasmic reticulum, lipid droplets, etc.) without, however, detectable qualitative difference in their organizations and interrelationships. The changes then are assumed to be quantitative rather than qualitative. Moreover, the extreme variability of fine structure of the interstitial cells in mature rabbits, complicated by the continuous new-formation of cells from atretic follicles, the widespread occurrence of degenerative changes, and the notorious sampling errors inherent in electron microscopy, make the detection of systematic fine structural alterations specifically related to pregnancy and pseudopregnancy impossible to define. This is in marked contrast to the corpus luteum in which systematic changes in the luteal cells occur in pregnancy and pseudopregnancy.

A feature of the interstitial cells as the rabbit approaches maturity (figs. 13, 14) is the presence of many lipid droplets crowding the cytoplasm. The droplets appear highly irregular in form and contain homogeneous material of a uniform electron density throughout the cytoplasm. Irregular stellate depots of lipid occur in some areas rich in free ribosomes but without membranes of the endoplasmic reticulum (fig. 14), suggesting that here they arise independently. In other areas (figs. 13, 14) the droplets of lipid are enveloped on all sides by vesicular and tubular elements of the endoplasmic reticulum, and here it is more difficult to make a case for their independent origin. In many regions the droplets are so close together that the intervening cytoplasm, containing small vesicles, ribosomes, glycogen, etc., is compressed and often attenuated, forming delicate septa. The irregularity of these droplets and contours of the cytoplasmic septa

between them impart to the cytoplasm a characteristically "lacy" appearance (fig. 13). Golgi areas are invariably present but less easily distinguished from the all-pervading network of endoplasmic membrane than in undifferentiated cells (c.p. fig. 12). The cells lie in intimate contact with each other except in the region of the perivascular space where folding of the plasma membranes occurs with the formation of slender processes (fig. 13). These processes are often devoid of lipid inclusions but are especially rich in free ribosomes and glycogen.

"Light" and "dark" cells are regularly but variably observed in the interstitial cell mass of the mature rabbit (see fig. 5). The differences between these two types of cells are seen in the electron microscope to be determined by the amount of agranular endoplasmic reticulum and to the resultant compression of the intervening cytoplasmic structures (fig. 16). In a typical "light" cell (fig. 15) the cytoplasmic structures are not compressed, and discrete Golgi areas are easily detected. The endoplasmic reticulum, moreover, is predominantly vesicular in such "light" cells and the electron dense contents of the vesicles are easily observed. The cytoplasm between the vesicles contains scattered ribosomes and occasional larger granules of glycogen. Small areas of granular endoplasmic reticulum occur, and in such areas continuity between it and the vesicles of the agranular endoplasmic reticulum is occasionally observed (fig. 15). In "dark" cells the agranular endoplasmic reticulum is extremely complex and appears to be made up of short tubules (fig. 16). In these cells the electron dense contents of the tubules of endoplasmic reticulum are less conspicuous or absent. All variations in cell type between "light" and "dark" cells exist. The differences are accentuated by fixation in hypertonic solutions, probably as a result of shrinkage and compression. The mitochondria are similar in both types of cells. They are numerous in mature cells and have the characteristic oval or spherical forms previously described. The folding of the plasma membrane and the formation of slender cytoplasmic processes which extend into the perivascular space are also more conspicuous in mature animals (fig.

and nucleolus, the organelles (Golgi, mitochondria, endoplasmic reticulum), a deposition of lipid droplets, and modifications of the plasma membrane. As the rabbit approaches maturity (about 5 months) the cells are crowded with lipid droplets and the agranular reticulum is abundant. Ribosomes appear to decrease relatively or absolutely, and there is an appearance of glycogen in monoparticulate form, recognized by its relative size and variability in comparison to ribosomes and its selective affinity for lead salts (Revel et al., '60). Blanchette ('66) observed glycogen during the differentiation of the granulosa cells under normal and experimental conditions in which luteinizing hormone was injected into the follicle of the rabbit; it was monoparticulate in the early stages, mostly in rosette-form in the later stages of luteal transformation.

The conformation of the organelles in fixed steroid-producing cells has been a subject of controversy. The form of the endoplasmic reticulum, vesicular or tubular, has been a particular problem, and several writers have concluded that the vesicular form is an indication of poor fixation, and that the tubular form more closely approximates to its condition in the living state (Enders, '62; Christensen, '65). Both types of agranular endoplasmic reticulum have been observed, however, by many investigators and there are undoubtedly marked variations in its form from one cell to another, from one zone to another (as in the adrenal cortex), and from one species to another. Blanchette ('66) observed both vesicular and tubular forms of the endoplasmic reticulum in the corpus luteum of the rabbit with all kinds of fixation and with all variations in osmolality within reasonable limits. Hypertonic fixatives, especially those containing sucrose, in our experience caused marked shrinkage of the cells with compression of the endoplasmic reticulum, which then appears predominantly tubular. However, in normal rabbits in which the ovarian interstitial tissue was fixed at a controlled osmolality (350 m.osmols) both vesicular and tubular forms of the agranular endoplasmic reticulum were observed and the cells in all other respects showed evidence of good fixation.^{*} "Light" and "dark" cells

were observed, similar to those described by Enders ('62) in the corpus luteum, the endoplasmic reticulum being sparse and vesicular in the former, densely packed and tubular in the latter. Since proliferation of the agranular reticulum has been shown to be a significant subcellular response of the interstitial cells to luteinizing hormone resulting in an almost complete transformation of all interstitial cells into "dark" cells (Davies, '66), we have tentatively concluded that "dark" cells may represent cells at a higher level of gonadotrophic stimulation than are "dark" cells.

A feature of the vesicular elements of the agranular endoplasmic reticulum in the interstitial cells, especially the "light" cells, was their content of electron dense material, possibly representing lipid. Similar material was observed in the dilated extremities of the Golgi cisterns and in the cisterns themselves. This material may have some relevance to the unsolved problem of how and where the steroidal hormones are synthesized or conveyed out of the cell. Hamilton et al. ('67) in our laboratory has shown that perfusion of the liver with free fatty acids results in the accumulation of electron dense bodies comparable in size to those observed in the interstitial cells of the rabbit. The Golgi cisterns and vesicles of the hepatic cell are also apparently involved in the synthesis or transport of this material which appears to represent "very low density" lipoprotein. It is possible that the application of methods and concepts widely developed in the field of hepatic lipid transport to the unsolved problems of steroidal hormone biosynthesis at the subcellular level may be of great value. The electron microscopic evidence is not inconsistent with the view that the vesicles of the agranular endoplasmic reticulum may be formed by "budding" from the Golgi area, a suggestion made by Mercer ('62) for cells in general and by Schwarz and Merker ('67) for

^{*} We have recently had the opportunity to study the interstitial cells of the opossum testis fixed in the same manner as described in this paper (2% osmic acid, approximately 0.15 phosphate buffer, 350 m.osmols). Tubular endoplasmic reticulum identical to that described by Christensen and Fawcett ('61) predominated but there were extensive areas of vesicular endoplasmic reticulum not only in different cells but also in the same cell. A similar conclusion was reached by de Kretzer ('67) from a study of the human testicular interstitial cells.

prolonged period (fig. 21). There is a disorganization of the regular pattern of organization of the endoplasmic reticulum (fig. 20). The vesicles, formerly occupied by electron dense material, are more often empty. In many areas the endoplasmic reticulum forms closely packed systems of parallel membranes, superficially resembling Golgi areas (fig. 20) but differing in essential particulars from them (c.p. fig. 15). Similar Golgi-like areas may be of mitochondrial origin (fig. 20). The formation of concentric whorls of membranes, having the unit-membrane structure when appropriately resolved, increase throughout the cytoplasm in degenerating cells and may ultimately become the predominant feature (fig. 21); these are the so-called "myelin" figures, and may result from the hydration of existing protein-phospholipid material.

The lipid droplets also show marked resistance to degeneration and may persist long after the formed elements of the cytoplasm are unrecognizable (figs. 20, 21). Aggregations of very electron dense granules are also observed in degenerating cells (fig. 21). Their nature cannot be ascertained. The granules appear too large and uniform and, in addition, are not selectively stained with lead salts, suggesting that they are not glycogen. They may represent pigmentary inclusions.

DISCUSSION

The interstitial cells of the rabbit ovary, as judged by light and electron microscopic criteria, are typical steroid-producing cells. Unlike the luteal cells, which are formed only as a result of an ovulatory stimulus, the interstitial cells are a permanent element of the ovary and constitute a significant mass of steroid-producing cells. Like the cells of the adrenal cortex and the interstitial cells of the testis, they form a stable population of cells, in contrast to the luteal cells which appear to have an inherently limited life span under normal conditions. The luteal cells, moreover, regress and degenerate after hypophysectomy, whereas the interstitial cells revert under these conditions to a resting or "basal" state in which they are capable of further response to gonadotrophins (Velardo, '59; Davies, '66). In terms of

pituitary-dependence the luteal cells are the most dependent; the ovarian interstitial cells, the interstitial cells of the testis and the outer zones of the adrenal cortex are the least dependent; and the cells of the inner zones of the adrenal cortex appear to be intermediate in dependence. The luteal cells appear to function normally at a maximal level of gonadotrophic stimulation and steroidal output, whereas the ovarian interstitial cells function at a lower level which can be raised by suitable gonadotrophic stimulation. Preliminary studies in our laboratory on the effects of luteinizing hormone on the interstitial cells of hypophysectomized rabbits (Davies, '66) indicate that under these circumstances the interstitial cells become fine structurally indistinguishable from luteal cells, with respect to the rich development of the endoplasmic reticulum and the complex folding of the plasma membrane. Though pregnancy appears to be associated with increased levels of gonadotrophic hormone (luteinizing hormone?, Davies et al. ('65)), it is of interest that no fine structural changes typical of pregnancy could be detected. The rate of turnover of the interstitial cells is unknown (Brambell, '62). The increase in size of the interstitial tissue in pregnancy is due to hypertrophy of individual cells and not to mitotic division (Claesson, '54).

The progressive differentiation of interstitial cells throughout the first five months of life in the rabbit ensures that a large mass of competent steroid-secreting cells is available to meet the demands of reproductive life. It is not known if this differentiation is governed wholly or in part by luteinizing hormone, as it appears in the luteal transformation of granulosa cells of the follicle. If so, luteinizing hormone or whatever other hormones are involved, must be regarded as morphogenetic hormones as well as trophic hormones. There is some evidence (Kilpatrick et al., '64) that luteinizing hormone is the trophic hormone of the ovarian interstitial cells in the rabbit.

In the differentiation of interstitial cells from cells of the theca interna of follicles and the stroma, all parts of the cells appear to change *pari passu*. The changes, in addition to growth, involve the nucleus

(minus corpora lutea) of the rabbit. They have demonstrated activity with 3 beta-, 17 beta-, and 20 alpha-hydroxysteroids. Preferences of one enzyme system for DPN or TPN were observed, and some were observed in the microsomal fraction and others in the supernatant. The role of the interstitial cells in the production of androgen or estrogen has not been substantiated (Moricard, '53; Eckstein, '62). Falck's observations on microtransplants of ovarian tissue in rats ('59) that these do not function independently but in synergy in the production of estrogen (e.g. granulosa cells plus theca interna cells, granulosa cells plus interstitial cells) may underlie the failure to ascribe a specific role to the ovarian interstitial tissue.

LITERATURE CITED

- Belt, W. D., and D. C. Pearce 1956 Mitochondrial structure in sites of steroid secretion. *J. Biophys. Biochem. Cytol.*, 2: Suppl., 369-374.
- Björkman, N. 1962 A study of ultrastructure of the granulosa cells of the rat ovary. *Acta anat. (Basel)*, 51: 125-147.
- Blanchette, J. E. 1966 Ovarian steroid cells. I. Differentiation of the lutein cells from the granulosa follicle cell during the preovulatory stage and under the influence of exogenous gonadotrophins. *J. Cell Biol.*, 31: 501-516.
- 1966 Ovarian steroid cells. II. The lutein cell. *J. Cell Biol.*, 31: 517-542.
- Björkman, H., and E. Odelblad 1952 Autoradiographic observations on the uptake of S^{35} in the genital organs of the female rat and rabbit after injection of labelled sodium sulphate. *Acta Endocr. (Copenhagen)*, 10: 89-96.
- Cambell, F. W. R. 1962 Ovarian changes. In: Marshall's Physiology of Reproduction, (A. S. Parkes, ed.). Longmans, Green and Co., London, vol. 1, pp. 397-542.
- Er, I., and J. Carr 1963 Membranous whorls in the testicular interstitial cell. *Anat. Rec.*, 144: 143-147.
- Ernst, P. M. 1965 Elektronenmikroskopische Probleme bei Strukturdeutungen von Einschlußkörpern im menschlichen Corpus luteum. *Arch. Gynäk.*, 200: 552-568.
- Ernstsen, A. K. 1965 The fine structure of testicular interstitial cell in guinea pigs. *J. Cell Biol.*, 26: 911-935.
- Ernstsen, A. K., and D. W. Fawcett 1961 The normal fine structure of opossum testicular cells. *J. Biophys. Biochem. Cytol.*, 9: 653-670.
- 1966 The fine structure of testicular interstitial cells in mice. *Am. J. Anat.*, 118: 51-57.
- Ernst, L. 1954 The intracellular localization of the esterified cholesterol in the living interstitial gland cell of the rabbit ovary. *Acta histol. Scand.*, 31: Suppl. 13, 53-78.
- Corner, G. W. 1963 Cytology of the ovum, ovary and fallopian tube. In: Special Cytology, (E. V. Cowdry, ed.). Hafner Publishing Co., New York, vol. 3, pp. 1565-1607.
- Crabo, B. 1963 Fine structure of the interstitial cells of the rabbit testis. *Z. Zellforsch.*, 61: 587-604.
- Davenport, G. R., and L. E. Mallette 1966 Some biochemical properties of rabbit ovarian hydroxysteroid dehydrogenases. *Endocrinology*, 78: 672-678.
- Davenport, G. R., P. I. C. Rennie and S. R. Longley 1967 Activities of phosphorylase in rabbit ovaries following mating. *Endocrinology*.
- Davies, J. 1962 Spontaneous vacuolar degeneration of the adrenal cortex in pregnant and pseudopregnant rabbits. *Endocrinology*, 71: 148-157.
- 1966 Electron microscopic criteria of function in steroid secreting cells of the rabbit ovary. Abstract, 1st Panamerican Congress of Anatomy, Mexico City.
- Davies, J., J. Falck Larsen, G. R. Davenport and B. Schmelling 1965 Plasma levels of ovarian ascorbic acid depleting material (luteinizing hormone?) in pregnant rabbits. *Proc. Soc. Exp. Biol. Med.*, 119: 925-930.
- Davies, J., G. R. Davenport, J. Norris and P. I. C. Rennie 1966 Histochemical studies of hydroxysteroid dehydrogenase activity in mammalian tissue. *Endocrinology*, 78: 667-671.
- Deane, H. W. 1958 Frontiers in Cytology, (S. L. Palay, ed.). Yale University Press, New Haven, p. 227.
- Eckstein, P. 1962 Ovarian physiology in the non-pregnant female. In: The Ovary, (Sir Solly Zuckerman, ed.). Academic Press, New York, vol. 1, pp. 317-318.
- Enders, A. C. 1962 Observations on the fine structure of lutein cells. *J. Cell Biol.*, 12: 101-113.
- Enders, A. C., and W. R. Lyons 1964 Observations on the fine structure of lutein cells. II. The effects of hypophysectomy and mammothrophic hormone in the rat. *J. Cell Biol.*, 22: 127-141.
- Falck, B. 1953 Occurrence of cholesterol and formation of oestrogen in the infantile rat ovary. *Acta Endocr. (Copenhagen)*, 12: 115-122.
- 1959 Site of production of oestrogen in rat ovary as studied in micro-transplants. *Acta physiol. Scand.*, 47: Suppl. 168, 1-101.
- Fawcett, D. W., and M. H. Burgos 1960 Studies on the fine structure of the mammalian testis. II. The human interstitial tissue. *Am. J. Anat.*, 107: 245-269.
- Flaks, B., and P. Bresloff 1966 Some observations on the fine structure of lutein cells of x-irradiated rat ovary. *J. Cell Biol.*, 30: 213-236.
- Gruraya, S. S., and G. S. Greenwald 1964 A comparative histochemical study of interstitial tissue and follicular atresia in the mammalian ovary. *Anat. Rec.*, 149: 411-434.

steroid-secreting cells in particular. Areas of granular endoplasmic reticulum are also commonly observed in steroid-producing cells, and direct continuity between it and vesicles or tubules of the agranular endoplasmic reticulum are also common, as shown in this study, and by others (Ross et al., '58; Enders, '62; Christensen, '65; Flaks and Bresloff, '66; Zelander, '59). These areas may be associated with regions of protein, or possibly lipoprotein, synthesis.

The mitochondria of steroid-secreting cells are also extremely varied in fine structure (Sheridan and Belt, '64), being of giant size in some cases, e.g. the fetal human adrenal cortex (Luse, '67), and in all cells often confused in phase-contrast microscopy with lipid droplets. The mitochondria of the ovarian interstitial cells become ovoid or spherical at an early stage in their differentiation and have an extremely complex system of internal cristae which are predominantly lamellar. Tubular or "villiform" cristae, though a regular feature of the zona fasciculata of the adrenal cortex and human fetal adrenal cortex, do not seem to be typical of all steroid-secreting cells. Internal membranes of this type are also seen in other organs (e.g. liver, placenta) not exclusively concerned with steroidal hormone production. Shrinkage and increased density of the mitochondrial matrix has been found to be an early indication of degeneration in interstitial cells. These shrunken forms resemble the "condensed" forms described in liver by Hackenbroeck ('66) and shown by him to be potentially reversible.

Information on the correlation of fine structure and function in the ovarian interstitial cells, as in all steroid-secreting cells, is fragmentary. Deane ('58) has emphasized that the number of lipid droplets is not necessarily a good criterion of functional activity. Isolation of the lipid droplets from the rabbit ovary (Claesson, '54) has shown that they are extremely stable over a wide range of time and physical conditions. About 75% of their lipid is esterified cholesterol, the remaining lipid being fatty acid (triglyceride, 23%), free cholesterol (1%), and phospholipid (1%). Following acute gonadotrophic stimula-

tion the droplets shrank slightly in size and showed a decrease in esterified cholesterol to about 25%, a rise in fatty acid, and a rise in phospholipid to 5%. These results, and those derived from histochemical studies (Rennels, '51; Falck, '53; Jacoby, '62) are consistent with the view that the droplets contain a depot of cholesterol to serve the needs of steroidal hormone biosynthesis. The depletion studies of Claesson are also consistent with the histochemical observation of a depletion of birefringent Schiff-positive and Schultz-positive material in the interstitial cells (not necessarily in the droplets) following gonadotrophic stimulation, and an accumulation after hypophysectomy. Boström and Odelblad ('52) observed an inverse relationship between the uptake of P^{32} and the amount of birefringent material in the interstitial tissue of the rabbit. Gonadotrophic stimulation, as after mating or the injection of luteinizing hormone, is also accompanied in the rabbit ovary by a depletion of ascorbic acid (Claesson, '54), by an almost total conversion of inactive to active phosphorylase (Davenport and Longley, '67), and by an outpouring of 20 α -hydroxyprogesterone into the ovarian venous blood (Hilliard et al., '63). This steroid appears to be the principal progestational steroid of the rabbit during the preovulatory and possibly the later stages of pregnancy. Though it has only about one-eighth the progestational activity of progesterone, it is produced in about ten times the amount (Rennie and Davies, '65). Rennie et al. ('65) have studied some of the enzymes of the glycolytic cycle in rabbit ovarian tissue for 8 days after mating, viz. glucose-6-phosphate dehydrogenase, phosphoglucosmutase, and phosphohexose isomerase. The activity of these enzymes showed no change that could be related to pregnancy but in those cases where variation was observed seemed to be related to the mass of interstitial tissue. Histochemically the rabbit's ovarian tissue shows marked hydroxysteroid dehydrogenase activity (Rubin et al., '63; Davies et al., '66), especially 3 β -ol dehydrogenase activity, essential for the conversion of pregnenolone to progesterone. Davenport and Mallette ('66) have made a study of hydroxysteroid dehydrogenase activity in the ovary

(minus corpora lutea) of the rabbit. They have demonstrated activity with 3 beta-, 17 beta-, and 20 alpha-hydroxysteroids. Preferences of one enzyme system for DPN or TPN were observed, and some were observed in the microsomal fraction and others in the supernatant. The role of the interstitial cells in the production of androgen or estrogen has not been substantiated (Morikard, '53; Eckstein, '62). Falck's observations on microtransplants of ovarian tissue in rats ('59) that these do not function independently but in synergy in the production of estrogen (e.g. granulosa cells plus theca interna cells, granulosa cells plus interstitial cells) may underlie the failure to ascribe a specific role to the ovarian interstitial tissue.

LITERATURE CITED

- Bel, W. D., and D. C. Pearse 1958 Mitochondrial structure in sites of steroid secretion. *J. Biophys. Biochem. Cytol.*, 2: Suppl., 269-374.
- Birkman, N. 1962 A study of ultrastructure of the granulosa cells of the rat ovary. *Acta anat. (Basel)*, 51: 125-147.
- Lochette, J. E. 1966 Ovarian steroid cells. I. Differentiation of the lutein cells from the granulosa follicle cell during the preovulatory stage and under the influence of exogenous gonadotrophins. *J. Cell Biol.*, 31: 501-516.
- . 1966 Ovarian steroid cells. II. The lutein cell. *J. Cell Biol.*, 31: 517-542.
- Burton, H., and E. Odelblad 1952 Autoradiographic observations on the uptake of S^{35} in the genital organs of the female rat and rabbit after injection of labelled sodium sulphate. *Acta Endocr. (Copenhagen)*, 10: 89-96.
- Burbell, F. W. R. 1962 Ovarian changes. In: *Marshall's Physiology of Reproduction*, (A. S. Parkes, ed.), Longmans, Green and Co., London, vol. 1, pp. 397-542.
- Carr, L. and J. Carr 1963 Membranous whorls in the testicular interstitial cell. *Anat. Rec.*, 141: 143-147.
- Casper, P. M. 1965 Elektronenmikroskopische Probleme bei Strukturdeutungen von Eizellenkörpern im menschlichen Corpus luteum. *Arch. Gynäk.*, 200: 552-568.
- Christensen, A. K. 1965 The fine structure of interstitial cell in guinea pigs. *J. Cell Biol.*, 25: 911-935.
- Christensen, A. K., and D. W. Fawcett 1961 The normal fine structure of opossum testicular cells. *J. Biophys. Biochem. Cytol.*, 9: 653-670.
- . 1966 The fine structure of testicular interstitial cells in mice. *Am. J. Anat.*, 118: 51-57.
- Cowan, L. 1954 The intracellular localization of the esterified cholesterol in the living interstitial gland cell of the rabbit ovary. *Acta physiol. Scand.*, 31: Suppl. 13, 53-78.
- Corner, G. W. 1963 Cytology of the ovum, ovary and fallopian tube. In: *Special Cytology*, (E. V. Cowdry, ed.), Hafner Publishing Co., New York, vol. 3, pp. 1565-1607.
- Crabo, B. 1963 Fine structure of the interstitial cells of the rabbit testis. *Z. Zellforsch.*, 61: 587-604.
- Davenport, G. R., and L. E. Mallette 1966 Some biochemical properties of rabbit ovarian hydroxysteroid dehydrogenases. *Endocrinology*, 78: 672-678.
- Davenport, G. R., P. I. C. Rennie and S. R. Longley 1967 Activities of phosphorylase in rabbit ovaries following mating. *Endocrinology*.
- Davies, J. 1962 Spontaneous vacuolar degeneration of the adrenal cortex in pregnant and pseudopregnant rabbits. *Endocrinology*, 71: 148-157.
- . 1966 Electron microscopic criteria of function in steroid secreting cells of the rabbit ovary. Abstract, 1st Panamerican Congress of Anatomy, Mexico City.
- Davies, J., J. Falck Larsen, G. R. Davenport and B. Schmelling 1965 Plasma levels of ovarian ascorbic acid depleting material (luteinizing hormone?) in pregnant rabbits. *Proc. Soc. Exp. Biol. Med.*, 119: 925-930.
- Davies, J., G. R. Davenport, J. Norris and P. I. C. Rennie 1966 Histochemical studies of hydroxysteroid dehydrogenase activity in mammalian tissue. *Endocrinology*, 78: 667-671.
- Deane, H. W. 1958 *Frontiers in Cytology*, (S. L. Palay, ed.), Yale University Press, New Haven, p. 227.
- Eckstein, P. 1962 Ovarian physiology in the non-pregnant female. In: *The Ovary*, (Sir Solly Zuckerman, ed.), Academic Press, New York, vol. 1, pp. 317-318.
- Enders, A. C. 1962 Observations on the fine structure of lutein cells. *J. Cell Biol.*, 12: 101-113.
- Enders, A. C., and W. R. Lyons 1964 Observations on the fine structure of lutein cells. II. The effects of hypophysectomy and mammothrophic hormone in the rat. *J. Cell Biol.*, 22: 127-141.
- Falck, B. 1953 Occurrence of cholesterol and formation of oestrogen in the infantile rat ovary. *Acta Endocr. (Copenhagen)*, 12: 115-122.
- . 1959 Site of production of oestrogen in rat ovary as studied in micro-transplants. *Acta physiol. Scand.*, 47: Suppl. 168, 1-101.
- Fawcett, D. W., and M. H. Burges 1960 Studies on the fine structure of the mammalian testis. II. The human interstitial tissue. *Am. J. Anat.*, 107: 245-269.
- Flaks, B., and P. Bresloff 1966 Some observations on the fine structure of lutein cells of x-irradiated rat ovary. *J. Cell Biol.*, 30: 213-236.
- Guraya, S. S., and G. S. Greenwald 1964 A comparative histochemical study of interstitial tissue and follicular atresia in the mammalian ovary. *Anat. Rec.*, 149: 411-434.

- Hackenbroeck, C. R. 1966 Ultrastructural basis for metabolically linked mechanical activity in mitochondria. *J. Cell Biol.*, 30: 269-297.
- Halliday, R. 1959 The occurrence of corpora lutea atretica in the ovaries of pregnant domestic rabbits. *J. Endocr.*, 19: 10-15.
- Hamilton, R. L., D. M. Regen, M. E. Gray and V. S. LeQuire 1966 Electron microscopic identification of very low density lipoproteins in perfused rat liver. *Lab. Invest.*, 16: 305-319.
- Hilliard, J., D. Archibald and C. H. Sawyer 1963 Gonadotrophic activation of preovulatory synthesis and release of progesterin in the rabbit. *Endocrinology*, 72: 59-66.
- Hilliard, J., R. Penardi and C. H. Sawyer 1967 A functional role for 20 α -hydroxy-pregnen-4-one in the rabbit. *Endocrinology*, 80: 901-909.
- Jacoby, F. 1962 Ovarian histochemistry. In: *The Ovary*, (Sir Solly Zuckerman, ed.). Academic Press, New York, vol. 1, pp. 189-245.
- Kilpatrick, R. D. T., D. T. Armstrong and R. O. Greep 1964 Maintenance of the corpus luteum by gonadotrophins in the hypophysectomized rabbit. *Endocrinology*, 74: 453-461.
- de Kretzer, D. M. 1967 The fine structure of the testicular interstitial cells in men of normal androgenic status. *Z. Zellforsch.*, 80: 594-609.
- Lane-Clayton, J. 1905 On the origin and life history of the interstitial cells of the ovary in the rabbit. *Proc. Roy. Soc. (London) B*, 77: 32-56.
- Leeson, C. R. 1963 Observations on the fine structure of rat interstitial tissue. *Acta anat. (Basel)*, 52: 34-48.
- Lever, J. D. 1956 Remarks on the electron microscopy of the rat luteum and comparison with earlier observations on the adrenal cortex. *Anat. Rec.*, 124: 111-125.
- 1959 Electron microscopic observations on the adrenal cortex. *Am. J. Anat.*, 97: 409-429.
- Limon, M. 1902 Etude histologique et histogénique de la glande interstielle de l'ovaire. *Arch. Anat. Micr. Morph. Exp.*, 5: 155-180.
- Luse, S. 1967 In: *The Adrenal Cortex*, (A. Eisenstein, ed.). Little, Brown and Co., Boston.
- Mercer, E. H. 1962 In: *The Interpretation of Ultrastructure* (R. J. C. Harris, ed.). Academic Press, New York, p. 369.
- Morleard, R. 1953 Effects of chorionic and equine gonadotrophins on hypophysectomized immature rats. *Ciba Found. Coll. Endocr.*, 5: 33-43.
- Muta, T. 1958 The fine structure of the interstitial cell in the mouse ovary studied with electron microscopy. *Kurume Med. J.*, 5: 167-185.
- Rennels, E. G. 1951 Influence of hormones on the histochemistry of ovarian interstitial tissue in the immature rat. *Am. J. Anat.*, 88: 63-100.
- 1966 Observations on the ultrastructure of luteal cells from PMS and PMS-HCG treated immature rats. *Endocrinology*, 79: 373-386.
- Rennie, P. I. C., and G. R. Davenport 1963 Glucose-6-phosphate dehydrogenase (G6PDH) phosphoglucosyltransferase (PGMT), and phosphoglucoisomerase (PGI) activities in rabbit ovarian tissue. Abstract, Endocrine Society, New York June.
- Rennie, P. I. C., and J. Davies 1965 Implantation in the rabbit following administration of 20 α -hydroxy-pregnen-3-one and 20 α -hydroxy-pregnen-3-one. *Endocrinology*, 76: 535-537.
- Revel, J. P., L. Napolitano and D. W. Fawcett 1960 Identification of glycogen in electron micrographs of thin tissue sections. *J. Biophys. Biochem. Cytol.*, 8: 575-589.
- Reynolds, E. S. 1963 The use of lead citrate at high pH as an electron-opaque stain in electron microscopy. *J. Cell Biol.*, 17: 209-212.
- Ross, J. H., G. D. Pappas, J. T. Lanman and J. Lind 1958 Electron microscopic observation on the endoplasmic reticulum in the human fetal adrenal. *J. Biophys. Biochem. Cytol.*, 4: 659-661.
- Rubin, L. B., H. W. Deane and J. A. Hamilton 1963 Biochemical and histochemical identification of Δ^4, β -hydroxysteroid dehydrogenase activity in the adrenal cortex and ovaries of diverse mammals. *Endocrinology*, 73: 748-763.
- Sabatini, D. D., and E. D. P. de Robertis 1965 Ultrastructural zonation of adrenocortex in the rat. *J. Biophys. Biochem. Cytol.*, 9: 105-119.
- Sabatini, D. D., E. D. P. de Robertis and H. Bleichman 1962 Submicroscopic study of the pituitary action on the adrenocortex of the rat. *Endocrinology*, 70: 390-406.
- Sainmont, G. 1906 Recherches relatives à l'organogénèse du testicule et de l'ovaire chez le chat. *Arch. Biol.*, 22: 71-153.
- Schwarz, W., and H. J. Merker 1967 Die Hodenzwischenzellen der Ratte nach Hypophysektomie und nach Behandlungen mit Choriongonadotropin und Amphipon B. *Z. Zellforsch.*, 65: 272-284.
- Sheridan, M. W., and W. D. Belt 1964 Fine structure of the guinea pig adrenal cortex. *Anat. Rec.*, 149: 73-78.
- Sluiter, J. W. 1945 Experimentelle Untersuchungen über die Funktion des Interstitiums der Gonade. I. Versuche an männlichen und weiblichen juvenilen Mäusen. *Z. Zellforsch.*, 33: 311-335.
- Velardo, J. L. 1959 Hormonal action of chorionic gonadotrophin. *Ann. N. Y. Acad. Sci.*, 80: 65-85.
- Wartenberg, H., and H. E. Stegner 1960 Über die Elektronenmikroskopische Feinstruktur der menschlichen ovarialen. *Z. Zellforsch.*, 52: 450-474.
- Zelander, T. 1959 Ultrastructure of the mouse adrenal cortex. An electron microscopical study in intact and hydrocortisone-treated male adults. *J. Ultrastruct. Res.*, 2: Suppl. 2.

PLATE 1

EXPLANATION OF FIGURES

- 1 Ovarian interstitial tissue of immature virgin rabbit (2 kilos). The cells are small with a relatively small area of cytoplasm which is uniformly acidophilic. The cells are arranged in clusters with thick septa of connective tissue between them. At the top left (arrow) is the remains of an atretic follicle. H and E, $\times 335$.
- 2 Interstitial tissue of non-pregnant ("estrous") rabbit (3 kilos). The cells are larger (c.p. fig. 1) and show a much greater ratio in area between cytoplasm and nucleus. The cytoplasm is vacuolated except for a small perinuclear zone of acidophilic material. The cells are in close mutual contact with only occasional capillaries which lie predominantly in the septa of connective tissue between clusters or lobules of interstitial tissue. H and E, $\times 335$.
- 3 Interstitial tissue of rabbit at the ninth day of pregnancy. The cells are hypertrophied (c.p. fig. 2). The perinuclear and acidophilic zone is particularly conspicuous. The peripheral cytoplasm is vacuolated. H and E, $\times 335$.
- 4 Interstitial tissue of rabbit at the twenty-fifth day of pregnancy. This area illustrates the lack of homogeneity in the cellular population of the interstitial tissue but also illustrates its essential development and final arrangement in clusters or lobules. To the right is an area of immature cells (c.p. fig. 1), arising in relation to the theca interna of an atretic follicle. To the left is a group of interstitial cells of mature type comparable to those in figure 3. H and E, $\times 335$.

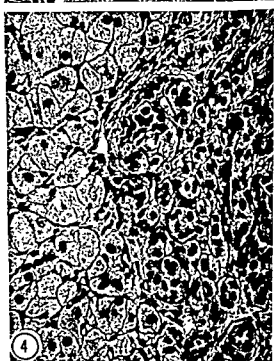
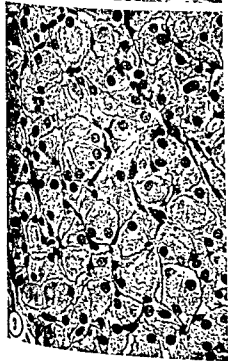
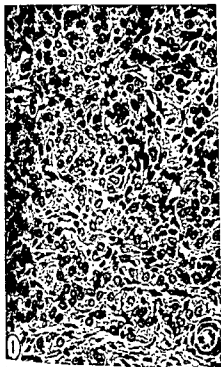
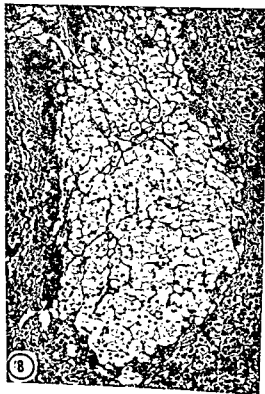
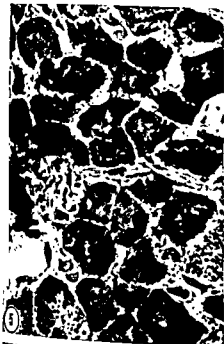


PLATE 2

EXPLANATION OF FIGURES

- 5 Phase-contrast photograph of ovarian interstitial tissue of a non-pregnant ("estrous") rabbit. The cells are packed with small droplets of osmophilic material (lipid). "Dark" and "light" cells are present, the difference being due to the density of the droplets and to the greater density of the background cytoplasm. The droplets vary in size but are constant in size within any one cell. Fixed in 2% osmic acid and buffered phosphate (350 m.osmols, pH 7.4), $\times 1,000$.
- 6 Phase-contrast photograph of ovarian interstitial tissue of pregnant rabbit at the sixteenth day. The cells are hypertrophied and there is less distinction between "dark" and "light" cells. The lipid droplets are numerous but more widely spaced. Fixation as in figure 6, $\times 1,000$.
- 7 Area of ovarian interstitial tissue of rabbit at the twenty-third day of pregnancy showing the occurrence of individual degenerating cells (at arrows). These cells are enlarged, showing nuclear pycnosis and an "empty" or "stippled" cytoplasm. The perinuclear acidophilic zone is absent in the degenerated cells (N.B. loss of this zone is a significant early sign of loss of function or of early degeneration). H and E, $\times 355$.
- 8 A different and rarer type of degeneration of interstitial cells in a non-pregnant ("estrous") rabbit. In this case the degeneration is "lobular" in pattern rather than "individual" and involves a large group of cells, presumably one once derived from the wall of an atretic follicle. The cellular appearance of the degenerating cells is as in figure 7. H and E, $\times 100$.



Abbreviations

b, electron dense body	m, mitochondrion
c, crystal	p, cell processes
d, dilatation of Golgi	n, nucleus
e, endothelium	nl, nucleolus
f, myelin figure	r, rough endoplasmic reticulum
g, Golgi	v, vesicle
l, lipid	

All succeeding figures are electron micrographs. They are all of ovarian interstitial tissue unless otherwise indicated, fixed in 2% osmic acid adjusted with 0.3 M phosphate buffer to a final osmolarity of about 350 m.osmols (final buffer concentration about 0.15 M) and at a pH of about 7.2. Tissues were embedded in English araldite and stained with uranyl acetate and lead citrate.

PLATE 3

EXPLANATION OF FIGURES

- 9 Interstitial cell from ovary of immature rabbit of 7.5 weeks. The appearance of such a cell in the light microscope is shown in figure 1. There are a few mitochondria, elongated or oval in shape, containing lamellar cristae. The Golgi areas are prominent. The cytoplasm contains vesicular bodies assumed to be representative of the smooth endoplasmic reticulum, which contain electron dense material (lipid?). An irregular and larger vesicle (at arrow) appears empty; it may have contained lipid before fixation. There are many cytoplasmic granules, one population being small and probably representing ribosomes, and a second population of larger size which is possibly glycogen. $\times 70,000$.
- 10 Details of immature interstitial cells from prepubertal rabbit of about five months. The cytoplasm in this area contains mitochondria, small vesicles of the endoplasmic reticulum which contain electron dense material and granules (probably ribosomes). $\times 65,000$.
- 11 Degenerating interstitial cell from immature rabbit of five months showing the loss of cytoplasmic organization (c.p. fig. 10). In addition there are spaces whose shape suggests that they were formerly occupied by crystals (cholesterol?). There are also "myelin figures" and other electron dense masses which may be lysosomes. $\times 33,000$.

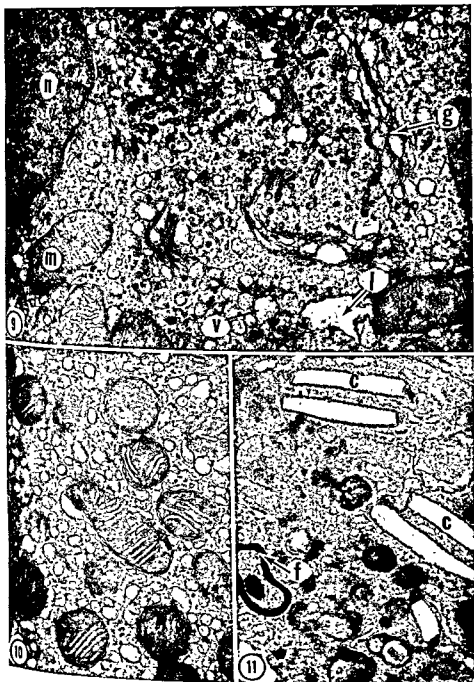


PLATE 4

EXPLANATION OF FIGURE

- 12 Partially differentiated (immature) interstitial cell of prepubertal rabbit of about 5.5 months. The mitochondria are predominantly spherical with the irregular cristae typical of mature cells (c.p. fig. 15). Large lipid droplets, partially or completely emptied of their contents, are observed at top right and bottom right. The cytoplasm contains a complex system of smooth membranes. Some are arranged in parallel rows enclosing cisternal spaces containing homogeneous electron dense material, and they are assumed to be Golgi areas. Regional dilatations of the Golgi cisterns are observed at d. Elsewhere the membranes are disposed in the form of roughly spherical vesicles or short tubules containing electron dense material. There are a few electron dense bodies within the Golgi area. Cytoplasmic granules probably represent ribosomes and glycogen. $\times 40,000$.



PLATE 5

EXPLANATION OF FIGURE

- 13 Almost fully differentiated interstitial cells from a young non-pregnant rabbit of about 5.5 months. Two cells are observed with their plasma membranes in close contact. There is an extensive extracellular space in relation to the blood vessels at the lower end of the figure, containing wisps of collagen, processes of other interstitial cells and traces of basement membrane in relation to the processes and to the endothelium of the vessels. The mitochondria are typical of mature interstitial cells. There are large lipid droplets, highly irregular in shape and containing homogeneous electron dense material. There are, in addition, small vesicles, also containing electron dense material. Ribosomes and glycogen are rare. $\times 45,000$.

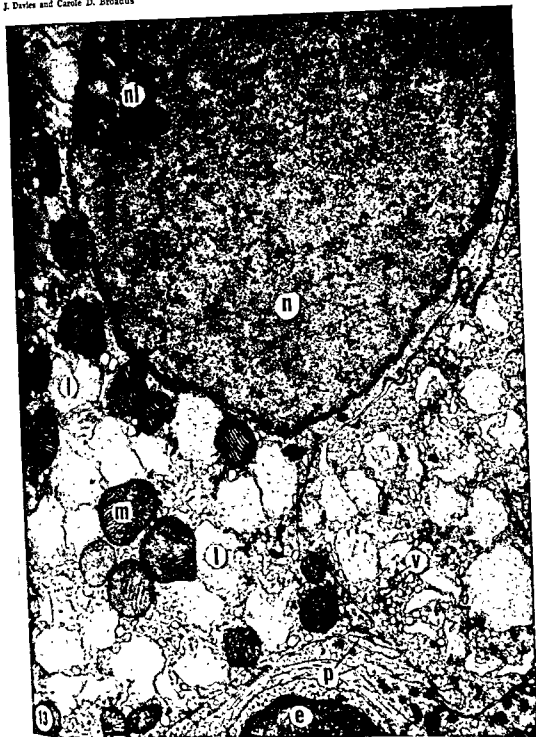
OVARIAN INTERSTITIAL CELLS OF RABBIT
J. Davies and Carole D. Broadus

PLATE 5

EXPLANATION OF FIGURE

- 13 Almost fully differentiated interstitial cells from a young non-pregnant rabbit of about 5.5 months. Two cells are observed with their plasma membranes in close contact. There is an extensive extracellular space in relation to the blood vessels at the lower end of the figure, containing wisps of collagen, processes of other interstitial cells and traces of basement membrane in relation to the processes and to the endothelium of the vessels. The mitochondria are typical of mature interstitial cells. There are large lipid droplets, highly irregular in shape and containing homogeneous electron dense material. There are, in addition, small vesicles, also containing electron dense material. Ribosomes and glycogen are rare. $\times 45,000$.

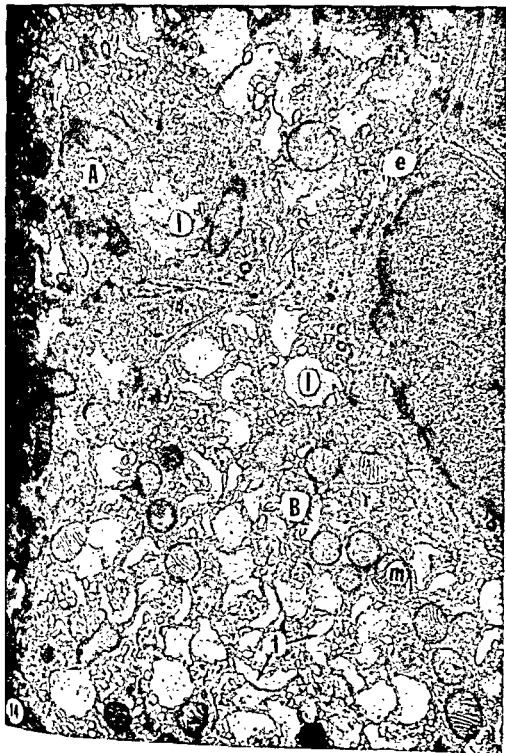


PLATE 6

EXPLANATION OF FIGURE

- 14 Cluster of interstitial cells from an immature rabbit of about five months in various stages of differentiation. Less differentiated cells (e.g. A) are characterized by the relative abundance of ribosomes and a paucity of lipid droplets and vesicles and by elongated mitochondria with simple cristae. More advanced cells (e.g. B) are characterized by an abundance of irregular lipid droplets, by many small endoplasmic vesicles also containing electron dense material, by spherical mitochondria with complex cristae, and by widely scattered and less dense accumulations of ribosomes and glycogen. The irregularity of the lipid droplets, presumably recently formed droplets, suggests that they may arise within dilated cisternae of the endoplasmic reticulum; a continuous and distinct limiting membrane is suggested here but is not always easy to define. In less differentiated cells (as A) in which there is little endoplasmic reticulum the lipid droplets are highly irregular and appear to arise freely within the cytoplasm with no limiting membrane. $\times 45,000$.

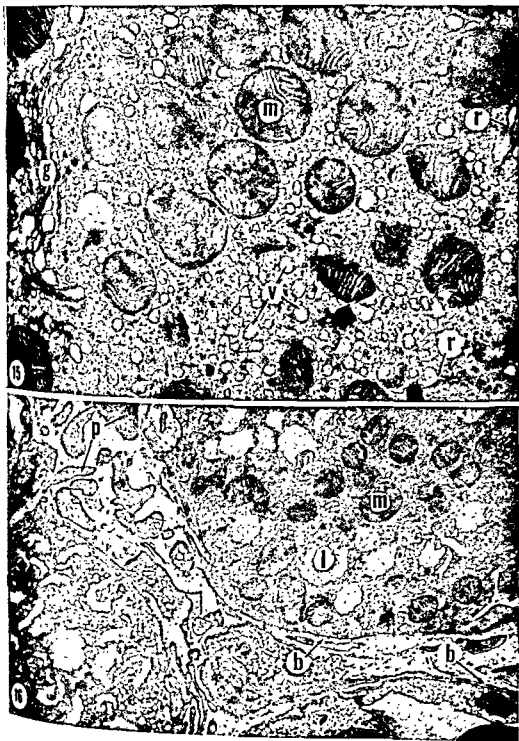


PLATE 7

EXPLANATION OF FIGURES

- 15 Mature interstitial cell of non-pregnant ("estrous") rabbit. This is typical "light" cell, as shown in figure 5. The Golgi area is prominent. Its component cisternae are dilated peripherally, forming vesicles with electron dense contents similar to those found elsewhere within the cytoplasm. The latter vary in size from about 500 to 1200 Angstroms. In some areas (e.g. r) there is direct continuity between rough endoplasmic reticulum and the smooth-walled vesicles. The mitochondria are typical of mature interstitial cells. The cristae are disposed in groups of parallel membranes, one group often being at an angle to another. There is a dense finely granular matrix. No large lipid droplets are shown in this figure though they are invariably present in mature interstitial cells. $\times 65,000$.
- 16 Two "dark" cells from the "interstitial gland" of a rabbit at the tenth day of pseudopregnancy. Similar "dark" cells are found in non-pregnant animals and so far are not to be interpreted as typical of pregnancy or pseudopregnancy. They are characterized by a closely packed network of smooth-walled endoplasmic reticulum in the form of compressed vesicles or short tubules. Irregular lipid droplets and mitochondria are scattered throughout the cytoplasm. An extensive extracellular space with collagen and processes of other interstitial cells is also shown. A thin discontinuous basement membrane (b) enveloped groups of interstitial cells and their processes. This is a continuous basement membrane in relation to the endothelium of the blood vessels. $\times 25,000$.

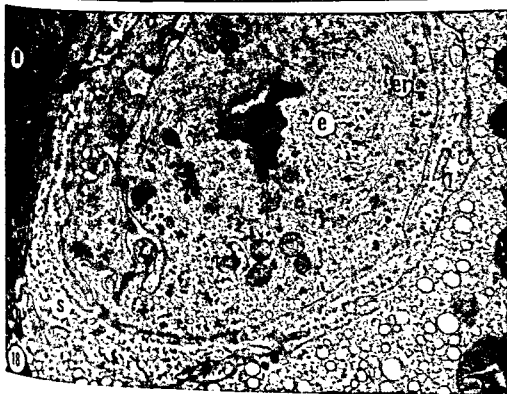


PLATE 8

EXPLANATION OF FIGURES

- 17 Portion of an interstitial cell from a rabbit at the sixth day of pregnancy showing the "microtubules" of the cytoplasm. They are only seen in material fixed in glutaraldehyde. Fixation, 1.25% glutaraldehyde with phosphate buffer, osmolarity about 350 m.osmols. $\times 90,000$.
- 18 Blood vessel of the ovarian interstitial tissue and adjacent cells of a rabbit at the thirtieth day of pregnancy. The lumen of the vessel is collapsed. The endothelial cells contain lipid droplets, endoplasmic reticulum and accumulations of monoparticulate glycogen. There is an extensive extracellular space containing wavy strands of material similar to that of basement membranes and also wisps of collagen. $\times 21,000$.

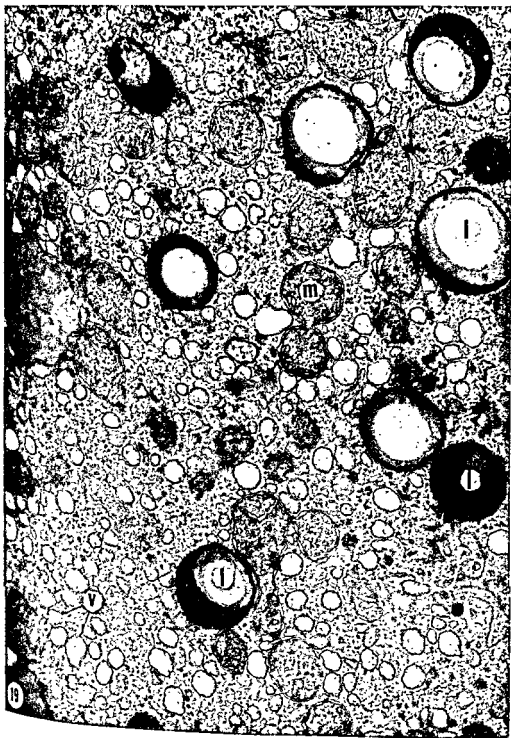


PLATE 9

EXPLANATION OF FIGURE

- 19 Interstitial cell of rabbit seven days after parturition. The cell depicted may be degenerating and was selected to show stages suggesting the transformation of lipid droplets into electron dense bodies. A general regression of the interstitial tissue in the post-partum period is not implied by the selection of this figure. Lipid droplets are shown in which electron dense material accumulates peripherally and gradually extends deeply into the center of the droplet which also shrinks. The empty area in the center of such droplets suggests poor penetration of the fixative. Mitochondria here are somewhat simpler in their pattern of cristae than in fully active cells and there is a suggestion that they may be tubular in type. Granules, probably of glycogen, are common. $\times 37,500$.



PLATE 10

EXPLANATION OF FIGURES

- 20 Degenerating interstitial cell of a rabbit at the thirtieth day of pregnancy. The mitochondria are shrunken and show simplification of their pattern of cristae and increased electron density of the matrix. The formation of parallel arrays of membranes superficially resembling Golgi areas may result from the degeneration of mitochondria. Some of these areas may be early stages in the formation of "myelin figures" (v. fig. 21). The lipid droplets vary in form from irregular masses of slight electron density (lower right) to rounded droplets having a peripheral condensation of very electron dense material (upper left). The small vesicles of the endoplasmic reticulum appear empty for the most part. $\times 21,000$.
- 21 Degenerating interstitial cell of the ovary of a non-pregnant ("estrous") rabbit. Such cells may be observed throughout the ovary of mature rabbits at any stage of the reproductive life (see figs. 7, 8). Here there is almost complete disorganization of the fine structure of the cell. Remnants of mitochondria may be recognized. "Myelin figures," apparently formed at the expense of the endoplasmic reticulum (f), are common and varied in morphology. Accumulations of extremely electron dense granules, larger than those assumed in previous figures to represent glycogen, are frequent; they lie free in the cytoplasm without limiting membranes (x). $\times 24,000$.

Fluid Flow in the Liver Demonstrated with Horse Radish Peroxidase

J. M. PAPADIMITRIOU AND M. N. L. WALTERS

Department of Pathology, University of Western Australia,
Perth, Western Australia

ABSTRACT Using horse radish peroxidase as a tracer for fluid flow, rapid diffusion was demonstrated between sinusoidal lumina and the interhepatocytic spaces of the murine liver. The marker passed rapidly between adjacent sinusoidal cells and filled the space of Disse. Appreciable amounts of peroxidase were also seen in pinocytotic and phagocytotic vacuoles within sinusoidal cells. Many junctions in the wall of bile canaliculi impeded the passage of the marker, but in some sites this hindrance did not occur. This provides a path for the direct exchange of material between vascular and biliary contents. Such a mechanism may be physiologically controlled. Junctions in bile ductules prevent diffusion of horse radish peroxidase.

For over a century the attention of morphologists and physiologists has been directed to the peculiarities of blood and fluid flow in the vertebrate liver. With the development of modern experimental techniques some of these problems are slowly being resolved. In this report ultrastructural histochemical techniques have been employed to trace the flow of fluid in the liver of the albino mouse; horse radish peroxidase (HRP) was used as the marker. This small haemoprotein has a molecular weight of approximately 40,000 (Keilin and Hartree, '65) which, in comparison with other plasma proteins, provides a more realistic picture of fluid flow than the use of larger, electron-dense markers such as ferritin. Horse radish peroxidase was first used as a marker by Straus ('57); it was later developed for ultrastructural histochemical techniques by Karnovsky ('63a).

Horse radish peroxidase activity can be demonstrated by its interaction with 3,3'-diaminobenzidine and H_2O_2 . The product of this reaction combines with osmium tetroxide and is deposited as electron-dense, easily seen material.

MATERIALS AND METHODS

Prince Henry albino mice weighing between 30-35 gm were injected intravenously with 3.0 mg of horse radish peroxidase dissolved in 0.5 ml of 0.9% saline. Hepatic biopsies were taken at 1, 2, 5, 10, 15 and 30 minute intervals. Specimens

from at least three mice were removed at each time interval. Small blocks of tissue were immersed in cold 6.25% glutaraldehyde in 0.1 M phosphate buffer (pH 7.5) and allowed to fix for four hours; they were then washed overnight in 0.1 M phosphate buffer containing 5% sucrose.

Sections 40 μ in thickness were cut on a freezing microtome and the tissue processed by the method of Graham and Karnovsky ('66). The sections were incubated for five to ten minutes in a saturated solution of 3,3'-diaminobenzidine in 0.05 M Tris HCl buffer (pH 7.6) containing 0.01% H_2O_2 . After washing in distilled water the sections were fixed in 1% osmium tetroxide in phosphate buffer (pH 7.3) for 90 minutes.

At the time of biopsy other portions of liver were immersed directly in osmium tetroxide in phosphate buffer (pH 7.3) and allowed to fix for 90 minutes. These were used as control examples of normal ultrastructure. After osmication the tissues were dehydrated in graded solutions of ethanol and embedded in Araldite according to the method of Luft ('61). Sections were cut with an LKB ultramicrotome and examined on a JEM T6 electron microscope. Mice injected with HRP served as controls.

OBSERVATIONS

A. Livers from uninjected mice. The sinusoidal cell layer is discontinuous, the gaps between adjacent cells measuring

passed (Farquhar and Palade, '63). It would appear that most of the intercellular space in the liver is available for rapid diffusion and exchange of substances. It has been suggested that this intercellular space may serve as a channel for conveying a protein-free filtrate of plasma from the hepatic sinusoids to the bile canaliculi (Ashworth and Sanders, '60). The findings in this study add some support to this belief. An intercellular aqueous pathway has been suggested for other tissues such as the choroid plexus (Maxwell and Pease, '56), ciliary epithelium of the eye (Pappas et al., '59), the kidney (Pease, '56; Sjostrom and Rhodin, '53), and the cornea (Kaye et al., '62).

Most bile canaliculi were free of the tracer. This may be due to the terminal bars of the interhepatocytic space situated along the length of the canaliculi (Carnethers and Steiner, '62); these may be similar to the zonulae occludentes described by Farquhar and Palade ('63). Such structures are said to be the sites of maximal constraint to the progress of diffusion in epithelial tissues. A few bile canaliculi, however, did exhibit horse radish peroxidase activity in their lumina, indicating that in some instances diffusion beyond the junction (terminal bar) can occur. Such a phenomenon may be due to faults in junctional regions and may depend on the physiological state of the liver and be temporary rather than permanent. Karnovsky ('65) has demonstrated the passage of the protein tracer through the junctions of vascular endothelium in myocardium. Cerebral capillaries, however, understood the passage of peroxidase (Fluse and Karnovsky, '67). Florey ('64) showed the entry of saccharated iron oxide into similar junctions in vascular endothelium, although it was uncommon. These findings indicate that such junctions may be patent under some physiological conditions; factors, as yet unknown, probably govern the patency of these junctions. On the other hand, morphologically similar structures may perhaps be functionally dissimilar in different cell types; this is suggested by the differences between the junctions of cerebral capillaries and those of myocardium and striated muscle. More recently, Graham and Karnovsky ('66) failed

to demonstrate entry of HRP into the luminal aspect of the intercellular space of renal tubular epithelium; such entry was probably impeded by the apical junction. Essentially similar results were obtained by Becker et al. ('67) for the choroid plexus. Thus the weight of evidence is that, with the exception of vascular endothelium in heart and skeletal muscle, zonular junctions generally impede diffusion of molecules of the size of horse radish peroxidase; small molecules such as water and electrolytes need not necessarily be hindered, this still remaining unproven. The apical junctions of ductular epithelium also obstruct the passage of HRP. We could not conclusively demonstrate the type of junctions in the walls of bile canaliculi, and a differentiation between zonula adherens and a zonula occludens could not be made.

The possibility of some dissolution of the intercellular material by the enzymatic effect of HRP needs also to be considered. Information on this is, however, lacking but, considering the data cited above, any such reaction would appear to be dependent on the type of junction encountered.

The disappearance of HRP from the extracellular space within 30 minutes indicates a pathway for rapid clearance. This may be accomplished by lymphatic drainage (Hampton, '58) and by drainage into a few selected bile canaliculi in which the patency of some junctions provides a means of direct exchange between the vascular and biliary compartments. This pathway may be under physiological control and may be disturbed in disease. The existence of connections between the space of Disse and bile canaliculi has been suggested by some electron microscopists (Rouiller, '54, '56; Cossel, '62; Schaffner and Popper, '59a,b). Rouiller and Simon ('62) and more recently Yodaiken ('66) have reaffirmed this, but state that the occurrence of such channels was rare. Other workers deny their presence. (Steiner, '61; Steiner et al., '61; Novikoff and Essner, '60; Goldfischer et al., '62). Although retrograde injection of colloidal particles did not demonstrate such a pathway (Hampton, '58), the size of the particles used was probably too great when compared with the relatively small molecular weight of

0.01–1 μ (fig. 1). In the space of Disse discontinuous strands of osmiophilic material reminiscent of the basement membrane of vascular endothelium are found (fig. 1). A few cells lining the sinusoidal wall also exhibit tight junctions of the type seen in vascular endothelium (fig. 2). Occasional fenestrae occur in some of the sinusoidal cells (fig. 2). These measure approximately 0.1 μ in diameter; those cells having them are unsupported by a basement membrane.

The ultrastructural morphology of hepatocytes resembles closely that described by various authors (Dalton et al., '50; Daems, '61; Novikoff and Essner, '60; Bruni and Porter, '65).

B. Livers from mice injected with horse radish peroxidase. Within one minute the reaction product is present in hepatic sinusoids and between adjacent sinusoidal cells. Sites of HRP activity are easily distinguished by their electron density. By two minutes activity occurs in pinocytic and phagocytic vacuoles within the cytoplasm of Kupffer cells. Small amounts of reaction product are also present in the space of Disse (figs. 3, 4).

After five minutes the marker completely fills the space of Disse and outlines the hepatocytic microvilli. At the sinusoidal border of the hepatocyte small pinocytic vesicles containing the tracer are forming (figs. 3, 5).

Reaction product is also present in the intercellular space between adjoining hepatocytes and is directly continuous with the material in the subsinusoidal space of Disse (fig. 5). The tracer is not uniformly distributed in the interhepatocytic space; thin strands measuring 40–50 Å in thickness and displaying marker activity are seen.

Despite the widespread distribution of reaction product in the interhepatocytic space, many of the bile canaliculi do not contain the tracer which appears to be impeded by the junctional region (terminal bar) of the canaliculus (fig. 6). This, however, is not invariable and several bile canaliculi do contain the marker which is directly continuous with that in the interhepatocytic space (figs. 7, 8).

After ten minutes the tracer lies within the periductular space between bile ductu-

lar cells and hepatocytes; once again it occurs in the intercellular space between adjacent ductular epithelial cells (fig. 9). The basement membrane at the base of the bile ductules does not impede diffusion from the periductular space into the intercellular space. However, there is no tracer in the lumen of the duct.

At 30 minutes the marker is absent from the intercellular spaces of the liver and the reaction product is confined solely to phagocytic vacuoles in Kupffer cells and to a few hepatocytic lysosomes.

DISCUSSION

On structural grounds it is unlikely that the discontinuous sinusoidal wall offers any resistance to the flow of fluid from within the sinusoidal space to the space of Disse. It is also unlikely that the fragmented basement membrane in the space of Disse is a source of impedence. This is demonstrated by the rapidity of appearance of HRP activity in the intercellular areas between the sinusoidal cells and in the space of Disse. Data from isotopic studies also confirm that the walls of the sinusoids are freely permeable to plasma protein (McCarrel and Drinker, '41).

Although peroxidase passed rapidly between adjacent sinusoidal cells we could not conclusively ascertain whether the sparse intercellular tight junctions in the sinusoidal wall impeded the diffusion of HRP. Fenestrae have been previously described in the vascular endothelium of the endocrine glands, in structures engaged in rapid exchange of fluids (such as the renal glomerulus and the choroid plexus) and also in retia mirabilia (Majno, '65) but have also been reported in the liver of normal rats (Burkel and Low, '66) and in the connective tissue proliferation during extra-hepatic cholestasis (Carruthers et al., '62). Whether fenestrae in hepatocytic sinusoids are permeable to the flow of fluid could not be established.

Diffusion of marker into the interhepatocytic space is rapid and unimpeded. This is not unexpected, for, apart from bile canaliculi, ultrastructural studies have shown only maculae adherens or desmosomes between adjoining hepatocytes. These are circumscribed areas of intercellular attachment and can be easily by-

assed (Farquhar and Palade, '63). It would appear that most of the intercellular space in the liver is available for rapid diffusion and exchange of substances. It has been suggested that this intercellular space may serve as a channel for conveying a protein-free filtrate of plasma from the hepatic sinusoids to the bile canaliculi (Ashworth and Sanders, '60). The findings in this study add some support to this belief. An intercellular aqueous pathway has been suggested for other tissues such as the choroid plexus (Maxwell and Pease, '56), ciliary epithelium of the eye (Pappas et al., '59), the kidney (Pease, '56; Sjöstrand and Rhodin, '53), and the cornea (Kaye et al., '62).

Most bile canaliculi were free of the tracer. This may be due to the terminal bars of the interhepatocytic space situated along the length of the canaliculi (Carnuthers and Steiner, '62); these may be similar to the zonulae occludentes described by Farquhar and Palade ('63). Such structures are said to be the sites of maximal constraint to the progress of diffusion in epithelial tissues. A few bile canaliculi, however, did exhibit horse radish peroxidase activity in their lumina, indicating that in some instances diffusion beyond the junction (terminal bar) can occur. Such a phenomenon may be due to faults in junctional regions and may depend on the physiological state of the liver and be temporary rather than permanent. Karnovsky ('65) has demonstrated the passage of the protein tracer through the junctions of vascular endothelium in myocardium. Cerebral capillaries, however, withstood the passage of peroxidase (Reese and Karnovsky, '67). Florey ('64) showed the entry of saccharated iron oxide into similar junctions in vascular endothelium, although it was uncommon. These findings indicate that such junctions may be patent under some physiological condition; factors, as yet unknown, probably govern the patency of these junctions. On the other hand, morphologically similar structures may perhaps be functionally dissimilar in different cell types; this is suggested by the differences between the junctions of cerebral capillaries and those of myocardium and striated muscle. Moreover, Graham and Karnovsky ('66) failed

to demonstrate entry of HRP into the luminal aspect of the intercellular space of renal tubular epithelium; such entry was probably impeded by the apical junction. Essentially similar results were obtained by Becker et al. ('67) for the choroid plexus. Thus the weight of evidence is that, with the exception of vascular endothelium in heart and skeletal muscle, zonular junctions generally impede diffusion of molecules of the size of horse radish peroxidase; small molecules such as water and electrolytes need not necessarily be hindered, this still remaining unproven. The apical junctions of ductular epithelium also obstruct the passage of HRP. We could not conclusively demonstrate the type of junctions in the walls of bile canaliculi, and a differentiation between zonula adherens and a zonula occludens could not be made.

The possibility of some dissolution of the intercellular material by the enzymatic effect of HRP needs also to be considered. Information on this is, however, lacking but, considering the data cited above, any such reaction would appear to be dependent on the type of junction encountered.

The disappearance of HRP from the extracellular space within 30 minutes indicates a pathway for rapid clearance. This may be accomplished by lymphatic drainage (Hampton, '58) and by drainage into a few selected bile canaliculi in which the patency of some junctions provides a means of direct exchange between the vascular and biliary compartments. This pathway may be under physiological control and may be disturbed in disease. The existence of connections between the space of Disse and bile canaliculi has been suggested by some electron microscopists (Rouiller, '54, '56; Cossel, '62; Schaffner and Popper, '59a,b). Rouiller and Simon ('62) and more recently Yodaiken ('66) have reaffirmed this, but state that the occurrence of such channels was rare. Other workers deny their presence. (Steiner, '61; Steiner et al., '61; Novikoff and Essner, '60; Goldfischer et al., '62). Although retrograde injection of colloidal particles did not demonstrate such a pathway (Hampton, '58), the size of the particles used was probably too great when compared with the relatively small molecular weight of

horse radish peroxidase. The present results would favour the existence of these intercommunicating channels.

LITERATURE CITED

- Ashworth, C. T., and E. Sanders 1960 Anatomical pathway of bile formation. *Amer. J. Path.*, 37: 33-350.
- Becker, N. H., A. B. Novikoff and H. M. Zimmerman 1967 Fine structure observations of the uptake of intravenously injected peroxidase by the rat choroid plexus. *J. Histochem. Cytochem.*, 15: 160-165.
- Bruni and K. R. Porter 1965 The fine structure of the parenchymal cell of the normal rat liver. I. General Observations. *Amer. J. Path.*, 46: 691-755.
- Burkel, W. E., and F. N. Low 1966 The fine structure of rat liver sinusoids, space of Disse and associated tissue space. *Am. J. Anat.*, 118: 769-784.
- Carruthers, J. S., S. R. Kalifat and J. W. Steiner 1962 The ductular cell reaction of rat liver in extrahepatic cholestasis. II. The proliferation of connective tissue. *Exptl. Molec. Path.*, 1: 377-396.
- Carruthers, J. S., and J. W. Steiner 1962 Fine structure of terminal branches of the biliary tree. III. Parenchymal cell cohesion and "intracellular bile canaliculi." *Arch. Path.*, 74: 117-126.
- Cossel, L. 1962 Über den submikroskopischen Zusammenhang der interzellulären Räume und Sinusoide in der Leber. *Z. Zellforsch.*, 58: 76.
- Daems, W. Th. 1961 The microanatomy of the smallest biliary pathways in mouse liver tissue. *Acta Anat.*, 46: 1-24.
- Dalton, A. J., H. Kahler, M. J. Striebich and B. Lloyd 1950 Fine structure of hepatic intestinal and renal cells of mouse as revealed by the electron microscope. *J. Natl. Cancer Inst.*, 11: 439-461.
- Farquhar, M. G., and G. E. Palade 1963 Junctional complexes in various epithelia. *J. Cell Biol.*, 17: 375-412.
- Florey, H. W. 1964 The transport of materials across the capillary wall. *Quart. J. Exptl. Physiol.*, 49: 117-128.
- Goldfischer, S., I. M. Arias, E. Essner and A. B. Novikoff 1962 Cytochemical and electron microscopic studies of rat liver with reduced capacity to transport conjugated bilirubin. *J. Exp. Med.*, 115: 467-474.
- Graham, R. C., Jr., and M. J. Karnovsky 1966 The early stages of absorption of injected horse radish peroxidase in the proximal tubules of mouse kidney: Ultrastructural cytochemistry by a new technique. *J. Histochem. Cytochem.*, 14: 291-302.
- Hampton, J. C. 1958 An electron microscope study of hepatic uptake and excretion of submicroscopic particles injected into the blood stream and into the bile duct. *Acta Anat.*, 32: 262-291.
- Karnovsky, M. J. 1965a A formaldehyde-glutaraldehyde fixative of high osmolality for use in electron microscopy (abst.). *J. Cell Biol.* 27: 137 A.
- 1965b Vesicular transport of exogenous peroxidase across capillary endothelium into the T-system of muscle. *J. Cell Biol.*, 27: 491.
- Kaye, G. L., G. D. Pappas, A. Donn and N. Malett 1962 Studies on the cornea. II. The uptake and transport of colloidal particles by the living rabbit cornea in vitro. *J. Biophys. Biochem. Cytol.*, 12: 481-501.
- Keilin, D., and E. F. Hartree 1951 Purification of horse-radish peroxidase and comparison of its properties with those of catalase and methaemoglobin. *Biochem. J.*, 49: 88-104.
- Luft, J. H. 1961 Improvements in epoxyresin embedding methods. *J. Biophys. Biochem. Cytol.*, 9: 409-414.
- McCarrel, T. S., and C. K. Drinker 1941 The lymph drainage of the gall bladder together with observations on the composition of liver lymph. *Amer. J. Physiol.*, 133: 79-81.
- Majno, G. 1965 Ultrastructure of the Vascular membrane. In: *Handbook of Physiology*, section 2 (circulation). W. F. Hamilton, ed., American Physiological Society, Washington, D. C., vol. 3, chap. 64, pp. 2293-2375.
- Maxwell, D. S., and D. C. Pease 1956 The electron microscopy of the choroid plexus. *Biophys. Biochem. Cytol.*, 2: 467-474.
- Novikoff, A. B., and E. Essner 1960 The liver cell: Some new approaches to its study. *Am. J. Med.*, 29: 102-131.
- Pappas, G. D., G. K. Smelser and P. W. Brinkman 1959 Studies on the ciliary epithelium and the zonule. II. Electron and fluorescence microscope observations on the function of the zonule. *Arch. Ophthalmol.*, 61: 959-965.
- Pease, D. C. 1956 Infolded basal plasma membranes found in epithelia noted for their water transport. *J. Biophys. Biochem. Cytol.*, 2 (Suppl.) 203-208.
- Reese, T. S., and M. J. Karnovsky 1967 Fine structural localization of a blood brain barrier to exogenous peroxidase. *J. Cell Biol.*, 34: 207-217.
- Rouiller, Ch. 1954 Les canalicules biliaires. Etude au microscope électronique. *Comp. rend. soc. biol.*, 148: 2008-2011.
- 1956 Les Canalicules biliaires. *Anat.*, 26: 94-109.
- Schaffner, F., and H. Popper 1959a Morphological studies of cholestasis. *Gastroenterology*, 37: 565-573.
- 1959b Electron microscopic study of human cholestasis. *Proc. Soc. Exptl. Biol. Med.* 101: 777-779.
- Sjöstrand, F. S., and J. Rhodin 1953 The ultrastructure of the proximal convoluted tubule of mouse kidney as revealed by high resolution electron microscopy. *Exptl. Cell Res.*, 4: 456.
- Steiner, J. W. 1961 Investigation of a liver injury. *Amer. J. Pathol.*, 38: 411-436.

Sejner, J. W., and J. S. Carruthers. 1961. Studies on the fine structure of the terminal branches of the biliary tree. I. The morphology of normal bile canaliculi, bile pre-ductules (ducts of Bering) and bile ductules. *Amer. J. Path.*, 38: 639-661.

Strauss, W. 1957. Segregation of an intravenously injected protein by "droplets" of the cells of rat kidney. *J. Biophys. Biochem. Cytol.*, 3: 1037-1041.

Yodaiken, R. E. 1966. The use of lead as a tracer in ultrastructural research. *Lab. Invest.*, 15: 402-411.

PLATE 1

EXPLANATION OF FIGURES

- 1 Liver from uninjected control. Cells lining the sinusoidal lumen (SIN) exhibit the presence of intercellular gaps (blank arrows). In the space of Disse fibrillar material (X) is seen. The hepatocyte (HEP) does not show any abnormalities. Mag. $\times 28,000$.
- 2 Liver from uninjected control. The cells lining the sinusoidal lumen (SIN) show in some instances tight junctions (J) and fenestrae (black arrows). Mag. $\times 24,000$.

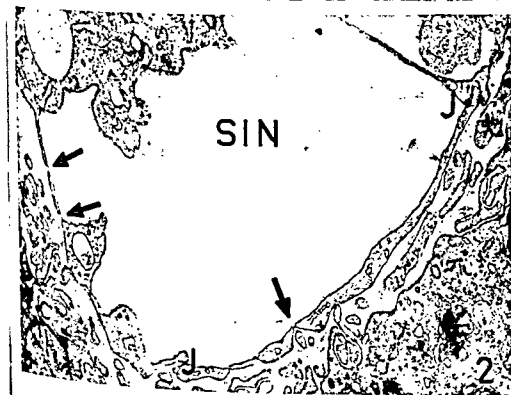
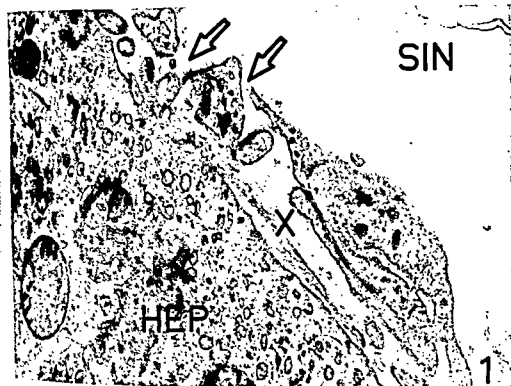


PLATE 1

EXPLANATION OF FIGURES

- 1 Liver from uninjected control. Cells lining the sinusoidal lumen (SIN) exhibit the presence of intercellular gaps (blank arrows). In the space of Disse fibrillar material (X) is seen. The hepatocyte (HEP) does not show any abnormalities. Mag. $\times 28,000$.
- 2 Liver from uninjected control. The cells lining the sinusoidal lumen (SIN) show in some instances tight junctions (J) and fenestrae (black arrows). Mag. $\times 24,000$.

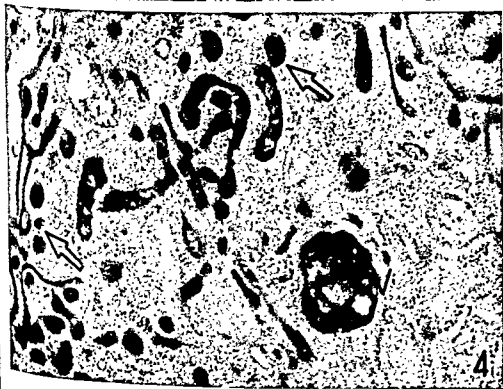


PLATE 2

EXPLANATION OF FIGURES

- 3 Liver five minutes after the injection of horse radish peroxidase. The electron dense deposits indicate areas of peroxidase activity. Reaction product is seen in micropinocytic vacuoles (black arrows) of both Kupffer cells (KUP) and hepatocytes (HEP). It is present in the junction (J) between adjacent sinusoidal cells and has entered the space of Disse (blank arrow). Mag. $\times 51,000$.
- 4 Kupffer cell two minutes after injection of horse radish peroxidase. Reaction product is present in small micropinocytic vacuoles (black arrows) and in larger vacuoles (V). Mag. $\times 40,500$.

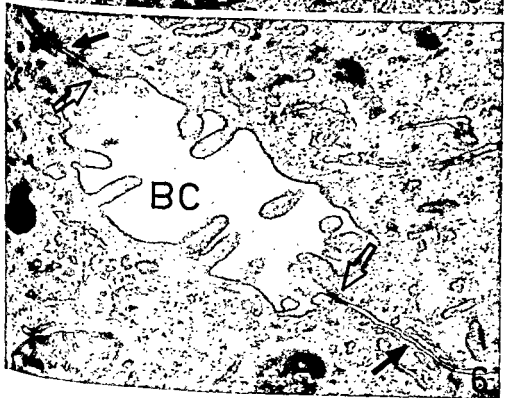
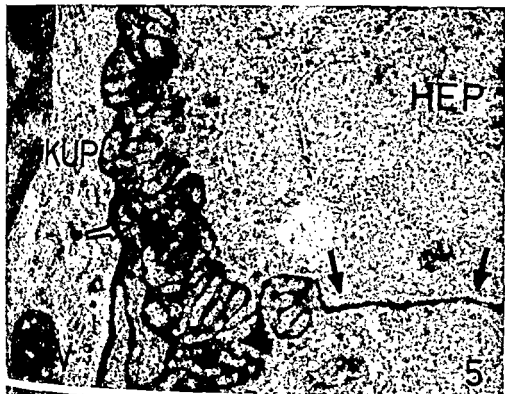


PLATE 3

EXPLANATION OF FIGURES

- 5 Liver five minutes after injection of horse radish peroxidase. The marker has entered into the space of Disse (blank arrow) and passed into the interhepatocytic space (black arrows) the reaction product is also present in a vacuole (V) of a Kupffer cell (KUP). Mag. $\times 41,000$.
- 6 Bile canaliculus (BC) showing terminal bars (blank arrows) and interhepatocytic spaces (black arrows). Mag. $\times 48,000$.

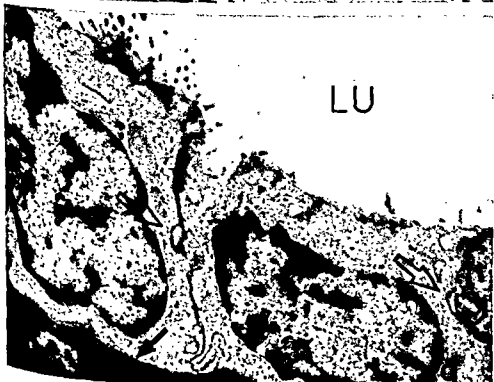


PLATE 4

EXPLANATION OF FIGURES

- 7 Bile canaliculus five minutes after injection of horse radish peroxidase. Reaction product is seen in the bile canaliculus (blank arrows) between adjacent hepatocytes (HEP). This is continuous with the marker in the interhepatocytic space (black arrows). Mag. $\times 24,000$.
- 8 Bile canaliculus five minutes after injection of horse radish peroxidase. The bile canaliculus (blank arrow) between adjacent hepatocytes (HEP) contains reaction product which is continuous with similar material in the interhepatocytic space (black arrows). Mag. $\times 40,000$.
- 9 Bile ductule ten minutes after injection of horse radish peroxidase. The marker is seen in the periductular space (black arrow) and passing between adjacent ductular cells (blank arrows). It does not, however, enter the lumen of the ductule (LU). Mag. $\times 28,000$.

Marginal Zone and Germinal Center Development in the Spleens of Neonatally Thymectomized and Nonthymectomized Young Rats¹

JAMES C. PETTERSEN AND ROBERT J. ROSE*

Department of Anatomy, University of Wisconsin, Madison, Wisconsin

ABSTRACT Spleens from neonatally thymectomized and nonthymectomized young rats were studied histologically and histochemically to elucidate the development of the splenic immune system with and without thymus.

In intact animals primitive germinal center activity could be elicited with antigen as early as 13 days of age. More definitive germinal centers lacking tingible body macrophages were observed at 18 days of age. Germinal centers containing tingible body macrophages did not develop until 35 days of age in response to antigenic stimulation. This coincided with maximal development of the marginal zone of medium-sized lymphocytes and the mature development of nodular macrophages possessing strong acid phosphatase activity.

Neonatally thymectomized rats developed marginal zones and germinal centers similar to control littermates when the young animals were maintained on tetracycline. Thymectomized animals not given tetracycline showed disturbances in splenic development. These are discussed.

The results suggest that the thymus may be critical to the immune system in rats from birth to about 30 days of age but is not essential to its function beyond this period. Marginal zone lymphocytes and germinal center cells proliferate normally and mature to the plasma cell stage in the absence of a thymus if the animals are maintained on tetracycline beyond this critical age.

Histological and histochemical evidence from our laboratory implicates the medium-sized, marginal zone lymphocytes as a major source of germinal center cells following antigenic stimulation (Pettersen, Borgen and Graupner, '67).

The present study was undertaken to determine when marginal zone lymphocytes migrate to the spleen, when they respond to antigenic stimulation and whether the thymus influences their development or maintenance.

MATERIALS AND METHODS

Fifty young Holtzman rats were used to study the development of the marginal zone and the time of appearance of germinal center activity in the spleen. Animals ranged from one hour to 64 days of age at autopsy and include some which received lateral tail vein injections of typhoid-paratyphoid vaccine (Eli Lilly and Co.) or of 055:B5 *E. coli* endotoxin (Difco) representative ages from 13 to 60 days. Intraperitoneal or intramedastinal injections were given to animals younger than 1 days of age.

Another series of rats was thymectomized on the day of birth. They were anesthetized by cooling in a freezer, the sternums were split with small surgical scissors and the thymic lobes were removed with forceps using clean but not sterile technique. Thirty percent of the animals died during or shortly following surgery. Forty-four animals survived the initial procedure.

At autopsy 12 animals were free of thymus and 13 had portions remaining. Nineteen died of runt disease or were victims of maternal cannibalism. Tetracycline hydrochloride (Pfizer Corp.) in the drinking water eliminated runting and was used routinely following a high mortality in our first four litters. Histological material was obtained from only three thymectomized animals not receiving the antibiotic. Two of these were runt animals 27 days of

¹This project received support from a General Research Support grant to the University of Wisconsin Medical School from the National Institutes of Health, Division of Research Facilities and Resources.

*Summer Research Fellow, National Institutes of Health Medical Student Training Grant.

imals were not available in the 30 to 60 day age group.

Thymectomized animals. Neonatal thymectomy retarded the development of the marginal zone in the spleens of animals not maintained on tetracycline. Figure 7 illustrates this in a spleen section stained for acid phosphatase activity from a 25 day old, non-runted, thymectomized animal. Figure 8 is a section from a litter-mate control. Runted animals lacked marginal zones (fig. 9).

Small lymphocytes were deficient but not entirely lacking in these spleens. Runted animals also showed decreased numbers of medium-sized lymphocytes (fig. 12). These latter cells were present in normal numbers in the spleen of the non-runted animal (fig. 11).

Spleens from thymectomized animals maintained on tetracycline developed marginal zones almost as rapidly as control animals and contained significant although reduced numbers of small lymphocytes. Cellular responses to antigenic stimulation were indistinguishable from control responses except for decreased numbers of mantle layer small lymphocytes. Recovery of the marginal zone population of medium-sized lymphocytes following initial depletion in response to antigenic stimulation was normal in thymectomized animals. Plasma cell proliferation was unaffected.

The 11 month old thymectomized animal responded like its control to antigen administered five hours before autopsy. Figure 16 shows a partial collapse of the marginal zone on a section from this spleen stained for macrophages. An additional thymectomized animal of this age was not available to test whether repopulation of the marginal zone occurs by four days following stimulation.

DISCUSSION

Two types of lymphocytes can be distinguished in the young lymphoid areas of the rat spleen. The first of these to enter the spleen is a medium-sized, slightly pyroninophilic lymphocyte that initially occupies a position adjacent to the arterial vessels (fig. 2). These are later located more peripherally as the second type, a small non-pyroninophilic lymphocyte, re-

places them around the vessels (fig. 4). There is some intermingling of the two types in spleen sections from animals less than ten days of age. By 13 days of age there is a definitive marginal zone (figs. 3, 4) of medium-sized lymphocytes enveloping an inner core of small lymphocytes. This relationship is disturbed within one day following the intravenous administration of antigen with suggestions of immature germinal center formation. Medium-sized lymphocytes invade the small lymphocyte mass and differentiation into hemocytoblasts occurs. Figures 5 and 6 illustrate splenic nodules from a control and an experimental animal 20 days of age. No plasma cell formation occurred at this age when animals were killed at later stages following antigenic stimulation.

Halliday ('56) reported an abrupt cessation of the ability of young rats to absorb antibodies through the gut wall at 20 days of age. This phenomenon was unrelated to the uptake of solid food. It was also shown (Halliday, '57) that young rats could produce antibodies in response to active immunization prior to the loss in absorptive capacity. Evidence indicated that these antibodies were located in the β -globulin fraction. Our results in young animals show that cellular changes occur in rats younger than 20 days of age following active immunization. These changes are similar to the response in adult spleens in certain respects. Marginal zone lymphocytes are the source of germinal center cells in both young and adult spleens and mitotic activity and hemocytoblast formation occur in both. Germinal centers in young spleens, however, did not contain tingible body macrophages and did not produce plasma cells. Additional studies in the 10-30 day age group employing immunohistochemical techniques would be desirable to determine what cell type produces antibodies during this stage of development. Our sections stained histochemically for macrophage distribution suggest that a follicular antigen trapping mechanism as described by Müller and Nossal ('64) in rat popliteal lymph nodes and by Hunter ('66) in the rat spleen may not be functional in young rats because of the paucity of macrophages in the white pulp at this age. MacFadden ('68) has studied the

age and the third was a 25 day old non-runted animal.

The 12 totally thymectomized animals were grouped with littermate controls and partially thymectomized animals of the same age. Some of the animals received typhoid-paratyphoid vaccine via the lateral tail vein. The injections were generally given five days before autopsy to allow a maximum cellular response to develop. Groups of animals were killed at 25, 27, 35, 41 and 64 days of age. One thymectomized animal was killed at 11 months of age five hours following antigenic stimulation. Histological material was obtained from 40 animals in this portion of the study.

All animals were killed with ether, spleens were rapidly removed and pieces fixed in Carnoy's fluid, in Helly's fluid and in 15% cold, neutral formalin. All suspicious mediastinal tissue was removed from the surgical animals and fixed in 15% formalin. The thorax was then held under running tap water to wash it free of blood for further inspection under a hand lens.

Tissue fixed in formalin was stained for acid phosphatase activity as previously described (Pettersen, '64). These sections were studied for macrophage distribution and general splenic topography. Mediastinal tissue stained in this manner was used to identify thymic remnants.

Tissue fixed in Helly's fluid was sectioned in paraffin at 5μ and stained with hematoxylin-eosin-azure II or with hematoxylin and eosin. Carnoy-fixed tissue was sectioned in paraffin at 5μ and stained with methyl green-pyronin.

RESULTS

Splenic development in nonthymectomized animals. Spleens of newborns were largely myeloid with an occasional small sheath of lymphocytes surrounding the arterial vessels. Macrophages were dispersed throughout the myelopoietic areas but were not present in the small lymphoid areas (fig. 1). At three days of age several tiers of lymphocytes surrounded the arterioles (fig. 2). These cells resembled the medium-sized lymphocytes found in the marginal zones of adult rats. Suggestions of a marginal zone were present at nine days of

age and it was definitive by 13 days of age (fig. 3). Small lymphocytes were then present in a position adjacent to the arteriole with medium-sized lymphocytes peripheral to them (fig. 4). A disturbance in this relationship occurred one day following intravenous injections of antigen in 13 day old animals. The two types of lymphocyte were commingled rather than segregate in these spleens. This phenomenon was suggested in animals eight or nine days of age following intraperitoneal injection but was difficult to assess because segregation was not complete in control spleens of this age. Figures 5 and 6 illustrate splenic nodules from a control and an injected animal 20 days of age.

Germinal centers developed in 18 day old rats following intravenous injection of 0.25 ml typhoid-paratyphoid vaccine at 14 days of age. They consisted of small nests of pyroninophilic cells surrounded by mantle layers of non-pyroninophilic small lymphocytes. Tingible body macrophages were not present and no plasma cells could be identified. About 30% of the lymphoid nodules contained such germinal center.

The marginal zone was the source of cells for early germinal centers. The width of this rim of cells reached adult size (800μ) by 35 days of age at which time tingible body macrophages were present in germinal centers of those spleens exposed to antigen for five days. About 20% of the nodules contained germinal centers with these macrophages (fig. 15). Up to this age tingible bodies were not present in response to antigen but there were increase in numbers of macrophages possessing acid phosphatase activity in the lymphoid areas of both stimulated and non-stimulated spleens. In 60 day old animals nearly 100% of the lymphoid nodules responded to similar antigenic stimulation by the formation of germinal centers containing tingible body macrophages.

Our data were not complete enough to establish the age of appearance of plasma cells. Sixty day old rats contained large numbers of plasma cells in the splenic red pulp five days following stimulation. Efforts to induce a similar response in 20 and 30 day old rats were negative. Sufficient numbers of antigenically stimulated and

imals were not available in the 30 to 60 day age group.

Thymectomized animals. Neonatal thymectomy retarded the development of the marginal zone in the spleens of animals not maintained on tetracycline. Figure 7 illustrates this in a spleen section stained for acid phosphatase activity from a 25 day old, non-runted, thymectomized animal. Figure 8 is a section from a litter-mate control. Runted animals lacked marginal zones (fig. 9).

Small lymphocytes were deficient but not entirely lacking in these spleens. Runted animals also showed decreased numbers of medium-sized lymphocytes (fig. 12). These latter cells were present in normal numbers in the spleen of the non-runted animal (fig. 11).

Spleens from thymectomized animals maintained on tetracycline developed marginal zones almost as rapidly as control animals and contained significant although reduced numbers of small lymphocytes. Cellular responses to antigenic stimulation were indistinguishable from control responses except for decreased numbers of mantle layer small lymphocytes. Recovery of the marginal zone population of medium-sized lymphocytes following initial depletion in response to antigenic stimulation was normal in thymectomized animals. Plasma cell proliferation was unaffected.

The 11 month old thymectomized animal responded like its control to antigen administered five hours before autopsy. Figure 16 shows a partial collapse of the marginal zone on a section from this spleen stained for macrophages. An additional thymectomized animal of this age was not available to test whether repopulation of the marginal zone occurs by four days following stimulation.

DISCUSSION

Two types of lymphocytes can be distinguished in the young lymphoid areas of the rat spleen. The first of these to enter the spleen is a medium-sized, slightly pyroninophilic lymphocyte that initially occupies a position adjacent to the arterial vessels (fig. 2). These are later located more peripherally as the second type, a small non-pyroninophilic lymphocyte, re-

places them around the vessels (fig. 4). There is some intermingling of the two types in spleen sections from animals less than ten days of age. By 13 days of age there is a definitive marginal zone (figs. 3, 4) of medium-sized lymphocytes enveloping an inner core of small lymphocytes. This relationship is disturbed within one day following the intravenous administration of antigen with suggestions of immature germinal center formation. Medium-sized lymphocytes invade the small lymphocyte mass and differentiation into hemocytoblasts occurs. Figures 5 and 6 illustrate splenic nodules from a control and an experimental animal 20 days of age. No plasma cell formation occurred at this age when animals were killed at later stages following antigenic stimulation.

Halliday ('56) reported an abrupt cessation of the ability of young rats to absorb antibodies through the gut wall at 20 days of age. This phenomenon was unrelated to the uptake of solid food. It was also shown (Halliday, '57) that young rats could produce antibodies in response to active immunization prior to the loss in absorptive capacity. Evidence indicated that these antibodies were located in the β -globulin fraction. Our results in young animals show that cellular changes occur in rats younger than 20 days of age following active immunization. These changes are similar to the response in adult spleens in certain respects. Marginal zone lymphocytes are the source of germinal center cells in both young and adult spleens and mitotic activity and hemocytoblast formation occur in both. Germinal centers in young spleens, however, did not contain tingible body macrophages and did not produce plasma cells. Additional studies in the 10-30 day age group employing immunochemical techniques would be desirable to determine what cell type produces antibodies during this stage of development. Our sections stained histochemically for macrophage distribution suggest that a follicular antigen trapping mechanism as described by Miller and Nossal ('64) in rat popliteal lymph nodes and by Hunter ('66) in the rat spleen may not be functional in young rats because of the paucity of macrophages in the white pulp at this age. MacFadden ('68) has studied the

phagocytic function of macrophages in the spleens of late fetal (17-18 days of gestation) to old (475 days) rats. Increased numbers of white pulp macrophages possessing phagocytic ability and hydrolytic enzyme activity were reported as the animals aged. Our results support his conclusions but also suggest that antigenic stimulation enhances the maturation of white pulp macrophages. Bauer et al. ('66) reported that the intracellular digestion of antigen was slower in macrophages of germfree versus conventional mice. Spleen sections from several germfree rats were stained for acid phosphatase activity in our laboratory. The white pulp contained relatively few cells exhibiting enzyme activity compared to spleen sections from untreated adult control rats. The red pulp did not differ from that of the controls. This suggests that ageing is not necessarily the variable in the maturation of white pulp macrophages but that some exogenous stimulation is required. Red pulp macrophages possess hydrolytic enzyme activity in the late fetal stages of development (MacFadden, '68) before such stimulation is likely to occur.

Williams and Nossal ('66) studied the antigen-trapping ability of the lymphoid tissues in young rats following footpad injections of 125 I-labelled polymerized flagellin from *Salmonella adelaide*. Autoradiographs showed initial signs of cortical localization in lymph nodes from animals between 10-14 days of age. True follicular retention did not occur until animals were four to six days older at the time of injection. Antigen was not retained by the lymphoid nodules of the spleen six days following an injection given at four weeks of age. An adult pattern of retention was observed in the spleen in animals injected at six weeks of age. The ability to retain antigen increased five fold per unit weight of lymphoid tissue between two and six weeks of age. Williams ('66) demonstrated a parallel development of the antigen-trapping mechanism and the ability to form antibodies.

White pulp macrophages may mature from reticular cells already present in the splenic anlage at the time lymphoid immigration begins. Their specialization into antigen-processing cells may be influenced

by their lymphoid environment and triggered upon initial exposure to antigen. Petersen ('64) reported that the number of cells in the white pulp reactive to Marshall's silver impregnation stain for macrophages does not increase following antigenic stimulation but the number of cells with active hydrolytic enzyme systems does increase following such treatment. This indicates that increases in macrophages represent maturation of existing cells. It is difficult to explain how macrophages get into the developing lymphoid areas. They may be incorporated from the red pulp as the lymphoid cells migrate into the spleen. This explanation is inconsistent with the following observations: (1) during development macrophages pile up at the marginal zone-red pulp junction but are rarely found in the marginal zone (fig. 3); (2) the marginal metallophils (Snook, '64) appear to migrate outward as the small lymphocytes move into the periarteriolar regions; (3) white pulp macrophages in newborns are not selectively localized near the periphery of the lymphoid masses; (4) macrophages in the red pulp possess hydrolytic enzyme activity at or before birth, whereas white pulp macrophages acquire this activity later in development.

Alternatively, one can postulate that the white pulp macrophages represent a breed that is different from those in the red pulp. They may migrate in with the lymphoid cells during development or may be products of maturation of certain of these cells. The data available suggest some form of this alternative hypothesis.

The retarded development of the marginal zone in young neonatally thymectomized rats not maintained on tetracycline may be related to deficiencies of small lymphocytes of thymic origin or to infectious processes that keep the marginal zone lymphocytes in a state of disorganization. There were no germinal centers and no hemocytoblasts in the white pulp of these animals to suggest a cellular response to invading organisms. Azar ('64) substantially reduced the incidence of runting in neonatally thymectomized rats by adding oxytetracycline HCl (Pfizer Corp.) to the drinking water. He believed that bronchopulmonary infections were the cause of

death in runted animals. Non-hemolytic streptococcus, a *Hemophilus* organism and diphtheroids were cultured from bronchopulmonary tissue. The spleens were atrophic, lacked well-formed follicles and contained no plasma cells. Plasma cells were present in the bronchopulmonary lesions and the serum gamma globulin level was increased. This suggests that the spleen was not involved in an immunological process in runted animals but that cells that normally would develop within the spleen were employed at the site of infection. This may be a possible explanation for the deficiency of medium-sized lymphocytes in spleens of our runted animals.

Schriever, Hsu and Azar ('67) found normal plasma cell formation and normal numbers of cells containing gamma globulin in the mesenteric lymph nodes of neonatally thymectomized animals. They concluded that, in their experience, "should neonatally thymectomized rats survive the first critical eight to ten weeks of life without succumbing to infection, they will then adequately cope with subsequent infections and compensate for the loss of thymus function."

Waksman, Arnason and Jankovic ('64) reported a complete absence of small lymphocytes in spleens of neonatally thymectomized rats. None of our spleens, with the exception of those from the two runted animals, showed small lymphocyte deficiencies of this magnitude. Tetracycline may have potentiated the development of small lymphocytes or may have permitted their development under less antigenically stressful conditions.

It is clear that the thymus is not essential in maintaining a marginal zone cell population in young adult rats once the splenic immune system has developed. It cannot be concluded from our data that the thymus is not the stem source of marginal zone medium-sized lymphocytes. The following observations are consistent with a thymic origin for these cells: (1) medium-sized lymphocytes appear in the spleen before small lymphocytes and can be found in spleens of one hour old rats corresponding to the time of our earliest thymectomies; (2) a 25 day old non-runted thymectomized animal showed retarded

development of the marginal zone and two 27 day old runted animals showed near absence of this region; (3) 35 day old neonatally thymectomized animals maintained on tetracycline showed subtle but distinguishable differences in the ability to repopulate the marginal zone following antigenic stimulation; (4) small lymphocytes entered the spleen in significant numbers in neonatally thymectomized animals maintained on tetracycline suggesting a potentiating influence.

The following are more consistent with a nonthymic origin: (1) a spleen from a non-runted thymectomized animal not maintained on tetracycline contained a sizable population of medium-sized lymphocytes although the deficiency of small lymphocytes disturbed the usual organization of the marginal zone; (2) marginal zone lymphocytes were present in normal numbers in the neonatally thymectomized animals maintained on tetracycline; (3) the marginal zone was reconstituted after the usual depletion following antigenic stimulation.

Moore and Owen ('67) recently presented evidence that the yolk sac in the chick furnishes blood-borne stem cells which enter the thymic rudiment. A sex chromosome marker and histological techniques used to study parabiosed chick embryos showed that a sizeable proportion of thymocytes came from the partner. Evidence suggested that the same type of cell migrates into the thymic rudiment of the mouse. The cell type shown on their illustrations closely resembles those we see in young germinal centers one day following antigenic stimulation (fig. 6, arrow). We have called this cell a hemocytoblast but it is believed by us to be a transitional form of the medium-sized marginal zone lymphocytes which migrate into the germinal centers in response to antigenic stimulation.

Several conclusions seem reasonable from our data: 1. The thymus plays some essential role in survival in young conventional rats. 2. Tetracycline permits normal development of the lymphoid structure in spleens of neonatally thymectomized rats except for relative deficiencies of small lymphocytes. 3. An intact thymus is not essential in maintaining these lymphoid structures once adult development has

phagocytic function of macrophages in the spleens of late fetal (17-18 days of gestation) to old (475 days) rats. Increased numbers of white pulp macrophages possessing phagocytic ability and hydrolytic enzyme activity were reported as the animals aged. Our results support his conclusions but also suggest that antigenic stimulation enhances the maturation of white pulp macrophages. Bauer et al. ('66) reported that the intracellular digestion of antigen was slower in macrophages of germfree versus conventional mice. Spleen sections from several germfree rats were stained for acid phosphatase activity in our laboratory. The white pulp contained relatively few cells exhibiting enzyme activity compared to spleen sections from untreated adult control rats. The red pulp did not differ from that of the controls. This suggests that ageing is not necessarily the variable in the maturation of white pulp macrophages but that some exogenous stimulation is required. Red pulp macrophages possess hydrolytic enzyme activity in the late fetal stages of development (MacFadden, '68) before such stimulation is likely to occur.

Williams and Nossal ('66) studied the antigen-trapping ability of the lymphoid tissues in young rats following footpad injections of 125 I-labelled polymerized flagellin from *Salmonella adelaide*. Autoradiographs showed initial signs of cortical localization in lymph nodes from animals between 10-14 days of age. True follicular retention did not occur until animals were four to six days older at the time of injection. Antigen was not retained by the lymphoid nodules of the spleen six days following an injection given at four weeks of age. An adult pattern of retention was observed in the spleen in animals injected at six weeks of age. The ability to retain antigen increased five fold per unit weight of lymphoid tissue between two and six weeks of age. Williams ('66) demonstrated a parallel development of the antigen-trapping mechanism and the ability to form antibodies.

White pulp macrophages may mature from reticular cells already present in the splenic anlage at the time lymphoid immigration begins. Their specialization into antigen-processing cells may be influenced

by their lymphoid environment and triggered upon initial exposure to antigen. Pettersen ('64) reported that the number of cells in the white pulp reactive to Marshall's silver impregnation stain for macrophages does not increase following antigenic stimulation but the number of cells with active hydrolytic enzyme systems does increase following such treatment. This indicates that increases in macrophages represent maturation of existing cells. It is difficult to explain how macrophages get into the developing lymphoid areas. They may be incorporated from the red pulp as the lymphoid cells migrate into the spleen. This explanation is inconsistent with the following observations: (1) during development macrophages pile up at the marginal zone-red pulp junction but are rarely found in the marginal zone (fir 3); (2) the marginal metallophilic (Snook '64) appear to migrate outward as the small lymphocytes move into the periarteriolar regions; (3) white pulp macrophages in newborns are not selectively localized near the periphery of the lymphoid masses; (4) macrophages in the red pulp possess hydrolytic enzyme activity at or before birth, whereas white pulp macrophages acquire this activity later in development.

Alternatively, one can postulate that the white pulp macrophages represent a breed that is different from those in the red pulp. They may migrate in with the lymphoid cells during development or may be products of maturation of certain of these cells. The data available suggest some form of this alternative hypothesis.

The retarded development of the marginal zone in young neonatally thymectomized rats not maintained on tetracycline may be related to deficiencies of small lymphocytes of thymic origin or to infectious processes that keep the marginal zone lymphocytes in a state of disorganization. There were no germinal centers and no hemocytoblasts in the white pulp of these animals to suggest a cellular response to invading organisms. Azar ('64) substantially reduced the incidence of runting in neonatally thymectomized rats by adding oxytetracycline HCl (Pfizer Corp.) to the drinking water. He believed that bronchopulmonary infections were the cause of

been attained. 4. Two types of lymphocytes migrate to the spleen during development of the lymphoid structures neither of which is entirely thymus dependent following birth.

LITERATURE CITED

- Azar, H. A. 1964 Bacterial infection and wasting in neonatally thymectomized rats. *Proc. Soc. Exp. Bio. and Med.*, 116: 817-823.
- Bauer, H., R. Horowitz, K. Watkins and H. Popper 1964 Immunologic competence and phagocytosis in germfree animals with and without stress. *J.A.M.A.*, 187: 715-718.
- Halliday, R. 1956 The termination of the capacity of young rats to absorb antibody from the milk. *Proc. Roy. Soc., B.*, 145: 179-185.
- 1957 The production of antibodies by young rats. *Proc. Roy. Soc., B.*, 147: 140-144.
- Hunter, R. L. 1966 Two patterns of splenic phagocytosis. *New Physician*, 15: 111-119.
- MacFadden, K. In press. *J. Reticuloendothel. Soc.*
- Miller, J. J., and G. J. V. Nossal 1964 Antigens in immunity. VI. The phagocytic reticulum of lymph node follicles. *J. Exp. Med.*, 120: 1075-1086.
- Moore, M. A. S., and J. Owen 1967 Experimental studies on the development of the thymus. *J. Exp. Med.*, 126: 715-726.
- Pettersen, J. C. 1964 A comparison of the metalophilic reticuloendothelial cells to cells containing acid phosphatase and nonspecific esterase in the lymphoid nodules of normal and stimulated rat spleens. *Anat. Rec.*, 149: 269-278.
- Pettersen, J. C., D. F. Borgen and K. C. Graupner 1967 A morphological and histochemical study of the primary and secondary immune responses in the rat spleen. *Am. J. Anat.*, 121: 305-317.
- Schriever, H. G., K. Hsu and H. Azar 1967 A Study of mesenteric lymph nodes in neonatally thymectomized rats with regard to cells types and gamma globulin content of cells. *Am. J. Path.*, 50: 177-185.
- Snook, T. 1964 Studies on the perifollicular region of the rat's spleen. *Anat. Rec.*, 143: 149-159.
- Waksman, B. H., B. Arnason and B. Jankovic 1962 The role of the thymus in immune reactions in rats. III. Changes in the lymphoid organs of thymectomized rats. *J. Exp. Med.*, 116: 187-206.
- Williams, G. M. 1966 Ontogeny of the immune response. II. Correlations between the development of the afferent and efferent limbs. *J. Exp. Med.*, 124: 57-67.
- Williams, G. M., and G. J. V. Nossal 1966 Ontogeny of the immune response. I. The development of the follicular antigen-trapping mechanism. *J. Exp. Med.*, 124: 47-56.

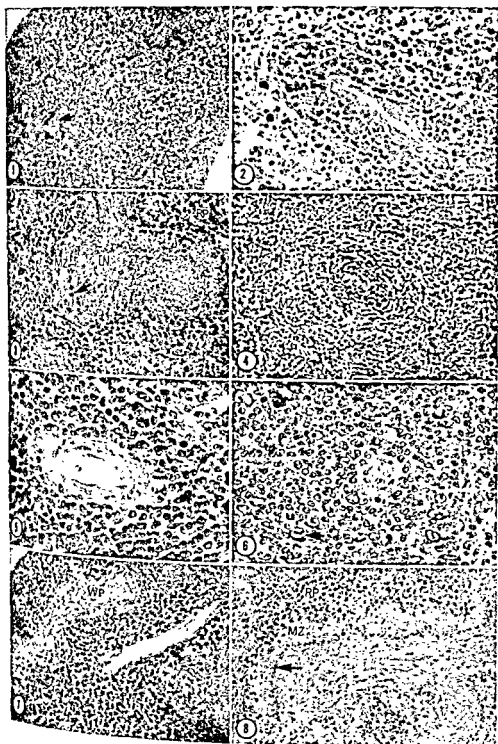


PLATE 1

EXPLANATION OF FIGURES

- 1 Section of spleen stained for acid phosphatase activity from a rat killed one hour after birth. Macrophages are dispersed throughout the red pulp which is entirely myeloid. Arrow identifies a small lymphoid area free of macrophages. $\times 70$.
- 2 Section of spleen from a three day old rat showing a sheath of medium-sized lymphocytes surrounding an obliquely sectioned arteriole. Methyl green-pyronin. $\times 270$.
- 3 Spleen section from a 13-day old rat showing developing marginal zone, MZ. A few macrophages are present in the nodules. RP, red pulp; LN, lymphoid nodule; MZ, marginal zone. Arrow identifies marginal metallophils. Acid phosphatase. $\times 70$.
- 4 Spleen section from a 16 day old rat showing an inner core of small lymphocytes surrounding an arteriole and a peripheral rim of medium-sized lymphocytes occupying the marginal zone. MZ, marginal zone. Methyl green-pyronin. $\times 170$.
- 5 A nodule in a spleen section from a 20 day old rat showing a core of small lymphocytes surrounding an arteriole. Methyl green-pyronin. $\times 400$.
- 6 A nodule in a spleen section of a 20 day old rat one day following an intravenous injection of 0.25 ml typhoid-paratyphoid vaccine. Medium-sized lymphocytes have invaded the mass of small lymphocytes. Arrow identifies a hemocytoblast. Methyl green-pyronin. $\times 400$.
- 7 Section of spleen from a 25 day old, neonatally thymectomized, nonrunted rat showing retarded development of the marginal zone, WP, white pulp. Acid phosphatase. $\times 70$.
- 8 Spleen section from a 25 day old littermate control. MZ, marginal zone; RP, red pulp. Arrow identifies marginal metallophils. Acid phosphatase. $\times 70$.

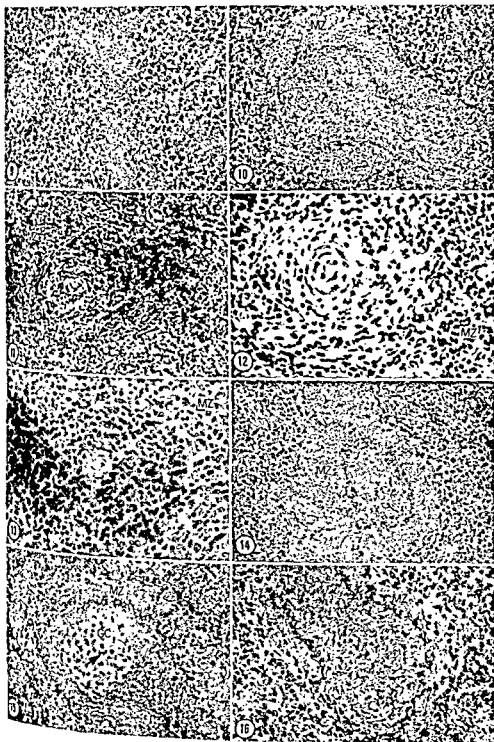


PLATE 2

EXPLANATION OF FIGURES

- 9 Spleen section from a 27 day old, thymectomized, runt rat showing poor development of lymphoid structures. Acid phosphatase. $\times 70$.
- 10 Spleen section from a 27 day old littermate control. MZ, marginal zone; RP, red pulp. Acid phosphatase. $\times 70$.
- 11 Splenic nodule from a 25 day old, thymectomized rat showing deficiency of small lymphocytes. Medium-sized lymphocytes show a normal population density in the marginal zone, MZ. H. and E. $\times 170$.
- 12 Splenic nodule from a 27 day old, thymectomized, runt rat showing marked depletion of small lymphocytes and a marginal zone, MZ, with a low population density of medium-sized lymphocytes. H. and E. $\times 330$.
- 13 Splenic nodule from a 27 day old control rat. MZ, marginal zone. Methyl green-pronin. $\times 330$.
- 14 Spleen section from a 32 day old, neonatally thymectomized rat maintained on tetracycline. Marginal zone, MZ, is well developed although slightly smaller than in controls. Compare to figure 10. Acid phosphatase. $\times 70$.
- 15 Spleen section from a 35 day old, neonatally thymectomized rat killed five days following an intravenous injection of typhoid-paratyphoid vaccine. The marginal zone, MZ, is reconstituted, a germinal center, GC, is present in the nodule and tingible body macrophages (arrow) have developed. Acid phosphatase. $\times 70$.
- 16 Ammoniacal silver-stained section of spleen from a neonatally thymectomized, 11 month old rat killed five hours after an intravenous injection of 1.0 ml typhoid-paratyphoid vaccine. The marginal zone, MZ, is constricted which is a characteristic response observed in spleens of nonthymectomized animals within one day following antigenic stimulation. $\times 70$.

Cell Division in Injured Spinal Cord¹

ERLE K. ADRIAN, JR.

Department of Anatomy, The University of Texas Medical Branch,
Galveston, Texas

ABSTRACT Thymidine-H³ radioautography was used to study the proliferative response to penetrating wounds of the mouse spinal cord. In one group of animals mononuclear leukocytes which infiltrate nervous tissue wounds were labeled by injecting thymidine-H³ prior to injury. In two other experimental groups the cells which synthesized DNA in the nervous tissue following the injury were labeled by giving either a single injection of isotope shortly before sacrifice or by giving four injections during the 24 hours prior to sacrifice. The animals were sacrificed over a five day period following spinal cord injury. Although the labeled nuclei in all three groups were similar in appearance, their distribution about the lesion was very different. The labeled blood cells were greatly concentrated at the wound, while the cells that responded to injury by DNA synthesis were much more evenly spread throughout the tissue. When these distributions were converted to straight lines and compared statistically, there was a very low probability that the group of cells labeled before injury and the two groups labeled after injury were samples from the same population. Although mononuclear leukocytes do proliferate in and around nervous tissue wounds, other cells originally present in the nervous tissue must also proliferate.

Although the cells in normal adult mammalian nervous tissue were long considered to be mitotically inert (Allen, '12; Ngow-yang, '30; Ries, '38; Leblond and Walker, '56), radioautography with tritiated thymidine has provided abundant evidence for the existence in normal nervous tissue of a small population of cells which undergo DNA synthesis and mitotic division (Messier et al., '58; Hain et al., '60; Messier and Leblond, '60; Schultze and Oehlert, '60; Smart, '61; Smart and Leblond, '61; Adrian and Walker, '62; Noetzel, '62; Altman, '63; Gavrilova, '64; Noetzel and Rox, '64; Hommes and Leblond, '67). Following injury the number of such cells is greatly increased, and it has been generally assumed that these cells are glial cells (Koenig, '60; Koenig et al., '62; Altman, '62; Adrian and Walker, '62; Samorajski et al., '64; Hassler, '66). A glial proliferative response has for many years been considered to be one of the characteristic reactions of nervous tissue to injury (Adams, '58). However, by labeling hemopoietic tissues with tritiated thymidine prior to injuring the nervous tissue, it has been possible to demonstrate that many labeled cells appear around the wound. These cells were taken to consist of large numbers of mononuclear leukocytes labeled before invading the injured

tissue (Adrian and Walker, '62), even though these invading cells could not be distinguished from glial cells on the basis of their appearance in paraffin sectioned material (Walker, '63). Since these invading cells have been shown to actively proliferate after entering the nervous tissue (Konigsmark and Sidman, '63; Kosunen et al., '63), the question is raised as to whether or not they can account for all the DNA synthesis that occurs in nervous tissue following injury.

Several lines of evidence have been presented which would support a position that most, if not all, of the observed DNA synthesis following local nervous tissue injury could be occurring in leukocytes. Konigsmark and Sidman ('63) demonstrated the leukocytic origin of a large percentage of the macrophages which appear at a site of nervous tissue injury. Most of the visible mitoses in injured nervous tissue occur in these macrophages, long thought to be derived from microglia (Penfield, '25; Del Rio-Hortega and Penfield, '27; Del Rio-Hortega, '32). Walker ('63) showed that although the number of labeled cells in injured nervous tissue increased with time following tritiated thymidine injection, there was no corresponding decrease in

¹ This investigation was supported by USPHS grant NB 03760.

nersion by moving back and fourth from side to side across the section covering consecutive bands or rows of tissue. The width of each row was the same as the diameter of the oil immersion objective, 0.18 mm. The area of each row was estimated by multiplying the number of oil immersion fields in the row by $(0.18 \text{ mm})^2$. A map was made for each section which showed the position of all radioactive nuclei, except those belonging to polymorphonuclear leukocytes. (A nucleus was considered to be radioactive if it had four or more silver grains superimposed over it.) The map was made initially on graph paper (10×10 per inch) by equating each oil immersion field to one 5×5 square. The corners of the square were observed as the field of view was changed. The borders of the section, the position of the wound, and other distinguishing features were included on each map.

To permit easier comparison of the distribution of radioactive cells in the three groups of animals, curves showing the number of radioactive cells in a band or row of tissue 0.18 mm wide extending across the width of the section were plotted as a function of the distance of the tissue band from the center of the lesion. A composite curve determined by averaging the values obtained from all the animals in the group was prepared for each day after injury.

The number of labeled cells in each two rows equidistant from and on either side of the lesion was then expressed as a ratio of the number of labeled cells in the two rows passing nearest the center of the lesion. Straight lines were fitted by the method of least squares to the ratios determined for the first five rows beyond those passing through the center of the lesion. A value for y-intercept and slope was determined for each animal. The hypothesis was made that the distribution of labeled cells (as represented by the straight lines) in the three groups of injured animals represented samples from the same population. A rank order analysis as described by Kruskal and Wallis ('52) was applied to the y-intercepts and to the slopes of the straight lines to test this hypothesis.

In a standard area of 1.25 mm^2 with the lesion at its center, the cell population of each spinal cord was analyzed. All nuclei of cells other than neurons, ependymal cells, and polymorphonuclear leukocytes were counted. All radioactive nuclei were classified according to their morphology. The nuclei of glial cells and of mononuclear blood cells which could not be distinguished from glial cells were classified in the following categories: (1) dark-staining round, ovoid, or irregular, (2) light-staining round, ovoid, or irregular, and (3) elongated. The light-staining nuclei were generally quite regular in shape and were larger than those of the other types. Nuclei were classified as elongated if their length was more than three times their width. Endothelial nuclei could be distinguished with considerable certainty in the material stained by the periodic-acid Schiff hematoxylin technique, and for this reason all of the nuclear classifications were done on slides stained by this method.

Sections from five of the animals in group I were chosen for mitotic counts. That part of each one of these sections lying within 3 mm from the lesion was scanned carefully under oil immersion for mitotic figures. Each mitotic figure observed was classified as to whether or not it was labeled, and its position was noted. The number of labeled mitotic figures lying within 0.7 mm from the center of the lesion and the total number of labeled cells within that same area were recorded. Likewise, the number of labeled mitotic figures between 0.7 mm and 3.0 mm from the center of the lesion and the total number of labeled cells in that area were recorded. Also, within these same two regions, the total number of mitotic figures was recorded. The χ^2 statistic as described by Dixon and Massey ('57) was used to test the hypothesis that in group I the ratio of the number of labeled mitotic figures to the total number of labeled cells within the same area is independent of their distance from the lesion. This same test was applied to the hypothesis that within a given area the ratio of the number of labeled mitotic figures to the total number of mitotic figures is independent of the distance from the lesion.

grain count, indicating an infiltration of labeled cells. Also, there was little difference in the number or in the grain count of the labeled cells regardless of whether the thymidine was given before or after injury. Since leukocytes must be virtually the only cells labeled before injury, it seemed likely that most of the cells incorporating the label after injury were also leukocytes. Finally, an experiment in which glial cells were labeled in new born mice gave no evidence for division of these cells two months later when the brain was injured (Smith and Walker, '67).

On the other hand, the observation had been made that the distribution of cells assumed to be mononuclear leukocytes around spinal cord wounds did not seem to be the same as the distribution of cells synthesizing DNA in response to injury (Adrian and Walker, '62). If these two distributions were in fact different from each other, it would seem unlikely that the two cell populations were identical. The present experiment has been designed to allowed an extensive comparison of the spatial distribution of labeled cells in injured spinal cords when labeled thymidine is injected before or after the injury. This has been done to determine whether or not the two groups of labeled cells could be samples from the same population.

MATERIALS AND METHODS

Fifty-three mice of known age were divided into three experimental groups. Group I consisted of four C57Bl adult females and seven A/J females. These animals were given three subcutaneous injections of 50 μ c tritiated thymidine (specific activity 1.9 c/mm) at four hour intervals starting 24 hours before spinal cord injury. Group II consisted of 20 A/J females, each of which was given a single injection of 50 μ c tritiated thymidine subcutaneously one hour before sacrifice. Group III consisted of 22 A/J females, of which each was given four subcutaneous injections of 50 μ c tritiated thymidine at six hour intervals starting 24 hours before sacrifice. The animals in all three experimental groups were sacrificed at either one, two, three, four, or five days after spinal cord injury.

All of the animals were subjected to the following operative procedure. After administration of ether anesthesia beginning between 9 A.M. and 11 A.M., the dorsal skin was shaved and washed. A midline dorsal incision was made in the region of the lower thoracic vertebral column. A sterile 30 gauge hypodermic needle was carefully inserted between two of the spinous processes of the lower thoracic vertebrae and pushed ventrally with a slight rotary motion through intervening structures and the spinal cord until it was felt to encounter the resistance of the vertebral body. The needle was then quickly removed, and the skin incision was closed with 6-0 silk sutures. After the animals recovered from anesthesia, they were observed for paralysis and at later times for wound infection. No wound infection was ever noticeable, and although two animals in group III showed some weakness of their hind legs, it did not interfere with their eating or drinking.

In group II four animals and in group III five animals, which will be considered as sham operated controls, were thought to be treated exactly as the others, but the spinal cord, as shown by subsequent detailed histological examination, was not injured.

All of the animals were sacrificed by intracardiac perfusion with 10% formalin made from paraformaldehyde according to the method described by Pease ('64). The caudal two-thirds of the vertebral column was removed and washed briefly in water. The spinal cord was dissected out, washed overnight in running water, dehydrated, embedded in paraffin, and sectioned at 7 μ . After removal of paraffin and staining by the periodic-acid Schiff technique, the slides were coated with either Kodak NTB3 nuclear emulsion or Ilford L-4 emulsion and exposed at 4°C for 3 to 12 weeks. Following three to five minute development in Kodak Microdol X the slides were additionally stained with hematoxylin or with hematoxylin and eosin, dehydrated, and mounted in Permount.

The sections chosen for study came from the central part of the spinal cord, and most of them contained segments of central canal. One complete section from each animal was scanned under oil im-

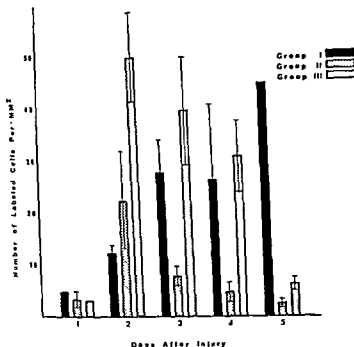


Fig. 1 Mean density of radioactive cells for each group on each of the five days after injury. The bar indicates the standard error of the mean. Controls (not shown) all had less than two labeled cells per mm². There was a progressive increase over the five day period in the number of pre-labeled cells (group I). The number of cells undergoing DNA synthesis in the spinal cord (groups II and III) reached a maximum on the second and third days after injury and by the fifth day was again near control levels.

three experimental groups most of the labeled cells fell into the category of dark-staining, round, ovoid, or irregular nuclei. Although there was a greater percentage of labeled cells in the light-staining category of group II than in group I, the difference was not significant. Table 3 shows the percentages of labeled endothelial cells found near the lesion in the three groups.

Forty-three mitotic figures were found in the five spinal cord sections studied for hem. Examples of these cells are shown in figures 11 through 14. There were 19 anaphases, 15 metaphases, eight anaphases, and one telophase. Table 4 shows the number of labeled mitotic figures and the total number of labeled cells in the same area in which the mitotic figures were observed. The proportion of labeled cells found in mitosis near the lesion was not significantly different from the proportion found at a distance from the lesion. Table 5 shows that the proportion of all mitotic

figures which were labeled is significantly higher in the region within 0.7 mm of the lesion than in the area more distant from the lesion.

DISCUSSION

The experiments described in this paper have been directed toward the following question: Does the DNA synthesis which occurs in nervous tissue following a local injury occur only in mononuclear leukocytes that have infiltrated the nervous tissue? The experimental approach to this question was based on the assumption that if a population of cells is distributed over a defined area of tissue in a manner that is the same in all animals treated the same way, then two independent and unbiased samples of this population should have similar distributions. The population of cells in question was the population of mononuclear leukocytes which infiltrate the spinal cord following a penetrating in-

RESULTS

In most of the sections examined the wound was located near the center of the section, although in some of the animals it was more caudally placed. In the animals killed the first day after injury the lesion contained mostly erythrocytes, necrotic debris and polymorphonuclear leukocytes. Cells with dark staining, irregular nuclei and macrophages containing erythrocytic debris were prominent on the second day, and mitotic figures were easily found near the wound on the second and third days after injury. By the fourth and fifth days the central core of the lesion was densely packed with nuclei, and the polymorphonuclear leukocytes had virtually disappeared.

The mean density of radioactive cells (as determined by dividing the total number of radioactive cells per section by the area of the section) is shown for each group on each day of the experiment in figure 1. The density of labeled cells in group I increased over the five day period. The radioactive cell densities in groups II and III reached maximum values on the second day after injury and on the fifth day were only slightly above control levels. The sham operated animals in groups II and III all had less than two radioactive cells per square millimeter of spinal cord.

Examples of the distribution of radioactive cells in the spinal cord sections from group I are shown in figure 2. The large concentration of labeled cells at the lesion, which appears to reach its peak on the third and fourth days after injury, is readily apparent. This distribution of labeled cells should be compared with that found in group II (fig. 3). Here on the second and third days after injury the labeled cells were more diffusely distributed. On the other days more of the labeled cells were located near the lesion, but the difference in radioactive cell density at the lesion from that over the rest of the section is not as high in group II as in group I. In group III the distribution of labeled cells (fig. 4) is similar to that in group II except for an increase in the total number of labeled cells and somewhat greater concentrations at the lesion on days three and four. Again, the labeled cells are seen

to be distributed throughout the section on the second day after injury.

The distribution curves which were determined from the maps of all animals in each group are shown in figures 5 through 9. In all cases group I has the highest value at the lesion with a sharp decline as one moves away from the lesion. Group II tends to be much less sharply peaked at the lesion, and group III is intermediate between the other two groups in this respect.

To emphasize the greater concentration of labeled cells at the lesion in group I as compared with the other two groups, the ratio of the density of labeled cells in the row passing through the lesion to the density of labeled cells over the entire section was calculated for each spinal cord. In group I this ratio ranged from 6.5 to 20.7. In group II the range was from 0.0 to 15.6 and in group III, from 0.8 to 14.6. Figure 10 shows the mean value of this ratio plotted for each group on each of the five days after injury. The values for groups II and III were not significantly different from each other. However, on the second and third days after injury the values for group I were significantly higher than the values for group II. (Days one and five were not included in the statistical analysis, since there was but a single animal in group I on each of these days).

Table 1 shows the values calculated for slope and y-intercept of the straight line for each animal. When these values were ranked and tested by the method of Kruskal and Wallis ('52), it was found that there is a very low probability that either the slopes ($p < 0.05$) or the y-intercepts ($p < 0.01$) from the three groups of straight lines represent samples from the same population. When group I was compared against group II, there were significant differences in both the slope ($p < 0.05$) and the y-intercept ($p < 0.01$). When group I was compared against group III, only the difference between the y-intercepts was significant ($p < 0.01$). In neither the slope nor the y-intercept were there significant differences when groups II and III were compared.

Table 2 shows the results of the nuclear classification of labeled cells that were indistinguishable from glial cells. In all

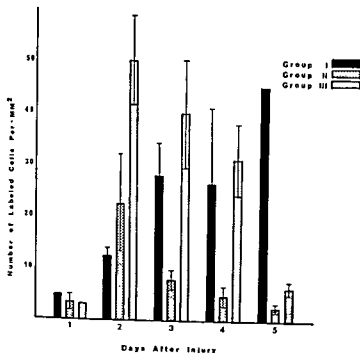


Fig. 1 Mean density of radioactive cells for each group on each of the five days after injury. The bar indicates the standard error of the mean. Controls (not shown) all had less than two labeled cells per mm². There was a progressive increase over the five day period in the number of pre-labeled cells (group I). The number of cells undergoing DNA synthesis in the spinal cord (groups II and III) reached a maximum on the second and third days after injury and by the fifth day was again near control levels.

ree experimental groups most of the labeled cells fell into the category of dark-staining, round, ovoid, or irregular nuclei. Although there was a greater percentage of labeled cells in the light-staining category in group II than in group I, the difference was not significant. Table 3 shows the percentages of labeled endothelial cells and near the lesion in the three groups. Forty-three mitotic figures were found in five spinal cord sections studied for 100 μ m. Examples of these cells are shown in figures 11 through 14. There were 19 metaphases, 15 metaphases, eight anaphases, and one telophase. Table 4 shows the number of labeled mitotic figures and the number of labeled cells in the same area in which the mitotic figures were observed. The proportion of labeled cells in mitosis near the lesion was not significantly different from the proportion at a distance from the lesion. Table 4 shows that the proportion of all mitotic

figures which were labeled is significantly higher in the region within 0.7 mm of the lesion than in the area more distant from the lesion.

DISCUSSION

The experiments described in this paper have been directed toward the following question: Does the DNA synthesis which occurs in nervous tissue following a local injury occur only in mononuclear leukocytes that have infiltrated the nervous tissue? The experimental approach to this question was based on the assumption that if a population of cells is distributed over a defined area of tissue in a manner that is the same in all animals treated the same way, then two independent and unbiased samples of this population should have similar distributions. The population of cells in question was the population of mononuclear leukocytes which infiltrate the spinal cord following a penetrating in-

RESULTS

In most of the sections examined the wound was located near the center of the section, although in some of the animals it was more caudally placed. In the animals killed the first day after injury the lesion contained mostly erythrocytes, necrotic debris and polymorphonuclear leukocytes. Cells with dark staining, irregular nuclei and macrophages containing erythrocytic debris were prominent on the second day, and mitotic figures were easily found near the wound on the second and third days after injury. By the fourth and fifth days the central core of the lesion was densely packed with nuclei, and the polymorphonuclear leukocytes had virtually disappeared.

The mean density of radioactive cells (as determined by dividing the total number of radioactive cells per section by the area of the section) is shown for each group on each day of the experiment in figure 1. The density of labeled cells in group I increased over the five day period. The radioactive cell densities in groups II and III reached maximum values on the second day after injury and on the fifth day were only slightly above control levels. The sham operated animals in groups II and III all had less than two radioactive cells per square millimeter of spinal cord.

Examples of the distribution of radioactive cells in the spinal cord sections from group I are shown in figure 2. The large concentration of labeled cells at the lesion, which appears to reach its peak on the third and fourth days after injury, is readily apparent. This distribution of labeled cells should be compared with that found in group II (fig. 3). Here on the second and third days after injury the labeled cells were more diffusely distributed. On the other days more of the labeled cells were located near the lesion, but the difference in radioactive cell density at the lesion from that over the rest of the section is not as high in group II as in group I. In group III the distribution of labeled cells (fig. 4) is similar to that in group II except for an increase in the total number of labeled cells and somewhat greater concentrations at the lesion on days three and four. Again, the labeled cells are seen

to be distributed throughout the section on the second day after injury.

The distribution curves which were determined from the maps of all animals in each group are shown in figures 5 through 9. In all cases group I has the highest value at the lesion with a sharp decline as one moves away from the lesion. Group II tends to be much less sharply peaked at the lesion, and group III is intermediate between the other two groups in this respect.

To emphasize the greater concentration of labeled cells at the lesion in group I as compared with the other two groups, the ratio of the density of labeled cells in the row passing through the lesion to the density of labeled cells over the entire section was calculated for each spinal cord. In group I this ratio ranged from 6.5 to 20.7. In group II the range was from 0.0 to 15.6, and in group III, from 0.8 to 14.6. Figure 10 shows the mean value of this ratio plotted for each group on each of the five days after injury. The values for groups II and III were not significantly different from each other. However, on the second and third days after injury the values for group I were significantly higher than the values for group II. (Days one and five were not included in the statistical analysis, since there was but a single animal in group I on each of these days).

Table 1 shows the values calculated for slope and y-intercept of the straight line, for each animal. When these values were ranked and tested by the method of Kruskal and Wallis ('52), it was found that there is a very low probability that either the slopes ($p < 0.05$) or the y-intercepts ($p < 0.01$) from the three groups, of straight lines represent samples from the same population. When group I was compared against group II, there were significant differences in both the slope ($p < 0.05$) and the y-intercept ($p < 0.01$). When group I was compared against group III, only the difference between the y-intercepts was significant ($p < 0.01$). In neither the slope nor the y-intercept were there significant differences when groups II and III were compared.

Table 2 shows the results of the nuclear classification of labeled cells that were indistinguishable from glial cells. In all

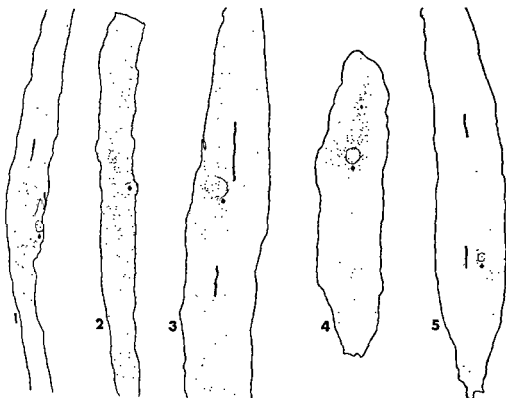


Fig. 3. Representative spinal cord sections from animals in group II. Here the black dots indicate the positions of cells synthesizing DNA at the time of injection, one hour before sacrifice. Numbers indicate the day after injury that the animal was sacrificed.

those which were in the blood, the vast majority of the labeled cells found in group I must be hematogenous. This method of tracing labeled leukocytes into tissues where there are normally only a low number of cells synthesizing DNA has been used previously in the study of wounded muscle (Bintliff and Walker, '60), injured spinal cord (Adrian and Walker, '62; Walker, '63) and injured brain (Konigsmark and Sidman, '63; Huntington and Terry, '66). That these infiltrating mononuclear leukocytes definitely do divide in nervous tissue is demonstrated by the numerous labeled mitotic figures found in group I (figs. 11 through 14; table 4 and 5).

The labeled leukocytes that were found within the nervous tissue were located within the neuropil and were not confined to vessels. The animals in all the experimental groups were sacrificed by perfusion

fixation, and the vessels were washed clear of cells. Only occasionally were labeled cells found in relation to vessel walls.

The labeled cells found in the spinal cords from the animals in group II, which received a single injection of tritiated thymidine one hour before sacrifice, represent sites of local DNA synthesis. The much higher number of labeled cells found in the spinal cords of the injured animals over that found in the sham-operated animals should be cells that have synthesized DNA in response to the injury. They cannot be cells that have acquired their label elsewhere before migrating into the nervous tissue, because there was insufficient time between the injection of the labeled thymidine and sacrifice for significant migration of labeled cells to occur.

When the drawings of the spinal cord sections from the animals in group I were

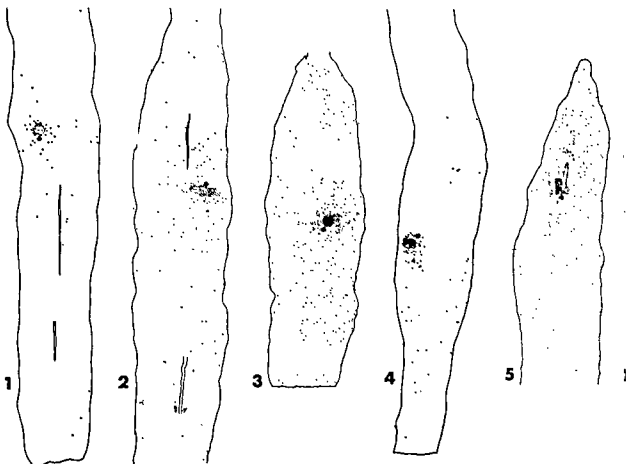


Fig. 2 Outline drawings of spinal cord sections from representative animals in the group injected with tritiated thymidine before injury (group I). Numbers indicate the day after injury when the animal was killed. Black dots show positions of radioactive cells, most of which entered the spinal cord after becoming labeled. Arrows indicate the position of the wounds.

jury. It has been shown that a substantial proportion of this cell population can be labeled by injecting tritiated thymidine several hours prior to injury (Walker, '63). If mononuclear leukocytes are the only cells in the spinal cord engaged in DNA synthesis following injury, then the cells labeled by injecting tritiated thymidine after injury should represent a second, independent sample of the population of mononuclear leukocytes. If the distributions of these two groups of labeled cells are dissimilar, then either the assumption stated above is false, or the hypothesis that only the leukocytes undergo DNA synthesis is false.

Tritiated thymidine is generally considered to label only DNA that is being synthesized in preparation for division (Cronkite et al., '59; Gall and Johnson, '60), and it is incorporated for only a short

time following injection (Hughes et al., '58). In normal adult nervous tissue, the number of labeled cells following tritiated thymidine injection is very low (Smart and Leblond, '61; Adrian and Walker, '62). In the spinal cord sections from the animals in group I, which received three injections of tritiated thymidine at 24, 20 and 16 hours before injury, most of the labeled cells at the wound must be due to an influx of labeled mononuclear leukocytes. Since the last injection of labeled thymidine was given 16 hours before the injury, none of it would have been available in the blood to label cells which began DNA synthesis after the injury. Therefore, the population of labeled cells which appeared at the site of injury must have migrated in from outside the nervous tissue. Since there was no large population of labeled cells close to the wound, except

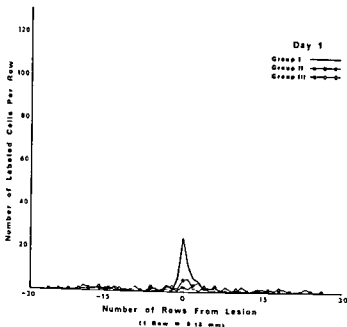


Fig. 5 Comparison of the distribution curves for the three groups of experimental animals sacrificed on the first day after injury. Each point was determined by averaging the individual values for a given row from all the animals in the group. Beyond three rows from the lesion the curves are indistinguishable. In the immediate vicinity of the lesion, the values for group I are much higher than those for the other two groups.

center of the wound. The number of labeled cells in the row passing through the lesion ranged from 25 on the first day to 213 on the third day after injury and averaged 91 for the eleven animals in the group. At a distance of more than four rows (0.7 mm) from the lesion the number of labeled cells per row did not exceed 15 on the first four days after injury and was usually less than ten. In contrast, the number of cells in the row through the lesion in group II ranged from zero to 21 and averaged 11. On the second day after injury the number of cells in DNA synthesis was greater than the number of labeled leukocytes at all places other than in the one or two rows nearest the lesion. On the other days, at a distance from the lesion, the number of cells in DNA synthesis was of comparable magnitude to the number of labeled leukocytes, except on the fifth day when there were more labeled cells in group I than in group II.

Since the exact percentages of the total cell population which the two samples of

labeled cells constituted were unknown, it seemed more meaningful to compare the distributions of the two samples about the lesion than to make a statistical comparison of absolute numbers of labeled cells in the two groups. To transform the data from the two samples to comparable forms, the number of labeled cells at a given distance from the lesion in each spinal cord section was expressed as a fraction of the number found in an equivalent area passing through the lesion. By this means the number of labeled cells at the lesion for every graph was set equal to 1.0, and the number of cells per row at a distance from the lesion was expressed as a fractional value of 1.0. When the best fitting straight line was computed for each set of these ratios, it was found that there was a very low probability that the family of lines from group I and the family of lines from group II represented samples from the same population. The distribution of labeled mononuclear leukocytes to a spinal cord lesion was signifi-

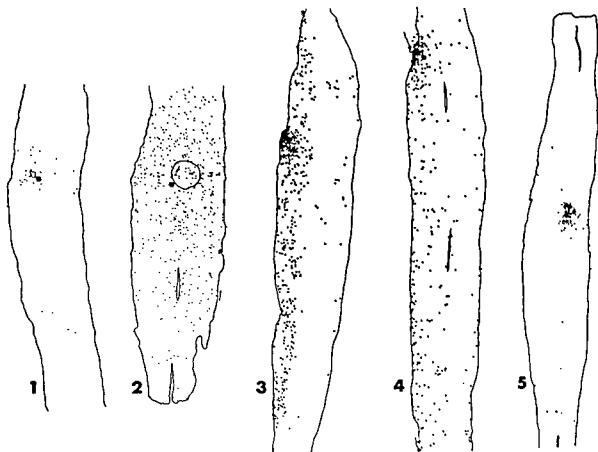


Fig. 4 Spinal cord sections from the animals in group III, which received four injections of tritiated thymidine during the 24 hour period prior to sacrifice. Although most of the dots represent cells that became labeled in the nervous tissue, there are probably some cells present that entered the nervous tissue after acquiring their label.

compared to those from the animals in group II, the patterns of distribution of radioactive cells were seen to be distinctly different. In all the sections from group I there was a large concentration of labeled leukocytes at the lesion compared to the numbers of such cells found at even short distances away. In most of the sections from group II there was an even distribution of cells in DNA synthesis over the entire section. At the wound the number of labeled infiltrating cells was very much greater than the number of cells in DNA synthesis on all five days. On the second day after injury there were more cells in DNA synthesis away from the wound than there were labeled leukocytes from the blood. By the fourth and fifth days after injury, while at the lesion there were still many more labeled leukocytes than there were cells in DNA synthesis, away from

the wound the number of leukocytes was of the same order of magnitude as the number of cells in DNA synthesis.

Although each spinal cord section was obviously only a two dimensional sample of a three dimensional distribution of labeled cells, the sections were comparable from animal to animal in that the plane of section was always at right angles to the needle track and the sections chosen for study all came from the central region of the cord. When the two dimensional maps were reduced to one dimensional graphs showing the number of labeled cells in a band or row across the width of the section plotted against the longitudinal dimension of the cord, the differences apparent on the maps were even more pronounced. All of the graphs from group had an extremely sharp peak that was limited to the one or two rows nearest the

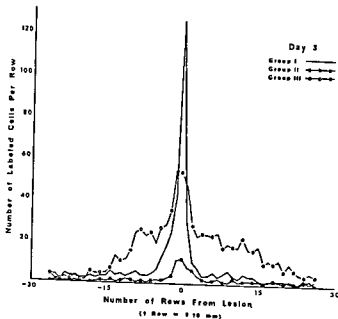


Fig. 7 Comparison of distribution curves on the third day after injury. The curve for group I is an average of the values from four animals. The curve for group II is an average of the values from five animals, and that for group III is an average from three animals. The curve for group III has become more sharply peaked at the lesion, but its values still remain high at a distance from the lesion. Most of the labeled cells in group I are within six rows of the center of the lesion, and the total number of labeled cells has increased over that found on the second day.

the spinal cord in groups II and III, they were seen to be very different in the area near the lesion. The straight lines plotted for group I were shown to be different from those plotted for either of the other groups. At the lesion there was a much greater difference in the density of leukocytes and the density of cells synthesizing DNA than there was elsewhere on the sections. A possible explanation for this difference in distribution of the leukocyte population and the population of cells synthesizing DNA was that the leukocytes had less tendency to divide near the lesion than elsewhere. To rule out this possibility, mitotic counts were made on several of the sections from group I. Table 4 shows that there is no significant difference in the percentage of leukocytes found in mitosis in the area within 0.7 mm from the lesion and the percentage found in mitosis between 0.7 mm and 3.0 mm from the lesion. Therefore, the leukocytes have just as much ability to divide, and presumably

to synthesize DNA, near the lesion as at a considerable distance from it. On the other hand, the leukocytes account for a significantly higher percentage of the total number of mitotic figures in the area within 0.7 mm from the lesion than they do at a greater distance from the lesion (table 5), which would indicate that some other type of cell is also dividing.

On the second day after injury it was only in the immediate vicinity of the lesion that there were a sufficient number of mononuclear leukocytes to account for the observed DNA synthesis in either group II or group III. Beyond a distance of 1.5 mm from the lesion there were roughly six times as many cells in which DNA synthesis was occurring in group II as there were labeled mononuclear leukocytes in group I. Beyond a distance of 0.7 mm from the lesion there were almost ten times as many labeled cells in group III as there were labeled mononuclear leukocytes in group I. If the mononuclear leukocytes

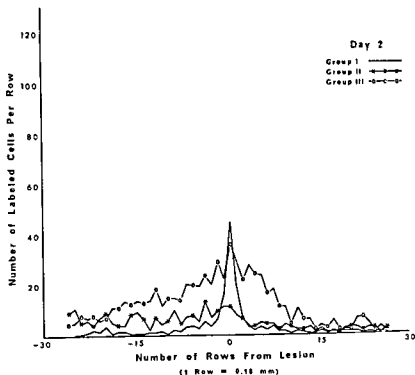


Fig. 6 Comparison of the distribution curves on the second day after injury. Each curve is an average of the values from three animals. Most of the labeled cells in group I are within four rows of the center of the lesion. Groups II and III are more evenly distributed; however, the curve for group III does reach its peak at the lesion.

cantly different from the distribution of cells synthesizing DNA in response to the injury.

The cells labeled in group III should include all of the cells that began DNA synthesis during the 24 hour period starting 30–32 hours before sacrifice, provided that the period of DNA synthesis in these cells is of the same duration (six to eight hours) as that found in most other mammalian cell types (Cameron and Greulich, '63). In the spinal cord this population is principally composed of cells that were in the spinal cord at the time DNA synthesis began. In addition, some mononuclear leukocytes which acquired their label elsewhere are probably among the labeled cells in group III, since a large percentage of these cells are labeled in the blood within 12 hours after beginning tritiated thymidine injection (Bintliff and Walker, '60). The relative magnitude of this infiltration of labeled cells in group III may be estimated by comparing the distribution curves for groups II and III on each of the five days. The cells labeled in group

II are known to be cells that were synthesizing DNA in the spinal cord shortly before sacrifice. Since the period of DNA synthesis is roughly six to eight hours there should be about three or four times as many of these cells labeled in group II as are found labeled in group III. The number of labeled cells in group III in excess of three or four times the number in group II could represent either an increase due to division of some of the earliest cells to be labeled or an infiltration of labeled leukocytes. Only on days three and four were there more than four times as many labeled cells in group III as were in group II. There was a significant difference between the y-intercepts of the straight lines computed for groups I and III, which would indicate that the component of labeled infiltrated cells in group III was probably quite small relative to the component of cells that had undergone DNA synthesis in the nervous tissue.

When the distribution of labeled leukocytes in group I was compared to the distribution of the cells synthesizing DNA in

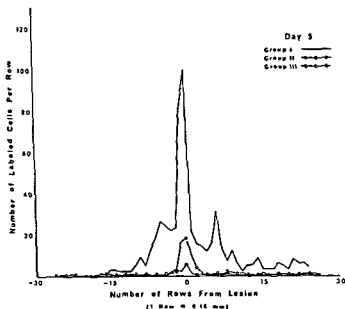


Fig. 9 Comparison of the distribution curves on the fifth day after injury. The curve for group I is based on a single animal. The curves for groups II and III are each based on four animals. The total number of labeled cells has increased in group I. Although most of them are still found close to the lesion, many more are found throughout the section than were found at the earlier times. The number of labeled cells in groups II and III has become quite small, and most of these are near the lesion.

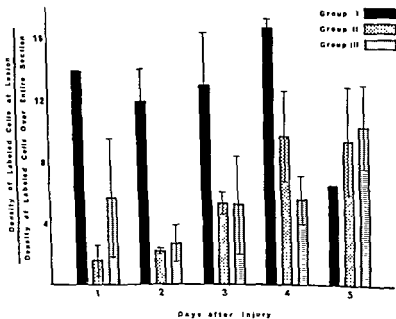


Fig. 10 Relative density of labeled cells at the lesion. The ratio of the density of labeled cells in the row passing through the lesion to the density of labeled cells throughout the entire spinal cord section is shown for each group on each day. Brackets indicate the standard error of the mean. The values for groups II and III are not significantly different from each other. On the second and third days after injury the values for group I are significantly higher than the values for group II ($p < 0.05$).

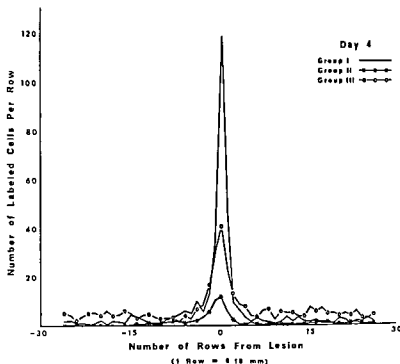


Fig. 8 Comparison of distribution curves on the fourth day after injury. The curve for group I is based on two animals. The curves for groups II and III are each based on four animals. There is little change in the distribution and in the number of labeled cells in group I from that found on the third day. The total number of labeled cells in group III is much smaller than on the previous two days, and the curve has become much more sharply peaked at the lesion.

were the only cells in the spinal cord undergoing DNA synthesis on the second day after injury, no more than 10% of them could have been labeled in group I, and all of them would have had to divide at least once during the second day after injury. However, from the work of others it is clear that a much higher percentage of the total population of mononuclear leukocytes must be labeled in group I by the second day after injury (Bintliff and Walker, '60; Konigsmark and Sidman, '63; Huntington and Terry, '66). Therefore, some type or types of cells other than the mononuclear leukocytes present in such large numbers at the lesion must also have been synthesizing DNA in the spinal cord on the second day after injury.

The exact nature of this cell has not been determined by this study. The possibility that some of the DNA synthesis may occur in small lymphocytes, in which the percentage labeled in the peripheral blood is known to be low, has not been completely excluded. Walker ('63) has

shown that these cells probably enter injured spinal cord but that they do not collect at the wound area in large numbers. Mononuclear leukocytes normally present in the nervous tissue, as opposed to those that infiltrated because of injury, may also be sites of DNA synthesis. Roessmann and Friede ('67) found labeled leukocytes in normal nervous tissue of recipient animals following transfusion of blood from animals that had received tritiated thymidine previously, indicating that some of these cells are in nervous tissue at all times. The number of such labeled cells was increased following injury. That endothelial cells must account for a portion of the non-leukocytic DNA synthesis is clear from the fact that a small number of endothelial cells were seen to be labeled in groups II and III throughout most of the five day period. However, the labeled endothelial cells were found almost entirely in the area of the lesion. Endothelial proliferation following nervous tissue injury has been previously reported by Bender ('25).

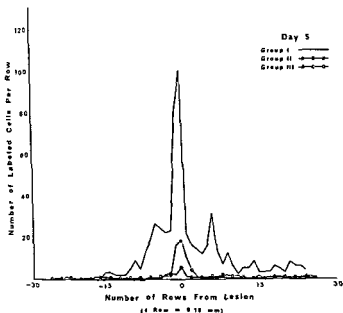


Fig. 9 Comparison of the distribution curves on the fifth day after injury. The curve for group I is based on a single animal. The curves for groups II and III are each based on four animals. The total number of labeled cells has increased in group I. Although most of them are still found close to the lesion, many more are found throughout the section than were found at the earlier times. The number of labeled cells in groups II and III has become quite small, and most of these are near the lesion.

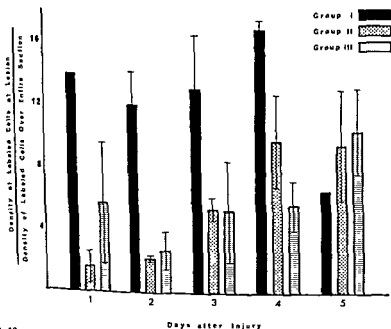


Fig. 10 Relative density of labeled cells at the lesion. The ratio of the density of labeled cells in the row passing through the lesion to the density of labeled cells throughout the entire spinal cord section is shown for each group on each day. Brackets indicate the standard error of the mean. The values for groups II and III are not significantly different from each other. On the second and third days after injury the values for group I are significantly higher than the values for group II ($p < 0.05$).

TABLE 1
Values for slope and y-intercept of the straight lines calculated for each animal

Day after injury	Group I		Group II		Group III	
	Slope	Y-intercept	Slope	Y-intercept	Slope	Y-intercept
1	-0.07	0.32	0.20 -0.06	1.40 1.62	-0.07 0.12	0.35 0.05
2	-0.02 -0.09 -0.02	0.21 0.43 0.17	0.02 -0.01 -0.13	0.76 0.99 0.92	-0.02 -0.06 -0.03	0.62 1.10 1.27
3	-0.03 -0.08 -0.14 -0.05	0.15 0.45 0.69 0.25	-0.33 -0.08 -0.18 -0.12 -0.15	1.46 0.53 0.96 0.53 0.81	-0.18 -0.10 -0.11	1.03 0.47 0.85
4	-0.06 -0.04	0.29 0.24	-0.18 -0.12 -0.11 -0.14	1.09 0.51 0.50 0.86	-0.20 -0.11 -0.16 -0.14	1.18 0.54 0.78 0.77
5	-0.01	0.25	-0.15 -0.07	0.75 0.44	-0.08 -0.08 -0.07 -0.06	0.36 0.35 0.34 0.29
Mean	-0.06	0.31	-0.10	0.88	-0.08	0.65

P y-intercepts < 0.01, P slopes < 0.05.

TABLE 2

Classification of radioactive nuclei indistinguishable from glial nuclei in 1.25 mm² around lesion

Group	No. of animals	Total area examined mm ²	Total ¹ no. of nuclei	Total R.A.	Types of radioactive nuclei		
					Round, oval or irregular		Elongated
					Dark	Light	
I	11	13.75	14,639	2,119	82.9 ± 9.5	9.5 ± 9.5	7.4 ± 5.9
II	17	21.25	22,573	500	61.8 ± 15.3	25.3 ± 10.5	12.9 ± 11.2
III	16	20.00	16,948	1,511	79.4 ± 10.9	11.0 ± 10.2	9.6 ± 7.6

¹ Excluding neurons, ependymal cells, polymorphonuclear leukocytes, and endothelial cells.

TABLE 3
Radioactive endothelial cells in 1.25 mm² around lesion

Group	Total no. of endothelial nuclei	Radioactive endothelial nuclei	
		no.	%
I	1,736	22	1.26
II	4,064	61	1.50
III	3,457	57	1.65

Baggenstoss et al. ('43) Klatzo et al. ('58), Levine and Stypulkowski ('59), and Cammermeyer ('65). Since the leukocytes in group I were distinguishable from the glial

nuclei among which they were found only by their label, the nuclear morphology of the labeled cells in groups II and III is of little value in distinguishing leukocytes from glial cells. A slightly higher percentage of the labeled cells in groups II and III fell into the categories of elongated and light staining nuclei than in group I, and it is possible that connective tissue cells and astrocytes may be responsible for some of the DNA synthesis that occurred. Several authors have maintained that a large portion of the population of macrophages that invade brain wounds are derived from vascular adventitial cells, and proliferation of these cells was usu-

TABLE 4

Labeled mitotic figures shown relative to the total number of labeled cells in group I

	Within 0.7 mm from lesion	Between 0.7 mm and 3.0 mm from lesion	Total
Labeled mitoses	19	6	25
Other labeled cells	914	312	1226
Total labeled cells	933	318	1251

$$\chi^2 = 0.005, p > 0.95.$$

TABLE 5

Labeled mitotic figures shown relative to the total number of mitotic figures in group I

	Within 0.7 mm from lesion	Between 0.7 mm and 3.0 mm from lesion	Total
Labeled mitoses	19	6	25
Unlabeled mitoses	5	13	18
Total mitoses	24	19	43

$$\chi^2 = 8.61, p < 0.01.$$

ally thought to be a necessary preliminary event (Cone, '28; Carmichael et al., '39; Baggenstoss et al., '43; Silver and Walker, '47). Following tritiated thymidine injection, Königsmark and Sidman ('64) found a few labeled nuclei in injured brains that stained with gold chloride sublimate and which they identified as astrocytes. The other reports of labeled glial cells following tritiated thymidine injection into animals with nervous tissue injuries have assumed either that no leukocytes were present to be labeled or that the glial cells could be distinguished from leukocytes on the basis of nuclear morphology (Koenig, '60; Koenig et al., '62; Altman, '62; Adrian and Walker, '62; Samorajski et al., '64; Hassler, '66).

On the basis of the results thus far presented it is concluded that although mononuclear leukocytes do freely invade the nervous tissue and synthesize DNA in and around sites of injury, they are not the only cells in which such DNA synthesis occurs. A substantial number of cells already present in the nervous tissue must engage in DNA synthesis during the five day period following injury. This synthe-

sis begins near the end of the first day after injury and is occurring in a large number of cells by the end of the second day. Many of these cells are located at relatively long distances from the lesion on that day. The number of such cells is considerably diminished by the fifth day after injury.

ACKNOWLEDGMENT

The author wishes to express his sincere thanks to Dr. Bruce E. Walker, who served as supervising professor during the preparation of the doctoral dissertation from which this paper developed, to Dr. Donald Duncan, who critically reviewed the manuscript, and to Mrs. Gwen Adrian, who prepared the illustrations.

LITERATURE CITED

- Adams, R. D. 1958 Implications of the biology of the neuroglia and microglia cells for clinical neuropathology. In: *Biology of Neuroglia*. Ed. by W. F. Windle Charles C Thomas, Springfield, Illinois, 245-287.
- Adrian, E. K., and B. E. Walker 1962 Incorporation of thymidine- H^3 by cells in normal and injured mouse spinal cord. *J. Neuropath. Exp. Neurol.*, 21: 597-609.
- Allen, E. 1912 The cessation of mitosis in the central nervous system of the albino rat. *J. Comp. Neur.*, 22: 547-568.
- Altman, J. 1962 Autoradiographic study of degenerative and regenerative proliferation of neuroglia cells with tritiated thymidine. *Exp. Neurol.*, 5: 302-318.
- 1963 Autoradiographic investigation of cell proliferation in the brains of rats and cats. *Anat. Rec.*, 145: 573-592.
- Baggenstoss, A. H., J. W. Kernohan and J. F. Drapiewski 1943 The healing process in wounds of the brain. *Amer. J. Clin. Path.*, 13: 333-348.
- Bender, L. 1925 Experimental production of gliosis. I. Effects on the nervous system of the rabbit of intravenous and intraspinal injections of cholesterol emulsion. *Amer. J. Path.*, 1: 657-666.
- Bindliff, S., and B. E. Walker 1960 Radioautographic study of skeletal muscle regeneration. *Am. J. Anat.*, 106: 233-246.
- Cameron, I. L., and R. C. Greulich 1963 Evidence for an essentially constant duration of DNA synthesis in renewing epithelia of the adult mouse. *J. Cell Biol.*, 18: 31-40.
- Cammermeyer, J. 1965 Endothelial and intramural karyokinesis during retrograde reaction in the facial nucleus of rabbits of varying age. *Ergebn. Anat. Entwicklungsgesch.*, 38: 23-45.
- Carmichael, F. A., J. W. Kernohan and A. W. Adson 1939 Histopathogenesis of cerebral abscess. *Arch. Neurol. Psychiat.*, 42: 1001-1029.

- Cone, W. 1928 Acute pathological changes in neuroglia and in microglia. *Arch. Neurol. Psychiat.*, 20: 34-68.
- Cronkite, E. P., V. P. Bond, T. M. Flidner and J. R. Rubini 1959 The use of tritiated thymidine in the study of DNA synthesis and cell turnover in hemopoietic tissues. *Lab. Invest.*, 8: 262-277.
- Del Rio-Hortega, P. 1932 Microglia. In: *Cytology and Cellular Pathology of the Nervous System*, Vol. II. Ed. by W. Penfield, Paul B. Hoeber, Inc., New York, N. Y., 482-534.
- Del Rio-Hortega, P., and W. Penfield 1927 Cerebral cicatrix; the reaction of neuroglia and microglia to brain wounds. *Bull. Johns Hopkins Hosp.*, 41: 278-303.
- Dixon, W. J., and F. J. Massey 1957 *Introduction to Statistical Analysis* 2nd edition, McGraw-Hill Book Company, Inc., New York, N. Y.
- Gall, J. G., and W. W. Johnson 1960 Is there "metabolic" DNA in the mouse seminal vesicle? *J. Biophys. Biochem. Cytol.*, 7: 657-665.
- Gavrilova, T. N. 1964 Vkluchenie H³-timidina v kletochnye elementy nervoi tkani vzroslkh myshei. *Tsitologiya*, 6: 622-626.
- Hain, R. F., W. O. Riecke and N. B. Everett 1960 Evidence of mitosis in neuroglia as revealed by radioautography employing tritiated thymidine. *J. Neuropath. Exp. Neurol.*, 19: 147-148.
- Hassler, O. 1966 Incorporation of thymidine-H³ into mouse brain after a single dose of X-rays. An autoradiographic study. *J. Neuropath. Exp. Neurol.*, 25: 97-106.
- Hommes, Otto R., and C. P. Leblond 1967 Mitotic division of neuroglia in the normal adult rat. *J. Comp. Neur.*, 129: 269-278.
- Hughes, W. L., V. P. Bond, G. Brecher, E. P. Cronkite, R. P. Painter, R. Quastler and F. G. Sherman 1958 Cellular proliferation in the mouse as revealed by autoradiography with tritiated thymidine. *Proc. Nat. Acad. Sci.*, 44: 476-483.
- Huntington, H. W., and R. D. Terry 1966 The origin of the reactive cells in cerebral stab wounds. *J. Neuropath. Exp. Neurol.*, 25: 646-653.
- Klatzo, I., A. Piraux and E. J. Laskowski 1958 The relationship between edema, blood-brain barrier and tissue elements in a local brain injury. *J. Neuropath. Exp. Neurol.*, 17: 548-564.
- Koenig, H. 1960 Autoradiographic studies of deoxyribonucleic acid (DNA) turnover in the feline neuraxis. *J. Histochem. Cytochem.*, 8: 337.
- Koenig, H., M. B. Bunge and R. P. Bunge 1962 Nucleic acid and protein metabolism in white matter. *Arch. Neurol.*, 6: 177-193.
- Konigsmark, B. W., and R. L. Sidman 1963 Origin of brain macrophages in the mouse. *J. Neuropath. Exp. Neurol.*, 22: 643-676.
- 1964 Response of astrocytes to brain injury. *J. Neuropath. Exp. Neurol.*, 24: 142.
- Kosunen, T. U., B. H. Waksman and I. K. Samuelsson 1963 Radioautographic study of cellular mechanisms in delayed hypersensitivity. II. Experimental allergic encephalomyelitis in the rat. *J. Neuropath. Exp. Neurol.*, 22: 367-380.
- Kruskal, W. H., and W. A. Wallis 1952 Use of ranks in one-criterion variance analysis. *J. Amer. Statistical Assn.*, 47: 583-621.
- Leblond, C. P., and B. E. Walker 1956 Renewal of cell populations. *Physiol. Rev.*, 36: 255-276.
- Levine, S., and W. Stypulkowski 1959 Experimental cyanide encephalopathy. *Arch. Path.*, 67: 306-323.
- Messier, B., and C. P. Leblond 1960 Cell proliferation and migration as revealed by radioautography after injection of thymidine-H³ into male rats and mice. *Am. J. Anat.*, 106: 247-285.
- Messier, B., C. P. Leblond and I. Smart 1958 Presence of DNA synthesis and mitosis in the brain of young adult mice. *Exp. Cell Res.*, 14: 224-226.
- Ngowyang, G. 1930 On the growth of the motor cells from birth to maturity at four levels in the spinal cord of the albino mouse. *J. Comp. Neur.*, 50: 231-245.
- Noetzel, H. 1962 Autoradiographische Untersuchungen über die physiologische Regeneration der Gliazellen. *Verh. Deutsch. Ges. Path.*, 46: 341-344.
- Noetzel, H., and J. Rox 1964 Autoradiographische Untersuchungen über Zellteilung und Zellentwicklung im Gehirn der erwachsenen Maus und des erwachsenen Rhesus-Affen nach Injektion von radioaktivem Thymidin. *Acta Neuropath.*, 3: 326-342.
- Pease, D. C. 1964 *Histological Techniques for Electron Microscopy*, 2nd Edition, Academic Press, New York, N. Y., 52.
- Penfield, W. 1925 Microglia and the process of phagocytosis in gliomas. *Amer. J. Path.*, 1: 77-90.
- Ries, E. 1938 Wann erlischt die mitotische Vermehrungsfähigkeit der Gewebe? *A. Mikr. Anat. Forsch.*, 43: 558-566.
- Roessmann, U., and R. L. Friede 1967 Entry of labeled donor cells from the bloodstream into the CNS. *J. Neuropath. Exp. Neurol.*, 26: 144-145.
- Samorajski, T., W. Zeman and J. M. Ordry 1964 Histochemistry of particle microbeam lesions in the brain of the mouse. *J. Neuropath. Exp. Neurol.*, 23: 264-279.
- Schultze, B., and W. Oehlert 1960 Autoradiographic investigation of incorporation of H³ thymidine into cells of the rat and mouse. *Science*, 131: 737-738.
- Silver, M. L., and A. E. Walker 1947 Histochemistry of thermocoagulation of the cerebral cortex. *J. Neuropath. Exp. Neurol.*, 6: 311-322.
- Smart, I. 1961 The subependymal layer of the mouse brain and its cell production as shown by radioautography after thymidine-H³ injection. *J. Comp. Neur.*, 116: 325-347.
- Smart, I., and C. P. Leblond 1961 Evidence for division and transformation of neuroglia cells in the mouse brain as derived from radioautography after injection of thymidine-H³. *J. Comp. Neur.*, 116: 349-367.

Smith, C. W., and B. E. Walker 1967 Glial and lymphoid cell response to tumor implantation in mouse brain. *Texas Rep. Biol. Med.*, 25: 585-600.

Walker, B. E. 1963 Infiltration and transformation of lymphoid cells in areas of spinal cord injury. *Texas Rep. Biol. Med.*, 21: 615-630.

- Cone, W. 1928 Acute pathological changes in neuroglia and in microglia. *Arch. Neurol. Psychiat.*, 20: 34-68.
- Cronkite, E. P., V. P. Bond, T. M. Fliedner and J. R. Rubini 1959 The use of tritiated thymidine in the study of DNA synthesis and cell turnover in hemopoietic tissues. *Lab. Invest.*, 8: 262-277.
- Del Rio-Hortega, P. 1932 Microglia. In: *Cytology and Cellular Pathology of the Nervous System*, Vol. II. Ed. by W. Penfield, Paul B. Hoeber, Inc., New York, N. Y., 482-534.
- Del Rio-Hortega, P., and W. Penfield 1927 Cerebral cicatrix; the reaction of neuroglia and microglia to brain wounds. *Bull. Johns Hopkins Hosp.*, 41: 278-303.
- Dixon, W. J., and F. J. Massey 1957 *Introduction to Statistical Analysis* 2nd edition, McGraw-Hill Book Company, Inc., New York, N. Y.
- Gall, J. G., and W. W. Johnson 1960 Is there "metabolic" DNA in the mouse seminal vesicle? *J. Biophys. Biochem. Cytol.*, 7: 657-665.
- Gavrilova, T. N. 1964 Vkluchenie ^3H -timidina v kletochnye elementy nervoi tkani vzrosplih myshek. *Tsitologiya*, 6: 622-626.
- Hain, R. F., W. O. Rieke and N. B. Everett 1960 Evidence of mitosis in neuroglia as revealed by radioautography employing tritiated thymidine. *J. Neuropath. Exp. Neurol.*, 19: 147-148.
- Hassler, O. 1966 Incorporation of thymidine- ^3H into mouse brain after a single dose of X-rays. An autoradiographic study. *J. Neuropath. Exp. Neurol.*, 25: 97-106.
- Hommes, Otto R., and C. P. Leblond 1967 Mitotic division of neuroglia in the normal adult rat. *J. Comp. Neur.*, 129: 269-278.
- Hughes, W. L., V. P. Bond, C. Brecher, E. P. Cronkite, R. P. Painter, R. Quastler and F. G. Sherman 1958 Cellular proliferation in the mouse as revealed by autoradiography with tritiated thymidine. *Proc. Nat. Acad. Sci.*, 44: 476-483.
- Huntington, H. W., and R. D. Terry 1966 The origin of the reactive cells in cerebral stab wounds. *J. Neuropath. Exp. Neurol.*, 25: 646-653.
- Klatzo, I., A. Piroux and E. J. Laskowski 1958 The relationship between edema, blood-brain barrier and tissue elements in a local brain injury. *J. Neuropath. Exp. Neurol.*, 17: 548-564.
- Koenig, H. 1960 Autoradiographic studies of deoxyribonucleic acid (DNA) turnover in the feline neuraxis. *J. Histochem. Cytochem.*, 8: 337.
- Koenig, H., M. B. Bunge and R. P. Bunge 1962 Nucleic acid and protein metabolism in white matter. *Arch. Neurol.*, 6: 177-193.
- Konigsmark, B. W., and R. L. Sidman 1963 Origin of brain macrophages in the mouse. *J. Neuropath. Exp. Neurol.*, 22: 643-676.
- 1964 Response of astrocytes to brain injury. *J. Neuropath. Exp. Neurol.*, 24: 142.
- Kosunen, T. U., B. H. Waksman and I. K. Samuelsson 1963 Radioautographic study of cellular mechanisms in delayed hypersensitivity. II. Experimental allergic encephalomyelitis in the rat. *J. Neuropath. Exp. Neurol.*, 22: 367-380.
- Kruskal, W. H., and W. A. Wallis 1952 Use of ranks in one-criterion variance analysis. *J. Amer. Statistical Assn.*, 47: 583-621.
- Leblond, C. P., and B. E. Walker 1956 Renewal of cell populations. *Physiol. Rev.*, 36: 255-276.
- Levine, S., and W. Stypulkowski 1959 Experimental cyanide encephalopathy. *Arch. Path.*, 67: 306-323.
- Messler, B., and C. P. Leblond 1960 Cell proliferation and migration as revealed by radioautography after injection of thymidine- ^3H into male rats and mice. *Am. J. Anat.*, 106: 247-285.
- Messler, B., C. P. Leblond and I. Smart 1958 Presence of DNA synthesis and mitosis in the brain of young adult mice. *Exp. Cell Res.*, 14: 224-226.
- Ngowyang, G. 1930 On the growth of the motor cells from birth to maturity at four levels in the spinal cord of the albino mouse. *J. Comp. Neur.*, 50: 231-245.
- Noetzel, H. 1962 Autoradiographische Untersuchungen über die physiologische Regeneration der Gliazellen. *Verh. Deutsch. Ges. Path.*, 46: 341-344.
- Noetzel, H., and J. Rox 1964 Autoradiographische Untersuchungen über Zellteilung und Zellentwicklung im Gehirn der erwachsenen Maus und des erwachsenen Rhesus-Affen nach Infektion von radioaktivem Thymidin. *Acta Neuropath.*, 3: 326-342.
- Pease, D. C. 1964 *Histological Techniques for Electron Microscopy*, 2nd Edition, Academic Press, New York, N. Y., 52.
- Penfield, W. 1925 Microglia and the process of phagocytosis in gliomas. *Amer. J. Path.*, 1: 77-90.
- Ries, E. 1938 Wann erlischt die mitotische Vermehrungsfähigkeit der Gewebe? *A. Mikr. Anat. Forsch.*, 43: 558-566.
- Roessmann, U., and R. L. Friede 1967 Entry of labeled donor cells from the bloodstream into the CNS. *J. Neuropath. Exp. Neurol.*, 26: 144-145.
- Samorajski, T., W. Zeman and J. M. Ord 1961 Histochemistry of particle microbeam lesions in the brain of the mouse. *J. Neuropath. Exp. Neurol.*, 23: 264-279.
- Schultze, B., and W. Oehlert 1960 Autoradiographic investigation of incorporation of ^3H -thymidine into cells of the rat and mouse. *Science*, 131: 737-738.
- Silver, M. L., and A. E. Walker 1947 Histopathology of thermocoagulation of the cerebral cortex. *J. Neuropath. Exp. Neurol.*, 6: 311-322.
- Smart, I. 1961 The subependymal layer of the mouse brain and its cell production as shown by radioautography after thymidine- ^3H injection. *J. Comp. Neur.*, 116: 325-347.
- Smart, I., and C. P. Leblond 1961 Evidence for division and transformation of neuroglia cells in the mouse brain as derived from radioautography after injection of thymidine- ^3H . *J. Comp. Neur.*, 116: 349-367.



PLATE I

EXPLANATION OF FIGURES

Examples of mitotic figures found in the spinal cord sections from the animals in group I, which were injected with tritiated thymidine before injury and sacrificed two (fig. 14) or three (figs. 11-13) days after injury.

- 11 Two prophases that were located near the lesion. Hematoxylin and eosin. $\times 1050$.
- 12 A prophase and a metaphase found near the lesion. Both mitotic figures were weakly labeled. Hematoxylin and eosin. $\times 1550$.
- 13 A labeled prophase and an unlabeled metaphase (arrow) found near the lesion. Hematoxylin and eosin. $\times 1550$.
- 14 Unlabeled anaphase (arrow) found at a considerable distance from the lesion on the second day after injury. Three neuronal nuclei and a capillary distended by the perfusion are also visible. Periodic acid Schiff hematoxylin. $\times 1050$.

Light and Electron Microscopic Observations on the Spleen and the Splenic Leukocytes of the Newt *Triturus cristatus*

J. TOOZE AND H. G. DAVIES

Department of Biophysics and Medical Research Council, Biophysics Research Unit, University of London, King's College, London, England

ABSTRACT The newt spleen has an outer region, the red pulp, that consists of reticular fibres, reticular cells, and fixed macrophages forming a framework within which erythropoiesis occurs, and an inner region, the white pulp, consisting of a reticular framework containing predominantly lymphocytes. The fine structure of the following leucocytes, namely lymphoid cells, reticular cells, macrophage, haemocyto-blasts, plasma cells and neutrophilic, basophilic and eosinophilic granulocytes is, in general, similar to that of the corresponding mammalian blood cells. However, in contrast, all the nuclei contain large numbers of interchromatin granules and a differentiated region termed the nuclear light-staining zone because of its electron-scattering properties. Furthermore the specific granules of the eosinophilic granulocytes are structureless whereas those of the basophilic granulocyte have crystalline regions. The structure and distribution of the granular, fibrillar, tubular and vesicular components of the cytoplasm of each cell type is described.

We have previously described the fine structure of the chromosomes in mitotic cells in the spleen of the newt *Triturus cristatus* (Davies and Tooze, '64, '66) and the cellular changes occurring during erythrocyte maturation in this organ (Tooze and Davies, '67). In this paper we describe electron microscopic observations of the fine structure of the non-erythrocytic cells in the newt spleen. We also examined these cells by light microscopy and as far as possible attempted to correlate the electron microscopic observations with our own and the earlier light microscopy of Jordan and Spiedel (see review Jordan, '38).

The early comparative haematologists (see especially Jordan, '32, '38; Jordan and Spiedel, '24, '30; and reviews by Foxon, '64; Andrew, '65) established the importance of the spleen as the primary haematopoietic organ in lower vertebrates. In adult mammals, the spleen is the exclusive site of erythropoiesis except in a few species, where most of the stem cells, the so-called haemocyto-blasts, leave the spleen and differentiate in the circulating blood (Jordan, '32). Development of thrombocytes also occurs in the spleen (Jordan and Spiedel, '30), whereas granulocytes usually develop in the subcapsular region of the liver, en-

tering the spleen presumably via the circulation (Jordan and Spiedel, '24).

Jordan ('32) commented on the striking similarity between the types of blood cells occurring in amphibians and mammals. Our observations on the fine structure of newt blood cells can be compared with those from many studies on mammalian, and from a few studies on avian, haematopoietic organs and blood cells, for example, Braunsteiner and Pakesch ('55); Low and Freeman ('58); Policard, Collet and Pregermain ('59); Bessis ('61); Bernhard and Granboulan ('60); Granboulan ('60); Sorenson ('60a,b); and Han ('61).

MATERIALS AND METHODS

The observations were made on spleens from the newt *Triturus cristatus*. The methods of preparation and study have been described in detail elsewhere (Davies and Tooze, '66; Tooze and Davies, '67). Briefly, smears were examined after staining in May-Grünwald-Giemsa (M.G.G.). Whole spleens or pieces were fixed in glutaraldehyde, post-fixed in OsO_4 (Sabatini, Bensch, and Barnett, '63) and embedded in araldite (Glauert and Glauert, '58; Luft, '61; Grimley, Albrecht and Michelitch, '65). Sections were stained with both uranyl

our. Reticular cells are not seen in smears and presumably remain behind in the reticular framework when the spleen is smeared as do most of the macrophages. Plasma cells have not been identified in smears. The three types of granulocytes are easily recognized. Neutrophilic granulocytes (fig. 9) have a highly polymorphic nucleus; the cytoplasm is unstained. Eosinophilic granulocytes (fig. 7) also have a highly lobed nucleus, and an extensive cytoplasm filled with orange staining eosinophilic granules. Basophilic granulocytes (fig. 8) can sometimes be seen to have a bilobed nucleus easily distinguishable from that of the eosinophil, and a cytoplasm filled with granules staining a deep bluish red.

Electron microscopy

1. Lymphoid cells

In the electron microscope a series of lymphoid cells with varying structure are seen. Typically small or medium sized lymphocytes appear round or slightly oval in cross section (fig. 14). Their nuclei, usually with several indentations, contain one or more large blocks of chromatin and many small regions of chromatin ranging in size from about 2500Å downwards, that is at about the limits of resolution of the light microscope. Chromatin blocks line the interior of the nuclear envelope. Also inside the nucleus are small lightly-stained regions partly bordered by chromatin, the structure of which is not well defined (fig. 14). Similar regions were found in the nuclei of erythroblasts (Tooze and Davies, '67) and were named nuclear light-staining zones. The nuclear sap contains numerous granules, referred to as interchromatin granules (Bernhard and Granboulan, '63), ranging in diameter from about 400Å downwards. These interchromatin granules are common in all the cell types described below, as well as in erythroblasts from *Triturus cristatus* (Davies and Tooze, '66; Tooze and Davies, '67). Occasionally groups of very large granules, about 1200Å in diameter, sometimes with hollow centres or U-shapes (figs. 14, 15), lie within the nuclear sap. Small nucleoli are common.

The cytoplasm forms a narrow rim about the nucleus and the surface is often thrown

into finger-like projections. Ribosomes are not very numerous; a few occur attached to endoplasmic reticulum, whilst smooth-surfaced endoplasmic reticulum in the form of flattened sheets and vesicles, is fairly common. There are a few mitochondria per section and usually granules, smaller than mitochondria, packed with homogeneous dark staining material (fig. 14).

The size and shape of the nucleus, the numbers of free ribosomes per unit area of cytoplasm and the amount of cytoplasm all vary in these lymphoid cells. Some of the lymphocyte-like cells that have elongated nuclei may correspond to the thrombocytes seen in the light microscope.

We have seen other cells which have a pronouncedly kidney-shaped nucleus. Centrioles as well as Golgi material almost invariably occur within the nuclear indentation forming a cytocentrum. Mitochondria and somewhat smaller electron-dense granules are also present within the cytocentrum. These cells may correspond to the monocytes seen in smears.

Another cell (fig. 16) with easily recognisable characteristics is found infrequently and we believe it corresponds to the haemocyctoblast seen in smears. This cell is characterised by a more abundant cytoplasm than is typical of the small lymphocytes; the cytoplasm is packed with ribosomal aggregates (polysomes) and many mitochondria. There is little granular or smooth-surfaced endoplasmic reticulum, but there is a Golgi zone, centrioles with pericentriolar bodies (Bernard and de Harven, '58; Bessis, '61; and Gall, '61) and a few microtubules about 230Å in diameter (see fig. 17). A few membrane-limited densely staining granules, smaller than mitochondria, also occur in the cytoplasm. The plasma membrane is often thrown into numerous projections. Much of the nuclear chromatin is distributed throughout the nucleus in small ($\leq 2500\text{\AA}$) blocks, and there is a narrow rim of condensed chromatin on the nuclear envelope (fig. 16). Nucleoli occur in these cells, as well as nuclear light-staining zones. In some cells, which have the cytoplasmic characteristics of haemocyctoblasts, the nuclear chromatin does not occur in small ($\leq 2500\text{\AA}$ diameter) blocks

acetate and lead citrate (Reynolds, '63) for electron microscopy or with various stains for light microscopy. The sections were examined in either a Zeiss E.M.9 or a Siemens Elmiskop I.

The problems of recognising the different types of blood cells in the electron microscope are well known (see e.g., Bernhard and Granboulan, '60) and we have discussed them previously (Tooze and Davies, '67).

RESULTS

Light microscopy

1. The structure of the spleen

The spleen of *Triturus cristatus* (figs. 1, 10) has a capsule consisting of an outer mesothelial cellular layer and an inner connective tissue sheath. The connective tissue extends inwards as trabeculae which join a reticular network (figs. 10, 11, 23, 24), so producing the framework of the organ. This reticular framework consists of groups of reticular fibres (figs. 11, 24) surrounded but often not enclosed by the cytoplasm of reticular cells, together with fixed macrophages (fig. 11). The extra-cellular reticular fibres each have a diameter of about 3000Å and an ill-defined banding (fig. 12). There is hardly any amorphous material surrounding these fibres, but there are fine threads lying between them (figs. 12, 13).

The distribution of red and white cells (fig. 1) is similar to that in the spleen of the newt *Triturus* (formerly *Diemyctylus*) *viridescens* described by Jordan and Speidel ('24). The outer region of the organ, the red pulp, consists partly of well defined venous sinuses, that is groups of red blood cells at various stages of development together with cells from circulating blood, such as lymphocytes and granulocytes, lying in irregularly shaped cavities outlined by the reticular framework. The venous sinuses (fig. 10) are interspersed among other areas of indefinitely arranged reticular fibres, reticular cells, macrophages and red and white blood cells, areas that may correspond to the cords thought to exist in the human spleen (Bloom and Fawcett, '62). In the outer regions of the red pulp the red blood cells are generally closely packed together (fig. 1). Well de-

fined blood vessels, circular or elliptical in section, that contain loosely packed erythrocytes are also present. The inner region of the spleen, the white pulp, consists of loosely arranged reticular fibres and reticular cells enclosing masses of lymphocytes and a few erythrocytes (see fig. 1).

As we reported elsewhere (Tooze and Davies, '67) the size of the spleen and the relative numbers of red and white cells varies greatly from animal to animal.

2. May-Grünwald-Giemsa smears

The various types of blood cells in the spleen were identified in M.G.G. stained smears. Lymphocytes of various sizes (figs. 2, 4) are characterized by a reddish, sometimes slightly reddish-blue (purple) nucleus usually containing well defined blocks of chromatin and a narrow band of cytoplasm, either hardly discernible or staining a light blue. In another type of cell (fig. 2), comparable in size with the largest lymphocytes, the nucleus is a definite purple and the cytoplasm is a distinct blue. Usually the nucleus appears more homogeneous in structure than that of the lymphocyte (compare figs. 2, 4) but blocks of chromatin are occasionally discernible (fig. 3). This cell appears to be similar to the haemocyto-blast described by Jordan and Speidel (30); haemocyto-blasts occur infrequently. There are also cells intermediate in appearance between haemocyto-blasts and the lymphocytes.

Cells identified as thrombocytes from criteria described by Jordan and Speidel ('30) and Andrew ('65) occur in clumps (fig. 5). Their nuclei, usually oval in shape, stain deep purple and occasionally appear grooved; the cytoplasm has numerous small projections and is very weakly stained; when the cells are in clumps their cytoplasm appears fused. Under oil-immersion some thrombocytes are seen to contain faint pink granules usually situated at one or both poles of the nucleus.

Monocytes (fig. 6) are readily distinguishable. They have an eccentrically placed nucleus, with a characteristic kidney-shape, staining a reddish colour, and a very weakly basophilic cytoplasm. Macrophages are seen very occasionally in smears, and are identified by the variety of their inclusion bodies, often green in

many groups of flattened sacs and circular vesicles.

4. Plasma cells

In the spleens we studied plasma cells were not common. They are characterised by a cytoplasm with enlarged cisternae of granular endoplasmic reticulum containing lightly-staining material (fig. 29). The ribosomes are usually more frequent on the membrane surfaces facing mitochondria (fig. 31) and this, no doubt, has physiological significance. There is extensive Golgi material and centrioles occur with pericentriolar bodies (fig. 29) as well as microtubules each about 230 Å diameter (fig. 30). Membrane-bound granules containing electron dense material are seen near the Golgi zone and scattered throughout the cytoplasm (fig. 29).

In the cells we examined the nucleus was eccentrically placed, contained clumped chromatin with a relatively large area of nuclear sap, and a small nucleolus. Interchromatin granules are prominent.

5. Granulocytes

(a) *Neutrophilic granulocytes.* The neutrophilic granulocytes are characterised by a highly polymorphic nucleus (fig. 9) causing the cell to appear multinucleate in thin sections (fig. 32). There are extensive regions of condensed chromatin on the interior surface of the nuclear envelope as well as small (≤ 2500 Å) blocks of chromatin throughout the nuclear sap. Small nucleoli and interchromatin granules are present.

Scattered throughout the cytoplasm are the characteristic neutrophilic granules. Like those in mammalian neutrophils (Palade, '55; Low and Freeman, '58; and Bessis, '61) they are shaped like rice grains or dumbbells and range in diameter from about 800–2000Å. They are membrane limited (fig. 37) and contain almost homogeneous material. There are also structures, interpreted as vesicles or sacs flattened or collapsed for most of their length, (figs. 32, 33, 35, 36), in which the two inner parts of the unit-membranes have fused to produce a darker line (fig. 35). These sacs have about the same circumference as the membranes limiting the neutrophilic granules. In some cells (fig. 33) empty sacs,

which are not collapsed, occur suggesting an intermediate stage between fully collapsed sacs and the neutrophilic granules.

According to Palade ('55) there is less endoplasmic reticulum in the neutrophilic granulocytes than in the basophilic and eosinophilic granulocytes of the rat. In those neutrophilic granulocytes of the newt, that we observed, however, there is more smooth and granular endoplasmic reticulum than in the other granulocytes. Occasionally (fig. 33) extensive regions of oriented granular endoplasmic reticulum occur. Scattered free throughout the cytoplasm are densely stained particles about the size of the ribosomes attached to the endoplasmic reticulum. Since after treatment with periodic acid and lead citrate some of these free particles had a granular substructure, resembling that of the glycogen granules in reticular cells, at least some of them may be small glycogen granules rather than ribosomes.

Like mammalian granulocytes (Policard and Bessis, '55) these cells have a large Golgi zone, with centrioles and microtubules about 230Å diameter (fig. 34) lying in this region. Bundles of fibrillar material, each fibril about 70Å diameter, are scattered throughout the cytoplasm (fig. 38).

(b) *Eosinophilic and Basophilic granulocytes.* The granules of eosinophilic granulocytes are generally understood to contain crystalline cores, whereas those of basophilic granulocytes are thought to be homogeneous (Low and Freeman, '58; Miller, de Harven and Palade, '66). Exceptionally, the granules in the basophilic granulocytes of guinea pig have been shown to contain lamellar structures (Pease, '55; Osaka, '59; Winquist, '60, '63; Fedorko and Hirsch, '65); similar crystalloid structure was found in human mast cells (Fedorko and Hirsch, '65). In *Triturus cristatus*, apart from the neutrophilic granulocytes, we see in the electron microscope two types of granulocytes. In one type (fig. 39) the cytoplasm contains dense homogeneous granules which are about 2–3 μ in diameter, larger than mitochondria, and approximately ovoid in shape. In cross section the cell (fig. 39) appears multinucleate presumably because the nucleus is lobed. These cells, as seen in the

but is in larger aggregates: these are however smaller than the large chromatin blocks that occur in lymphocyte nuclei.

2. Reticular cells

The characteristic features of the reticular cells are their association with the extra-cellular fibres of the reticular network and their highly indented nuclei, giving the surface of the nucleus a corrugated appearance (fig. 18). The chromatin is distributed partly in a thin layer on the inner surface of the nuclear envelope, but is mainly scattered in small clumps throughout the interior of the nucleus with occasionally a few larger blocks. There are small nuclear light-staining zones, large nucleoli and interchromatin granules.

The cytoplasm usually forms a fairly thin layer about the nucleus, and characteristically projects over long distances (fig. 23) bounding but not completely enclosing reticular fibres (figs. 11, 24). A striking feature of the cytoplasm is the large amount of fibrillar material it contains (fig. 18, 19), which is often aggregated into bundles and sometimes forms a continuous layer about the cell nucleus just within the plasma membrane. The individual fibrils are about 70Å thick (figs. 19, 20). There is a well-developed Golgi region with paired centrioles and pericentriolar bodies (fig. 18). Many profiles of granular endoplasmic reticulum are scattered throughout the cytoplasm, together with free ribosomes, mitochondria and few membrane-bounded granules, smaller than mitochondria, packed with densely-staining material.

The cytoplasm of the reticular cell also contains large amounts of glycogen which we identified with the periodic acid/lead citrate technique of Perry and Waddington ('66). In material fixed in glutaraldehyde and osmium tetroxide and stained with uranyl acetate and lead citrate, the glycogen in these cells normally appears as densely stained homogeneous granules about 250Å in diameter (see fig. 19) but very occasionally they show a granular substructure (see fig. 21). After periodic acid treatment and staining in lead citrate however all the granules have this substructure (fig. 22).

3. Macrophages

These large cells are readily identified in the electron microscope by the presence in the cytoplasm of dense granules and phagocytosed material (fig. 24). The nucleus appears elongate, and sometimes has deep indentations so that in thin sections it may appear bilobed. A layer of condensed chromatin is associated with the nuclear envelope; the interior of the nucleus is filled with many small regions of condensed chromatin and a few larger blocks. Light-staining zones are often seen, the one shown in figure 25 being rather larger than usual. Small nucleoli and interchromatin granules are present. Dense granules (figs. 25, 27) about 500Å diameter, which lie embedded in, or closely adjacent to, chromatin, but separated from it by a less dense annulus, are presumably perichromatin granules (Swift, '62; Watson, '62a,b).

The cytoplasmic inclusion bodies show a wide range of size and structure; some are recognisably phagocytosed erythrocytes which themselves contain cytosomes or polar bodies (fig. 24), while other bodies contain extensive myelin figures (fig. 25). There are at least four classes of roughly ovoid bodies or granules distinguishable within the cytoplasm after staining with uranyl acetate and lead citrate; large granules (g1) each of which contains variable concentrations of dense particles, presumably ferritin, the regions free from ferritin appearing dark-grey in stained sections (fig. 24; see the region of the granule g3 surrounding the eccentric dense granule, fig. 26); ovoid granules of varying size (g2) which appear electron-opaque (fig. 24) and sometimes membrane limited (fig. 24, 28); granules (g3) like g1 granules but containing within them very dense structures similar to g2 granules (fig. 26); smaller dark-grey granules (g4) without ferritin and sometimes seen to be membrane limited (figs. 25, 28). In some cells small electron dense particles, presumably ferritin, are scattered throughout the cytoplasm and nucleus, being excluded however from mitochondria (fig. 26) and chromatin.

The cytoplasm contains extensive profiles of smooth and granular endoplasmic reticulum and a few free ribosomes. The Golgi zone is often extensive consisting of

many groups of flattened sacs and circular vesicles.

4. Plasma cells

In the spleens we studied plasma cells were not common. They are characterised by a cytoplasm with enlarged cisternae of granular endoplasmic reticulum containing lightly-staining material (fig. 29). The ribosomes are usually more frequent on the membrane surfaces facing mitochondria (fig. 31) and this, no doubt, has physiological significance. There is extensive Golgi material and centrioles occur with pericentriolar bodies (fig. 29) as well as microtubules each about 230 Å diameter (fig. 30). Membrane-bound granules containing electron dense material are seen near the Golgi zone and scattered throughout the cytoplasm (fig. 29).

In the cells we examined the nucleus was eccentrically placed, contained clumped chromatin with a relatively large area of nuclear sap, and a small nucleolus. Interchromatin granules are prominent.

5. Granulocytes

(a) *Neutrophilic granulocytes.* The neutrophilic granulocytes are characterised by a highly polymorphic nucleus (fig. 9) causing the cell to appear multinucleate in thin sections (fig. 32). There are extensive regions of condensed chromatin on the interior surface of the nuclear envelope as well as small ($\approx 2500\text{Å}$) blocks of chromatin throughout the nuclear sap. Small nucleoli and interchromatin granules are present.

Scattered throughout the cytoplasm are the characteristic neutrophilic granules. Like those in mammalian neutrophils (Palade, '55; Low and Freeman, '58; and Bessis, '61) they are shaped like rice grains or dumbbells and range in diameter from about 800–2000 Å. They are membrane limited (fig. 37) and contain almost homogeneous material. There are also structures, interpreted as vesicles or sacs flattened or collapsed for most of their length, (figs. 32, 33, 35, 36), in which the two inner parts of the unit-membranes have fused to produce a darker line (fig. 35). These sacs have about the same circumference as the membranes limiting the neutrophilic granules. In some cells (fig. 33) empty sacs,

which are not collapsed, occur suggesting an intermediate stage between fully collapsed sacs and the neutrophilic granules.

According to Palade ('55) there is less endoplasmic reticulum in the neutrophilic granulocytes than in the basophilic and eosinophilic granulocytes of the rat. In those neutrophilic granulocytes of the newt, that we observed, however, there is more smooth and granular endoplasmic reticulum than in the other granulocytes. Occasionally (fig. 33) extensive regions of oriented granular endoplasmic reticulum occur. Scattered free throughout the cytoplasm are densely stained particles about the size of the ribosomes attached to the endoplasmic reticulum. Since after treatment with periodic acid and lead citrate some of these free particles had a granular substructure, resembling that of the glycogen granules in reticular cells, at least some of them may be small glycogen granules rather than ribosomes.

Like mammalian granulocytes (Policard and Bessis, '55) these cells have a large Golgi zone, with centrioles and microtubules about 230 Å diameter (fig. 34) lying in this region. Bundles of fibrillar material, each fibril about 70 Å diameter, are scattered throughout the cytoplasm (fig. 38).

(b) *Eosinophilic and Basophilic granulocytes.* The granules of eosinophilic granulocytes are generally understood to contain crystalline cores, whereas those of basophilic granulocytes are thought to be homogeneous (Low and Freeman, '58; Miller, de Harven and Palade, '66). Exceptionally, the granules in the basophilic granulocytes of guinea pig have been shown to contain lamellar structures (Pease, '55; Osaka, '59; Winquist, '60, '63; Fedorko and Hirsch, '65): similar crystalloid structure was found in human mast cells (Fedorko and Hirsch, '65). In *Triturus cristatus*, apart from the neutrophilic granulocytes, we see in the electron microscope two types of granulocytes. In one type (fig. 39) the cytoplasm contains dense homogeneous granules which are about 2–3 μ in diameter, larger than mitochondria, and approximately ovoid in shape. In cross section the cell (fig. 39) appears multinucleate presumably because the nucleus is lobed. These cells, as seen in the

but is in larger aggregates: these are however smaller than the large chromatin blocks that occur in lymphocyte nuclei.

2. Reticular cells

The characteristic features of the reticular cells are their association with the extra-cellular fibres of the reticular network and their highly indented nuclei, giving the surface of the nucleus a corrugated appearance (fig. 18). The chromatin is distributed partly in a thin layer on the inner surface of the nuclear envelope, but is mainly scattered in small clumps throughout the interior of the nucleus with occasionally a few larger blocks. There are small nucleolus light-staining zones, large nucleoli and interchromatin granules.

The cytoplasm usually forms a fairly thin layer about the nucleus, and characteristically projects over long distances (fig. 23) bounding but not completely enclosing reticular fibres (figs. 11, 24). A striking feature of the cytoplasm is the large amount of fibrillar material it contains (fig. 18, 19), which is often aggregated into bundles and sometimes forms a continuous layer about the cell nucleus just within the plasma membrane. The individual fibrils are about 70Å thick (figs. 19, 20). There is a well-developed Golgi region with paired centrioles and pericentriolar bodies (fig. 18). Many profiles of granular endoplasmic reticulum are scattered throughout the cytoplasm, together with free ribosomes, mitochondria and few membrane-bounded granules, smaller than mitochondria, packed with densely-staining material.

The cytoplasm of the reticular cell also contains large amounts of glycogen which we identified with the periodic acid/lead citrate technique of Perry and Waddington ('66). In material fixed in glutaraldehyde and osmium tetroxide and stained with uranyl acetate and lead citrate, the glycogen in these cells normally appears as densely stained homogeneous granules about 250Å in diameter (see fig. 19) but very occasionally they show a granular substructure (see fig. 21). After periodic acid treatment and staining in lead citrate however all the granules have this substructure (fig. 22).

3. Macrophages

These large cells are readily identified in the electron microscope by the presence in the cytoplasm of dense granules and phagocytosed material (fig. 24). The nucleus appears elongate, and sometimes has deep indentations so that in thin sections it may appear bilobed. A layer of condensed chromatin is associated with the nuclear envelope; the interior of the nucleus is filled with many small regions of condensed chromatin and a few larger blocks. Light-staining zones are often seen, the one shown in figure 25 being rather larger than usual. Small nucleoli and interchromatin granules are present. Dense granules (figs. 25, 27) about 500Å diameter, which lie embedded in, or closely adjacent to, chromatin, but separated from it by a less dense annulus, are presumably perichromatin granules (Swift, '62; Watson, '62a,b).

The cytoplasmic inclusion bodies show a wide range of size and structure; some are recognisably phagocytosed erythrocytes which themselves contain cytolysomes or polar bodies (fig. 24), while other bodies contain extensive myelin figures (fig. 25). There are at least four classes of roughly ovoid bodies or granules distinguishable within the cytoplasm after staining with uranyl acetate and lead citrate; large granules (g1) each of which contains variable concentrations of dense particles, presumably ferritin, the regions free from ferritin appearing dark-grey in stained sections (fig. 24; see the region of the granule g3 surrounding the eccentric dense granule, fig. 26); ovoid granules of varying size (g2) which appear electron-opaque (fig. 24) and sometimes membrane limited (fig. 24, 28); granules (g3) like g1 granules but containing within them very dense structures similar to g2 granules (fig. 26); smaller dark-grey granules (g4) without ferritin and sometimes seen to be membrane limited (figs. 25, 28). In some cells small electron dense particles, presumably ferritin, are scattered throughout the cytoplasm and nucleus, being excluded however from mitochondria (fig. 26) and chromatin.

The cytoplasm contains extensive profiles of smooth and granular endoplasmic reticulum and a few free ribosomes. The Golgi zone is often extensive consisting of

many groups of flattened sacs and circular vesicles.

4. Plasma cells

In the spleens we studied plasma cells were not common. They are characterised by a cytoplasm with enlarged cisternae of granular endoplasmic reticulum containing lightly-staining material (fig. 29). The ribosomes are usually more frequent on the membrane surfaces facing mitochondria (fig. 31) and this, no doubt, has physiological significance. There is extensive Golgi material and centrioles occur with pericentriolar bodies (fig. 29) as well as microtubules each about 230 Å diameter (fig. 30). Membrane-bound granules containing electron dense material are seen near the Golgi zone and scattered throughout the cytoplasm (fig. 29).

In the cells we examined the nucleus was eccentrically placed, contained clumped chromatin with a relatively large area of nuclear sap, and a small nucleolus. Interchromatin granules are prominent.

5. Granulocytes

(a) *Neutrophilic granulocytes*. The neutrophilic granulocytes are characterised by a highly polymorphic nucleus (fig. 9) causing the cell to appear multinucleate in thin sections (fig. 32). There are extensive regions of condensed chromatin on the interior surface of the nuclear envelope as well as small (≈ 2500 Å) blocks of chromatin throughout the nuclear sap. Small nucleoli and interchromatin granules are present.

Scattered throughout the cytoplasm are the characteristic neutrophilic granules. Like those in mammalian neutrophils (Palade, '55; Low and Freeman, '58; and Bessis, '61) they are shaped like rice grains or dumbbells and range in diameter from about 800–2000 Å. They are membrane limited (fig. 37) and contain almost homogeneous material. There are also structures, interpreted as vesicles or sacs flattened or collapsed for most of their length, (figs. 32, 33, 35, 36), in which the two inner parts of the unit-membranes have fused to produce a darker line (fig. 35). These sacs have about the same circumference as the membranes limiting the neutrophilic granules. In some cells (fig. 33) empty sacs,

which are not collapsed, occur suggesting an intermediate stage between fully collapsed sacs and the neutrophilic granules.

According to Palade ('55) there is less endoplasmic reticulum in the neutrophilic granulocytes than in the basophilic and eosinophilic granulocytes of the rat. In those neutrophilic granulocytes of the newt, that we observed, however, there is more smooth and granular endoplasmic reticulum than in the other granulocytes. Occasionally (fig. 33) extensive regions of oriented granular endoplasmic reticulum occur. Scattered free throughout the cytoplasm are densely stained particles about the size of the ribosomes attached to the endoplasmic reticulum. Since after treatment with periodic acid and lead citrate some of these free particles had a granular substructure, resembling that of the glycogen granules in reticular cells, at least some of them may be small glycogen granules rather than ribosomes.

Like mammalian granulocytes (Policard and Bessis, '55) these cells have a large Golgi zone, with centrioles and microtubules about 230 Å diameter (fig. 34) lying in this region. Bundles of fibrillar material, each fibril about 70 Å diameter, are scattered throughout the cytoplasm (fig. 38).

(b) *Eosinophilic and Basophilic granulocytes*. The granules of eosinophilic granulocytes are generally understood to contain crystalline cores, whereas those of basophilic granulocytes are thought to be homogeneous (Low and Freeman, '58; Miller, de Harven and Palade, '66). Exceptionally, the granules in the basophilic granulocytes of guinea pig have been shown to contain lamellar structures (Pease, '55; Osaka, '59; Winquist, '60, '63; Fedorko and Hirsch, '65): similar crystalloid structure was found in human mast cells (Fedorko and Hirsch, '65). In *Triturus cristatus*, apart from the neutrophilic granulocytes, we see in the electron microscope two types of granulocytes. In one type (fig. 39) the cytoplasm contains dense homogeneous granules which are about 2–3 μ in diameter, larger than mitochondria, and approximately ovoid in shape. In cross section the cell (fig. 39) appears multinucleate presumably because the nucleus is lobed. These cells, as seen in the

electron microscope, closely resemble the eosinophilic granulocytes seen in M.G.G. stained smears (compare figs. 39, 7). For this reason we conclude that they are eosinophilic granulocytes even though the fine structure of their granules differs from the generally understood structure of eosinophilic granules (Low and Freeman, '58; Miller et al., '66).

Most of the chromatin in these eosinophils is condensed on the inner surface of the nuclear envelope, but sometimes (fig. 39) both large and small (2500A) blocks of chromatin occur in the nuclear sap. Nucleoli have not been seen but interchromatin granules are numerous (fig. 39).

The eosinophils have little endoplasmic reticulum but very small vesicles occur throughout the cytoplasm (these are not easily seen in low power micrographs such as fig. 39). Aggregates of free ribosomes are scattered throughout the cell and there are a few mitochondria. Extensive Golgi zones, centrioles and microtubules have been seen; frequently there are finger-like projections from the cytoplasm.

The third type of granulocytes occurs less frequently than the neutrophilic and eosinophilic granulocytes; the shape of the nucleus in thin sections (fig. 40) is easily distinguished from that of the eosinophils and is what would be expected from sectioning the bilobed nucleus of the basophilic granulocytes seen in smears (fig. 8); therefore we identify these cells as basophilic granulocytes. The large dense granules characteristic of the cytoplasm contain crystalline regions (fig. 41) seen as spaced lines (dark lines of variable intensity separated by lighter stained spacings about 60-90A wide). We did not attempt to elucidate their structure further.

DISCUSSION

The fine structural features of the cells termed haemocytoblasts (fig. 16), namely the lack of a well developed endoplasmic reticulum, numerous free ribosomes, moderate numbers of mitochondria and the absence of any specialised cell structures are characteristic of undifferentiated cells (Porter, '54). The structure of these so-called haemocytoblasts in *Triturus cristatus* is similar to that of the primitive cells in popliteal nodes of rabbits described by

Sorenson ('60b), to cells in erythropoietic tissues of certain mammals (Sorenson, '60a, '63; Grasso, Swift and Ackerman, '62), and to the lymphoblasts in mammalian lymph nodes (Bernhard and Granboulan, '60). These cells also probably correspond to the haemocytoblasts or lymphoid haemoblasts described by Jordan and Speidel in light microscopic studies of newt spleen (see review Jordan, '38). These variously named cells are similar in appearance, and are thought to give rise to the different types of blood cell. According to the Unitarian theory of haematopoiesis which Jordan held, a single stem cell the haemocytoblast is multipotent, its differentiation into different types of blood cells depending on environmental factors; lymphocytes, although morphologically distinct from haemocytoblasts, also have multiple developmental potency according to this theory. Thus Jordan concluded from the presence of intermediate stages that in the urodele spleen haemocytoblasts or lymphocytes give rise to erythrocytes, thrombocytes and monocytes. Although we have seen a wide variety of lymphoid cells, some intermediate in appearance between the easily recognised lymphocyte (fig. 14) and the so-called haemocytoblast (fig. 16) our data are insufficient to support the theories of Jordan and Speidel.

The fine structure of the white blood cells found in the spleen of *Triturus cristatus*, in general, resembles that of their counterparts in mammalian tissues; this is seen when mammalian plasma cells (Braunsteiner, Fellingner and Pakesch, '53; Braunsteiner and Pakesch, '55; Thiry, '60; Bernhard and Granboulan, '60), small lymphocytes (Low and Freeman, '58; Bernhard and Granboulan, '60), and macrophages (Policard, Bessis and Breton-Gorius, '57; Sorenson, '60b; Han, '61; Thiry, '62) are compared with the same cell types of the newt. Interesting exceptions are eosinophilic and basophilic granulocytes.

In mammalian bone marrow (Policard and Bessis, '58; Bessis, '58, '59) reticular cells and macrophages occur almost exclusively surrounded by erythroblasts forming the so-called erythroblastic islands, and according to some authors (Bessis, '61; Sorenson, '62) there appears to be a direct transfer of material from the macrophage

to the surrounding cells. In newt spleen there are no recognisable cell islands, but basophilic erythroblasts usually occur close to the macrophage and reticular cells of the reticular framework (Tooze and Davies, '67); however, as we have discussed elsewhere (Tooze and Davies, '67), no evidence was seen of a transfer of material such as ferritin from the reticular cells or fixed macrophages to erythroblasts.

A variable amount of fine fibrillar material occurs in the cytoplasm of several types of mammalian blood cells including macrophages, monocytes, neutrophils and eosinophilic granulocytes, and various blood cells in leukemic animals (de Petris, Karlsbad and Pernis, '62); this material also occurs in basophilic erythroblasts of the newt (Tooze and Davies, '67). The reported diameters of these fibrils vary from about 40-80 Å in these different cell types and usually they are aggregated into bundles. We have not seen such fibrils in macrophages of newt, but they are occasionally present in neutrophilic granulocytes and are a striking feature of the cytoplasm of reticular cells.

We have observed membrane-bounded granules containing densely staining material in all the cell types recognised in the electron microscope. In lymphocytes, haemocytoblasts, reticular cells and plasma cells these granules are usually smaller than mitochondria and their contents appear homogeneous. These structures may be storage lysosomes similar to those thought to occur in immature erythroblasts (Tooze and Davies, '67) but evidence that they contain lysosomal enzymes is required to confirm this interpretation. We have been able to classify the cytoplasmic granules of macrophage into four distinct types on the basis of their fine structure. Since biochemical studies have shown that macrophages contain lysosomes (Cohn, Hirsch and Wiener, '63) it is likely that some if not all of the types of granules we identify are lysosomes, but whether differences in structure reflect differences in function remains to be seen. Polymorphonuclear granulocytes are known to be rich in hydrolytic enzymes (Cohn et al., '63) and Archer and Hirsch ('63) have shown several lysosomal enzymes in the specific granules of mammalian eosinophilic granulocytes.

According to Miller et al. ('66) it is probable that the crystalline cores in the granules of mammalian eosinophilic granulocytes consist of a specific peroxidase. We did not observe crystals in the cytoplasmic granules of newt eosinophilic granulocytes but they are present in the granules of newt basophilic granulocytes. In this respect these cells resemble the basophilic granulocytes of the guinea pig which, alone amongst the mammalian basophilic granulocytes so far studied, have cytoplasmic granules with crystalline cores (Winquist, '60; Fedorko and Hirsch, '65). As Miller et al. ('66) suggest, the presence of crystals within such granules may depend on the types and amounts of enzymes that they contain.

The presence of many interchromatin granules appears to be a characteristic feature of the nuclei of amphibian cells, and we have observed them in all the cell types described here; they also occur in pancreatic cells of the salamander (Swift, '59), in newt erythroblasts and mature erythrocytes of the newt and the frog *Rana esculenta* (Tooze and Davies, '67). We have discussed the electron staining properties and the nature of these granules elsewhere (Davies and Tooze, '66; Tooze and Davies, '67). Because of the large number of interchromatin granules it was sometimes difficult to decide whether granules associated with chromatin in the special manner of perichromatin granules (Swift, '62; Watson, '62a,b) occur in most of the cells described here; however, they are certainly present in macrophages. The significance of the so-called light-staining zones found in the nuclei of many types of leucocytes as well as erythroblasts (Tooze and Davies, '67) is unknown.

ACKNOWLEDGMENTS

We are grateful to Professor Sir John Randall, F. R. S. for continued encouragement and facilities, as well as to Professor Dame Honor Fell, F. R. S. and Dr. R. A. Rifkind for discussions. We are also indebted to Dr. W. Jacobson for discussion and advice on May-Grünwald-Giemsa stained material. We gratefully acknowledge technical help from Miss Pamela Rush, Miss Margaret Blade, and expert photographic help from Mrs. Freda Collier.

LITERATURE CITED

- Andrew, W. 1965 Comparative Haematology. Grune and Stratton, Inc., New York and London.
- Archer, G. T., and J. G. Hirsch 1963 Isolation of granules from eosinophil leukocytes and study of their enzyme content. *J. Exp. Med.*, 118: 277-286.
- Behnke, O. 1964 A preliminary report on 'microtubules' in undifferentiated and differentiated vertebrate cells. *J. Ultrastruct. Res.*, 11: 139-146.
- Bernhard, N., and N. Granboulan 1960 Ultrastructure of immunologically competent cells. In: C.I.B.A. Symposium on Cellular Aspects of Immunity. G. E. W. Wolstenholme and M. O'Connor, eds. Churchill Ltd., London. 92-116.
- 1963 The fine structure of the cancer cell nucleus. *Exptl. Cell Res.*, 9: (Suppl.): 19-53.
- Bernhard, W., and E. de Harven 1958 L'ultrastructure du centriole et d'autres éléments de l'appareil achromatique. *Proc. 4th Int. Cong. Electron Microsc.*, Berlin, 2: 217-227.
- Bessis, M. 1958 L'îlot érythroblastique, unité fonctionnelle de la moelle osseuse. *Revue Hemat.*, 13: 8-11.
- 1959 Erythropoiesis as seen with the electron microscope. In: Kinetics of Cellular Proliferation. F. R. Stohlman, Jr., ed. Grune Stratton, Inc., New York. 22-30.
- 1961 The blood cells and their formation. In: The Cell. J. Brachet and A. E. Mirsky, eds. Academic Press, London and New York, 5: 163-217.
- Bloom, W., and D. W. Fawcett 1962 A Textbook of Histology. Eighth edition. W. B. Saunders and Co., Philadelphia and London. 112-143, 303-316.
- Braunsteiner, H., K. Fellingner and F. Pakesch 1953 Demonstration of a cytoplasmic structure in plasma cells. *Blood*, 8: 916-922.
- Braunsteiner, H., and F. Pakesch 1955 Electron microscopy and the functional significance of a new cellular structure in plasmacytes: A review. *Blood*, 10: 650-654.
- Cohn, Z. A., J. G. Hirsch and E. Wiener 1963 Lysosomes and endocytosis. The cytoplasmic granules of phagocytic cells and the degradation of bacteria. In: C.I.B.A. Symposium "Lysosomes." A. V. S. de Rueck and M. P. Cameron, eds. Churchill, London, 126-150.
- Davies, H. G., and J. Tooze 1964 Electron microscope observations on mitotic chromosomes in erythroblasts of the newt, *Triturus cristatus cristatus*. *Nature*, 203: 990-992.
- 1966 Electron- and light-microscope observations on the spleen of the newt *Triturus cristatus*: the surface topography of the mitotic chromosomes. *J. Cell Sci.*, 1: 331-350.
- dePetrìs, S., G. Karlsbad and B. Pernis 1962 Filamentous structures in the cytoplasm of normal mononuclear phagocytes. *J. Ultrastruct. Res.*, 7: 39-55.
- Fedorko, M. E., and J. G. Hirsch 1965 Crystalloid structure in granules of guinea pig basophils and human mast cells. *J. Cell Biol.*, 26: 973-976.
- Foxon, G. E. H. 1964 Blood and respiration. In: Physiology of the Amphibia. J. A. Moore, ed. Academic Press, London and New York, 151-209.
- Gall, J. G. 1961 Centriole replication: A study of spermatogenesis in the snail *Vitellina*. *J. Cell Biol.*, 10: 163-193.
- Glauert, A. M., and R. H. Glauert 1958 Araldite as an embedding medium for electron microscopy. *J. biophys. biochem. Cytol.*, 4: 191-194.
- Granboulan, N. 1960 Etude au microscope électronique des cellules de la lignée lymphocytaire normale. *Revue Hemat.*, 15: 52-71.
- Grasso, J. A., H. Swift and G. A. Ackerman 1962 Observations on the development of erythrocytes in foetal liver. *J. Cell Biol.*, 14: 235-254.
- Grimley, P. M., J. M. Albrecht and H. J. Michelich 1965 Preparation of large epoxy sections for light microscopy as an adjunct to fine-structure studies. *Stain Tech.*, 40: 357-366.
- Han, S. S. 1961 The ultrastructure of the mesenteric lymph node of the rat. *Am. J. Anat.*, 109: 183-197.
- Jordan, H. E. 1932 The histology of the blood and the blood forming tissues of the urodele, *Proteus anguineus*. *Am. J. Anat.*, 51: 215-251.
- 1938 Comparative haematology. In: Handbook of Hematology. Vol. 2. H. Downey, ed. Hoeber, New York. 700-862.
- Jordan, H. E., and C. G. Speldel 1924 Studies on lymphocytes. III. Granulocytopenia in the salamander, with special reference to the monophyletic theory of blood-cell origin. *Am. J. Anat.*, 33: 485-505.
- 1930 The hemocytopoietic effect of splenectomy in the salamander, *Triturus viridescens*. *Am. J. Anat.*, 46: 55-80.
- Low, F. N., and J. A. Freeman 1958 Electron Microscopic Atlas of Normal and Leukemic Human Blood. McGraw-Hill, New York.
- Luft, J. H. 1961 Improvements in epoxy resin embedding methods. *J. biophys. biochem. Cytol.*, 9: 409-414.
- Miller, F. E., de Harven and G. E. Palade 1966 The structure of eosinophil leukocyte granules in rodents and in man. *J. Cell Biol.*, 31: 349-362.
- Osako, R. 1959 An electron microscopic observation on the specific granules of eosinophil leukocytes of vertebrates. *Acta Haematol. Japan*, 22: 134-147.
- Palade, G. E. 1955 Studies on the endoplasmic reticulum. II. Simple dispositions in cells in situ. *J. biophys. biochem. Cytol.*, 1: 567-582.
- Pease, D. C. 1955 Marrow cells seen with the electron microscope after thin sectioning. *Revue Hemat.*, 10: 300-313.
- Perry, M. M., and C. H. Waddington 1966 The ultrastructure of the cement gland in *Xenopus laevis*. *J. Cell Sci.*, 1: 193-200.
- Pollicard, A., and M. Bessis 1955 Etude au microscope électronique de la centrophère de leucocytes des mammifères. *Exptl. Cell Res.*, 8: 583-585.
- 1958 Sur un mode d'incorporation des macromolécules par la cellule, visible au microscope électronique la raphécytose. *Compt. Rend. Acad. Sci.*, 246: 3194-3197.

- Pelcard, A., M. Bessis and J. Breton-Gorius 1957 Structures myéliniques observées au microscope électronique sur des coupes des plaquettes rouges en voie de lyse. *Expl. Cell. Res.*, 13: 184-186.
- Pelcard, A., A. Collet and S. Pregermain 1959 Les cellules basophiles et éosinophiles du sang et des tissus chez le rat. Etude au microscope électronique. *Revue Hemat.*, 14: 278-293.
- Porter, K. R. 1954 Electron microscopy of basophilic components of cytoplasm. *J. Histochem. Cytochem.*, 2: 346-373.
- 1965 Cytoplasmic microtubules and their function. In: C.I.B.A. Symposium on the Principles of Biomolecular Organization. G. E. W. Wolstenholme and M. O'Connor, eds. 308-345.
- Reynolds, E. S. 1963 The use of lead citrate at high pH as an electron opaque stain in electron microscopy. *J. Cell Biol.*, 17: 208-212.
- Sabatini, D. D., K. Bensch and R. J. Barnett 1963 Cytochemistry and electron microscopy. *J. Cell Biol.*, 17: 19-58.
- Sorenson, G. D. 1960a An electron microscopic study of hematopoiesis in the liver of the fetal rabbit. *Am. J. Anat.*, 106: 27-40.
- 1960b An electron microscopic study of popliteal lymph nodes from rabbits. *Am. J. Anat.*, 107: 73-96.
- 1962 Electron microscopic observations of bone marrow from patients with sideroblastic anemia. *Amer. J. Path.*, 40: 297-314.
- 1963 Hepatic hematocytopenia in the fetal rabbit: A light and electron microscopic study. *Ann. N. Y. Acad. Sci.*, 111: 45-69.
- Swift, H. 1959 Studies on nuclear fine structure. *Brookhaven Symp. Biol.*, 12: 134-151.
- 1962 Nucleoprotein localisation in electron micrographs: metal binding and radioautography. In: *Symp. Int. Soc. Cell. Biol., Interpretation of Ultrastructure*. Berne, 1961. R. J. C. Harris, ed. Academic Press, New York and London. 213-232.
- Thiery, J. P. 1960 Microcinematographic contributions to the study of plasma cells. In: C.I.B.A. Symposium on Cellular Aspects of Immunity. G. E. W. Wolstenholme and M. O'Connor, eds. Churchill, London. 59-91.
- 1962 Etude au microscope électronique de l'ilot plasmocytaire. *J. de Microscopie*, 1: 275-286.
- Tooze, J., and H. G. Davies 1967 Electron and light microscope observations on the spleen of the newt *Triturus cristatus*. The fine structure of erythropoietic cells. *J. Cell Sci.*, in press.
- Watson, M. L. 1962a Observations on a granule associated with chromatin in the nuclei of cells of rat and mouse. *J. Cell Biol.*, 13: 162-167.
- 1962b Considerations of nucleic acid and morphology in fixed tissues. In: 5th Int. Congr. Electron Microscopy, Philadelphia. Vol. 2. Academic Press, New York and London. 0.5.
- Winquist, G. 1960 The ultrastructure of the granules of the basophilic granulocytes. *Zeit für Zellforsch.*, 52: 475-481.
- 1963 The electron microscopy of the basophilic granulocyte. *Ann. N.Y. Acad. Sci.*, 103: 352-375.

Abbreviations

be, basophilic erythroblast	l, lymphocyte
c, cytoplasm	lz, nuclear light-staining zone
ce, centriole	m, mitochondrion
e, erythrocyte	ma, macrophage
er, endoplasmic reticulum	M.G.G., May-Grünwald-Giemsa
fe, ferritin	mm, membrane material
fi, fibrils	mt, microtubules
gb, basophilic granule	nu, nucleolus
gc, cytoplasmic granules	pe, polychromatic erythroblast
ge, eosinophilic granule	r, ribosomes
gi, interchromatin granules	re, reticular cell
gn, neutrophilic granules	rf, reticular fibres
go, Golgi substance	rp, red pulp
gp, perichromatin granules	si, venous sinus
g1, g2, g3, g4, granules of macrophage cytoplasm	vc, collapsed vesicles
	wp, white pulp

All sectioned material, unless otherwise stated, was fixed in glutaraldehyde + OsO_4 , embedded in araldite and stained in uranyl acetate, plus lead citrate.

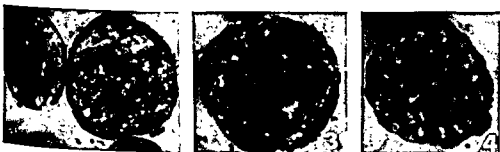
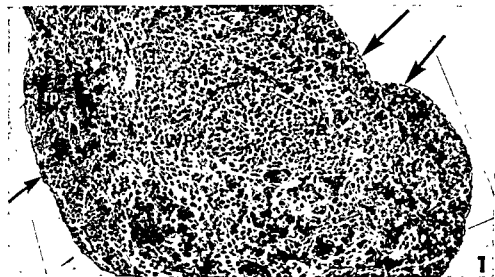
PLATE 1

EXPLANATION OF FIGURES

- 1 Light micrograph of $1\ \mu$ section through a segment of spleen fixed in glutaraldehyde only, stained with MacCullum's stain followed by toluidine blue. The outer regions, the red pulp, stain more densely than the inner region, the white pulp. The flattened nuclei of the outer mesothelial cell layer (arrowed) and the underlying connective tissue sheath are seen. $\times 120$.

Figs. 2-9 Light micrographs of cells from a spleen smear stained with May-Grünwald-Giemsa. $\times 1540$.

- 2 The large cell on the right is a so-called haemocytoblast with a small lymphocyte on the left.
- 3 Another cell with the staining properties of the haemocytoblast but with a somewhat more granular nucleus.
- 4 A large lymphocyte, the nucleus containing well-defined chromatin blocks.
- 5 A group of thrombocytes with their cytoplasm apparently fused together.
- 6 A monocyte with characteristic kidney shaped nucleus and lightly stained cytoplasm.
- 7 An eosinophilic granulocyte with highly lobed nucleus.
- 8 A basophilic granulocyte with a characteristic bilobed nucleus and cytoplasmic granules.
- 9 A neutrophilic granulocyte with a highly lobed nucleus and unstained cytoplasm.



Abbreviations

be, basophilic erythroblast	l, lymphocyte
c, cytoplasm	lz, nuclear light-staining zone
ce, centriole	m, mitochondrion
e, erythrocyte	ma, macrophage
er, endoplasmic reticulum	M.G.G., May-Grünwald-Giemsa
fe, ferritin	mm, membrane material
fi, fibrils	mt, microtubules
gb, basophilic granule	nu, nucleolus
gc, cytoplasmic granules	pe, polychromatic erythroblast
ge, eosinophilic granule	r, ribosomes
gi, interchromatin granules	re, reticular cell
gn, neutrophilic granules	rf, reticular fibres
go, Golgi substance	rp, red pulp
gp, perichromatin granules	sl, venous sinus
gl, g2, g3, g4, granules of macrophage cytoplasm	vc, collapsed vesicles
	wp, white pulp

All sectioned material, unless otherwise stated, was fixed in glutaraldehyde + OsO₄, embedded in araldite and stained in uranyl acetate, plus lead citrate.

PLATE 1

EXPLANATION OF FIGURES

- 1 Light micrograph of 1 μ section through a segment of spleen fixed in glutaraldehyde only, stained with MacCullum's stain followed by toluidine blue. The outer regions, the red pulp, stain more densely than the inner region, the white pulp. The flattened nuclei of the outer mesothelial cell layer (arrowed) and the underlying connective tissue sheath are seen. $\times 120$.

Figs. 2-9 Light micrographs of cells from a spleen smear stained with May-Grünwald-Giemsa. $\times 1540$.

- 2 The large cell on the right is a so-called haemocytoblast with a small lymphocyte on the left.
- 3 Another cell with the staining properties of the haemocytoblast but with a somewhat more granular nucleus.
- 4 A large lymphocyte, the nucleus containing well-defined chromatin blocks.
- 5 A group of thrombocytes with their cytoplasm apparently fused together.
- 6 A monocyte with characteristic kidney shaped nucleus and lightly stained cytoplasm.
- 7 An eosinophilic granulocyte with highly lobed nucleus.
- 8 A basophilic granulocyte with a characteristic bilobed nucleus and cytoplasmic granules.
- 9 A neutrophilic granulocyte with a highly lobed nucleus and unstained cytoplasm.

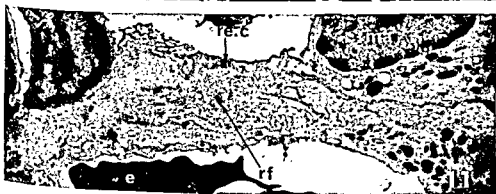
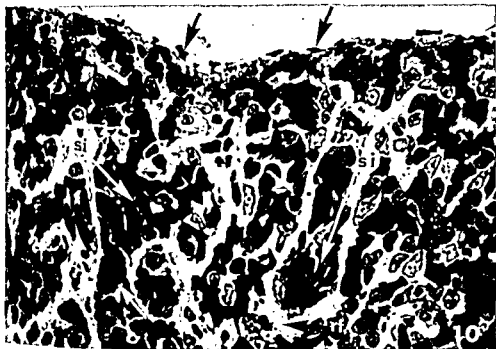


PLATE 2

EXPLANATION OF FIGURES

- 10 Light micrograph of a $1\ \mu$ section through the red pulp of the spleen. The venous sinuses are clearly outlined by lightly stained reticular fibres. The arrows mark cells of the mesothelial layer and the underlying connective tissue sheath. A mitotic polychromatic erythroblast is arrowed (white). $\times 500$.
- 11 Electron micrograph of part of the reticular framework of the red pulp. Numerous reticular fibres cut transversely and longitudinally are surrounded by reticular cell cytoplasm. $\times 5,000$.
- 12 Electron micrograph of reticular fibres cut longitudinally. $\times 90,000$.
- 13 Electron micrograph of reticular fibres cut transversely. $\times 108,000$.



PLATE 3

EXPLANATION OF FIGURES

- 14 Electron micrograph of a small or medium-sized lymphocyte, the cytoplasm of which abuts on that of other cells, probably a macrophage and two erythrocytic cells. Very large ($\sim 1200\text{\AA}$) granules within the nucleus are arrowed. $\times 14,000$.
- 15 Electron micrograph of part of a nucleus of a lymphocyte which shows adjacent groups of very large ($\sim 1200\text{\AA}$) granules (arrow) and interchromatin granules ($\sim 400\text{\AA}$). $\times 15,000$.



PLATE 4

EXPLANATION OF FIGURES

- 16 Electron micrograph of a haemocytoblast, the cytoplasm of which abuts on that of a macrophage and a polychromatic erythroblast. The haemocytoblast cytoplasm is packed with ribosomes and contains numerous mitochondria and a few membrane-limited densely staining granules. $\times 10,500$.
- 17 Electron micrograph of the microtubule arrowed in figure 16. $\times 33,000$.

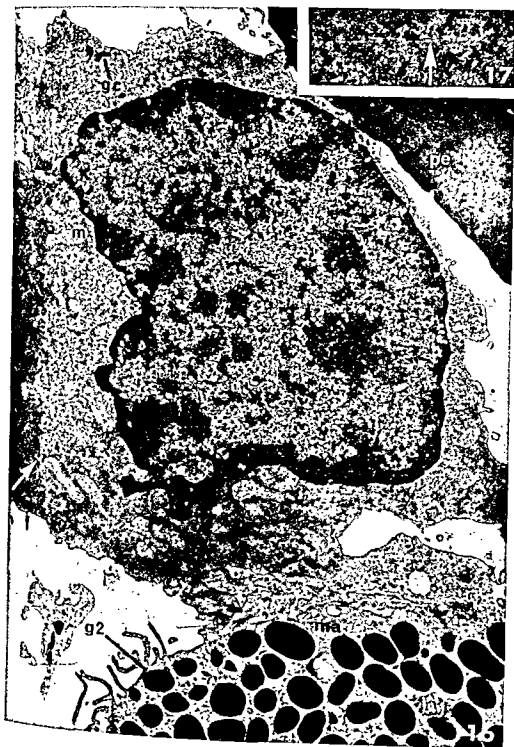


PLATE 5

EXPLANATION OF FIGURE

- 18 Electron micrograph of a reticular cell showing centrioles lying within Golgi material. Groups of glycogen granules in the cytoplasm are arrowed (see also figs. 19, 21, 22). Profiles of ribosome-studded endoplasmic reticulum are prominent at the bottom of the micrograph. The surface of the nucleus has the characteristic corrugated appearance. $\times 14,000$.



PLATE 6

EXPLANATION OF FIGURES

- 19 Electron micrograph of part of a reticular cell showing intracellular fibrils lying near the cell periphery (see fig. 18). Clusters of glycogen granules about 250Å diameter are arrowed. $\times 108,000$.
- 20 Electron micrograph of transversely sectioned fibrils in the cytoplasm of a reticular cell. $\times 125,000$.
- 21 Electron micrograph of part of a reticular cell with clusters of glycogen granules: each granule contains small particles about 40Å diameter. $\times 125,000$.
- 22 Electron micrograph of a reticular cell showing glycogen granules after treatment with periodic acid and lead citrate. $\times 120,000$.

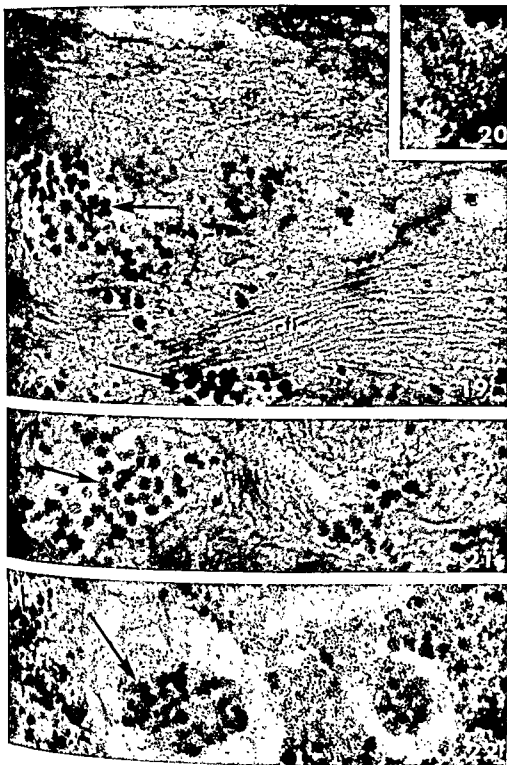


PLATE 6

EXPLANATION OF FIGURES

- 19 Electron micrograph of part of a reticular cell showing intracellular fibrils lying near the cell periphery (see fig. 18). Clusters of glycogen granules about 250Å diameter are arrowed. $\times 108,000$.
- 20 Electron micrograph of transversely sectioned fibrils in the cytoplasm of a reticular cell. $\times 125,000$.
- 21 Electron micrograph of part of a reticular cell with clusters of glycogen granules; each granule contains small particles about 40Å diameter. $\times 125,000$.
- 22 Electron micrograph of a reticular cell showing glycogen granules after treatment with periodic acid and lead citrate. $\times 120,000$.

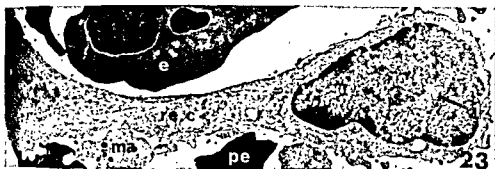


PLATE 7

EXPLANATION OF FIGURES

- 23 Electron micrograph of part of a reticular cell showing a cytoplasmic extension. $\times 5,000$.
- 24 Electron micrograph of a macrophage containing a phagocytosed erythrocyte. A cytolysome (polar body) arrow is present within the erythrocyte. Within the cytoplasm of the macrophage lie large dark-grey ferritin-containing granules (g1) and electron opaque granules (g2) (see fig. 28), g1 granules at higher magnification appear like the g3 granule shown in figure 26, but without the large dense inclusion. Note the reticular fibres and associated reticular cell cytoplasm which form the framework of the spleen. $\times 7,300$.

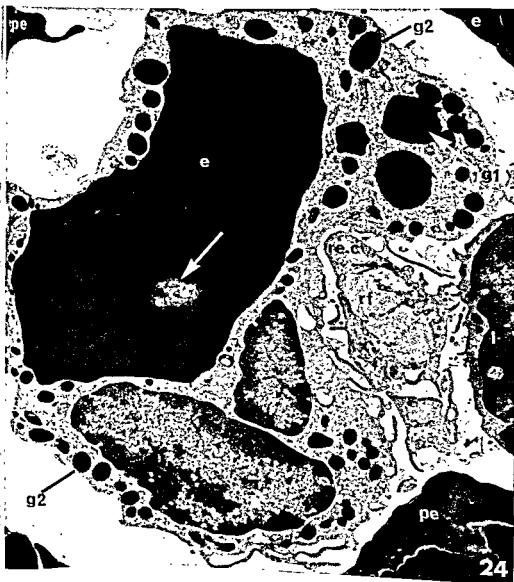
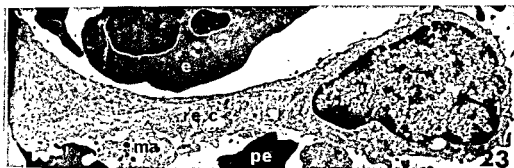


PLATE 8

EXPLANATION OF FIGURES

- 25 Electron micrograph of a macrophage showing cytoplasmic bodies containing extensive myelin formations (arrows) and adjacent g4 and g2 granules (see fig. 28). The cell has long finger-like cytoplasmic extensions. $\times 15,000$.
- 26 Electron micrograph of part of a macrophage showing a granule (type g3, see text) also containing profiles of stacked membranes (arrow). Note that ferritin is excluded from the mitochondrion. $\times 88,000$.
- 27 Electron micrograph of part of a macrophage nucleus showing perichromatin granules (arrow) and smaller interchromatin granules (gi). $\times 42,000$.
- 28 Electron micrograph of an almost electron-opaque granule (g2) with surrounding membrane: the smaller dark-grey granules (g4) are also membrane limited. $\times 40,000$.

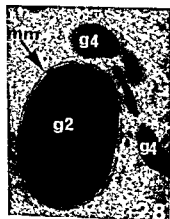
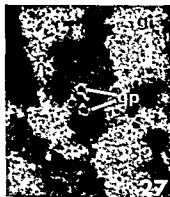
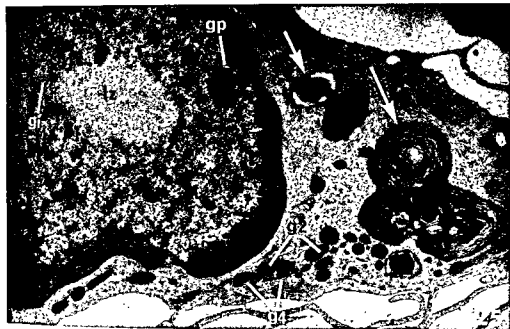


PLATE 8

EXPLANATION OF FIGURES

- 25 *Electron micrograph of a macrophage showing cytoplasmic bodies containing extensive myelin formations (arrows) and adjacent g4 and g2 granules (see fig. 28). The cell has long finger-like cytoplasmic extensions. $\times 15,000$.*
- 26 *Electron micrograph of part of a macrophage showing a granule (type g3, see text) also containing profiles of stacked membranes (arrow). Note that ferritin is excluded from the mitochondrion. $\times 88,000$.*
- 27 *Electron micrograph of part of a macrophage nucleus showing perichromatin granules (arrow) and smaller interchromatin granules (gi). $\times 42,000$.*
- 28 *Electron micrograph of an almost electron-opaque granule (g2) with surrounding membrane: the smaller dark-grey granules (g4) are also membrane limited. $\times 40,000$.*



PLATE 9

EXPLANATION OF FIGURES

- 29 Electron micrograph of a plasma cell showing a centriole embedded in Golgi material and numerous extended sacs of endoplasmic reticulum. The boxed area is enlarged in fig. 30. $\times 15,000$.
- 30 Electron micrograph of part (see box) of the cytoplasm of the cell shown in figure 29 showing microtubules and a membrane-bound cytoplasmic granule (gc). $\times 15,000$.
- 31 Electron micrograph of part of a plasma cell showing distended endoplasmic reticulum, the cavity of which contains electron scattering material; the membranes which face and partially enclose the mitochondria are preferentially studded with ribosomes. $\times 57,000$.



PLATE 10

EXPLANATION OF FIGURE

- 32 Electron micrograph of a neutrophilic granulocyte, the specific granules (see figs. 33, 37) of which have only stained faintly: flattened vesicles (see figs. 35, 36) are numerous. $\times 13,000$.

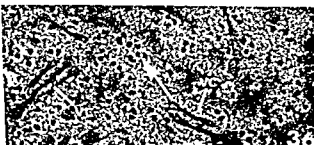
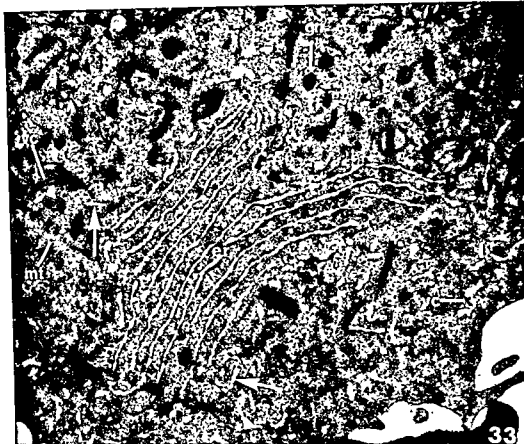


PLATE 11

EXPLANATION OF FIGURES

- 33 Electron micrograph of a neutrophilic granulocyte showing specific granules (see fig. 37), empty sacs or vesicles (arrows), collapsed vesicles (see figs. 35, 36) and an array of ribosome-studded endoplasmic reticulum. $\times 37,000$.
- 34 Electron micrograph of the microtubule at site marked mt in figure 33. $\times 60,000$.
- 35 Electron micrograph of a collapsed vesicle from a neutrophil showing tripartite structure. $\times 360,000$.
- 36 Electron micrograph showing collapsed vesicles and particles, possibly glycogen (arrowed) lying in the cytoplasm of a neutrophil. $\times 120,000$.
- 37 Electron micrograph of neutrophilic granules showing limiting membrane (arrows). $\times 120,000$.
- 38 Electron micrograph of a bundle of fibrils lying in the cytoplasm of a neutrophilic granulocyte. $\times 120,000$.



PLATE 12

EXPLANATION OF FIGURE

- 39 Electron micrograph of an eosinophilic granulocyte. Cytoplasmic vesicles are arrowed. $\times 9,000$.

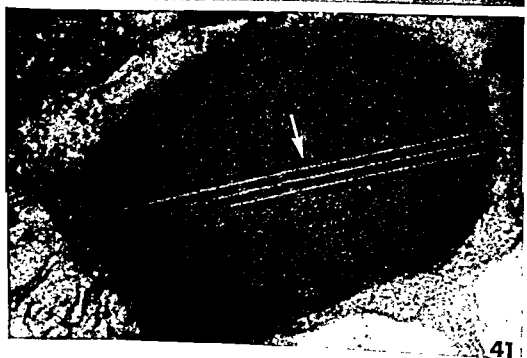
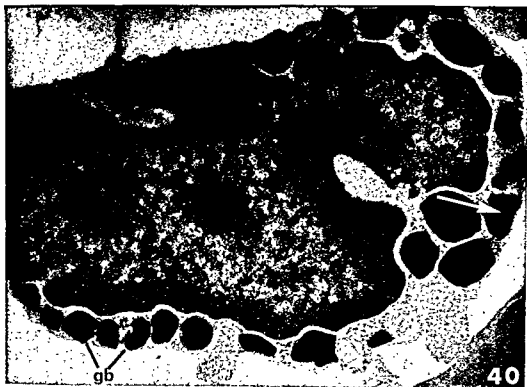


PLATE 13

EXPLANATION OF FIGURES

- 40 Electron micrograph of a basophilic granulocyte. A crystalline region in one of the granules is arrowed. $\times 6,000$.
- 41 Electron micrograph of a granule from a basophilic granulocyte which contains a crystalline region (arrow). $\times 128,000$.

A

- absorptive cells in suckling rats, the uptake of ferritin by fetal. An electron microscope study 297
- adipose cell maturation in vivo and in vitro, morphological features of brown 255
- adrenal cortex of the 13-lined ground squirrel, the fine structure of the 297
- ADAMS, ELLA K., JR. Cell division in injured spinal cord 501
- ADAMS, ERNEST N., AND LANTIER, C. FRANK. An electron microscopic study of uterine arteries during pregnancy 195
- animals, the innervation of the bone marrow in laboratory 315
- Arteries during pregnancy, an electron microscopic study of uterine 195
- ASHBURN, ALLEN D. See Clarke, Thomas D.
- Autogenous rat molars, the subcutaneous implantation of 113
- Autoradiographic investigation of calvarial growth in the rat 359

B

- BENFORD, J. M. Ultrastructural changes in the sperm head during fertilization in the rabbit 329
- BO, WALTER J., D. LOUISE OGDEN AND MARTHA NOTHROCK. The fine structure of uterine smooth muscle of the rat uterus at various time intervals following a single injection of estrogen 369
- BOND, JAMES A. See Irving, James T.
- Bone marrow in laboratory animals, the innervation of the 315
- BONNEVILLE, MARY A. Observations on epidermal differentiation in the fetal rat 147
- BROADUS, CAROLE D. See Davies, J.
- Brown adipose cell maturation in vivo and in vitro, morphological features of 255
- BULGER, RUTH ELLEN, AND BENJAMIN F. TRUMP. Renal morphology of the English sole (*Parophrys retulus*) 195

C

- Calvarial growth in the rat, autoradiographic investigation of 359
- CALVO, WENCESLAO. The innervation of the bone marrow in laboratory animals 315
- Cardiovascular lesions in mice, cortisone-induced hypertension and 429
- CARPENTER, MALCOLM B., BENNETT M. STEIN AND JOYCE E. SHRIVER. Central projections of spinal dorsal roots in the monkey. II. Lower thoracic, lumbosacral and coccygeal dorsal roots 75

- CARPENTER, MALCOLM B. See SHRIVER, JOYCE E.
- Cat gingiva, the ultrastructure of the crevicular epithelium of 283
- Central projections of spinal dorsal roots in the monkey. I. Cervical and upper thoracic dorsal roots 19
- II. Lower thoracic lumbosacral and coccygeal dorsal roots 17
- Cervical and upper thoracic dorsal roots, central projections of spinal dorsal roots in the monkey. I. 19

- Cells in suckling rats, the uptake of ferritin by fetal absorptive. An electron microscope study 297
- Cells in the rabbit, studies on the fine structure of ovarian steroid-secreting. I. The normal interstitial cells 441
- Cell division in injured spinal cord 501
- Cell maturation in vivo and in vitro, morphological features of brown adipose 255
- CLARKE, THOMAS D., ALLEN D. ASHBURN AND W. LANE WILLIAMS. Cortisone-induced hypertension and cardiovascular lesions in mice 429
- Coccygeal dorsal roots, central projections of spinal dorsal roots in the monkey. II. Lower thoracic lumbosacral and 75
- Cortex of the 13-lined ground squirrel, the fine structure of the adrenal 297
- Cortisone-induced hypertension and cardiovascular lesions in mice 429
- Crevicular epithelium of cat gingiva, the ultrastructure of the 283

D

- DAVIES, H. G. See Tootze, J.
- DAVIES, J., AND CAROLE D. BROADUS. Studies on the fine structure of ovarian steroid-secreting cells in the rabbit. I. The normal interstitial cells 441
- DE ANGELIS, VINCENT. Autoradiographic investigation of calvarial growth in the rat 359
- Development of the gonads in the female Japanese quail 131
- Differentiation in the fetal rat, observations on epidermal 147
- Division in injured spinal cord, cell 501
- DOMM, L. V. See Kannankeril, J. V.
- Dorsal roots in the monkey, central projections of spinal. I. Cervical and upper thoracic dorsal roots 27
- II. Lower thoracic lumbosacral and coccygeal dorsal roots 75
- DYER, ROBERT F. Morphological features of brown adipose cell maturation in vivo and in vitro 255

Index

A

- Absorptive cells in suckling rats, the uptake of ferritin by ileal. An electron microscope study 227
- Adipose cell maturation *in vivo* and *in vitro*, morphological features of brown 255
- Adrenal cortex of the 13-lined ground squirrel, the fine structure of the 297
- ADRIAN, ERLE K., JR. Cell division in injured spinal cord 501
- ALBERT, ERNEST N., AND DANIEL C. PEASE. An electron microscopic study of uterine arteries during pregnancy 165
- Animals, the innervation of the bone marrow in laboratory 315
- Arteries during pregnancy, an electron microscopic study of uterine 165
- ASHBURN, ALLEN D. See Clarke, Thomas D.
- Autogenous rat molars, the subcutaneous implantation of 429
- Autoradiographic investigation of calvarial growth in the rat 119

B

- BEDFORD, J. M. Ultrastructural changes in the sperm head during fertilization in the rabbit 329
- BO, WALTER J., D. LOUISE ODOR AND MARTHA ROTHROCK. The fine structure of uterine smooth muscle of the rat uterus at various time intervals following a single injection of estrogen 369
- BOND, JAMES A. See Irving, James T.
- Bone marrow in laboratory animals, the innervation of the 119
- BONNEVILLE, MARY A. Observations on epidermal differentiation in the fetal rat 147
- BROADUS, CAROLE D. See Davies, J.
- Brown adipose cell maturation *in vivo* and *in vitro*, morphological features of 255
- BULGER, RUTH ELLEN, AND BENJAMIN F. TRUMP. Renal morphology of the English sole (*Parophrys vetulus*) 195

C

- Calvarial growth in the rat, autoradiographic investigation of 359
- CALVO, WENCESLAO. The innervation of the bone marrow in laboratory animals 315
- Cardiovascular lesions in mice, cortisone-induced hypertension and 429
- CARPENTER, MALCOLM B., BENNETT M. STEIN AND JOYCE E. SHRIVER. Central projections of spinal dorsal roots in the monkey. II. Lower thoracic, lumbosacral and coccygeal dorsal roots 75

- CARPENTER, MALCOLM B. See Shriver, Joyce E. 27
- Cat gingiva, the ultrastructure of the crevicular epithelium of 283
- Central projections of spinal dorsal roots in the monkey. I. Cervical and upper thoracic dorsal roots 27
- II. Lower thoracic lumbosacral and coccygeal dorsal roots 75
- Cervical and upper thoracic dorsal roots, central projections of spinal dorsal roots in the monkey. I. 27
- Cells in suckling rats, the uptake of ferritin by ileal absorptive. An electron microscope study 227
- Cells in the rabbit, studies on the fine structure of ovarian steroid-secreting. I. The normal interstitial cells 441
- Cell division in injured spinal cord 501
- Cell maturation *in vivo* and *in vitro*, morphological features of brown adipose 255
- CLARKE, THOMAS D., ALLEN D. ASHBURN AND W. LANE WILLIAMS. Cortisone-induced hypertension and cardiovascular lesions in mice 429
- Coccygeal dorsal roots, central projections of spinal dorsal roots in the monkey. II. Lower thoracic lumbosacral and 75
- Cortex of the 13-lined ground squirrel, the fine structure of the adrenal 297
- Cortisone-induced hypertension and cardiovascular lesions in mice 429
- Crevicular epithelium of cat gingiva, the ultrastructure of the 283

D

- DAVIES, H. G. See Tooze, J. 521
- DAVIES, J., AND CAROLE D. BROADUS. Studies on the fine structure of ovarian steroid-secreting cells in the rabbit. I. The normal interstitial cells 441
- DE ANGELIS, VINCENT. Autoradiographic investigation of calvarial growth in the rat 359
- Development of the gonads in the female Japanese quail 131
- Differentiation in the fetal rat, observations on epidermal 147
- Division in injured spinal cord, cell 501
- DOMM, L. V. See Kannankeril, J. V. 131
- Dorsal roots in the monkey, central projections of spinal. I. Cervical and upper thoracic dorsal roots 27
- II. Lower thoracic lumbosacral and coccygeal dorsal roots 75
- DYER, ROBERT F. Morphological features of brown adipose cell maturation *in vivo* and *in vitro* 255

Maturation in vivo and in vitro, morphological features of brown adipose cell	255
Membranes of the tree shrews (family Tupaiidae), morphogenesis of the placenta and fetal	385
Mice, cortisone-induced hypertension and cardiovascular lesions in	429
Microscope study, the uptake of ferritin by ileal absorptive cells in suckling rats. An electron	227
Microscopic observations on the spleen and the splenic leukocytes of the newt <i>Triturus cristatus</i> , light and electron	521
Microscopic study of uterine arteries during pregnancy, an electron	165
Molars, the subcutaneous implantation of autogenous rat	119
Monkey, central projections of spinal dorsal roots in the	
I. Cervical and upper thoracic dorsal roots	27
II. Lower thoracic lumbosacral and coccygeal dorsal roots	75
Morphogenesis of the placenta and fetal membranes of the tree shrews (family Tupaiidae)	385
Morphological features of brown adipose cell maturation in vivo and in vitro	255
Morphology of the English sole (<i>Parophrys vetulus</i>), renal	195
Movement of muscles by Galen of Pergamon, on	1
Muscle of the rat uterus at various time intervals following a single injection of estrogen, the fine structure of uterine smooth	369
Muscles by Galen of Pergamon, on movement of	1

N

Neonatally thymectomized and nonthymectomized young rats, marginal zone and germinal center development in the spleens of	489
Newt <i>Triturus cristatus</i> , light and electron microscopic observations on the spleen and the splenic leukocytes of the	521
Nonthymectomized young rats, marginal zone and germinal center development in the spleens of neonatally thymectomized and	489
Normal interstitial cells, studies on the fine structure of ovarian steroid-secreting cells in the rabbit. I. The	441

O

Observations on epidermal differentiation in the fetal rat	147
Odor, D. LOUISE. See Bo, Walter J.	369
On movement of muscles by Galen of Pergamon	1
Ovarian steroid-secreting cells in the rabbit, studies on the fine structure of. I. The normal interstitial cells	441

P

PAPADIMITRIOU, J. M., AND M. N-I. WALTERS. Fluid flow in the liver demonstrated with horse radish peroxidase	475
(<i>Parophrys vetulus</i>), renal morphology of the English sole	195
PEASE, DANIEL C. See Albert, Ernest N.	165
Peroxidase, fluid flow in the liver demonstrated with horse radish	475
PETTERSEN, JAMES C., AND ROBERT J. ROSE. Marginal zone and germinal center development in the spleens of neonatally thymectomized and nonthymectomized young rats	489
Placenta and fetal membranes of the tree shrews (family Tupaiidae), morphogenesis of the	385
Pregnancy, an electron microscopic study of uterine arteries during	165
Projections of spinal dorsal roots in the monkey, central.	
I. Cervical and upper thoracic dorsal roots	27
II. Lower thoracic lumbosacral and coccygeal dorsal roots	75

Q

Quail, development of the gonads in the female Japanese	131
---	-----

R

Rabbit, studies on the fine structure of ovarian steroid-secreting cells in the. I. The normal interstitial cells	441
Rabbit, ultrastructural changes in the sperm head during fertilization in the	329
Rat, autoradiographic investigation of calvarial growth in the	359
Rat molars, the subcutaneous implantation of autogenous	119
Rat, observations on epidermal differentiation in the fetal	147
Rat uterus at various time intervals following a single injection of estrogen, the fine structure of uterine smooth muscle of the	369
Rats, marginal zone and germinal center development in the spleens of neonatally thymectomized and nonthymectomized young	489
Rats, the uptake of ferritin by ileal absorptive cells in suckling. An electron microscope study	227
Renal morphology of the English sole (<i>Parophrys vetulus</i>)	195
Roots in the monkey, central projections of spinal dorsal.	
I. Cervical and upper thoracic dorsal roots	27
II. Lower thoracic lumbosacral and coccygeal dorsal roots	75
ROSE, ROBERT J. See Pettersen, James C.	489
ROTHROCK, MARTHA. See Bo, Walter J.	369

E

- Electron microscope study, the uptake of ferritin by ileal absorptive cells in suckling rats. An 227
- Electron microscopic observations on the spleen and the splenic leukocytes of the newt *Triturus cristatus*, light and 521
- Electron microscopic study of uterine arteries during pregnancy, an 165
- English sole (*Parophrys vetulus*), renal morphology of the 195
- Epidermal differentiation in the fetal rat, observations on 147
- Epithelium of cat gingiva, the ultrastructure of the crevicular 283
- Estrogen, the fine structure of uterine smooth muscle of the rat uterus at various time intervals following a single injection of 369

F

- Female Japanese quail, development of the gonads in the 131
- Ferritin by ileal absorptive cells in suckling rats, the uptake of. An electron microscope study 227
- Fertilization in the rabbit, ultrastructural changes in the sperm head during 329
- Fetal membranes of the tree shrews (family Tupaiidae), morphogenesis of the placenta and 385
- Fetal rat, observations on epidermal differentiation in the 147
- Fine structure of the adrenal cortex of the 13-lined ground squirrel, the 297
- Fine structure of uterine smooth muscle of the rat uterus at various time intervals following a single injection of estrogen, the 369
- Fluid flow in the liver demonstrated with horse radish peroxidase 475

G

- Galen of Pergamon, on movement of muscles by 1
- GAVIN, J. B. The ultrastructure of the crevicular epithelium of cat gingiva 283
- Germinal center development in the spleens of neonatally thymectomized and nonthymectomized young rats, marginal zone and 489
- Gingiva, the ultrastructure of the crevicular epithelium of cat 283
- Gonads in the female Japanese quail, development of the 131
- Goss, CHARLES MAYO. On movement of muscles by Galen of Pergamon 1
- GRANEY, DANIEL O. The uptake of ferritin by ileal absorptive cells in suckling rats. An electron microscope study 227
- Ground squirrel, the fine structure of the adrenal cortex of the 13-lined 297
- Growth in the rat, autoradiographic investigation of calvarial 359

H

- Horse radish peroxidase, fluid flow in the liver demonstrated with 475
- Hypertension and cardiovascular lesions in mice, cortisone-induced 429

I

- Ileal absorptive cells in suckling rats, the uptake of ferritin by. An electron microscope study 227
- Implantation of autogenous rat molars, the subcutaneous 119
- Injured spinal cord, cell division in 501
- Innervation of the bone marrow in laboratory animals, the 315
- Interstitial cells, studies on the fine structure of ovarian steroid-secreting cells in the rabbit. I. The normal 441
- In vitro*, morphological features of brown adipose cell maturation *in vivo* and 255
- In vivo* and *in vitro*, morphological features of brown adipose cell maturation 255
- IRVING, JAMES T., AND JAMES A. BOND. The subcutaneous implantation of autogenous rat molars 119

J

- Japanese quail, development of the gonads in the female 131

K

- KANNANKERIL, J. V., AND L. V. DOMM. Development of the gonads in the female Japanese quail 131

L

- Laboratory animals, the innervation of the bone marrow in 315
- Leukocytes of the newt *Triturus cristatus*, light and electron microscopic observations on the spleen and the splenic 521
- Lesions in mice, cortisone-induced hypertension and cardiovascular 429
- Light and electron microscopic observations on the spleen and the splenic leukocytes of the newt *Triturus cristatus* 521
- Liver demonstrated with horse radish peroxidase, fluid flow in the 475
- LUCKETT, WINTER PATRICK. Morphogenesis of the placenta and fetal membranes of the tree shrews (family Tupaiidae) 385
- Lumbosacral and coccygeal dorsal roots, central projections of spinal dorsal roots in the monkey. II. Lower thoracic 75

M

- Marginal zone and germinal center development in the spleens of neonatally thymectomized and nonthymectomized young rats 489

Maturation <i>in vivo</i> and <i>in vitro</i> , morphological features of brown adipose cell	255
Membranes of the tree shrews (family Tupaiidae), morphogenesis of the placenta and fetal	385
Mice, cortisone-induced hypertension and cardiovascular lesions in	429
Microscope study, the uptake of ferritin by ileal absorptive cells in suckling rats. An electron	227
Microscopic observations on the spleen and the splenic leukocytes of the newt <i>Triturus cristatus</i> , light and electron	521
Microscopic study of uterine arteries during pregnancy, an electron	165
Molars, the subcutaneous implantation of autogenous rat	119
Monkey, central projections of spinal dorsal roots in the.	
I. Cervical and upper thoracic dorsal roots	27
II. Lower thoracic lumbosacral and coccygeal dorsal roots	75
Morphogenesis of the placenta and fetal membranes of the tree shrews (family Tupaiidae)	385
Morphological features of brown adipose cell maturation <i>in vivo</i> and <i>in vitro</i>	255
Morphology of the English sole (<i>Parophrys vetulus</i>), renal	195
Movement of muscles by Galen of Pergamon, on	1
Muscle of the rat uterus at various time intervals following a single injection of estrogen, the fine structure of uterine smooth	369
Muscles by Galen of Pergamon, on movement of	1

N

Neonatally thymectomized and nontymectomized young rats, marginal zone and germinal center development in the spleens of	489
Newt <i>Triturus cristatus</i> , light and electron microscopic observations on the spleen and the splenic leukocytes of the	521
Nontymectomized young rats, marginal zone and germinal center development in the spleens of neonatally thymectomized and	489
Normal interstitial cells, studies on the fine structure of ovarian steroid-secreting cells in the rabbit. I. The	441

O

Observations on epidermal differentiation in the fetal rat	147
ODOR, D. LOUIS. See Bo, Walter J.	369
On movement of muscles by Galen of Pergamon	1
Ovarian steroid-secreting cells in the rabbit, studies on the fine structure of. I. The normal interstitial cells	441

P

PAPADIMITRIOU, J. M., AND M. N. I. WALTERS. Fluid flow in the liver demonstrated with horse radish peroxidase	475
(<i>Parophrys vetulus</i>), renal morphology of the English sole	195
PEASE, DANIEL C. See Albert, Ernest N. ..	165
Peroxidase, fluid flow in the liver demonstrated with horse radish	475
PETTERSEN, JAMES C., AND ROBERT J. ROSE. Marginal zone and germinal center development in the spleens of neonatally thymectomized and nontymectomized young rats	489
Placenta and fetal membranes of the tree shrews (family Tupaiidae), morphogenesis of the	385
Pregnancy, an electron microscopic study of uterine arteries during	165
Projections of spinal dorsal roots in the monkey, central.	
I. Cervical and upper thoracic dorsal roots	27
II. Lower thoracic lumbosacral and coccygeal dorsal roots	75

Q

Quail, development of the gonads in the female Japanese	131
---	-----

R

Rabbit, studies on the fine structure of ovarian steroid-secreting cells in the. I. The normal interstitial cells	441
Rabbit, ultrastructural changes in the sperm head during fertilization in the	329
Rat, autoradiographic investigation of calvarial growth in the	359
Rat molars, the subcutaneous implantation of autogenous	119
Rat, observations on epidermal differentiation in the fetal	147
Rat uterus at various time intervals following a single injection of estrogen, the fine structure of uterine smooth muscle of the	369
Rats, marginal zone and germinal center development in the spleens of neonatally thymectomized and nontymectomized young	489
Rats, the uptake of ferritin by ileal absorptive cells in suckling. An electron microscope study	227
Renal morphology of the English sole (<i>Parophrys vetulus</i>)	195
Roots in the monkey, central projections of spinal dorsal.	
I. Cervical and upper thoracic dorsal roots	27
II. Lower thoracic lumbosacral and coccygeal dorsal roots	75
ROSE, ROBERT J. See Pettersen, James C. ..	489
ROTHEROCK, MARTHA. See Bo, Walter J.	369

E

- Electron microscope study, the uptake of ferritin by ileal absorptive cells in suckling rats. *An* 227
- Electron microscopic observations on the spleen and the splenic leukocytes of the newt *Triturus cristatus*, light and 521
- Electron microscopic study of uterine arteries during pregnancy, *an* 165
- English sole (*Parophrys vetulus*), renal morphology of the 195
- Epidermal differentiation in the fetal rat, observations on 147
- Epithelium of cat gingiva, the ultrastructure of the crevicular 283
- Estrogen, the fine structure of uterine smooth muscle of the rat uterus at various time intervals following a single injection of 369

F

- Female Japanese quail, development of the gonads in the 131
- Ferritin by ileal absorptive cells in suckling rats, the uptake of. *An electron microscope study* 227
- Fertilization in the rabbit, ultrastructural changes in the sperm head during 329
- Fetal membranes of the tree shrews (family Tupaiidae), morphogenesis of the placenta and 385
- Fetal rat, observations on epidermal differentiation in the 147
- Fine structure of the adrenal cortex of the 13-lined ground squirrel, the 297
- Fine structure of uterine smooth muscle of the rat uterus at various time intervals following a single injection of estrogen, the 369
- Fluid flow in the liver demonstrated with horse radish peroxidase 475

G

- Galen of Pergamon, on movement of muscles by 1
- GAVIN, J. B. The ultrastructure of the crevicular epithelium of cat gingiva 283
- Germinal center development in the spleens of neonatally thymectomized and nonthymectomized young rats, marginal zone and 489
- Gingiva, the ultrastructure of the crevicular epithelium of cat 283
- Gonads in the female Japanese quail, development of the 131
- Goss, CHARLES MAYO. On movement of muscles by Galen of Pergamon 1
- GRANEY, DANIEL O. The uptake of ferritin by ileal absorptive cells in suckling rats. *An electron microscope study* 227
- Ground squirrel, the fine structure of the adrenal cortex of the 13-lined 297
- Growth in the rat, autoradiographic investigation of calvarial 359

H

- Horse radish peroxidase, fluid flow in the liver demonstrated with 475
- Hypertension and cardiovascular lesions in mice, cortisone-induced 429

I

- Ileal absorptive cells in suckling rats, the uptake of ferritin by. *An electron microscope study* 227
- Implantation of autogenous rat molars, the subcutaneous 119
- Injured spinal cord, cell division in 501
- Innervation of the bone marrow in laboratory animals, the 315
- Interstitial cells, studies on the fine structure of ovarian steroid-secreting cells in the rabbit. I. The normal 441
- In vitro*, morphological features of brown adipose cell maturation *in vivo* and 255
- In vivo* and *in vitro*, morphological features of brown adipose cell maturation 255
- IRVING, JAMES T., AND JAMES A. BOND. The subcutaneous implantation of autogenous rat molars 119

J

- Japanese quail, development of the gonads in the female 131

K

- KANNANKERIL, J. V., AND L. V. DOMM. Development of the gonads in the female Japanese quail 131

L

- Laboratory animals, the innervation of the bone marrow in 315
- Leukocytes of the newt *Triturus cristatus*, light and electron microscopic observations on the spleen and the splenic 521
- Lesions in mice, cortisone-induced hypertension and cardiovascular 429
- Light and electron microscopic observations on the spleen and the splenic leukocytes of the newt *Triturus cristatus* 521
- Liver demonstrated with horse radish peroxidase, fluid flow in the 475
- LUCKETT, WINTER PATRICK. Morphogenesis of the placenta and fetal membranes of the tree shrews (family Tupaiidae) 385
- Lumbosacral and coccygeal dorsal roots, central projections of spinal dorsal roots in the monkey. II. Lower thoracic 75

M

- Marginal zone and germinal center development in the spleens of neonatally thymectomized and nonthymectomized young rats 485

S

- SELIGER, WILLIAM G., AND WAYNE F. SMITH.
The fine structure of the adrenal cortex
of the 13-lined ground squirrel 297
- Shrews (family Tupaiidae), morphogenesis
of the placenta and fetal membranes of
the tree 385
- SHRIVER, E. JOYCE, BENNETT M. STEIN AND
MALCOLM B. CARPENTER. Central projec-
tions of spinal dorsal roots in the monkey.
I. Cervical and upper thoracic dorsal roots 27
- SHRIVER, JOYCE E. See Carpenter, Malcolm
B. 75
- SMITH, WAYNE F. See Seliger, William G.
Sole (*Paraphrys vetulus*), renal morphology
of the English 297
- Sperm head during fertilization in the rab-
bit, ultrastructural changes in the 195
- Spinal cord, cell division in injured 329
- Spinal dorsal roots in the monkey, central
projections of.
I. Cervical and upper thoracic dorsal
roots 501
- II. Lower thoracic lumbosacral and coc-
cygeal dorsal roots 27
- Spleen and the splenic leukocytes of the
newt *Triturus cristatus*, light and electron
microscopic observations on the 75
- Spleens of neonatally thymectomized and
nonthymectomized young rats, marginal
zone and germinal center development
in the 521
- STEIN, BENNETT M. See Carpenter, Malcolm
B. 489
- STEIN, BENNETT M. See Shriver, Joyce E.
Steroid-secreting cells in the rabbit, studies
on the fine structure of ovarian. I. The
normal differentiating cells 75
- Structure of ovarian steroid-secreting cells
in the rabbit, studies on the fine. I. The
normal interstitial cells 27
- Structure of the adrenal cortex of the 13-
lined ground squirrel, the fine 441
- Structure of uterine smooth muscle of the
rat uterus at various time intervals fol-
lowing a single injection of estrogen, the
fine 441
- Studies on the fine structure of ovarian
steroid-secreting cells in the rabbit. I. The
normal interstitial cells 297
- Subcutaneous implantation of autogenous
rat molars, the 369

T

- Thoracic dorsal roots, central projections of
spinal dorsal roots in the monkey. I. Cer-
vical and upper 1
- Thoracic lumbosacral and coccygeal dorsal
roots, central projections of spinal dorsal
roots in the monkey, II. Lower 7
- Thymectomized and nonthymectomized
young rats, marginal zone and germinal
center development in the spleens of
neonatally 46
- Time intervals following a single injection
of estrogen, the fine structure of uterine
smooth muscle of the rat uterus at vari-
ous 36
- TOOZE, J., AND H. G. DAVIES. Light and
electron microscopic observations on the
spleen and the splenic leukocytes of the
newt *Triturus cristatus* 52
- Triturus cristatus*, light and electron micro-
scopic observations on the spleen and the
splenic leukocytes of the newt 52
- TRUMP, BENJAMIN F. See Bulger, Ruth
Ellen 18
- Tupaiidae, morphogenesis of the placenta
and fetal membranes of the tree shrews
(family 36

U

- Ultrastructural changes in the sperm head
during fertilization in the rabbit 32
- Ultrastructure of the crevicular epithelium
of cat gingiva, the 28
- Uptake of ferritin by ileal absorptive cells
in suckling rats, the. An electron micro-
scope study 22
- Uterine arteries during pregnancy, an elec-
tron microscopic study of 16
- Uterine smooth muscle of the rat uterus at
various time intervals following a single
injection of estrogen, the fine structure of 361
- Uterus at various time intervals following
a single injection of estrogen, the fine
structure of uterine smooth muscle of the
rat 361

W

- WALTERS, M. N-I. See Papadimitriou, J. M. 471
- WILLIAMS, W. LANE. See Clarke, Thomas D. 425

